An evaluation of the neurotoxicity of pesticides and alcohol using human neuroblastoma cells and human progenitor cortical neural stem cells

By

Wijesekara Mudiayanselage Anusha Udayangani Kumari Manike Wijesekara

The thesis is submitted to the University of Nottingham for the degree Doctor of Philosophy



Special thanks to

Commonwealth Scholarship Commission, UK

(Commonwealth PhD scholarships)

DECLARATION

I declare that this thesis has been completed by myself under the supervision of Dr. Wayne Grant Carter and Dr. Ian Mellor at the Division of Medical Sciences and Graduate Entry Medicine, School of Medicine, University of Nottingham, Royal Derby Hospital Centre. This thesis is a record of work that has not been submitted previously for a higher degree.

Wijesekara Mudiyanselage Anusha Udayangani Kumari Manike Wijesekara

PUBLICATIONS

- **Wijesekara W. M. A. U. K. M**, Wijamunige W.B.C, Kocoń, A and Carter W.G (2019). Alcohol damages and kills neurons in a concentration and exposure duration dependent fashion (in preparation).
- **Wijesekara, W. M. A. U. K. M** and Carter W.G (2019). Neurotoxicity evaluation of acute pesticide exposure on Human progenitor neural stem cells, Letters of toxicology, Volume 314S1; S221 (ISSN 0378-4274 314 (S1) S1–S339 (2019).

Oral presentations

- **Wijesekara, W. M. A. U. K. M.** (2018). Evaluation of neurotoxicity of pesticides using neuroblastoma cells, CSC scholar's symposium. 3rd August 2018, Trent building, University of Nottingham.UK.
- **Wijesekara W. M. A. U. K. M** (2019)**.** Acute exposure of organophosphate pesticides triggers neuronal cell death in human neural progenitor cells. Sue Watson Presentation event, 24th of May School of Medicine, room no B28, Queens medical centre, University of Nottingham.
- **Wijesekara W. M. A. U. K. M, Wijamunige W.B.C, Knagg C and Carter W.G** (2019) Alcohol induced oxidative stress damages in neuronal cells, Post transitional protein modification and cell signalling, Life sciences conferences, East Midland conference centre, 17-18th March, Nottingham.

Poster presentations

- **Wijesekara W. M. A. U. K. M, Wijamunige W.B.C, Knagg C and Carter W.G** (2018). Alcohol related neuronal cell damage, Europhysiology 2018, London, UK.
- **Wijesekara W. M. A. U. K. M, Wijamunige W.B.C, Knagg C and Carter W.G** (2019)**.** Treatment of neuronal cells with Alcohol and pesticides triggers neurite retraction cell damage and cell death. BNA festival 2019, Dublin, Ireland.
- **Wijesekara W. M. A. U. K. M and Carter W.G (2019)** Acute alcohol exposure disrupts the neuronal contacts before cell death, N and N event, University of Nottingham.
- **Wijesekara W. M. A. U. K. M and Carter W.G (2019)** Mapping the redox stress damages to developing neuronal cells by organophosphate pesticides, Early carrier research symposium, Engineering and learning centre, 13th June, University of Nottingham.
- **Wijesekara W. M. A. U. K. M and Carter W.G (2019)** Mapping the redox stress damages to developing neuronal cells by organophosphate pesticides and alcohol, Medicine & Health Sciences Faculty Postgraduate Research Forum,

25th June, Queens medical centre, University of Nottingham

Wijesekara W. M. A. U. K. M and Carter W.G (2019) Neurotoxicity evaluation of acute pesticide exposure on Human progenitor neural stem cells Eurotox 2019, Finlandia hall, 8-11th September, Finland

ACKNOWLEDGEMENTS

I am very grateful to my supervisors Dr. Wayne Grant Carter and Dr. Ian Mellor for their continuous support, guidance, patience, and supervision during this work. My special thanks go to Dr. Wayne for his support throughout the period not only for my academic work but for the willpower he provided for me and my family throughout the period in the United Kingdom for undertaking my Ph.D. degree.

My sincere thanks go to all the staff member's in clinical sciences laboratory specially Averill Warren and Rebecca Tarbox who helped me in many ways by teaching protocols and giving me the relevant training since this was a completely new area for me to study and without their constant support, this would be a dream. I would like to appreciate the helping hand given by Mr. Artur Kocon, as a colleague and as a new laboratory technician for me to undertake my alcohol study and teaching me the Western blotting protocols. I am grateful for my husband, my child, and my parents who give me caring support and motivation during this time. Their stimulation, constant support, encouragement, and understanding cannot be expressed in words. Special thanks go to my little daughter for fading away my stresses during the study with her adorable work. I would like to thank my lab mates who give their helping hands and their motivational thoughts during the study. Their loving friendships and their constant contribution by providing suggestions and comments for some points to improve the study during the discussions help me to improve my work in many ways. I also appreciated the constant support of Ms. Karen Kirkland, Postgraduate administrator, who help me throughout the way from beginning to end. Finally, I would like to give a big thank to my colleague Mr. Eranga Wimalasiri for teaching me connecting the microscopic images into one image.

ABSTRACT

Health concerns have been raised that the developing brain may be particularly vulnerable to the toxic effects of organophosphate (OP) and carbamate pesticides and alcohol. Invariably, many of the adult population are co-exposed to both pesticides and alcohol over the course of a lifetime, and for some individuals, also exposed in an acute setting. Chlorpyrifos and Azamethiphos are commonly used OP pesticides and Aldicarb is a commonly used carbamate pesticide. Safety testing of these commonly encountered neurotoxicants is a challenge to the area of development neurotoxicity. Induction of reactive oxygen species (ROS) has been proposed as a mechanism of acute OP, carbamate and alcohol induced poisoning cases, but there is uncertainty related to the cytotoxic responses associated with oxidative stress induced by these neurotoxicants. Herein, SH-SY5Y neuroblastoma cells and human embryonic progenitor cortical neuronal stem cells (hNPC) were used for evaluating ROS-mediated oxidative stress and cellular damage including elevation of protein carbonylation.

Both undifferentiated and differentiated cells of neuroblastoma SH-SY5Y and hNPCs were challenged with active (oxon) metabolites of chlorpyrifos (CPO), azamethiphos (AZO) and Aldicarb from (1 - 200 µM) for 24 hours, and ethanol for 10 - 200 mM for 3, 6, 12 and 24 hours to mimic episodic binge drinking. Undifferentiated and differentiated neuroblastoma SH-SY5Y cells were also co-exposed to pesticides such as concentrations producing 5,10, 20, or 50% cell death (IC_5 IC_{10}, IC_{20} and IC_{50}) of CPO, AZO and Aldicarb in combination with 10 - 200 mM ethanol for 24 hours. The effect of pesticides and ethanol on cell metabolic activity and viability was determined by (4,5 dimethylthiazol-2-yl)-2,5-diphenyl-tetrazolium bromide (MTT), lactate dehydrogenase (LDH), and ATP assays. Cellular morphological changes that arose from the exposures were

recorded by phase contrast microscopy. The effect of pesticides and ethanol on cellular differentiation was assessed by neurite outgrowth inhibition. The effect of the three pesticides on acetylcholinesterase inhibition was determined by Elman's assay. The generation of ROS was quantified using a 2',7'-dichlorofluorescein diacetate (DCFDA) assay. Cellular protein modification and damage was determined using spectrophotometric protein carbonyl content (PCC) assay. Specific targets of oxidatively damaged proteins were identified using gel electrophoresis, and oxyblots.

CPO, AZO and Aldicarb was cytotoxic to both cell lines in a concentration-dependent fashion. Alcohol induced concentration and time dependent increases in cytotoxic responses in both cell lines. Cellular energy supply (ATP levels) decreased in a concentration-dependent manner in cells exposed to the three tested pesticides and in a concentration and time dependent manner for ethanol treatments. CPO, AZO and Aldicarb induced AChE inhibition in both SH-SY5Y and hNPCs cells. ROS levels increased, with an associated increase of protein carbonylation, particularly within cytosolic proteins of 35 - 120 kDa. All pesticides exposures including those at low levels (IC_{10}) induced oxidation of an ~50 kDa protein, while low concentrations of ethanol (such as 10 mM) also induced protein carbonylation in hNPCs. Co-exposure of low doses of pesticides and ethanol induced cell metabolic and cell viability loss in neuroblastoma SH-SY5Y cells with increasing pesticide and ethanol concentration and induced a mix of synergistic or antagonistic effects. Co-exposure of pesticides and ethanol induced oxidative damage to both undifferentiated and differentiated cells as evidenced by DCFDA assay, PCC and oxyblots.

This study provides evidence that ROS generation correlates with induction of cytotoxicity in neuronal cells after exposures to CPO, AZO, Aldicarb and

ethanol. Furthermore, specific protein targets were subjected to oxidative damage after acute pesticide and alcohol exposures to neuronal cells. The cytotoxic responses are dependent not only on the concentration and duration, but also on the developmental stage. hNPC and SH-SY5Y neuroblastoma cells provided *in-vitro* model systems for the better understanding of cellular and molecular mechanisms involved in development neurotoxicity studies and can be regarded as complementary to animal testing in a cost and time effective manner.

TABLE OF CONTENTS

ACKNOWLEDGEMENTS i
ABSTRACT ii
TABLE OF FIGURES xi
TABLE OF TABLES xv
LIST OF ABBREVIATIONS xix
1 INTRODUCTION 1
1.1 The rationale of the study 3
1.2 Aims of the study 3
2 BACKGROUND OF THE STUDY 5
2.1 Human nervous system and cells 5
2.1.1 Neuronal cells 5
2.1.2 Glial cells 6
2.2 Organophosphates and carbamate pesticides 7
2.2.1 Chlorpyrifos-oxon (CPO) 10
2.2.2 Azamethiphos-oxon (AZO) 11
2.2.3 Aldicarb 12
2.2.4 Routes of exposure to CPO, AZO and Aldicarb 13
2.2.5 CPO, AZO and Aldicarb biotransformation 14
2.2.6 Organophosphate and carbamate neurotoxicity 17
2.2.7 Developmental neurotoxicity of OP and carbamate pesticides 19
2.2.8 Candidate mechanisms of OP and carbamate neurotoxicity 21
2.2.9 Role of oxidative stress in OP and carbamate cytotoxicity 27
2.3 Alcohol 41
2.3.1 Human alcohol exposure 41
2.3.2 Alcohol metabolism in humans 43
2.3.3 Alcohol neurotoxicity 44
2.3.4 Developmental neurotoxicity of alcohol 45
2.3.5 Role of oxidative stress in alcohol-induced neurotoxicity 47
2.4 Oxidative stress induced protein carbonylation 53
2.5 The use of *in vitro* human cell models for assessment of organophosphate, carbamate, and alcohol neurotoxicity 56
2.5.1 Human neuroblastoma SH-SY5Y cells 57
2.5.2 Human progenitor cortical neuronal cells (ReNcell CX) 58
3 MATERIAL AND METHODS 60

3.1 Materials....60
3.1.1 Reagents used for the study....60
3.1.2 Test compounds....65
3.1.3 Cell lines used for the study....66
3.1.4 Brain samples used for the study....66
3.2 Methodology....67
3.2.1 SH-SY5Y cell culture....67
3.2.2 Human cortical neuronal progenitor cell culture (ReNcell CX / hNPCs)....68
3.2.3 Seeding and counting cells for experiments....71
3.2.4 Cell differentiation....72
3.2.5 Cryopreservation of cell lines....73
3.2.6 Cell density standard curves....74
3.2.7 Exposure of cells to pesticides and alcohol....74
3.3 Measurement of cell viability in cells exposed to pesticides and ethanol....77
3.3.1 Preparation of MTT....78
3.3.2 Assay protocol....78
3.4 Lactose dehydrogenase assay for measurement of cell death or cytotoxicity (LDH)....79
3.4.1 Assay protocol....80
3.5 Detection of cellular ATP production....81
3.5.1 Preparation of cell lysis buffer....82
3.5.2 Assay protocol....82
3.6 Morphological measurements of cells exposed to pesticides and ethanol....83
3.7 Measurements of neurite length in differentiated cells....83
3.8 Measurement of reactive oxygen species generation....83
3.8.1 Preparation of reagents....84
3.8.2 Assay protocol....85
3.9 Colorimetric determination of acetylcholinesterase activity of cells exposed to pesticides....85
3.9.1 Preparation of reagents....86
3.9.2 Assay protocol....86
3.10 Preparation of cell lysates for one dimensional polyacrylamide gel electrophoresis (SDS- PAGE)....87
3.11 Protein quantification by modified Lowry assay....88
3.12 One dimensional polyacrylamide gel electrophoresis (SDS-PAGE)....88
3.12.1 Preparation of buffers and reagents....89

3.12.2 Sample preparation for SDS 90
3.12.3 SDS -PAGE 90
3.12.4 Western transfer and immunoblotting 91
3.13 Spectrophotometric detection of carbonylated proteins 92
3.14 Preparation of cell lysates for Oxyblot 93
3.14.1 Derivation of protein mixture 93
3.14.2 SDS-PAGE, Western transfer and immunodetection of carbonylated proteins 94
3.15 Statistical analysis 94
4 NEUROTOXICITY EVALUATION OF ORGANOPHOSPHATE AND CARBAMATE PESTICIDES USING HUMAN NEUROBLASTOMA SH-SY5Y CELLS 96
4.1 Introduction 96
4.2 Results 99
4.2.1 Phenotypic characterization of undifferentiated and differentiated SH-SY5Y cells 99
4.2.2 Determination of linear correlation between the optical signal and cell seeding density 100
4.2.3 CPO, AZO and Aldicarb reduced cell viability in a concentration-dependent manner. 102
4.2.4 CPO, AZO and Aldicarb induced cytotoxicity in SH-SY5Y cells in a concentration-dependent fashion. 107
4.2.5 Morphological observation of CPO, AZO and Aldicarb treated cells 112
4.2.6 CPO, AZO and Aldicarb reduced neurite outgrowth of pre-differentiated SH-SY5Y cells. 112
4.2.7 Effect of CPO, AZO and Aldicarb on AChE inhibition in SH-SY5Y cells 118
4.2.8 CPO, AZO and Aldicarb decreased cellular ATP levels. 122
4.2.9 CPO, AZO, and Aldicarb induced ROS generation in SH-SY5Y cells. 128
4.2.10 Effect of CPO, AZO, and Aldicarb on cellular protein carbonylation and association between ROS generation and ATP depletion in cells 132
4.3 Discussion 140
5 NEUROTOXICITY EVALUATION OF ORGANOPHOSPHATE AND CARBAMATE PESTICIDES USING HUMAN PROGENITOR CORTICAL NEURONAL STEM CELLS 147
5.1 Introduction 147
5.2 Results 150
5.2.1 Phenotypic characterisation of undifferentiated and differentiated HNPCs 150

5.2.2 Determination of linear correlation between the optical signal and cell seeding density 151

5.2.3 CPO, AZO, and Aldicarb reduced cell metabolic activity and cell viability in a concentrations-dependent manner in ReNcell CX cells. 153

5.2.4 CPO, AZO, and Aldicarb induced cytotoxicity responses in a concentration-dependent fashion in ReNcell CX. 158

5.2.5 Morphological observation of CPO, AZO and Aldicarb treated cells 163

5.2.6 CPO, AZO, and Aldicarb inhibit AChE in a concentration-dependent manner in ReNcell CX. 171

5.2.7 CPO, AZO, and Aldicarb decreased cellular ATP levels in ReNcell CX cells. 175

5.2.8 CPO, AZO, and Aldicarb induced ROS generation in ReNcell CX cells. 180

5.2.9 Effect of CPO, AZO and Aldicarb on cellular protein carbonylation and association between ROS generation and ATP depletion in cells 185

5.3 Discussion 191

6 NEUROTOXICITY EVALUATION OF ALCOHOL USING HUMAN NEUROBLASTOMA SH-SY5Y CELLS 200

6.1 Introduction 200

6.2 Results 202

6.2.1 Alcohol reduced cell metabolic activity and cell viability in a concentration and time-dependent manner in SH-SY5Y cells. 202

6.3 Alcohol induced cytotoxicity in SH-SY5Y cells. 208

6.3.1 Alcohol altered SH-SY5Y cell morphology. 214

6.3.2 Alcohol effect on cell differentiation of SH-SY5Y cells. 217

6.3.3 Alcohol affected energy levels of SH-SY5Y cells in a concentration and time dependent manner. 221

6.3.4 Alcohol induced ROS generation in SH-SY5Y cells. 226

6.3.5 Alcohol-induced oxidative damage to proteins 232

6.4 Discussion 241

7 NEUROTOXICITY EVALUATION OF ALCOHOL USING HUMAN PROGENITOR NEURONAL STEM CELLS 246

7.1 Introduction 246

7.2 Results 249

7.2.1 Alcohol reduced cell metabolic activity and cell viability in hNPCs. 249

7.2.2 Alcohol induced cell death in hNPCs in a concentration and time-dependent manner. 255

7.2.3 Alcohol-induced morphological alterations to hNPCs 261

7.2.4 Alcohol effect on cellular ATP production in hNPCs.....264
7.2.5 Alcohol-induced oxidative stress in hNPCs.....270
7.2.6 Alcohol induced oxidative stress damage to proteins and associated elevation of ROS. 275
7.3 Discussion.....283
8 EFFECT OF PESTICIDES AND ETHANOL CO-EXPOSURES ON HUMAN NEUROBLASTOMA SH-SY5Y CELLS.....289
8.1 Introduction.....289
8.2 Results 291
8.2.1 Effect of co-exposure of ethanol with low doses of OP and carbamate pesticides on cell metabolic activity and cell viability of SH-SY5Y cells.....291
8.2.2 Interactive effect of ethanol and low doses of OP and carbamate pesticide on cell death of SH-SY5Y cells.....305
8.2.3 Co-exposure of ethanol with low doses of OP and carbamate pesticide causes morphological impairments of SH-SY5Y cells.....316
8.2.4 Impact of co-exposure of ethanol with low doses of OP and carbamate pesticide on energy levels of SH-SY5Y cells. 323
8.2.5 Co-exposure of ethanol with low doses of OP and carbamate pesticide, effects on SH-SY5Y cell differentiation. 333
8.2.6 Co-exposure of ethanol with low doses of OP and carbamate pesticide on induction of oxidative stress in SH-SY5Y. 343
8.2.7 Oxidative stress-induced protein damage in SH-SY5Y cells by the co-exposure of ethanol with low doses of OP and carbamate pesticides. 355
8.3 Discussion.....369
9 GENERAL DISCUSSION.....376
9.1 Summary of findings.....376
9.2 Limitations of the study and future work.....388
9.3 Conclusions.....394
REFERENCES.....396
ANNEXURE I.....429
CHPATER IV.....429
Effect of NAC on ROS generation of CPO, AZO and Aldicarb treated SH-SY5Y cells.....429
Quantification of β tubulin II changes in undifferentiated and differentiated SH-SY5Ycells upon exposure of CPO, AZO and Aldicarb for 24 h.....430
CHAPTER V.....432
Effect of NAC on ROS generation of CPO, AZO and Aldicarb treated hNPCs cells. 432

Quantification of β tubulin III in differentiated hNPCs cells upon exposure of CPO, AZO and Aldicarb for 24 h. 433
CHAPTER VI.....434
Cellular proliferation of SH-SY5Y cells in response to alcohol exposure. 434
Effect of NAC on ROS generation of SH-SY5Y cells exposed ethanol for 24 h. 436
Quantification of β tubulin II in SH-SY5Y cells exposed ethanol for 24 h. 437
CHAPTER VII. 439
Effect of NAC on ROS generation of hNPCs cells exposed ethanol for 24 h. 439
Identification of major cytosolic protein targets of protein carbonylation.439

TABLE OF FIGURES

Figure 2-1: General structures of (A) Organophosphates (B) carbamates 9
Figure 2-2: Chemical structures of Chlorpyrifos-oxon, Azamethiphos-oxon, and Aldicarb 11
Figure 2-3: Biotransformation of OP pesticides in humans.....15
Figure 2-4: Metabolic bioactivation of chlorpyrifos (proposed by Eaton et al. 2008). 16
Figure 2-5: Metabolism of Aldicarb in humans (proposed by Giri et al. 2018).17
Figure 2-6: AChE inhibition by OP and carbamates. 24
Figure 2-7: ROS generation pathways OP and carbamate pesticide exposure. 28
Figure 2-8: Cellular targets of ROS generated by the OP and carbamate pesticides in neuronal cells 31
Figure 2-9: Main pathways of alcohol metabolism. 43
Figure 4-1: Undifferentiated and differentiated SH-SY5Y cells. 99
Figure 4-2: Direct correlation of absorbance and SH-SY5Y cell number. 101
Figure 4-3: Mean comparison of two-way ANOVA results of MTT signal development with time in SH-SY5Y cells 102
Figure 4-4: Cell viability inhibition dose-response curves of CPO, AZO and Aldicarb on undifferentiated and differentiated SH-SY5Y cells. 105
Figure 4-5: Cell viability inhibition dose-response curves of undifferentiated and differentiated SH-SY5Y cells.....106
Figure 4-6: Cytotoxicity of CPO, AZO and Aldicarb on SH-SY5Y cells determined by LDH assay.....110
Figure 4-7: Cytotoxicity of undifferentiated and differentiated SH-SY5Y cells assessed by LDH assay. 111
Figure 4-8: Morphological observation of CPO, AZO, Aldicarb exposure to cells for 24 h. 114
Figure 4-9: Quantitative analysis of the effect of CPO, AZO and Aldicarb on neurite out growth. 116
Figure 4-10: Effect of CPO, AZO and Aldicarb on pre-differentiated SH-SY5Y cells. 118
Figure 4-11: Assay linearity with the reaction and cell sample volume for Sh-SY5Y cells. 119
Figure 4-12: Effect of CPO, AZO and Aldicarb on inhibition of AChE in SH-SY5Y cells. 122
Figure 4-13: Effect of CPO, AZO and Aldicarb on cellular ATP level of SH-SY5Y cells. 125
Figure 4-14: Effect of CPO, AZO and Aldicarb on ATP levels in undifferentiated and differentiated SH-SY5Y cells. 127
Figure 4-15: Effect of CPO, AZO and Aldicarb in cellular ROS generation...131
Figure 4-16: Effect of CPO, AZO and Aldicarb on cytosolic protein carbonylation in SH-SY5Y cells. 133
Figure 4-17: Cytosolic protein carbonylation of CPO, AZO and Aldicarb exposure for 24 h in SH-SY5Y cells. 136
Figure 5-1: Representative images for undifferentiated and differentiated ReNcell CX cells and expression of βIII tubulin. 150
Figure 5-2: Direct correlation of absorbance and ReNcell CX cell number…151

Figure 5-3: Effect of incubation time on MTT signal development in ReNcell CX cells. 152
Figure 5-4: Cell viability inhibition dose-response curves of CPO, AZO, and Aldicarb on undifferentiated and differentiated ReNcell CX cells. 156
Figure 5-5: Effect of CPO, AZO, and Aldicarb on undifferentiated and differentiated cell viability. 157
Figure 5-6: Cytotoxicity dose-response curves of CPO, AZO, and Aldicarb on undifferentiated and differentiated ReNcell CX cells. 159
Figure 5-7: Effect of CPO,AZO and Aldicarb on undifferentiated and differentiated cell cytotoxicity. 162
Figure 5-8: Morphological changes of undifferentiated ReNcell CX exposed to CPO,AZO and Aldicarb. 166
Figure 5-9: Morphological changes of differentiated ReNcell CX exposed to CPO,AZO and Aldicarb. 169
Figure 5-10: Assay linearity with the reaction and cell sample volume of ReNcell CX cells 172
Figure 5-11: Effect of CPO, AZO and Aldicarb on inhibition of AChE in ReNcell CX. 174
Figure 5-12: Effect of CPO, AZO, and Aldicarb on cellular ATP levels. 177
Figure 5-13: Effect of CPO,AZO and Aldicarb on cellular ATP levels on undifferentiated and differentiated ReNcell CX. 179
Figure 5-14: Effect of CPO,AZO and Aldicarb in cellular ROS generation. 184
Figure 5-15: Effect of CPO, AZO, and Aldicarb on cytosolic protein carbonylation in ReNcell CX cells. 186
Figure 5-16: Cytosolic protein carbonylation of CPO, AZO and Aldicarb exposed undifferentiated and differentiated ReNcell CX cells for 24 h. 188
Figure 6-1: Cell metabolic and cell viability in responses to alcohol by SH-SY5Y cells. 204
Figure 6-2: Effect of ethanol on undifferentiated and differentiated SH-SY5Y cells. 207
Figure 6-3: LDH activity of alcohol exposed SH-SY5Y cells. 211
Figure 6-4: LDH activity of Undifferentiated and differentiated SH-SY5Y cells 213
Figure 6-5: Morphological alteration of ethanol exposed SH-SY5Y cells. 216
Figure 6-6: Effect of ethanol on neurite outgrowth of differentiating SH-SY5Y cells. 217
Figure 6-7: Effect of ethanol for differentiating SH-SY5Y cells. 219
Figure 6-8: Effect of ethanol on cellular ATP levels in SH-SY5Y cells. 223
Figure 6-9: Effect of ethanol on cellular ATP levels of undifferentiated and differentiated SH-SY5Y cells. 225
Figure 6-10: Effect of ethanol on cellular ROS generation in SH-SY5Y cells. 229
Figure 6-11: Effect of ethanol on ROS generation of undifferentiated and differentiated SH-SY5Y cells. 231
Figure 6-12: Quantitation of oxidatively damaged proteins as protein carbonyl content. 232
Figure 6-13: Protein carbonyl contents of alcoholic and control brain samples. 235
Figure 6-14: Cytosolic protein carbonylation of differentiated cells, alcoholic and control brain samples. 236

Figure 7-1: Cell metabolic and cell viability responses to alcohol by hNPCs. 252
Figure 7-2: Effect of ethanol on undifferentiated and differentiated hNPCs. .253
Figure 7-3: LDH activity of undifferentiated and differentiated hNPCs.....257
Figure 7-4: LDH activity of alcohol exposed hNPCs.....259
Figure 7-5: Effect of ethanol on undifferentiated and differentiated hNPCs. .264
Figure 7-6: Effect of ethanol on cellular ATP levels of undifferentiated and differentiated hNPCs.....266
Figure 7-7: Effect of ethanol on cellular ATP levels in hNPCs.....268
Figure 7-8: Effect of ethanol on ROS generation in hNPCs.....272
Figure 7-9: Effect of ethanol on ROS generation in undifferentiated and differentiated hNPCs.....274
Figure 7-10: Cytosolic protein carbonylation of undifferentiated and differentiated hNPCs exposed to ethanol.....275
Figure 7-11: Cytosolic protein carbonylation of alcohol treated undifferentiated and differentiated hNPCs.....279
Figure 8-1: Co-exposure to ethanol and CPO SH-SY5Y cells for 24 h.....292
Figure 8-2: Co-exposure to ethanol and AZO for SH-SY5Y cells for 24 h. ...299
Figure 8-3: Co-exposure to ethanol and Aldicarb SH-SY5Y cells for 24 h....304
Figure 8-4: Co-exposure to ethanol and CPO and LDH production in differentiated SH-SY5Y cells after 24 h.....306
Figure 8-5: Co-exposure to ethanol and AZO and LDH production for undifferentiated SH-SY5Y cells for a 24 h exposure. 311
Figure 8-6: Co-exposure to Aldicarb and ethanol and LDH production for differentiated SH-SY5Y cells after 24 h exposure. 315
Figure 8-7: Co-exposure of CPO, AZO and Aldicarb with ethanol on SH-SY5Y cells for 24 h. 322
Figure 8-8: Co-exposure to ethanol and CPO and cellular ATP production in differentiated SH-SY5Y cells for 24 h.....325
Figure 8-9: Co-exposure to ethanol and AZO and cellular ATP production in differentiated SH-SY5Y cells after 24 h.....329
Figure 8-10: Co-exposure to ethanol and Aldicarb and effect on cellular ATP production in differentiated SH-SY5Y cells after 24 h.....332
Figure 8-11: Effect of co-exposure of ethanol and CPO on neurite outgrowth of differentiating SH-SY5Y cells.....334
Figure 8-12: Effect of co-exposure of ethanol and AZO on neurite outgrowth of differentiating SH-SY5Y cells.....336
Figure 8-13: Effect of co-exposure of ethanol and Aldicarb on neurite outgrowth of differentiating SH-SY5Y cells. 337
Figure 8-14: Effect of joint toxicity of CPO, AZO and Aldicarb on differentiating SH-SY5Y cells. 342
Figure 8-15: Effect of co-exposure to ethanol and CPO on ROS generation in undifferentiated and differentiated SH-SY5Y cells after 24 h.....345
Figure 8-16: Effect of co-exposure to ethanol and AZO on ROS generation in undifferentiated SH-SY5Y cells after 24 h.....349
Figure 8-17: Effect of co-exposure to ethanol and Aldicarb on ROS generation in undifferentiated SH-SY5Y cells after 24 h. 352
Figure 8-18: Effect of co-exposure to ethanol and CPO on cellular protein carbonyl levels of undifferentiated SH-SY5Y cells for 24 h.....357
Figure 8-19: Effect of co-exposure to ethanol and AZO on cellular protein carbonyl levels of undifferentiated SH-SY5Y cells for 24 h.....360

Figure 8-20: Effect of co-exposure to ethanol and Aldicarb on cellular protein carbonyl levels of undifferentiated SH-SY5Y cells for 24 h.....363
Figure 8-21: Cytosolic protein carbonylation of joint toxicity of CPO or AZO or Aldicarb treated differentiated SH-SY5Y cells with ethanol. 366
Figure 9-1: Possible pathways of oxidative stress and other protein adducts resulting in cellular toxic responses after alcohol and pesticides exposure in neuronal cells. 376
Figure 9-1 Possible pathways of oxidative stress and other protein adducts resulting in cellular toxic responses after alcohol and pesticides exposure in neuronal cells 376
Figure 9-2: Schematic diagram of common mechanisms underlying the cytotoxicity of exposure to CPO, AZO, Aldicarb and alcohol in human neuroblastoma SH-SY5Y cells and human cortical progenitor neuronal cells. 381
Figure 1: Effect of NAC on ROS generation of CPO, AZO and Aldicarb on undifferentiated and differentiated SH-SY5Y cells for 24 h exposure. 429
Figure 2: Detection of β II tubulin on western blots of undifferentiated and differentiated neuroblastoma SH-SY5Y cells upon exposure of CPO,AZO and Aldicarb for 24 h. 430
Figure 3: Effect of NAC on ROS generation of CPO, AZO and Aldicarb on undifferentiated and differentiated hNPCs cells for 24 h exposure. 432
Figure 4: Detection of β III tubulin on western blots of undifferentiated and differentiated hNPCs cells upon exposure of CPO, AZO and Aldicarb for 24 h. 433
Figure 5: BrdU incorporation of ethanol treated undifferentiated and differentiated SH-SY5Y cells.....435
Figure 6: Effect of NAC on ROS generation of ethanol on undifferentiated and differentiated SH-SY5Y cells for 24 h exposure 436
Figure 7: Detection of β II tubulin on western blots of undifferentiated and differentiated neuroblastoma SH-SY5Y cells upon exposure of CPO,AZO and Aldicarb for 24 h. 437
Figure 8: Effect of NAC on ROS generation of ethanol on undifferentiated and differentiated hNPCs cells for 24 h exposure. 439
Figure 9: 2D analysis of protein carbonylation in differentiated SH-SY5Y cells exposed to CPO, AZO and Aldicarb. Vehicle control shows total protein staining. CPO, AZO and Aldicarb showed 2D oxyblots. 443

TABLE OF TABLES

Table 2-1: Summary of published literature on organophosphate and carbamate induced oxidative stress responses of human neuronal and glial cell models. 33
Table 2-2: Summary of published literature on ethanol effect on human neuronal cells and neurospheres....50
Table 3-1: Reagents used for the cell culture....60
Table 3-2: List of other reagents and materials....62
Table 3-3: Plastic culture ware used for the study....65
Table 3-4: Loading cell density for experiments with SH-SY5Y and ReNcell CX cells....72
Table 4-1: Toxicity of CPO, AZO and Aldicarb to undifferentiated and differentiated SH-SY5Y cells....115
Table 4-2: 10, 20, 50 and 80% inhibition concentrations interpolated from concentration-response curves....123
Table 4-3: Comparison of individual concentrations at 6 h and 24 h ROS generation by the exposure of CPO, AZO, and Aldicarb on SH-SY5Y cells. 132
Table 4-4: Correlation analysis between ROS generation vs protein carbonyl content, and ROS generation vs ATP production in SH-SY5Y cells for 24 h exposure of CPO, AZO, and Aldicarb. 137
Table 4-5: Comparison of the cytotoxicity induced by CPO, AZO and Aldicarb to undifferentiated Vs differentiated SH-SY5Y cells. 138
Table 4-6: Comparison of AChE activity of undifferentiated and differentiated SH-SY5Y inhibition by CPO, AZO and Aldicarb. 139
Table 5-1: Toxicity of CPO, AZO, and Aldicarb to undifferentiated and differentiated HNPCs. 170
Table 5-2: 10, 20, 50 and 80% inhibition concentrations interpolated from dose-response curves. 175
Table 5-3: Comparison of individual concentrations at 6 h and 24 h ROS generation by the exposure of CPO, AZO and Aldicarb on ReNcell CX. 181
Table 5-4: Correlation analysis of ROS generation vs protein carbonyl content and ROS generation vs ATP production in ReNcell CX cells. 189
Table 5-5: Toxicity of CPO, AZO and Aldicarb on undifferentiated vs differentiated ReNcell CX cells....190
Table 6-1: Comparison of ethanol toxicity at different time points in undifferentiated and differentiated SH-SY5Y cells measured by MTT assay. 205
Table 6-2: Comparison of ethanol toxicity at different time points in undifferentiated and differentiated SH-SY5Y cells measured by LDH assay. 212
Table 6-3: Comparison of effect of ethanol on neurite outgrowth with exposure duration. 220
Table 6-4: Comparison of ethanol toxicity in different time points in undifferentiated and differentiated SH-SY5Y cells measured by ATP assay. 224
Table 6-5: Comparison of ethanol induced ROS generation at different time points in undifferentiated and differentiated SH-SY5Y cells measured by DCFDA assay....230

Table 6-6: Correlation between the ROS generation and protein carbonyl content / ATP production in SH-SY5Y cells. 237
Table 6-7: Comparison of ethanol toxicity at different time points in undifferentiated and differentiated SH-SY5Y cells for protein carbonyl content. 238
Table 6-8: Comparison of the cytotoxicity of alcohol to undifferentiated vs differentiated SH-SY5Y cells.....239
Table 6-9: Toxicity of alcohol to undifferentiated or differentiated SH-SY5Y cells. 240
Table 7-1: Comparison of ethanol toxicity in different time points in undifferentiated and differentiated hNPCs measured by MTT assay.....254
Table 7-2: Comparison of ethanol toxicity in different time points in undifferentiated and differentiated hNPCs measured by LDH assay.....260
Table 7-3: Comparison of ethanol toxicity at different time points in undifferentiated and differentiated hNPCs measured by ATP assay. 269
Table 7-4: Comparison of ethanol induced ROS generation at different time points in undifferentiated and differentiated hNPCs cells measured by DCFDA assay. 273
Table 7-5: Comparison of ethanol toxicity in different time points in undifferentiated and differentiated hNPCs for protein carbonyl content.....278
Table 7-6: Correlation between the ROS generation and protein carbonyl content / ROS generation or ATP production in hNPCs. 280
Table 7-7: Comparison of the cytotoxicity of alcohol to undifferentiated vs differentiated hNPCs.....281
Table 7-8: Toxicity of alcohol to undifferentiated or differentiated hNPCs. ...282
Table 8-1: Comparison of treatment combinations of ethanol and CPO with their corresponding non-treated controls. Results were analysed by two-way ANOVA and means comparison was done by Tukey's multiple comparison tests.....293
Table 8-2: Synergistic and antagonistic effect of joint toxicity of CPO and alcohol in SH-SY5Y cells. 295
Table 8-3: Comparison of treatment combinations of ethanol and AZO with their corresponding non-treated control. Results were analysed by two-way ANOVA and means comparison was done by Tukey's multiple comparison tests.....298
Table 8-4: Synergistic and antagonistic effect of joint toxicity of AZO and alcohol in SH-SY5Y cells. 300
Table 8-5: Comparison of treatment combinations of ethanol and Aldicarb with their corresponding non-treated controls. Results were analysed by two-way ANOVA and means comparison was done by Tukey's multiple comparison tests.....302
Table 8-6: Synergistic and antagonistic effects of joint toxicity of Aldicarb and alcohol for SH-SY5Y cells.....303
Table 8-7: Comparison of treatment combinations of ethanol and CPO with their corresponding non-treated controls. Results were analysed by two-way ANOVA and means comparison was done by Tukey's multiple comparison tests.....307
Table 8-8: Comparison of treatment combinations of ethanol and AZO with their corresponding non-treated controls. Results were analysed by two-way ANOVA and means comparison was done by Tukey's multiple comparison tests.....312

Table 8-9: Comparison of treatment combinations of Aldicarb with ethanol and their corresponding non-treated controls. Results were analysed by two-way ANOVA and means comparison by Tukey's multiple comparison tests.....314
Table 8-10: Comparison of treatment combinations of ethanol and CPO with their corresponding non-treated controls. Results were analysed by two-way ANOVA and means comparison was done by Tukey's multiple comparison tests.....326
Table 8-11: Comparison of treatment combinations of ethanol and AZO with their corresponding non-treated controls. Results were analysed by two-way ANOVA and means comparison was done by Tukey's multiple comparison tests.....330
Table 8-12: Comparison of treatment combinations of ethanol and Aldicarb with their corresponding non-treated controls. Results were analysed by two-way ANOVA and means comparison was done by Tukey's multiple comparison tests. 333
Table 8-13: Comparison of treatment combinations of ethanol and pesticides with their corresponding non-treated controls. Results were analysed by two-way ANOVA and means comparison was done by Tukey's multiple comparison tests. 339
Table 8-14: Comparison of treatment combinations of ethanol and CPO with their corresponding non-treated controls. Results were analysed by two-way ANOVA and means comparison was done by Tukey's multiple comparison tests.....346
Table 8-15: Comparison of treatment combinations of ethanol and AZO with their corresponding non-treated controls. Results were analysed by two-way ANOVA and means comparison was done by Tukey's multiple comparison tests.....350
Table 8-16: Comparison of treatment combinations of ethanol and Aldicarb with their corresponding non-treated controls. Results were analysed by two-way ANOVA and means comparison was done by Tukey's multiple comparison tests. 353
Table 8-17: Synergistic and antagonistic effect of joint toxicity of CPO and alcohol on ROS generation in SH-SY5Y cells.....354
Table 8-18: Comparison of treatment combinations of ethanol and CPO with their corresponding non-treated controls. Results were analysed by two-way ANOVA and means comparison was done by Tukey's multiple comparison tests.....358
Table 8-19: Comparison of treatment combinations of ethanol and AZO with their corresponding non-treated controls. Results were analysed by two-way ANOVA and means comparison was done by Tukey's multiple comparison tests.....361
Table 8-20: Comparison of treatment combinations of ethanol and Aldicarb with their corresponding non-treated controls. Results were analysed by two-way ANOVA and means comparison was done by Tukey's multiple comparison tests. 364
Table 8-21: Synergistic and antagonistic effect of joint toxicity of CPO and alcohol on PCC in SH-SY5Y cells.....365
Table 8-22: Joint toxicity of CPO, AZO, and Aldicarb with alcohol on undifferentiated vs differentiated cells. 367
Table 1: Densiometric analysis of western blots probed with β II tubulins in undifferentiated and differentiated cells.....431

Table 2: Densitometric analysis of western blots probed with β II tubulins in undifferentiated and differentiated cells.....436
Table 3: Psychiatric diagnosis, age, gender, post-mortem delay (PMD), cause of death, and toxicological characteristics of Control (C), Alcoholic (A) subjects used in this study.....438

LIST OF ABBREVIATIONS

AChE	Acetylcholinesterase
ACh	Acetylcholine
ADHD	Attention deficit hyperactivity disorder
ANOVA	Analysis of variance
ATCI	Acetylthiocholine iodide
ATP	Adenosine triphosphate
AZA	Azamethiphos
AZO	Azamethiphos-oxon
BAC	Blood alcohol concentration
BDNF	Brain derived growth factor
Ca^{2+}	Calcium
CNS	Central nervous system
COPIND	Chronic organophosphate induce neuropsychiatric disorder
CPF	Chlorpyrifos
CPO	Chlorpyrifos-oxon
Cyt C	Cytochrome C
DCFDA	2′,7′-Dichlorofluorescin diacetate
DMEM	Dulbecco’s modified Eagle’s medium
DMSO	Dimethyl sulfoxide
DNA	Deoxyribonucleic acid
DNT	Development neurotoxicology
DNPH	2,4-Dinitrophenylhydrazine
DTNB	5,5'-Dithiobis-(2-Nitrobenzoic Acid)
EGF	Epidermal growth factor
EPA	Environmental Protection Agency
FBS	Foetal bovine serum
FGF	Fibroblast growth factor
FMO	Flavin monooxygenase
h	hour
GAPDH	Glyceraldehyde 3-phosphate dehydrogenase

GSH	Glutathione
H_2O_2	Hydrogen peroxide
HRP	Horseradish peroxidase
IC_{50}	50% inhibition concentration
IQ	Intelligence quotient
JNK	JUN-N-terminal kinase
kg	Kilogram
kDa	Kilodalton
M	Molar
Mg	Milligram
Min	Minute
Ml	Millilitre
mM	Millimolar
nM	Nanomolar
nm	Nanometre
MTT	3-(4,5-Dimethylthiazol-2-yl)-2,5-Diphenyltetrazolium Bromide
OP	Organophosphate
PON1	Paraoxonase 1
PBS	Phosphate Buffered Saline
ReNcell CX	Human cortical progenitor neuronal stem cell line
ROS	Reactive oxygen species
RPMI	Roswell Park Memorial Institute
RNA	Ribonucleic acid
SDS	Sodium dodecyl sulphate
SDS-PAGE	Sodium dodecyl sulphate-polyacrylamide gel electrophoresis
SEM	Standard error of mean
SH-SY5Y	Human neuroblastoma SH-SY5Y cell line
UK	United Kingdom
v/v	Volume/volume
w/v	Weight/volume
WHO	World Health Organization

µM	Micromolar
µm	Micron
µl	Microliter

1 INTRODUCTION

Humans are exposed to thousands of different chemicals simultaneously from their natural surroundings and lifestyles, and for some individuals, additional chemicals from occupational environments. The toxicological consequences and potential risk of exposure to these chemicals are gaining attention, and adverse health risks associated with them become social and economic burdens to the world. Pesticide and alcohol are two of the most common neurotoxicants that are heavily studied, and adverse effects on health in adults and young children is one of the biggest burdens, and recognizing their potential toxicological consequences is a challenge to modern toxicology.

The world pesticide usage is ever increasing with the growing population due to the immense need for food production in line with the growing population (FAOSTAT, 2019). Pesticides are vital to control pests in agriculture, domestic settings, industrial settings, and animal husbandry. Hence, the general population are exposed to low concentrations of pesticides during their lifetime, occupationally or generally. On the other hand, human alcohol consumption is increasing in the modern world, and is a component of the social fabric in some countries (WHO 2019). However, adverse health consequences by pesticides and alcohol exposure make a considerable impact on the economy of developed and developing countries in the world.

Organophosphates (OPs), carbamate pesticides, and alcohol are considered as neurotoxic substances which may lead to neurodegeneration. Pesticides and alcohol are bio-transformed in the human liver and the toxicity of each may also be compounded by toxic metabolites produced in the liver or toxicity directly to neuronal cells. The mechanism of neurotoxicity of both above pesticides and alcohol were found to be similar in the literature as both induced neuronal cell

death in a dose-dependent fashion by apoptosis or necrosis and mediated by oxidative stress.

The safety testing of these neurotoxicants including their metabolic products have been widely studied using animal dosing and is therefore extremely time-consuming and expensive. Furthermore, animal models cannot be used to interpret the toxicological consequences on individual cells including mechanisms and species differences that exist in vulnerability to pesticides or alcohol in humans. Recently, cell lines were used to study the mechanism of toxicity of these neurotoxicants which showed advantages over the traditional paradigms of *in vivo* animal dosing as less time consuming and can be used for high throughput screening studies. On the other hand, the cell model allowed scientists to control and manipulate the environment and attributes that are essential to understand the underlying mechanism of toxicity. Therefore, multiple pathways in cellular level effects on single toxicological consequences can be studied. Human neuroblastoma cell line and human cortical progenitor neuronal stem cell lines are emerging cell models currently use in neurotoxicological studies that mimic the effect of environmentally toxic chemicals on cell viability, proliferation, and differentiation in humans.

However, considerable evidence demonstrated that both pesticides and alcohol effects depend upon the development stage at which exposure occurs. Nevertheless, a plethora of literature has showed that most *in vitro* studies challenged with pesticides or alcohol on neuronal cells that have been committed to undifferentiated or differentiated cells. Hence, this study was designed to investigate the neurotoxicity mechanism of oxon metabolites of commonly used organophosphate pesticides (OP) Chlorpyrifos, Azamethiphos, the carbamate pesticide, Aldicarb, and alcohol using human neuroblastoma SH-SY5Y cells and human embryonic progenitor cortical neuronal stem cells

(hNPCs). Cellular mechanisms of induced toxicity and functional cell loss by the acute exposure of these neurotoxicants were studied using undifferentiated cells and the differentiated cells to mimic the toxicological consequences to different stages of neuronal development.

1.1 The rationale of the study

In vitro, neurotoxicological studies are important to mimic the cellular mechanism of neurotoxicity of pesticides and alcohol in humans. The use of a wide concentration of compounds with small quantities is cost-effective for toxicological studies than using a large number of rodents for predicting the effect of results on humans. The safe limit of these neurotoxic compounds should be studied to prevent the potential risk of using them and understand the mechanism of neuronal damage in humans for the development of potential therapeutics. To explore the biological basis of neurotoxic compounds, this study was designed to determine the effect of OP and carbamate pesticides on cell viability of both cell lines. Besides, the molecular mechanism driving cellular damages was studied. These neurotoxic compounds target cellular proteins and morphological impairments are common due to the formation of new adducts. Furthermore, cellular protein damages arose from the exposure were investigated using immunoblotting.

1.2 Aims of the study

Human neuroblastoma SH-SY5Y cell and human cortical progenitor neuronal cells are used to examine:

1. Neurotoxicity of selected organophosphates and carbamate pesticides, and alcohol.

2. Determine the doses producing 50% cell response/cell viability/death (IC_{50}s).

3. Examine the molecular mechanism driving cell damage such as redox stress.

4. Evaluate the cellular oxidative damage protein changes arising from exposures.

2 BACKGROUND OF THE STUDY

2.1 Human nervous system and cells

The human nervous system is a complex biological network of cells and organs. It consists of the brain, spinal cord, and nerves. Collectively, the nervous system governs all functions of the body including control over muscles, glands, organs, and physiological processes. The brain and the spinal cord constitute the central nervous system (CNS). The nerves arise from the spinal cord (peripheral nerves), cranial nerves, and the autonomic structures compromise the peripheral nervous system (PNS) (Franklin, 2017). The human nervous system is composed of two common cell types, neuronal cells, and glial cells.

2.1.1 Neuronal cells

The neuronal cell is the structural and functional unit of the human nervous system while glial cells play an important role in neuronal regulation and function. Neuronal cells being responsible for the perception of impulses, responding to the impulse and transmitting nerve impulses to other neighbouring neuronal cells or effector cells through synaptic transmission. Neuronal cells are highly polarised cells, and possess single long neurite axon and shorter processes, dendrites upon differentiation. The morphological and structural attributes of the axon reflect their role in nerve impulse transmission and the system to mediate axonal transport. The structure of differentiated neurons processes have three main elements: growth cone, axon, and cell body. The cell body is comprised of a nucleus and cytoplasmic organelles. The length of the axon varies and is usually longer than that of the cell body (Barres and Barde, 2000).

2.1.2 Glial cells

Glial cells are considered as supporters of neuronal cells and actual numbers in the nervous system are greater than that of the neurons (Barone et al., 2000). Approximately 90% of the human brain cells are glial cells (Allen and Barres, 2009). Glial cells lack single long axons and are not involved in nerve impulse transmission, but they provide spatial accompaniment to neuronal cells by providing fundamental homeostasis, nutritional, structural, and defensive support to the neurons. Glial cells in the central nervous system are composed of a heterogeneous array of cell types of different origins. Microglia derived from the immune system and act as specialized macrophages that remove the debris and neuronal cells which have undergone apoptosis (Compston et al., 1997). The other glial cell lineages in the central nervous system are known as astrocytes and oligodendrocytes which are developed in the cell differentiation process in neurogenesis (Compston et al., 1997).

Astrocytes support the functionality of neurons, playing a role in differentiation and proliferation and neuronal migration. Astrocytes separate synaptic connection by acting as a barrier between the neuronal cells and protect the neurons from excitotoxicity (Hassel et al., 1997). These cells also protect neuronal cells from oxidative stress by releasing antioxidants such as glutathione (Sagara et al., 1993).

Oligodendrocytes synthesise a myelin sheath around the neuronal cells and this insulation supports impulse transmission and increases the efficiency of impulse transmission (Compston et al., 1997, Allen and Barres, 2009).

Glial cells present in the peripheral nervous system are known as enteric glia and Schwann cells (Allen and Barres, 2009). Two types of Schwann cells found in the peripheral nervous system: myelinated and non-myelinated Schwann

cells. Myelinated Schwann cells have similar functions as oligodendrocytes while non-myelinated cells provide mechanical and metabolic support to the neuronal cells. Enteric glia is found in the autonomic ganglia of the gut and plays a role in the synaptic impulse transmission process (Jessen and Mirsky, 2005).

Thus, spatial activity of neuronal cells and glial cells in the human nervous system helps to regulate neuronal function and targeting any of them with a toxic insult of neurotoxins, such as pesticides and alcohol, could have a detrimental effect on the nervous system.

2.2 Organophosphates and carbamate pesticides

Worldwide pesticide usage was estimated as 6 billion sterling pounds according to the EPA report 2016 (Ock, Kim and Choi 2020). Organophosphates (OP) and carbamate pesticides are widely used pesticides in the world accounting for 64% of the world's pesticide market (Sapbamrer and Hongsibsong 2019, Schmitt et al. 2019). The main use of OPs is as an insecticide in agriculture and animal husbandry. However, OPs are also used in many medical, residential, and industrial settings as lubricants, solvents, and fire retardants (Hargreaves, 2012) due to their cost-effectiveness and broad-spectrum activity on pests. Four billion kg of OP insecticides such as chlorpyrifos, are applied to agriculture fields in different parts of the world each year, but a small amount of applied pesticides effects the target pest, while a considerable portion pollutes the environment (Gavrilescu et al., 2015). Carbamate pesticides are used in agriculture, veterinary, and in households and used second to the OPs in the world due to their low mammalian toxicity (Barr and Buckley, 2011).

The consumption of OP and carbamate contaminated foods is the main body burden. The intake of OP and carbamate contaminated foods with residues of deposits of pesticide active ingredients, its metabolites or breakdown products, can bioaccumulate in the human body during the lifetime and are potentially

detrimental to health. Several foods including fresh fruits, vegetable, baby food, and processed foods are contaminated with OP pesticides has been reported in Europe. Besides, 50% of fruits and vegetables and cereals are contaminated with pesticides (Bjørling-Poulsen et al., 2008b). Although Europe and the USA restricted the use of certain pesticides, other countries in the world heavily used carbamate pesticides in food production. For instance, China has used 12,438 metric tonnes of carbofuran for their agriculture fields according to the China pesticide web 2016 (Zhang et al., 2019). According to the European Union report of pesticide residue analysis in foods, this showed most of the imported food products from third world countries exceeded the residue level that has to be in those foods (Authority, 2019) implying overuse of OP and carbamate pesticides in food production by those countries.

The widespread use of OPs and carbamate pesticides and the underlying hazards are posing potential health risks to the public. Exposure of these pesticides not only affects the occupational workers including farmers, formulators, manufacturers, but also the public. Several epidemiological studies showed that low dose exposure of OP and carbamates through the environmental exposures and contaminated food for a longer time may cause chronic damage to the nervous system in humans (Mearns et al., 1994, Stephens et al., 1995, Eaton et al., 2008).

Most cases of pesticide poisoning were recorded as accidental or occupational exposures for both pesticide groups in humans. 1 to 2 million suicidal poisonings were recorded in each year as per WHO reports (Boucaud-Maitre et al., 2019). A recent review showed that carbamate poisoning was reported due to intentional oral ingestion or dermal occupational exposure, while most of the OP poisoning cases were due to accidental exposure and suicidal attempts (Lee et al., 2014a, Vale and Lotti, 2015). The figures were comparatively higher in

developing countries to the developed countries, with free usage of highly toxic pesticides in conventional agriculture due to lack of legislative or industrial control. 20% to 30% intentional exposures cause respiratory arrests as a result of carbamate and OP poisoning respectively in the Asian region and suicidal attempts of about 200,000 per year (Taylor, 2020).

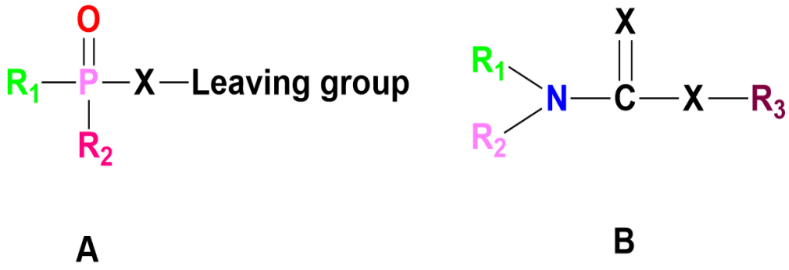


Figure 2-1: General structures of (A) Organophosphates (B) carbamates

OPs are synthetic in origin and are esters, amides, or thiol derivatives of phosphoric, phosphates, phosphorothioate, or phosphorothioic acids. The general structure of OP pesticides is characterized by central phosphorus atom connected with sulphur or oxygen atom with a double bond and R_1, R_2, and leaving group, where R_1 and R_2 are usually dimethyl or diethyl groups. The X group can be any one of the wide variety of substituted or branched aliphatic, aromatic, or heterocyclic groups linked to phosphorous atom through a labile bond usually O or S and is referred to as the leaving group (Figure 2-1 A) (Sogorb and Vilanova, 2002).

Carbamates are derived from carbamic acid and have higher biocidal activities. In carbamates, the central carbon atom is either bonded to X, which can be sulphur or oxygen and R_1 and R_2 are organic radicals or hydrogen (Figure 2-1 B). If carbamate is an insecticide, then R_1 is hydrogen while R_2 is a methyl group. When R_1 contains an aromatic group then it is used as herbicide while R_1 is a benzimidazole moiety then it is used as a fungicide. R_3 is usually an organic radical or a metal (Sogorb and Vilanova, 2002).

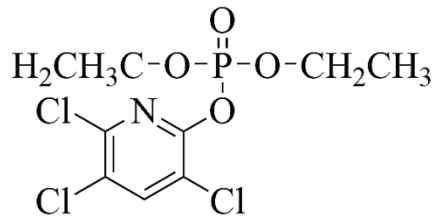
Even though OP and carbamate pesticides are different in their chemical structure and physical properties, both groups have a common mechanism of inducing toxicity in humans. However, their effectiveness as neurotoxicity inducers varies widely and depends on the chemical presentation of the OP or carbamate pesticides active ingredient with the surfactant used for the formulation (Zerin et al., 2017).

2.2.1 Chlorpyrifos-oxon (CPO)

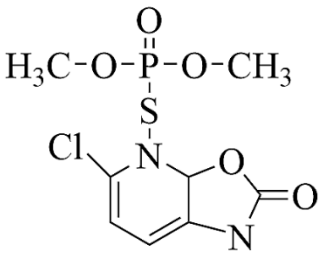
Chlorpyrifos (CPF) is the most extensively used organophosphorothionate insecticide worldwide (Satoh and Gupta, 2011). This potent neurotoxic compound was first synthesised by the Dow Elanco Company in 1965 (Cox, 1994). CPF is widely used in crop protection, landscaping pest control, and in domestic settings to control insect pests due to its potent biocidal nature to kill a large number of pests (Testai et al., 2010). It has been distributed in the world market as different brand names and 850 products were registered in the USA in 1997 (Salyha, 2010). Currently, CPF use is banned in the USA since 2017 and European Union has banned its sale from 2020. However, CPF is still authorized for use in Southeast Asian countries including Japan. Chlorpyrifos is converted into Chlopyrifos-oxon (CPO) which is the active metabolite of the CPF, by desulphuration and this has more potent toxicity than the CPF (Flaskos, 2012). CPO is more soluble in water than parent CPF and easily penetrates into the brain and other organs in the body (Sogorb and Vilanova, 2011). Furthermore, CPO is more chemically reactive than CPF and reacts with a multitude of molecules in cells, and also interferes with cellular events (Flaskos, 2012).

CPO (O, O-diethyl O-3,5,6-trichloro-2-pyridyl phosphate, $C_9H_{11}Cl_3NO_4P$) has a molecular weight of 334.5 g/mol (Figure 2-2) and exists as an off-white

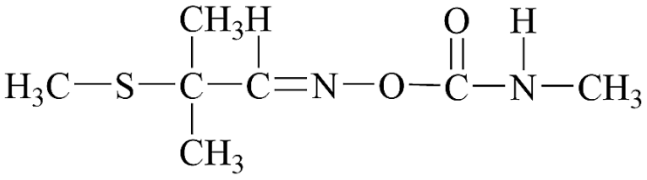
crystalline solid and is odourless. CPF is used as an active ingredient in many chemical formulations in a variety of forms, such as granules, powders, suspensions, emulsifiable concentrates, and in gel-based products and baits (Whang et al. 1993). However, the photolysis of CPF yields CPO in soil (Ishag et al. 2019) and volatilization also generates CPO in the environment (Whang et al. 1993), where humans can directly be exposed to the CPO. The half-life of CPF is recorded as 60 -120 h in soil but can be varied upon the soil condition from 2 weeks to 1 year (Eaton et al., 2008). It has been proved that half-life depends on the pH of the solvent (Lockridge, Verdier and Schopfer 2019).



Chlorpyrifos-oxon



Azamethiphos-oxon



Aldicarb

Figure 2-2: Chemical structures of Chlorpyrifos-oxon, Azamethiphos-oxon, and Aldicarb

2.2.2 Azamethiphos-oxon (AZO)

Azamethiphos (AZA) S-[(6-chloro-2-oxooxazolo [4,5–b] pyridine-3(2H)-yl)methyl] O, O-dimethyl phosphorothioate) is the active ingredient found in Salmosan®, Ciba–Geigy 18809; Snip; and Alfacron, and is a synthetic organophosphate pesticide from the phosphorothioate class. This has been

approved in several countries in the world for sea lice control in salmon farming (O'Halloran and Hogans, 1996, Roth et al., 1996). However, it is also used for the control of ectoparasites in crustaceans and eel, seabass or trout aquaculture to control monogenean (Intorre et al., 2004). In some European and North American countries, and Canada, it is licensed to use AZA for the control of pre-adult to adult sea lice in salmon farming (O'Halloran and Hogans, 1996, Revie et al., 2002, Roth et al., 1996). It has been documented, AZA is biotransformed to its oxon metabolite (Azamethiphos-oxon- (AZO, S-6-chloro-2,3-dihydro-2-oxo-1,3-oxazolo[4,5-b]pyridin-3-ylmethyl O,O-dimethyl phosphorothioate, $C_9H_{10}ClN_2O_5PS$) in salmons by CYP 450 enzymes (Moulton et al., 1996). The molecular weight of AZO is 324.7 mg/mol and it is a colourless crystal in structure (Figure 2-2). AZA is also used to control flies and cockroaches primarily in Europe. Other than that, it has been used as a fly bait by US troops in the Gulf War. AZA has a lower potential for bioaccumulation in soil and is moderately degraded in water (Richardson, 2014). However, AZA in water and air have been found to be toxic to non-target organisms and also cause low to moderate environmental risk (Ernst et al., 2001). The half-life of Azamethiphos is recorded as 6 hrs in soil (Richardson, 2014).

2.2.3 Aldicarb

Aldicarb, (2-Methyl-2-(methylthio) propanalaldehyde O-(methylcarbamoyl) oxime, $C_7H_{14}N_2O_2S$) is an oxime carbamate insecticide. It was first produced by the Union Carbide Cooperation, labelled as Temik (Figure 2-2). It is used to control insects and nematodes and in animal husbandry as an acaricide (Risher et al., 1987, de Bertrand and Barceló, 1991, Feist et al., 2020) and utilized as a soil applicant in agriculture. It is currently registered to use in field crops, plantation crops, and horticultural crop cultivations. The half-life of Aldicarb in laboratory conditions is about 1 to 2 weeks but it is much longer in soil and

water. It undergoes photodegradation after exposure to light and produces Aldicarb sulphoxide (de Bertrand and Barceló, 1991) which is similar to the metabolic product in mammals (Risher et al., 1987), and humans can be exposed to Aldicarb sulphoxide from the environment. The molecular weight of Aldicarb is 190.27 g/mol and it exists as white crystals with a slightly sulphurous odour. It is commercially available as granule formulations (EPA, 1998), and is soluble in organic solvents like methanol, ethanol, or acetone (Williams, 2013). Aldicarb can bioaccumulate in vegetables and fruits by absorption from soil (Todd, 2003, Bjørling-Poulsen et al., 2008b) and by consumption of contaminated fruits, vegetable, and cereals, but generally the public are exposed to low levels of this pesticide (Vale and Lotti, 2015).

2.2.4 Routes of exposure to CPO, AZO and Aldicarb

Humans are exposed to CPO, AZO, and Aldicarb in three exposure settings that are occupational, ambient, and indoor settings. All who deal with CPF, AZA, and Aldicarb and their active metabolites, for instance agricultural workers and their family members, manufacturers, chemical industry workers, transporters, and those involved in the formulation of pesticides, are exposed (Rawn et al., 2009, Saunders et al., 2012). The general public are exposed to these pesticides through consumption of contaminated foods and water (Reiss et al., 2015), inhalation of contaminated air, and industrial dust (Gurunathan et al. 1998, Morgan et al. 2005, Saunders et al. 2012). Direct exposure to CPF showed a positive relationship with neurological effects in adults (Macintosh et al., 2001) and also the development of neurological disorders in children (Rauh et al., 2006). Pesticides absorb through the skin after dermal contact, oral mucosa through ingestion and airways by inhalation of contaminated air (Damalas and Eleftherohorinos, 2011). The soil application of CPF and Aldicarb undergoes photodegradation and metabolites are volatilised to the atmosphere (Risher et

al., 1987, Whang et al., 1993, Blacker et al., 2010) and the people who work in fields can be exposed to their active metabolites directly. Although there was no recorded studies that indicate that AZA bioaccumulation contaminates surface water or volatilise from the surface water to the surrounding atmosphere (Roth et al., 1993).

Despite the chemical class of the pesticide, the level of exposure can be varied according to the duration of exposure, the concentration of the pesticide exposed, chemical nature of the pesticide, and the physical properties of the pesticide (Damalas and Eleftherohorinos, 2011).

2.2.5 CPO, AZO and Aldicarb biotransformation

Neurotoxicity of organophosphate and carbamate pesticides in humans depends on the chemical structure of the pesticide and the metabolic product of the parental compound (Jokanović, 2001). On the other hand, inherent characters such as age, sex, and the genetic makeup of the person exposed will also affect neurotoxicity development by the pesticides (Gupta and Milatovic, 2012). After absorption of CPF, AZA, and Aldicarb by the body, they undergo many biotransformation reactions inside the body. Moreover, all three pesticides are lipophilic and easily penetrates through the skin and they make polar conjugates.

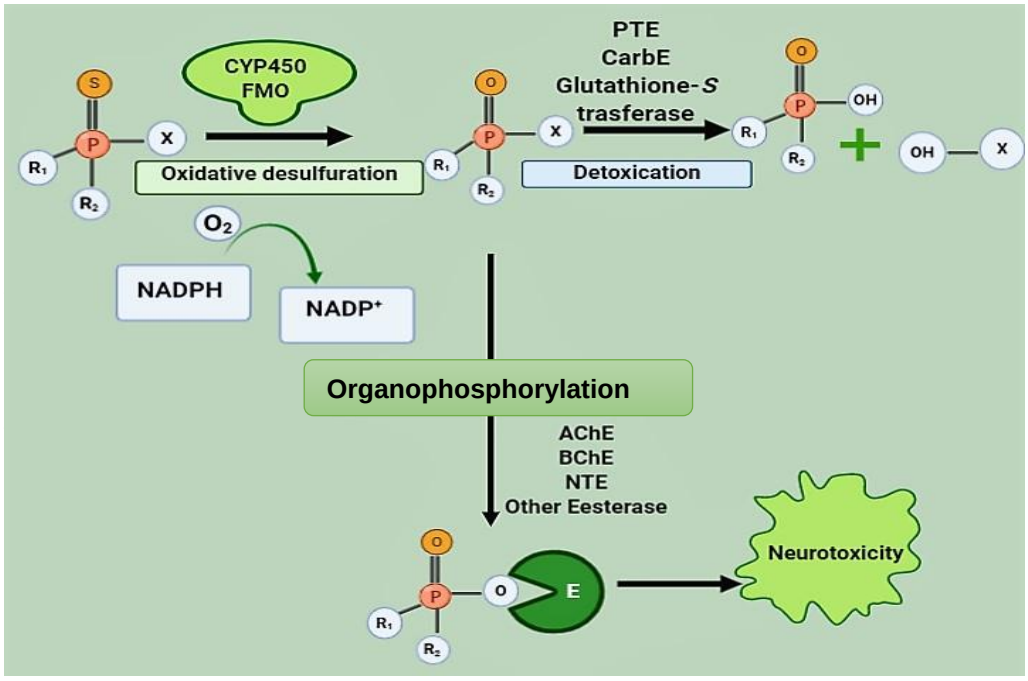


Figure 2-3: Biotransformation of OP pesticides in humans.
The biotransformation of OP that has entered into the body takes place in the liver as an enzyme-dependent reaction. Metabolic activation of inactive OP to its oxygen analogs and then converted to non-toxic compounds which are eliminated by the body. The OP is first converted to its oxon metabolite by the oxidative desulfurization where its double bonded sulphur atom is replaced from oxygen atom which is a potent AChE inhibitor due to its electron withdrawing ability. The reaction is primarily carried out by the cytochrome P450 (CYP) enzymes depended on the monooxygenase system which mainly exist in the liver (Jokanović, 2001).
CYP450-Cytochrome P450; FMO- Flavin-containing monooxygenase, PTE-Phosphotriesterase, CarbE - Carboxylesterase; AChE- Actylcholinesterase; BChE-Butylcholinestease; NTE-neuropathytargetesterase; E- Enzyme; X- lLeaving group.

However, different metabolic conversion in different OP compounds by the CYP450 system shows variability in toxic insults as sometimes the parental compound is more toxic than the bioactivated compound, or bioactivated compound further converted into more toxic compounds. Moreover, other than the involvement of CYP450 enzymes, CPO detoxification occurs by A-esterase such as paraoxonase 1 (PON1). Low level of detoxifying enzymes can also increase the human susceptibility to the OP neurotoxicity as discovered by *in vivo* studies (Costa et al., 2013).

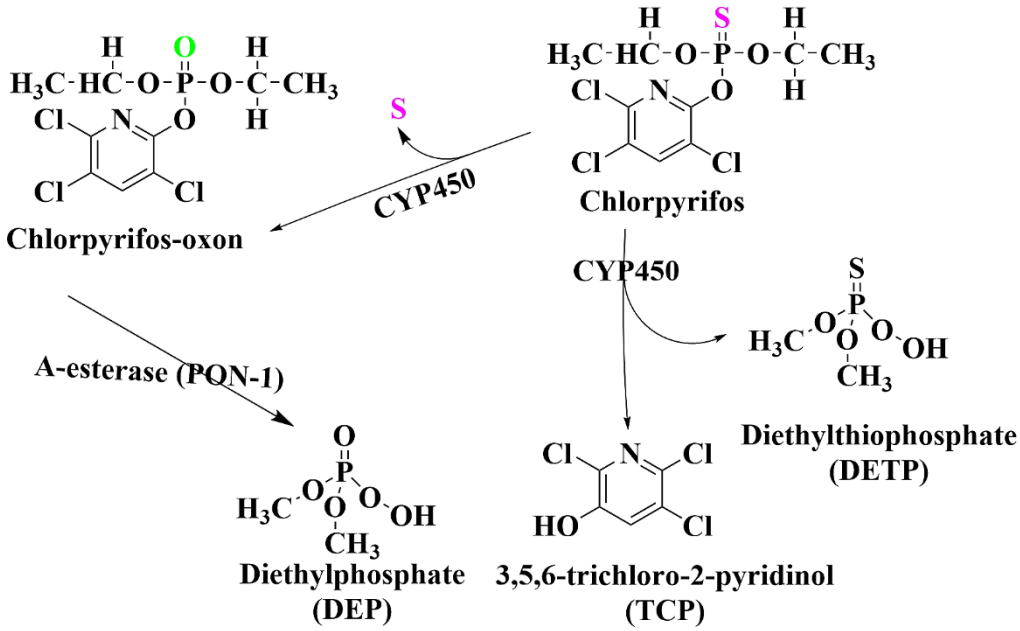


Figure 2-4: Metabolic bioactivation of chlorpyrifos (proposed by Eaton et al. 2008).

Aldicarb is readily bio-transformed in the liver in most organisms including rats, cows, and dogs (Risher et al., 1987, Perkins et al., 1999). Although there are no demonstrations available for humans, however, an *in vitro* study suggested that Aldicarb is metabolically activated by the CYP450 monooxygenase system (Giri et al., 2018). All animal model studies suggested that it is detoxified and eliminated through the urine as oximes and nitrite metabolites. Aldicarb is converted to its metabolite Aldicarb sulfoxide by an oxidation reaction and is mediated by CYP450 and flavin monooxygenases due to thioether bonds in Aldicarb. The aforementioned study with liver microsomes suggested that isoforms CYP2C8 and CYP2C9 are involved in oxidative desulphuration. The resultant Aldicarb sulfoxide can be further oxidised to Aldicarb sulfone by the presence of CYP2C19, CYP3A4 as the study suggested (Giri et al., 2018). Both Aldicarb sulfoxide and Aldicarb sulfone are potent inhibitors of AChE in humans (Damalas and Eleftherohorinos, 2011).

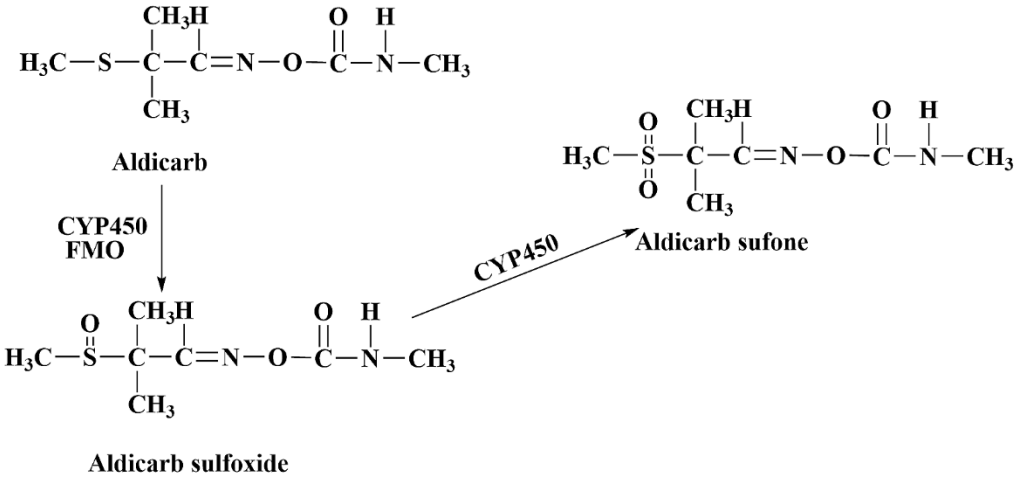


Figure 2-5: Metabolism of Aldicarb in humans (proposed by Giri et al. 2018).

2.2.6 Organophosphate and carbamate neurotoxicity

OPs and carbamates are proven AChE inhibitors that effect chemistry, structure, and function of the nervous system during development or at maturity. The change can be an effect on morphological, neurochemicals, neurologic or behavioural aspects of the nervous system. The effect can be transitory or persistent (Costa, 1998). Organophosphates including CPO can cause neurotoxicity due to excess accumulation of ACh at synapses of PNS and this hyper-stimulates the cholinergic receptors in the CNS. The resulting “cholinergic syndrome” is the main mechanism underlying organophosphate neurotoxicity.

The neurotoxic disorders resulting from organophosphorus esters exposure includes cholinergic syndrome, intermediate syndrome, organophosphate-induced delayed neuropathy (OPIDN), and chronic organophosphate-induced neuropsychiatric disorder (COPIND). The cholinergic syndrome is directly related to the OPs' acute toxicity and induced inhibition of AChE. The condition further develops with nicotinic and muscarinic symptoms. Muscarinic symptoms include miosis, sweating, lacrimation, salivation, abdominal cramps, and

respiratory difficulties, whereas the nicotinic symptoms include hyperreflexia and paralysis (Karczmar, 2007, Jokanović and Kosanović, 2010)

OP-induced delayed neuropathy (OPIDN) is due to single-dose exposures, and usually symptoms appear after 1-2 weeks. This includes axon and myelin degeneration in CNS and PNS. Additionally, the condition is dependent on AChE inhibition (Singh and Sharma, 2000, Ray and Richards, 2001). The symptoms of this condition include muscle cramps, tingling feet, and hands after numbness and paraesthesia (Lotti and Moretto, 2005, Jokanović et al., 2011). The OPIDN is characterised by inhibition of the activity of neuropathy target esterase (NTE) which is found on neuronal cell membranes as proposed by Martin Johnson (Johnson, 1974, Glynn et al., 1999). Most studies of developmental neurotoxicity (DNT) focus on the activity of NTE and the development of OPIDN. The condition is subsequently developed with the chemical ageing of NTE. According to the studies it was pointed out the ageing reaction may lead to disturbances of phospholipid homeostasis in the endoplasmic reticulum in cells. This may ultimately cause impairment of axonal transport and interaction with glial cells (Glynn, 2006).

Chronic organophosphate-induced neuropsychiatric disorder (COPIND) is a condition that affects the CNS interfering with its neurobehavioral performance (Ray and Richards, 2001). It is a long-lasting condition that is a permanent impairment of the CNS. The common symptoms of this condition include the cognitive deficit, mood change, chronic fatigue, autonomic dysfunction, and rigidity of facial muscles (Salvi et al., 2003, Kamel and Hoppin, 2004, Roldán-Tapia et al., 2005, Davies, 2009)

Acute exposures to carbamates show minor health or serious health problems depending on the dose and length of exposure. Minor effects such as discomfort or chest pain and serious effects include convolution, seizures, coma, and

death. Muscarinic symptoms of acute poisoning include hypersalivation, gastrointestinal cramps, overproduction of bronchial fluids due to the accumulation of ACh via AChE inactivation. High dose exposures shows tremors, convolutions, mental disturbances, cyanosis, and coma (Gupta and Milatovic, 2012, Gupta, 2014). Chronic exposure reports include skin irritations, eye irritations, and reproductive matters such as low sperm production in men or endocrine system disruption (Gupta and Milatovic, 2012). It has been reported that severe Aldicarb exposure causes acute cholinergic syndrome in humans (Baron, 1994, Blacker et al., 2010). Interestingly, studies reported the combined use of OPs and carbamates to have cumulative subacute neurotoxicity in humans than exposure to each pesticide individually (Gupta and Milatovic, 2012).

2.2.7 Developmental neurotoxicity of OP and carbamate pesticides

During gestational development of humans and the early childhood exposure of organophosphates, carbamate pesticide, and their metabolites can cause severe brain defects, abnormalities, and permanent impairments, even if the exposure occurs at lower concentrations than those required to produced clinical signs of acute neurotoxicity in adults (Grandjean and Landrigan, 2014). Many studies have proved that the gestational and early development exposure to CPF and its metabolite CPO are linked with the development of attention deficit hyperactivity disorder (ADHD), autism, learning difficulties, and other emotional and behavioural problems and intimately linked with socio-behavioural problems (González-Alzaga et al., 2014). These neurodevelopment disorders called a “silent pandemic” has major health, economic, and social impact on developed and developing countries. Nearly one in six children worldwide has been diagnosed with developmental disorders worldwide.

Low and chronic exposure to the organophosphate pesticide CPF and its metabolite CPO at early development stages caused severe neurodevelopmental effects, such as premature births, and other clinically obvious conditions. The main source of exposing the foetus to oxon metabolites is through the mother's tissues. CYP2B enzymes present in the placenta also have the capability of converting CPF to CPO, but this is not significant in humans at physiologically relevant insecticide concentrations (Flaskos, 2012). The generated oxon metabolites can readily be passed to the foetus due to their high-water solubility. The growing brain has the highest oxygen demand over other organs, rich in unsaturated fatty acids, high content of iron and low levels of antioxidants compared to the adult brains, because of this, there is an increase in vulnerability to oxon metabolite induced neurotoxicity damage (Flaskos 2012). Another factor that increases the vulnerability of these pesticides in prenatal stages is less of a developed blood-brain barrier. So, it cannot prevent the transfer of some toxic chemicals from the maternal blood to the foetal or infant brain in early life (Costa et al. 2004). The studies done with different development stages with young children has shown prenatal exposure of CPF caused a decline in the intelligent quotient (IQ), working memory and increased attention problems and ADHD (Rauh et al., 2006, Horton et al., 2012, Philippat et al., 2018). CPO susceptibility of newborns was also explained by variation in A-esterase PON 1 for a cohort study in Latina farmworkers (Furlong et al., 2006).

Exposure of carbamates like Aldicarb and carbaryl showed development neurotoxicity defects in young children (Bjørling-Poulsen et al., 2008b). However, the exposure of carbamates caused reversible inhibition of AChE, unlike OPs. Also it has been reported young children showed CNS depression and hypotonia (Lifshitz et al., 1997) upon exposure and developed symptoms

similar to those developed in OP poisoning (Lifshitz et al., 1999). Exposure of carbamate pesticides causes long term neurological defects in children including cognitive deficit in attention, memory, perceptual, and motor domains (Roldan-Tapi et al., 2005), but there is no epidemiological studies that have observed a long-term effect related to developmental neurotoxicity from carbamate poisoning.

The brain development process involves a sequence of events such as neural cell proliferation, migration and differentiation, axonogenesis, neurite outgrowth, synaptogenesis, gliogenesis, and apoptosis, which starts from embryonic life and continues to late adolescence (Grandjean and Landrigan, 2014). These critical events can be disrupted by OP or carbamate exposure at any stage of development. Therefore, OP and carbamate neurotoxicity are mainly dependent on neurodevelopment stages at which the exposure occurs. The timing at which the exposure occurs to these pesticides determines the affected region and function (Flaskos, 2011, Pizzurro et al., 2014).

2.2.8 Candidate mechanisms of OP and carbamate neurotoxicity

Numerous mechanisms have been proposed as the underlying mechanisms of pesticide neurotoxicity. Many *in vitro* studies proved that both parent compounds and the metabolic product damage the neuronal cells and then have a direct link or indirect link to the toxicity induction in neuronal cells (Yang et al., 2008, Raszewski et al., 2015). Hence, a recent literature review confirmed that there is no single mechanism that can account for inducing neurotoxicity (Naughton and Terry, 2018) .

Pesticide effects on the brain and developing brain are complex. For certain cell types, pesticides can induce cell death while other groups interfere with cellular functions. Also, OP and carbamate pesticides induce neurodegeneration in a

given cell population, depending on the developmental stage of cells. For instance, developing neuronal cells multiply by cell division, and migrate to an appropriate location where they are fully differentiated and functional as neuronal cells. If the cells are exposed during the cell division, the proliferation ability of cells may be affected. If those cells are exposed at a later stage their migration and differentiation may be affected (Sandoval et al., 2019). Therefore, multiple mechanisms are associated with organophosphates and carbamate related neuronal cell damages dependent upon the stage of development. Depending on the group of cells affected by pesticides such as functionality changes or depletion of cells, there will be a relationship with the development of neurotoxicity related disorders in humans (Chang et al., 2018).

Experimental approaches using animal models, *in vitro* cell culture models and new technologies such as microarray experiments has helped to identify the numerous mechanisms related to OP and carbamate induced neurotoxicity at the cellular levels (Lukaszewicz-Hussain, 2008, Lukaszewicz-Hussain, 2010, Terry, 2012, Lukaszewicz-Hussain, 2013).

2.2.8.1 ***Cholinergic mechanism***

The key mechanism of organophosphate and carbamate toxicity in humans is cholinesterase inhibition in the nervous system (Miller, 1982, Mangas et al., 2017). Acute toxicity by both groups of pesticides is induced by AChE inhibition in insects, mammals, and humans (Risher et al., 1987, Blacker et al., 2010, Carr et al., 2018). AChE is the governing enzyme that terminates the neurotransmission at central and peripheral cholinergic synapses and is a serine hydrolase embedded in the postsynaptic membranes of neuromuscular junctions (Miller, 1982, Carr et al., 2018). Persistent inhibition of AChE activity causes decreased degradation of the neurotransmitter acetylcholine (ACh) into choline and acetate, and the gradual accumulation of ACh in the synaptic cleft

cause perturbations of nerve impulse transmission (Figure 2-6). The organophosphorylation of AChE by OPs leads to the inhibition of its normal function and reduced degradation of the major neurotransmitter acetylcholine (ACh) at the cholinergic nerve endings in the central and peripheral nervous system (Eaton et al., 2008, Carr et al., 2018). Several hours later, reactivation of AChE usually occurs by hydrolysis of OP compounds. Consequently, ACh is accumulated in cholinergic synapses and causes excessive stimulation of receptors in the CNS and nicotinic receptors which cause the clinical manifestations of OP neurotoxicity. Azamethiphos is also a cholinesterase inhibitor, but there is no recorded data for humans and only recorded for fish and lobsters (Burridge et al., 2014, Couillard and Burridge, 2015). (Figure 2-6).

Carbamate pesticides have a similar mechanism to OP pesticides of AChE inhibition, carbamylation of the active site of the enzyme which reduces the affinity of ACh to bind to the active site. Unlike the AChE-OP conjugate, however, the carbamylated enzyme does not undergo the ageing process and hydrolyses within a few hours. Therefore, the action is considered as reversible inhibition. However, the rate of hydrolysing of the carbamylated enzyme is lower than hydrolysing the ACh molecules by AChE. Toxicity of carbamates occurs when the rate of carbamylation of AChE is greater than that of the hydrolysing the carbamylated enzyme during acute high dose pesticide exposure (Figure 2-6). As a result, ACh accumulates on the synapses and overstimulates the receptors as in OP pesticides. Clinical manifestations associated with carbamate pesticide exposure is generally more short-lived with recovery within 36-48 hours (Vale and Lotti, 2015).

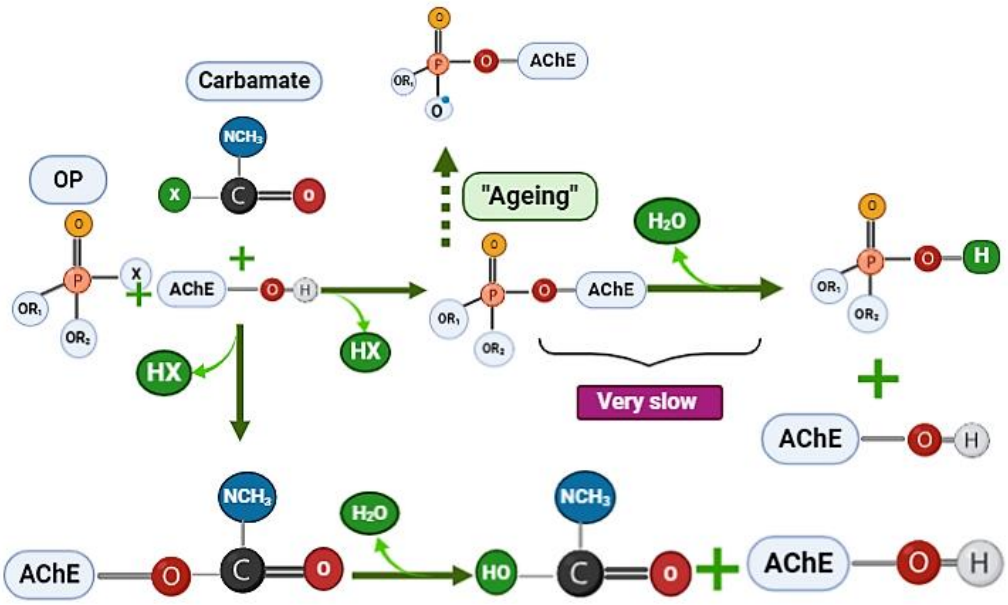


Figure 2-6: AChE inhibition by OP and carbamates.
At the molecular level, OP which has a P=O moiety, is a potent inhibitor of AChE. When OP binds to the active site of the AChE, the covalent bond is formed between the phosphate group of the OP compound and the hydroxyl group of the serine within the active site of AChE. This bond is stable and usually persists for hours or weeks depending on the OP involved (Estevez and Vilanova, 2009, Carr et al., 2018). However, the AChE-OP bond complex can subsequently undergo an "ageing" mechanism where it loses one or two alkoxy liable groups (R_1 and R_2) by non-enzymatic hydrolysis process (Vilanova et al., 1987, Worek et al., 2007). When the AChE-OP undergoes the ageing process, inhibition of AChE by OP is considered as irreversible as the enzyme conjugation is more resistant for the reactivation (Mangas et al., 2017) and is regarded as permanently inhibited.

2.2.8.2 *Non-cholinergic mechanisms*

AChE inhibition undoubtedly plays a key role in the neurotoxicity mechanism of OP and carbamate pesticides, however, a plethora of literature has suggested that AChE inhibition is not the sole mechanism for the symptom and disorders that arise from the exposure to OP and carbamates. The high reactivity of CPO and Aldicarb account for several cellular targets other than inhibiting cholinesterase enzymes (Grigoryan et al., 2009b, Luqman et al., 2019). Wider literature has suggested that these non-cholinergic mechanisms contribute to the more delayed and persistent effect of OPs and carbamate pesticide neurotoxicity along with the AChE inhibition (Terry, 2012). Oxidative stress, neuroinflammation (Lee et al., 2014b), mitochondrial dysfunction (Dai et al.,

2015, de Oliveira et al., 2016, Fu et al., 2019), endoplasmic reticulum dysfunction and stress (Reyna et al., 2017, Xia et al., 2020), Ca^{2+} imbalance, apoptosis, and necrosis are widely studied as non-cholinergic mechanisms of neurotoxicity.

Table 2-1 shows potential cellular mechanisms induced by OP and carbamate pesticides in human neuronal cells. However, cytotoxicity of both OP and carbamate pesticides can induce more than one mechanism, and these mechanisms are interconnected with each other and collectively play a role in inducing the long-term functional changes in neuronal cells.

Apoptosis is known as programmed cell death, where neuronal cells shrink their cell body, DNA becomes fragmented and then the cell becomes fragmented, and organelles remain intact. Then cells are surrounded by apoptotic bodies, and later engulfed by scavenging cells after the toxic insult of pesticides. However, its onset can be delayed after toxic insult until the activation of gene-mediated programmed cell death (Elmore 2007, de Oliveira et al. 2016). CPF and CPO induced cellular apoptosis has been widely recorded and is mediated by apoptotic enzymes/protein/gene expression and apoptotic signalling pathways induced upon CPO and CPF exposure, as demonstrated in human neuronal cells (Table 2-1). Cellular apoptosis occurs mainly in two pathways. The extrinsic pathway or death receptor pathway and the intrinsic pathway or mitochondrial pathway (Elmore, 2007). According to the summarised data in Table 2-1 it is suggested that the CPF and CPO can induce apoptosis in neuronal cells in both ways, consistent with the fact that the two pathways are interconnected, and one pathway can influence the other. For instance, de Olivera and colleagues in 2016 suggested that CPF can induce cell death by the death receptor pathway in SH-SY5Y cells and also DNA fragmentation

which is a marker of apoptosis induced by oxidative stress-mediated mitochondrial dysfunction.

Necrosis occurs when neuronal cells are exposed to pesticides at high acute doses. This has been demonstrated with human neuroblastoma SH-SY5Y cells exposed to Zeneb, a dithiocarbamate fungicide. Cells undergoing necrosis initially swell and then internal organelles break down. The cells then rupture and spill debris while triggering inflammation (Elmore 2007). The cells exposed to Zeneb show necrotic cell death at a higher concentration by flow cytometric studies with propidium iodide (Jia and Misra, 2007).

Mitochondrial dysfunction is one of the major non-cholinergic mechanisms suggested in OP and carbamate induced cytotoxicity. Loss of mitochondrial function attributed by loss of energy generated by the electron transport chain and reduction of synthesis of energy molecules, rupture of mitochondrial membrane and cytochrome c release in cells. This results in reduced ATP production, which is used as a biomarker of viable mitochondrial functioning. CPF and carbamate exposure cause mitochondrial dysfunction by interfering with the electron transport chain and this is followed by ATP depletion. Massicotte and colleagues (2005) showed that OP pesticides target mitochondria and induce effects on Complex I and Complex IV in SH-SY5Y neuroblastoma cells and the associated production of ATP (Karami-Mohajeri and Abdollahi, 2013).

Neuroinflammation has been demonstrated in CPF exposed human neuronal cells as a mechanism inducing cytotoxicity. Low-level repeated exposure of CPF upregulated inflammatory responses in cultures of astrocytes (increased IL-6, GFAP, and p-ERK1/2) (Mense et al., 2006) and also upregulated inflammatory cytokines has been demonstrated in human neuroblastoma cells (Lee et al., 2014b). Neuroinflammatory responses caused by pesticide

exposure caused significant impairment in spatial memory as demonstrated by Wenk et al. (2003). But still ill-defined in the literature is the link between inflammatory responses and functional impairments (Wenk et al., 2003).

Ferroptosis is a newly revealed form of regulated cell death which is characterized with iron accumulation and production of ROS (Xie et al., 2016, Stockwell et al., 2017). Ferroptosis is morphologically marked with smaller mitochondria with condensed mitochondrial densities, and mitochondrial membrane rupture according to Xie et al. (2016). Lipid peroxidation is linked to NADPH oxidase depended oxidative stress and has been identified as one cause of cell ferroptosis related cell death by the toxic insult of pesticides (Hou et al., 2019).

A key component of pesticide-induced cellular apoptosis/necrosis, and mitochondrial dysfunction is oxidative stress. OP or carbamates are able to induce all of these cellular toxicity responses with a concentration-dependent or dose-dependent effects as detailed in Table 2-1, via the interaction of several mechanisms.

2.2.9 Role of oxidative stress in OP and carbamate cytotoxicity

Oxidative stress is a key factor that can induce pesticide-related apoptosis in neuronal cells. Oxidative stress can be described as an imbalance between the production of free radicals and the cellular antioxidant system. Free radicals are highly reactive molecules produced from various biochemical reactions in cells. Many free radicals contain oxygen and are termed reactive oxygen species (ROS). Various scavenger molecules known as antioxidants control the free radicals produced in cells (Lukaszewicz-Hussain, 2010). ROS are short-lived molecules and can undergo various biochemical reactions inside the cells to eliminate them. ROS are important for typical cell functioning since they act as

mediators in various signalling pathways and cell cycle progression (Boonstra and Post, 2004, Ferreira et al., 2018). Acute and chronic OP exposure induced oxidative stress is reported as the main mechanism of its toxicity (Ranjbar et al., 2005).

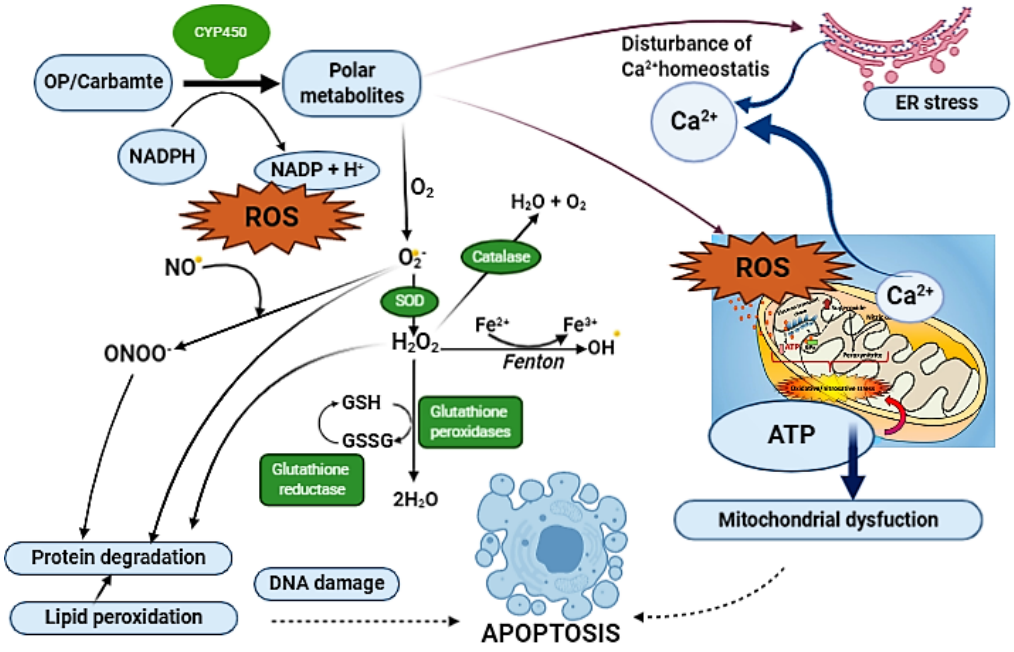


Figure 2-7: ROS generation pathways OP and carbamate pesticide exposure.

ROS are produced through two main pathways by the toxic insult of pesticides as reported in the literature. OP metabolism by CYP450 which is a catalytic pathway that introduces one oxygen atom to an OP molecule by the electron transport chain and ROS are generated from this reaction through conversion of NADPH to NADP (Chambers et al., 2010, White, 1991). Hence, if a continuous supply of antioxidants are not maintained to eliminate resultant ROS, a redox imbalance occurs in cells (Banerjee et al., 1999, Vidyasagar, 2004, Possamai et al., 2007). The other way of ROS generation in OP toxicity is the oxidative phosphorylation that demands higher energy as described by Milatovic and colleagues (Milatovic et al., 2006). High energy requirements release ATP from cells which accelerate the glycogenesis in the cell (Rahimi

and Abdollahi, 2007). High energy consumption after toxic insult causes depletion of ATP molecules in cells and generates considerable levels of ROS (Milatovic et al., 2006) (Figure 2.7).

There are two antioxidant systems available in humans to counteract the redox stress, namely, an enzymatic system which consists of superoxide dismutase (SOD), catalase (CAT), glutathione peroxidase (GPx) and glutathione reductase (Gr), and a non-enzymatic system via the reduced form of glutathione (GSSG), vitamins including E, C, and beta carotene, and coenzyme Q(10) (Gerard-Monnier and Chaudiere, 1996, Spolarics and Wu, 1997, MatÉs et al., 1999, Michael J. Morgan, 2007, Rahimi and Abdollahi, 2007, Das and Roychoudhury, 2014, Su et al., 2019). Toxicity of acute and chronic exposure of OP and carbamate pesticide in humans and in human cell models *in vitro* displayed changes in the antioxidant system (Table 2-1), altering the levels of non-enzymatic or enzymatic antioxidants in cells regarded as oxidative stress markers (SOD, GSH, CAT). OP induced hyperglycaemia also caused an increase of non-enzymatic glycation which produces adducts with amino groups of proteins and alters the function and structure of proteins. These glycated proteins can induce oxidative stress by interfering with the membrane receptors in cells and are considered as an oxidative stress mechanism (Basiri et al., 2007, Rahimi and Abdollahi, 2007).

ROS can damage cellular components such as membrane lipids, nucleic acids, and proteins due to their unstable nature. Neuronal cell membranes are highly susceptible to ROS damage due to their polyunsaturated nature. Therefore, the brain, which is rich in unsaturated fatty acids can be a good target for the ROS and cause oxidative stress after pesticide exposure. Free radical species such as oxyl radicals, peroxyl radicals, and hydroxyl radicals remove electrons from lipids and subsequently produce reactive intermediates that can undergo further

reactions, a process known as lipid peroxidation (Su et al., 2019). The products of lipid peroxidation cause chain reaction damage to cellular macromolecules such as DNA and proteins due to their high reactivity. The main aldehyde product of lipid peroxidation is a 3-carbon dialdehyde species, malondialdehyde (MDA), and 4-hydroxy-2-nonenal (HNE) which can be used as a marker of lipid peroxidation. Chlorpyrifos and other OPs induced lipid peroxidation in human neuronal cells as demonstrated by both *in vivo* and *in vitro* studies (Vidyasagar, 2004, Ranjbar et al., 2005, Ki et al., 2013) (Figure 2-8).

OP and carbamate pesticide-induced ROS damage to DNA has been demonstrated in several *in vivo* and *in vitro* studies. Oxidative damages to DNA are remarkable because this changes the genetic makeup of the cells irreversibly. This has been widely recorded in development neurotoxicity studies with OP and carbamates that make epigenetic changes after exposure of pesticides in early life. ROS species induced by acute and chronic low doses of pesticides oxidize DNA bases. Guanine is the most vulnerable to oxidative damage with its high potential for oxidation. Cytokines have the potential to damage second to the guanine. Frequently, studies have shown DNA damage by pesticides as 7,8-dihydro-8-oxoguanine (8-oxoG). Specific sites of DNA accumulate oxidized bases and cause mutations that can be transferred into the next generation of cells. A study concludes that occupational exposure of low chronic doses increased oxidative damage to DNA by assessing 8-OHdg levels (Shadnia et al., 2005, Calviello et al., 2006, Tope and Panemangalore, 2007)

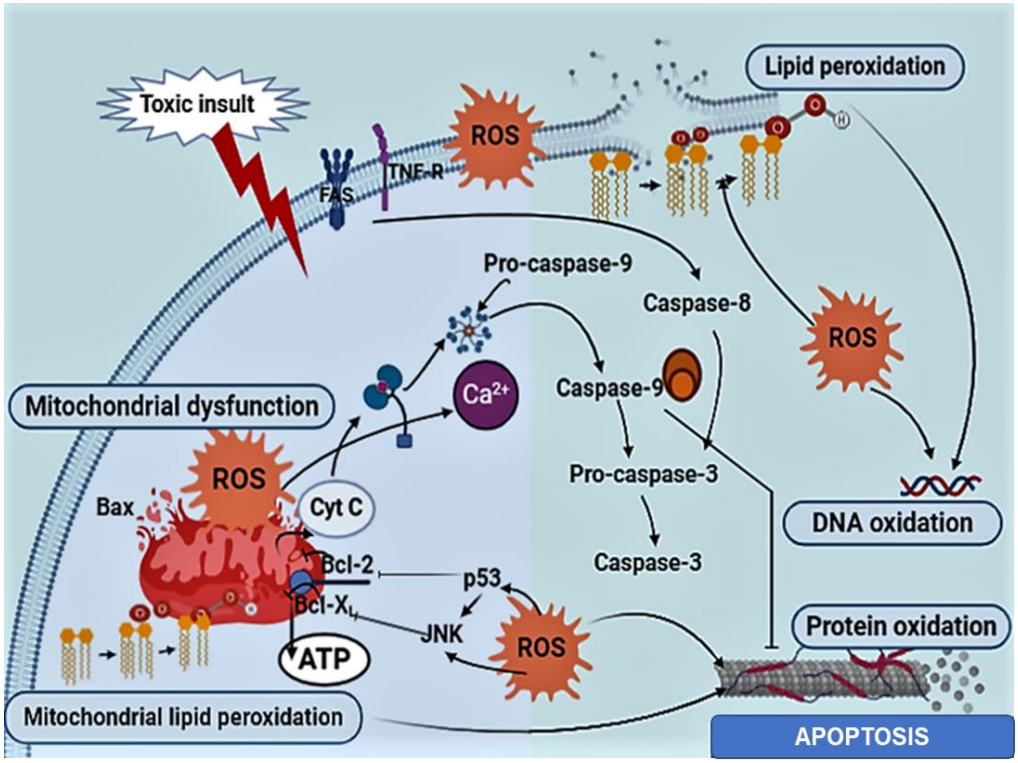


Figure 2-8: Cellular targets of ROS generated by the OP and carbamate pesticides in neuronal cells .
ROS activates mitochondrial pathway of apoptosis. ROS generated exogenously or endogenously activates p53, C-JUN-N terminal kinase (JNK) which then activates Anti-apoptotic Bcl-2 proteins that inhibits Pro-apoptotic proteins. ROS cause oxidation of lipids, proteins, and nuclear and mitochondrial DNA in cells. Damaged mitochondria release cytochrome c (Cyt c), then form an apoptosome complex leading to caspase-9 activation. Activation of death receptors such as FAS can lead to induced caspase-9 activation.

Oxidative modification of protein alters the structure and function of proteins. Redox damage occurs in three ways after exposure of OP or carbamate pesticides. Oxidative modification of specific amino acids, free radical-mediated peptide cleavage, and formation of protein cross-linkage due to reaction with lipid peroxidation products. The protein modifications can be reversible or irreversible. Irreversible protein modifications include protein carbonylation and tyrosine nitration. Reversible protein modification by ROS species is protein cysteine modification, protein sulfenic acid formation, *S*-nitrosylation, *S*-glutathionylation, and protein disulphides. OP exposure induces protein carbonylation, peptide cleavage, and formation of cross-linkages. CPF and CPO induced all these protein modifications in proteins in cells (Schopfer and

Lockridge, 2018). Protein oxidation can be detrimental to cell function. Although some studies showed reversible protein oxidation is beneficial to cellular functions (Wall et al., 2012, Cai and Yan, 2013). For instance, cysteine oxidation products include disulfide formation, and this has been demonstrated to involve oxidative stress and regulation of protein functions by ROS. It has also been shown that reversible protein modifications boost the defence mechanism to counteract toxic insults and prevent further oxidation of target proteins (Lou et al., 2008, Madian et al., 2012, Wang et al., 2012b).

Table 2-1: Summary of published literature on organophosphate and carbamate induced oxidative stress responses of human neuronal and glial cell models.

Pesticide type	Cell type	Treatments	Cytotoxicity mechanism	Cytotoxic effects	Reference
Malathion	Human Astrocytes (GHA cells)	10–25 μM for 24 h	Oxidative stress-induced Apoptosis	Concentration-dependent induced cytotoxicity and cell cycle arrest. Induced apoptotic protein expressions. Increase ROS production in a concentration-dependent manner. Weakening of cellular antioxidant defences.	(Shieh et al., 2019)
Monocrotophos (MCP) Chlorpyrifos (CPF)	Human neuroblastoma IMR-32 and SH-SY5Y	0.1-1000 μM For 24 h and 48 h	Oxidative stress	Reduced cell survival both concentration- and time-dependently. Increase ROS production. Down-regulation of the nuclear factor erythroid 2-related factor 2 (Nrf2).	(Sarkar et al., 2017)
Chlorpyrifos (CPF)	Human dopaminergic neuronal cells (LUHMES cells)	100 nM–100 μM for 24 h 10 μM for 24, 48, 72, 96 hrs	Mitochondria-mediated oxidative stress mechanisms Autophagy	A dose-dependent decrease in cell viability and an increase in DNA fragmentation. Time-dependent increase in STAT1 activation. Collapse of mitochondrial transmembrane potential. Time-dependent increase in ROS generation.	(Singh et al., 2018)

				Inhibition of the mitochondrial basal oxygen consumption rate (OCR). Chromatin immunoprecipitation. Increase in Bax/Bcl-2 ratio. Decreased cellular ATP level. Decreased cellular antioxidants.	
Monocrotophos	Human neuroblastoma SHSY-5Y	100 µM 24, 48, 72 and 96 h	Autophagy, Mitochondrial dysfunctions	Increased mitochondrial fission and decrease mitochondrial membrane potential. Effect on cell viability, oxidative stress. Induced apoptotic cell death.	(Srivastava et al., 2018)
Maneb	Human SK-N-AS cells	0 – 400 µM 1 or 24 h 50 µM for 1 or 24 h	Oxidative stress-induced Apoptosis	Dose and time-dependent reduction of cell viability. Increase ROS generation. ATP depletion. Bioenergetics disruption outside of the mitochondria.	(Anderson et al., 2018)
Monocrotophos	Human neural (SH-SY5Y) and glial (U373-MG)	10^{-3}–10^{-7} M and 0.5-8 mM 24, 48, 72 and 96 h	Oxidative stress-induced Apoptosis	Time and dose-dependent decrease in cell viability. Increased ROS generation and lipid peroxidation in a time-dependent manner. Reduced antioxidant enzymes in a time-dependent manner. Fragmentation in chromosomes.	(Tripathi et al., 2017)
Chlorpyrifos (CPF)	Human neuroblastoma cell line SH-SY5Y	40 or 80 µM	Mitochondria damage and oxidative stress	Decrease of mitochondrial potential. Increased ROS level.	(Xu et al., 2017)

Chlorpyrifos (CPF)	Human neuroblastoma cell line SH-SY5Y	5–500 μM 17.5, 25, 30 μM 24, 48 and 72 hr	Apoptotic mechanisms	Time and concentration dependent decrease in cell viability. A dose-dependent increase in DNA fragmentation.	(Raszewski et al., 2015)
Chlorpyrifos (CPF) CPF-oxon (CPO) 3, 5, 6-trichloropyridinol (TCP)	hNPs, NeuroNet pure human neurons (DIV 28 neurons) and hAstroPro human astrocyte cells	2.5, 5, 10, 20, and 40 μM for 48 h	-	CPF reduced cell density only at the highest concentration tested. CPF inhibited neurites per neuron, neurite length per neuron, and branch points per neuron at 10 μM without reducing cell density. CPO reduced neurite length, neurites per neuron, branch points per neuron in a concentration-dependent manner at which cell viability not effected. TCP has no effect on neuronal cells. Astrocytes reduced the effect on neurons.	(Wu et al., 2017)
Chlorpyrifos (CPF)	Human neuroblastoma SH-SY5Y cells	25–100 μM	Mitochondrial dysfunction and redox impairment	Decrease cell viability, LDH activity in a concentration-dependent manner. ROS generation at higher concentration. Induced protein carbonylation. Increases lipid peroxidation. The reduced antioxidant level in cells and ATP levels.	(de Oliveira et al., 2016)

				DNA fragmentation.	
Chlorpyrifos (CPF)	Human neuroblastoma SH-SY5Y cells	25-200 μM 50, 100 μM 6, 12, 24 or 48 h	Mitochondrial dysfunction and redox stress	Cell viability reduction in time and a concentration-dependent manner. Increased ROS generation and decreased mitochondrial membrane potential.	(Dai et al., 2015)
Mipafox Paraoxon Phenyl saligenin phosphate (PSP) phenylmethylsulfonyl fluoride (PMSF)	SH-SY5Y neuroblastoma cells	100, 500, 750, 1000 and 5000μM 0.5 and 6 hrs	Mitochondrial dysfunction and ATP depletion	Decreased ATP concentrations. Effect on the mitochondrial respiratory chain, including Complexes, I, II, III, and IV.	(Massicotte et al., 2005)
Chlorpyrifos (CPF)	Human iPSC line 253G1 (differentiated cells)	0–30 μM for 24 hours 30 μM for 2, 4, 6, and 8 days	Mfn1-mediated mitochondrial dysfunction	Inhibition of neural induction. Mitochondrial fragmentation.	(Yamada et al., 2017)
Chlorpyrifos, dichlorvos or methamidophos	human SK-N-SH neuroblastoma cells	Concentration causing 20% cell death for 24 h 1/20 of LC_{20}	Apoptosis	Dose-dependent variation of the toxicity for each OP. Downregulation MAPK signalling pathways. Downregulation of cell cycle and growth genes.	(Li et al., 2012)
Chlorpyrifos (CPF)	SH-SY5Y cells	(0–200 μM)	ROS mediated apoptosis	Reduced cell viability in a concentration-dependent manner. Increased cytotoxicity in a time-dependent manner. Increased ROS generation.	(Lee et al., 2014b)

				induced COX-2 expression and Pro-inflammatory cytokine production.	
Chlorpyrifos-oxon (CPO) Chlorpyrifos (CPF)	ReNcell CX undifferentiated and pre-differentiated	(0, 1, 3, 10 µM) For 2 hours, 8 hours	-	No significant reduction of cell viability. Significant AChE inhibition at 10 µM for CPF 2 hours and 8 hours. CPO inhibits AChE in all concentrations tested. (IC_{50} =1-2 µM) Concentration-dependent reduction of neurite lengths in pre-differentiated cells and glial cells for 2 and 8 h. No significant effect on β III tubulin proteins. Reduced Ta51 activity. Neurofilament heavy chain (NFH) phosphorylation.	(Sindi, 2015)
Chlorpyrifos-oxon (CPO) Chlorpyrifos (CPF) phenyl saligenin phosphate (PSP)	ReNcell CX differentiating cells	0, 1, 3, 10 µM for 2 h	-	Significant reduction of cell viability only for CPO for all concentration tested. β III tubulin, NEFH (Neurofilament heavy chain), *GFAP* mRNA reduction at 10 µM CPO.	(Alyamani, 2018)
Chlorpyrifos (CPF)	Human neuroblastoma SH-SY5Y cells	25–200 µM For 24 h	Oxidative stress-induced Apoptosis	Increased ROS generation. Reduced cell viability. Increased LDH activity in a concentration-dependent manner.	(Ki et al., 2013)

				IC_{50} value for CPF was about 100 µM. Increased lipid peroxidation in a concentration-dependent manner. Increased the level of cytosolic cytochrome c. Caspase-9, cleaved caspase-3, and cleaved PARP increased in a dose-dependent manner.	
Chlorpyrifos (CPF)	K-N-SH (human Neuroblastoma cell)	100-500 µmol/L for 48 h	Apoptosis	Reduced cell viability in a dose-dependent manner IC_{50}= 777.8 µmol/L.	(Fu et al., 2019)
Chlorpyrifos (CPF)	Human foetal astrocytes	30–100 µM 24 h	Oxidative stress	A concentration-dependent increase in TBARS. Decreased DNA synthesis in cells.	(Qiao et al., 2005)
Chlorpyrifos (CPF)	Human neuroblastoma cell line SH-SY5Y	25,50,100, 200 µM for 24 h and 50 µM 6, 12, 24, and 48 h	Apoptosis and oxidative stress	Dose and time-dependent decrease in cell viability. Caspase-1and TUNEL upregulated in a dose and time-dependent manner. ROS increased in a concentration-dependent manner. Expression of miR-181 and pyroptosis proteins enhanced Nrf2 significantly upregulated.	(Zhao et al., 2019)
Chlorpyrifos (CPF)	Human neuroblastoma cell line SH-SY5Y	25, 50, or 100 µM 24 h	mitochondrial-dependent apoptosis	Reduced cell viability in a dose-dependent manner.	(Park et al., 2015)

				Increased cytotoxicity in a dose-dependent manner. Enhanced the activities of cleaved caspase-9 and cleaved caspase-3 in a dose-dependent manner. 50 μM CPF significantly decreased the Tyrosine hyroxylase (TH) expression. ROS increased in a concentration-dependent manner.	
Parathion Paraoxon Phenyl saligenin phosphate (PSP)	Human neuroblastoma cell line SH-SY5Y	10 μM, 100 μM and 1 mM for 4, 8, 12, 24, 48, and 72 h	Apoptosis	Time-dependent cell death. Nuclear condensation, budding, and fragmentation. Caspase 3 activation.	(Carlson et al., 2000)
Parathion	Human neuroblastoma cell line SH-SY5Y	0 μM to 1 mM for 7.5 to 960 minutes	Mitochondrial dysfunction	Induced concentration-dependent mitochondrial hyperpolarization. Increase in DNA fragmentation.	(Carlson and Ehrich, 1999)
Trichlorfon Dichlorvos	Human neuroblastoma cell line SH-SY5Y	10–500 μM 1-50 μM 48 h	Apoptosis	Concentration-dependent cell viability decrease. Induced apoptosis in a dose-dependent manner. Concentration-dependent decrease in AChE. Induced apoptosis via an ER-dependent pathway. [Ca2+] increased.	(Liu et al., 2009)

Chlorpyrifos (CPF)	Human neuroblastoma cell line SH-SY5Y	25, 50, 100 μM	Redox stress and mitochondrial dysfunction	Concentration-dependent ROS generation. Reduced mitochondrial membrane potential/ mitochondrial complex I in concentration -dependant fashion. ATP depletion.	(Park et al., 2017)
Chlorpyrifos (CPF)	Human neural stem cells	30,60,120 μM and 240 μM for 4 and 7 days	Apoptosis	Altered cellular morphology. Effect on the phenotypic specification. Irreversible condensation of chromatin.	(Sandoval et al., 2019)

2.3 Alcohol

Alcohol, also called ethanol, or ethyl alcohol, is a clear colourless liquid and is the principal ingredient in alcoholic beverages like beer, wine, or spirits. Alcohol readily dissolves in water and other organic compounds (Das and Vasudevan, 2007). Ethanol is the most common psychoactive drug, and drinking alcohol is an element of the social fabric of many western cultures. This small, uncharged, polar molecule can cross cell membranes by passive diffusion to reach the CNS via transport from the bloodstream (Shield et al., 2020, Abdel-Salam et al., 2018). There are serious health consequences that can arise from excessive alcohol usage in humans, with alcohol consumption high in many countries around the world (WHO, 2019). The relationship between alcohol and human health effects is complex and multidimensional but increases monotonically with consumption (Shield et al. 2020). According to the WHO, approximately half of the adult population in the world consume alcoholic beverages (Di Rocco et al., 2019). The number of global deaths attributed to the harmful use of alcohol was over 3 million in 2016, constituting 1 in 20 deaths. In terms of disability-adjusted life years (DALYs), over 5% of the global burden of disease is causally linked to alcohol usage (WHO, 2018).

2.3.1 Human alcohol exposure

People are exposed to alcohol mainly by ingestion. Harmful effects of alcohol drinking arise due to the pattern of drinking and the quantity of drinking (Brocardo et al., 2011). However, this can vary due to sex, body weight, and genetic makeup (Brady, 2014). Moderate alcohol drinking may have a beneficial effect on human health as discovered by some literature studies (Davies et al., 2002, Reynolds et al., 2003, Fillmore et al., 2007). According to the National Institute of Alcohol abuse and Alcoholism (NIAAA), 4 standard drinks on any

one of the days while not exceeding the 14 standard drinks (≈14 g pure alcohol according to NIAAA) for a week is considered as relatively low risk drinking for men, and for women, 3 standard drinks per day while not exceeding 7 standard drinks for a week. However, heavy drinkers lose their control over drinking behaviours and become a significant psychological, medical, and physiological state that they cannot live without alcohol called “alcohol dependency” (Brady, 2014). This is depending on individual desires and long-term persistence with alcohol as a drug. Alcohol dependency and low to moderate alcohol usage has been linked with more than 200 somatic disease and disorders including cancer (Rehm et al., 2017a). Several epidemiological studies done with humans established an association with disease development and problematic or hazardous use of alcohol or alcohol dependency (Brust, 2010). The impact of alcohol on humans depends on the blood alcohol concentration level (BAC) where BAC increases, cognitive abilities, psychomotor functions, vital physiological functions may change (Brady, 2014). Although chronic use of alcohol develops a tolerance to the effect of alcohol and the functional impact is dependent on the rate of intake, body weight, percentage of fat, and gender. Clinical manifestation develops in humans is largely dependent on the BAC level. For instance, 20-99 mg% showed loss of muscular functions while higher intoxications like 600-800 mg% are fatal. In England alone, over 10 million people drink alcohol at levels associated with increased risk of harms, with over 1 million annual alcohol-related hospital admissions, and close to 600,000 requiring treatment for alcohol dependence. Besides, the rate of alcohol metabolism has a direct link to the developing alcohol-associated diseases (Di Rocco et al., 2019).

2.3.2 Alcohol metabolism in humans

Alcohol is metabolised in the liver after the absorption through the gastrointestinal tract. 90% of alcohol is metabolised in the liver in humans (Di Rocco et al., 2019). Alcohol is converted to acetaldehyde by alcohol dehydrogenase and microsomal CYP450 2EI, 1A2, and 3A4 isoforms (Niemelä et al., 2000, Salmela et al., 1998). In the next step, acetaldehyde is metabolised to acetate through the catalytic action of acetaldehyde dehydrogenase (Figure 2-10). Finally, acetate is transformed into carbon dioxide and water and eliminated from the body. In addition to liver biotransformation, CYP450 2EI and catalase enzymes present in the brain convert alcohol to acetaldehyde. However, alcohol directly induces neurotoxicity and the metabolically generated acetaldehyde also plays a role in inducing neurotoxicity (Brocardo et al., 2011).

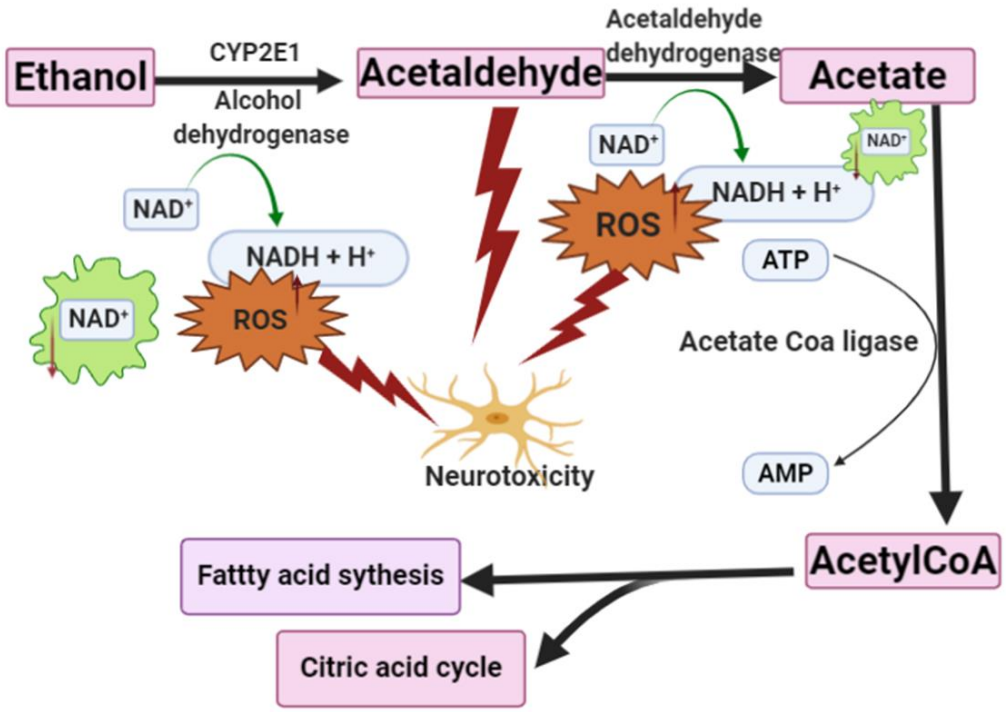


Figure 2-9: Main pathways of alcohol metabolism.

Additionally, it has been shown that heavy alcohol drinkers metabolize alcohol through peroxisomal activity. Here, the acetate generated by the acetaldehyde

metabolism converts to acetyl-CoA by the enzyme acetate-CoA-ligase and is dependent on ATP. Acetyl-CoA is then used in the TCA cycle or it is used in the synthesis of fatty acids or cholesterol (Das and Vasudevan, 2007) (Figure 2-10).

2.3.3 Alcohol neurotoxicity

Brain is the major target of alcohol intoxication of moderate or heavy drinkers. Studies have demonstrated alcohol is neurotoxic to neuronal cells in the brain (Harper, 2007). Alcohol Amnesic Syndrome is a condition associated with chronic heavy drinking, and the cause of short term memory loss, impairments of decision making, and deficits in motor skill leading to dementia (Harper, 2007). Alcohol-related dementia is also observed more in alcoholics than non-alcoholics, and causes long term memory loss (Smith and Atkinson, 1995). One study showed that heavy alcohol use is a contributing factor in 21-24% of cases of dementia. However, ethanolic dementia accounts for 10 % of all dementia (Gupta and Warner 2008, Harper, Kril and Daly 1987). Alcohol intoxication also causes brain trauma, and persistent alcohol-related brain injuries that can lead to Wernicke-Korsakoff Syndrome (WKS). Harper in 2007, 2009 has observed a reduction of brain weight and atrophy in alcoholic brains compared to non-drinkers (Harper 2009). WKS is another condition related to heavy alcohol drinking which shows characteristic brain swelling. Nutrition deficiencies of thiamine, nicotinic acid, other B vitamins, and folate often develop in alcoholics and are related to this condition (Serdaru et al., 1988). Damage to the frontal lobe of the brain is a serious condition in alcohol-related brain damages. Loss of critical thinking, incompetence of motor function, other emotional behaviours occur due to the alcohol effect on the frontal lobe of the brain. The cortex is also damaged from alcohol exposure and this has been widely reported in studies with humans and in animal models (Kubota et al., 2001, Dirksen et al., 2006).

Brain images have showed that alcohol exposure causes volume loss, brain shrinkage, and neuropathies compared to non-alcoholics in studies that have used alcoholic human brain and non-alcoholic *post-mortem* brains (Harper 2009). All these pathologies are linked to changes in neuronal structure and function. Neuronal cell loss has been observed in alcoholic brain slices (Crews and Nixon, 2009), neuronal cell injuries and functionality changes have also been observed in many studies (Harper et al., 1987, Erdozain et al., 2014, Crews and Nixon, 2009, Harper, 2007, Harper, 1998). Neuronal density decreased in the frontal cortex and 15–23% of cortical neurons were lowered in alcoholics (Harper, 1998, Pfefferbaum et al., 1997, Harper and Matsumoto, 2005). Alcohol intoxication affects neurotransmitter function in the nervous system such as dopamine, glutamate, and gaba-aminobutric acid (GABA) neurotransmitters, and this is also linked with many of the clinical manifestations related to alcohol (Davis and Wu, 2001).

2.3.4 Developmental neurotoxicity of alcohol

Alcohol is considered as a teratogen and its consumption during pregnancy affects the developing foetus. Even mild to moderate drinking of alcohol affects brain development and behavioural alterations in the foetus (Zhang, Hashimoto and Guizzetti 2018). Alcohol can directly affect the growing foetus or indirectly affect the foetus by altering the placental ability to provide nutritional support and impairing the mother's physiology, such as leading to malnutrition (Goodlett and Horn, 2001). Alcohol consumption is the third leading factor of premature birth in the world (Di Rocco et al., 2019). The severity of the effects depends on the gestational stage, the pattern of drinking, dose of ethanol consumed and age of the mother, hormonal level, and the genetic makeup of the mother (Abel and Hannigan, 1995, Gil-Mohapel et al., 2010). Several epidemiological studies in humans and experiments with animal models have shown that alcohol

consumption during pregnancy causes severe CNS developmental defects (Zhang et al., 2018). The broad spectrum of this teratogenicity is known as Foetal Alcohol Syndrome Disorders (FASD) which encompass a variety of pathological conditions depending upon the gestation period and consumption (Warren et al., 2011). The FASD includes alcohol-related birth defects (Burd and Martsolf, 1989), alcohol-related neurological disorders (May et al., 2009), and foetal alcohol syndrome (FAS) (Warren, Hewitt and Thomas 2011). FAS is attributed to craniofacial dysmorphologies, growth retardation, and CNS impairments, which is the condition caused from *in utero* alcohol exposure (Warren, Hewitt and Thomas 2011). All these deficits cause structural and functional damages to the brain (Ikonomidou et al., 2000, Roebuck et al., 1998, West et al., 1994). Furthermore, it has been shown that CNS dysfunction of the growing foetus increases with the increasing alcohol dose and exposure time (Zhang, Hashimoto and Guizzetti 2018). Children who display FASD show brain structure abnormalities which is attributed to behavioural and cognitive deficits (McGee and Riley, 2006). Their brain size, shape, symmetry and decreased volumes of grey and white matter have been recorded as alterations due to exposure, as revealed by MRI (McGee and Riley, 2006, Petrenko and Riley, 2006). Autopsies of infants heavily exposed to alcohol showed microcephaly, effects on neuronal migration, basal ganglia, brain stem, and cerebellar anomalies which is a severe form of FAS, and they are very unlikely to survive. Alcohol effects on neurogenesis, cell migration, cell adhesion, neuron survival, axon outgrowth, synapse formation, and neurotransmitter function have all been reported for the developing brain even at mild exposures (Goodlett and Horn, 2001).

Alcohol effects on the growing brain is complex, and certain group of cells change their functions, and other group of cells are depleted depending on the

growing stage of the cells and the BAC of the mother (Goodlett and Horn, 2001, West et al., 1990). This suggests functionality changes in remaining cells may affect the development of neurotoxicity symptoms or other clinical manifestation related to FAS in children. Different mechanisms cause consequences of alcohol exposure in cells depending on the stage of cell development. For instance, cells are more vulnerable to alcohol damages during differentiation rather than in within the undifferentiated stage. Collectively, this suggests that the cytotoxicity is dependent upon multiple mechanisms that operate simultaneously and sequentially over time to develop FASD (Goodlett and Horn, 2001).

2.3.5 Role of oxidative stress in alcohol-induced neurotoxicity

Several cytotoxic mechanisms of alcohol exposure have been documented in the literature. Neurotoxicity studies done with alcohol *in vitro* demonstrated that the key mechanism behind the cytotoxicity of alcohol is triggering apoptosis (Das et al., 2011, Balaszczuk et al., 2011, von Haefen et al., 2011, Sari et al., 2012). However, signalling mechanisms that induced apoptosis in neuronal cells upon alcohol exposure remain unclear. Molecular-level studies suggest cellular apoptosis by both intrinsic and/or extrinsic pathways. Several agents including caspase 3, and caspase 9 have been recorded as mediators of apoptosis in neuronal cells highlighting the intrinsic pathway (Haorah et al., 2008). Few studies using human neuronal cells showed that death receptor kinases are involved in the signalling mechanism to induce the extrinsic apoptotic pathway (Moon et al., 2013). Numerous pathways can induce neuronal apoptosis by a direct effect of alcohol including mitochondrial dysfunction, disruption of normal calcium level, and oxidative stress (Table 2.2). This has been demonstrated in both animal and human cell models. Other than apoptosis, some studies emphasise necrosis as a mechanism of cell

dysfunction and cell death due to the direct effect of alcohol on neuronal cells. However, alcohol-related neurotoxicity in adults and development neurotoxicity in the foetus, infants, and young children, and the clinical manifestations and disorders, are related to the functionality changes of neuronal cells due to the above mentioned molecular mechanisms (Donadoni et al., 2019).

Oxidative stress plays a vital role in cytotoxicity induced by alcohol. Numerous studies have been shown an increase of oxidative markers such as products of lipid peroxidation, proteins adduct, oxidative markers on DNA damage, and alterations of cellular antioxidants upon exposure of alcohol in both animal models and *in vitro* studies (Das and Vasudevan, 2007, Hernández et al., 2016).

Alcohol induces ROS during its metabolism. The biotransformation of alcohol by alcohol dehydrogenase, microsomal ethanol oxidation system (MEOS), and catalase induce ROS which affects the antioxidant system in cells (Zimatkin et al., 2006). The generated NADH molecule utilised in the respiratory (electron transport) chain yields ROS (Xu et al., 2005). The resultant acetaldehyde also forms adducts with cellular lipids, proteins, and nucleic acids (Das and Vasudevan, 2007) (Figure 2-9).

The CYP450 2EI leads to an increase of hydroxyl radicals which can then trigger lipid peroxidation. Catalase conversion also generate ROS in brain cells due to increased activity of the respiratory chain (Das and Vasudevan 2007). However, the direct generation of ROS due to mitochondrial dysregulation has also been suggested by Chu et al 2007 in immature neurons (Chu et al., 2007). This evidence is further supported by experiments that used cerebral tissue of rat foetuses, that ethanol exposure reduces mitochondrial volume, proliferation, as well as alters respiratory chain complexes, and thus results in reduced cellular ATP production (Liu et al., 2014). This can lead to an imbalance of Ca^{2+} levels in cells, which can interfere with the cell neurotransmission process, and a

higher level of Ca^{2+} is toxic to neuronal cells (Goodlett and Horn, 2001). Oxidative stress induced by alcohol exposure causes cellular morphological changes like cell shrinkage due to loss of cell structural rigidity. DNA fragmentation was also observed in some studies after exposing cells to alcohol (Goodlett and Horn, 2001) (Figure 2-8).

Several lines of evidence showed that the underlying mechanism of FASD is oxidative stress (Brocardo et al., 2011). However, most of the evidence from rat models showed indirect involvement of ROS in disease development. These studies showed an increase of oxidative damage markers of lipids, proteins (Marino et al., 2004), and DNA (Shirpoor et al., 2009) as well as imbalances of the antioxidant system (Shirpoor et al., 2009). Oxidative stress has been demonstrated in several brain regions of rodent brain and effects that arose from ethanol are long-lasting and induce memory deficits (Dong et al., 2010), and neuronal cell death (Ramachandran et al., 2001). However, the involvement of oxidative stress in cell death has only been recorded in a few studies using human neuronal cell models (Wang et al. 2015a).

Table 2-2: Summary of published literature on ethanol effect on human neuronal cells and neurospheres

Cell type	Treatments	Cytotoxicity mechanism	Major findings	Reference
Primary cortical neurons (Foetal brain)	17.5 mM EtOH /ACh	Oxidative stress	3-fold induction of CYP2E1 activity after EtOH treatment. ROS and nitric oxide (NO) generated via induction of NADPH/xanthine oxidase (NOX/XOX) and nitric oxide synthase (NOS). Marked increase in the lipid peroxidation product (4-hydroxy-2-nonenal).	(Haorah et al., 2008)
Human neuroblastoma cells	100, 300, 500 and 700 mM 24 h	Apoptosis	Reduced cell viability and increase LDH release in a concentration-dependent manner. Decrease intracellular ATP production in a concentration-dependent manner. Reduced mitochondrial respiration.	(Liu et al., 2014)
Human neuroblastoma SK-N-SH cells	100 mM ethanol for one to three days	Apoptosis	Ethanol-induced changes in lipid metabolism.	(Saito et al., 2005)
iPS cellular model	70 mM for 24 h or 7 days	Inflammasome pathway	Increase of microtubule-associated proteins. No effect on cell proliferation. Impairment of the mitochondrial and lysosomal distribution.	(De Filippis et al., 2016)
Human embryonic stem cell (hESC)-derived cortical neurons	50 mM 7 days exposure followed by a 24-hour ethanol withdrawal treatment	-	MDA receptor genes, play an important role in regulating neuronal function and mediating chronic alcohol consumption-induced neuroadaptations. Induced DNA methylation and correlated gene expression changes.	(Xiang et al., 2015)

Human foetal neuron cultures and neurospheres (hNSPs)	0, 10, 25, 50, and 75 mM for 6, 24, and 48 h	Apoptosis	Concentration-dependent cell viability loss. Immature neurones are highly sensitive to ethanol than mature neurones. EtOH-mediated pre-mRN splicing of antiapoptotic Mcl-1L isoform.	(Donadoni et al., 2019)
SH-SY5Y cells and cultured primary cortical neurons	50 mM 2 h and 24 h	Inflammasome signalling	NOX2 subunits increased the activation of NLRP1 inflammasome. Ethanol-induced HMGB1 release was oxidative stress-dependent. Time-dependent increase in ROS generation.	(Wang et al., 2015a)
Human neuroblastoma cells SH-SY5Y	0.4% (400 mg/dl) 0.5,1,3,6,12 and 24h	Oxidative stress	Duration-dependent increase in NADPH oxidase activity. NOX is an important mediator of ethanol-induced ROS generation.	(Wang et al., 2012a)
SH-SY5Y cells	50 and 100 mM for 48 h	Apoptosis	Increased cleaved caspase 3 expression. PKA pathway is required to increase Sim2 in response to ethanol.	(Wang et al., 2015b)
Human embryonic carcinoma (NCCIT) cells	50 mM for 48 h	-	EtOH-mediated transcriptional alterations. Transcription alteration in differentiating cells.	(Mandal et al., 2018)
Human neural stem cells (NSC)	0.1-10 mM 12 hrs and 12 days	Apoptosis	Colony-forming ability NSC was completely inhibited by 5 mM EtOH treatment. Protein kinase C (PKC) mediate the susceptibility of NSC to EtOH.	(Hao et al., 2003)
Human embryoid bodies Neural progenitors Mature neurones	0%, 0.1% or 0.3% 4 days	Apoptosis	Significant changes to the metabolome profile of human embryoid bodies, neural progenitors, and neurons.	(Palmer et al., 2012)

Human glioblastoma U-118 MG and Neuroblastoma SH-SY5Y	75 mM for 48 hours	Apoptosis	Ethanol-elicited nuclear GAPDH augments TIEG2-mediated Monoamine Oxidase B Cascade cause cell damage.	(Ou et al., 2010)
Neurospheres from Neural progenitor cells	0, 1, 10 or 100 mM 72 h	-	ETOH dose-dependently increased the diameter of neurospheres. No significant increase in apoptosis in cultures after 72 hours ETOH exposure. Cell cycle progression was not significantly stimulated by ETOH at any of the doses.	(Vangipuram et al., 2008)
Neuroblastoma SH-SY5Y	50–500 mM 24 h	Apoptosis	Concentration above 100 mM induced apoptosis in cells. Concentration-dependent toxicity in cells. Induced AChE in concentration-dependent manner.	(Sun et al., 2017)

2.4 Oxidative stress induced protein carbonylation

Protein oxidation by ROS occurs as irreversible or reversible modifications. One of the irreversible mechanisms of protein oxidation is protein carbonylation. Protein carbonylation is an irreversible, non-enzymatic metal-catalysed modification of proteins (Dalle-Donne et al. 2006, Suzuki, Carini and Butterfield 2010). ROS can directly or indirectly oxidise proteins. Direct oxidation of proteins by ROS produces highly reactive carbonyl derivatives by introducing carboxyl groups to protein side chains including prolines, arginine, lysine, and threonine known as “primary protein carbonylation” (Stadtman 1990). Indirect protein carbonylation occurs by the reaction of ROS with conjugated sugars and lipids generating products which are reactive carbonyl species (RCS) including secondary products of carbonylated primary amino lysine residues, subsequently oxidised glycation end products, and lipid peroxidation products such as malondialdehyde (MDA) known as “secondary protein carbonylation” (Esterbauer, Schaur and Zollner 1991, Uchida and Stadtman 1999). Notably, both ways of carbonylation change protein structure and function.

Primary protein carbonylation is also generated via cleavage of peptide bonds by the α-amination pathway or glutamyl oxidative modification pathway, which is the most common type of protein carbonylation in cells (Uchida and Stadtman 1999). Primary carbonylated products can be reacted with 2,4-dinitrophenylhydrazine (DNPH) to form hydrazones which can be readily detected as oxidative stress and protein oxidation markers which reflect cellular damages induced by ROS (Butterfield and Stadtman, 1997, Levine, 2002, Stadtman and Levine, 2000). However, oxidatively modifies proteins are not repaired and cells remove them through proteolytic degradation by the proteasome. A decrease in proteolytic degradation of carbonylated proteins in cells accumulates the modified proteins leading to “carbonyl stress” which can

be detrimental to cells. The degree of protein carbonylation is dependent on the relative availability of proteins, the proximity of protein to the site of ROS generated due to their short life (10^{-9} s for hydroxyl radicals, 10^{-6} s for superoxide, 10^{-3} s for peroxynitrite, 100 s peroxyl radicals and 102 s for hydrogen peroxide) (Reth, 2002) and the presence of the metal binding site in the protein which is the key factor to vulnerability to the protein carbonylation. Other than that, molecular conformation and availability of amino acid residues make the protein a candidate for the reaction.

Cytoskeleton proteins are vulnerable to ROS induced carbonylation as a common target. For instance, 4-2 HNE forms Michael adducts with tubulins, causes microtubule assembly loss, blocking neurite outgrowth in neuroblastoma cells (Neely et al., 1999) and PC12 cells after H_2O_2 exposure (Zhang et al., 2016). The intermediate filament is a target of protein carbonylation as explained by Wataya and colleagues (Wataya et al., 2002), oxidation of neurofilament heavy chain, and microfilaments as actin are carbonylated as shown in *in vitro* and *in vivo* studies (Dalle-Donne et al., 2001, Aldini et al., 2005). Furthermore, protein carbonyls produce lipid peroxidation by-products like HNE adducts, and can result in a loss of protein function (Dalle-Donne et al., 2006, Smerjac and Bizzozero, 2008).

Carbonylated protein has been shown to have a great impact upon general cell functioning. The ROS induced carbonylation effect on protein folding (Wilson and Easterbrook-Smith, 2000), and proteolytic protein degradation process (Grune et al., 2004, Butterfield and Perluigi, 2017), plays a role in early events of cell dysfunction and cell functionality loss. Carbonylated proteins in cell-induced apoptosis act as signals for caspase activation, cytochrome c release, and elevation of p53 expression in cells by interfering with cell signalling pathways (Ding and Keller, 2001). Also, carbonylated proteins are involved in

DNA fragmentation and DNA laddering in both neuronal and glial cells (Ding and Keller, 2001). Aggregation of high molecular weight carbonylated proteins which are not degraded, are toxic to the cell and fast-track apoptosis. Indeed, protein carbonylation is regarded as one of the key factors that could contribute to neurodegeneration (Dalle-Donne et al., 2006).

OP pesticide exposure induced oxidative stress and mediated protein carbonylation has been recorded in a few *in vitro* and *in vivo* studies. Chlorpyrifos at 100 µM concentration induced protein carbonylation as detected by DNPH derivatization spectrophotometric assay and authors stated that CPF induced ROS and lipid peroxidation by-products of MDA induced protein carbonylation in SH-SY5Y cells (de Oliveira et al. 2016).

Previous neurotoxicity studies have contextualized the implications of protein alterations in neurogenesis and cognitive functioning, particularly βIII-tubulin expression, a neuronal cytoskeleton protein necessary for correct guidance and migration of NPCs and correlates with the earlier stages of neuronal differentiation. Therefore, ethanol reduced the expression of βIII tubulin in differentiating neural cells on a proteomic level, implying ethanol's post-translational modifications on βIII tubulin (Maxi et al., 2016). Associations with a disorganised cytoskeletal architecture, loss in neurite outgrowth, and dendritic connections were also observed, bridging the protein dynamics and the morphological brain deficits, relevant to FAS (Labisso et al., 2018). *In vivo* studies involving subcutaneous administration of ethanol to pregnant mice during the last trimester (gestational days 16-17) and harvesting the foetuses following 24 hours of ethanol exposure, demonstrated a sharp increase in foetal brain carbonyl content, while the ethanol-exposed maternal brain was resistant to protein oxidation (Akhtar et al., 2017). Thereby, demonstrating the oxidative protein damage elicited by acute alcohol exposure and highlighting the foetuses'

increased susceptibility to alcohol toxicity during the neurodevelopmental window of vulnerability.

2.5 The use of *in vitro* human cell models for assessment of organophosphate, carbamate, and alcohol neurotoxicity

Human cell models are widely use in neurotoxicity studies over the traditional paradigms of animal and animal-derived cell models due to the species differences. Recently human neuroblastoma cells: SH-SY5Y, SH-N-SH, IMR-32, LA-N-5, and human embryonal carcinoma cells NT2, human embryonic neural stem cell models, such as human neuronal stem cell, immortalised human neuronal cortical stem cells (ReNcell CX), human cortical ventricle neuronal cells (ReNcell VM) have been used as cell lines. However, primary neuronal cells have also used for the studies including brain-derived neuronal cells, human embryonic neural stem cells. The use of commercial cell lines for neurotoxicity studies is more advantageous over the use of primary cell lines. Maintaining primary cell lines is more expensive than maintaining commercial cell lines, and it is challenging to obtain and requires ethical approvals. Although they are more relevant to human neuronal cells which are physiologically and biologically similar to human conditions. The later explained embryonic stem cell models provide an opportunity to study neurodevelopmental toxicity while homogenous cell lines are used to study single-cell studies that are relevant to human molecular pathways (Heusinkveld and Westerink, 2017).

A cell line which is developed from human tissues can be maintained in culture media for an extended period and these cell lines provide a homogeneous population of cells, easy to obtain and that can stored in liquid nitrogen indefinitely, are easy to maintain in plastic culture ware and rapidly proliferate to give a larger number of cells and can be easily passaged to get cells as required. Also, they can be differentiated readily using growth factors, or

removal of serum from media (Radio and Mundy, 2008). Opposed to these benefits, intrinsic limitations such as diminished metabolic capability, lack of cell to cell interaction representing the CNS are limitations of cell lines. However, *in vitro* studies have generally focused on mechanisms of toxicity of neurotoxicant than the protection of hazard outcomes as in human involved experiments (Heusinkveld and Westerink, 2017).

2.5.1 Human neuroblastoma SH-SY5Y cells

According to the literature, human neuroblastoma SH-SY5Y cells are widely used for mechanistic *in vitro* studies to investigate OP and carbamate pesticide neurotoxicity (Table 2-1). SH-SY5Y cells are derived from SK-N-SH which originated from a metastatic biopsy. SH-SY5Y is the last subclone of this parental line, which is was first subcloned to SH-SY, then to SH-SY5, and then to SH-SY5Y which was deposited as a cell line by Biedler in 1983. SH-SY5Y cells can be grown using *in vitro* conditions and yield both neuroblastomas like cells and epithelial cells which are then classified as “N” type and “S” type by Encinas et al. (2000). Neuroblastoma like cells are more neuronal-like and positive for tyrosine hydroxylase (TH) and dopamine-β-hydroxylase while epithelial cells lack enzymatic activities (Biedler et al., 1978). Cells can be differentiated to get more neuronal-like cells by all-*trans*-retinoic acid (RA) by manipulating the culture medium serum levels (Encinas et al., 2000, Kovalevich and Langford, 2013) in a cost-effective way. Differentiation of SH-SY5Y yields a homogenous population of neuronal-like cells and is a great advantage over the other cell lines (Ross et al., 1983). Serum withdrawal results in differentiated cells that extend neurites with morphological characteristics like neuronal cells and are suitable to study effects of neurotoxins for neuronal differentiation. Undifferentiated cells are more neuroblast like and have proliferative ability with polarized cell bodies and truncated processes and mimic the immature neuronal

stages (Lopes et al., 2010). Differentiation of SH-SY5Y yields a more cholinergic neuron phenotype containing long processes/neurites, neuronal-specific enolase positive, with functioning synapses, formation of synaptophysin, neuronal-specific neurotransmitter production, and produce enzymes and neuronal makers including βIII tubulin (Cheung et al., 2009). However, discrepancies between the neuronal-like phenotype and effect of culture maintained for a longer time yields variations of N and S type cells, but this has been answered by Encinas et al. (2000), that showed that the addition of 50 ng/ml brain-derived growth factor (BDNF) mitigated this problem (Encinas et al., 2000). RA and BDNF treated differentiated cells displayed a marked difference in expressing AChE than undifferentiated cells (Goldie et al., 2014). All these factors have justified the suitability of SH-SY5Y cells for neurotoxicity evaluation studies, using both undifferentiated and differentiated cells to mimic single cell effects of immature and mature neuronal stages in humans.

2.5.2 Human progenitor cortical neuronal cells (ReNcell CX)

The ReNcell CX cell line was isolated by the ReNeuron group (Guildford, UK). The cell line is commercially available by Merk Millipore and has the ability of self-renewal and differentiation to produce co-cultures of neuronal and glial cell types including oligodendrocytes and astrocytes (Chalmers-Redman et al., 1997, Donato et al., 2007). The cell line has been immortalized by retroviral transduction of the c-*myc* oncogene to produced unlimited clonal human progenitor cortical neuronal stem cells and maintain the attributes of original cells (Dang et al., 1999, Villa et al., 2004). ReNcell CX showed cobblestone-like growth behaviour in laminin-coated culture ware surfaces with growth factors and can maintain its normal diploid karyotype even after long passages. After differentiation, cells are more likely a rounded shape with long processes and specified to three cell lineages in CNS including neurons, astrocytes, and

oligodendrocytes. Therefore, ReNcell CX can be used to study the early neurodevelopmental processes such as proliferation, migration, differentiation, and apoptosis being a more relevant model to study human-related toxicity studies in developmental neurotoxicity (Radio and Mundy, 2008, Bal-Price et al., 2010). Hence, this avoids the interspecies extrapolation of results and represents spacial and temporal coordination of glial cells in neuronal toxicity as in the CNS.

3 MATERIAL AND METHODS

3.1 Materials

3.1.1 Reagents used for the study

All reagents used for the cell culture and other experiments are listed in Table 3-1 and 3-2 which were of the highest analytical grade available.

Table 3-1: Reagents used for the cell culture

Reagent	Product Number	Supplier	Storage Conditions
Minimum Essential Medium Eagle (EMEM)	M4655	Sigma-Aldrich Poole, UK	2°C to 8°C
F12 Nut mix (Ham) (1X)	217650-29	Life Technologies, Paisley, UK	2°C to 8°C
Heat inactivated Foetal Bovine Serum (FBS) Non-USA origin	F9665	Sigma-Aldrich Poole, UK	-5°C to -20°C
Penicillin/ streptomycin (Penicillin 10,000 units/ml streptomycin 10 mg /ml)	P4333	Sigma-Aldrich Poole, UK	-5°C to -20°C
Non-Essential Amino Acid Solution (NEAA) (100X), without L-Glutamine	M7145	Sigma-Aldrich Poole, UK	2°C to 8°C
L-Glutamine (100x)	01077	Life Technologies, Paisley, UK	-5°C to -20°C
Hanks' Balanced Salt Solution (HBSS) (1X)	14170088	Life Technologies, Paisley, UK	15°C to 30° C
Trypsin-EDTA (0.05%), phenol red	25300062	Life technologies, Paisley, UK	-5°C to -20°C
Poly-D-lysine Hydrobromide	P6407	Sigma-Aldrich Missouri, USA	-20°C
Brain-Derived Neurotrophic Factor human (BDNF)	B3795	Sigma-Aldrich Missouri, USA	-20°C
All-*trans*-retinoic acid (RA)	R2625	Sigma-Aldrich Missouri, USA	-20°C
Phosphate Buffered Saline (PBS pH 7.4 (1X)	10010-015	Life Technologies, Paisley, UK	15°C to 30° C
99% IMS	32221	Scientific Laboratory Supplies, Nottingham, UK	18°C to 25° C

ReNcell CX NSC maintenance medium	SCM005	EMD Millipore Cooperation, Temecula, USA	-20°C until ready to use. Upon thawing, the maintenance medium should be stored at 2-8°C
ReNcell CX NSC freezing medium	SCM007	EMD Millipore Cooperation, Temecula, USA	-20^{o}C
Basic fibroblast growth factor (bFGF) Specific activity ≥ 2x10^{6} units/mg	GF003	EMD Millipore Cooperation, Temecula, USA	-20°C
Epidermal growth factor (EGF) Specific activity ≥1x10^{7} units/mg	GF001	EMD Millipore Cooperation, Temecula, USA	-20°C
Laminin	CC095	EMD Millipore Cooperation, Temecula, USA	20°C
DMEM/F12 1:1 w/o HEPES, 2.5 mM w/ L-Glutamine	DF-042-B	EMD Millipore Cooperation, Temecula, USA	2° to 8°C, away from light
Accutase™	SCR005	EMD Millipore Cooperation, Temecula, USA	-20°C After thawing can be stored for up to 2 months at 4°C
Dimethyl sulphoxide (DMSO) for cell culture	BP231100	FisherScientific	Room temperature
Trypan blue	T10282	FisherScientific	18°C to 25° C

Table 3-2: List of other reagents and materials

Reagents	Code No	Supplier	Storage Conditions
(3-(4,5-Dimethylthiazol-2-yl)-2,5-Diphenyltetrazolium Bromide) (MTT)	M5655	Sigma-Aldrich Poole, UK	Room temperature, storage of reconstituted MTT solution at 2-8°C (protected from light)
Dimethyl sulphoxide (DMSO)	D8418	Sigma-Aldrich Poole, UK	Room temperature
2-propanol	279544	Sigma-Aldrich Poole, UK	Room temperature
Ethylenediaminetetraacetic acid disodium salt dehydrate (EDTA)	E5134	Sigma-Aldrich Poole, UK	Room temperature
Tris base	T1503	Sigma-Aldrich Poole, UK	Room temperature
2′,7′-Dichlorofluorescin diacetate (DCFDA)	D6883	Sigma-Aldrich Poole, UK	−20°C
Hanks' Balanced Salt solution (Modified, with sodium bicarbonate, without phenol red, liquid, sterile-filtered, suitable for cell culture)	H8264	Sigma-Aldrich Poole, UK	2°C to 8°C
N-Acetyl-L-cysteine	A9165	Sigma-Aldrich Poole, UK	2°C to 8°C
Hydrogen Peroxide (H_2O_2)	H1009	Sigma-Aldrich Poole, UK	2°C to 8°C
Potassium dihydrogen phosphate	P5655	Sigma-Aldrich Poole, UK	Room temperature
Potassium phosphate dibasic	P8281	Sigma-Aldrich Poole, UK	Room temperature
Triton™ X-100	T9284	Sigma-Aldrich Poole, UK	Room temperature
Acetylthiocholine iodide (ACTI)	A5751	Sigma-Aldrich Poole, UK	2°C to 8°C
5,5'-Dithiobis-(2-Nitrobenzoic Acid) DTNB	D8130	Sigma-Aldrich Poole, UK	Room temperature
Radioimmunoprecipitation assay Lysis Buffer, 10X	20-188	EMD Millipore Cooperation, Temecula, USA	Room temperature
Phosphatase inhibitors	P0044	Sigma-Aldrich Poole, UK	2°C to 8°C
Protease inhibitor cocktail tablets	0469312400	Roche, Germany	2°C to 8°C

Bovine Serum Albumin standards (2 mg/ mL)	500-0206	Bio-Rad Laboratories Ltd, Hertfordshire, UK	4°C
MOPS (20X)	NP0002-02	Invitrogen™ Novex™, Life technologies, Paisley, UK	4°C to 25°C.
NuPAGE™ Sample Reducing Agent (10X)	NP0009	Invitrogen™ Novex™, Life technologies, Paisley, UK	4°C
NuPAGE™ LDS Sample Buffer (4X)	NP0007	Invitrogen™ Novex™, Life technologies, Paisley, UK	4°C to 25°C
NuPAGE™ Antioxidant	NP0005	Invitrogen™ Novex™, Life technologies, Paisley, UK	4°C
Glycine	G8898	Sigma-Alrich Poole, UK	Room temperature
Methanol	M/4056/17	ThermoFisher Scientific, Loughborough, UK	Room temperature
Acetic acid	200-580-7	Scientific Laboratory Supplies, Nottingham, UK	Room temperature
2-Mercaptoethanol	M7154	Sigma-Aldrich Poole, UK	Room temperature
TWEEN® 20	P1379	Sigma-Aldrich Poole, UK	Room temperature
Marvel Original Dried Skimmed Milk		Premier Foods, Thame, UK	Room temperature
Bovine Serum Albumin powder	A7906	Sigma-Aldrich Poole, UK	2°C to 8°C
2,4-Dinitrophenylhydrazine (DNPH)	D199303	Sigma-Aldrich Poole, UK	Room temperature (Protected from light)
Glycerol	G5516	Sigma-Aldrich Poole, UK	Room temperature
5N HCL	231-5957	ThermoFisher Scientific, Loughborough, UK	Room temperature
Trichloroacetic acid solution (TCA)	T0699	Sigma-Aldrich Poole, UK	Room temperature
Diethyl ether	676845	Sigma-Aldrich Poole, UK	Room temperature

Guanidine hydrochloride	50950	Sigma-Aldrich Poole, UK	Room temperature
Ethyl acetate	270989	Sigma-Aldrich Poole, UK	Room temperature
Sodium dodecyl sulfate (SDS)	L3771	Sigma-Aldrich Poole, UK	Room temperature
Ammonium persulfate (APS)	A3678	Sigma-Aldrich Poole, UK	Room temperature
DL-Dithiothreitol (DTT)	D9779	Sigma-Aldrich Poole, UK	2°C to 8°C
DC™ Protein Assay Reagent A	500-0113	Bio-Rad Laboratories Ltd, Hertfordshire, UK	Room temperature
DC™ Protein Assay Reagent B	500-0114	Bio-Rad Laboratories Ltd, Hertfordshire, UK	Room temperature
PBS Phosphate buffered saline tablet	P4417	Sigma-Aldrich Poole, UK	Room temperature
Sodium chloride	S9888	Sigma-Aldrich Poole, UK	Room temperature
Sodium phosphate dibasic	S3264	Sigma-Aldrich Poole, UK	Room temperature
Potassium chloride	P9541	Sigma-Aldrich Poole, UK	Room temperature
Clarity™ Western ECL Substrate Luminol/enhancer peroxide solution Clarity Western Peroxide Reagent	170-5061	Bio-Rad Laboratories Ltd, Hertfordshire, UK	Room temperature
Pierce™ Reversible Protein Stain Kit for PVDF Membranes	24585	ThermoFisher Scientific, Loughborough, UK	Room temperature
Immobilon-PSQ Membrane, PVDF	ISEQ85R	EMD Millipore Cooperation, Temecula, USA	Room temperature
Page ruler prestained protein ladder	26619	ThermoFisher Scientific	-20°C
Prestained protein molecular weight marker	26612	ThermoFisher Scientific	-20°C
βIII tubulin antibody	MAB1637	Merk Millipore	-20°C
βII tubulin antibody	sc-55529	Santa Cruz Biotechnology	-4°C
Anti-GAPDH antibody	ab181602	Abcam, UK	-4°C
Polyclonal goat Anti Rabbit IgG (HRP)	P0448	DAKO-Cytomation, Denmark	-4°C

Polyclonal goat Anti Rabbit IgG (HRP)	P0447	DAKO-Cytomation, Denmark	-4^{o}C

All sterile culture plastic ware were supplied by Scientific Laboratory Supplies (Nottingham, UK) was used unless specified in Table 3-3.

Table 3-3: Plastic culture ware used for the study

Plasticware	Catalog Number	Supplier
Vented cap, Angled neck T25 flasks	130189	ThermoFisher Scientific, Rochester, UK
Vented cap, Angled neck T75 flasks	130190	ThermoFisher Scientific, Rochester, UK
Vented cap, Angled neck T125 flasks	130191	ThermoFisher Scientific, Rochester, UK
Sterile, clear bottom, tissue culture treated 96 well plates	167425	ThermoFisher Scientific, Rochester, UK
Sterile, clear bottom, tissue culture treated 24 well plates	662940	Greiner Bio-One North America Inc. USA
Sterile, clear bottom, tissue culture treated 12 well plates	CC682-7512	STARLAB International GmbH, Hamburg, Germany
Sterile, clear bottom, tissue culture treated 6 well plates	CC7682-7506	STARLAB International GmbH, Hamburg, Germany
Corning® 96 Well Poly-D-Lysine Treated Microplate	CLS3842-100EA	Sigma, Poole, UK
Sterile, clear bottom, tissue culture treated black 96 well plates	165305	ThermoFisher Scientific Rochester, UK

All other materials required for cell culture were purchased from Scientific Laboratory Supplies including disposable pipettes, and 15 ml and 50 ml falcon tubes.

3.1.2 Test compounds

Azamethiphos-oxon (AZO) (S-6-Chloro-2, 3–dihydro-2-oxo-1, 3-oxazolo (4, 5b) pyridine-3-ylmethyl O,O-dimethyl, $C_9H_{10}ClN_2O_5PS$) was purchased (10340000, Dr, Ehrenstorfer-Schafers) with purity at 95-99.5%, Chlorpyrifos–oxon (CPO) (Diethyl-,5,6-trichloro-2-pyridinyl phosphate, $C_9H_{11}C_{l3}NO_4P$), purity at 97.2-99.1% and Aldicarb (2-Methyl-2-(methylthio) propanalaldehyde O-(methylcarbamoyl) oxime, $C_7H_{14}N_2O_2S$ from chem service Inc. (West Chester, PA, USA) were supplied by Greyhound Chromatography, Birkenhead, UK and

used for pesticide treatments. 99.5% pure ethyl alcohol (459844, Sigma) was used for alcohol treatments.

3.1.3 Cell lines used for the study

The SH-SY5Y cell line is derived from the original cell line, called SK-N-SH, from which it was subcloned and isolated from a bone marrow biopsy taken from a four-year-old female with neuroblastoma. SH-SY5Y cells are often used as an *in vitro* model of neuronal function and differentiation studies, and these cells were obtained from the European Collection of Authenticated Cell Culture (ECACC) (ECACC-94030304) for the current study.

Immortalized human cortical neural progenitor stem cells (hNPCs) (ReNcell CX) (SCC007) derived from cortical brain tissue of a 14-week gestating foetus following normal terminations and following nationally UK approved ethical and legal guidelines were obtained from EMD Millipore Cooperation, UK.

3.1.4 Brain samples used for the study

The human brain samples used in this study were supplied by the Neuropsychopharmacology Research Group from the Department of Pharmacology of the University of the Basque Country (UPV/EHU). (https://www.ehu.eus/en/web/neuropsicofarmacologia/home). Brain collection is registered in the National Biobank Register of the Spanish Health Department with the number C.0000035. Six control brain samples were used, matched by age and sex, to 6 alcoholic subjects, as detailed in previous studies (Erdozain et al., 2014, Labisso et al., 2018a) (refer to Annexure1; Table 3). Brain collection was conducted in compliance with policies of research and ethical review boards for *post-mortem* brain studies (Basque Institute of Legal Medicine, Bilbao, Spain) and tissues were regulated, handle and stored according to the

human tissue act 2004 (HTA). The diagnosis of alcoholism was carried out according to the Diagnostic and Statistical Manual of Mental Disorders (DSM-III-R, DSM-IV or DSM-IV-TR; American Psychiatric Association) or International Classification of Diseases criteria (ICD-10; World Health Organization). All diagnoses were established by clinicians in charge of the patients before death. The brain samples used were all from the prefrontal cortex (Brodmann's area 9) (BA 9), macroscopically dissected at the time of autopsy, and immediately stored at -70ºC until utilised.

3.2 Methodology

3.2.1 SH-SY5Y cell culture

3.2.1.1 *SH-SY5Y culture media preparation*

SH-SY5Y cells were grown in a culture medium prepared from using 43.5% Eagle's Minimum Essential Medium supplemented with 43.5% Ham's F12 nutrient mix, 10% heat-inactivated Foetal Bovine Serum (FBS),1% MEM Non-Essential Amino Acid Solution (NEAA), 2 mM glutamine and 1% penicillin-streptomycin solution containing 10,000 IU penicillium and 10 mg/ml streptomycin (p/s) in autoclaved sterile Durham bottles.

3.2.1.2 *SH-SY5Y resuscitation from liquid nitrogen storage*

When it was required for experiments, a frozen vial of passage 12 was obtained from liquid nitrogen storage, wiped with 70% IMS, and thawed quickly by incubation in a 37ºC water bath for 2 minutes. The outside of the vial was wiped with 70% IMS and the content was transferred to a pre-warmed culture media and centrifuged to get rid of any cryopreserved media by spinning at 800 rpm for 5 minutes. The resultant supernatant was removed, and cell pellets were resuspended in 1 ml of pre-warmed culture media and mixed thoroughly with a sterile plastic pipette before transferring into T75 flasks containing 14 ml of

culture media. Cells were maintained at 37ºC with an atmosphere of 5% CO_2 and 95% humidity for 24 hours. The medium was changed every other day until cell growth reached 80% confluency and passaged as needed or cryopreserved.

3.2.1.3 *SH-SY5Y cell culture*

Cell culture was passaged after they attained 80% confluence. Spent culture media was aspirated and washed with HBSS twice to remove the spent media containing FBS. 1.5 ml (for T25) / 3 ml (T75) / 6 ml (for T175) of Trypsin-EDTA was added and incubated for 3 mins in 37ºC with an atmosphere of 5% CO_2 and 95% humidity to detach cells. The activity of trypsin-EDTA was terminated by adding an equal volume of FBS to the flask and cells were harvested into a 15 ml falcon tube, then centrifuged at 800 rpm for 5 minutes and the supernatant was removed. The resultant cell pellet was resuspended in 10 ml of HBSS using the pipette and the centrifugation repeated as above. The supernatant was discarded, and the cell pellet was resuspended using 1 ml of media with 1000 µl Gilson pipette to break up the pellet. Cells were introduced into a new cell culture flask with fresh media after cell counting. All the experiments were done using passage 13 to prevent the morphological changes and genetic drift associated with multiple passages.

3.2.2 Human cortical neuronal progenitor cell culture (ReNcell CX / hNPCs)

All tissue culture flasks or plates were coated with laminin at 37ºC with an atmosphere of 5% CO_2 and 95% humidity for 4 hours. Coated plastic cell culture ware was washed with PBS twice. Laminin is an extra cellular matrix ECM protein, which supports and enhances the neural progenitor stem cell adhesion, proliferation, differentiation, and neurite elongation (Flanagan et al., 2006). A 1

mg/ml laminin vial was thawed at 4ºC after taking from -20ºC for 45 minutes to prevent the gelatinization and thawed at room temperature before use. Laminin was diluted to 20 µg/ml final concentration by adding DMEM (DF-042-B). The prepared laminin is used to coat the flasks or plates: 2 ml for T25, 6 ml for T75, 50 µl for one well of 96 well plate, 250 µl for one well of 24 well plates, and 500 µl for one well of 6 well plates. Coated flasks or plates were stored at 4 ºC for 24 hours if not used on the same day for passaging. Flasks were washed with sterile PBS used for cell culture just before use if not used on the same day of coating.

3.2.2.1 *Preparation of ReNcell CX maintenance media*

ReNcell CX cell culture media was prepared by adding 5% penicillin-streptomycin to ReNcell CX NSC maintenance media. Growth factors, 20 ng/ml of EGF or 20 ng/ml bFGF was added to media before seeding or changing media freshly just before use. bFGF (50 µg) was prepared after a quick spin to collect the liquid in a vial, and then the vial was reconstituted to 10 µg/ml in a filtered solution of 0.5% bovine serum albumin (BSA), 1 mM DTT (1,4-dithiothreitol), and 10% glycerol in Dulbecco's PBS. These were then aliquoted and stored at -20°C for up to six months. EGF was prepared in sterilized filtered distilled water and aliquoted and stored at -20°C for up to six months.

3.2.2.2 *ReNcell CX resuscitation from liquid nitrogen storage*

Cells were thawed when the laminin-coated flasks were on hand to seed. A vial of ReNcell CX was removed from liquid nitrogen storage and incubated in a 37ºC water bath for 1 minute after loosening the lid halfway and wiped out with 70% IMS. When the cells were completely thawed, the vial was wiped with 70% IMS to sterilize. Cells were transferred into a 15 ml sterile flacon tube gently using a plastic pipette. After that 9 ml of ReNcell CX NSC maintenance medium without growth factors were added into the tube drop by drop to avoid the

osmotic stress that may result in reduced cell viability. The cell suspension was gently mixed by slow pipetting up and down with a 1000 µl Gilson pipette and centrifuged at 300 x g for 5 mins. The supernatant was aspirated gently and 2 ml freshly prepared media with 20 ng/ml FGF and 20 ng/ml EGF was added to the vial drop by drop and the cell pellet was resuspended in the media with 1000 µl Gilson pipette gently up and down. Cells were then introduced to a flask containing fresh media with growth factors and maintained at 37ºC with an atmosphere of 5% CO_2 and 95% humidity for 24 hours. Then medium was changed, and subsequent media changes were done every 48 hours until 60% confluence was reached and then cells were passaged as needed or cryopreserved.

3.2.2.3 ***Culturing of ReNcell CX***

Cells were subcultured or passaged by carefully removing the maintenance medium from flasks and rinsing with the PBS and then, accutase (1.5 ml (for T25) / 3 ml (T75) / 6 ml (for T175) was added for 3 mins and incubated at 37ºC with an atmosphere of 5% CO_2 and 95% humidity. The reaction was terminated by adding an equal volume of ReNcell CX NSC maintenance medium without growth factors and collected into a 15 ml sterile falcon tube. The tube was topped up with 9 ml of ReNcell CX NSC maintenance medium, and then centrifuged at 300 x g for 5 mins. The supernatant was discarded gently and 2 ml of ReNcell CX NSC maintenance medium with freshly supplied growth factors were added to the pellet dropwise and gently mixed. Cells were introduced to the laminin-coated flasks with 3 ml (for T25) or 13 ml (for T75) growth factor supplied ReNcell CX NSC maintenance medium after cell counting. The flask was monitored at 37ºC with an atmosphere of 5% CO_2 and 95% humidity for 24 hours and media was refreshed with freshly prepared growth factor supplied ReNcell CX NSC maintenance medium. Then

subsequent media changes were done every 48 hours until cells reached 60% confluency and passaged as required. All experiments were done using passage 4 to prevent genetic drift and morphological differences.

3.2.3 Seeding and counting cells for experiments

Cell monolayers were grown to reach 80% confluence for SH-SY5Y cells and 60% confluence for ReNcell CX cells, and then harvested and centrifuged accordingly. Cell pellets were resuspended in respective culture media. Then cells were prepared for counting using an automated cell counter. This technique is more accurate, produces reproducible results, and assesses cell viability in a single step, by comparison with manual hemocytometers. A countess II Automated Cell Counter (AMQAX1000, Thermofisher Scientific, Rochester, UK) was used for the cell counting. Trypan blue was used as a dye to distinguish live and dead cells. The dye-based on the blue acid chromophores reacts and passes through a dead cell's damaged membrane, whereas live cells did not absorb the dye.

10 µl of cell suspension was used and added to 10 µl of Trypan blue solution in a sterile Eppendorf tube and left for a couple of minutes to allow the cells to mix with the dye. 10 µl of this mixture was then loaded by a pipette tip into a chamber of disposable counting slides. The slide was inserted into the chamber of the cell counter and counting initiated. The result of live cell counting was recorded and used for the calculations or dilution preparation in experiments by multiplying by 2 as the suspension was diluted 1:1 with Trypan blue. A cell count for 1 ml was used for determination of the volume necessary to seed the required cell density in corresponding growth medium (Table 3-4).

Table 3-4: Loading cell density for experiments with SH-SY5Y and ReNcell CX cells

Type of cell culture ware	SH-SY5Y		ReNcell CX	
	Loading volume	Total number of cells	Loading volume	Total number of cells
T25	5 ml	250,000	5 ml	350,000
T75	15 ml	750,000	15 ml	1,000,000
T175	45 ml	175,000,000	45 ml	200,000,000
96 well plate	200 µl/well	30000/ well	200 µl/well	30000/ well
12 well plate	1 ml/ well	38000/ well	1 ml/ well	50000/well
6 well plate	2 ml/ well	100,000/ well	2 ml/well	200,000/ well

3.2.4 Cell differentiation

Differentiation of SH-SY5Y were performed according to Encinas et al. (2000) using media prepared with 48% Eagle's Minimum Essential Medium supplemented with 48% Ham's F12 nut mix, 1% heat-inactivated Fetal Bovine Serum (FBS),1% MEM Non-Essential Amino Acid Solution (NEAA), 2 mM glutamine and 1% penicillin–streptomycin solution containing 10,000 IU penicillium and 10 mg/ml streptomycin (p/s), collectively known as low serum media. All -*trans*-retinoic acid (RA) was prepared as a 5 mM stock in ethanol and 10 µM RA was added to low serum media just before adding the media to the cells in light-protected conditions to prevent the photodegradation of RA. RA has been used for SH-SY5Y cells differentiation to generate more neuronal-like cells including production of neurite outgrowth and morphological features (Påhlman et al., 1984, Lopes et al., 2010). Cell culture plastic ware was either coated with 50 µg/ml poly-D-lysine (PDL) before introducing the cells or PDL-coated culture wares were used for seeding. SH-SY5Y cells were passaged with trypsin-EDTA after they reached 80% confluence and then seeded on PDL-coated culture ware, as required with SH-SY5Y cell culture media (10% FBS), at 60,000 cells/ml. Media was changed 24 hours after seeding and subsequent

media change was done every other day until cells reached 60% confluency. Media was then replaced with low serum media with freshly supplied 10 µM RA under light protected conditions. Cells were maintained in low serum media for 6 days, after that low serum media with RA was added with 20 ng/ml BDNF for a further two days to generate more neuronal-like cells. Addition of RA and BDNF to low serum media induces cell differentiation by decreasing cell division and increasing production of neurofilaments, and opioid, muscarinic, and nerve growth factor receptors which mark the development of neuronal like cells (Xie et al., 2010).

ReNcell CX cell differentiation was induced upon growth factor removal which is the standard method of cell differentiation. ReNcell CX were passaged with accutase and seeded on laminin coated culture ware at 100, 000 cells/ml with ReNcell CX NSC maintenance medium with freshly supplied growth factors. Media was replaced with ReNcell CX NSC maintenance medium with freshly supplied growth factors the next day, and after three days ReNcell CX NSC maintenance media with growth factors was replaced with differentiation media (ReNcell CX NSC maintenance medium without growth factors).

3.2.5 Cryopreservation of cell lines

Cells were preserved in liquid nitrogen by expanding cells at the same passage number as used for each experiment use. Briefly, the contents of a T175 flask was harvested and resuspended in freezing medium. For SH-SY5Y cells, freezing medium was prepared by adding 10% DMSO (for cell culture use only) into the SH-SY5Y cell culture media. ReNcell CX was cryopreserved by adding ReNcell CX freezing medium after cell counting. Then, the cell suspension was placed in cryovials and placed in an ice box prepared in advanced for 20 minutes, and then into the Cryo cell freezing container (12 X 1-2 ml, BCS-405S,

Sigma) and stored in a -80ºC freezer overnight. The rate of cooling is approximately -1ºC/minute, and then the following day, cryovials were transferred to the cryobox in the liquid nitrogen for long term storage at approximately – 200 ºC.

3.2.6 Cell density standard curves

A MTT standard curve was generated in order to establish the relationship between cell number and linearity of signal produced, to determine the optimum number of cell density that should be plated on 96 well microtiter culture plates. Cells were counted using an automated cell counter and cells were serially diluted in SH-SY5Y cell growth media or ReNcell CX NSC maintenance medium with freshly supplied growth factors to a range of cell densities of 1x 10^3, 2.5 x 10^3, 5 x 10^3,1 x 10^4, 2.5 x 10^4, 5 x 10^4 and 7.3 x 10^4 SH-SY5Y cells, or ReNcell CX were seeded in replicates of three wells per seeding at the same densities in four separated 96 well plates, with each comprising a total working volume of 100 µl. Three wells of each plate were left cell free for background controls. Culture plates were then transferred to a humidified CO_2 incubator at 37ºC. After 24 hours, cells were checked for attachment using an inverted microscope. Cell viability was assessed using an Dimethylthiazol-2-yl)-2,5-Diphenyltetrazolium Bromide (MTT) assay at four different time points in order to establish the relationship between cell number and signal produced at 0.5 hours, 1 hour, 2 hour and 4 hour after addition of MTT reagent into media. The background corrected absorbance readings obtained were used to generate the cell density standard curve and determine the linearity of signal.

3.2.7 Exposure of cells to pesticides and alcohol

Chlorpyrifos-oxon, Azamethiphos-oxon, and Aldicarb were prepared as 50 mM stocks in ethanol. Pesticides were diluted in SH-SY5Y cell culture media to

various concentrations (1, 10, 20, 50, 100 and 200 µM) for treatment of undifferentiated SH-SY5Y cells. SH-SY5Y cell culture media containing the same concentration of ethanol 0.01% (v/v) served as control treatment (vehicle control) for 24 hours.

Differentiated SH-SY5Y cells were treated with pesticide concentrations of 1, 10, 20, 50, 100 and 200 µM diluted in low serum media containing freshly added 10 µM RA and 20 ng/ml BDNF for 24 hours. Vehicle control treatment was done using ethanol 0.01% (v/v) in low serum media containing freshly added 10 µM RA and 20 ng/ml BDNF for 24 hours. The effect of pesticides on differentiation of SH-SY5Y cells were done by diluting pesticides in low serum media containing 10 µM RA, and media containing freshly added 10 µM RA and ethanol 0.01 (v/v) served as a vehicle control.

Pesticides were diluted in ReNcell CX NSC maintenance medium with freshly added growth factors used for undifferentiated cell treatment with various concentrations (0.3, 1, 3, 10, 30, 100 and 200 µM) of pesticides for 24-hour treatment. ReNcell CX NSC maintenance medium with freshly added growth factors containing ethanol 0.01% (v/v) served as vehicle control treatment in these experiments. Differentiated ReNcell CX cells were treated with (0.3, 1, 3, 10, 30, 100 and 200 µM) pesticides by diluting pesticides stock in ReNcell CX NSC maintenance medium for 24 hours. Control treatments (vehicle control treatments) were with 0.01% ethanol in ReNcell CX NSC maintenance medium without growth factors.

Ethanol neurotoxicity evaluation was done in SH-SY5Y cells by diluting stock ethanol (17.2 M) in SHSY5Y cell culture media (to prepare final concentrations of 10, 20, 50, 100 and 200 mM) for undifferentiated cells, with cell culture media only as a control treatment. Cells were treated for 3, 6, 12 and 24 hours. Differentiated cells were treated with the same concentration range of alcohol

for 3, 6, 12 and 24 hours by diluting alcohol in low serum media with freshly supplied 10 µM RA and 20 ng/ml BDNF. Only low serum media with freshly supplied 10 µM RA and 20 ng/ml BDNF served as control for each time point. Differentiation inducing experiments were done with using low serum media with freshly supplied 10 µM RA under light protective conditions.

ReNcell CX undifferentiated cells were treated with ethanol for 3, 6, 12 and 24 hours by diluting stock ethanol in ReNcell CX NSC maintenance medium with freshly added growth factors in the rage of 10, 20, 50, 100 and 200 mM, and ReNcell CX NSC maintenance medium with freshly added growth factors as a control for treatments. Differentiated ReNcell CX were treated in the same alcohol concentration range for the same time points as for undifferentiated cells by diluting stock ethanol only in ReNcell CX NSC maintenance medium. ReNcell CX NSC maintenance medium served as a control treatment.

Treated cells were incubated in a humidified CO_2 incubator at 37^{o}C for time points and cell lysates or pellets were prepared according to the required assay.

For evaluation of the combination effects of both pesticide and alcohol on SH-SY5Y undifferentiated and differentiated cells, an IC_5, IC_{10}, IC_{20} and IC_{50} concentration of pesticides were interpolated from corresponding viability curves and respective concentrations were prepared by diluting the corresponding culture media. Ethanol concentrations of 10, 20, 50, 100 and 200 mM were prepared in corresponding culture media of undifferentiated or differentiated SH-SY5Y cells (Low serum media + 10 µM RA +/- 20 ng/ml BDNF). The corresponding culture media only was treated as the control treatment for alcohol while ethanol at 0.01% was treated as a pesticide vehicle control.

3.3 Measurement of cell viability in cells exposed to pesticides and ethanol

Measurement of cell viability is a foundation stone for most *in vitro* studies of cellular responses to toxic agents. The effect of pesticides and alcohol on the viability of both SH-SY5Y and ReNcell CX were determined by the MTT reduction assay, as described by (Mosmann, 1983). MTT is a colorimetric assay based upon the ability of cellular dehydrogenase enzymes (mainly succinate dehydrogenase) from viable cells to split the tetrazolium ring of the pale yellow MTT to form purple colour formazan crystals. These crystals are largely impermeable to the cell membrane resulting in their accumulation within healthy cells. Accumulated crystals were dissolved by the action of a DMSO:isopropanol mixture as this results in their liberation, and this can be read spectrophotometrically. The ability of cells to reduce MTT to formazan provides a readout of metabolic activity, as quantified level of the formazan product is directly proportional to the number of metabolically active cells. In turn, this is a measurement of the number of viable cells.

Cell viability has been commonly measured using variety of tetrazolium compounds such as MTT, MTS, XTT and WST-1. MTT is a positively charged molecule and easily penetrates through the cell membrane of eukaryotic cells while others are negatively charged and act as intermediate electron acceptors from the cytoplasm or plasma membranes to facilitate the reaction. MTT is a homogenous cell viability assay which was developed for 96 well format and highly recommended for high throughput screening studies (Riss et al., 2004). Moreover, the reagents yield a stable colour and with a low background absorbance value in the blanks (no cells) observed. The quantification of a linear relationship with cell number and MTT signal provides a more accurate quantification of cell growth. Therefore, the MTT assay is widely accepted

among neurotoxicity testing studies and considered a reliable tool of measuring cell viability after cellular treatments (Mosmann, 1983).

3.3.1 Preparation of MTT

MTT powder was dissolved in sterile cell culture PBS solution to prepare a 5 mg/ml stock. Aliquots of 1 ml were stored at -20^{o}C and used as required by thawing at room temperature.

3.3.2 Assay protocol

Cells were plated in microtiter 96 well plates (transparent or clear bottom PDL coated black well plates) and grown until they reached the required cell density. Cells allowed to settle for 24 hours and treatments were done according to the experiments as explained in section 3.2.7. At the end of the treatment period spent culture media was replaced with 0.5 mg/ml MTT containing cell growth media prepared in advanced. Plates were protected with aluminium foil to prevent the photodegradation of MTT and placed inside the incubator at 37^{o}C for 4 hours, and then spent media with MTT was replaced with 1:1 (v/v) DMSO:isopropanol. Each well with DMSO:isopropanol was resuspended until the formazan crystals had been dissolved thoroughly by mixing using a multichannel pipette. Plates were then incubated for 15 minutes at room temperature. Following incubation, the optical density (OD) was measured at 570 nm using a Spectramax plate reader (Multiskan Spectrum, Thermo Electron Corporation). Readings were imported to Microsoft Excel (2016) and average OD values obtained after subtracting blanks (cell free control wells) to correct for background OD values. Corrected OD readings for each treatment were normalized to the mean of the vehicle control (or control in ethanol treatments), and the percentage cell viability calculated as a percentage relative to the vehicle control.

3.4 Lactose dehydrogenase assay for measurement of cell death or cytotoxicity (LDH)

Reduction of MTT to formazan by non-mitochondrial and mitochondrial oxidoreductase enzymes directly correlates with cellular metabolic activity and thereby acts as a surrogate of cell viability or cell proliferation (Slater et al., 1963, Mshana et al., 1998, Riss et al., 2004). However, to further confirm changes in cell viability, LDH assay was used. Loss of membrane integrity of cells exposed to toxic insult leads to released lactate dehydrogenase (LDH) into the surrounding extracellular space. This is very stable enzyme and does not lose activity in cell viability assays, and only is only released if the cell membrane integrity is damaged. The presence of this enzyme in culture medium is used as a cell death marker in neuronal cell culture the relative amounts of live and dead cells within the medium quantitated by measuring the amount of released LDH using a colorimetric LDH cytotoxicity assay. This has been used to measure the apoptosis or necrosis of neuronal cell cultures (Koh and Cotman, 1992, Gwag et al., 1995, Lobner, 2000). NAD^+ converted to NADH and H^+ by LDH that has been liberated into the cell culture media by the damaged cells, through the oxidation of lactate to pyruvate. The catalyst (diaphorase) then transfers H/H^+ from NADH and H^+ to the iodonitrotetrazolium or INT (a tetrazolium salt) to form the red coloured formazan salt. The amount of colour is measured at 490 nm by standard spectroscopy and is proportional to the number of damaged cells in the culture which is a measure of number of dead cells. This assay can accurately measure cell death due to its inherent linearity. Simplicity, reliability and reproducibility of the assay make it useful in high throughput screening of neurotoxic chemicals.

3.4.1 Assay protocol

Undifferentiated or differentiated cells were prepared as described above for the MTT assay and similarly treated with pesticides. After 24 hours of each pesticide treatment, 50 µL of spent media from each treatment was removed into a microtiter plate. LDH activity was measured using an assay kit (ab 65393 (cytotoxicity), Abcam, Cambridge, UK) according to the manufacturer's guidelines. Briefly, LDH released from the toxic insult of the pesticides as oxidized lactate was converted to pyruvate generating NADH, and this reacts with [2-(4-Iodophenyl)-3-(4-nitrophenyl)- 5-(2,4-disulfophenyl)-2H-tetrazolium] (WST) reagent which is a tetrazolium salt that readily dissolves in water in the kit to generate a yellow colour. 50 µl of treated culture media in each assay was allowed to react with WST reaction mix, prior to an incubation for 30 minutes. Blank treatment (culture media without cells) was similarly mixed with WST. An LDH positive control in the kit was used in the same plate. Plates were read at 450 nm using a spectrophotometer (Multiskan Spectrum, Thermo Electron Corporation, Finland) at 37^{o}C, protected from light. Readings were imported to Microsoft Excel (2016) and average OD values obtained after subtracting blanks (cell free control wells) to correct for background OD values. Corrected OD readings for each treatment were normalized to the mean of the vehicle control, and a percentage cell death relative to the vehicle control calculated.

Undifferentiated or differentiated SHSY-5Y cells or ReNcell CX cells were treated with ethanol as described above for the MTT assay. After ethanol treatment, 50 µL of spent media was removed and LDH activity measured using an assay kit (ab102526, Abcam, Cambridge, UK) according to the manufacturer's guidelines. NADH standards were prepared according to the manufacturer's protocol and were transferred into the same assay plate. Assays were performed at 450 nm using a spectrophotometer (Multiskan Spectrum,

Thermo Electron Corporation, Finland) in kinetic mode, with readings taken every 2 minutes at 37^{o}C, protected from light, for a total of 60 minutes. A NADH standard curve was generated and LDH activity measurements interpolated from the NADH standard curve. Experiments were performed in triplicates from which an average was taken, and blank values subtracted to correct for background OD values. Corrected OD readings for each treatment were normalized to the mean of the control as a minimum value providing the LDH activity percentage as a percentage relative to the vehicle control.

3.5 Detection of cellular ATP production

An ATP assay is a reliable method of measuring cell viability used in high throughput screening assays, since the concentration of ATP is a valid marker for viable cells. Measurement of cell viability exposed to the selected low and high concentration of pesticides (IC_{10}, IC_{20}, IC_{50} and IC_{80}) and alcohol was done using an ATP assay. In turn, ATP assays provide a measurement about mitochondrial functions of cells. Cells lose their membrane integrity when cells are exposed to toxic insult from a neurotoxicant and lose their ability to synthesise ATP. The ATP assay is based on the conversion of luciferin to oxyluciferin which is found in fireflies. The reaction is catalysed by Mg+ ions and ATP to generate a luminescence signal in the presence of oxygen. As a result, ATP is converted to AMP. The green luminescence can be determined using a luminometric plate reader. The number of cells with active mitochondria is propositional to the quantified luminescence level. In turn this provides a number of viable cells as a function of luminescence. The rapidity and stability of the signal within 10 minutes provides this assay with high accuracy and sensitivity. Furthermore, there is not any assay chemistry changes during the reaction in the assay (Riss et al., 2004).

3.5.1 Preparation of cell lysis buffer

1 L of cell lysis buffer was prepared using 100 mM Tris and 4 mM EDTA and the pH was adjusted to 7.75.

3.5.2 Assay protocol

Undifferentiated and differentiated cells were seeded in 6 well plates and treated with pesticide or alcohol as explained in section 3.2.7. Plates were washed with ice cold PBS for three times and extracted into the 500 µl of Tris/EDTA assay buffer via agitation on ice for 5 minutes, before scraping the cells into the buffer. The extracted cell suspension was then added to 9 volumes of boiling Tris/EDTA buffer, and then incubated for 10 minutes at 100^{o}C. After that, samples were centrifuged at 1000 x g and the supernatant transferred into a fresh tube and placed on ice until required. ATP levels were quantified using an ATP luminescence assay kit (ATP Bioluminescence Assay Kit CLS II (11 699 695 001, Roche, Germany), according to the manufacturer's protocol. Briefly, ATP standards were prepared according to the kit protocol across a concentration range of 1 x 10^{-4} to 1 x 10^{-10} moles. Samples were added to white opaque 96 well plates. After addition of luciferase reagent to each well, the luminescence was measured using a luminometric plate reader (Thermo Fisher Scientific, Fluoroskan Ascent FC, Finland) at 562 nm using an integration time of 1 second. The ATP content in vehicle controls and treated samples were interpolated from the ATP standard curve. Experiments were performed in triplicates from which an average was taken, and blank values subtracted. Corrected luminometric readings for each treatment was normalized to the mean of the vehicle controls as a highest value providing the ATP level as a percentage relative to the vehicle control.

3.6 Morphological measurements of cells exposed to pesticides and ethanol

Cell culture plates after pesticide and alcohol treatments were monitored with an Olympus inverted microscope, which phase-contrast optics (DP70, London, UK) to compare the general morphological changes after pesticide or ethanol treatments with (vehicle) control treatments.

3.7 Measurements of neurite length in differentiated cells

Neurite outgrowth is considered a marker of cell differentiation. SH-SY5Y cells were cultured in 12 well PDL coated plates in media and incubated for 24 hours to ensure cell adhesion. Cells were then treated with pesticides or ethanol as described in section 3.2.7. Cell images were captured using a phase contrast microscope (Olympus, DP70, London, UK) at the end of the treatment period. Cells were considered to be differentiated if each neuronal cell contained at least one process that was longer than its cell body (Raghunath et al., 2000). The neurite length from 200 randomly chosen cells were measured in 5 selected quadrants per well using the neurite tracer tool from Image J (Image J 1.49k, National Institute of Health, USA) in three independent wells for one treatment (Pool et al., 2008). Five independent experiments were conducted for each experiment with three replicates. Results are expressed as mean percentage neurite length (± SD) relative to vehicle control cells.

3.8 Measurement of reactive oxygen species generation

Cellular ROS generation is a marker of the cellular oxidative stress induced by neurotoxicants in neuronal cells. SH-SY5Y cells and ReNcell CX exposed to pesticides and ethanol were assayed for cellular ROS production after agent exposure. ROS assays were performed using 2',7'-Dichlorofluorescein diacetate (DCFDA). DCDFA is a non-fluorescent dye which is readily permeable through the cell membrane due to the hydrophobic nature of the dye. After

absorption it is deacetylated by cellular esterases to a non-fluorescent moiety and later oxidised in to 2', 7'–dichlorofluorescein (DCF) by ROS produced in cells. DCF is a highly fluorescent compound and the magnitude of the signal can be quantified by fluorescence spectroscopy with maximum excitation and emission spectra of 495nm and 529nm, respectively. The magnitude of the DCF fluorescence signal produced is proportional to the formation of ROS produced in the cells: for instance, $OH^{\bullet}$, and molecules that include peroxyl, alkoxyl, carbonate ($CO_3^{\bullet -}$) and $NO_2^{\bullet}$ groups. The dye has been used for both *in vivo* and *in vitro* experiments and also for fluorescence microscopy (Halliwell and Whiteman, 2004). The only drawback of DCFDA assay is that serum esterase in the cell culture media can convert it to DCFA other than ROS in cells (Korystov et al., 2007, Boulton et al., 2011, Subramaniam et al., 2002). However, this problem can be eliminated by analysis in serum-free media, or serum containing media with dye separately and the values from the treatments and controls subtracted (Tetz et al., 2013).

3.8.1 Preparation of reagents

DCFDA dye was dissolved in ethanol to prepare a 25 mg/ml stock solution and aliquots were stored at -20^{o}C. Just before the assay, DCFDA was reconstituted in phenol red free HBSS to achieve the concentration of 1 mM.

1 mM H_2O_2 was reconstituted in sterile filtered distilled water on the same day before use in the experiments as a positive control.

N-Acetyl-L-cysteine used as antioxidant in assay and prepared as 100 mg/ml stock in sterile filtered distilled water and was reconstituted to 1 mM before use in assay.

3.8.2 Assay protocol

Cell were cultured in clear bottomed sterile, black 96 well plates for undifferentiated cells and PDL coated clear bottom 96 well, black microtiter plates for differentiated cells, and grown to a desired density as explained in section 3.2.4. Cells were treated with IC_{10}, IC_{20}, IC_{50} and IC_{80} concentrations of agent for pesticides or 10, 20, 50, 100 and 200 mM concentrations for ethanol experiments with their corresponding media. 50 µM DCFDA with cell culture media added 30 min before each experiment. Media and dye served treatment was used to check the serum effect on DCFDA and only cell and media with dye served as a blank in the same experiment plate. The highest concentration (IC_{80} for pesticide and 200 mM) of the test compound and cells treated with 1mM *N*-Acetyl-L-cysteine to check the accuracy of assay in the same well plate as a separate treatment with replicates. 30 mins before end of the experiment 500 µM H_2O_2 treated to the cells with 50 µM DCFDA. After end of the treatment period plates were washed three times with PBS and florescence signal was measured in PBS. Blanks and serum effect are subtracted from the fluorescence values and normalized to the values of mean of the vehicle control. ROS generation was then calculated as a percentage relative to the vehicle control.

3.9 Colorimetric determination of acetylcholinesterase activity of cells exposed to pesticides

The measurement of AChE activity after treatment of cells with pesticides was used to model the mechanism associated with OP and carbamate neurotoxicity *in vitro* (Flaskos, 2012). Inhibition of the enzymatic activity of AChE is one of the key mechanisms of OP and carbamate neurotoxicity. The AChE inhibition was assessed using a modified Ellman's assay (Flaskos et al., 2007). The activity of enzyme in cells exposed to OP compounds was measured in a

spectrophotometric assay developed by Ellman and colleagues in 1961.This method is based on production of thiocholine by the action of AChE on acetylthiocholine, which forms a yellow coloured product with 5,5'-Dithiobis-(2-Nitrobenzoic Acid) (DTNB). The colour intensity can be quantified at 412 nm and it is proportional to the AChE enzyme activity within the sample.

3.9.1 Preparation of reagents

Potassium phosphate buffer was prepared in a total volume of 200 ml containing 100 mM sodium phosphate (monobasic)/potassium phosphate (dibasic) containing 0.1% Triton X-100 at pH 8.

The substrate was prepared in a total volume of 20 ml containing 1.25 mM acetylthiocholine iodide (ATCI).

5,5'-Dithiobis-(2-Nitrobenzoic Acid) (DTNB) was freshly prepared for every experiment in a total volume of 20 ml containing 1.25 mM DTNB in potassium phosphate buffer at pH 8 and kept in ice until used.

3.9.2 Assay protocol

Both undifferentiated and differentiated cells were cultured in T25 flasks and cells were harvested to establish the relationship with sample volume and linearity of signal produced. Cells are harvested into ice cold potassium phosphate buffer and centrifuged at 13000 x g for 5 minutes at 4^{o}C. Then the supernatant was discarded, and resultant cell pellet was resuspended in 1 ml of potassium phosphate buffer. A volume of 10, 20, 50, 80, 100 and 150 µl was assayed with 1:1 mixture of ATCI and colour indicator DTNB. Absorbance was immediately measured at 412 nm using a spectrophotometer (Multiskan Spectrum, Thermo Electron Corporation, Finland) in kinetic mode, with readings every 1 minute at 37^{o}C, protected from light, for a total of 30 minutes.

Cells were plated in 6 well plates for treatment as described in Sections 3.2.3 and 3.2.4 and pesticide treatments were done according to Section 3.2.7 in the concentration range of 0.1, 0.3, 1, 3,10 µM for both SH-SY5Y and ReNcell CX cells for 24 hours. Cells were harvested into ice cold potassium phosphate buffer and centrifuged at 13000 x g for 5 minutes at 4^{o}C. Then the supernatant was discarded, and resultant cell pellet was resuspended in 1 ml of potassium phosphate buffer. A volume of 100 µl was assayed with 1:1 mixture of ATCI and colour indicator DTNB. Absorbance was immediately measured in 412 nm using a spectrophotometer (Multiskan Spectrum, Thermo Electron Corporation, Finland) in kinetic mode, with readings every 1 minute at 37^{o}C, protected from light, for a total of 10 minutes. The absorbance of blank (only assay buffer) values were subtracted from the absorbance readings of treatments. As the absorbance background was increasing with time, the absorbance intensity value of the blank well was subtracted for each data point. Corrected absorbance readings for each treatment were normalized to the mean of the vehicle control as a highest value providing the AChE activity as a percentage relative to the vehicle control.

3.10 Preparation of cell lysates for one dimensional polyacrylamide gel electrophoresis (SDS- PAGE)

After pesticide or ethanol treatments of differentiated or undifferentiated SH-SY5Y cells or ReNcell CX cells, cells were washed three times with ice cold PBS. After that 0.5 ml of RIPA buffer containing protease inhibitors (1:100 diluted stock) and 1:100 diluted phosphatase inhibitor cocktail (prepared in advance and kept on ice) was added and flasks were placed and agitated on ice for 5 minutes. Cells were scraped into RIPA buffer and collected to a pre-labelled Eppendorf tube and vortexed thoroughly. A 28g needle was used for passage of the cell lysate 25 times. Cell lysates were centrifuged at 500 x g for 10 minutes at 4^{o}C in a bench top centrifuge to pellet the nuclear fraction. The

supernatants were then centrifuged at 21,300 x g for 40 min at 4^{o}C to produce crude cytosolic preparations. Each fraction was stored at -80^{o}C until needed.

3.11 Protein quantification by modified Lowry assay

To determine the amount of protein in all treated cell samples, a modification of the Lowry assay (Lowry et al., 1951) was used. Bovine serum albumin protein was used as a standard. The Lowry assay was performed in 96 well plates by using protein standard amounts of 1.25, 2.5, 5, 7.5, and 10 µg of protein. Every time, fresh standards were prepared along with the samples and then Lowry protein assays performed. The cytosolic fractions were thawed at room temperature and vortexed. 40 µl cell lysates were diluted 1:5 or 1:8 in the study with 10 mM Tris buffer for loading into a 96 well plate as duplicates along with standards. Then, 20 µl of Reagent A (Alkaline copper tartrate solution) was added to each well and 160 µl of Reagent B (Folin reagent). After 15 minutes the plate was agitated in a Spectramax plate reader (Multiskan Spectrum, Thermo Electron Corporation) for 5 minutes before taking the readings at 740 nm. The protein yield is expressed as mg/ml and data was imported to Microsoft Excel (2016) for analysis. A standard curve was plotted on Microsoft Excel (2016) to calculate the amount of protein concentration in each sample from linearity of the equation of line of best fit.

3.12 One dimensional polyacrylamide gel electrophoresis (SDS-PAGE)

SDS- PAGE and western blotting allows characterisation and visualisation of denatured proteins with molecular weights characterised against similar passage of molecular weight standards.

3.12.1 Preparation of buffers and reagents

500 ml of 1 M of Tris-HCl buffer was prepared by dissolving 60.57 g of Tris base in 350 ml of ultrapure water and stirred until completely dissolved, then 32.5 mL of 12 M HCl was added slowly, while monitoring the pH to reach 7.4 and then the volume topped up with ultrapure water to make up to 500 ml.

Running buffer was prepared by diluting 20X MOPS in ultrapure water. 1000 ml of running buffer was prepared by adding 50 ml of MOPS in 950 ml of ultrapure water and made up fresh on the day of use.

2000 ml 10X stock of transfer buffer was prepared by dissolving 288g of glycine and 60.4 g of Tris base in 1500 ml of ultrapure water and dissolved and topped up to 2000 ml with ultrapure water.

2000 ml of 1X transfer buffer was prepared on the day of working by adding 200 ml of stock into 400 ml of methanol and 1400 ml of ultrapure water and chilled at 4^{o}C.

PBS-Tween buffer (Wash buffer) was prepared by dissolving 8 g of NaCl, 0.2 g of KCl, 1.44 g of Na_2HPO_4 and 0.2 g of KH_2PO_4 in 800 ml of ultrapure water. After compounds were completely dissolved the pH was adjusted to 7.4 with HCl and topped up to 1000 ml with ultrapure water and 0.05% (v/v) Tween 20 was added to make PBS-T.

Fixative solution was prepared by mixing 10% (v/v) acetic acid, 50% methanol (v/v) and 40% (v/v) ultrapure water.

Blocking buffers; 5% (w/v) of Marvel – semi skimmed dried milk powder or 1% (w/v) or 2.5 (w/v) BSA (lyophilised powder) was dissolved in PBS-T to make 200 ml of blocking buffer. Blocking buffers were prepared fresh before use.

3.12.2 Sample preparation for SDS

Cell lysates were prepared to a concentration of 1µg/µl. Then samples were mixed with 10 mM Tris buffer, Novex reducing agent and 4x LDS sample buffer and heated at 70^{o}C for 10 minutes on a block heater (DB100/3, Stuart Scientific). Samples were allowed to cool to room temperature, and then pulsed in a centrifuge for 5 seconds to collect the material for gel loading.

3.12.3 SDS -PAGE

Precast gels (10% Bis-Tris Gels, 1.0mm x 10 well (NP0301BOX) and 10% Bis-Tris Gels, 1.0 mm x 12 well (NP0322BOX) were used in this study. Gels were placed vertically in an Xcell surelock Mini-cell, and the electrophoresis chamber was filled with running buffer (MOPS). 0.5 ml of antioxidant was added to the inner chamber and then buffer filled it to the top. Prepared samples were loaded into wells as required (typically 15-25 µl loaded per gel well) using gel loading pipette tips. The first lane of the gel was loaded with 10 µl of a pre-stained protein molecular weight marker and any unused wells were loaded with 1X loading buffer. Electrophoresis was performed at 125V (constant voltage) for approximately 100 minutes. Then gel plates were carefully separated by using a purposely made gel knife and placed in fixative solution for staining. The gel ridge and comb were carefully removed using a scalpel. After 15 minutes, gels were stained with Colloidal Blue staining Kit overnight. The next day gels were destained by washing with double distilled water for one hour on a rocking platform. When gels were fully destained, pictures were taken using a ChemiDoc imaging system (BioRad). If gel staining was not performed, then the separated gel was transferred for Western blotting.

3.12.4 Western transfer and immunoblotting

8.5 x 8.5 cm polyvinyl difluoride (PVDF) membranes were pre-soaked in 100% methanol for 5 minutes and equilibrated in 100% transfer buffer for 15 minutes by changing the buffer in every 5 minutes. A Bio Rad Mini Trans-Blot cell was placed on ice within a polystyrene container and a frozen block of transfer buffer inserted into the end compartment. A transfer sandwich was prepared on a supporting grid usually on the black side (anode) as transfer buffer soaked sponge, 3 of 8.5 x 8.5 cm squares of filter paper (Whatman filter papers, Sigma-Alrich), SDS–PAGE gel, PVDF membrane, and then 3 of 8.5 x 8.5 cm squares of filter paper and sponge again. Proteins were transferred for 120 minutes at 80V constant voltage.

Thereafter, the PVDF membrane was removed and washed in 20 ml of Coomassie blue safestain for 30 minutes for visualize the protein bands or stained with reversible stain kit for protein visualization. Then the PVDF membrane was placed on cling film overnight to dry at room temperature. The following day the membrane was detained as previous in a fixative for 5 minutes and placed on a rocking platform for shaking with a wash buffer of PBS-T until equilibrated for three times for 10 minutes each time. Membranes were then blocked with blocking buffer to prevent non-specific protein (antibody) binding for 1 hour at room temperature. Then membranes were incubated overnight with primary antibody (β II/ βIII or GAPDH) diluted in blocking buffer in a sealed polythene packet attached to a rotary mixer at 4^{o}C. The following day membranes were washed in PBS-T for three times as previous for 10 minutes each and probed with a corresponding horseradish conjugated anti-species secondary antibody at room temperature for 1 hour. After that, membranes were washed in washing buffer for three times as previous and placed on a cling film. 4 ml of 1:1 Clarity Western Enhanced Chemiluminescence substrate reagent A

and B was poured over the membrane and left for 5 minutes. Immunoreactive bands were captured by placing the membrane on the imaging platform of a ChemiDoc imaging system (BioRAD). Membranes were stored for later use by washing in wash buffer as previous and dried overnight on cling film. Dosimetric analysis of proteins were done using Biorad Imagelab^{TM} software version 6.0.1 build 34. Band measurement was corrected for background for normalisation with total protein present, and values presented as averages to corresponding controls ± SEM.

3.13 Spectrophotometric detection of carbonylated proteins

Protein carbonylation is a biomarker of protein oxidation. Carbonylated proteins are relatively stable and can be derivatized to DNPH which leads to a stable dinitrophenyl (DNP) hydrazine product which can be spectrophotometrically quantified and standardised to protein concentration. Quantitation of the levels of cellular protein carbonyl content (PCC) was performed according to (Colombo et al., 2016).

Undifferentiated or differentiated pesticide or ethanol treated cells in 6 well plates were washed with ice cold PBS three times and then solubilized and lysed with RIPA buffer containing protease and phosphatase inhibitors. Samples were vortexed for 30 seconds and then sonicated for 15 minutes on ice cold water. Samples were spun at 500 x g for 10 minutes at 4^{o}C, and the supernatant retained and centrifuged at 23,100 x g for 40 minutes at 4^{o}C to prepare crude cytosolic fractions. Protein concentration was determined using a modified Lowry assay and then adjusted to 1 mg/ml for each sample. An equivalent volume of 10 mM 2,4-dinitrophenylhydrazine (DNPH) prepared in 2N HCl was added to samples or blanks, vortex mixed, and then samples left in the dark for 1 hour at room temperature, with vortex mixing every 10 minutes. An equivalent volume of ice cold 20% (w/v) trichloroacetic acid was added and

samples incubated for 15 minutes on ice. Samples were then spun at 10,000 x g for 5 min, at 4^{o}C, supernatant discarded, and pellets washed with 1:1 ethanol: ethyl acetate (v/v) by vortex-mixing. Samples were spun at 10,000 x g for 5 min, at 4^{o}C, and the supernatant discarded. Washing with 20% ice cold TCA and then 1:1 ethanol: ethyl acetate was repeated, and then samples air dried for 5 minutes to allow complete evaporation of solvents. Protein pellets were resuspended in an equal volume of 6 M guanidine hydrochloride in 50 mM phosphate buffer, pH 2.3, with incubation at 37^{o}C for 30 mins and with vortex mixing. Protein carbonyl contents (PCC) of test samples were determined via spectrophotometric reading at 366 nm using a molar absorption coefficient of 22,000 M-1cm^{-1} after subtraction of blanks (phosphate buffer with 6 M guanidine hydrochloride only). Assays were performed in triplicate from which an average was calculated.

3.14 Preparation of cell lysates for Oxyblot

The DNPH derivatized proteins were further separated by SDS-PAGE and immunoblotted to identify the specific protein targets of oxidative stress. The OxyBlot^{TM} Protein Oxidation Detection Kit (S7150, Millipore) was used for Oxyblots.

3.14.1 Derivation of protein mixture

Samples were prepared with after pesticide or ethanol treated cells as mentioned in section 3.10, and protein quantification was done as mentioned in 3.11. Samples are prepared at 2mg/ml concentration and 20 µg of protein samples were used for derivatization. Samples were denatured by adding an equal volume of 12% SDS, and then derivatization solution in the kit added to each sample and incubated for 15 minutes in room temperature. Then, samples were neutralized by adding neutralization solution from the kit. Then, 0.05%

(v/v) of β-mercaptoethanol was added to prevent further oxidation of samples. A negative control was prepared by adding the derivatization control solution instead of DNPH. A 500 µM H_2O_2 treated cells along with the experimental treatments (positive control) for the experiment was prepared in the same way that treated samples were prepared. Samples for the Oxyblot were prepared just after treatments and SDS-PAGE and Western transfer done in the same day to limit sample degradation. Derivatized proteins were stored up to five days at 4ºC.

3.14.2 SDS-PAGE, Western transfer and immunodetection of carbonylated proteins

Proteins were separated by gel electrophoresis and immunoblotted to PVDF membranes as explained in section 3.12.3 and 3.12.4. Membranes were blocked with 1% BSA (w/v) in PBS-T for one hour, and then incubated overnight with rabbit anti-DNP antibody at a 1:150 dilution, before incubation with goat anti-rabbit IgG (HRP-conjugated) secondary antibody at a 1:300 dilution in 5% milk (w/v) in PBS-T, according to the manufacture's protocol. Specific carbonylated proteins were visualized as explained in section 3.12.4 using a ChemicDoc imaging system (BioRad).

3.15 Statistical analysis

All sets of data were based on minimum of 5 separate experiments and expressed as mean ± standard error of mean (SEM). The analysis was conducted using Graph Pad Prism 8.4.1 (Graph Pad Prism, San Diego, California USA). Dose-response curves were generated to interpolate the inhibition concentrations in each experiment by using a nonlinear regression curve fit model. Comparison between control and treatment groups was performed using either one-way analysis of variance (ANOVA) or two-way

ANOVA with Dennett's multiple comparison test and Tukey's multiple comparisons, respectively. Correlation analysis was done using Pearson's correlation analysis. Combination index (CI) was calculated using the CompuSyn software and Chou-Talalay method provide quantitative definition for an additive (CI=1), synergistic (CI<1) or antagonistic (CI>1) effect of ethanol and pesticide combinations. Results were considered significant at a $p < 0.05$.

4 NEUROTOXICITY EVALUATION OF ORGANOPHOSPHATE AND CARBAMATE PESTICIDES USING HUMAN NEUROBLASTOMA SH-SY5Y CELLS

4.1 Introduction

OP and carbamate pesticides remain the most extensively used pesticides in the world. Despite strict bands on its household applications, OP and carbamate pesticides are still used in fruit crops, plantation crops and animal farming, thereby posing a high risk to people who work with them, such as applicators, families, and children living close proximity to agricultural areas where they are used (Gupta and Milatovic, 2012). The key mechanism of neurotoxicity of OP and carbamate pesticides is AChE inhibition (Gupta and Milatovic, 2012).

However, metabolic products resulted from the biotransformation of OP and carbamate pesticides can directly affect neuronal cells (Flaskos, 2012). Cellular and molecular level studies suggested that AChE inhibition is not the single mechanism responsible for OP and carbamate neurotoxicity. For instance, OP and carbamate acute exposure affects general biological processes of cells such as cell cycle, apoptosis, DNA synthesis or induces oxidative stress (Flaskos, 2012). Oxidative stress damages DNA and other cellular proteins as well as affects critical genes involved in cell differentiation which in turn are linked with neuronal communication, growth, and neuronal plasticity which effects motor abilities and cognitive abilities. Several lines of studies point out that CPF and CPO can deplete neuronal cells or induce neurodegeneration (Sarkar et al. 2017, Xu et al. 2017, Singh et al. 2018).

In light of these uncertainties, human risk assessment of commonly used OP and carbamate pesticides and their underlying mechanism of toxicity at the cellular level has gained attention to clarify whether the possible

neuropathological effects found in the literature occur at low doses than the doses currently considered safe for the population and occupational workers. Despite a large body of evidence available for the toxicity mechanisms of CPO, AZA and Aldicarb on animal models, some of these data are not sensitive enough to compare the effect of highly reactive metabolites of these pesticides on humans. These deficits are important to address to establish safety levels of these hazardous pesticides. *In vitro* systems have been widely accepted for neurotoxicity testing of environmental chemicals using human neuronal cell lines such as human neuroblastoma cells (Chapter II, Table 2-1). According to Bal-Price et al. (2010), a critical mechanism of neurotoxicity should have to cover neuronal-specific endpoints, and initial toxicity testing should cover the concentration-dependent curve and generate IC_{20}, IC_{50} and IC_{80} concentrations should be further tested with other specific endpoints to address the deficits in neurotoxicity studies (Bal-Price et al., 2010). However, cytotoxicity of different pesticides and their metabolic compounds are cell type and stage-specific (Heusinkveld and Westerink, 2017). Also, mechanisms inducing toxicity are significantly different from one to the other. However, there is a deficit in neurotoxicity evaluation using oxon metabolites in human neuronal cell models and their underlying mechanisms of inducing neurotoxicity and the functional changes in cells that arise from the exposure. This chapter focuses on a study designed to investigate the neurotoxicity of oxon metabolites commonly used, the OP pesticides Chlorpyrifos and Azamethiphos and carbamate pesticide Aldicarb, using human neuroblastoma cells. Morphological changes that arose after exposure were captured using a phase-contrast microscope. 50% inhibition concentrations of cell viability were interpolated using dose-response curves and general cell functional tests such as ATP assay, and oxidative stress were quantified using low and high viability inhibiting concentrations (IC_{10}, IC_{20},

IC_{50} and IC_{80}) to evaluate the low dose exposure effects on cells, and oxidative stress-mediated protein oxidation.

4.2 Results

4.2.1 Phenotypic characterization of undifferentiated and differentiated SH-SY5Y cells

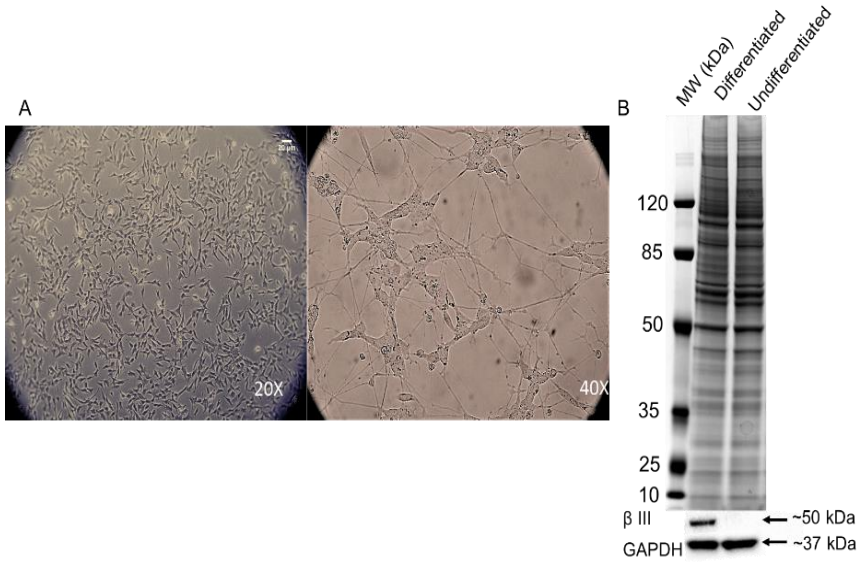
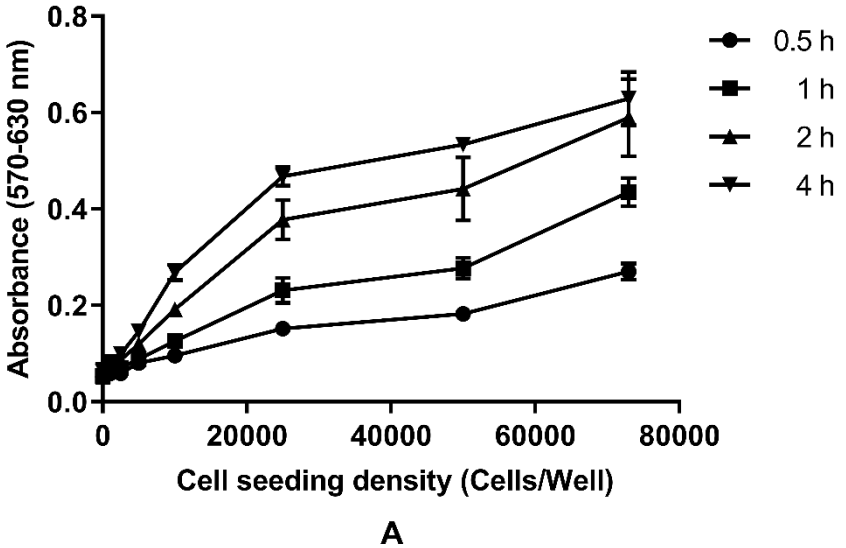


Figure 4-1: Undifferentiated and differentiated SH-SY5Y cells.
A- Undifferentiated SH-SY5Y cells have truncated processes while differentiated cells have more long neurites; B- Differentiated cells (RA and BDNF treated cells) express neuronal marker β III tubulin but undifferentiated cells did not express detectable β III tubulin. RA- All-*trans* -retinoic acid; BDNF- Brain derived growth factor. Experiments were repeated as three independent experiments with three replicates.

SH-SY5Y cells were grown in normal 10% FBS media and differentiated with 10 µM RA and 20 ng/ BDNF according to Encinas et.al (2000). SH-SY5Y cells were treated with 10 µM RA for 6 days and then treated with 20 ng/ BDNF for a further two days. Differentiated neurons with longer and more robust neurites were obtained as shown in Figure 4-1 A. To confirm the differentiated cells are more neuronal-like, crude cytosolic fractions of differentiated cells were Western blot analysed to observe β III tubulin expression which is a specific neuronal cell marker. In Figure 4-1 B showed representative images of undifferentiated and differentiated cells of SH-SY5Y and the expression of β III tubulin.

4.2.2 Determination of linear correlation between the optical signal and cell seeding density

Quantification of the linear range of MTT intensity for the SH-SY5Y cell line was important for optimising parameters for cells that would be subjected to neurological treatments. Linear correlation between the optical signal (OD signal at 570 nm) and the cell number was established using MTT assay for different cell densities. As depicted in Figure 4-2 A, OD increased with increasing cell density in a time-dependent manner and at higher densities the curve eventually flattened. At cell densities of 1x 10^4 - 3 x 10^4 cells showed a linear correlation between the optical signal (OD signal at 570 nm) and the cell number (Figure 4-2 B).



A

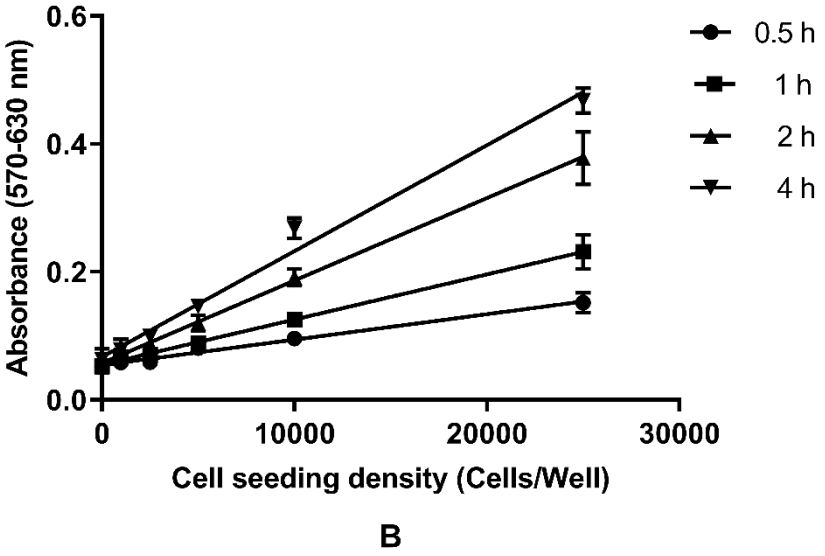


Figure 4-2: Direct correlation of absorbance and SH-SY5Y cell number. Determination of linear correlation between the optical signal and cell seeding density was done using MTT assay. Cell viability readings for each time point was obtained from one plate (A) SH-SY5Y cells were seeded at different cell concentrations ($1x10^3$-$7.3x10^4$) and MTT assay was performed to establish the linearity of signal at 4 different time points. (B) The graph illustrates the best signal can be obtained in log phase of cell growth phases after 4-hour incubation period (R^2= 0.9812). Viability readings were obtained from a total of 5 repeated plates for each time point with three replicates (n= 5). Results analysed using two-way ANOVA with Tukey's multiple comparison and expressed as the mean ± standard error of the mean (SEM). OD- Optical density.

Two-way ANOVA confirmed that there was a significant interaction between the cell number and time taken to develop the signal (p<0.0001). Also, there was a significant difference in all time points with 0.5 hours (p<0.0001) (Figure 4-3). According to the results revealed from two-way ANOVA and multiple mean comparisons by Tukey's multiple mean comparison test, all the treatments above 2.5 $x10^4$ cells/well resulted in a significant interaction between mean cell number and time taken to develop the signal. Optimal seeding density selection at the beginning of experiments of the most linear range of the standard curve ensured that the cells run over 24 hours would still be within the detectable region for MTT, without reaching the saturation point and the best signal can be obtained with a 4 h incubation period.

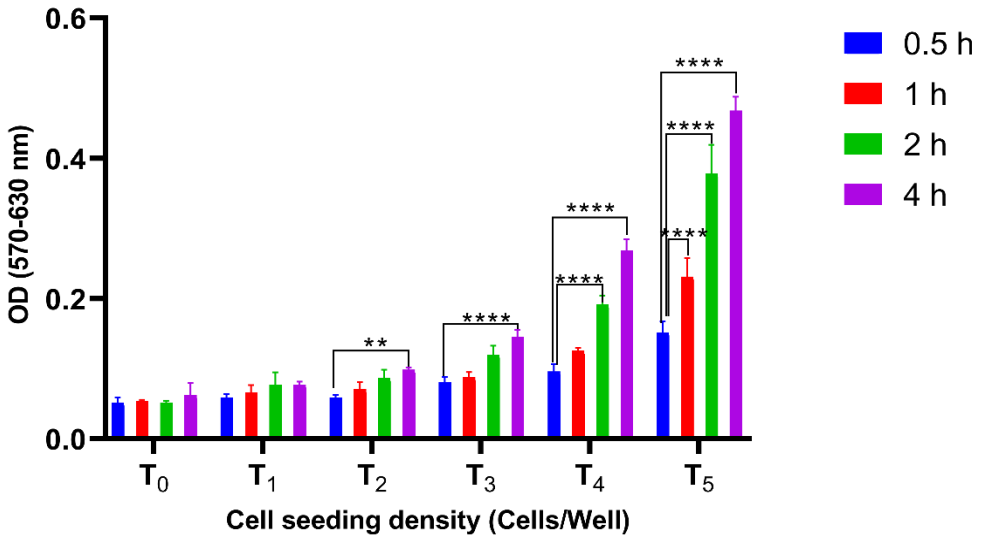


Figure 4-3: Mean comparison of two-way ANOVA results of MTT signal development with time in SH-SY5Y cells

Cell viability readings for each time point was obtained from one plate with different cell densities (1 x10^3 - 7.3 x10^4) and MTT assay. Viability readings were obtained from total of 5 repeated plates for each time point with three replicates (n=5). Results analysed using two-way ANOVA with Tukey's multiple comparison and expressed as the mean ± standard error of the mean (SEM); OD Optical density; For significance; ** p<0.01, **** p<0.0001.T_0 - No cells, T_1 - 1000, T_2 - 2500, T_3 -5000, T_4 - 10000, T_5 - 25000.

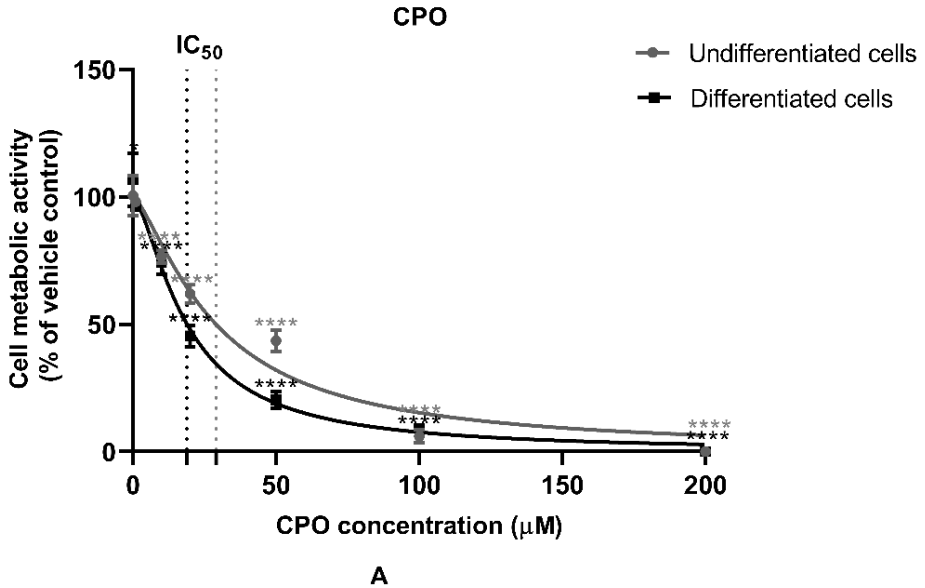
4.2.3 CPO, AZO and Aldicarb reduced cell viability in a concentration-dependent manner.

The impact of CPO, AZO and Aldicarb on the viability of undifferentiated and differentiated cells were determined using the MTT assay. Both phenotypes were exposed to 0, 1, 10, 20, 50, 100 and 200 µM concentrations for 24 h. Metabolic activities of the cultures were monitored by MTT assay at 24 h post-exposure as shown in Figure 4-4. The figure shows CPO, AZO and Aldicarb's influence on cell metabolic activity by curve exhibiting various degrees of deviation from 100% cell viability in a concentration-dependent fashion. Cell viability responses exhibit higher sensitivity for SH-SY5Y cells to CPO, AZO and Aldicarb at higher concentrations such as 50, 100 and 200 µM. The effect was dramatic at 200 µM concentration for both phenotypes with all three pesticides. Notably, 1 µM concentration only showed a significant increase in cell viability

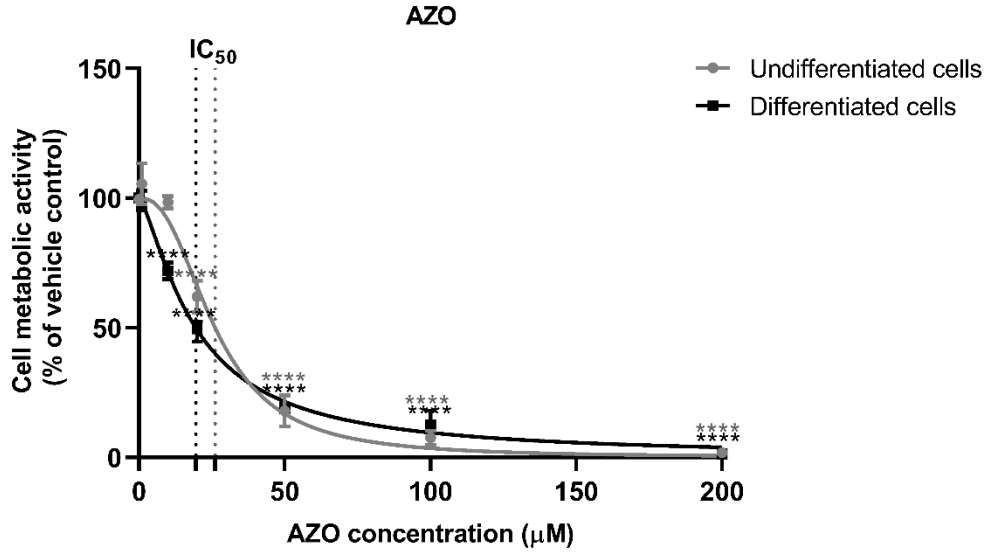
in undifferentiated cells for AZO that is about 5.4% increase compared to the vehicle control treatment, however, it is not statistically significant (p=0.3848), but there is no significant effect from CPO and Aldicarb on cell viability compared to vehicle controls. All three pesticides showed an initial significant decrease in cell viability from 10 µM except AZO treatment for undifferentiated cells. Furthermore, undifferentiated cells treated with 10 µM CPO, AZO and Aldicarb showed 23.9%, 1.08% and 17.6% decrease in cell viability, respectively. Differentiated cells do not exhibit significant toxic responses on cell viability at 1 µM compared to vehicle controls. Differentiated cells showed responses of metabolic rates and loss of cell viability at 10 µM concentration for CPO, AZO and Aldicarb as 10.5%, 26.6%, and 17.6%, respectively. This suggested that toxic responses are minimal until concentrations reach 10 µM, which is a threshold concentration for the three pesticides in both phenotypes. AZO shows more potent toxicity to differentiated cells than in undifferentiated cells at 10 µM (Table 4-5).

The concentration (dose)-response curves exhibit a sharp decrease in cell metabolic rates and viability loss after 10 µM for both phenotypes. Aside from 1 and 10 µM treatments for 24 h, similar concentration-dependent responses for both phenotypes were observed, with a slope of curves that became steeper as the dose continued to increase. Comparison of metabolic rates and viability loss responses of undifferentiated vs differentiated cells for 24 h exposure of CPO, AZO and Aldicarb showed a similar pattern of toxic responses for the three pesticides. Although there was a difference in metabolic activity and viability reduction induced by CPO (p<0.0001), AZO (p<0.0001) and Aldicarb (p<0.0001) that was significant between undifferentiated and differentiated cells (Table 4-5). Notably, undifferentiated cells were more resistant to the toxic effect of pesticides for 24 h exposure than differentiated cells. 50% inhibition

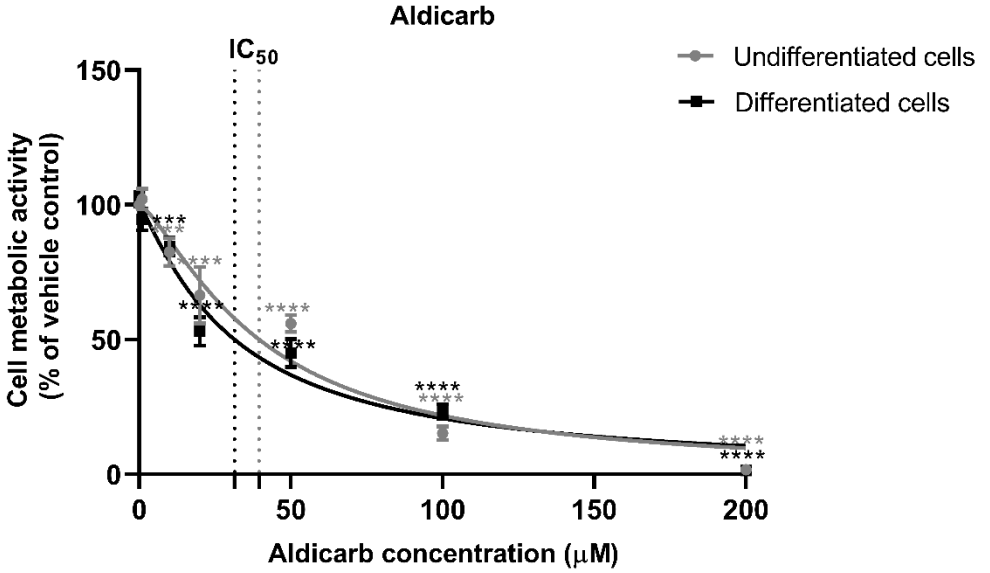
concentration (IC_{50}) values were interpolated from corresponding dose-response curves, and also confirmed that the potency of toxicity decreased as AZO>CPO>Aldicarb for undifferentiated cells and differentiated cells are more sensitive to toxicity (Table 4-1; Figure 4-5 A). However, CPO exerts more potent toxicity in differentiated cells compared to AZO and Aldicarb, where the order of toxic potency was descending as CPO>AZO>Aldicarb (Table 4-1; Figure 4-5 B). When comparing the toxic responses of undifferentiated and differentiated cells, each pesticide showed similar decreasing cell metabolic rates and loss of viability. Two way ANOVA showed there was a significant interaction between the pesticides and cell phenotype indicating differential sensitivity of pesticides (CPO, AZO and Aldicarb interaction was $p<0.0001$, $p<0.0001$ and $p<0.0007$, respectively) and Table 4-5 indicates the individual concentration comparison for both phenotypes where 200 µM concentration showed toxicity to both phenotypes without significant difference. Undifferentiated and differentiated cells exhibited a difference in toxic response at 1 and 10 µM treatments in AZO ($p<0.0001$) (Table 4-5).



A



B



C

Figure 4-4: Cell viability inhibition dose-response curves of CPO, AZO and Aldicarb on undifferentiated and differentiated SH-SY5Y cells.

Undifferentiated and differentiated cells were treated with CPO (A), AZO (B), and Aldicarb (C) for 24 h over the range of 1,10, 20, 50,100 and 200 μM. Viability was assessed using MTT assay. Readings were normalized to the viability of vehicle control, providing cell viability percentage, as a percentage value to the vehicle control. Readings were obtained from 5 individual experiments (n=5) with triplicates in each treatment. Results were analysed using one-way ANOVA with Dunnett's multiple comparison and expressed as the mean ± standard error of the mean (SEM). When SEM bar is not apparent, this means that error is smaller than the symbol size. For significance; ***p<0.001, ****p<0.0001.

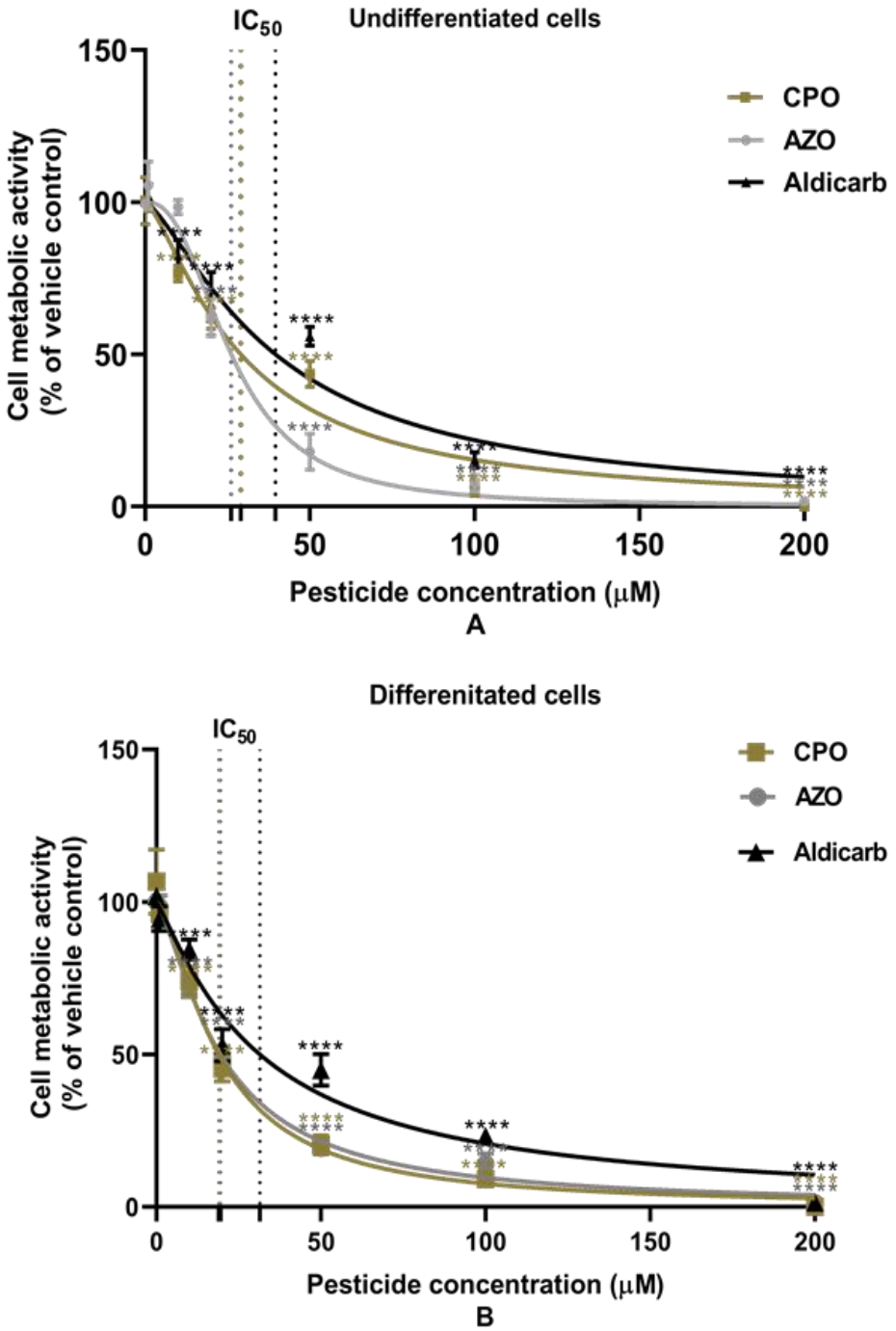


Figure 4-5: Cell viability inhibition dose-response curves of undifferentiated and differentiated SH-SY5Y cells

(A)- undifferentiated and (B)- differentiated cells were treated with CPO, AZO, and Aldicarb for 24 h over the range of 1,10, 20, 50, 100 and 200 µM. Viability was assessed using MTT assay. Readings were obtained from 5 individual experiments (n=5) with triplicates in each treatment. Results were analysed using one-way ANOVA with Dunnett's multiple comparison and expressed as the mean ± standard error of the mean (SEM). When SEM bar is not apparent, this means that error is smaller than the symbol size. For significance; ***p<0.001, ****p<0.0001.

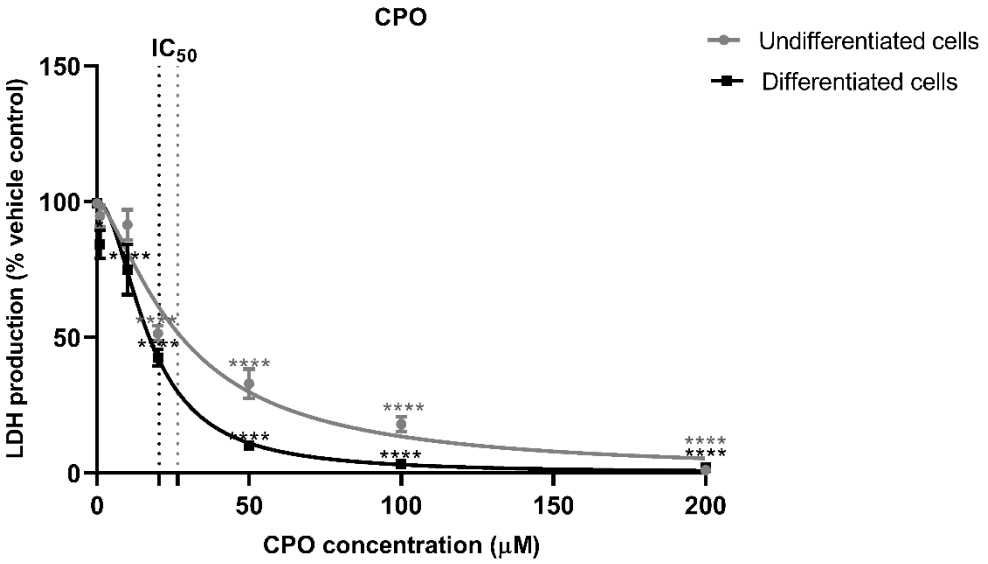
4.2.4 CPO, AZO and Aldicarb induced cytotoxicity in SH-SY5Y cells in a concentration-dependent fashion.

Although MTT assay can measure the cell viability of pesticide-treated cells by assessing the metabolic activity of cells, a change in metabolic activity could potentially reflect cytostatic activity induced by pesticides. Therefore, to gain more insight into cytotoxicity/cell death induced by pesticides on SH-SY5Y cells, an LDH assay was done. Both undifferentiated and differentiated cells were treated with 1,10, 20, 50,100, 200 µM concentrations of CPO, AZO and Aldicarb for 24 h and LDH assay were carried out using spent media as stated in the manufacturer's protocol. LDH assay shows the cytotoxicity of each pesticide, in turn, it indicates cell death upon pesticide exposure.

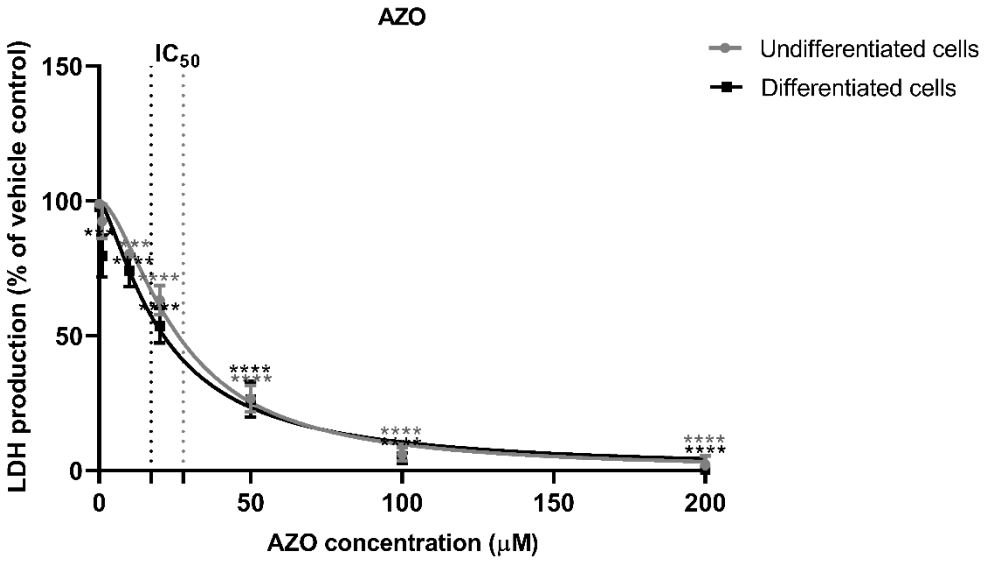
CPO, AZO and Aldicarb induced cytotoxicity of SH-SY5Y cells in a concentration-dependent manner as depicted in Figure 4-6. Cytotoxicity of higher concentrations such as 50,100, 200 µM in both undifferentiated and differentiated cells show a dramatic increase (Figure 4-6). There is no significant LDH production observed at 1 µM in undifferentiated cells compared to vehicle control treatments in all pesticide treatments, confirming 1 µM concentration is not cytotoxic to the undifferentiated cells in CPO, AZO and Aldicarb exposure (Figure 4-6). However, 1 µM increased LDH production in differentiated cells indicating that CPO (p=0.0013) (Figure 4-6 A) and AZO (p=0.0008) (Figure 4-6 B) induced cytotoxicity in differentiated cells even at 1 µM concentration, but there is no significant difference in Aldicarb (p=0.9428) (Figure 4-6 C) compared to the vehicle control treatments. 10 µM induced cytotoxicity by AZO (p=0.0006), except CPO and Aldicarb in undifferentiated cells. Therefore, this result suggested cytotoxicity response was minimal until 10 µM treatment of CPO and Aldicarb in undifferentiated cells, but AZO induced cytotoxicity starts significantly from 10 µM concentration which implies opposite behaviour to that

observed in MTT assays in undifferentiated cells. The potency of cytotoxicity descended as AZO>CPO>Aldicarb for undifferentiated cells. LDH production dose-repose curves in CPO, AZO and Aldicarb show a sharp rise after the 10 µM concentration suggesting 20 - 200 µM concentrations of all three pesticides induced potent toxicity in both phenotypes of SH-SY5Y cells. Nevertheless, the results revealed that the threshold concentration of cytotoxicity is 10 µM for both phenotypes of SH-SY5Y cells by CPO, AZO and Aldicarb, and after that there was a sharp rise in cytotoxicity observed for all pesticides in both phenotypes.

A comparison of undifferentiated cells vs differentiated cells for their cytotoxic responses towards the CPO, AZO and Aldicarb exposure (Table 4-5) showed that there is a significant interaction of pesticides exposure and cell phenotype for CPO (p<0.0001) and Aldicarb (p<0.0001) exposure, but there is no significant interaction on cell phenotypes and AZO exposure (p=0.1691). That suggests that AZO is a potent cytotoxic inducer in both phenotypes without a marked difference. However, similar results were recorded in MTT assay for undifferentiated cells showing more potent toxicity by AZO exposure than CPO and Aldicarb (Figure 4-7 A and Figure 4-5 A). According to Figure 4-7 B, CPO induced more potent cytotoxic responses in differentiated cells than AZO and Aldicarb. Therefore, undifferentiated cells demonstrated the potency of pesticides in descending order as AZO>CPO>Aldicarb (Figure 4-7 A) whereas in differentiated cells it is CPO>AZO>Aldicarb (Figure 4-7 B) (Table 4-1 and 4-5). IC_{50} values for each pesticide that induced 50% cell death were interpolated from the corresponding LDH concentration-response curve (Table 4-1) indicate that CPO can exert more toxicity than other pesticides on differentiated cells.


CPO
Undifferentiated cells
Differentiated cells
IC50
LDH production (% vehicle control)
150
100
50
0
0
50
100
150
200
CPO concentration (μM)

A


AZO
Undifferentiated cells
Differentiated cells
IC50
LDH production (% of vehicle control)
150
100
50
0
0
50
100
150
200
AZO concentration (μM)

B

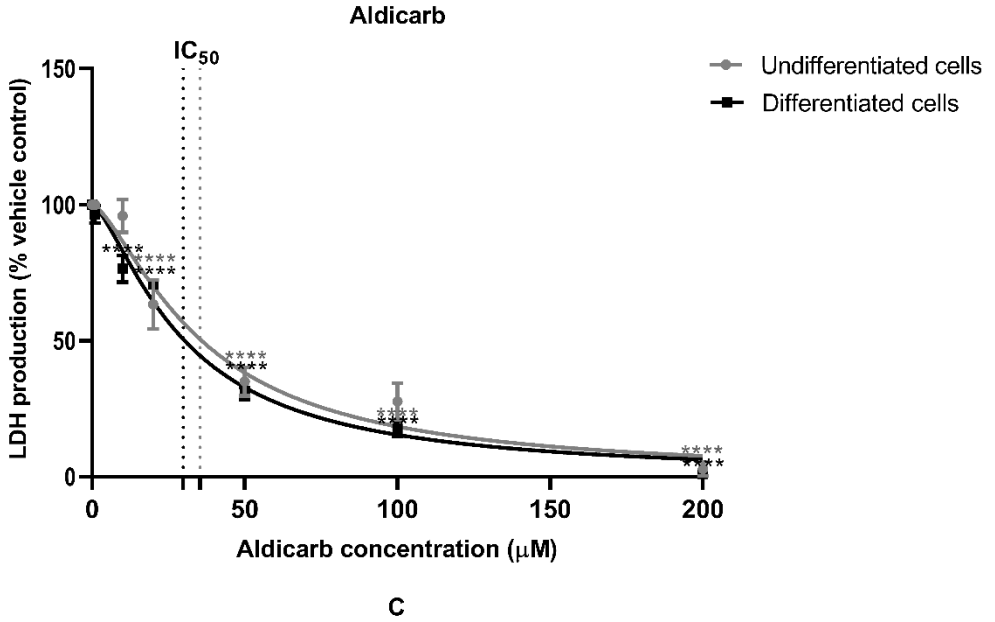


Figure 4-6: Cytotoxicity of CPO, AZO and Aldicarb on SH-SY5Y cells determined by LDH assay.

Undifferentiated and differentiated cells were treated with (A) CPO, (B) AZO, and (C) Aldicarb for 24 h over the range of 1 ,10, 20, 50, 100 and 200 µM. LDH production was assessed using LDH cytotoxicity assay. Readings were normalized to the viability of vehicle control, providing LDH production percentage, as a percentage value to the vehicle control. Vehicle control and treatments were performed as triplicates in 5 individual experiments (n=5). Results were analysed using one-way ANOVA with Dunnett's multiple comparison and expressed as the mean ± standard error of the mean (SEM), when SEM bar is not apparent, this means that error is smaller than the symbol size. For significance; ****p*<0.001, *****p*<0.0001.

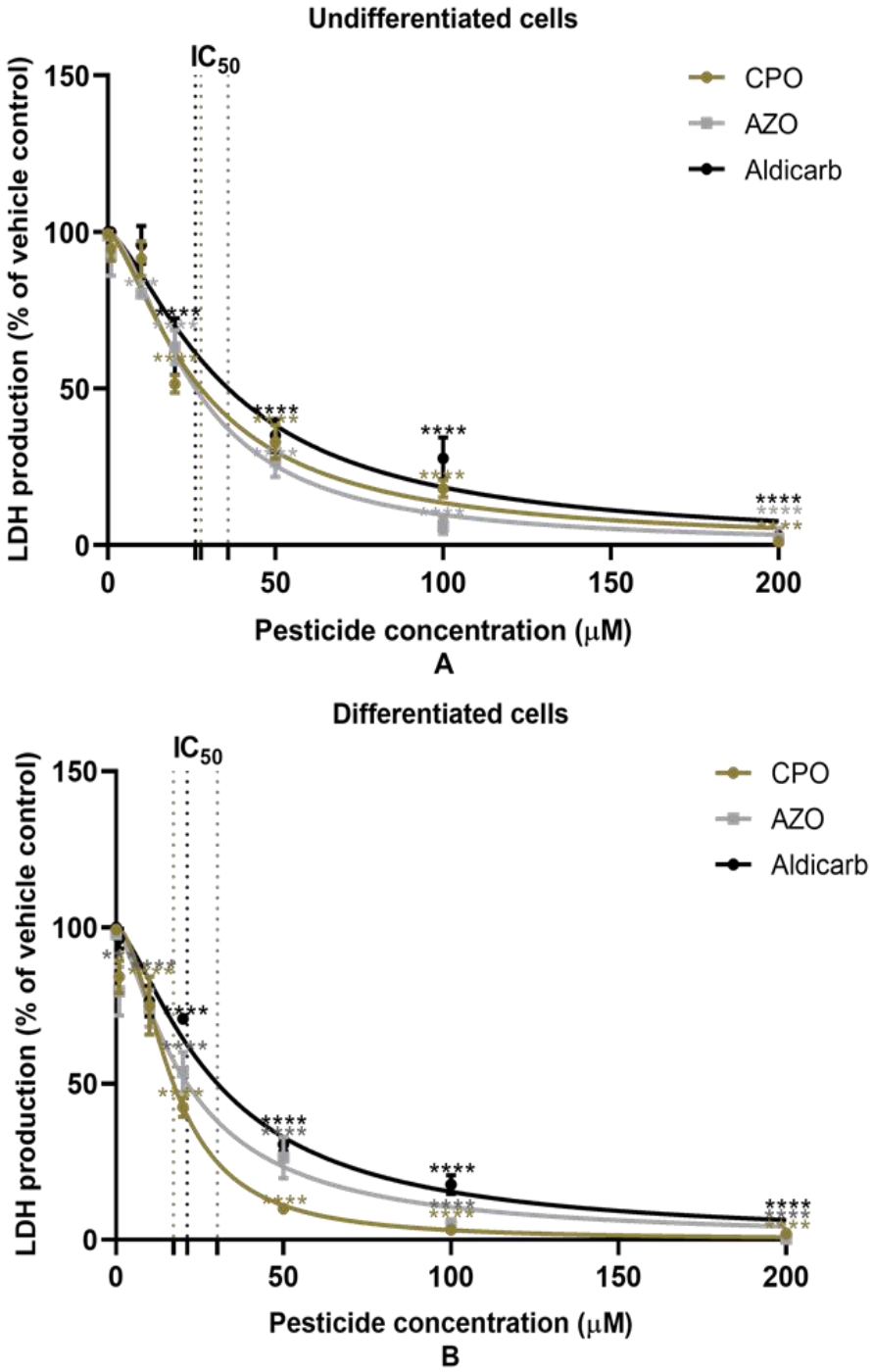


Figure 4-7: Cytotoxicity of undifferentiated and differentiated SH-SY5Y cells assessed by LDH assay.

(A)- undifferentiated and (B)- differentiated cells were treated with CPO, AZO, and Aldicarb for 24 h over the range of 1,10, 20, 50,100 and 200 µM. LDH production was assessed using LDH cytotoxicity assay. Readings were normalized to the viability of vehicle control, providing LDH production percentage, as a percentage value to the vehicle control. Vehicle control and treatments were performed as triplicates in 5 individual experiments (n=5). Results were analysed using one-way ANOVA with Dunnett's multiple comparison and expressed as the mean ± standard error of the mean (SEM), When SEM bar is not apparent, this means that error is smaller than the symbol size. For significance; ***p<0.001, ****p<0.001.

4.2.5 Morphological observation of CPO, AZO and Aldicarb treated cells

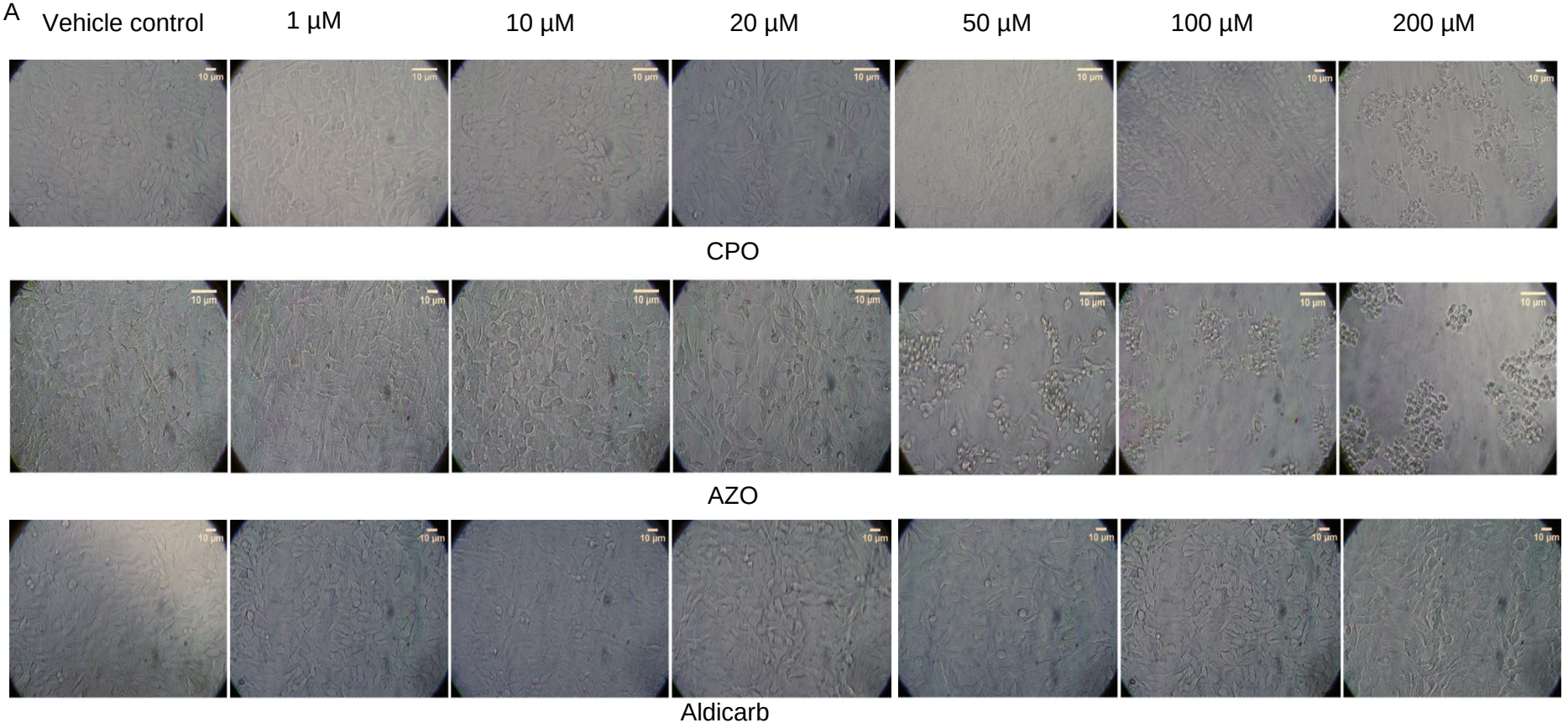
Cells exposed to CPO, AZO or Aldicarb were observed under phase-contrast microscopy to gain an insight into the morphological differences in cells after a 24 h exposure. Figure 4-8 (A-B) showed the undifferentiated cells and differentiated cells exposed to pesticides after 24 hours. Images clearly showed a concentration-dependent increase in cytotoxicity of pesticides. Cell shrinkage and decrease in cell number and loss of cell contacts was observed when the concentration of pesticides increased. However, neurite retraction was observed in differentiated cells as a morphological impairment by CPO, AZO and Aldicarb exposure for 24 h.

4.2.6 CPO, AZO and Aldicarb reduced neurite outgrowth of pre-differentiated SH-SY5Y cells.

To investigate the impact of CPO, AZO and Aldicarb on neurite outgrowth in pre-differentiated SH-SY5Y cells, cells were exposed to 0-200 µM concentrations at the same time of induction of cell differentiation as explained by (Raghunath et al., 2000). This method is known as co-differentiation (Flaskos, 2011). Cells were allowed to differentiate with CPO, AZO and Aldicarb and after 24 h images were captured using the phase-contrast microscope (Olympus, DP70, London, UK) in high resolution with maximum power (40 X), and neurite lengths were measured by neurite tracer tool using Image J (Image J 1.49k, National Institute of Health, USA).

The images showed that the absence of pesticides had typical cell morphology of pre-differentiated cells with cell body and long extending processes. After exposure of different concentrations of CPO, AZO and Aldicarb, inhibition of

A


Vehicle control
1 µM
10 µM
20 µM
50 µM
100 µM
200 µM
CPO
AZO
Aldicarb

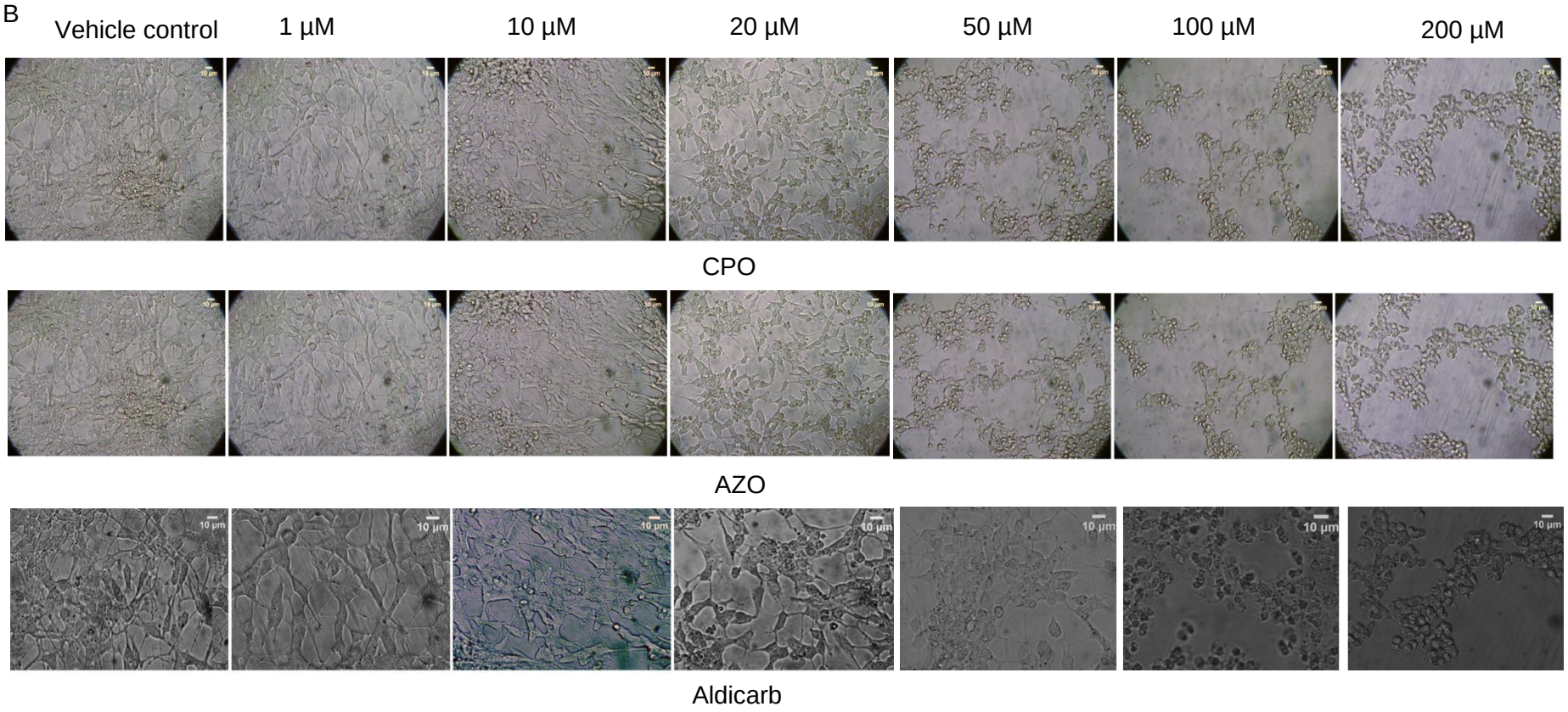


Figure 4-8: Morphological observation of CPO, AZO, Aldicarb exposure to cells for 24 h.
A-undifferentiated cells; B-differentiated cells. Image were taken from Olympus phase contrast microscope after 24 h. Scale bar-10 µM.

Table 4-1: Toxicity of CPO, AZO and Aldicarb to undifferentiated and differentiated SH-SY5Y cells.

Cell type	Pesticides	MTT assay		LDH assay		ATP assay		50% Neurite retraction		AChE inhibition	
		IC_{50} (µM)	R^2	IC_{50} (µM)	R^2	IC_{50} (µM)	R^2	IC_{50} (µM)	R^2	IC_{50} (µM)	R^2
Undifferentiated	CPO	29.39 ± 2.1	0.9702	27.75 ± 2.1	0.9713	29.57 ± 2.1	0.9561	N/A	-	0.2757 ± 0.0	0.9955
Differentiated		17.30 ± 0.9	0.9866	17.15 ± 1.1	0.9672	18.84 ± 0.1	0.9988	10.84 ± 0.1	0.9135	0.1916 ± 0.00	0.9873
Undifferentiated	AZO	26.85 ± 1.1	0.9870	26.50 ± 0.9	0.9923	25.98 ± 0.6	0.9948	N/A	-	0.2968 ± 0.01	0.9919
Differentiated		19.63 ± 0.5	0.9956	20.45 ± 1.6	0.9539	20.69 ± 0.1	0.9996	16.48 ± 1.3	0.8939	0.2195 ± 0.00	0.9861
Undifferentiated	Aldicarb	39.55 ± 3.6	0.9506	35.38 ± 1.4	0.9897	40.17 ± 2.9	0.9452	N/A	-	0.6189 ± 0.04	0.9672
Differentiated		31.60 ± 2.2	0.9733	29.91 ± 1.6	0.9811	32.44 ± 1.2	0.9870	30.18 ± 4.7	0.7026	0.3792 ± 0.02	0.9702

IC_{50}- 50% inhibition concentration, all values are interpolated from corresponding concentration-response curves and expressed as means ± 95% confidence interval in five independent experiments. MTT- (4,5-dimethylthiazol-2-yl)-2,5-diphenyltetrazolium bromide, LDH- Lactate dehydrogenase, ATP-Adenosine triphosphate, AChE- Acetylcholinesterase. N/A- not applicable for undifferentiated cells.

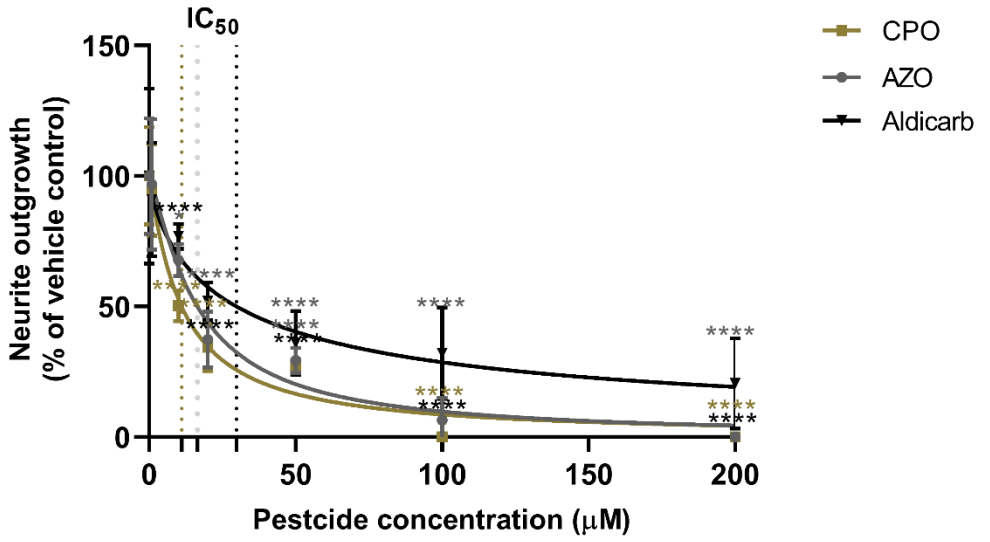
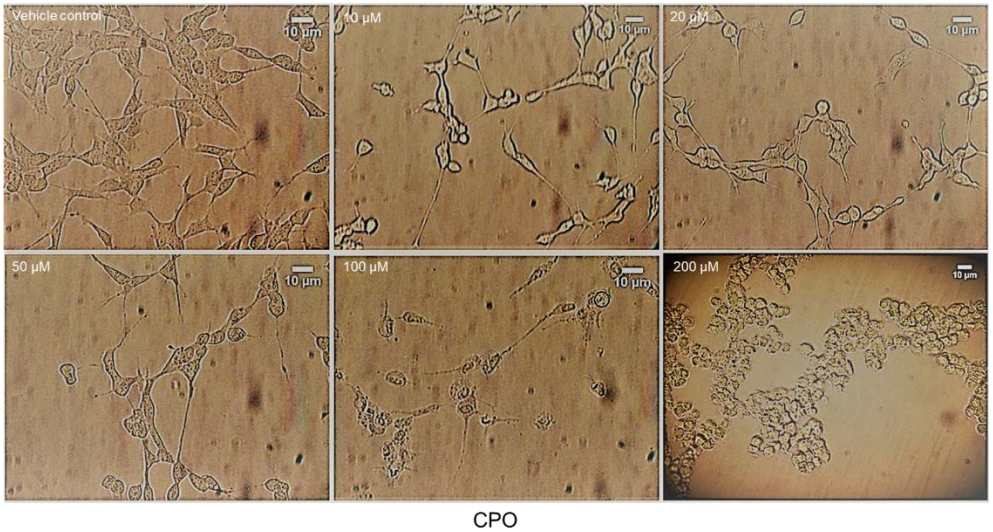


Figure 4-9: Quantitative analysis of the effect of CPO, AZO and Aldicarb on neurite out growth.
SH-SY5Y cells were induced to differentiate for 24h with 0 - 200 µM concentrations of CPO, AZO and Aldicarb for 24 h. Images were captured from a phase contrast microscope and neurite lengths were quantified using neurite tracer tool in ImageJ. Data are expressed as mean lengths per 200 cells and normalised to the lengths of vehicle control treatments and expressed as a percentage to the vehicle controls of five independent experiments with three replicates in each treatment (n=5). Results were analysed using one-way ANOVA with Dunnett's multiple comparison and expressed as the mean ± standard error of the mean (SEM), when SEM bar is not apparent, this means that error is smaller than the symbol size. For significance; *p<0.05, ****p<0.0001.

Neurite outgrowth was apparent compared to vehicle control treatments (Figure 4-10). However, alteration of neurite outgrowth was more pronounced in CPO treated cells compared to AZO and Aldicarb treated cells after a 24 h exposure. There was a dramatic increase in neurite outgrowth inhibition compared to vehicle control treatments when the pesticide concentration continues to increase. These findings were further confirmed by quantitative analysis of the effects of each pesticide on neurite outgrowth as depicted in Figure 4-9, which showed a significant reduction of neurite outgrowth of pre-differentiated cells in a concentration-dependent manner by CPO, AZO and Aldicarb exposure. However, there was no significant neurite length outgrowth inhibition in 1 µM treatments for CPO (p=0.7343), AZO (p=0.9899) and Aldicarb (p=0.7668) compared to vehicle control treatments. Neurite length retraction was significant

at 10 µM concentrations for all pesticides, and the curve gets steeper when concentration continues to increase. However, there were no apparent neurites in 200 µM treatments for CPO and AZO exposure, while there was a significant reduction of neurite lengths in remaining cells exposed to Aldicarb at 200 µM treatment. These results suggested that 1 µM is the threshold concentration that induced neurite inhibition of all pesticides. The results of MTT and LDH assay demonstrated that 200 µM induced a dramatic loss of cell viability and cell death and this proves cell lose their contacts before losing their viability.

There is significant interaction (p=0.0031) between each pesticide treatment and induction of neurite inhibition in pre-differentiated cells as showed using a two-way ANOVA, and the potency of toxicity descended as CPO>AZO> Aldicarb. There was no significant difference between CPO and AZO (p=0.1779) but Aldicarb showed a significant difference (p<0.0001) compared with CPO and AZO on neurite inhibition in pre-differentiated SH-SY5Y cells. There was no significant difference between the AZO and CPO for inducing neurite outgrowth pre-differentiated cells as revealed by two-way ANOVA. IC_{50} values were interpolated from dose-response curves and showed that CPO had the lowest values (Table 4-1).



CPO

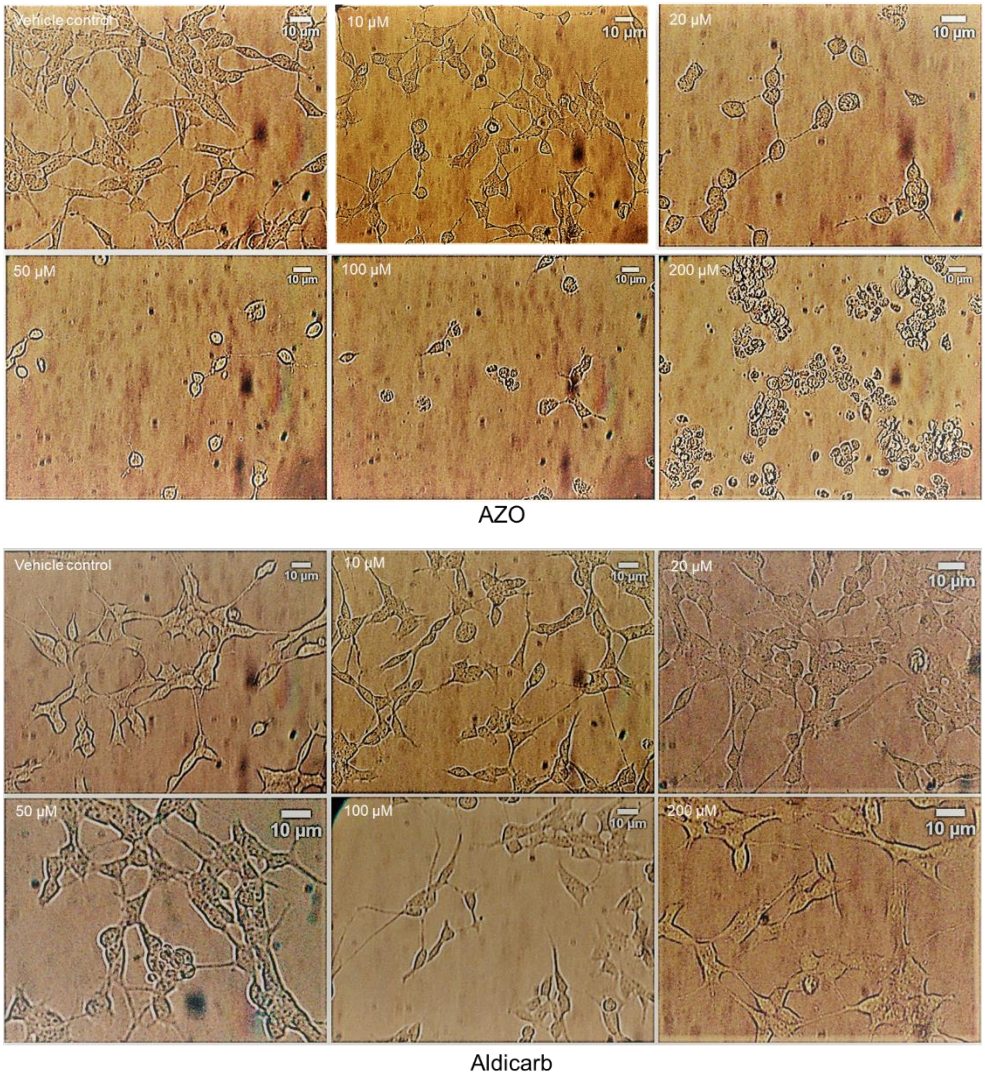


Figure 4-10: Effect of CPO, AZO and Aldicarb on pre-differentiated SH-SY5Y cells.
SH-SY5Y cells were induced to differentiate for 24 h with CPO, AZO and Aldicarb over the range of 0 - 200 µM. The morphological changes were captured with phase-contrast microscopy and neurite lengths were quantified using the neurite tracer tool in ImageJ from five independent experiments with three replicates.

4.2.7 Effect of CPO, AZO and Aldicarb on AChE inhibition in SH-SY5Y cells

To gain insight into AChE inhibition in SH-SY5Y cells exposed to CPO, AZO, and Aldicarb for 24 h, a modified Ellman's assay was used as explained in Flaskos et al. (2007), adapted for microtiter plates. Assay linearity with reaction

time and the amount of sample volume was established before the assay and 100 µl extracted cell sample was used for the assay (Figure 4-11). Figure 4-11 indicates that there was a significant difference in the linearity of signal in undifferentiated and differentiated cells, and 150 µl volume showed absorbance that reached up to maximum value after limited reagents in the reaction. On that basis, 100 µl volume of cells was selected for the study.

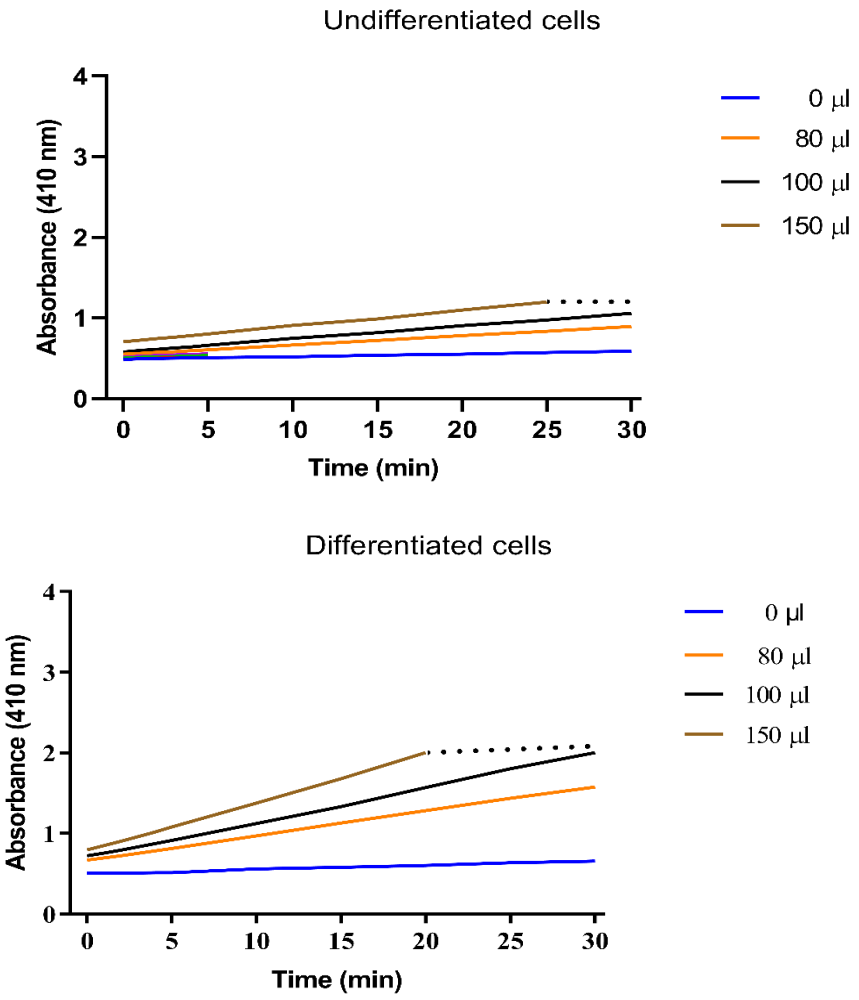
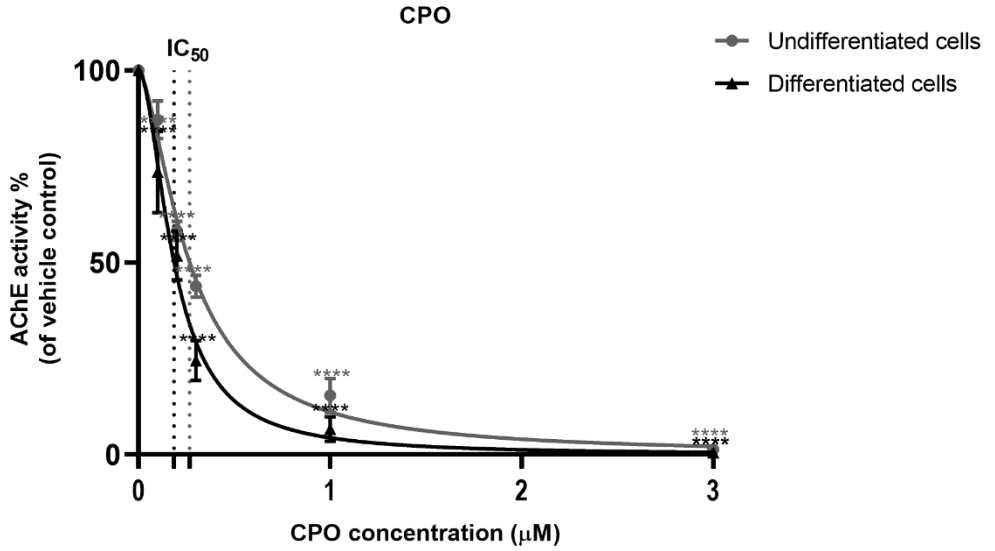


Figure 4-11: Assay linearity with the reaction and cell sample volume for Sh-SY5Y cells.
Figure shows the absorbance versus the reaction (time) for each different volume of cell samples in undifferentiated and differentiated cells. AChE activity was measured by Ellman's assay. Points represent the five independent experiments with three replicates each sample (n=5).

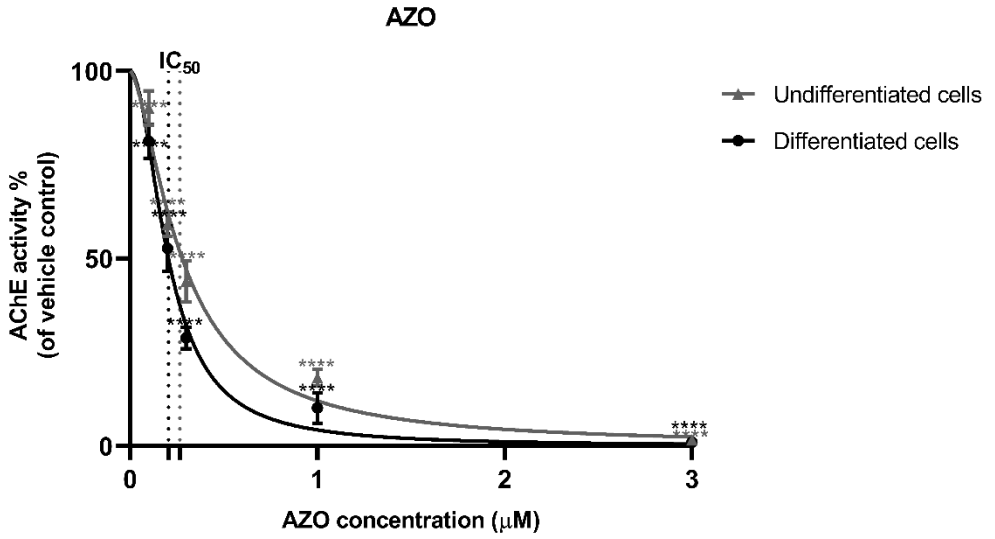
CPO, AZO and Aldicarb showed different patterns of inhibition of AChE in SH-SY5Y cells as depicted in Figure 4-12. CPO, AZO and Aldicarb induced a significant reduction of AChE activity in both undifferentiated and differentiated cells within 24 h exposure in a concentration-dependent fashion. The inhibition started from nanomolar concentrations as shown in Figure 4-12. After a 24 h exposure at 0.1 µM, CPO, AZO and Aldicarb showed a significant reduction in AChE compared to non-pesticide treated controls (p<0.0001) in both undifferentiated and differentiated cells. At 0.1 µM treatment, undifferentiated cells showed 16.7%, 12. 51% and 8.5 % inhibition by CPO, AZO and Aldicarb, respectively (Figure 4-12). Differentiated cells showed 29.7%, 22.06% and 9.5% inhibition by CPO, AZO and Aldicarb, respectively. Aldicarb induced 18.8% AChE inhibition in undifferentiated cells and 36.2% in differentiated cells at 0.2 µM treatment. CPO and AZO induced more than 20% inhibition at 0.2 µM compared to non-treated controls in both phenotypes. However, inhibition accelerated until 1 µM before the curve begins to plateau at 1-3 µM range, suggesting that complete inhibition of AChE at higher concentrations by all three pesticides. IC_{50} values were interpolated from concentration-response curves of both undifferentiated and differentiated cells and were nanomolar levels in the range between 200 nM-700 nM for the three pesticides (Table 4-1).

Comparison of each pesticide for undifferentiated and differentiated cells showed that there was a significant interaction between pesticide and cell phenotypes (CPO (p<0.0001), AZO (p<0.0001) and Aldicarb (p=0.0003). A comparison of the three pesticides on individual cell phenotypes showed an interaction, implying each pesticide has a selective effect on AChE inhibition (Table 4-6). However, there was no significant difference in inhibition of AChE between CPO and AZO (p>0.9999) but a significant difference (p<0.0001) with Aldicarb for undifferentiated cells indicating the potency of toxicity descending

as CPO>AZO>Aldicarb. CPO, AZO, and Aldicarb induced AChE inhibition in differentiated cells without any significant differences when a comparison was made between the pesticides.



A



B

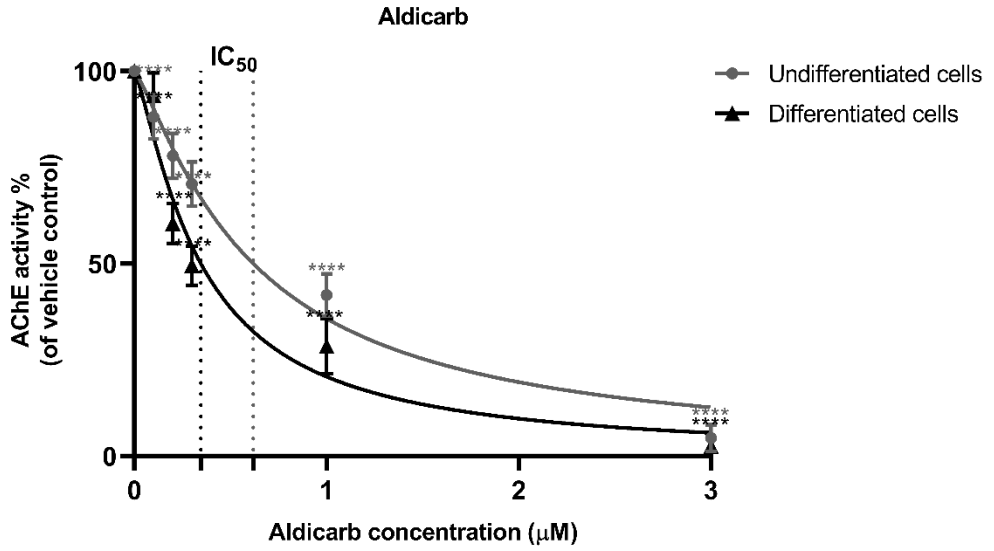


Figure 4-12: Effect of CPO, AZO and Aldicarb on inhibition of AChE in SH-SY5Y cells.

Undifferentiated and differentiated cells were treated with CPO (A), AZO (B) and Aldicarb (C) for 24 h over the range of 0.1 - 3 µM. AChE activity was measured by Ellman's assay and the readings were normalised to the vehicle control values by subtracting the blank values and expressed as percentages to the corresponding vehicle control. Readings obtained from 5 individual experiments (n=5) with three replicates in each treatment. Results were analysed using one-way ANOVA with Dunnett's multiple comparison and expressed as the mean ± standard error of the mean (SEM), when SEM bar is not apparent, this means that error is smaller than the symbol size. For significance; **** p<0.0001.

4.2.8 CPO, AZO and Aldicarb decreased cellular ATP levels.

To gain insight into the impact of low dose responses of CPO, AZO, and Aldicarb on cellular functions in SH-SY5Y cells, an ATP assay was performed. First IC_{50} values of MTT and LDH assays were compared and IC_{10}, IC_{20}, $IC_{50,}$ and IC_{80} concentrations selected for the subsequent experiments.

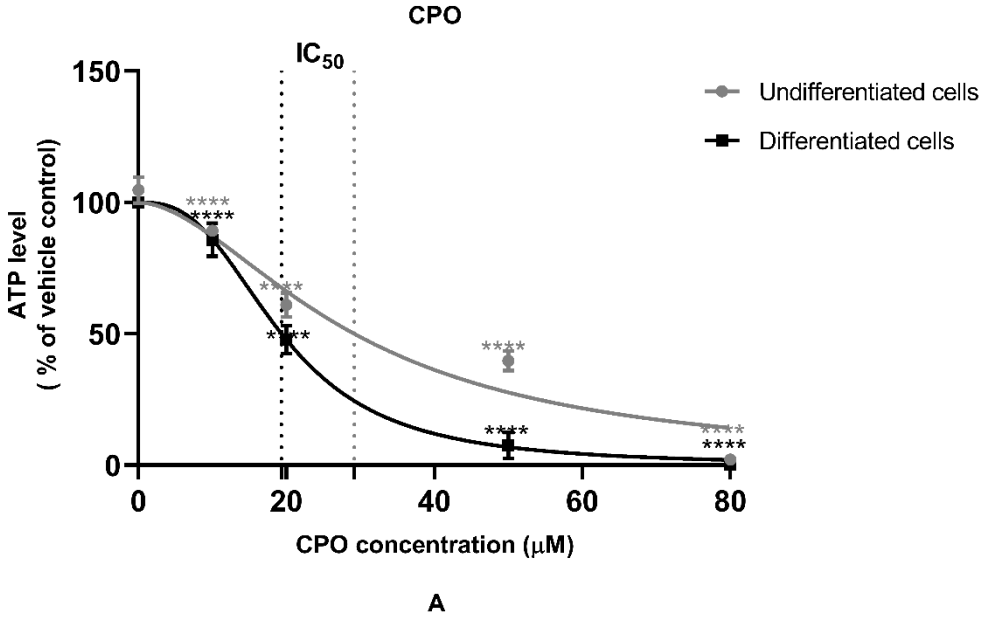
Table 4-2: 10, 20, 50 and 80% inhibition concentrations interpolated from concentration-response curves.

	Pesticides			
Cell type	IC value (µM)	CPO (µM)	AZO (µM)	Aldicarb (µM)
Undifferentiated	IC_{10}	07	11	08
	IC_{20}	11	15	14
	IC_{50}	29	27	40
	IC_{80}	75	46	108
Differentiated	IC_{10}	04	04	05
	IC_{20}	08	07	10
	IC_{50}	17	20	32
	IC_{80}	44	52	99

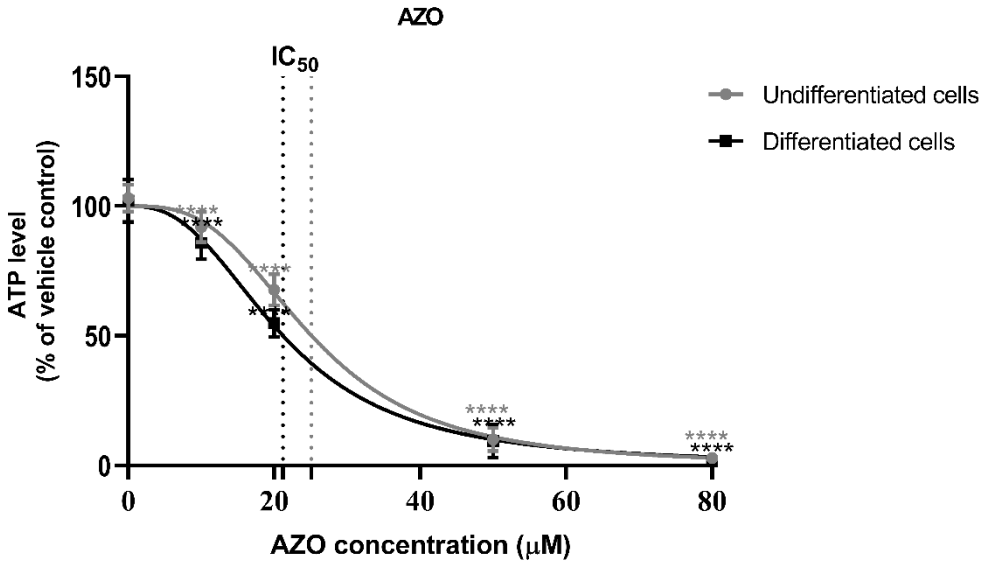
IC_{10}- 10%, inhibition concentration; IC_{20}- 20 % inhibition concentration; IC_{50}-50% inhibition concentration; IC_{80}- 80% inhibition concentration

The cell metabolic activity/cell viability measured by MTT assay proved that there was a concentration-dependent decrease in metabolic activity with pesticides. This MTT assay relies upon the mitochondrial function of cells, as the viability measurement is based on mitochondrial NAD(P)H-dependent cellular oxidoreductase enzymes. Since one of the major function of mitochondria is ATP production, then IC_{10}, IC_{20}, IC_{50} and IC_{80} concentrations were treated to both undifferentiated and differentiated cells for 24 h to verify the dose-dependent cell viability loss and to gain insight into the impact of CPO, AZO and Aldicarb on cellular ATP production.

Similar to the cell viability assays, CPO, AZO and Aldicarb induced a concentration-dependent decrease in cellular ATP levels in SH-SY5Y cells. Figure 4-13 illustrated cellular ATP level changes with pesticide exposure in SH-SY5Y cells for 24h.


CPO
IC50
Undifferentiated cells
Differentiated cells
ATP level
(% of vehicle control)
150
100
50
0
0
20
40
60
80
CPO concentration (μM)

A


AZO
IC50
Undifferentiated cells
Differentiated cells
ATP level
(% of vehicle control)
150
100
50
0
0
20
40
60
80
AZO concentration (μM)

B

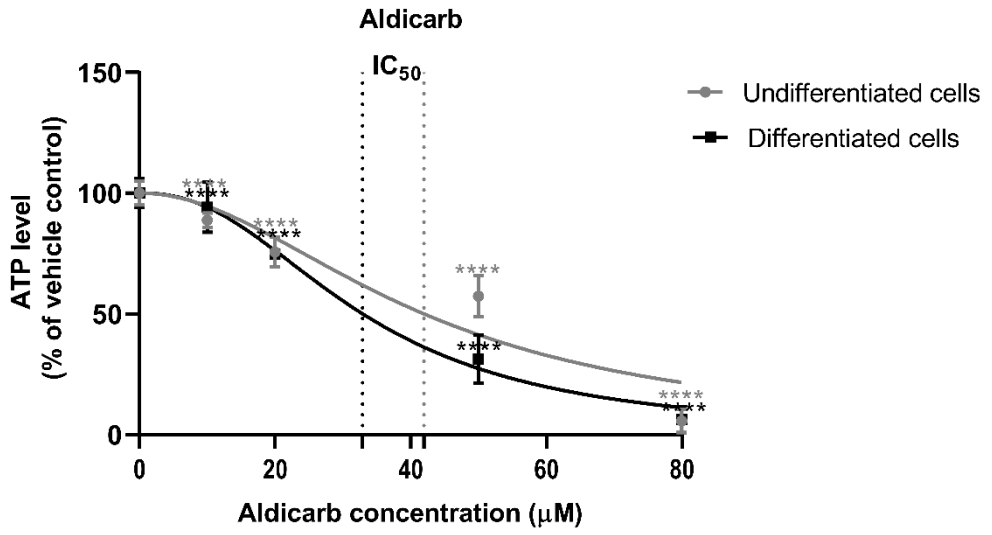


Figure 4-13: Effect of CPO, AZO and Aldicarb on cellular ATP level of SH-SY5Y cells.

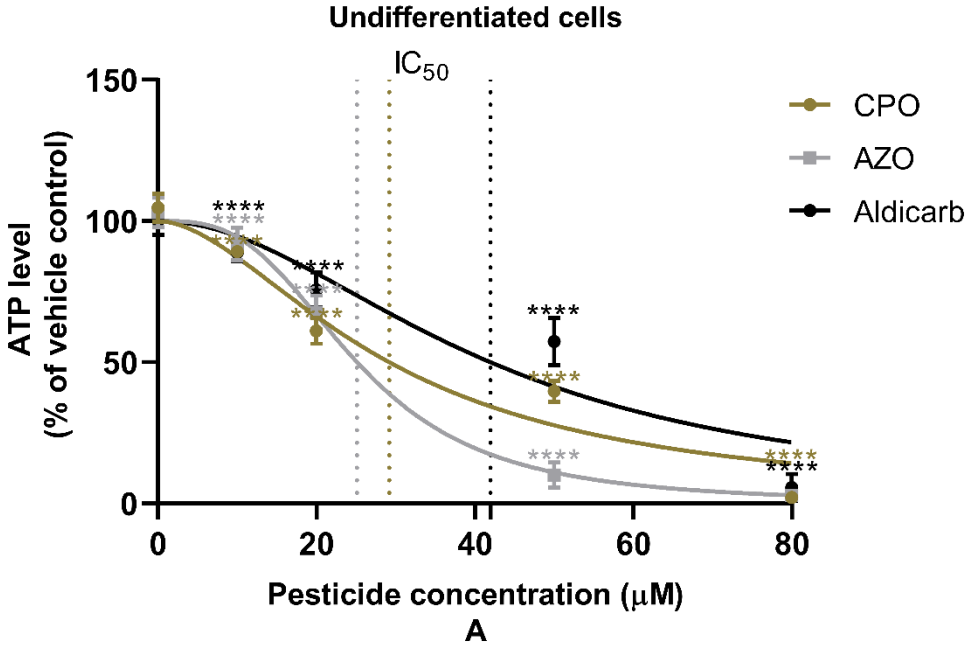
Undifferentiated and differentiated cells were exposed IC_{10}, IC_{20}, IC_{50}, and IC_{80} concentrations of CPO (A), AZO (B), and Aldicarb (C) for 24 h. Cellular ATP levels were measured using an ATP assay and the resultant values normalised to vehicle control treatments and presented as a percentage of vehicle control. Readings were obtained from 5 individual experiments (n=5) with triplicates in each treatment. Results were analysed using one-way ANOVA with Dunnett's multiple comparison and expressed as the mean ± standard error of the mean (SEM). When SEM bar is not apparent, this means that error is smaller than the symbol size. For significance; **** p <0.0001.

IC_{10}, IC_{20}, IC_{50} and IC_{80} concentrations influenced cellular ATP levels, and exhibited various degrees of deviation from 100% vehicle control treatments. However, cellular ATP levels dropped significantly starting from IC_{10} concentration and generated a curve that got steeper indicating IC_{20}, IC_{50}, IC_{80} concentrations significantly affected cellular ATP levels in both phenotypes of SH-SY5Y cells, as in MTT and LDH assays. The IC_{80} concentration of CPO, AZO and Aldicarb showed the greater impact on cellular ATP levels (Figure 4-13).

However, the MTT viability curve indicates there is a minimal effect on viability until 10 µM on undifferentiated cells, but cellular ATP levels start to drop in CPO and Aldicarb at 7 and 8 µM concentration. AZO induced significant ATP level drop in undifferentiated cells compared to non-treated controls at 11 µM,

supporting the MTT assay results that it induced significant viability loss in cells at a higher concentration than 10 µM. This consideration is consistent with the LDH assay results, 10 µM induced a significant LDH increase after AZO exposure to undifferentiated cells but this was not observed for CPO or Aldicarb. This suggests that CPO, AZO and Aldicarb alter cellular ATP levels at concentrations slightly lower than those that induce a significant loss of cell viability and cell death in undifferentiated cells.

Comparison of the ATP level drop in differentiated cells upon CPO, AZO, and Aldicarb exposure contextualized that the drop in cellular ATP levels is inconsistent with the results of MTT and LDH assay. This showed that significant viability loss and cell death in differentiated cells was apparent even at 10 µM. In line with that, significant ATP level reduction was apparent at 4, 4 and 5 µM pesticide concentrations for CPO, AZO, and Aldicarb, respectively.



A

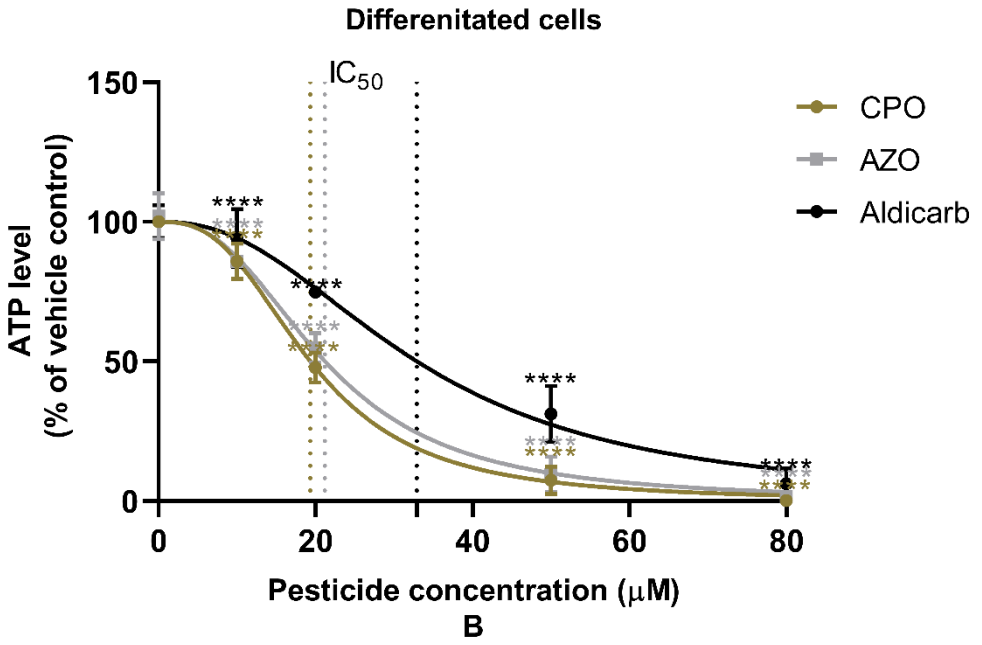


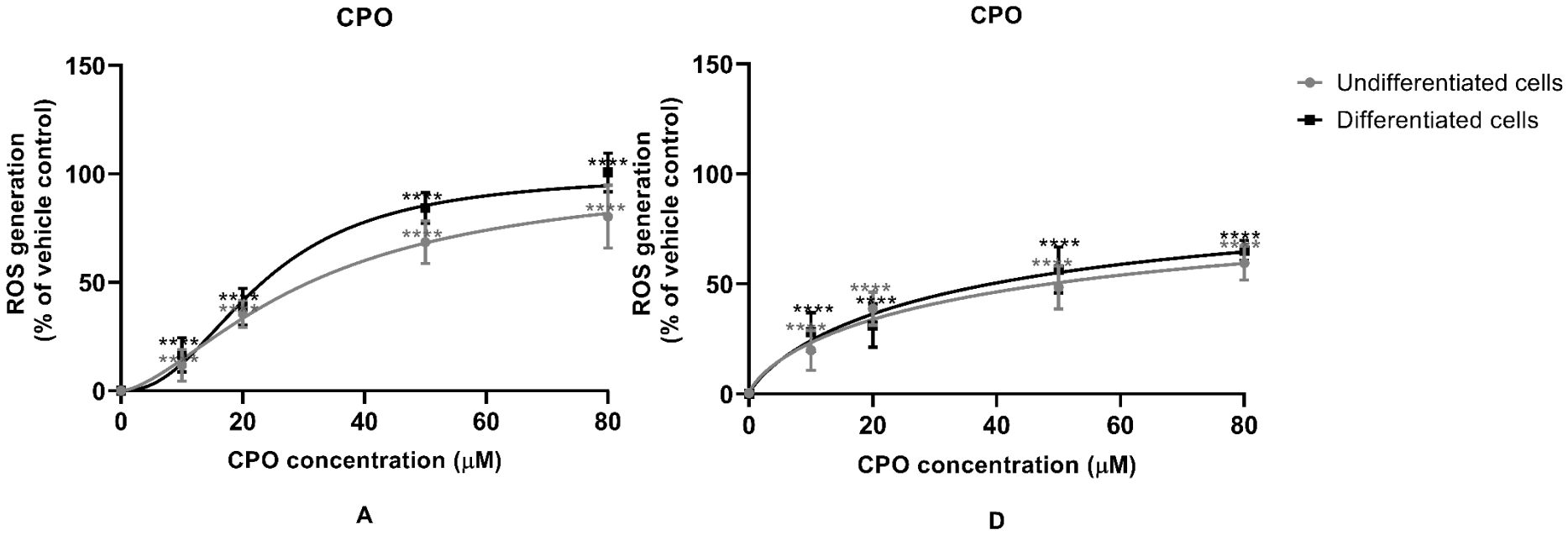
Figure 4-14: Effect of CPO, AZO and Aldicarb on ATP levels in undifferentiated and differentiated SH-SY5Y cells.
A- Undifferentiated and B- differentiated cells were exposed IC_{10}, IC_{20}, IC_{50}, and IC_{80} concentrations of CPO, AZO, and Aldicarb for 24 h. Cellular ATP levels were measured using an ATP assay and the resultant values normalised to vehicle control treatments and presented as a percentage of vehicle control. Readings were obtained from 5 individual experiments (n=5) with triplicates in each treatment. Results were analysed using one-way ANOVA with Dunnett's multiple comparison and expressed as the mean ± standard error of the mean (SEM). When SEM bar is not apparent, this means that error is smaller than the symbol size. For significance; **** p<0.0001.

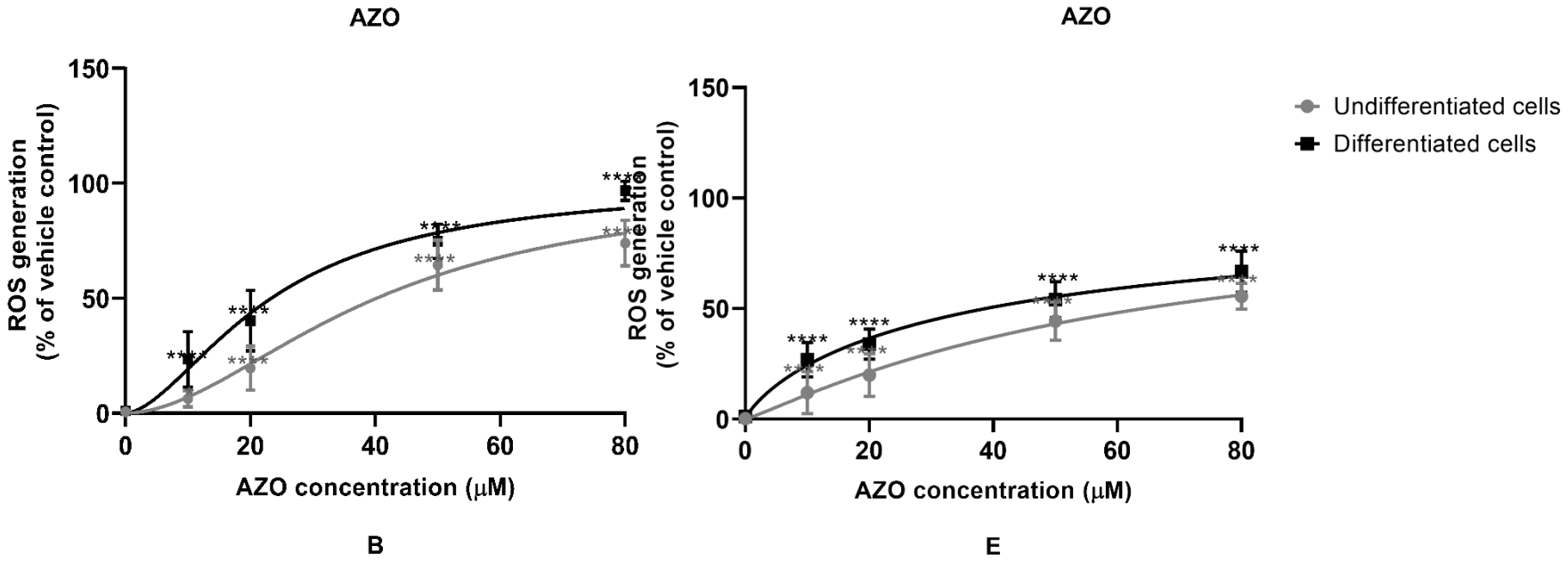
According to the graph, significant ATP levels dropped in the order AZO>CPO>Aldicarb for undifferentiated cells (Figure 4-14 A). In line with the MTT and LDH data, for differentiated cells the order of potency of pesticides for induction of reduced ATP levels was CPO>AZO>Aldicarb (Figure 4-14 B). However, there was a significant interaction with CPO, AZO, and Aldicarb exposure and the impact on cellular ATP levels revealed by two-way ANOVA and Tukey's multiple comparisons of each concentration on both cell phenotypes (Table 4-5).

4.2.9 CPO, AZO, and Aldicarb induced ROS generation in SH-SY5Y cells.

Next, to gain insight into oxidative stress induced by CPO, AZO, and Aldicarb in SH-SYY cells, intracellular ROS generation was quantified by exposing cells to IC_{10}, IC_{20}, IC_{50} and IC_{80} pesticide concentrations. ROS have a relatively short half-life and cells were incubated for both 6 h and 24 h time points for this reason. Both undifferentiated and differentiated cells were treated with IC_{10}, IC_{20}, IC_{50}, and IC_{80} concentrations of CPO, AZO, and Aldicarb for 6 h and 24 h to quantify the ROS generation by a DCFDA assay. The ROS generated with increasing concentrations of CPO, AZO, and Aldicarb at 6 h and 24 h time points are depicted in Figure 4-15.

Concentration-dependent ROS generation was observed in both cell phenotypes exposed to CPO, AZO and Aldicarb for 6 h (Figure 4-15 A-C) and 24 h (Figure 4-15 D-E). All concentrations induced significant (p<0.05) ROS production compared to their untreated control in both 6 h and 24 h. However, the comparison of 6 h and 24 h ROS generation indicates that CPO, AZO and Aldicarb induced ROS generation in both undifferentiated and differentiated cells (Table 4-3), but ROS generation decreased with increasing incubation time such that the curves flattened at higher pesticide concentrations at 24 h (Figure 4-15). CPO, AZO, and Aldicarb significantly induced more ROS generation in differentiated cells than in undifferentiated cells at both time points. Comparison of 6 hours and 24 hours exposure of CPO, AZO and Aldicarb on individual phenotypes indicated that there was a significant difference at IC_{50} and IC_{80} (Figure 4-15; Table 4-3).


CPO
ROS generation (% of vehicle control)
150
100
50
0
0
20
40
60
80
CPO concentration (μM)
A
CPO
ROS generation (% of vehicle control)
150
100
50
0
0
20
40
60
80
CPO concentration (μM)
D
Undifferentiated cells
Differentiated cells


AZO
ROS generation (% of vehicle control)
150
100
50
0
0
20
40
60
80
AZO concentration (μM)
B
AZO
ROS generation (% of vehicle control)
150
100
50
0
0
20
40
60
80
AZO concentration (μM)
E
Undifferentiated cells
Differentiated cells

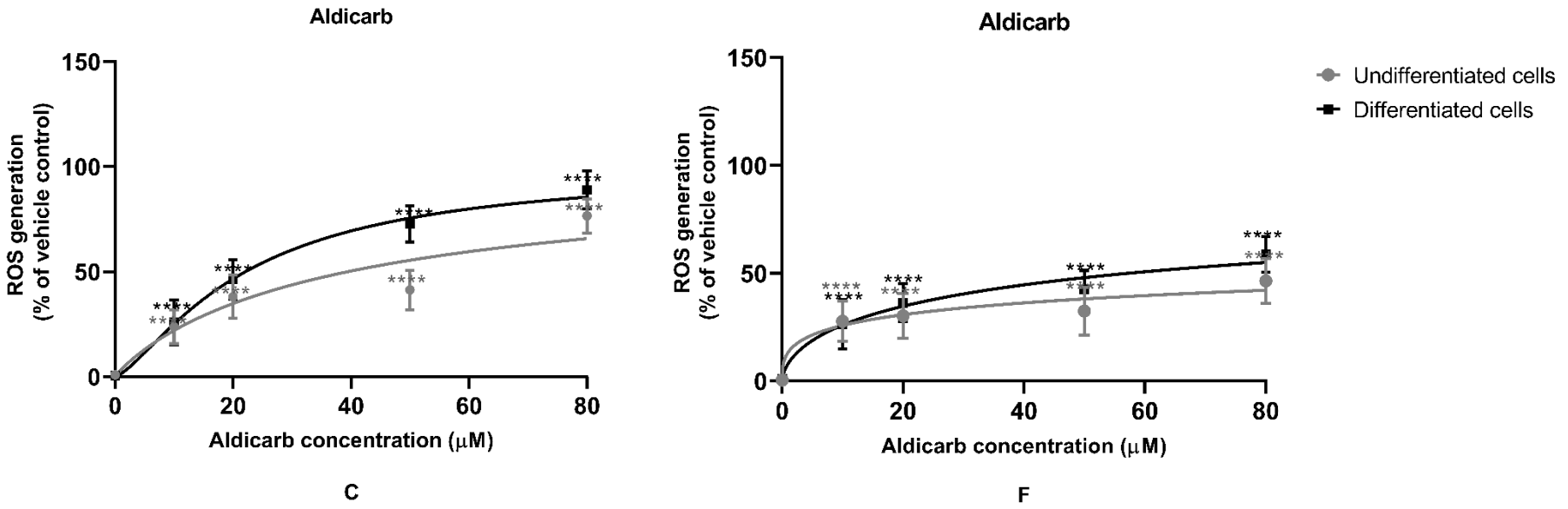


Figure 4-15: Effect of CPO, AZO and Aldicarb in cellular ROS generation.
Undifferentiated and differentiated cells were exposed IC_{10}, IC_{20}, IC_{50} and IC_{80} concentrations CPO, AZO, and Aldicarb for 6h (A-C) and 24 h (D-E). Cellular ROS generation was quantified using DCFDA and readings were normalised to the vehicle control treatments and presented as a percentage of vehicle control. Readings including vehicle control and treatments were obtained from 5 individual experiments (n=5) with triplicates in each treatment. Results were analysed using one-way ANOVA with Dunnett's multiple comparison and expressed as the mean ± standard error of the mean (SEM), When SEM bar is not apparent, this means that error is smaller than the symbol size. For significance; **** p<0.0001.

Table 4-3: Comparison of individual concentrations at 6 h and 24 h ROS generation by the exposure of CPO, AZO, and Aldicarb on SH-SY5Y cells.

Pesticide	Concentration (µM)	Undifferentiated cells	Differentiated cells
CPO	IC_{10}	NS	NS
	IC_{20}	0.0386	NS
	IC_{50}	0.0008	0.0010
	IC_{80}	0.0006	<0.0001
AZO	IC_{10}	NS	NS
	IC_{20}	NS	NS
	IC_{50}	0.0260	0.0260
	IC_{80}	0.0460	0.0010
Aldicarb	IC_{10}	NS	NS
	IC_{20}	NS	NS
	IC_{50}	NS	0.0015
	IC_{80}	0.0019	0.0015

NS- not significant; IC-inhibition concentration; IC_{10}- 10% inhibition concentration; IC_{20}- 20% inhibition concentration; IC_{50}- 50% inhibition concentration; IC_{80}- 80% inhibition concentration

4.2.10 Effect of CPO, AZO, and Aldicarb on cellular protein carbonylation and association between ROS generation and ATP depletion in cells

Proteins are one of the targets of ROS generated by the toxic insult of pesticides in cells. Protein carbonylation is an irreversible protein oxidation mediated by oxidative stress in neuronal cells and used as an oxidative stress marker in response to neurotoxicant exposures. Next, to gain insight into oxidative protein damages in SH-SY5Y cells induced as a response to CPO, AZO, Aldicarb exposure, protein carbonylation levels were quantified using a spectrophotometric protein carbonylation assay as explained by Colombo et al (2016). Specific protein targets vulnerable to oxidative damage were characterized by SDS-PAGE gel electrophoresis of crude cytosolic fractions and immunoblotting.

Protein carbonylation levels were increased in a concentration-dependent manner with increasing concentration of pesticides in CPO, AZO and Aldicarb in both phenotypes of SH-SY5Y cells. Interestingly, increased protein

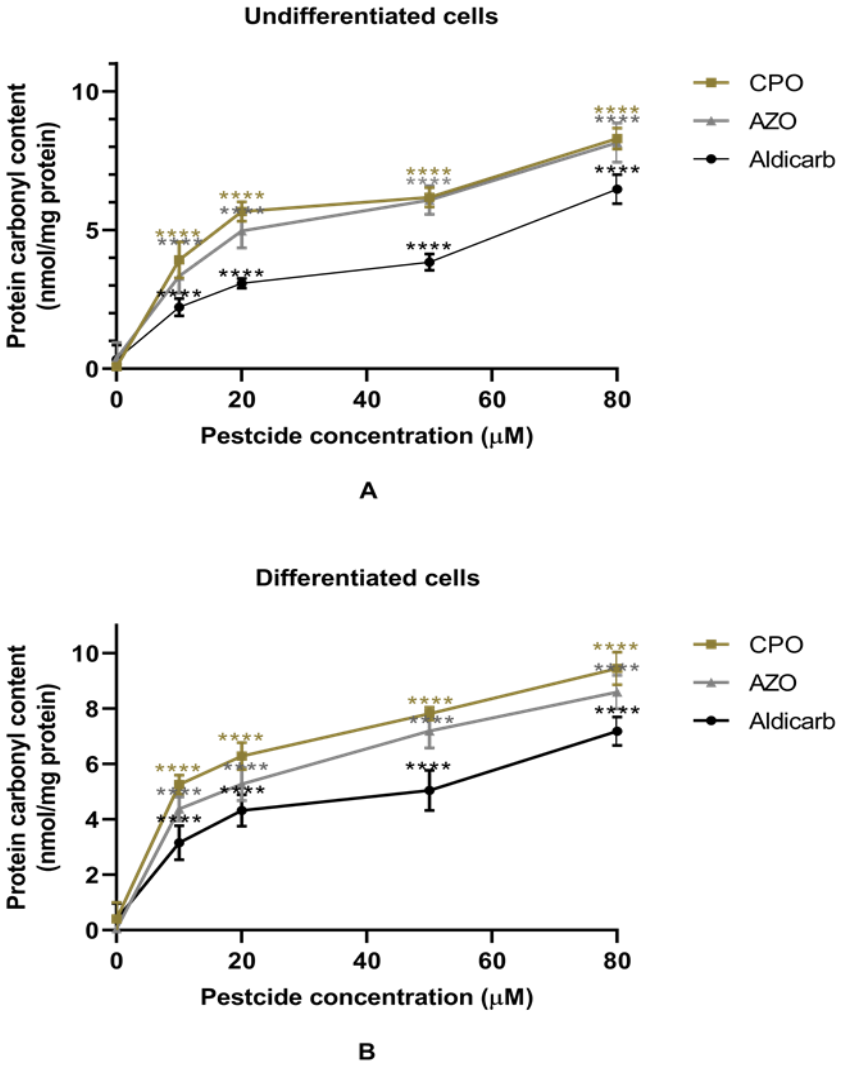


Figure 4-16: Effect of CPO, AZO and Aldicarb on cytosolic protein carbonylation in SH-SY5Y cells.

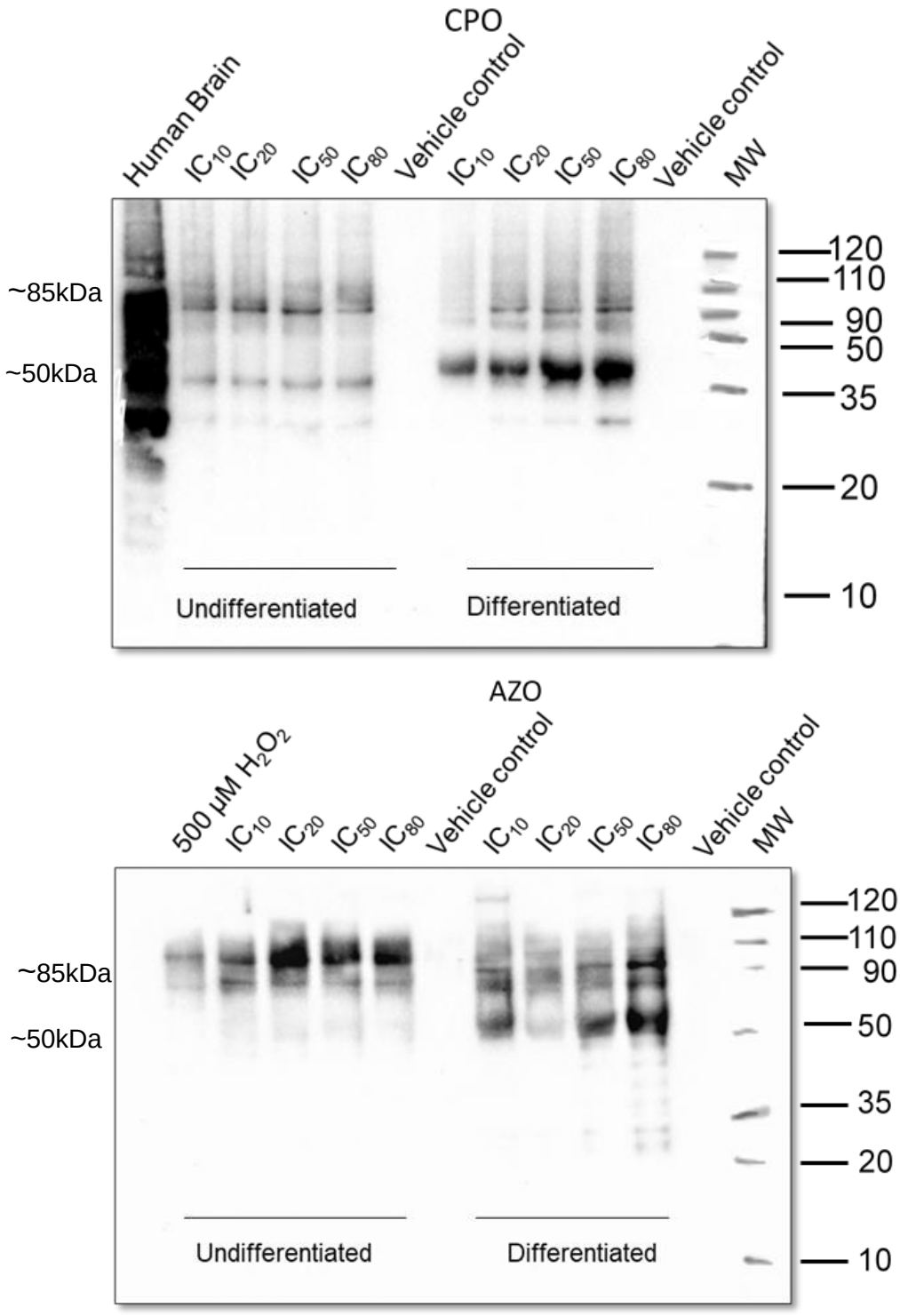
(A)- undifferentiated and (B)- differentiated cells were exposed to IC_{10}, IC_{20}, IC_{50} and IC_{80} concentrations CPO, AZO and Aldicarb for 24 h. Protein carbonylation levels were quantified using DNPH derivatization of crude cytosolic fraction of treated cells and spectrophotometric readings normalised to vehicle control treatments after subtracting the blanks. Readings including vehicle control and treatments were obtained from 5 individual experiments (n=5) with triplicates in each treatment. Results were analysed using one-way ANOVA with Dunnett's multiple comparison and expressed as the mean ± standard error of the mean (SEM), when SEM bar is not apparent, this means that error is smaller than the symbol size. For significance; **** p<0.0001.

carbonylation was observed at IC_{80} with all three pesticides in both phenotypes of SH-SY5Y cells compared to corresponding non-treated controls. (Figure 4-16 A and B). Even at the low doses like IC_{10}, there was still an induction of a significant level of protein carbonylation in both phenotypes as a response to CPO, AZO and Aldicarb exposure. However, there was a marked difference

between CPO and Aldicarb *(p* <0.0001), and AZO and Aldicarb *(p*<0.0001) on undifferentiated cells revealed by two-way ANOVA. But there was no significant difference between induction of protein carbonylation by CPO and AZO (*p*=0.3555). Protein carbonylation responses in three pesticides for differentiated cells were significantly different from each other as revealed by two-way ANOVA and potency of order was CPO>AZO>Aldicarb.

Oxyblots of CPO, AZO and Aldicarb showed a concentration-dependent increase of protein carbonyls in both undifferentiated and differentiated cells compared to vehicle control treatments and there was a marked level of protein carbonylation in the positive control treatment (500 µM H_2O_2). All three pesticides extensively carbonylated proteins over the molecular weight range of ~50-120 kDa, with a major band of ~50 and 85 kDa. Notably the ~50 and 85 kDa proteins were carbonylated even at IC_{10} in undifferentiated and differentiated cells. Carbonylation of ~50 kDa protein was much stronger in differentiated cells than in undifferentiated cells in all three pesticides for 24 h (Figure 4.17).

Association between the cellular ATP levels, ROS and protein carbonylation were analysed using Pearson correlation analysis. The results revealed that there was a negative correlation with cellular ATP levels with protein carbonyl levels and there was a positive correlation with ROS generation and protein carbonyl levels. This suggested that protein carbonylation induced by ROS increased with the increasing ROS generation, and when a depletion of ATP levels was ongoing (Table 4-4).


CPO
Human Brain
IC10
IC20
IC50
IC80
Vehicle control
IC10
IC20
IC50
IC80
Vehicle control
MW
~85kDa
~50kDa
120
110
90
50
35
20
10
Undifferentiated
Differentiated
AZO
500 µM H2O2
IC10
IC20
IC50
IC80
Vehicle control
IC10
IC20
IC50
IC80
Vehicle control
MW
~85kDa
~50kDa
120
110
90
50
35
20
10
Undifferentiated
Differentiated

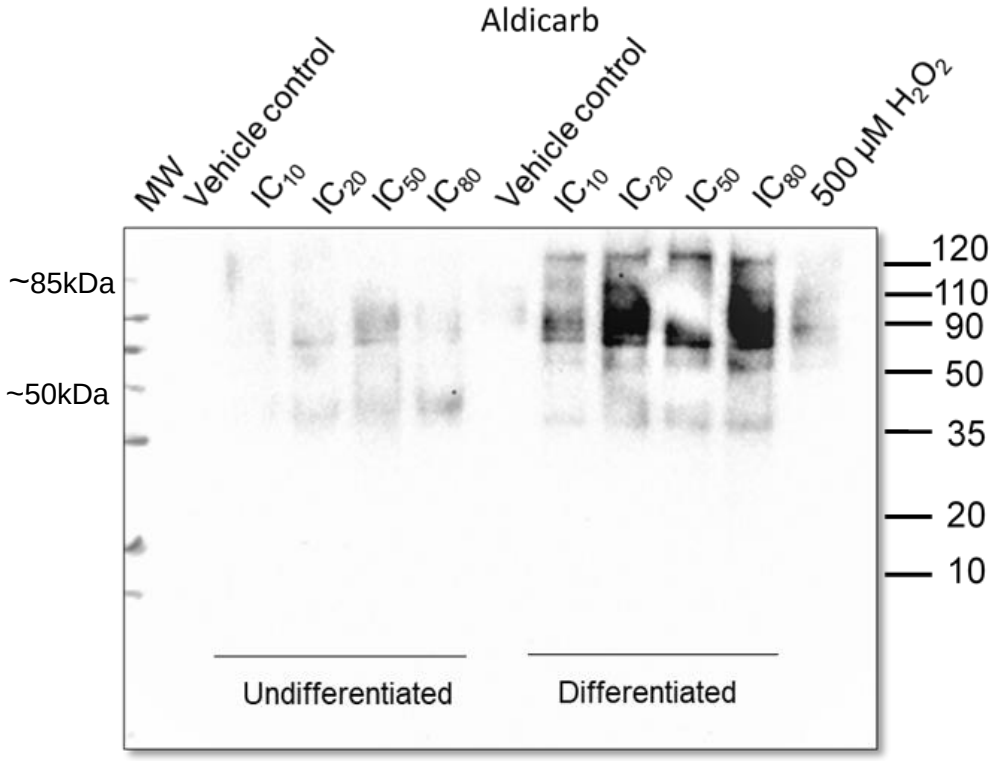


Figure 4-17: Cytosolic protein carbonylation of CPO, AZO and Aldicarb exposure for 24 h in SH-SY5Y cells.

Undifferentiated and differentiated cells were exposed to IC_{10}, IC_{20}, IC_{50} and IC_{80} concentrations CPO, AZO and Aldicarb for and 24 h. DNPH derivatized crude cytosolic fractions were analysed with gel electrophoresis and immunoblotted with anti-DNPH antibody to identify the specific protein targets of protein carbonylation of CPO,AZO and Aldicarb exposure. Each experiment was conducted as 5 independent experiments with three replicates.

Table 4-4: Correlation analysis between ROS generation vs protein carbonyl content, and ROS generation vs ATP production in SH-SY5Y cells for 24 h exposure of CPO, AZO, and Aldicarb.

Pesticide	Cell type	ROS vs PCC			ROS vs ATP		
		r	**R^2**	***p* value**	***r***	**R^2**	***P* value**
CPO	Undifferentiated	0.982	0.965	0.002	-0.930	0.865	0.022
	Differentiated	0.974	0.948	0.005	-0.905	0.819	0.034
AZO	Undifferentiated	0.953	0.908	0.012	-0.914	0.836	0.029
	Differentiated	0.988	0.977	0.001	-0.927	0.860	0.023
Aldicarb	Undifferentiated	0.941	0.886	0.016	-0.899	0.808	0.037
	Differentiated	0.998	0.997	<0.0001	-0.922	0.850	0.025

PCC- Protein carbonyl content; ROS- Reactive oxygen species; *r*- Pearson's correlation coefficient

Table 4-5: Comparison of the cytotoxicity induced by CPO, AZO and Aldicarb to undifferentiated Vs differentiated SH-SY5Y cells.

Pesticide	Treatments	MTT assay	LDH assay	Treatments	ATP assay	ROS assay		PCC assay
	1	NS	0.0216			6 hours	24 hours	
	10	NS	0.0002	IC_{10}	NS	0.0022	0.0002	<0.0001
CPO	20	0.0005	NS	IC_{20}	0.0031	NS	NS	0.0004
	50	<0.0001	<0.0001	IC_{50}	<0.0001	<0.0001	0.0002	<0.0001
	100	NS	0.0008	IC_{80}	NS	<0.0001	0.0012	<0.0001
	200	NS	NS					
	1	0.0253	0.0056					
	10	<0.0001	NS	IC_{10}	NS	<0.0001	<0.0001	<0.0001
AZO	20	0.0006	0.0145	IC_{20}	0.0444	<0.0001	<0.0001	<0.0001
	50	NS	NS	IC_{50}	NS	<0.0001	<0.0001	<0.0001
	100	NS	NS	IC_{80}	0.0270	<0.0001	<0.0001	<0.0001
	200	NS	NS					
	1	NS	NS					
	10	NS	<0.0001	IC_{10}	Ns	NS	NS	<0.0001
Aldicarb	20	0.0361	NS	IC_{20}	Ns	0.0006	0.0066	<0.0001
	50	0.0015	NS	IC_{50}	0.0005	<0.0001	<0.0001	<0.0001
	100	NS	NS	IC_{80}	Ns	<0.0001	<0.0001	0.1945
	200	Ns	NS					

NS- not significant; IC_{10} - 10%, inhibition concentration; IC_{20}- 20 % inhibition concentration; IC_{50}- 50% inhibition concentration; IC_{80}- 80% inhibition concentration, MTT- (4,5-dimethylthiazol-2-yl)-2,5-diphenyltetrazolium bromide, LDH- Lactate dehydrogenase, ATP- Adenosine triphosphate.

Table 4-6: Comparison of AChE activity of undifferentiated and differentiated SH-SY5Y inhibition by CPO, AZO and Aldicarb.

Pesticide concentration (µM)		Undifferentiated vs Differentiated cells
CPO	0.1	NS
	0.2	NS
	0.3	0.0013
	1	NS
	3	NS
AZO	0.1	NS
	0.2	NS
	0.3	0.0002
	1	NS
	3	NS
Aldicarb	0.1	NS
	0.2	0.0011
	0.3	0.0001
	1	0.0171
	3	NS

NS- Not significant

4.3 Discussion

This study evaluated oxidative stress-induced cellular responses in human neuroblastoma SH-SY5Y cells, focussing on cellular metabolic activities, morphological impairments, and protein oxidation in response to commonly used OP and carbamate pesticides. The utilization of human neuroblastoma SH-SY5Y cells for neurotoxicity and neurodegenerative diseases studies with pesticides has been demonstrated in a number of studies due to their metabolic and biochemical features related to neurons and their human origin (Heusinkveld and Westerink 2017, Chapter II,Table 2-1).

The toxic effect of three pesticides is related to the indirect or direct covalent modification of AChE and thereby inducing cellular responses as suggested in earlier studies (Rishe et al.1987, Flaskos 2012, Christen et al. 2017). More recently, some studies have focused upon OP effects and the adduction of non-AChE cellular targets and protein adduction as a possible mechanism of other cellular responses and development of OP related pathologies (Chapter II, Table 2-1). Although CPF and Aldicarb were evaluated on SH-SY5Y cell lines, there are no recorded studies found that relate to acute exposure of their active metabolites on human cell lines in the literature. However, the toxicity of oxon-metabolites was studied in animal models and mouse neuroblastoma cells (Betancourt and Carr, 2004, Middlemore-Risher et al., 2011, Yang et al., 2011, He et al., 2017). These data were not sensitive to interpret the effect on human cells due to the species differences. The current study utilized both undifferentiated and differentiated cells to study the oxidative stress-induced toxicological consequences of oxon metabolites of Chlorpyrifos, Azamethiphos and the carbamate pesticide, Aldicarb.

Characterization of differentiated neuronal cells showed that SH-SY5Y cells can be successfully differentiated to human neuronal-like cells (Figure 4-1) (Encinas

et al. 2000, Lopes et al. 2010,). Therefore, SH-SY5Y can be used to mimic the effect of pesticides on developmental stages including immature and mature neurons and provide an opportunity to study the effect of pesticides on non-cholinesterase targets and underlying mechanisms of toxicity on single cell type studies.

This study first focussed on the evaluation of the vulnerability of SH-SY5Y cells to CPO, AZO, and Aldicarb-induced toxicity using MTT and LDH assays and further confirmed by ATP assay. MTT assays reported a concentration-dependent decrease of cell viability after exposure to CPO, AZO, and Aldicarb after 24 h. In turn, MTT assays provided a measurement of cell metabolic activities and acted as a surrogate of cell viability and cell proliferation responses related to CPO, AZO and Aldicarb exposure. CPO, AZO, and Aldicarb decreased cell metabolic activities and reduced cell viability in both undifferentiated and differentiated cells. This is supported by the observations of LDH assays which showed a concentration-dependent increase of cell death (loss or membrane integrity) in both phenotypes. Notably, differentiated cells were sensitive to CPO, AZO, and Aldicarb exposure as revealed by both MTT and LDH assays. The current study revealed that there was a dramatic cell viability loss and cell death at the highest concentrations tested for all pesticides. Moreover, AZO showed more potent toxicity in undifferentiated cells than CPO and Aldicarb, while CPO exerts more potent toxicity to differentiated cells. This suggested that cytotoxicity of AZO, CPO, and Aldicarb are cell type and stage-specific. Results from cell viability and cell cytotoxicity suggested that CPO and AZO induced cytotoxicity in both undifferentiated and differentiated cells at a concentration range of 10 - 30 µM whereas Aldicarb caused cytotoxicity of both pesticides at a concentration range of 10 - 40 µM. In contrast, CPF caused cytotoxicity at a concentration range of 25 - 100 µM in SH-SY5Y

cells (Chapter II, Table 2-1) consistent with other studies (Singh et al. 2018, Xu et al. 2017; Raszewski et al. 2015, de Oliveira et al. 2016, Dai et al. 2015, Yamada et al. 2017).

Neurite retraction in pre-differentiated SH-SY5Y cells can be used as *in vitro* morphological biomarker of neuronal differentiation to evaluate the toxicological responses of cells. This study showed that the reduction of neurite outgrowth starts at 10 µM concentration of CPO, AZO, and Aldicarb, and also that neurite retraction increases with increasing concentration. This result is complemented with previous data demonstrating concentration-response relationships of CPO and Azamethiphos inhibiting neurite outgrowth in PC12 cells (Christen et al. 2017). CPO is a potent inhibitor of neurite outgrowth as revealed by studies with mouse neuroblastoma cells (Sindi 2015, Alyamani 2018). Chlorpyrifos inhibits neurite outgrowth at concentrations ranging from 1 - 50 µM (Flaskos, 2011). CPO was 1000 times more potent than CPF in inhibiting neurite and axonal outgrowth (Howard et al., 2005, Yang et al., 2008). As shown by Sindi, (2015), CPO inhibits neurite outgrowth significantly than CPF in a concentration-dependent manner in mouse neuroblastoma cells treated 2, 4, and 8 h. Treatment of, 3 µM treatment of CPO on N2a cells showed neurite outgrowth inhibition of differentiating cells from at 2 h postexposure and that was significant compared to 3 µM treatment with CPF in N2a cells. Azamethiphos induced a significant reduction of neurite outgrowth in PC12 cells treated for 48 h at 10 µM concentration (Christen et al. 2017). A 50 µM concentration of Aldicarb reduced neurite lengths in SK-N-SH cells significantly without affecting viability after 7 days (Chang et al. 2006). However, there was a clear superiority of CPO and AZO over Aldicarb effects on pre-differentiated SH-SY5Y cells after a 24 h exposure according to this study. The oxon-metabolite of OP pesticides directly inhibits neurite outgrowth presumably by directly interfering with

cytoskeleton proteins and/or AChE (Flaskos 2012). This has been further supported by Sindi, (2015) that showed that CPO significant altered cytoskeleton protein expression after an 8 h exposure, and Christen et al. (2017) showed significant cytoskeleton protein phosphorylation upon CPO exposure such as βIII tubulins and microtubule-associated proteins in human cell models. These results suggested that differentiating cells are susceptible to CPO, AZO, and Aldicarb induced toxicity and these pesticides can influence cell differentiation.

This study showed significant inhibition of AChE in undifferentiated and differentiated cells exposed to CPO, AZO, and Aldicarb which is in line with previous studies with SH-SY5Y cells exposed to paraoxon and CPF (Cho and Tiffany-Castiglioni, 2004). However, there is a deficit in results found for human neuronal cells with CPO, AZO and Aldicarb related to AChE inhibition. 50 % AChE inhibition of CPO within 8 hr in human neuronal progenitor cells was recorded as between 1 - 2 µM (Sindi, 2015). Ehrich and Correll (1997) reported that 50% AChE inhibition with CPO for 1 hour was 0.00034µM and further the inhibition curve reaches a plateau after 0.5 and 4 h treatments (Ehrich et al., 2011). The IC_{50} of CPO in mouse brain has been recorded as 4.6 nM which is smaller than that revealed by this study, but this can be due to species differences. When comparing the AChE inhibition concentrations and neurite length retraction concentrations, AChE inhibition with all pesticides occurs at a lower concentration. Literature screening revealed that the CPO induced neurite or axonal growth inhibitory effects are due to interference with AChE, but not with the enzymatic activity, instead these compounds effect the morphogenic activity of the AChE (Howard et al., 2005).

One of the most striking effects of CPO, AZO and Aldicarb in this study is the direct alteration of ATP production in SH-SY5Y cells in a concentration-

dependent manner. The study suggests oxon forms of CPF, AZA, and the carbamate pesticide, Aldicarb, influence cellular energy metabolism at low concentrations in both undifferentiated and differentiated SH-SY5Y cells. In turn, this suggests that toxicity induced by exposure of these pesticides could be via a blunting of the mitochondrial function in cells. This influences reduction of the metabolic activities and viability of cells observed in cell viability assays. This observation is in accordance with the previous studies done with SH-SY5Y undifferentiated cells exposed to CPF and carbamate pesticides for different time points that have shown concentration and time-dependent depletion of ATP levels (Faria et al., 2016, Anderson et al., 2018, Singh et al., 2018). However, CPO, AZO and Aldicarb showed selective and stage-specific inhibition of ATP levels in SH-SY5Y cells according to this study.

CPO, AZO and Aldicarb toxicity (IC_{10}, IC_{20}, IC_{50} and IC_{80}) was speculated to influence oxidative stress via two studies. First, ROS generation in undifferentiated and differentiated cells were quantified after CPO, AZO and Aldicarb exposure and cytosolic protein carbonylation levels were determined. Growing lines of evidence have showed that CPF induced ROS generation in a concentration-dependent manner using human neuronal cells (Ki et al., 2013, Park et al., 2015, Zhao et al., 2019). The current study showed increased ROS generation but decreased ATP levels in cells in a concentration-dependent manner. This suggested that excessive levels of ROS generation alter cellular energy metabolism and influence on mitochondrial functions of undifferentiated and differentiated cells. In agreement with this statement, Dettbarn et al. (2006) showed OP induced ROS generation is the mechanism of cholinergic stimulations and leading to higher energy consumption and gradual depletion of ATP levels of cells. This is further supported by a demonstration that a 30 - 40% drop in cellular ATP levels for several hours upon OP exposure can cause

a significant fall in mitochondrial membrane potential which supports the suppression of the activity of complex I and IV of electron transport chain which in turn causes depleted ATP (Milatovic et al., 2006). The output of this is to cause imbalance in cellular Ca^{2+} homeostasis, and activation of the caspase cascade in cells (Milatovic et al., 2006).

Interestingly, this study revealed that even at low pesticide doses such as those associated with a loss of 10% of cell viability, this still caused significant protein carbonylation in both undifferentiated and differentiated cells. CPF induced protein carbonylation at an increasing concentration in human neuroblastoma SH-SY5Y cells over the concentration range of 20 - 100 µM, but CPO induced protein carbonylation even at 7 µM in undifferentiated cells and 4 µM for differentiated cells. Correlation analysis showed that there was a strong positive correlation in ROS generation and protein carbonylation in both phenotypes. A similar observation was made in PC12 cells treated with rotenone for 24 hours, with increased protein carbonylation along increasing ROS generation in cells (Chiaradia et al., 2019). Protein carbonylation causes irreversible alterations in the structure and functions of cells. Protein carbonylation can also alter specific cell signalling pathways. Furthermore, protein carbonyls are associated with higher molecular weight protein aggregates and show resistance to proteolysis and are toxic to cells (Stadtman and Levine, 2000, Dalle-Donne et al., 2006, Dasgupta et al., 2012). Herein, oxyblots revealed that a number of relatively higher molecular weight proteins were carbonylated by the exposure of CPO, AZO and Aldicarb, and more robust damage was observed in differentiated cells than in undifferentiated cells. It seems likely that ROS induced protein carbonylation contributes to the pesticide cellular toxicity to SH-SY5Y cells. This notion is supported by a proteomic study that considered the protein carbonyls in PC12 cells which showed carbonylation of proteins involved in metabolic

pathways and ATP synthesis, as a response to rotenone exposure (Chiaradia et al. 2019). Furthermore, cytoskeleton protein aggregation via peptide crosslinking has been demonstrated by CPO exposure even at 1.5 µM (Schopfer and Lockridge, 2018). This suggests protein carbonylation causes an alteration in cell morphology in SH-SY5Y cells exposed to CPO, AZO and Aldicarb even at IC_{10} concentration. These alterations can lead to losing the rigidity of neuronal cells, and potentially alter the neurotransmission by inhibiting neurite outgrowth in differentiating cells. Therefore, the current study suggested that AChE inhibition stimulates cellular cytotoxic responses of SH-SY5Y cells and CPO, AZO and Aldicarb evoked ROS induced protein damages that also contributed to the toxic responses within cells.

In conclusion, this study suggested that CPO, AZO, and Aldicarb induced cellular damage though ACh excitotoxicity and induced ROS mediated protein carbonylation, and that these effects alter cellular functions and induced toxic responses of both undifferentiated and differentiated cells.

5 NEUROTOXICITY EVALUATION OF ORGANOPHOSPHATE AND CARBAMATE PESTICIDES USING HUMAN PROGENITOR CORTICAL NEURONAL STEM CELLS

5.1 Introduction

Organophosphate and carbamate pesticides are widely used pesticides and their adverse effects on growing brain is getting attention due to the potential short and long-term damage to the nervous system. Prenatal and postnatal OP and carbamate exposure has shown association with neurodevelopmental disorders such as attention deficit hyperactivity disorder (ADHD), autism, and neurodevelopmental delays (Flaskos, 2012). The main mechanism behind all these disorders and associated with OP and carbamate exposure is AChE inhibition (Flaskos, 2011). However, a plethora of literature has suggested that there is an association between oxidative stress and neurodevelopmental disorders (Bjørling-Poulsen et al., 2008a, Flaskos, 2012, Mostafalou and Abdollahi, 2018, Philippat et al., 2018). Epidemiological studies has been also concluded an association of oxidative stress with ADHD (Flaskos, 2012, González-Alzaga et al., 2014, Philippat et al., 2018). Hence, growing lines of evidences have shown that AChE inhibition is not the sole mechanism of induced developmental neurotoxicity. Direct or indirect effects of OP or carbamate exposure interfere with general cell function but the major mechanisms underlying the toxicity (apart from AChE inhibition) is still in debate (Lukaszewicz-Hussain, 2010, Lukaszewicz-Hussain, 2013, de Oliveira et al., 2016). Hence, neurotoxicity modelling of OP and carbamate pesticides in more human CNS related cell lines is important to establish the safety levels and to provide exhaustive information about the mechanism of action of OP and carbamates in humans.

Although the previous chapter of this thesis focused upon CPO, AZO and Aldicarb neurotoxicity on human neuroblastoma cells, it only represents the neuronal cells population within the CNS. However, human progenitor neuronal cells more closely resemble the complexity of the human nervous system, representing three cell lineages such as neurons, astrocytes and oligodendrocytes (Donato et al., 2007). Astrocytes in brain plays a role in eliminating and metabolism of toxins as a part of the blood-brain barrier, and function as a second line defences to protect neurones in the CNS. Studies have highlighted a protective role of astrocytes against OP neurotoxicity in neuronal cultures (Guizzetti et al., 2005, Mense et al., 2006, Pizzurro et al., 2014, Wu et al., 2017, Shieh et al., 2019). Thus it is very important to consider developmental neurotoxicity studies as critical developmental events within the nervous system are precisely temporarily and spatially coordinated (Cowan, 1998, Sanes et al., 2000). On this basis human progenitor neuronal stem cells can be more effectively used to predict the chemical-related changes *in vivo* (Radio and Mundy, 2008). However, the use of these cells become limited due to the lack of possibility to maintain stable phenotypic features throughout passages. This has been eliminated with immortalized cell lines that can be maintained for longer passages with self-renewal and multi-potentiality characteristics along with stable genotype and phenotype (Dang et al., 1999, Donato et al., 2007).

ReNcell CX cells are a commercially available immortal human progenitor cortical neuronal stem cell line (HNPCs) with *c-myc* transgene (Donato et al., 2007). ReNcell CX can differentiate into a mixed population of neurones, astrocytes, and oligodendrocytes upon mitogen removal (Gage, 2000, Donato et al., 2007). The oxidative stress responses of chemical and herbicide exposures have been widely studied using ReNcell CX cells (Chang et al., 2013,

Zhao et al., 2018). Although CPO induced neurite outgrowth has been shown in the literature (Sindi, 2015, Alyamani, 2018), CPO, AZO, and Aldicarb induced oxidative stress responses in human cortical neuronal progenitor cells have not yet received attention. The aim of this study was to explore the mechanism underlying the effect of CPO, AZO, and Aldicarb on viability, cytotoxicity, ROS production, cellular ATP production and study the protein damages that arose from oxidative stress in undifferentiated and differentiated ReNcell CX cells.

5.2 Results

5.2.1 Phenotypic characterisation of undifferentiated and differentiated HNPCs

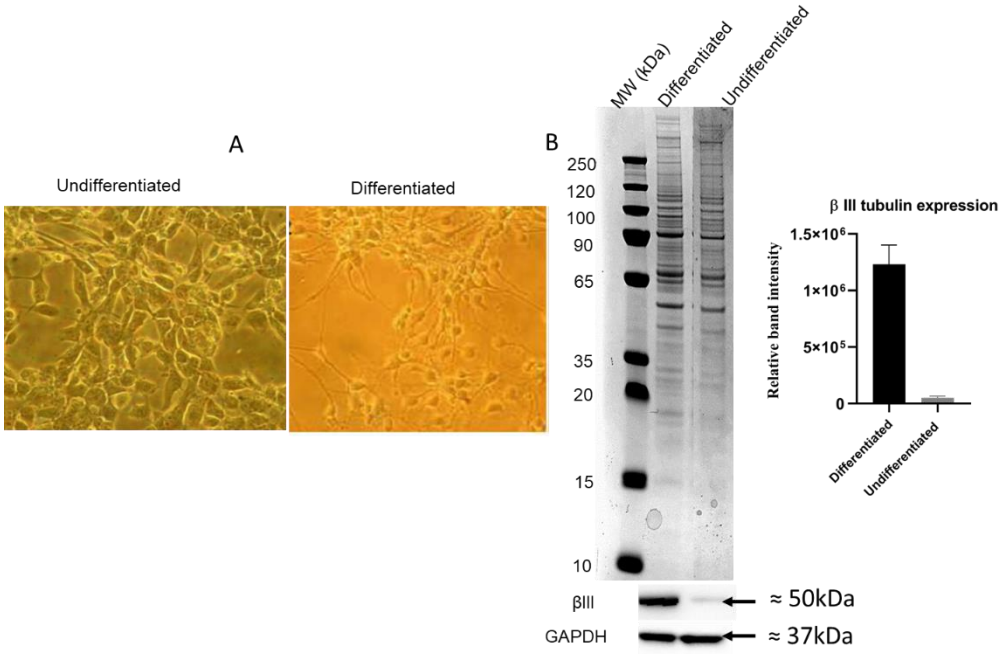


Figure 5-1: Representative images for undifferentiated and differentiated ReNcell CX cells and expression of βIII tubulin.
A- morphological difference of undifferentiated and differentiated cells captured by phase contrast microscopy B- Expression of βIII tubulin expression in differentiated cells revealed by gel electrophoresis and Western blotting. Equal levels of protein were loaded and the blot reversibly stained (upper panel), with βIII and GAPDH detected via immunoblotting. Proteins were quantified using total protein normalization. Images captured at maximum power of 40X.

Characterisation of undifferentiated and differentiated HNPCs was performed using the expression of the specific neuronal marker βIII tubulin by Western blotting. Crude cytosolic fractions of undifferentiated or differentiated cells were separated by gel electrophoresis and immunoblotted with βIII tubulin antibody to confirm expression levels. According to Figure 5-1 A undifferentiated ReNcell CX cells are expanded as an island showing their cobblestone (phenotypic) nature on a laminin-coated surface. Differentiated cells displayed migration properties with spindle shape morphology with extensive neurite outgrowths as

shown in Figure 5-1 A. Results of Western blotting indicated that differentiated cells expressed high levels of βIII tubulin confirming, their differentiated into neuronal cells after mitogen removal as shown by Donato et al. (2007).

5.2.2 Determination of linear correlation between the optical signal and cell seeding density

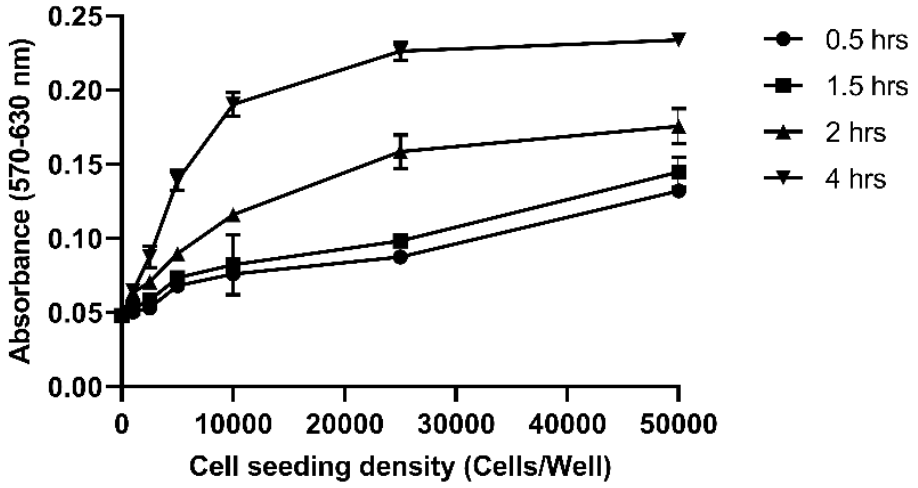


Figure 5-2: Direct correlation of absorbance and ReNcell CX cell number. Determination of linear correlation between the optical signal and cell seeding density to find the linear relationship with MTT signal. Cell viability readings at each time point obtained from one plate. ReNcell CX cells were seeded at different cell concentrations ($1x10^3$ - $7.3x10^4$) and MTT assay performed to establish the linearity of signal at 0.5, 1, 2 and 4 h. The graph illustrates the best signal can be obtained in log phase of cell growth phases after 4-hour incubation period (p<0.0001). Each data points represent mean ± standard error of the mean (SEM) 5 repeated experiments. OD- Optical density.

Quantification of the linear range of MTT intensity for the ReNcell CX cells line was done to optimise parameters for cells before subjecting them to pesticide treatments. A linear correlation between the optical signal (OD signal at 570 nm) and the cell number was established using MTT assay for different cell densities. As depicted in Figure 5-2, OD increase with increasing cell density in a time-dependent manner and at higher densities the curve eventually flattened. At cell densities of $1x\ 10^4$ - $3\ x\ 10^4$ cells showed a linear correlation

between the optical signal (OD signal at 570 nm) and the cell number (Figure 5-2).

Comparison of signal generation and the time of incubation showed there was a significant (p<0.0001) difference between time of incubation and the OD value generated. Optimal seeding density selection at the beginning of experiments within the most linear range of the standard curve ensured that the cells run over 24 hours would still be within the detectable region for MTT without reaching the saturation point. According to results the best signal can be obtained by a 4 h incubation period (Figure 5-3).

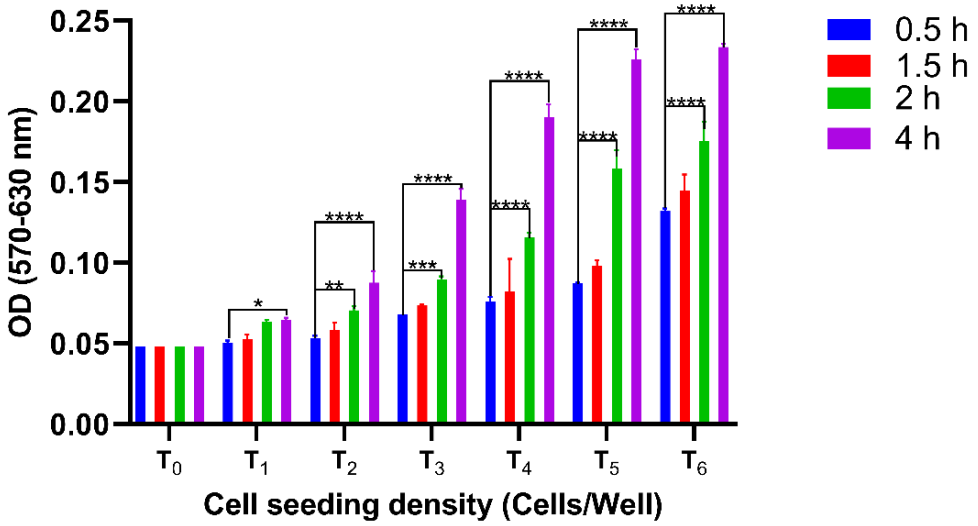


Figure 5-3: Effect of incubation time on MTT signal development in ReNcell CX cells.
Cell viability readings for each time point was obtained from one plate with different cell densities (1x10^3- 7.3x10^4) and MTT assay. Viability readings were obtained from total of 5 repeated plates for each time point with three replicates (n=5). Results were analysed using two-way ANOVA with Tukey's multiple comparison and expressed as the mean ± standard error of the mean (SEM); OD Optical density; For significance; *p<0. 05, **p<0. 01, ***p<0. 001, ****p<0. 0001. T_0- No cells, T_1-1000, T_2- 2500, T_3-5000, T_4- 10000, T_5- 25000, T_6- 30000.

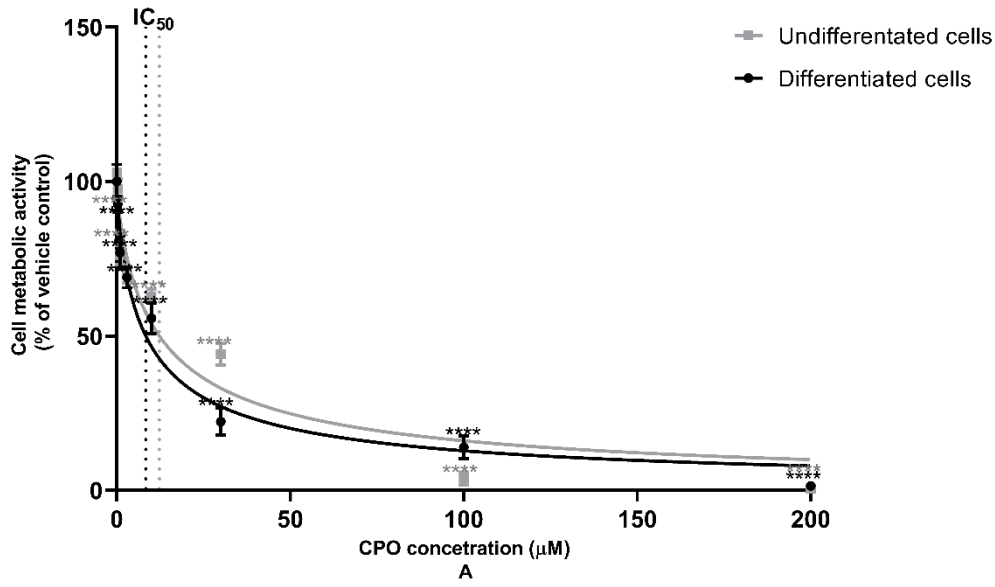
5.2.3 CPO, AZO, and Aldicarb reduced cell metabolic activity and cell viability in a concentrations-dependent manner in ReNcell CX cells.

Undifferentiated and differentiated ReNcell CX were treated at 0.3,1, 3, 10, 30, 100 and 200 µM for 24 h to determine the effect of CPO, AZO, and Aldicarb on cell viability. The concentration ranges for the viability study were selected from preliminary experiments with a broad range of concentrations of pesticides and narrowed down to the most effective range of concentrations. Cell metabolic activities of cells were determined by the MTT assay.

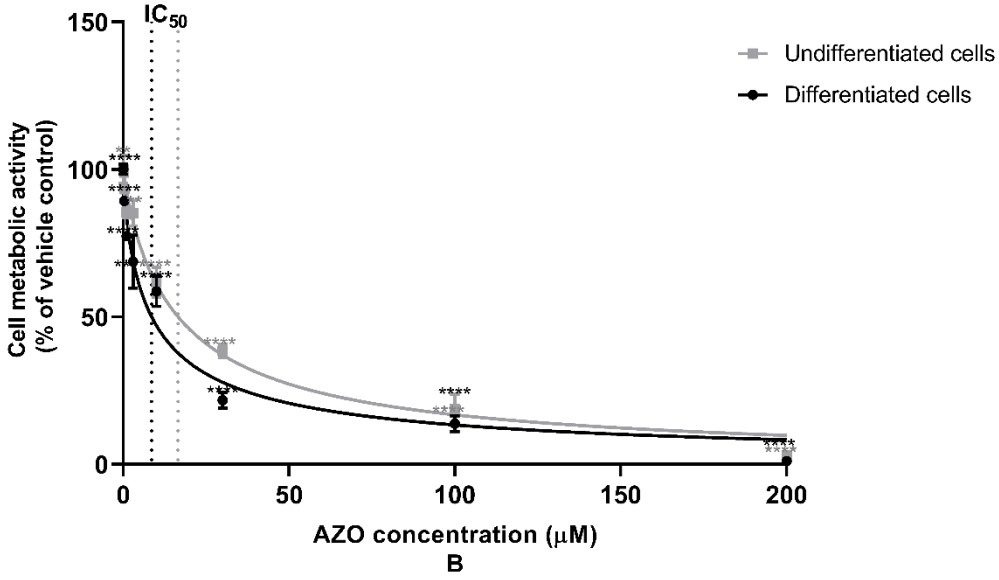
Figure 5-4 illustrated the effect of CPO, AZO, and Aldicarb on cell metabolic activity and cell viability of undifferentiated and differentiated ReNcell CX cells. The Figure 5-4 shows CPO, AZO, and Aldicarb influence cell metabolic activity in a concentrations-dependent manner. ReNcell CX cells were highly sensitive to the toxic responses of CPO, AZO, and Aldicarb at higher concentrations such as 30, 100 and 200 µM. Interestingly, undifferentiated cells did not show significant toxic responses at 0.3 µM for 24 h exposure for CPO (p=0.6211), AZO (p=0.7245) and Aldicarb (p=0.0548) compared to non-treated controls. At 0.3 µM concentration, undifferentiated cells showed a 5.38%, 6.7% and 11.1% drop in cell metabolic and cell viability in CPO, AZO and Aldicarb treatments, respectively. However, a strong concentration-dependent decrease in cell viability of undifferentiated cells arose after 1 µM concentration, and all pesticides tested show a dramatic decrease in cell metabolic activities and cell viability loss with increasing concentrations of pesticide. There was a dramatic fall in cell viability between 1-30 µM concentrations and then the curve flattened, with similar strong toxic effects at higher concentrations like 100 and 200 µM in undifferentiated cells. Notably, AZO had a similar effect at 1 µM and 3 µM concentration on undifferentiated cells. A two way-ANOVA and Tukey's multiple

comparison of cell metabolic activity and cell viability of three pesticides showed that Aldicarb induced potent toxicity in undifferentiated cells compared to AZO and CPO (Figure 5-5 A and B), initially. However, when concentrations continue to increase, CPO and AZO showed more dramatic effects on cell viability compared to the corresponding controls than Aldicarb (Figure 5-5). IC_{50} values interpolated from concentration-response curves showed CPO at 11.95 ± 1.942 µM; AZO at 16.50 ± 1.404 µM; Aldicarb at 14.79 ± 2.964 µM for undifferentiated cells. However, all three pesticides showed a minimal effect until 1 µM and then the cell viability decrease accelerated from 1 µM, suggesting 1 µM is the threshold concentration for undifferentiated cells in all three pesticides tested.

Differentiated cells elicit strong concentration-dependent effects on cell metabolic activity and cell viability loss (Figure 5-5) for 24 h compared to the corresponding non-treated controls. All three pesticides showed similar behaviour in decreasing cell viability in differentiated cells. Notably, 0.3 µM does not induce significant cell viability loss in differentiated cells by CPO (p=0.3182), AZO (p=0.0573), or Aldicarb (p=0.8846), showing 7.3%, 10.7% and 4.5% drop in cell viability, respectively, compared to their non-treated control treatments (Figure 5-4). Initial significant viability drop starts at 1 µM implying it is the threshold concentration for CPO, AZO, and Aldicarb in differentiated cells. At 1 µM there was a 23.0%, 22.7% and 21.6% reduction of cell metabolic activity and viability loss in CPO, AZO, and Aldicarb, respectively. However, CPO showed potent toxicity on cell viability loss compared to AZO and Aldicarb in differentiated cells, and this property remains when the concentration continues to increase within 24 h. IC_{50} values interpolated from corresponding cell viability concentration-response curve for differentiated cells were CPO: 8.172 ± 0.8702 µM, AZO: 8.588 ± 1.059 µM; and Aldicarb:12.29 ± 1.775 µM.


IC50
Undifferentiated cells
Differentiated cells
Cell metabolic activity
(% of vehicle control)
150
100
50
0
0
50
100
150
200
CPO concetration (µM)

A


IC50
Undifferentiated cells
Differentiated cells
Cell metabolic activity
(% of vehicle control)
150
100
50
0
0
50
100
150
200
AZO concentration (µM)

B

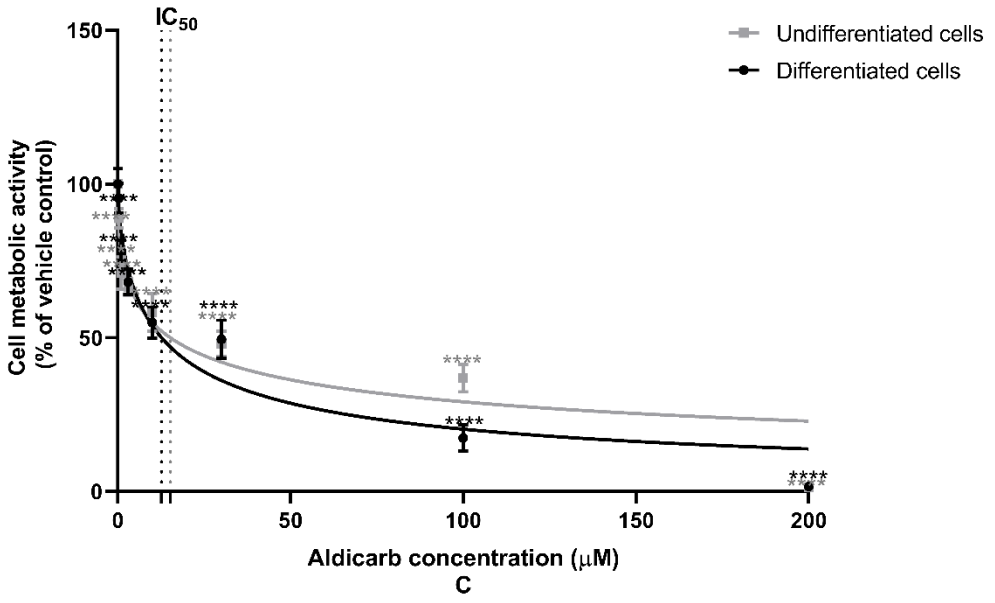


Figure 5-4: Cell viability inhibition dose-response curves of CPO, AZO, and Aldicarb on undifferentiated and differentiated ReNcell CX cells.
Undifferentiated and differentiated cells were treated with CPO (A), AZO (B), and Aldicarb (C) for 24 h over the concentration range of 0, 0.3, 1, 3, 10, 30, 100 and 200 µM. Viability was assessed using MTT assay. Readings were normalized to the viability of vehicle control, providing cell viability percentage, as a percentage value to the vehicle control. Vehicle control and treatments were performed as triplicates in 5 independent experiments (n=5). Results were analysed using one-way ANOVA with Dunnett's multiple comparison and expressed as the mean ± standard error of the mean (SEM), when SEM bar is not apparent, this means that error is smaller than the symbol size. For significance; **p<0.01, ****p<0.0001.

The toxic potency of pesticides shows CPO>AZO>Aldicarb in order of descending toxicity to differentiated cells. A comparison of individual pesticide effects on undifferentiated vs differentiated cells implied there was a significant interaction (p<0.05) between the pesticide and cell phenotype (Table 5-5). The individual concentration comparison for both undifferentiated vs differentiated cells showed that there is not any significant difference at 0.3, 1, 10, 200 µM concentrations. Notably at 200 µM, there was a dramatic effect on both phenotypes, exhibiting significant cell viability loss and inducing cell death by all tested pesticides.

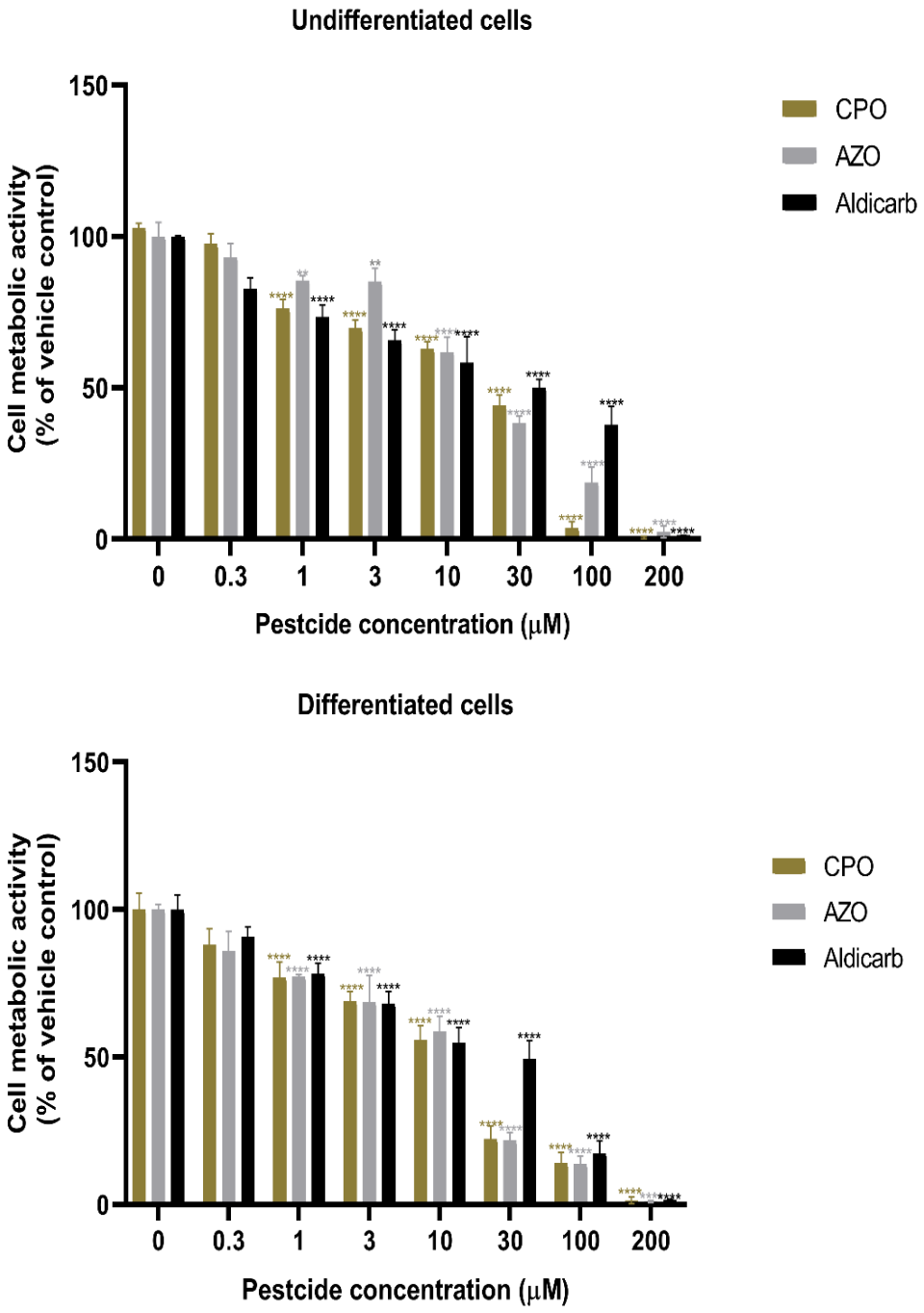
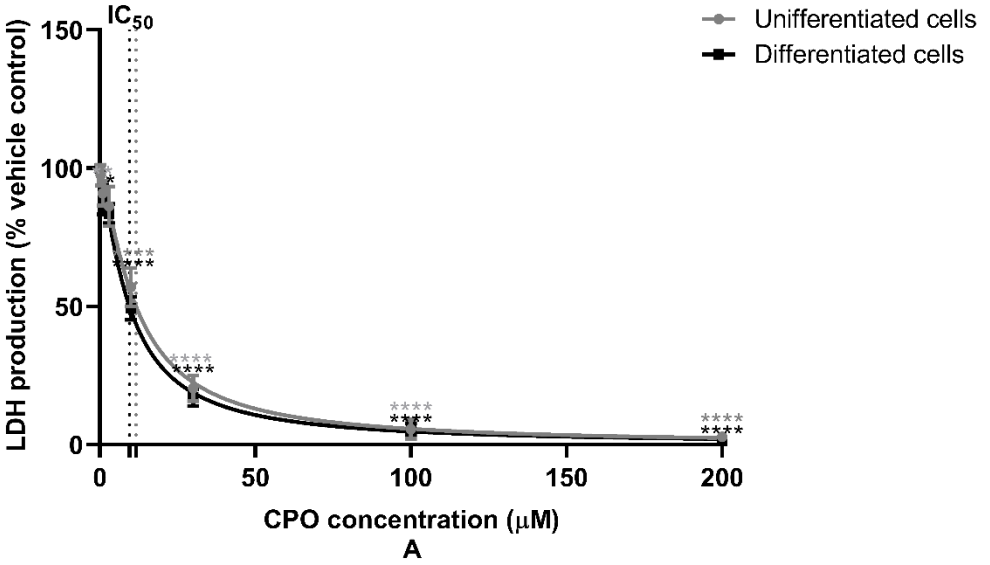


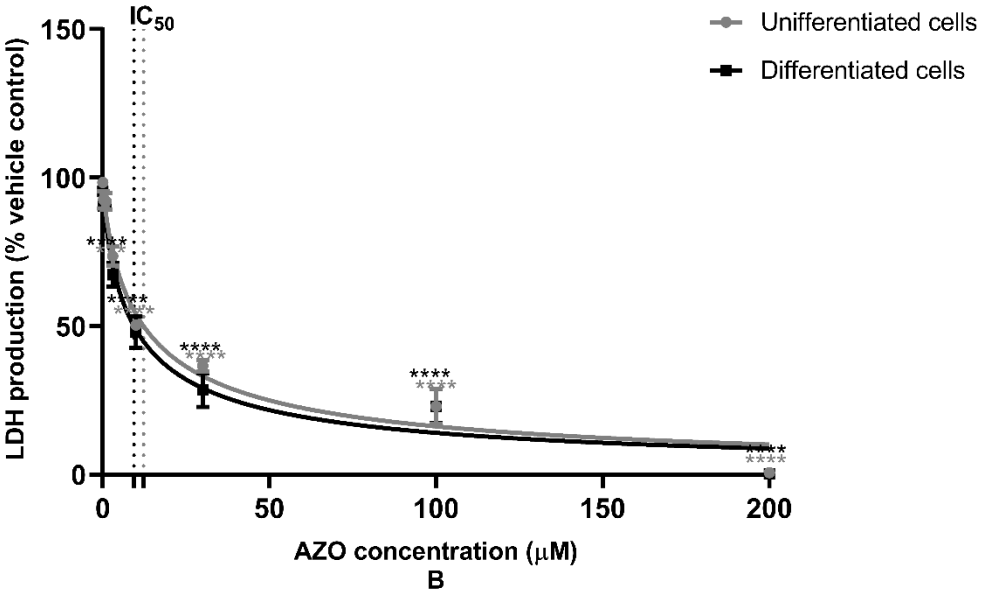
Figure 5-5: Effect of CPO, AZO, and Aldicarb on undifferentiated and differentiated cell viability.

A- Undifferentiated and B- differentiated cells were treated with CPO, AZO, and Aldicarb for 24 h over the range of 0, 0.3, 1, 3, 10, 30, 100 and 200 µM. Viability was assessed using MTT assay. Readings were normalized to the viability of vehicle control, providing cell viability percentage, as a percentage value to the vehicle control. Cell viability readings including vehicle control and treatments were performed as triplicates in 5 independent experiments (n=5). Results were analysed using one-way ANOVA with Dunnett's multiple comparison and expressed as the mean ± standard error of the mean (SEM), when SEM bar is not apparent, this means that error is smaller than the symbol size. For significance; **p<0.01, ****p<0.0001.

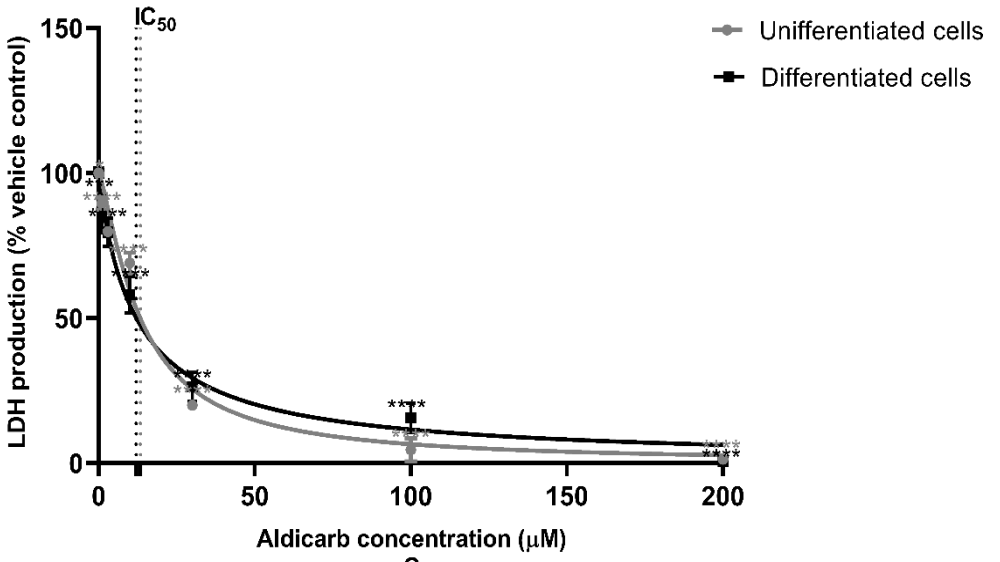
5.2.4 CPO, AZO, and Aldicarb induced cytotoxicity responses in a concentration-dependent fashion in ReNcell CX.



A



B



C

Figure 5-6: Cytotoxicity dose-response curves of CPO, AZO, and Aldicarb on undifferentiated and differentiated ReNcell CX cells.

Undifferentiated and differentiated cells were treated with CPO (A), AZO (B), and Aldicarb (C) for 24 h over the range of 0, 0.3, 1, 3,10, 30, 100 and 200 µM. Cytotoxicity was assessed using LDH assay. Readings were normalized to the LDH production of vehicle control, providing LDH production percentage, as a percentage value to the vehicle control. Vehicle control and treatments were performed as triplicates in 5 independent experiments (n=5). Results were analysed using one-way ANOVA with Dunnett's multiple comparison and expressed as the mean ± standard error of the mean (SEM), when SEM bar is not apparent, this means that that error is smaller than the symbol size. For significance; **p<0.01, ***p<0.001, ****p<0.0001.

Although MTT assays were used to measure the loss of cell viability it can measure the number of cells that shift from proliferation to quiescence (cytostatic activity) of cells induced by CPO, AZO, or Aldicarb exposures. Therefore, to gain more insight into CPO, AZO, and Aldicarb induced cytotoxicity in different phenotypes of ReNcell CX cells, cells were treated with 0, 0.3, 1, 3,10, 30, 100 and 200 µM of CPO, AZO and Aldicarb for 24 h and an LDH assay was performed.

As shown Figure 5-6, dose-response curves of CPO, AZO, and Aldicarb for LDH assay over 24 h exposure clearly indicates pesticides induced cytotoxicity in both phenotypes in a concentration-dependent manner. Cell cytotoxicity responses of undifferentiated cells were highly sensitive to CPO, AZO, and Aldicarb in the concentration range of 30 - 200 µM compared to non-treated controls. The effect was more dramatic at 200 µM which showed higher LDH

production compared to the vehicle control treatments. However, LDH production at 0.3 µM was not significant compared to the vehicle control in all three pesticides tested: CPO (p>0.9999); AZO (p>0.7021); Aldicarb (p>0.9999), suggesting that until a concentration of 0.3 µM is reached, CPO, AZO and Aldicarb induced minimal cytotoxicity in undifferentiated cells, which is consistent with the MTT assay. At 1 µM, only Aldicarb (p<0.001) induced statistically significant cytotoxicity compared to the non-treated control with a 10.4% increase of LDH production compared to vehicle control treatment. CPO (p>0.5213) and AZO (p>0.1897) did not induce significant cell death in undifferentiated cells compared to the corresponding non-treated controls. At 1 µM, CPO showed 9.3% and AZO showed 6.3% increase in LDH production compared to vehicle control treatments according to Figure 5-6. CPO and AZO induced significant LDH production at 3 µM concentration to a percentage of 13.8% and 24.7%, respectively, suggesting that undifferentiated cells are slightly resistant to the toxic insult of CPO and AZO up to 3 µM. The cytotoxicity of CPO, AZO and Aldicarb accelerated mainly at 3 µM to 200 µM, with the rate of increasing cytotoxicity decreased from 100 to 200 µM showing quite similar cytotoxic effect at both 100 and 200 µM (Figure 5-7). However, AZO induced less LDH production at 100 µM compare to AZO and Aldicarb. IC_{50} values interpolated from corresponding concentration-repose curves for undifferentiated cells are CPO: 12.19 ± 0.6393 µM; AZO: 12.15 ± 1.207 µM; and Aldicarb: 14.21 ± 1.087 µM.

Differentiated cells showed a similar response to CPO, AZO and Aldicarb as undifferentiated cells in terms of cytotoxicity responses. Concentration-dependent increases in cytotoxicity were observed for the three pesticides in differentiated cells. However, at 0.3 µM differentiated cells showed similar responses to that shown for the MTT assay. Differentiated cells did not show

significant LDH production at 0.3 µM CPO (p>0.9999), AZO (p>0.09011), or Aldicarb (p>0. 0.9999) with a percentage increase for CPO of 0.13%; AZO: 4.9%; and Aldicarb: 0.7% compared to the non-treated controls. Furthermore, only CPO (p<0.0455) and Aldicarb (p<0.003) showed significant effects on differentiated cells displaying 11.02% and 14.8% increase in LDH production, respectively, compared to their non-treated controls after a 1 µM exposure, whereas AZO (p>0.9445) was not significant at 1 µM, generating a 4.3% increase in LDH production compared to the non-treated control. Differentiated cells displayed a sharp increase in LDH production over the concentration range of 3-200 µM, with a dramatic effect apparent at 200 µM treatment compared to vehicle treatments. Therefore, CPO and Aldicarb showed minimal cytotoxic effect until 1 µM while AZO does not induce cytotoxicity until 3 µM (AZO-27.9%). This suggested that three pesticide showed differential sensitivity on differentiated cells in inducing cytotoxic responses (Figure 5-7). IC_{50} values interpolated from concentration-responses curves for differentiated cells were CPO: 9.833 ± 0.3710 µM; AZO: 11.41 ± 1.081 µM; and Aldicarb: 13.51 ± 0.7432 µM.

A comparison of undifferentiated vs differentiated cells for LDH production showed marked interaction between the cell phenotype and the pesticides (p<0.05). However, when the main pesticides effects for each phenotype are considered, CPO and AZO induced cytotoxicity in both undifferentiated and differentiated cells without significant difference, but when compared to that from Aldicarb there was a significant difference between AZO and CPO (Figure 5-7; Table 5-5).

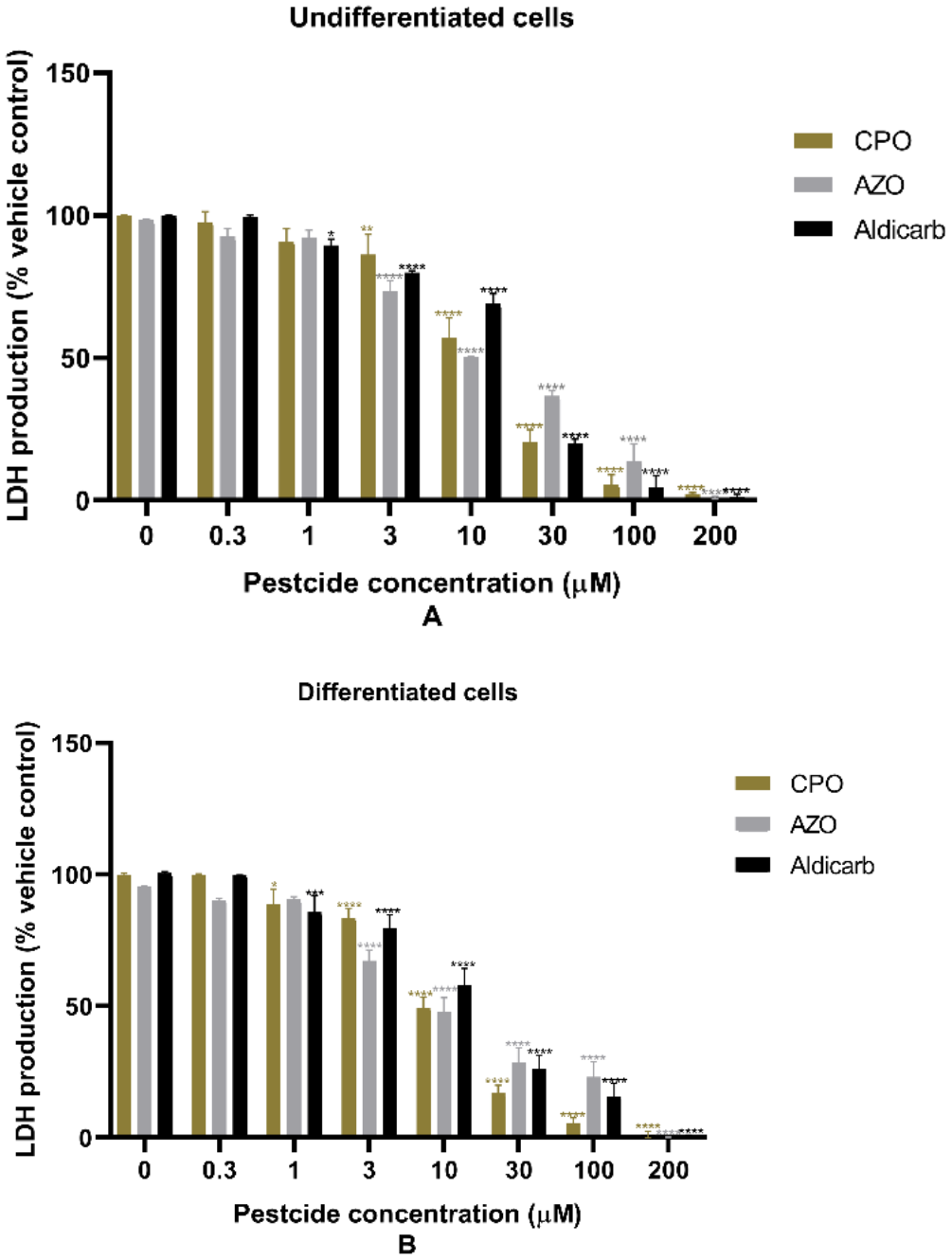
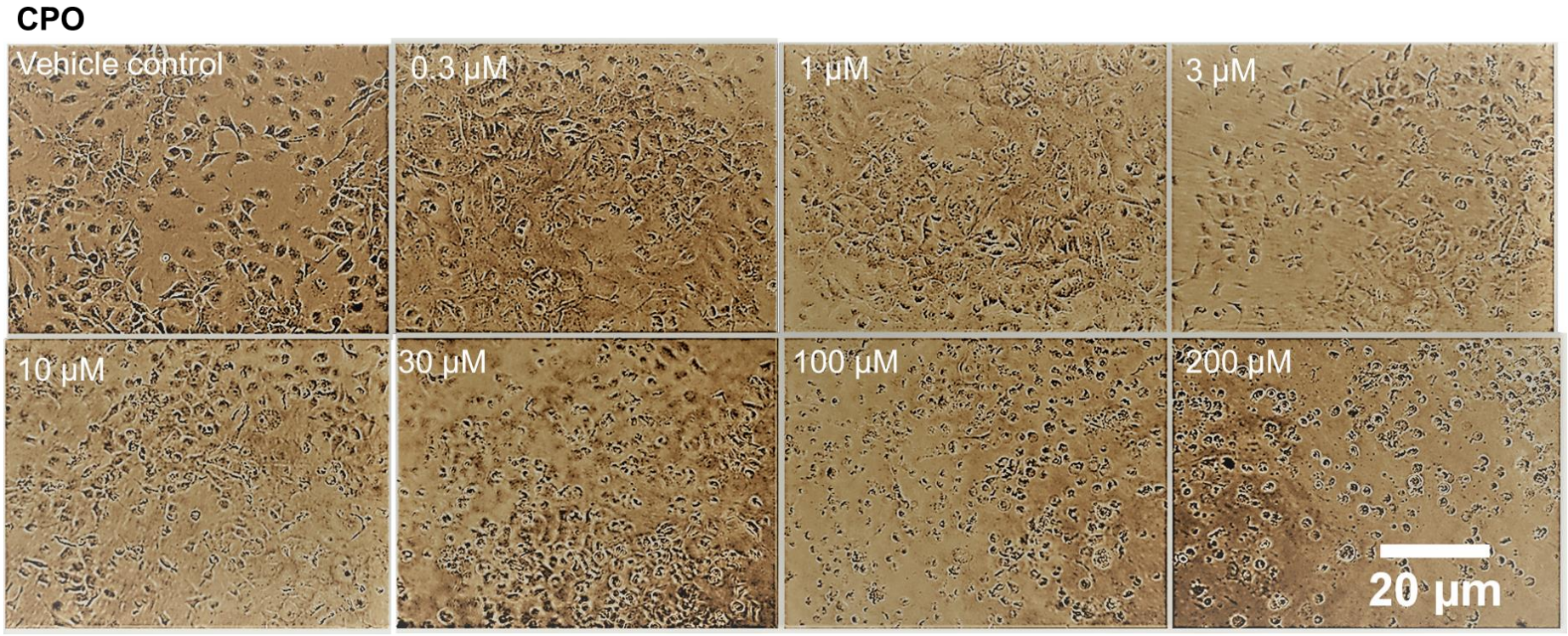


Figure 5-7: Effect of CPO,AZO and Aldicarb on undifferentiated and differentiated cell cytotoxicity.

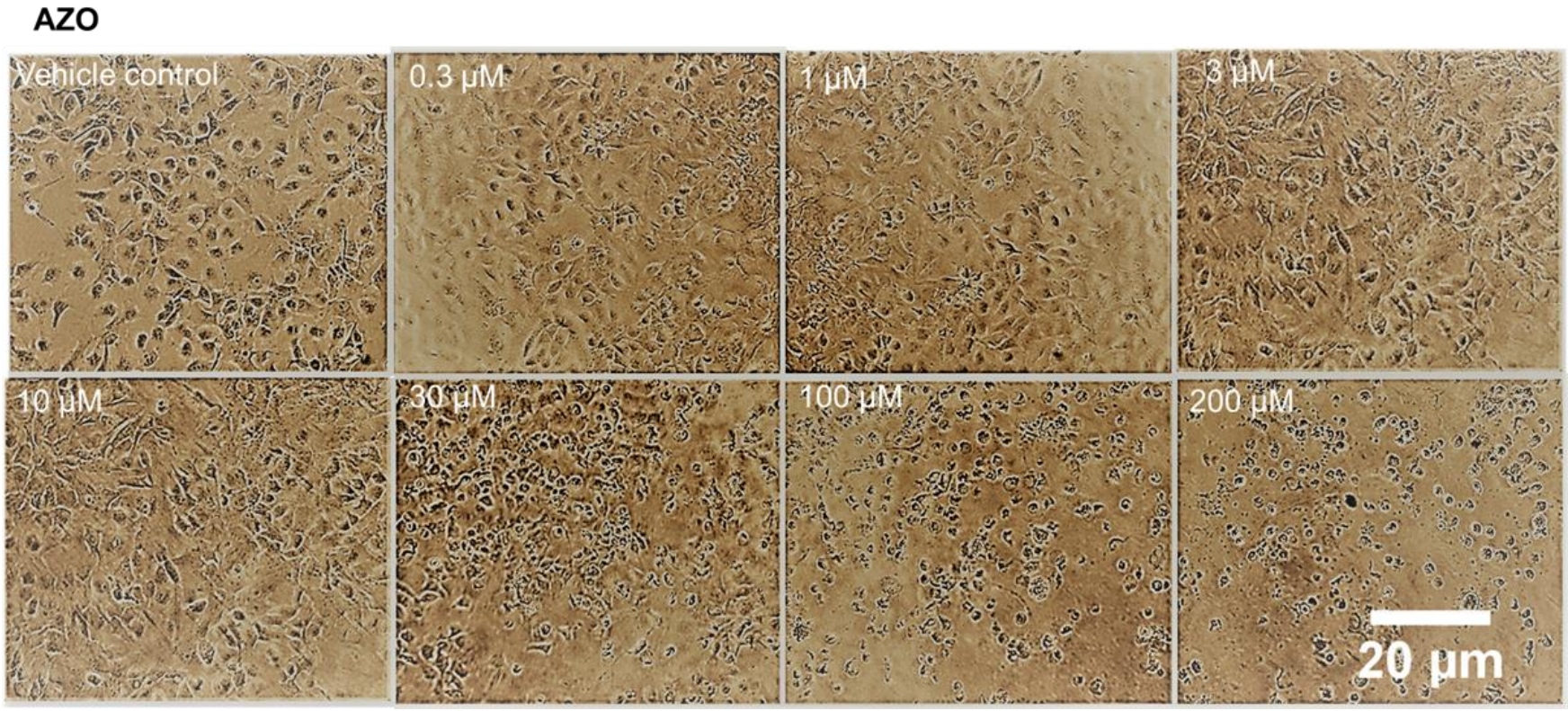
A- Undifferentiated and B- differentiated cells were treated with CPO, AZO, and Aldicarb for 24 h over the range of 0, 0.3, 1, 3, 10, 30, 100 and 200 µM. Cytotoxicity was assessed using a LDH assay. Readings were normalized to the LDH production of vehicle control, providing cell viability percentage, as a percentage value to the vehicle control. Readings including vehicle control and treatments were performed as triplicates in 5 independent experiments (n=5). Results analysed using one-way ANOVA with Dunnett's multiple comparison and expressed as the mean ± standard error of the mean (SEM), when SEM bar is not apparent, this means that error is smaller than the symbol size. For significance; *p<0.05, **p<0.01, ***p<0.001, ****p<0.0001.

5.2.5 Morphological observation of CPO, AZO and Aldicarb treated cells

Cellular morphological changes arose after exposure to CPO, AZO, or Aldicarb was captured using a phase contrast microscope. Consistent with MTT and LDH assays, there was a decrease in cell number and loss of cell contacts apparent when the concentration of pesticides was increased in both undifferentiated and differentiated ReNcell CX cells as illustrated in Figure 5-8 and Figure 5-9. According to images, at 100 and 200 µM exposures visible cell death (reduced numbers) was apparent after exposure to all pesticides in both undifferentiated and differentiated cells. Also, there was an apparent loss of neuronal connections by retraction/degeneration of existing neurites in cells.



A



B

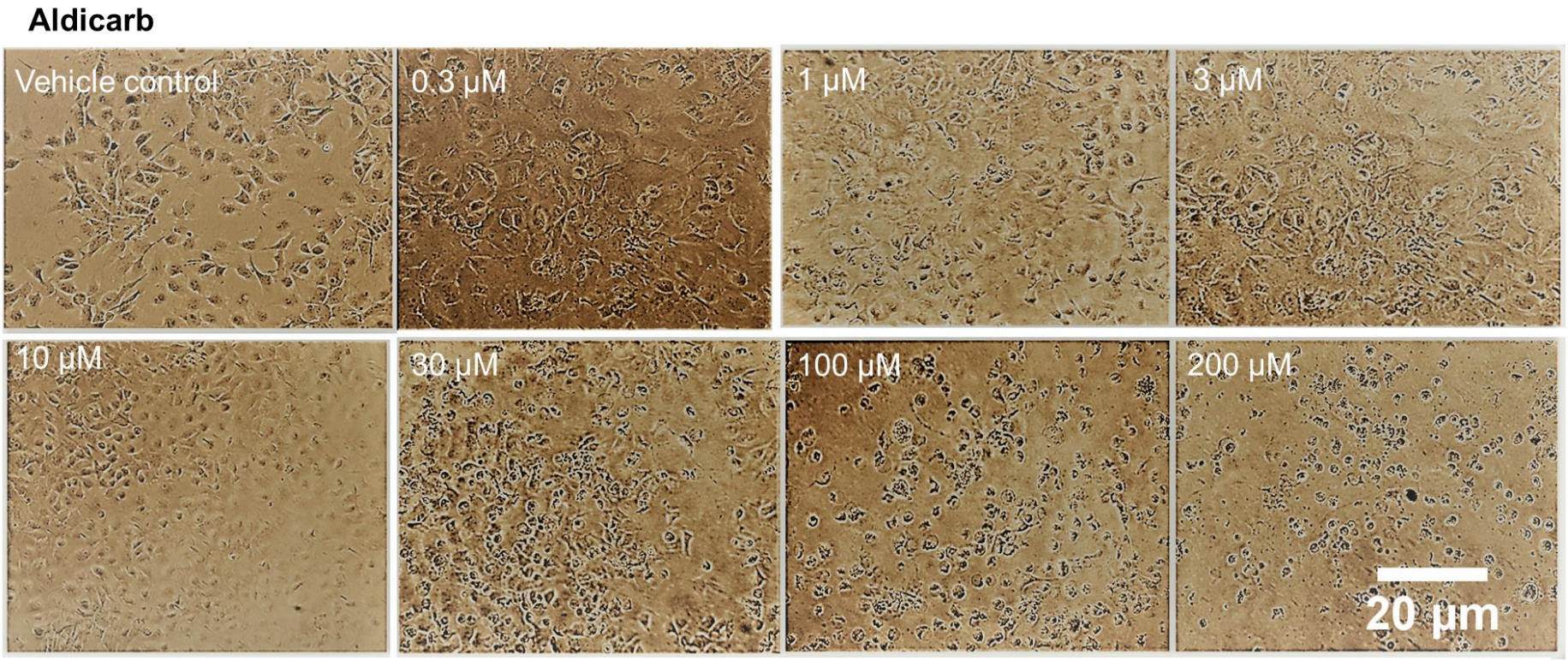
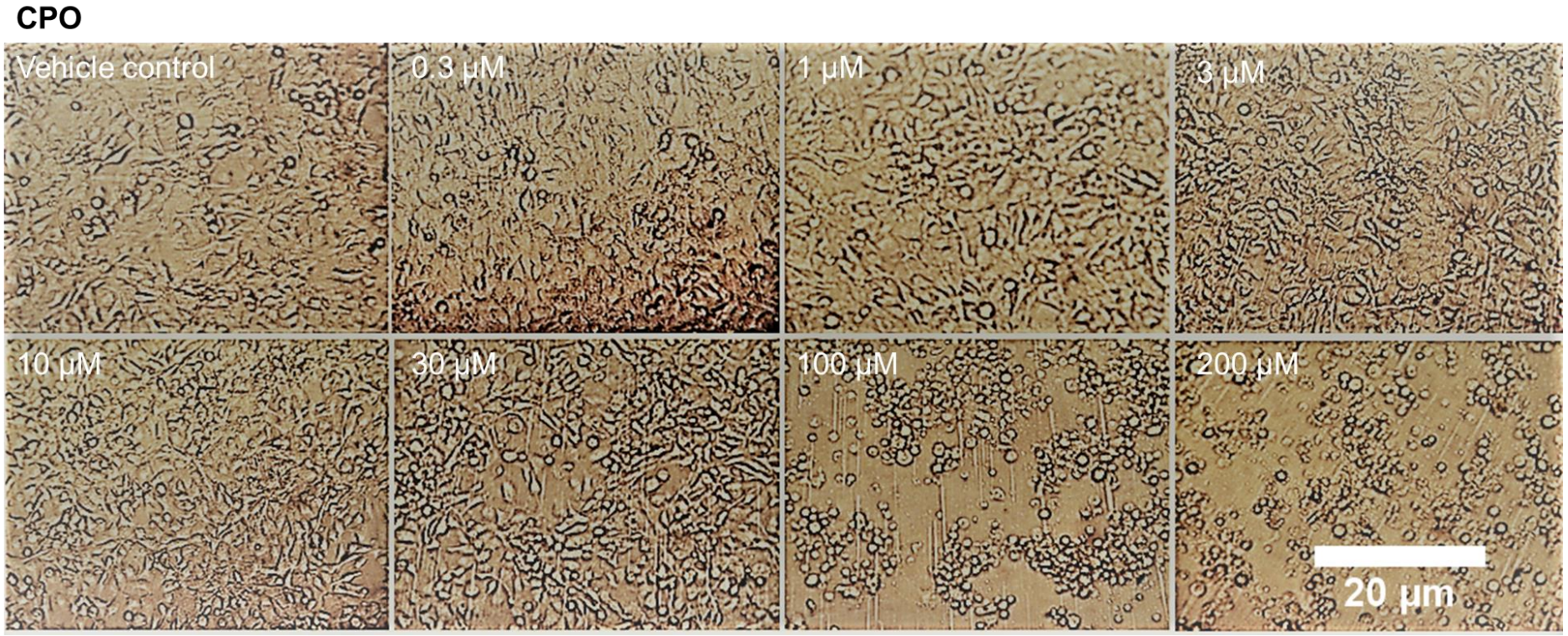


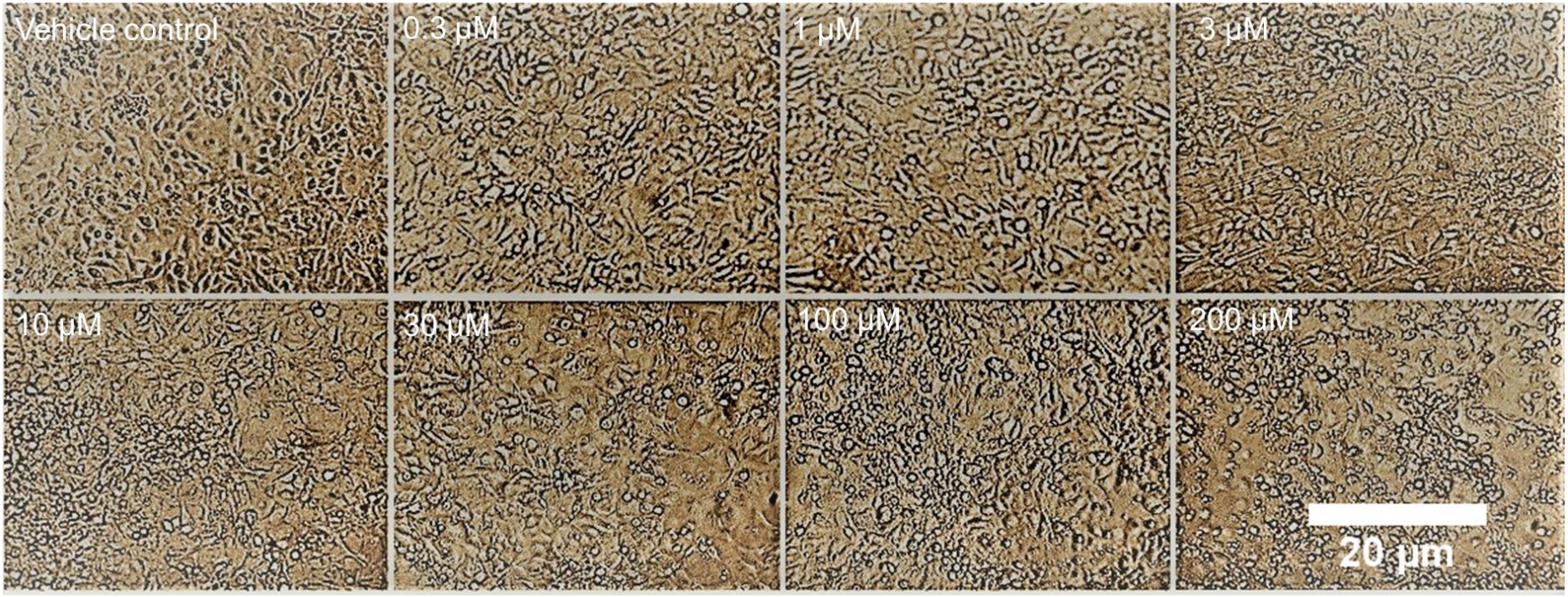
Figure 5-8: Morphological changes of undifferentiated ReNcell CX exposed to CPO,AZO and Aldicarb.
Undifferentiated cells were exposed to CPO, AZO and Aldicarb over the concentration range of 0 - 200 µM and cells imaged using an Olympus phase contrast microscope after 24 h. Scale bar: 20 µM.

C



A

AZO



B

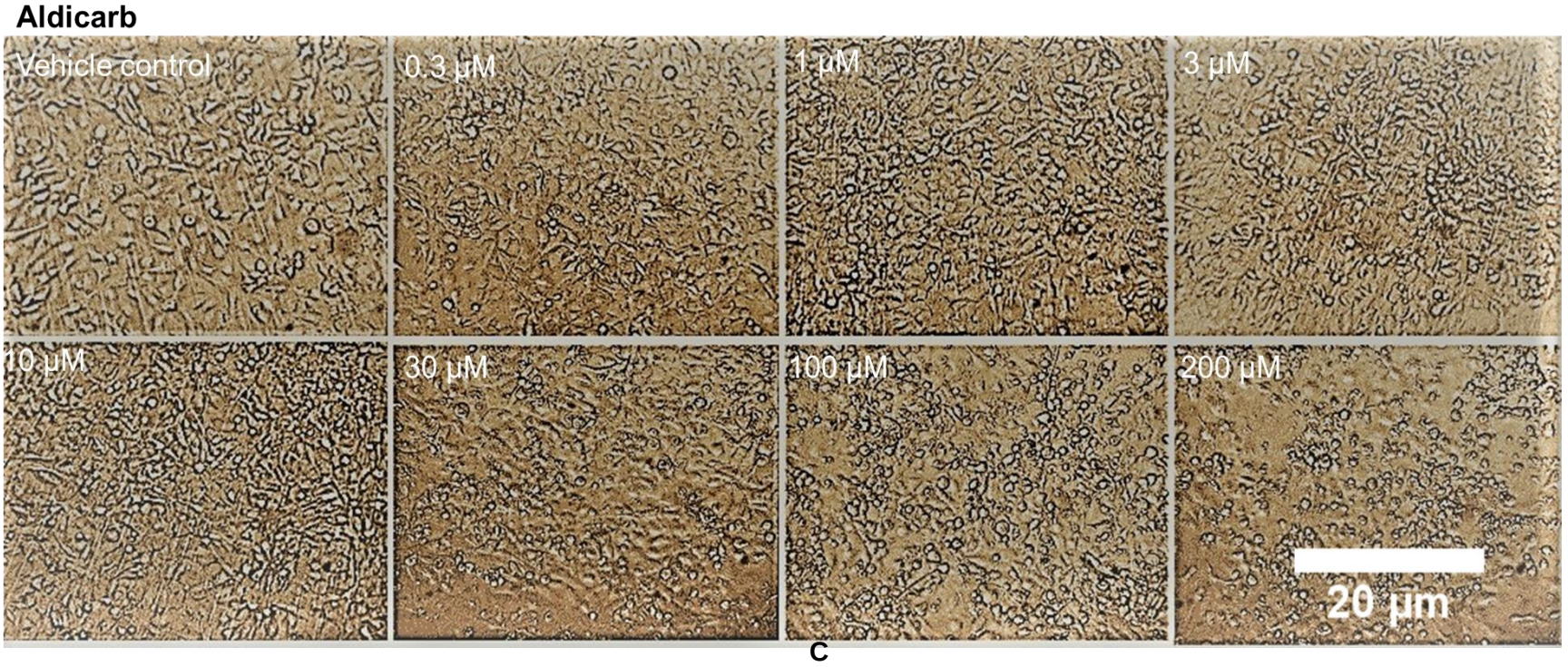


Figure 5-9: Morphological changes of differentiated ReNcell CX exposed to CPO,AZO and Aldicarb.
Differentiated cells exposed to CPO, AZO and Aldicarb over the concentration range of 0 - 200 µM and cells imaged using an Olympus phase contrast microscope after 24 h. Scale bar: 20 µM.

Table 5-1: Toxicity of CPO, AZO, and Aldicarb to undifferentiated and differentiated HNPCs.

Cell type	Pesticides	MTT assay		LDH assay		ATP assay		AChE inhibition	
		IC_{50} (µM)	R^2	IC_{50} (µM)	R^2	IC_{50} (µM)	R^2	IC_{50} (µM)	R^2
Undifferentiated	CPO	11.95 ± 1.9	0.9373	12.19 ± 0.6	0.9955	12.49 ± 1.4	0.9614	0.2263 ± 0.02	0.9493
Differentiated		8.172 ± 0.8	0.9716	9.833 ± 0.3	0.9906	9.184 ± 0.9	0.9784	0.1266 ± 0.01	0.9497
Undifferentiated	AZO	16.50 ± 1.4	0.9772	12.15 ± 1.2	0.9735	12.81 ± 0.2	0.9977	0.2053 ± 0.02	0.9252
Differentiated		8.588 ± 1.0	0.9624	11.41 ± 1.0	0.9748	11.02 ± 0.3	0.9956	0.1855 ± 0.01	0.9649
Undifferentiated	Aldicarb	14.79 ± 2.9	0.9108	14.21 ± 1.0	0.9794	14.81 ± 1.2	0.9703	0.2207 ± 0.01	0.9932
Differentiated		12.29 ± 1.7	0.9490	13.51 ± 0.7	0.9908	13.84 ± 1.4	0.9615	0.2120 ± 0.01	0.9976

IC_{50}- 50%inhibition concentration producing; all values are interpolated from corresponding dose-reposes curves and expressed as means ± 95% confidence interval in five independent experiments, MTT- (4,5-dimethylthiazol-2-yl)-2,5-diphenyltetrazolium bromide, LDH- Lactate dehydrogenase, ATP- Adenosine triphosphate, AChE- Acetylcholinesterase.

5.2.6 CPO, AZO, and Aldicarb inhibit AChE in a concentration-dependent manner in ReNcell CX.

The key mechanism of CPO, AZO and Aldicarb induced cytotoxicity is via inhibition of AChE in neuronal cells. Therefore, to gain insight into AChE inhibition in ReNcell CX cells, cells were exposed to CPO, AZO, and Aldicarb for 24, and then a modified Ellman's assay was used as explained in Flaskos et al. (2007) using a microtiter plate assay. Assay linearity with reaction time and the amount of sample volume was established before the assay. According to Figure 5-10, there was a significant difference in the linearity of signal in undifferentiated and differentiated cells. The use of a volume of up to 150 µl showed that absorbance reached up to maximum values, hence on that basis, 100 µl volume of cells was selected for the study.

Preliminary experiments were done over the range of 0 - 200 µM and then this was narrowed down to 0 - 1 µM for further experimentation. CPO, AZO, and Aldicarb showed concentration-dependent inhibition of AChE for 24 h according to Figure 5-11. CPO, AZO, and Aldicarb induced AChE inhibition in the nanomolar range. CPO, AZO and Aldicarb induced significant inhibition (p<0.0001) at 0.1 µM compared to the vehicle control treatments in both undifferentiated and differentiated cells. At 0.1 µM treatment, CPO, AZO and Aldicarb inhibited 30.9%, 20.8% and 14.8% of AChE, respectively, in undifferentiated cells compared to their corresponding vehicle controls (Figure 5-11). The response in differentiated cells was 38.26% by CPO, 25.40% by AZO and 10.1% by Aldicarb for AChE inhibition after a 24 h exposure compared to their non-treated controls. Aldicarb induced 39.2% AChE inhibition in undifferentiated cells and 42.8 % AChE inhibition for differentiated cells at 0.2 µM treatment. CPO and AZO induced more than 20% inhibition at 0.2 µM compared to non-treated controls in both phenotypes (Figure 5-11). However,

inhibition accelerated until 1 µM and the curve then plateaued at 0.3 - 1 µM range, suggesting complete inhibition of AChE at higher concentrations by all three pesticides. IC_{50} values interpolated from concentration-response curves of both undifferentiated and differentiated cells were in the nanomolar range (100-230 nM) for the three pesticides (Figure 5-11, Table 5-1).

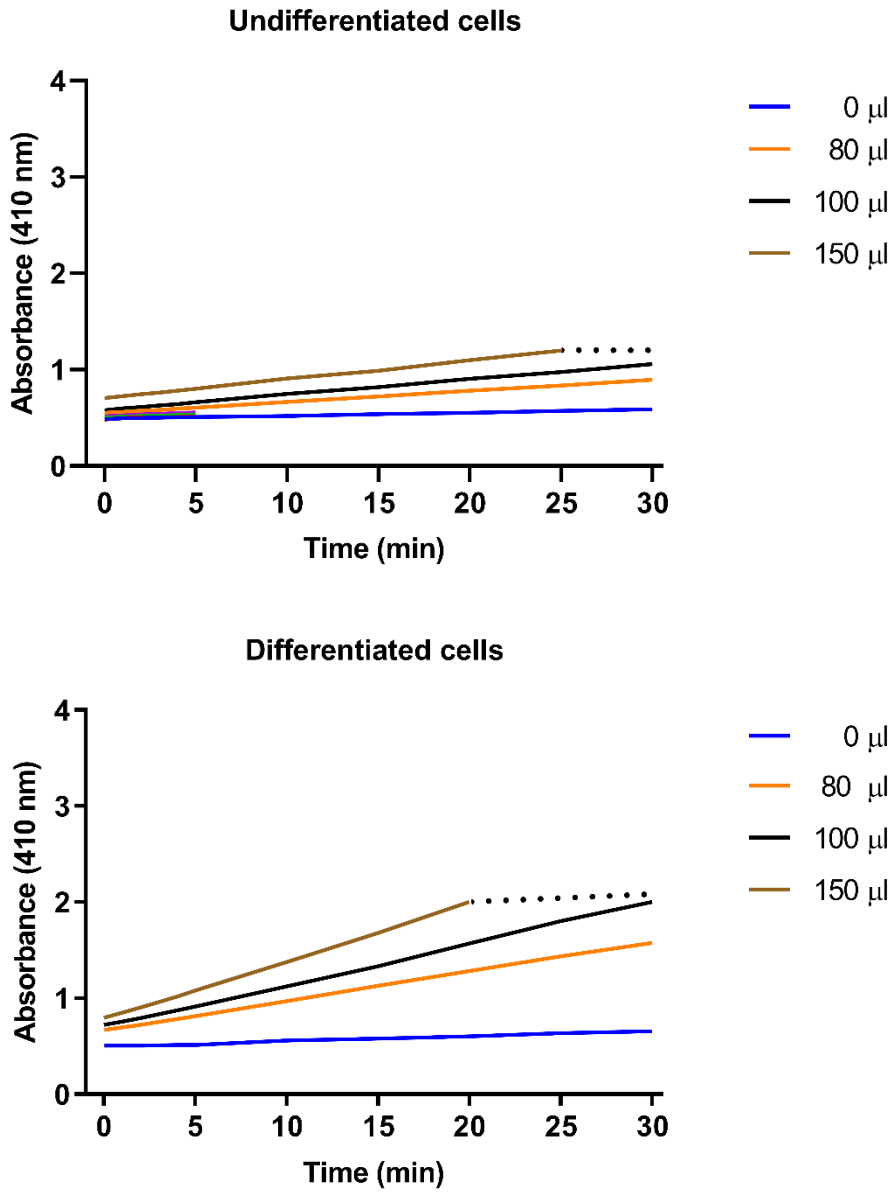
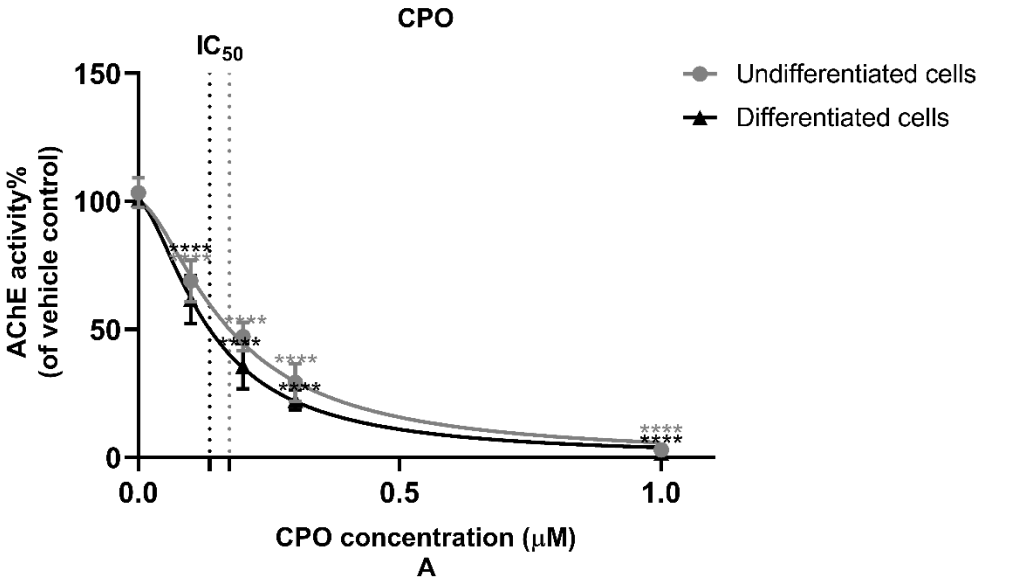
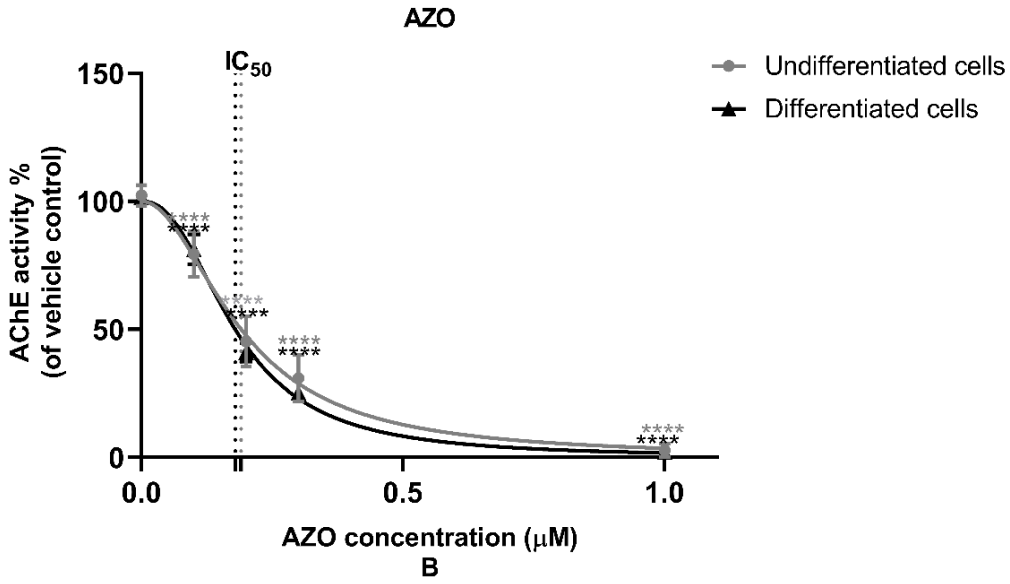


Figure 5-10: Assay linearity with the reaction and cell sample volume of ReNcell CX cells

Figure shows the absorbance versus the reaction time for each different volume of cell samples in undifferentiated and differentiated cells. AChE activity was measured by Ellman's assay. Points represent the five independent experiments with three replicates each sample (n=5).


CPO
IC50
Undifferentiated cells
Differentiated cells
AChE activity%
(of vehicle control)
150
100
50
0
0.0
0.5
1.0
CPO concentration (μM)
A


AZO
IC50
Undifferentiated cells
Differentiated cells
AChE activity %
(of vehicle control)
150
100
50
0
0.0
0.5
1.0
AZO concentration (μM)
B

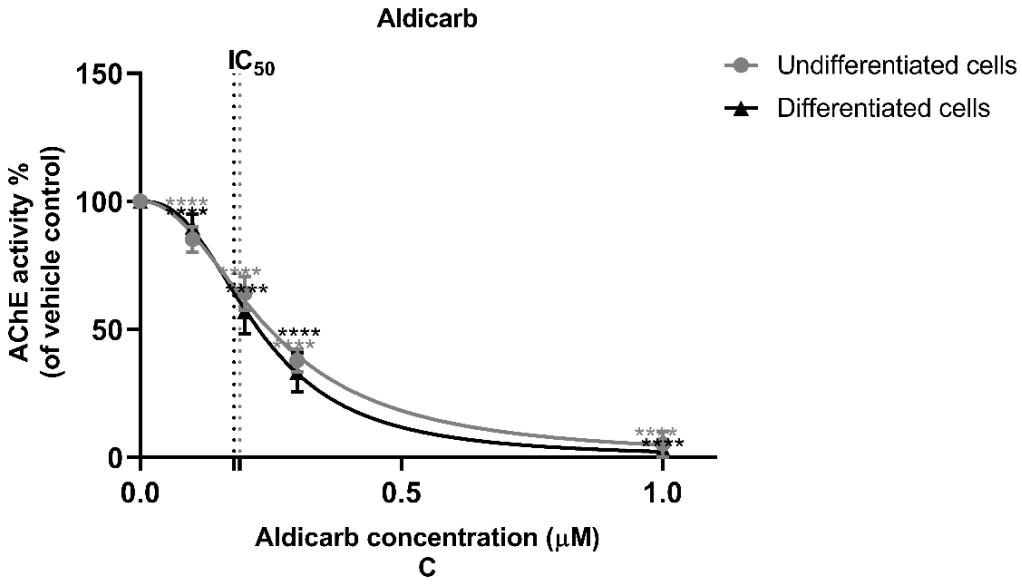


Figure 5-11: Effect of CPO, AZO and Aldicarb on inhibition of AChE in ReNcell CX.

Undifferentiated and differentiated cells were treated with CPO (A), AZO (B), and Aldicarb (C) for 24 h over the pesticide concentration range of 0, 0.1, 0.2, 0.3, and 1 µM. AChE inhibition was measured by Ellman's assay and the readings were normalised to the vehicle control values by subtracting the blank values and expressed as percentages to the corresponding vehicle control. Readings including vehicle control and treatments obtained from 5 independent experiments (n=5) with three replicates in each treatment. Results were analysed using one-way ANOVA with Dunnett's multiple comparison and expressed as the mean ± standard error of the mean (SEM), when SEM bar is not apparent, this means that error is smaller than the symbol size. For significance; **** p<0.0001.

Comparison of each pesticide's effects on undifferentiated and differentiated cells showed that there was a significant interaction between pesticide and cell phenotypes (CPO (p<0.0001), AZO (p<0.0001), and Aldicarbs (p<0.0001)) for AChE inhibition. A comparison of three pesticides on individual cell phenotype showed an interaction implying each pesticide has a selective effect on AChE inhibition. However, there is no significant difference in inhibition of AChE between CPO and AZO (p>0.7109) but a significant difference (p<0.0001) with Aldicarb for undifferentiated cells indicating the potency of toxicity descending as CPO>AZO>Aldicarb. CPO, AZO, and Aldicarb induced AChE inhibition in differentiated cells without any significant differences when compared to the main effects of each pesticide.

A pesticide concentration of 0.3 µM of CPO, AZO, or Aldicarb induced nearly 70% inhibition of AChE in both undifferentiated and differentiated cells, although more than 80% inhibition of AChE was observed at 1 µM in both phenotypes implying that the significant cell viability loss and cytotoxicity (apparent in MTT and LDH assays) was correlated to strong inhibition of AChE.

5.2.7 CPO, AZO, and Aldicarb decreased cellular ATP levels in ReNcell CX cells.

Next, to gain insight into the effects of low, moderate, and high dose exposure to undifferentiated and differentiated cells: IC_{10}, IC_{20}, IC_{50} and IC_{80} concentrations were interpolated from corresponding cell viability and cell cytotoxicity concentration-response curves and used to compare inhibition of ATP production: values as detailed in Table 5-2.

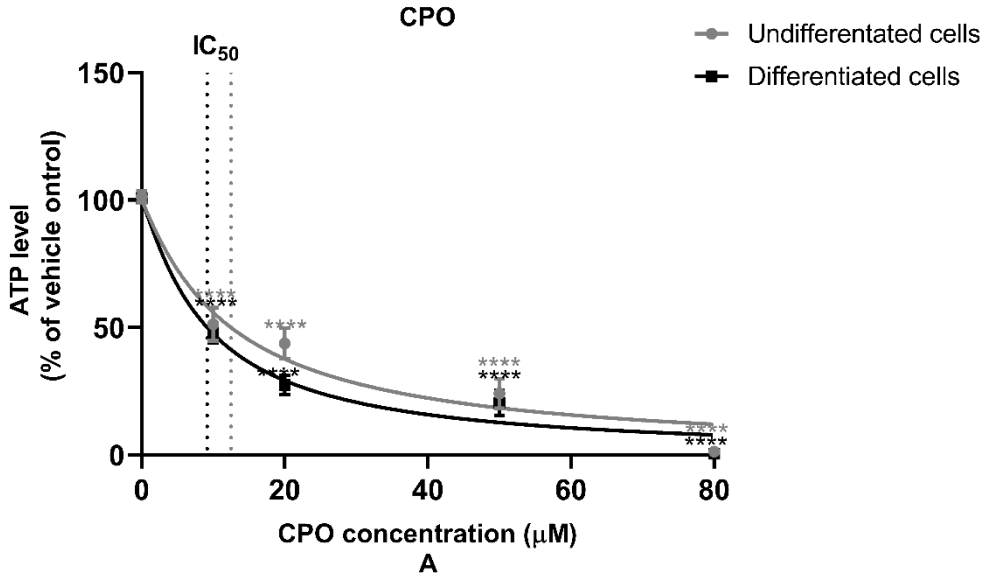
Table 5-2: 10, 20, 50 and 80% inhibition concentrations interpolated from dose-response curves.

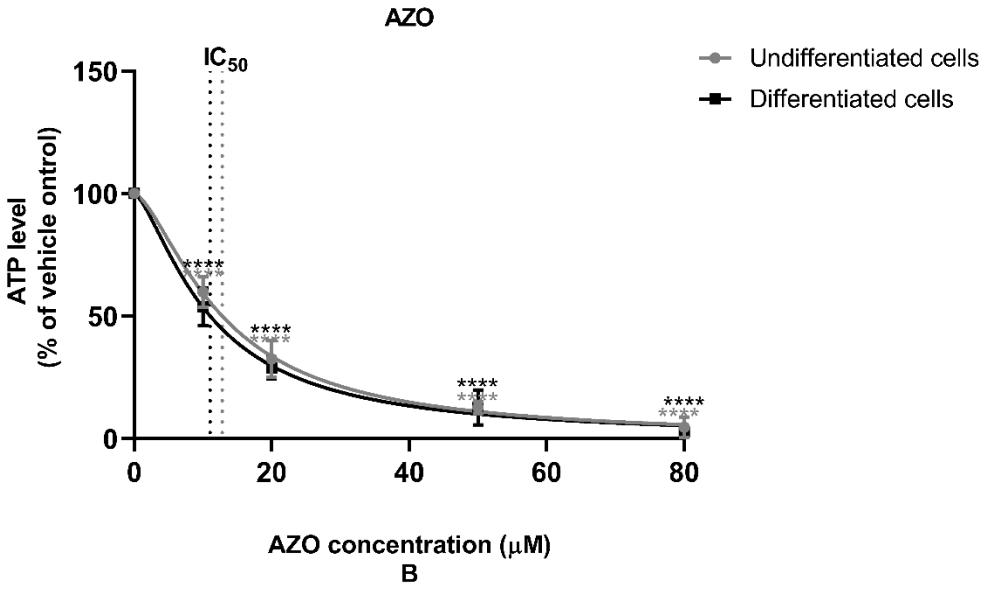
	Pesticides			
Cell type	IC value (µM)	CPO (µM)	AZO (µM)	Aldicarb (µM)
Undifferentiated	IC_{10}	0.7	1.4	0.9
	IC_{20}	2.1	4.8	1.5
	IC_{50}	12.2	14.1	15.1
	IC_{80}	71.1	78.5	285.3
Differentiated	IC_{10}	0.4	0.5	1.5
	IC_{20}	1.5	2.3	4.5
	IC_{50}	09	10.5	12.6
	IC_{80}	50	57.9	102.4

IC_{10}- 10%, inhibition concentration; IC_{20}- 20 % inhibition concentration; IC_{50}- 50% inhibition concentration; IC_{80}- 80% inhibition concentration

Functional cell survival when plotted against the pesticide concentrations showed that there was a concentration-dependent decrease in metabolic activity (MTT assay), and likewise, in turn, that the mitochondrial function of cells

was depleted as evidenced by reduced mitochondrial NAD(P)H-dependent cellular oxidoreductase enzymes and ATP production. Since one of the major functions of mitochondria is ATP production, then low, moderate and high concentrations of pesticide treatments were selected (Table 5-2) and applied to both undifferentiated and differentiated cells for 24 h to confirm the dose-dependent cell viability loss, and to gain insight into the impact of CPO, AZO and Aldicarb on cellular ATP production.





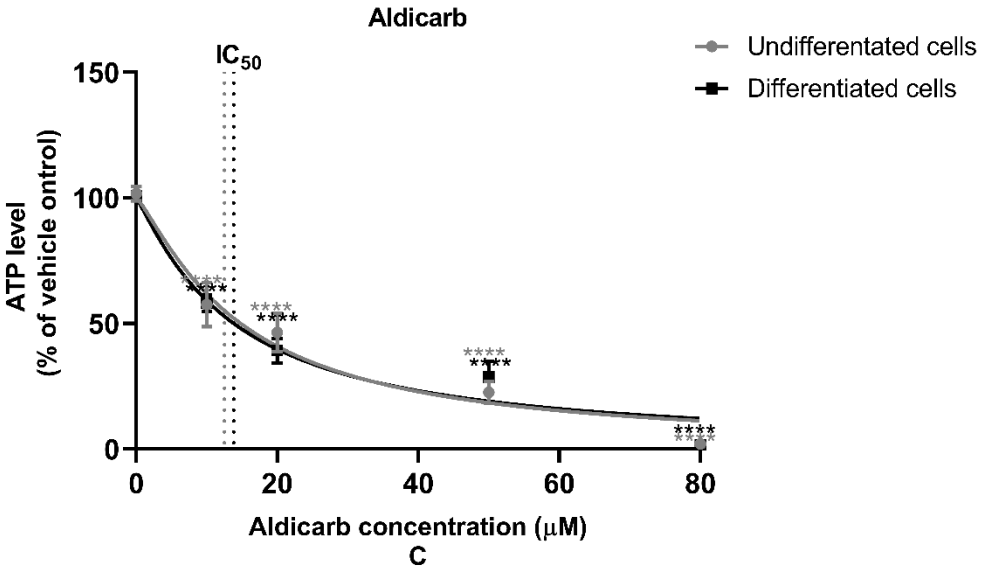


Figure 5-12: Effect of CPO, AZO, and Aldicarb on cellular ATP levels. Undifferentiated and differentiated cells were treated with CPO (A), AZO (B), and Aldicarb (C) for 24 h over the range of IC_{10}, IC_{20}, IC_{50} and IC_{80} µM. ATP levels were measured by ATP luminescence assay and the readings were normalised to the vehicle control values by subtracting the blank values and expressed as percentages to the corresponding vehicle control. Readings including vehicle control and treatments obtained from 5 independent experiments (n=5) with three replicates in each treatment. Results analysed using one-way ANOVA with Dunnett's multiple comparison and expressed as the mean ± standard error of the mean (SEM), when SEM bar is not apparent, this means that error is smaller than the symbol size. For significance; **** p<0.0001.

IC_{10}, IC_{20}, IC_{50} and IC_{80} concentrations influenced cellular ATP levels in both undifferentiated and differentiated cells with a response curve exhibiting various degrees of deviation from 100% vehicle control treatments as depicted in Figure 5-12. However, cellular ATP levels drops significantly starting from IC_{10} concentration and curve gets more steeper, indicating IC_{20}, IC_{50}, IC_{80} concentrations significantly influence cellular ATP production in both phenotypes of ReNcell CX cells, in support of the MTT assays and LDH dose-response curves. IC_{80} concentration of CPO, AZO and Aldicarb showed a dramatic effect on cellular ATP production in both phenotypes (Figure 5-12).

However, for the MTT viability curve, there is a minimal effect until 1µM on undifferentiated cells, but cellular ATP levels start to drop in CPO and Aldicarb at 0.7 and 0.9 µM concentrations. AZO induced significant ATP level drops in

undifferentiated cells compared to non-treated controls at 1.4 µM justifying MTT assay results that it induced significant viability loss in cells at higher concentration than 0.3 µM. In contrast to the LDH assay results, 1 µM induced significant LDH production in Aldicarb in undifferentiated cells, but this was not observed for CPO and AZO treatments. Significant level of LDH production in CPO and LDH treated cells were observed in 3 µM treatment (Figure 5-7).

A comparison of the ATP level drop in differentiated cells upon CPO, AZO, and Aldicarb exposure contextualized that the drop in cellular ATP levels is inconsistent with the results of MTT and LDH assay, and showed that significant viability loss and cell death in differentiated cells was apparent at 1 µM only for CPO and Aldicarb. In line with that, there was a significant ATP level reduction apparent at 0.4, 0.5 and 0.6 µM for CPO, AZO, and Aldicarb, respectively. This further suggested that differentiated cells are more sensitive to toxic insult of CPO, AZO and Aldicarb.

CPO and AZO reduced ATP levels in undifferentiated cells with marked difference at higher concentrations which is similar in MTT and LDH assays. According to the graph, there was a significant ATP level drop in the order: AZO>CPO>Aldicarb for undifferentiated cells (Figure 5-13 A). In line with the MTT and LDH data, differentiated cells showed an order of potency of the pesticide in terms of reduced ATP level production as CPO>AZO>Aldicarb (Figure 5-13 B). However, there is a significant interaction with CPO, AZO, and Aldicarb exposure impact on cellular ATP levels revealed by two-way ANOVA and Tukey's multiple comparisons of each concentration on both cell phenotypes (Table 5-5).

This result suggested that CPO, AZO and Aldicarb alter cellular ATP levels at concentrations slightly lower than that able to induce significant viability loss and

cell death in undifferentiated and differentiated cells implying mitochondrial activity blunting before cell death upon pesticide exposure.

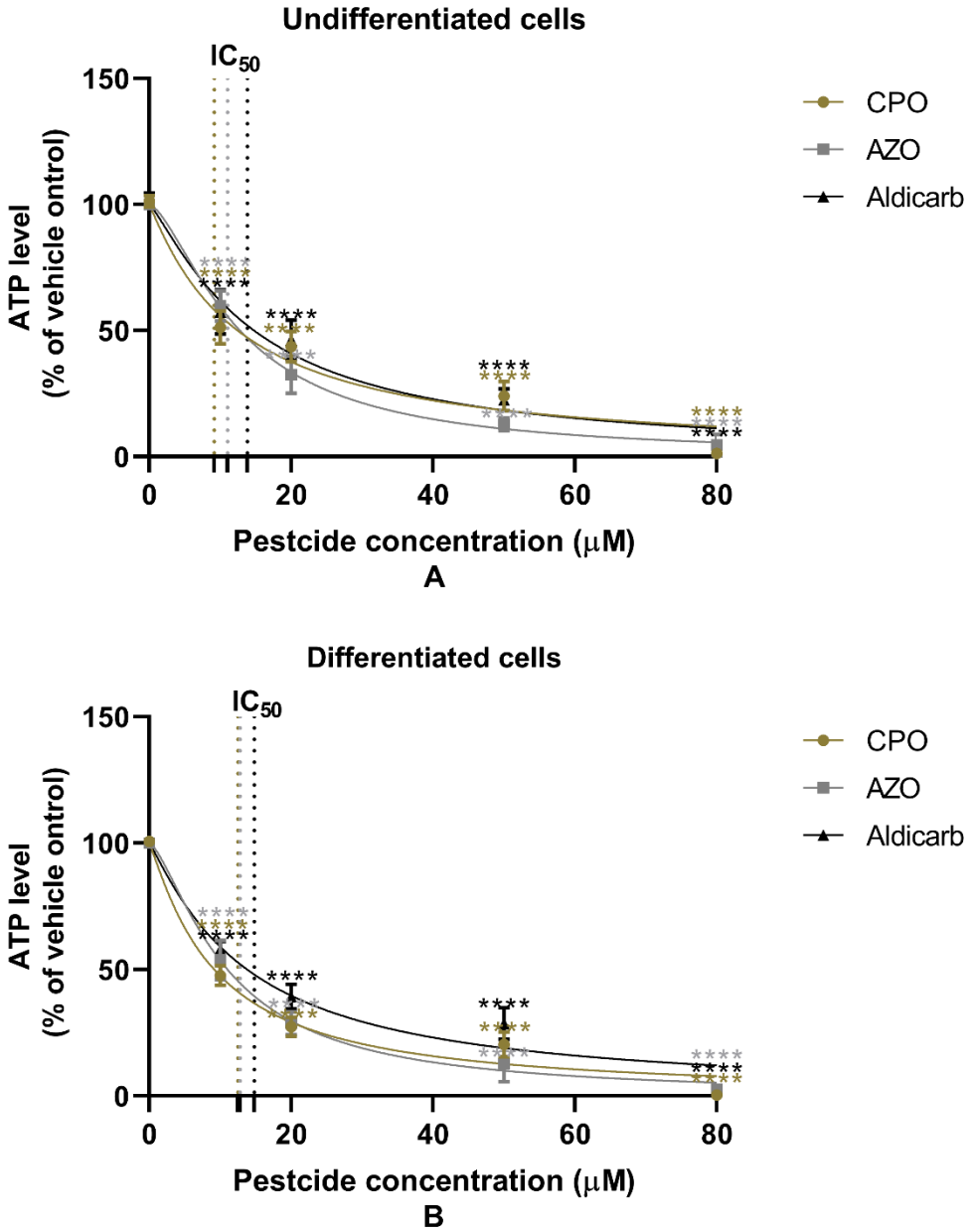


Figure 5-13: Effect of CPO,AZO and Aldicarb on cellular ATP levels on undifferentiated and differentiated ReNcell CX.

A- Undifferentiated and B- differentiated cells were treated with CPO, AZO and Aldicarb for 24 h with IC_{10}, IC_{20}, IC_{50} and IC_{80} concentrations. ATP levels were measured by ATP luminescence assay and the readings were normalised to the vehicle control values by subtracting the blank values and expressed as percentages to the corresponding vehicle control. Readings including vehicle control and treatments obtained from 5 independent experiments (n=5) with three replicates in each treatment. Results were analysed using one-way ANOVA with Dunnett's multiple comparison and expressed as the mean ± standard error of the mean (SEM), when SEM bar is not apparent, this means that error is smaller than the symbol size. For significance; **** p<0.0001.

5.2.8 CPO, AZO, and Aldicarb induced ROS generation in ReNcell CX cells.

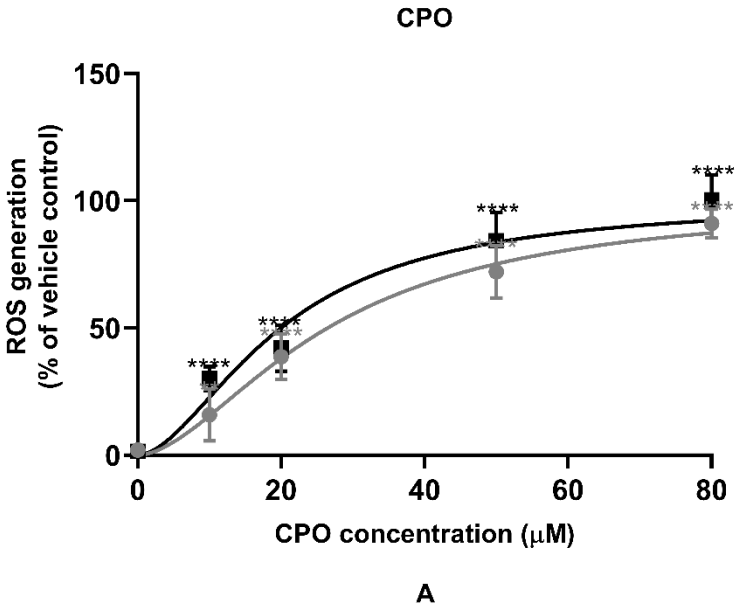
Next, to gain insight into the effects of CPO, AZO and Aldicarb on ROS generation in differentiated and undifferentiated ReNcell CX cells, a DCFDA assay was used. DCDFA assay was done for both 6 and 24 h time points (due to the short half-life of ROS), by exposing both phenotypes to IC_{10}, IC_{20}, IC_{50} and IC_{80} concentrations of CPO, AZO and Aldicarb.

CPO, AZO and Aldicarb induced ROS in both undifferentiated and differentiated cells in dose-dependent manner for 6 h (Figure 5-14 A-C) and 24 h (Figure 5-14 D-E). All concentrations induced significant (p<0.05) ROS production compared to their untreated control at both 6 h and 24 h. However, the comparison of 6 h and 24 h ROS generation indicates that CPO, AZO and Aldicarb induced significant levels of ROS in both undifferentiated and differentiated cells (Table 5-3). Although, ROS generation decreased with increasing incubation time and curves were flattened at higher concentrations at 24 h (Figure 5-15 D-E). CPO, AZO and Aldicarb significantly induced ROS generation in differentiated cells with levels higher than those in undifferentiated cells at both time points. Notably, ROS generation increased at lower concentrations after 24 h compared to 6 h in both phenotypes. Comparison of 6 h and 24 h exposure of CPO, AZO and Aldicarb on individual phenotypes indicated that there was a significant difference at IC_{50} and IC_{80} (Figure 5-14; Table 5-5).

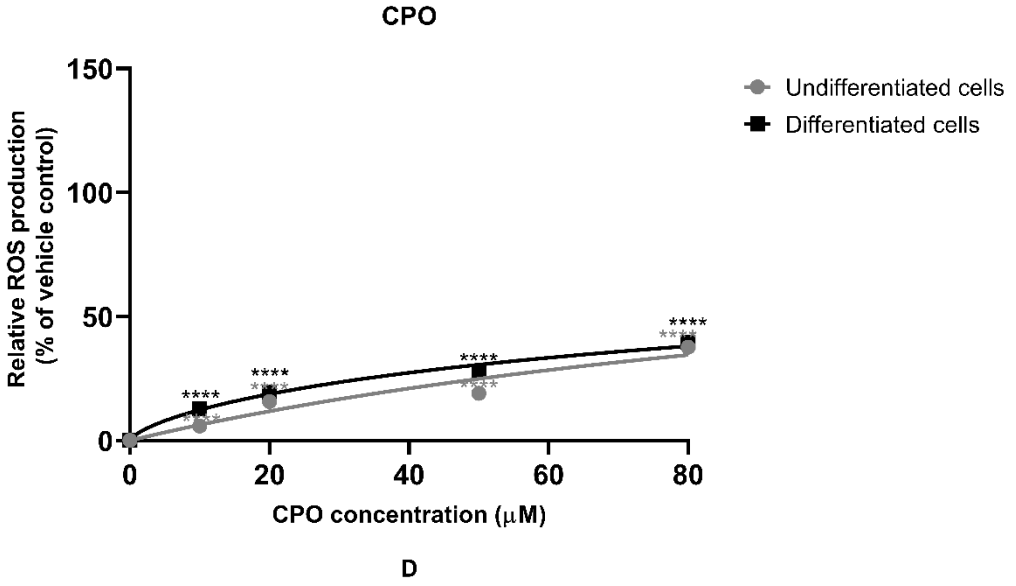
Table 5-3: Comparison of individual concentrations at 6 h and 24 h ROS generation by the exposure of CPO, AZO and Aldicarb on ReNcell CX.

Pesticide	Concentration (µM)	Undifferentiated cells	Differentiated cells
CPO	IC_{10}	NS	NS
	IC_{20}	0.0372	0.0180
	IC_{50}	<0.0001	<0.0001
	IC_{80}	<0.0001	<0.0001
AZO	IC_{10}	0.0015	<0.0001
	IC_{20}	NS	<0.0001
	IC_{50}	NS	<0.0001
	IC_{80}	<0.0001	<0.0001
Aldicarb	IC_{10}	NS	NS
	IC_{20}	<0.0001	0.0180
	IC_{50}	<0.0001	<0.0001
	IC_{80}	<0.0001	<0.0001

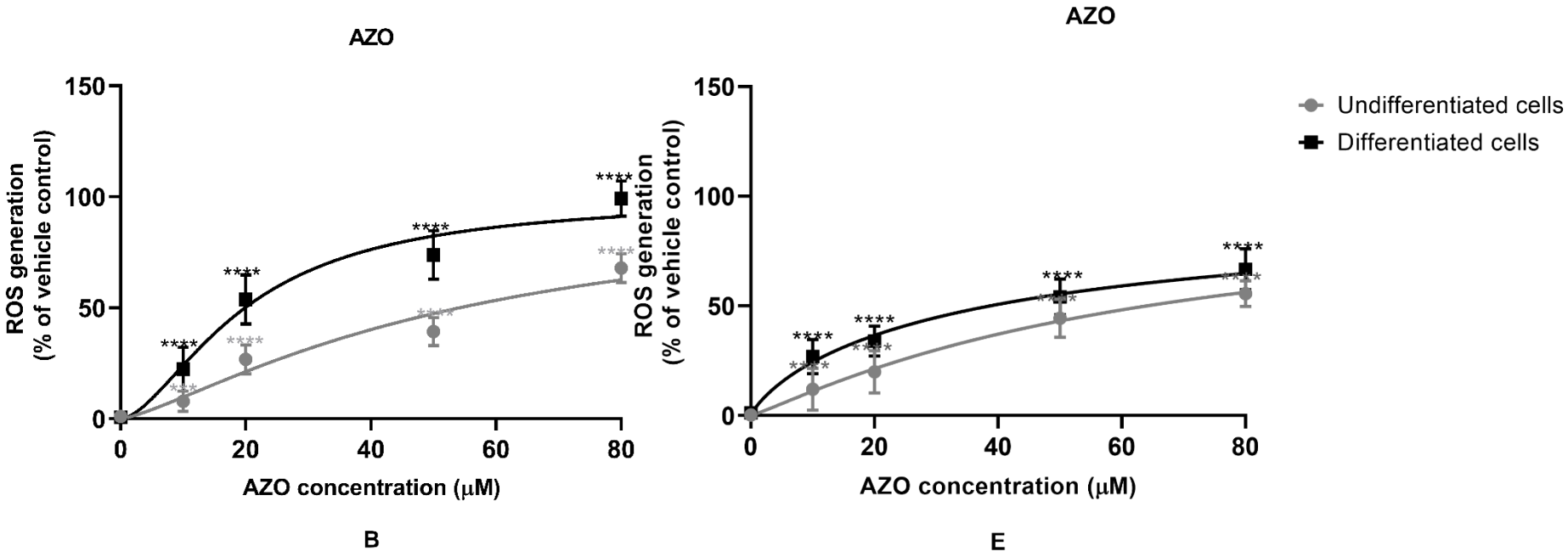
IC- inhibition concentration; IC_{10}- 10% inhibition concentration; IC_{20}- 20% inhibition concentration; IC_{50}- 50% inhibition concentration; IC_{80}- 80% inhibition concentration.


CPO
ROS generation
(% of vehicle control)
150
100
50
0
0
20
40
60
80
CPO concentration (μM)
****
****
****
****

A


CPO
Relative ROS production
(% of vehicle control)
150
100
50
0
0
20
40
60
80
CPO concentration (μM)
****
****
****
****
Undifferentiated cells
Differentiated cells

D


AZO
ROS generation (% of vehicle control)
150
100
50
0
0
20
40
60
80
AZO concentration (μM)
****
B
AZO
ROS generation (% of vehicle control)
AZO concentration (μM)
E
Undifferentiated cells
Differentiated cells

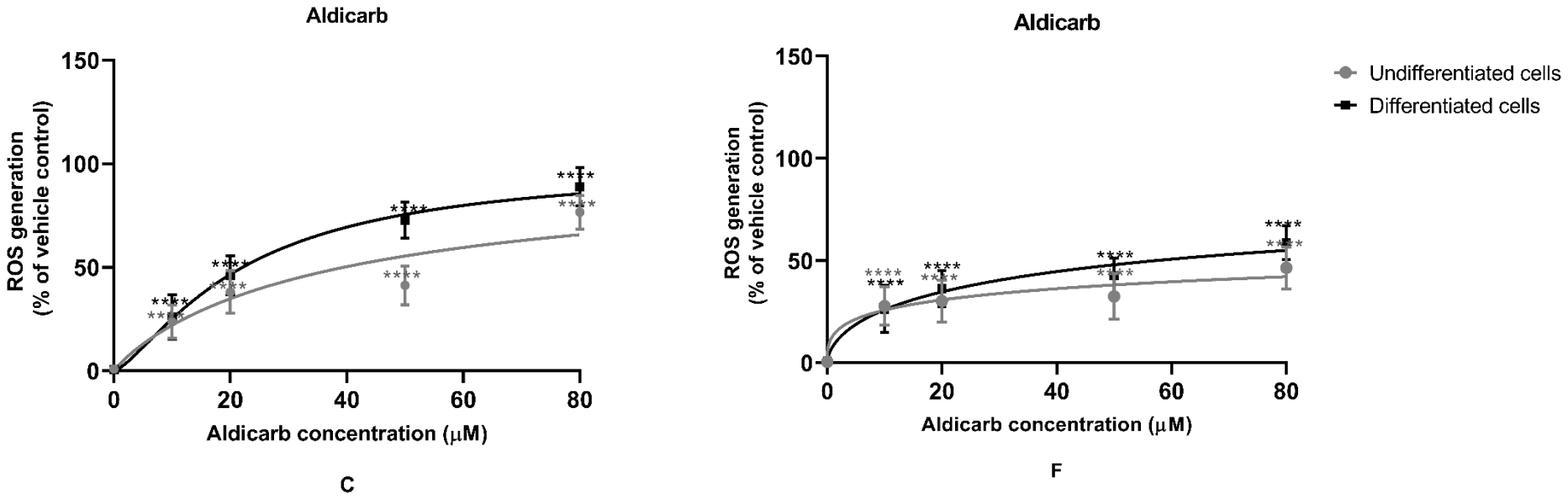


Figure 5-14: Effect of CPO,AZO and Aldicarb in cellular ROS generation.
Undifferentiated and differentiated cells were exposed IC_{10}, IC_{20}, IC_{50} and IC_{80} concentrations CPO, AZO and Aldicarb for 6h (A-C) and 24 h (D-E). Cellular ROS generation was quantified using DCFDA and readings were normalised to the vehicle control treatments and presented a percentage of vehicle control. Readings including vehicle control and treatments were obtained from 5 independent experiments (n=5) with triplicates in each treatment. Results were analysed using one-way ANOVA with Dunnett's multiple comparison and expressed as the mean ± standard error of the mean (SEM), when SEM bar is not apparent, this means that error is smaller than the symbol size. For significance; * p<0.05, ** p<0.01, *** p<0.001, **** p<0.0001.

5.2.9 Effect of CPO, AZO and Aldicarb on cellular protein carbonylation and association between ROS generation and ATP depletion in cells

Protein carbonylation is an irreversible protein oxidation mediated by oxidative stress in neuronal cells and is used as an oxidative stress marker in response to neurotoxicants exposures. Next, to gain insight into potential oxidative protein damages to proteins in ReNcell CX cells induced as a response to CPO, AZO or Aldicarb exposure, protein carbonylation levels were quantified. Specific protein targets of oxidative damage were identified after gel electrophoresis and immunoblotting of crude cytosolic fractions.

Protein carbonylation levels were increased in a concentration-dependent manner with increasing concentration of pesticides for CPO, AZO, and Aldicarb in both phenotypes of ReNcell CX cells. However, marked increased carbonylation was observed at IC_{80} for all three pesticides in both phenotypes of ReNcell CX cells compared to corresponding non-treated controls (Figure 5-15 A and B). Even at low doses, like IC_{10}, a significant (p<0.05) level of protein carbonylation was observed in both phenotypes as a response to CPO, AZO and Aldicarb exposure. The three pesticides exhibited differential effects on induction of protein carbonylation in both phenotypes of ReNcell CX. There was a marked difference between CPO and Aldicarb (p<0.0001), and AZO and Aldicarb (p<0.0001) on undifferentiated cells revealed by two-way ANOVA, and also there was a significant difference between induction of protein carbonylation by CPO and AZO (p=0.0001). Differentiated cells showed specificity of pesticide to induction of carbonylation responses as evidenced by a two-way ANOVA (CPO and AZO (p=0.0354), CPO and Aldicarb (p<0.0001) and AZO and Aldicarb (p<0.0001).

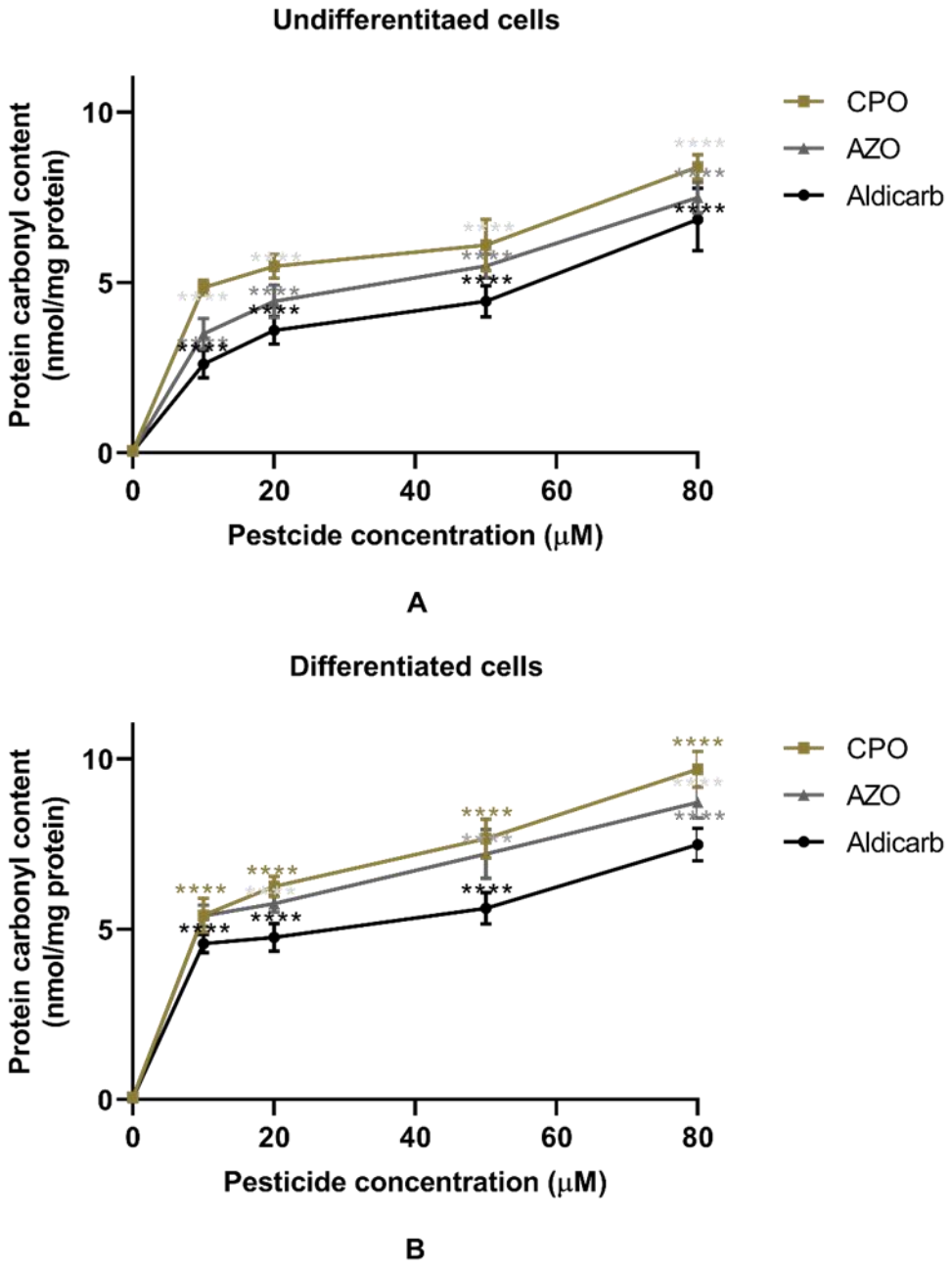
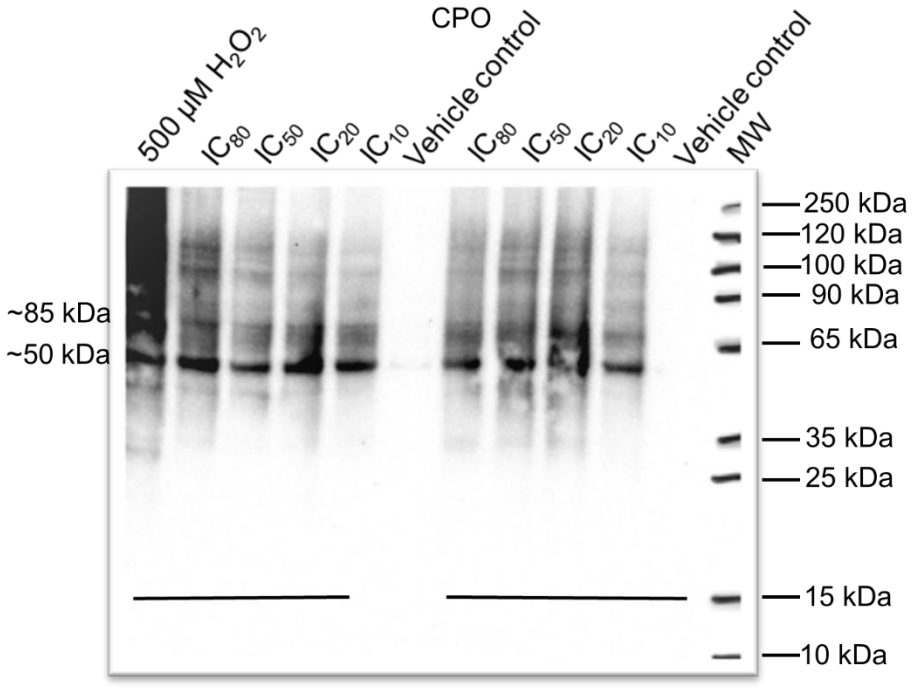


Figure 5-15: Effect of CPO, AZO, and Aldicarb on cytosolic protein carbonylation in ReNcell CX cells.

A- Undifferentiated and B- differentiated cells were exposed to IC_{10}, IC_{20}, IC_{50} and IC_{80} concentrations CPO, AZO, and Aldicarb for 24 h. Protein carbonylation levels were quantified using DNPH derivatization of crude cytosolic fraction of treated cells and spectrophotometric analysis. Readings were normalised to the vehicle control treatments after subtracting the blanks. Readings including vehicle control and treatments were obtained from 5 independent experiments (n=5) with triplicates in each treatment. Results were analysed using one-way ANOVA with Dunnett's multiple comparison and expressed as the mean ± standard error of the mean (SEM), when SEM bar is not apparent, this means that error is smaller than the symbol size. For significance; **** p<0.0001.

Oxyblots of CPO, AZO, and Aldicarb showed a concentration-dependent increase of protein carbonyls in both undifferentiated and differentiated cells compared to vehicle control treatments and there was also a marked difference (p<0.05) between the positive control treatment (500 µM H_2O_2). All pesticides resulted in an extensive carbonylation of proteins in the molecular weight range of ~50-250 kDa, with major bands at ~50 and 85 kDa. Particularly the ~50 kDa protein was carbonylated even at IC_{10} in undifferentiated and differentiated cells. Carbonylation of ~50 kDa protein was much stronger in differentiated cells than in undifferentiated cells with all three pesticides for 24 h (Figure 5-16).

An association between cellular ATP levels, ROS and protein carbonylation were analysed using Pearson's correlation analysis. The results revealed that there is a negative correlation with cellular ATP levels and protein carbonyl levels as well as there is a positive correlation with ROS generation and protein carbonyl levels for 24h. This suggested that protein carbonylation induced by ROS increased, and with increasing ROS generation there is a corresponding reduction of ATP levels in cells, consistent with reduced metabolic activity and viability (Table 5-4).



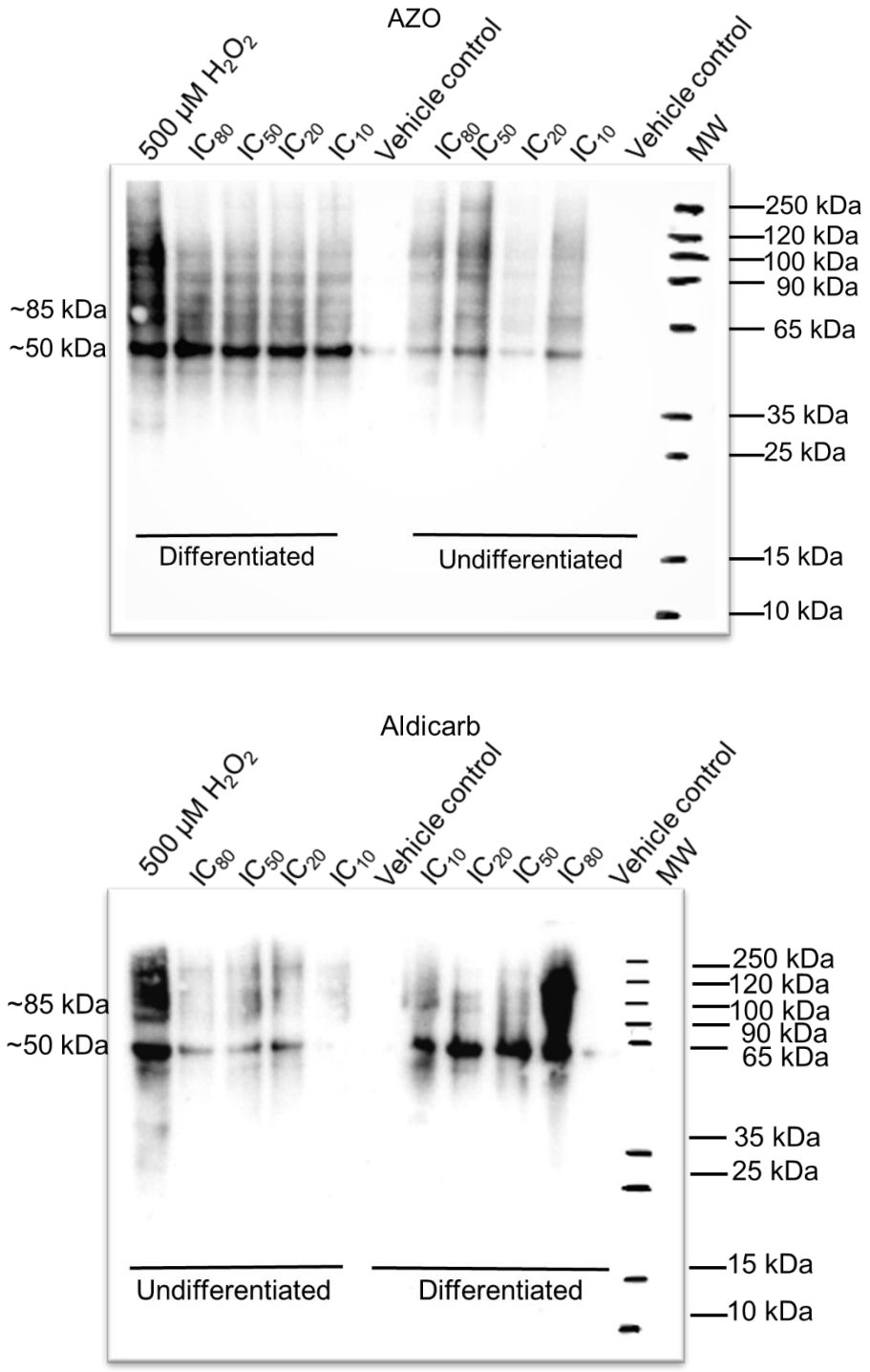


Figure 5-16: Cytosolic protein carbonylation of CPO, AZO and Aldicarb exposed undifferentiated and differentiated ReNcell CX cells for 24 h.
Undifferentiated and differentiated cells were exposed to IC_{10}, IC_{20}, IC_{50} and IC_{80} concentrations CPO, AZO and Aldicarb for and 24 h. DNPH derivatized crude cytosolic fractions were analysed with gel electrophoresis and immunoblotted with anti-DNPH antibody to identify the specific protein targets of protein carbonylation of CPO, AZO and Aldicarb exposure. Each experiment was conducted as 3 independent experiments with three replicates.

Table 5-4: Correlation analysis of ROS generation vs protein carbonyl content and ROS generation vs ATP production in ReNcell CX cells.

Pesticides	Cell type	ROS vs PCC			ROS vs ATP		
		r	R^2	*p* value	*r*	R^2	*p* value
CPO	Undifferentiated	0.90	0.8237	0.0332	-0.98	0.9656	0.0027
	Differentiated	0.96	0.9159	0.0106	-0.95	0.9177	0.0103
AZO	Undifferentiated	0.98	0.9543	0.0042	-0.98	0.9765	0.0015
	Differentiated	0.95	0.9126	0.0113	-0.96	0.9375	0.0068
Aldicarb	Undifferentiated	0.88	0.7766	0.0482	-0.96	0.9388	0.0066
	Differentiated	0.98	0.9529	0.0044	-0.93	0.8726	0.0201

r- Pearson's correlation coefficient; ROS- reactive oxygen species generation; PCC- Protein carbonyl content; ATP- Adenosine triphosphate production

Table 5-5: Toxicity of CPO, AZO and Aldicarb on undifferentiated vs differentiated ReNcell CX cells.

Pesticide	Treatments	MTT assay	LDH assay	Treatments	ATP assay	ROS assay		PCC assay
						6 hours	24 hours	
CPO	0.3	NS	NS	IC_{10}	0.0017	<0.0001	<0.0001	0.0003
	1	NS	NS	IC_{20}	0.0456	0.0017	0.0013	0.0012
	3	NS	NS	IC_{50}	NS	0.0011	<0.0001	<0.0001
	10	Ns	NS	IC_{80}	NS	NS	NS	0.0001
	30	<0.0001	NS					
	100	0.0079	NS					
	200	NS	NS					
AZO	0.3	NS	NS					
	1	NS	NS	IC_{10}	0.0043	<0.0001	NS	<0.0001
	3	<0.0001	NS	IC_{20}	<0.0001	<0.0001	0.0438	0.0004
	10	NS	NS	IC_{50}	0.0029	<0.0001	NS	<0.0001
	30	<0.0001	0.0441	IC_{80}	NS	<0.0001	0.0055	0.0004
	100	NS	NS					
	200	NS	NS					
Aldicarb	0.3	NS	NS					
	1	NS	NS					
	3	NS	NS	IC_{10}	NS	NS	NS	<0.0001
	10	NS	0.0041	IC_{20}	0.0006	0.0017	NS	0.0012
	30	NS	NS	IC_{50}	0.0030	<0.0001	<0.0001	0.0017
	100	<0.0001	NS	IC_{80}	NS	<0.0001	<0.0001	NS
	200	NS	NS					

IC_{50}- 50% inhibition concentration, MTT- (4,5-dimethylthiazol-2-yl)-2,5-diphenyltetrazolium bromide, LDH- Lactate dehydrogenase, ATP- Adenosine triphosphate, ROS- reactive oxygen species, PCC- protein carbonyl content.

5.3 Discussion

Organophosphate and carbamate pesticides are widely used in pest control. Chlorpyrifos, Azamethiphos and Aldicarb are extensively used pesticides in agriculture, veterinary, medical and public health practices (Baron, 1994, Lionetto et al., 2013, Struger et al., 2016). Although these pesticides are considered as neurotoxic, their widespread usage in agricultural and household practices has raised concern over their potential damage to health in different species including humans. Numerous studies have indicated a higher risk of developing neurodevelopmental disorders in humans exposed to OP and carbamates with special attention drawn to chlorpyrifos in this regard (Flaskos, 2012). Furthermore, *in vivo* studies with rats and epidemiological studies in occupational workers in some areas in the world showed association of neurodevelopmental disorders such as ADHD, autism and other neurobehavioral alteration in adults and children (Flaskos, 2012, González-Alzaga et al., 2014). However, the mechanisms underlying the neurotoxicity and cellular responses that arise from exposures, apart from AChE inhibition, in human progenitor cortical neuronal stem cells are unknown. Therefore, this study was designed to investigate the cytotoxic effect and the underlying mechanism of oxidative stress induced by oxon metabolites of commonly used OP pesticides, Chlorpyrifos, Azamethiphos and the carbamate pesticide Aldicarb, on human progenitor cortical neuronal stem cells. This study was also designed to evaluate the protein damages mediated by ROS that arose from the pesticide exposures as potential targets from oxidative stress.

Results from cell metabolic and cell viability assays revealed that CPO, AZO and Aldicarb reduced cell metabolic activities and cell viability of HNPCs in a concentration-dependent fashion. These finding suggested that a concentration range of 1 - 20 µM and after a 24 h exposure in HNPCs; CPO, AZO and Aldicarb

induced cytotoxicity (Table 5-1). In line with the finding of the study, Alyamani, (2018) showed that 1, 3, and 10 µM exposures to CPO for 24 h reduced cell viability of ReNcell Cx cells in a concentration dependent manner for pre-differentiated cells. The study results reported here are consistent with those undertaken in Chapter IV with human neuroblastoma SH-SY5Y cells; that showed that CPO, AZO and Aldicarb induced cell cytotoxicity in a concentration-dependent manner. Differing here is that the IC_{50} values for SH-SY5Y cells were higher than those generated for HNPCs. This can be explained by the cell specific effect of OP and carbamate pesticides and that their cytotoxicity responses are different. Furthermore, cell types derived from different origins have different cell functions, and the toxicity induced by CPO, AZO and Aldicarb appear to vary among different cell models. However, the IC_{50} value for human brain cells exposed to CPF is in the range of 0.8 - 56 µM (Eaton et al., 2008, Burke et al., 2017), but CPO should be lower than that due to the toxic potency of CPO over that for CPF (Flaskos, 2012).

Cell death was evaluated using a LDH assay, and this showed that cell death was induced in a concentration-dependent fashion and that the higher pesticide concentrations induced dramatic cell loss. In line with this, Alyamani, (2018), showed that cell death was evident at 1 µM and then increased continuously up to 10 µM after a 24 h exposure to CPO. Herein, at 1 µM only CPO induced significant LDH production exposed differentiated cells but not in undifferentiated cells (Figure 5-7). This difference reflects that Alyamani, (2018) reported that significant cell death was observed in pre-differentiated cells, not in differentiated cells. However, SH-SY5Y cells exposed to CPO, AZO and Aldicarb in the previous study (Chapter IV) showed that all three pesticides induced cell death in a concentration-dependent manner for 24 h exposure similar to this study, and that 1 µM induced cytotoxicity in differentiated cells by

AZO and CPO but, not in undifferentiated cells. Herein, only CPO and AZO did not induce cytotoxicity in undifferentiated cells at this concentration, but Aldicarb induced significant LDH production. In contrast, 1 µM did not induce cytotoxicity of differentiated cells by AZO, but CPO and Aldicarb induced cytotoxicity. However, SH-SY5Y cells showed significant level of LDH production in differentiated cells by exposure of CPO and AZO at 1 µM except Aldicarb. This can be justified as the differences of cell models, that show different cellular responses at different growth stages. Differentiated HNPCs can display more resistance to low pesticide concentrations (Delp et al. 2018) as cells adapt to mitochondrial toxicants at lower concentrations during their phenotypic specifications and changes to their energy generation. In contrast, differentiated cells were more susceptible to higher pesticide concentrations. This has been observed due to the activation of more apoptotic genes in differentiated cells than undifferentiated cells in CPF treated neural stem cells in mouse and PC12 cells (Slotkin and Seidler, 2012). This has been supported by the findings of Alyamani, (2018) which showed that mRNA level changes in differentiating ReNcell CX was associated with viability and morphological changes in cells even at 3 and 10 µM exposure of CPO.

AChE activity of ReNcell CX cells was significantly reduced when pesticide concentrations continue to increase; similar to the responses observed in SH-SY5Y cells for both phenotypes. However, the effective range is slightly lower than that in SH-SY5Y cells (200 - 700 nM). IC_{50} values generated from the concentration-response curves for 24 h exposure is higher in SH-SY5Y cells for the three pesticides. Herein, more than 80% AChE inhibition was observed for CPO, AZO, or Aldicarb exposed undifferentiated or differentiated cells within 24 h, and cell morphological changes and cell viability loss was apparent at this concentration due to ACh excitotoxicity. This has been supported by the study

of Sindi (2015), showed that differentiated ReNcell Cx cells showed an IC_{50} in between 1 - 2 µM for 8 h exposure, and no significant viability loss apparent even at 3 µM, but apparent at 10 µM when nearly 62.5% AChE inhibition occurs in differentiating cells. However, CPO development effects could relate to an effect on the morphogenic activity of AChE, which is known to be displayed during the normal process of neurodevelopment, rather than the enzymatic activity of the AChE protein (Howard et al., 2005). Therefore, this could suggest that AChE inhibition in ReNcell CX cells by CPO, AZO or Aldicarb induces morphological or biochemical effects upon undifferentiated or differentiated cells. However, CPO, AZO and Aldicarb induced severe effects on certain parameters, including viability, suggesting AChE inhibition has at least some influence in the severity of the effect.

A basis of CPO, AZO and Aldicarb toxicity is the production of oxidative stress and this has been examined in two elements in this study. Firstly, ROS was generated upon pesticide exposures with selected low, moderate, or high doses that induce viability loss, and secondly, via an evaluation of protein carbonylation as a potential target mediated by oxidative stress. ROS generation due to the exposure to CPO, AZO or Aldicarb in both undifferentiated and differentiated cells showed concentration-dependent increased ROS, but levels reduced after longer time points (24 hours). This could be due to two main reasons: the ROS produced could react with other cellular macromolecules and make stable products, and this would result in a reduction of ROS generation due to their relatively short half-lives and reactive nature. Secondly, DCFDA may not be stable for 24 h time courses and could degrade with time, limiting the availability of DCFDA for the reaction (Tarpey and Fridovich, 2001). However, the concentration of DCFDA was optimized before the assay and a high concentration effected for the viability of cells that has been observed by

others (Figueroa et al., 2018). To gain insight into ROS generation two time points were selected. In line with the previous study with SH-SY5Y cells, ROS generation in both undifferentiated and differentiated cells showed a marked increase with increasing pesticide concentration after 6h and 24 h, but the levels of ROS generated were lower at 24 h than at 6 hours. ROS generation after CPF exposure was in a concentration dependent manner in human neuroblastoma cells (Ki et al. 2013, Park et al. 2015, Zhao, Yang and Zhao 2019). However, the lack of uniformity in experimental conditions makes it difficult to directly compare the ROS generation data with other studies. Therefore, it is suggested that CPO, AZO and Aldicarb induced cytotoxicity does still correlate with ROS levels in ReNcell CX cells.

Cellular mitochondria are majorly responsible for the generation of free radicals, in addition to their role in energy metabolism (Karami-Mohajeri and Abdollahi, 2013). OP pesticides can damage mitochondria and liberate ROS (Xu et al., 2017, Srivastava et al., 2018). Mitochondrial dysfunction alters the cellular energy metabolism and can be detected by measuring the impact upon cellular ATP levels. Herein, MTT assays showed cellular metabolic activities were decreased in a pesticide concentration-dependent manner, and in turn, there was blunting of mitochondrial activity with reduced cellular ATP levels and a corresponding increase of ROS generation. This suggested that CPO, AZO and Aldicarb could potentially interact with cellular mitochondria. This is supported by Chapter IV with SH-SY5Y cells, that showed increased ROS generation, and decreased cellular ATP levels in a pesticide concentration-dependent manner. However, there are insufficient similar studies with HNPCs, and differences in experiment conditions, such that ROS generation and levels cannot be compared directly. It has been reported that mouse neural stem cells show oxidative stress upon CPO exposure with increasing concentration

(Lukaszewicz-Hussain, 2010). In agreement with this statement, Dettbarn et al. (2006) showed OP induced ROS generation is the mechanism of cholinergic stimulations and leading to higher energy consumption and gradual depletion of ATP levels of cells. This is further supported by statement that a 30-40% drop in cellular ATP levels for several hours upon OP exposure can be cause a significant fall in mitochondrial membrane potential which supports the suppression of the activity of complex I and IV of electron transport chain which in turn causes depleted ATP production (Milatovic et al., 2006).

The second notable effect on ReNcell CX cells after exposure to CPO, AZO, or Aldicarb was the positive correlation in ROS generation and protein carbonylation in both undifferentiated and differentiated cells, confirming the primary target of ROS generated are specific proteins in both phenotypes. A concentration-dependent increase in protein carbonyls in both phenotypes was apparent, that was initiated even at very low concentrations of CPO, AZO, or Aldicarb (IC_{10} values). The ~50 kDa protein modified by carbonylation could be tubulin. This would be supported by a study with brain hippocampal slices that showed that cytosolic tubulin proteins are one of the major protein targets of CPO (Prendergast et al., 2007). Tubulin phosphorylation was also demonstrated in a study with CPO which showed that CPO targets isoforms of α and β tubulins in cells at multiple sites, although high pesticide concentrations were used (Schopfer and Lockridge, 2018) . Also, Sindi, (2015) showed that β tubulin III, which is a neuronal marker, can be organophosphorylated by exposure to sublethal levels of CPO for 6 h and 8 h exposure in both pre-differentiated ReNcell CX cells. Furthermore, the possibility of formation of adducts with lipid peroxidation products has been suggested for carbonylated tubulins (Grigoryan et al., 2009a, Grigoryan et al., 2008). Hence, further work

is required to delineate the relationship between CPO, AZO and Aldicarb exposure and tubulin carbonylation in hNPCs.

The levels of protein carbonyls could alter specific cell signalling pathways. With increasing pesticide concentration, there will be induction of progressively higher ROS levels and a potential imbalance with the antioxidant system in cells, and the cell's abilities to mitigate the redox stress. Low levels of generated ROS can effect cell signalling but higher levels can act as mediators of inducing apoptotic cell death (Redza-Dutordoir and Averill-Bates, 2016). This notion is supported by a proteomic study of protein carbonyls in PC12 cells, which showed carbonylation of proteins related to metabolic pathways and ATP synthesis by rotenone exposure (Chiaradia et al. 2019). Furthermore, protein carbonyls associated with higher molecular weight proteins aggregated and showed resistance to proteolysis, with potential toxicity to cells (Dalle-Donne et al. 2006). Herein, oxyblots revealed that higher molecular weight proteins were carbonylated after exposure to CPO, AZO or Aldicarb. Carbonylation and aggregation of these proteins could contribute to impairment of the cell morphology of neurons including axonal and dendritic processes, particularly if these are cytoskeletal proteins such as tubulins. It has been suggested that the microtubules serve as a track of neurotransmission process in cells and perturbations of these proteins disturbs cellular neurotransmission, receptor sites and ion channels (Flaskos, 2014).

Accumulation of carbonated proteins is likely to be detrimental to cellular activities and induce viability loss (Fucci et al., 1983, Abdel-Salam et al., 2018). Toxic protein carbonyls are eliminated from the cell by the 20S proteasome in an ATP dependent manner (Divald and Powell, 2006). Herein, ATP levels decreased at higher pesticide concentrations, and so this could influence the proteolytic degradation of the carbonylated proteins, due to the deficit of ATP,

promoting their toxic persistence. Hence, these oxidized proteins are likely to contribute to cellular dysfunction and alteration of metabolic rates, and impairment of cellular morphology.

Accumulation of heavily carbonylated, cross linked proteins aggregates in cells can eventually induce apoptosis, and inhibit the proteasome and cause further protein aggregation and crosslinking (Ding and Keller, 2001). CPO exposure can induce tubulin protein cross linking and aggregation even at very low concentrations such as 1.5 μM (Schopfer and Lockridge, 2018). An imbalance between the rate of production and detoxification of protein carbonyls causes carbonyl stress in cells (Dalle-Donne et al., 2006). This carbonyl stress condition further increases the accumulation and cross linking of carbonylated proteins (Curtis et al., 2012, Schopfer and Lockridge, 2018). A subsequent loss of cell dysfunction and alteration of metabolic pathways is linked with several neurodegenerative disorders (Dalle-Donne et al., 2006). Hence, neurodevelopment disorders could in part be caused by the accumulation of damaged proteins, such as those with high levels of protein carbonyls, as a response to pesticide exposures in the developing brain, according to the current study. However, further studies are needed to clarify cross linking and protein aggregation at these concentrations, and the persistent toxicity of these proteins needs to be tested.

In conclusion, this part of the current study investigated the effect of CPO, AZO and Aldicarb on undifferentiated and differentiated hNPCs model. CPO, AZO and Aldicarb induced cytotoxicity in a concentration-dependent manner and cytotoxicity was in part mediated by oxidative stress in both undifferentiated and differentiated cells. AChE inhibition increased the severity of cytotoxic responses of cells, and proteins at ~50 kDa were prominent targets of oxidative stress in both undifferentiated and differentiated neuronal cells. Protein

carbonylation occurred even at very low pesticide concentrations, below those that show significance cell viability loss or cell death. This may be of particular importance to humans exposed to pesticides at low (sub-clinical) concentrations, as cellular effects and impacts upon cellular functions may still be observed. The protein carbonylation induced in human progenitor cortical neuronal cells, particularly after expose to high concentrations of CPO, AZO or Aldicarb will induce severe carbonyl stress due to accumulation of protein carbonyls and further cross linking that may contribute to the induction of apoptotic cell death.

6 NEUROTOXICITY EVALUATION OF ALCOHOL USING HUMAN NEUROBLASTOMA SH-SY5Y CELLS

6.1 Introduction

Alcohol consumption among young people is increasing in the world. The WHO has been recently published alcohol consumption data that showed that the rate of alcohol consumption increased among young people and women (WHO, 2019). The toxicological consequences of alcohol consumption can lead to liver damage and disease but are also associated with damage to the CNS (Zhang et al., 2018). Numerous studies have demonstrated that binge drinking of alcohol has been linked with foetal alcohol syndrome (FAS), development delays, cognitive impairment, and neurobehavioral changes. The most destructive and intense toxicological consequence of alcohol exposure is the neuronal cell loss due to exacerbation of programmed cell death. Excessive neuronal death interrupts the development of the normal neuronal network and may lead to structural changes along with cognitive and behavioural impairments (May et al., 2014, Zhang et al., 2018). It has been proved that excessive neuronal death in certain human brain areas is due to alcohol exposure such as cerebellar abnormalities with developmental and motor deficits (Riley and McGee, 2005, Goodlett et al., 2005), hippocampal abnormalities linked with learning and memory deficits, and hypothalamic abnormalities associated with stress hyper-responses and anxiety (Berman and Hannigan, 2000, Hamilton et al., 2003, González-Burgos et al., 2006).

Alcohol can have direct or indirect effects on neuronal cells. Indirect alcohol effects arise from alcohol related metabolic products, such as acetaldehyde or alcohol effects on other body systems such as the endocrine system can adversely effect neuronal cells (de la Monte et al., 2012). The severity of

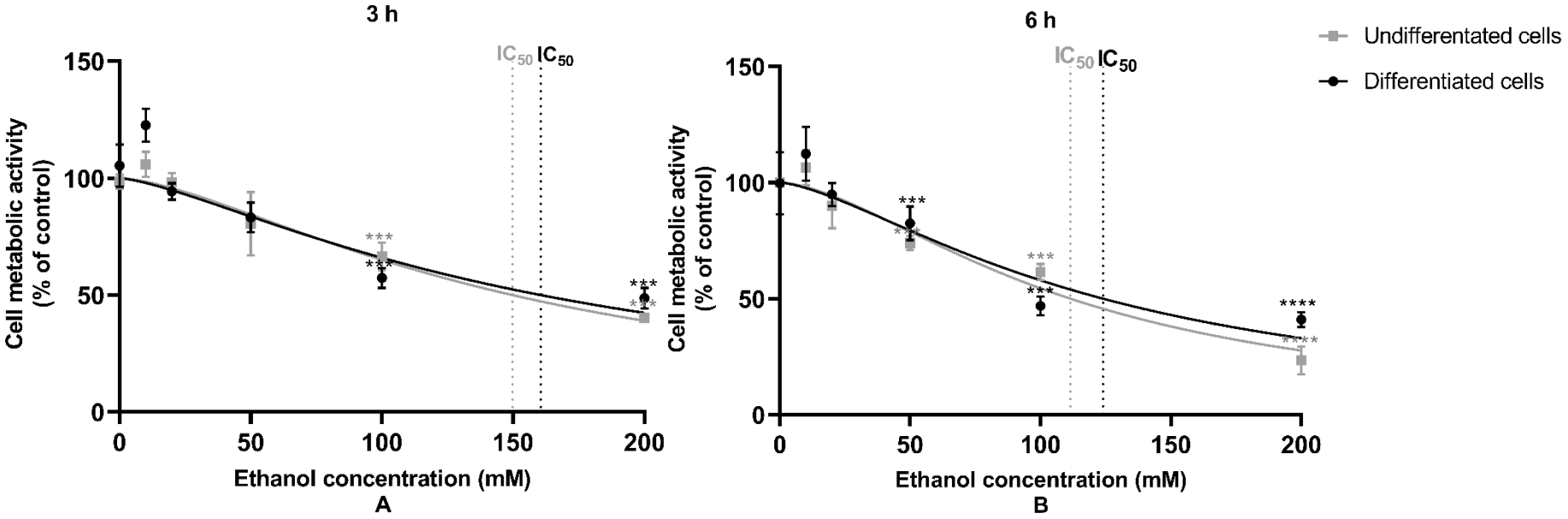
neuronal damages from alcohol depends on the timing, pattern and the dose of alcohol consumed. The cellular mechanisms involved in increased neuronal death and functionality changes in remaining cells that lead to altered structural and functionality changes in the ethanol exposed offspring or adult are not clearly demonstrated. However, it has been proved that the main mechanism involved in consequences of alcohol exposure is neuronal cell death via apoptosis (Goodlett and Horn, 2001). Few studies have reported alcohol induced oxidative stress in neuronal cells (Wang et al., 2012a) using human neuronal cell models. The mechanism of alcohol damage to neuronal cells are stage specific and cell specific (Goodlett and Horn, 2001, Goodlett et al., 2005). Nevertheless, the mechanism of inducing neuronal cell damage upon alcohol exposure may operate both simultaneously or sequentially over time to interact together to induce toxicological consequences or cell death (Goodlett and Horn, 2001, Goodlett et al., 2005).

Therefore, to gain insight to the direct toxic effects of alcohol, and to determine the exposures that may be considered safe for neurones, human neuroblastoma SH-SY5Y cells were exposed to low and high alcohol concentrations and for the durations consistent with acute episodes of drinking. To determine this, ethanol exposure of 3, 6, 12 and 24 h time points and cytotoxic responses that arose from the exposures were evaluated. Also, the effect of alcohol on cellular oxidative stress and its impact on cellular protein damages were studied.

6.2 Results

6.2.1 Alcohol reduced cell metabolic activity and cell viability in a concentration and time-dependent manner in SH-SY5Y cells.

The impact of alcohol exposure on the viability of undifferentiated and differentiated cells were measured using a MTT assay by exposing cells to 0, 10, 20, 50, 100, 200 mM for 3, 6, 12 and 24 h. Figure 6.1 illustrates cell viability responses in undifferentiated and differentiated SH-SY5Y cells exposed to ethanol for 3, 6, 12 and 24 h. Cell viability responses varied compared to their corresponding controls by exhibiting concertation and time dependent decrease in both cell phenotypes. Cell metabolic activity and cell viability of both undifferentiated and differentiated cells showed a linear relationship with increasing concentration at both 3 and 6 h time points (Figure 6-2 A and B). Curves got steeper at 12 and 24 h exposures exhibiting classical dose repose curves of alcohol in both phenotypes. However, at 100 and 200 mM concentrations, cell metabolic activity and cell viability decreased significantly. At 50 mM cells showed significantly reduced cell metabolic activity and cell viability decreased at 3 h and 6 h in both differentiated and undifferentiated cells. Cell metabolic activities and cell viability loss were highly sensitive at 12 h and 24 h time points over the concentration range of 50 - 200 mM (Figure 6-1 A and D). The effect was dramatic for 12 and 24 h post exposures and nearly 76.5% cells lost their viability at 200 mM after a 6 h post exposure. The effect was stronger at 12 and 24 h exposures compared with 3 and 6 h exposures, with nearly 75% - 90% cell viability lost at 200 mM at 12 and 24 h exposures. Undifferentiated cells showed a significant cell metabolic activity and viability loss in each time points at the range of 20 - 200 mM, and significant viability loss obvious at 50,100 and 200 mM in both 12 h and 24 h exposure.


3 h
6 h
Undifferentated cells
Differentiated cells
Cell metabolic activity (% of control)
Ethanol concentration (mM)
IC50
A
B

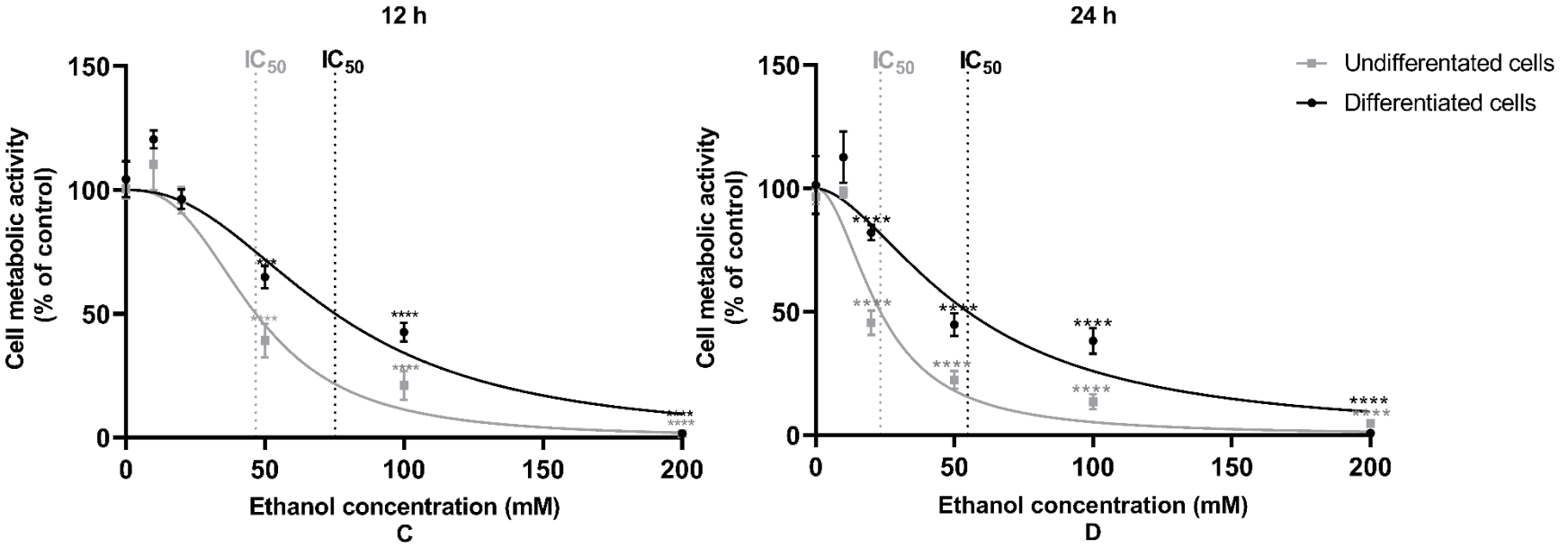


Figure 6-1: Cell metabolic and cell viability in responses to alcohol by SH-SY5Y cells.
Undifferentiated and differentiated cells were challenged with 0 - 200 mM for durations of 3 h (A), 6 h (B), 12 h (C) and 24 h (D). Viability was assessed using MTT assay. Readings were normalized to the viability of control, providing cell viability percentage, as a percentage value to the control. Control and treatments were performed as triplicates in 5 independent experiments (n=5). Results were analysed using one-way ANOVA with Dunnett's multiple comparison and expressed as the mean ± standard error of the mean (SEM), when SEM bar is not apparent, this means that error is smaller than the symbol size. For significance; ***p*<0.01, ****p*<0.01, *****p*<0.0001.

Table 6-1: Comparison of ethanol toxicity at different time points in undifferentiated and differentiated SH-SY5Y cells measured by MTT assay.

Cell type	Treatments (mM)	3h vs 6 h	3h vs 12 h	3 h vs 24 h	6 h vs 12 h	6 h vs 24 h	12 h vs 24 h
Undifferentiated	10	NS	NS	NS	NS	NS	NS
	20	NS	NS	<0.0001	NS	<0.0001	<0.0001
	50	NS	<0.0001	<0.0001	<0.0001	<0.0001	0.0067
	100	NS	<0.0001	<0.0001	<0.0001	<0.0001	NS
	200	NS	<0.0001	0.0007	0.0003	0.0437	NS
Differentiated	10	NS	NS	NS	NS	NS	NS
	20	NS	NS	NS	NS	NS	NS
	50	NS	0.0085	<0.0001	0.0122	<0.0001	0.0037
	100	NS	0.0483	0.0061	NS	NS	NS
	200	NS	<0.0001	<0.0001	<0.0001	<0.0001	NS

NS- Not significant, $p<0.05$.

Cell loss was worsening at 24 h than 12 h exposure at 50,100 and 200 mM compared to control in differentiated cells. Furthermore, differentiated cells cultures exhibited moderate toxic responses for alcohol initially at 6 h treatment and then 12 h and 24 h, but significant cell loss was apparent at higher concentrations of 12 h and 24 h compared to corresponding control treatments.

Interestingly, 10 mM concentration induced a 6 - 11% increase in cell metabolic activity of differentiated cells for all treatment time points. Similarly, a 1 - 10% increase in metabolic activity compared to the control treatments was apparent for undifferentiated cells. A comparison of undifferentiated and differentiated cells at each of time points showed a significant difference in cell metabolic and cell viability reduction in undifferentiated and differentiated cells (Table 6-8). Comparison of each concentration at different time points showed that at 50 - 200 mM, cells exhibit significant differences at each time point tested for both phenotypes of SH-SY5Y cells (Table 6-1).

The reduction of viability in undifferentiated cells was not significantly different from differentiated cells exposed to ethanol up to 50 mM for 6 h post exposure and then a significant difference in rate of cell metabolic activity and cell viability was apparent for 12 and 24 h (Table 6-1 and Table 6-8). Hence, the concentration of alcohol that produced 50% inhibition of cell viability for undifferentiated cells was lower than similarly treated differentiated cells (Figure 6-1, Table 6-9).

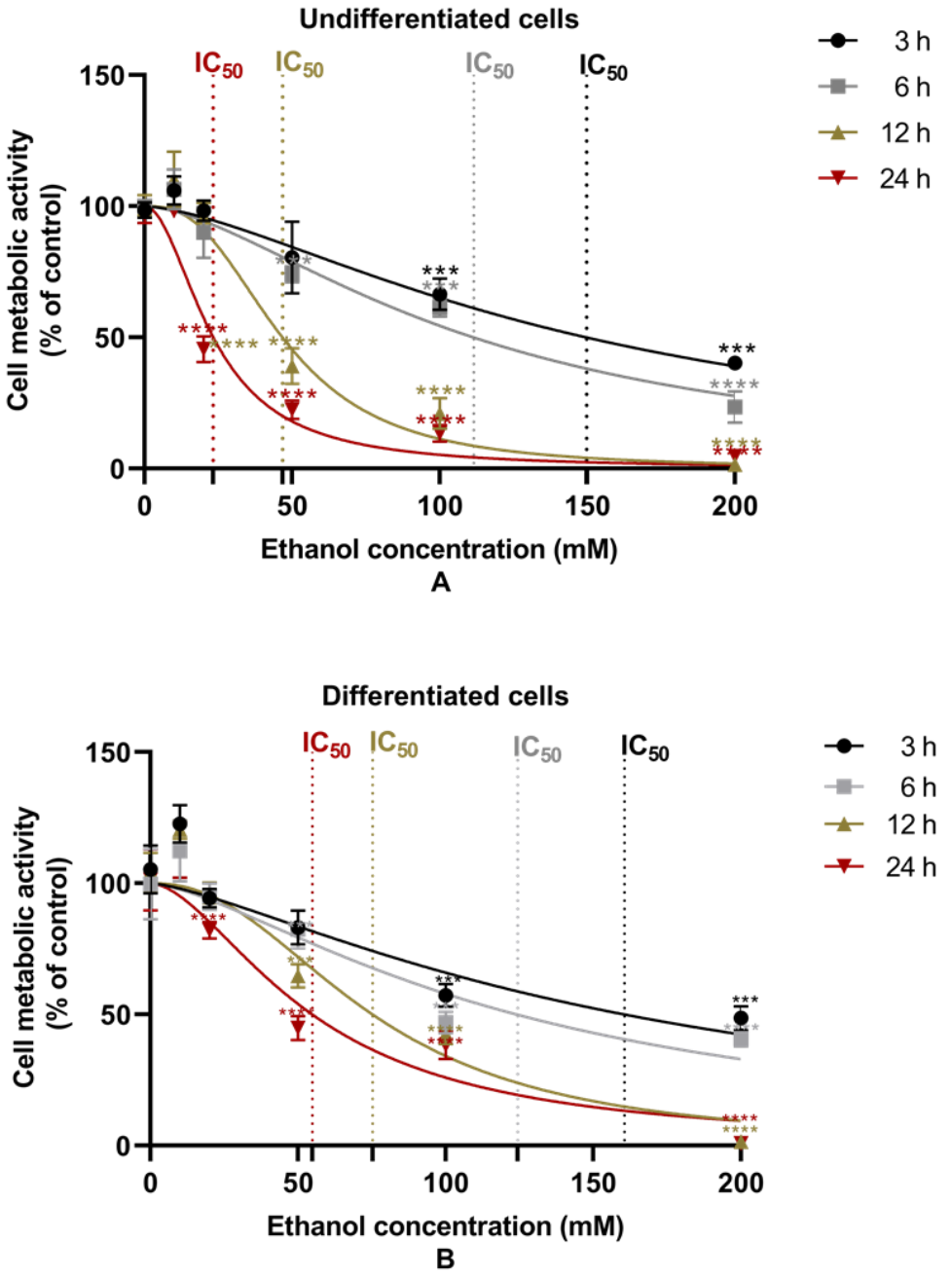


Figure 6-2: Effect of ethanol on undifferentiated and differentiated SH-SY5Y cells.

A- undifferentiated and B- differentiated cells were challenged with 0 - 200 mM for durations of 3, 6, 12 and 24 h. Viability was assessed using MTT assay. Readings were normalized to the viability of control, providing cell viability percentage, as a percentage value to the control. Control and treatments were performed as triplicates in 5 independent experiments (n=5). Results were analysed using one-way ANOVA with Dunnett's multiple comparison and expressed as the mean ± standard error of the mean (SEM), when SEM bar is not apparent, this means that error is smaller than the symbol size. For significance; **p<0.01, ***p<0.01, ****p<0.0001.

6.3 Alcohol induced cytotoxicity in SH-SY5Y cells.

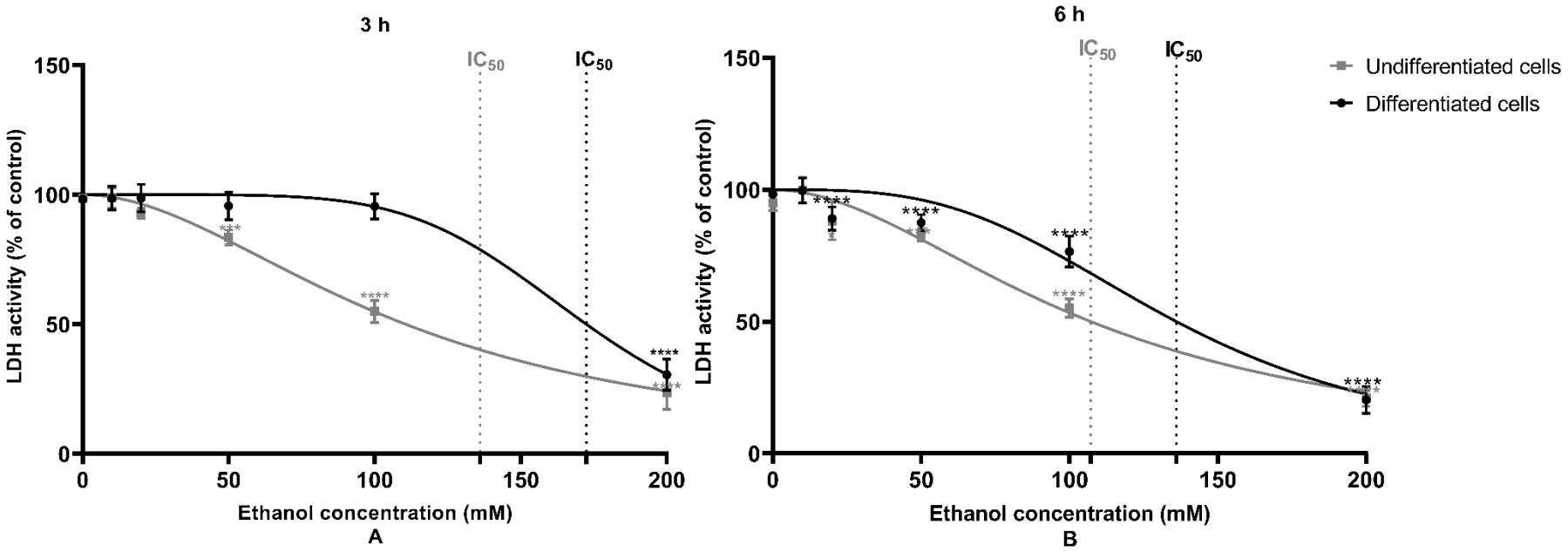
The MTT assay results suggested growth and proliferation inhibition by alcohol exposure to SH-SY5Y cells, but to confirm that these were cytotoxic effects rather than cytostatic effects, a LDH assay was done for 3, 6, 12 and 24 h exposed undifferentiated and differentiated cells at 0 - 200 mM alcohol concentrations.

Undifferentiated and differentiated cells showed cytotoxic responses to ethanol exhibiting various degrees of deviation from control treatments. Cytotoxicity of both undifferentiated and differentiated cells increased with increasing concentration and time of exposure. The cytotoxic responses at 200 mM were significant compared to all other treatments and all other time points. The reduction in cell viability when considered for ethanol concentrations at 3 and 6 h post exposures, showed a linear relationship in both phenotypes; a similar response to that detected by the MTT assay. Interestingly, the rate of inducing cytotoxic responses at 10 -100 mM remains unchanged, and then there was a significant increase after 100 mM in differentiated cells compared to control treatment. Undifferentiated cells showed sensitive cytotoxic responses compared to differentiated cells, and a significant LDH activity increase was apparent from 50 mM compared with controls. At 100 mM concentration, differentiated cells were significantly reduced after a 6 h exposure. Undifferentiated cells showed significant cytotoxic responses at 20 mM compared to control treatments for this exposure duration (Figure 6-3 A and B).

Extended exposure durations of ethanol on SH-SY5Y cells exhibited classical dose-response relationships. Undifferentiated cells exhibited strong cytotoxic responses against the ethanol exposure compared to differentiated cells at both 12 h and 24 h exposures. A 10 mM concentration increased LDH activity by 48% (p<0.05) compared to its control, while at 24 h exposure the LDH activity

increased up to 84% compared to its controls (p<0.01). The analysis of 12 h and 24 h mean comparison showed a 6.3% rise in LDH at 10 mM compared with that of a 24 h exposure (Table 6-2; Figure 6-4). More than an 80% reduction in cell viability was apparent at higher concentrations such as 100 and 200 mM for both 12 and 24 h exposures (p<0.0001). Differentiated cells were more resistant to ethanol exposure than undifferentiated cells at both 12 h and 24 h exposures. However, 100 mM concentration showed strong cytotoxic effects on differentiated cells at all time points considered in the study (Table 6-2). Comparison of undifferentiated vs differentiated cells for their LDH activity upon ethanol exposure showed that at 200 mM, cells responded without a marked difference (Table 6-8).

LDH assay results suggested that undifferentiated cells were highly susceptible to the toxicity of ethanol exposure at every time point tested, and thereby confirming the MTT results. Hence, IC_{50} values for LDH activity were lower in undifferentiated cells than differentiated cells (Table 6-9). Also, results proved that differences in LDH activity induced by ethanol in SH-SY5Y cells were significant between undifferentiated and differentiated cells. There was an increased rate of cell cytotoxicity in undifferentiated cells and significant difference at 3 h from differentiated cells at concentrations of 10 - 200 mM, but not significantly different at 6, 12 and 24 h exposures (Table 6-8, Figure 6-4).


3 h
6 h
IC50
IC50
IC50
IC50
150
100
50
0
LDH activity (% of control)
0
50
100
150
200
Ethanol concentration (mM)
A
B
Undifferentiated cells
Differentiated cells
****
***

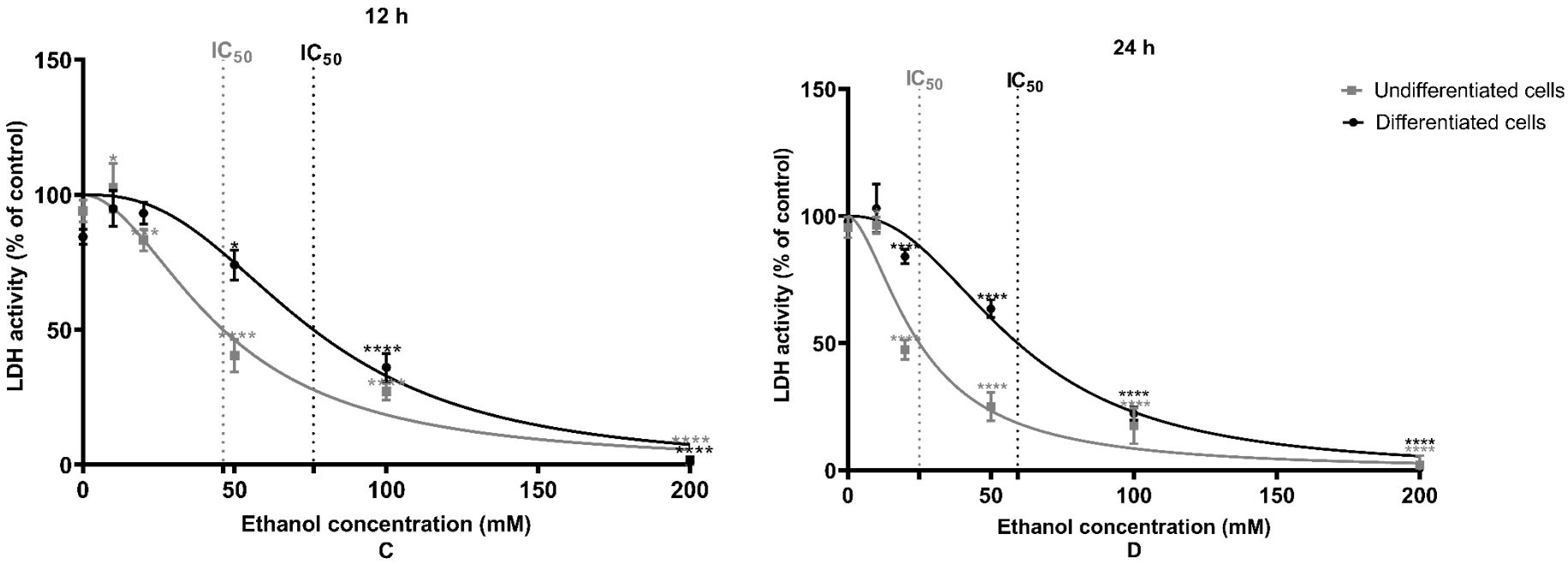


Figure 6-3: LDH activity of alcohol exposed SH-SY5Y cells.
Undifferentiated and differentiated cells were challenged with 0 - 200 mM ethanol for durations of 3 h (A), 6 h (B), 12 h (C) and 24 h (D). Viability was assessed using LDH assay. Readings were normalized to the LDH activity of control, providing LDH activity percentage, as a percentage value to the control. Control and treatments were performed as triplicates in 5 independent experiments (n=5). Results were analysed using one-way ANOVA with Dunnett's multiple comparison and expressed as the mean ± standard error of the mean (SEM), when SEM bar is not apparent, this means that error is smaller than the symbol size. For significance; *p<0.05, **p<0.01, ***p<0.001, ****p<0.0001.

Table 6-2: Comparison of ethanol toxicity at different time points in undifferentiated and differentiated SH-SY5Y cells measured by LDH assay.

Cell type	Treatments (mM)	3h vs 6 h	3h vs 12 h	3 h vs 24 h	6 h vs 12 h	6 h vs 24 h	12 h vs 24 h
Undifferentiated	10	NS	NS	NS	NS	NS	NS
	20	NS	NS	<0.0001	NS	<0.0001	<0.0001
	50	NS	<0.0001	<0.0001	<0.0001	<0.0001	0.0007
	100	NS	<0.0001	<0.0001	<0.0001	<0.0001	NS
	200	NS	<0.0001	<0.0001	<0.0001	<0.0001	NS
Differentiated	10	NS	NS	NS	NS	NS	NS
	20	NS	NS	0.0015	NS	NS	NS
	50	NS	<0.0001	<0.0001	0.0037	<0.0001	0.0318
	100	<0.0001	<0.0001	<0.0001	<0.0001	<0.0001	0.0029
	200	0.0002	<0.0001	<0.0001	NS	NS	NS

NS- Not significant, $p<0.05$.

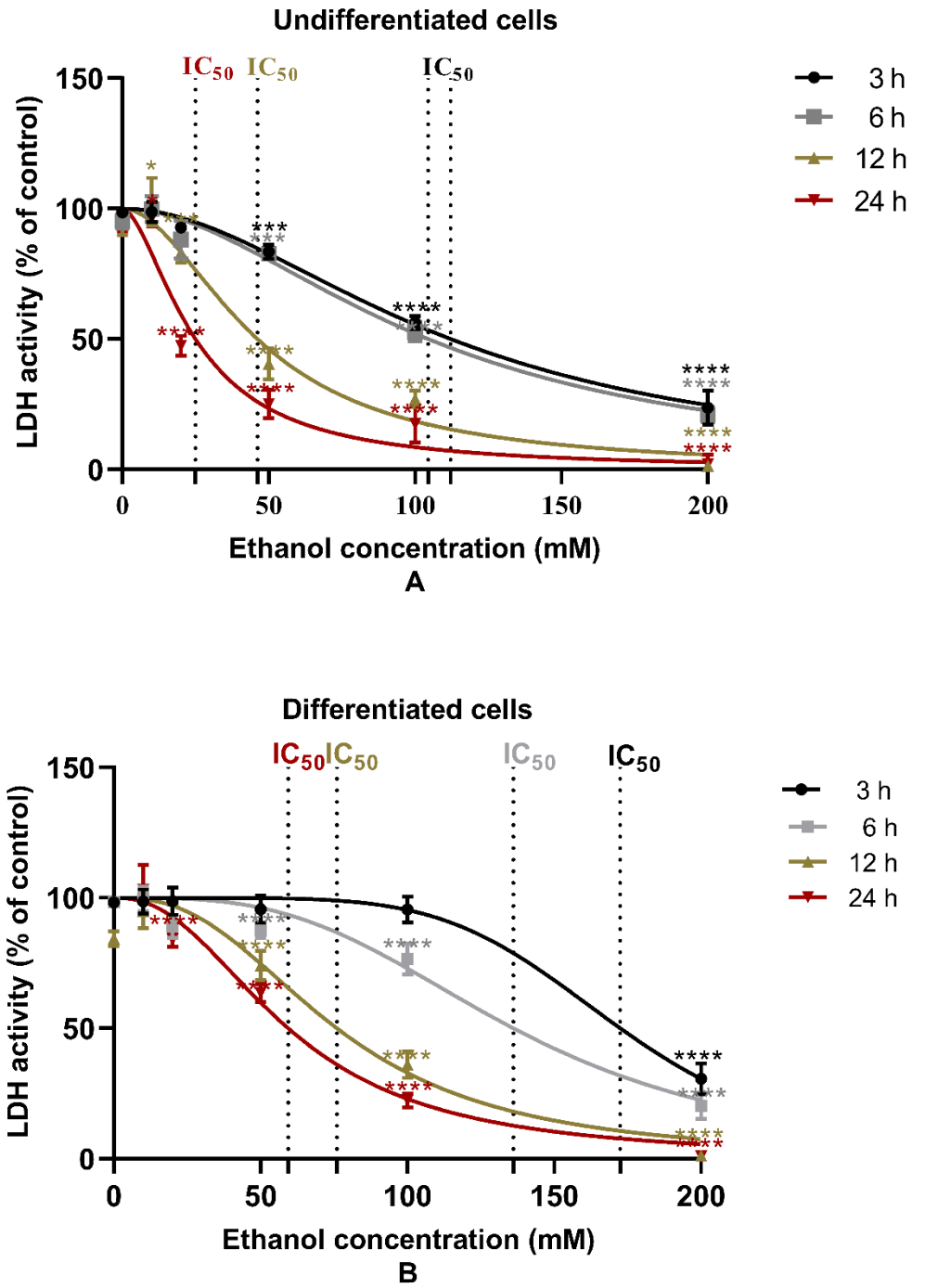
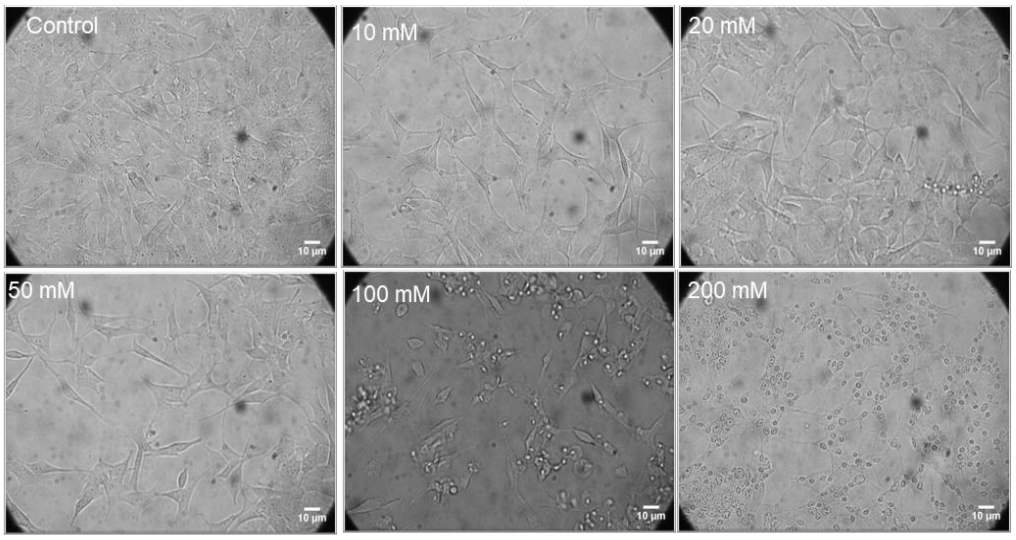


Figure 6-4: LDH activity of Undifferentiated and differentiated SH-SY5Y cells

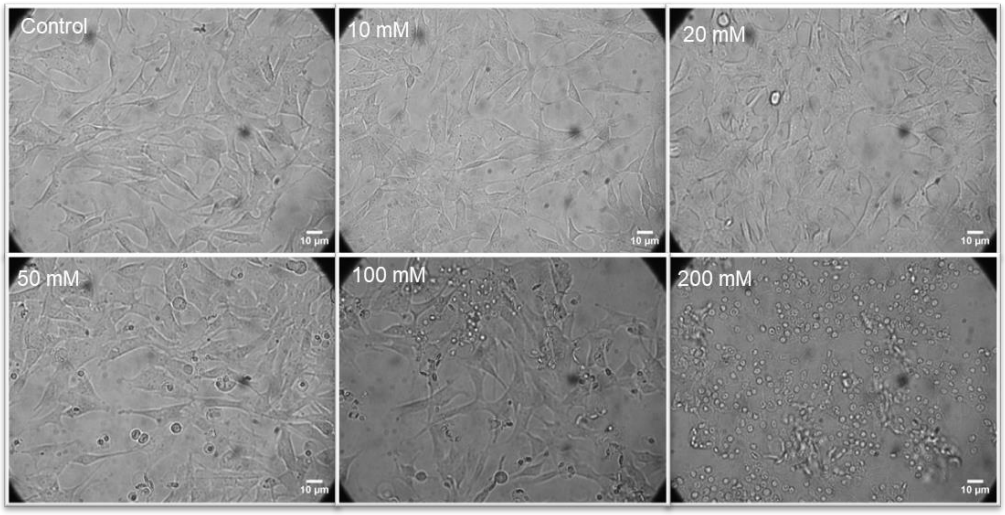
A- undifferentiated and B- differentiated cells were challenged with 0 - 200 mM ethanol for durations of 3, 6, 12 and 24 h. Viability was assessed using LDH assay. Readings were normalized to the LDH activity of control, providing LDH activity percentage, as a percentage value to the control. Control and treatments were performed as triplicates in 5 independent experiments (n=5). Results were analysed using one-way ANOVA with Dunnett's multiple comparison and expressed as the mean ± standard error of the mean (SEM), when SEM bar is not apparent, this means that error is smaller than the symbol size. For significance; *p<0.05, **p<0.01, ***p<0.001, ****p<0.0001.

6.3.1 Alcohol altered SH-SY5Y cell morphology.

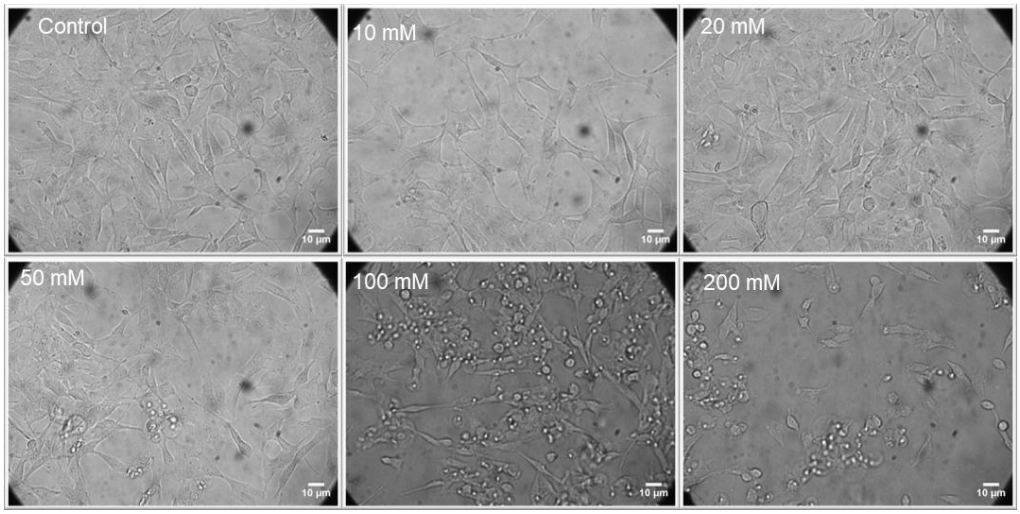
The results obtained from MTT and LDH assays were further confirmed by exposing undifferentiated and differentiated cells to ethanol for 3, 6, 12 and 24 h at 0 - 200 mM concentrations. Images clearly indicated a concentration and exposure duration-dependent decrease in cell number, cell shrinkage, neurite, and neuronal contact loss in undifferentiated and differentiated SH-SY5Y cells (Figure 6-5).



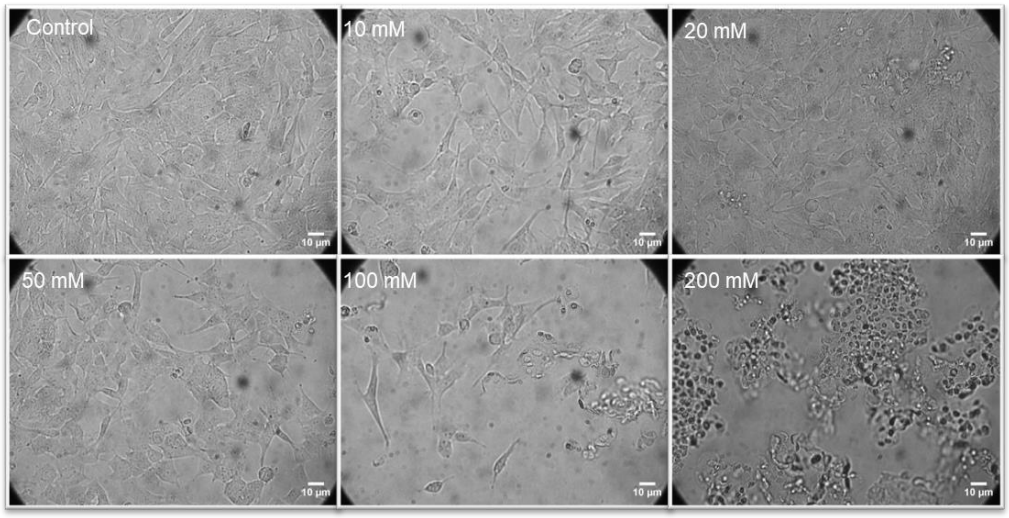
A



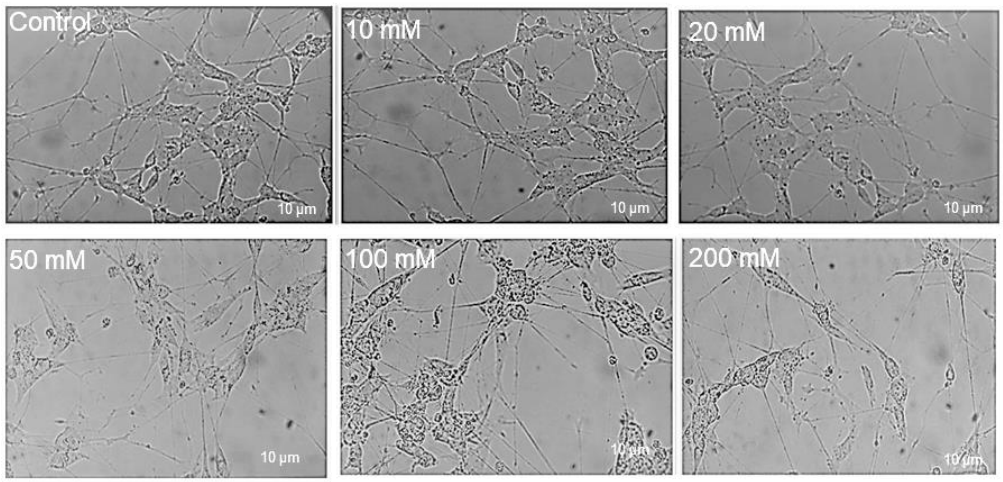
B


Control
10 mM
20 mM
50 mM
100 mM
200 mM
10 µm

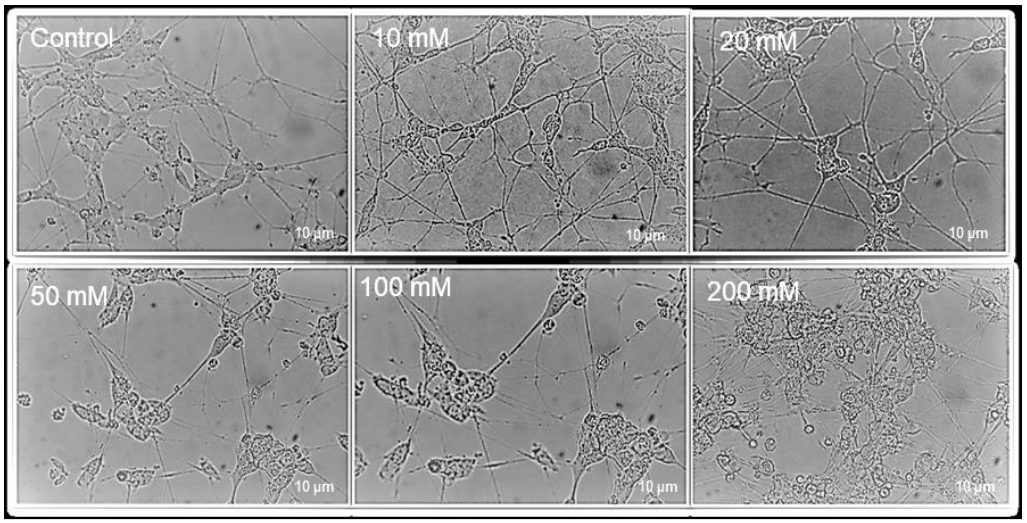
C


Control
10 mM
20 mM
50 mM
100 mM
200 mM
10 µm

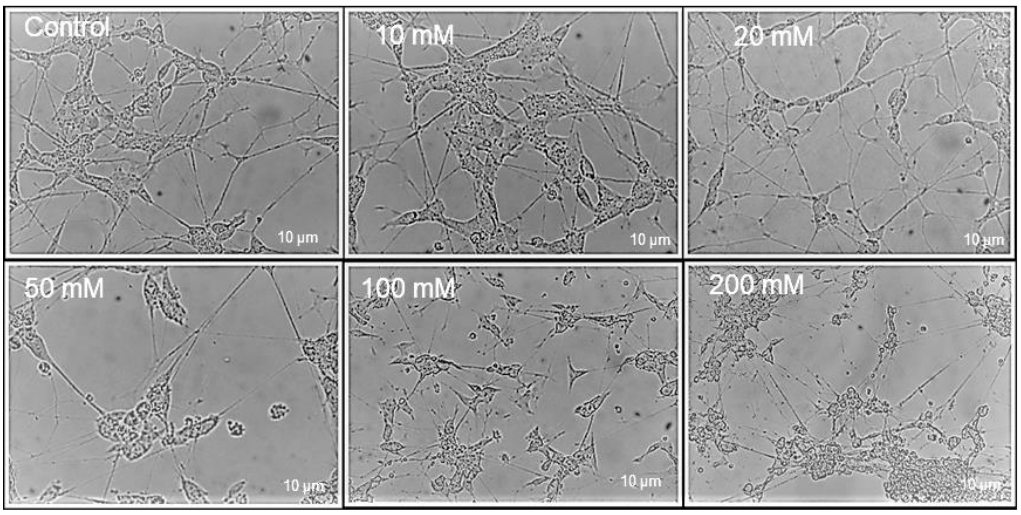
D


Control
10 mM
20 mM
50 mM
100 mM
200 mM
10 µm

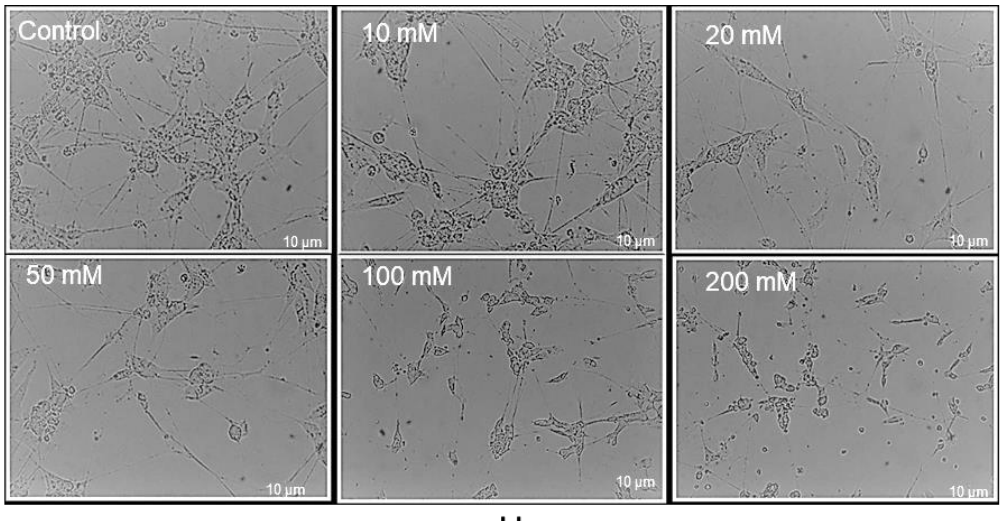
E



F



G



H

Figure 6-5: Morphological alteration of ethanol exposed SH-SY5Y cells. Undifferentiated cells: A- 3 h; B- 6 h; C- 12 h; D- 24 h. Differentiated cells: E- 3 h; F- 6 h; G- 12 h; H- 24 h. Images were captured using a phase contrast microscope. Scale bar: 10 µM.

6.3.2 Alcohol effect on cell differentiation of SH-SY5Y cells.

The effect of alcohol on differentiation of SH-SY5Y cells was quantified by a neurite outgrowth inhibition assay. Neurite outgrowth is considered as an *in vitro* biomarker of neuronal differentiation. SH-SY5Y differentiation was induced under conditions of exposure to 0 - 200 mM ethanol, to evaluate the effect of ethanol on cellular differentiation. Morphological impairments of neurite outgrowth were captured by phase contrast microscopy and further quantified by analysing neurite lengths and compared with control treatments.

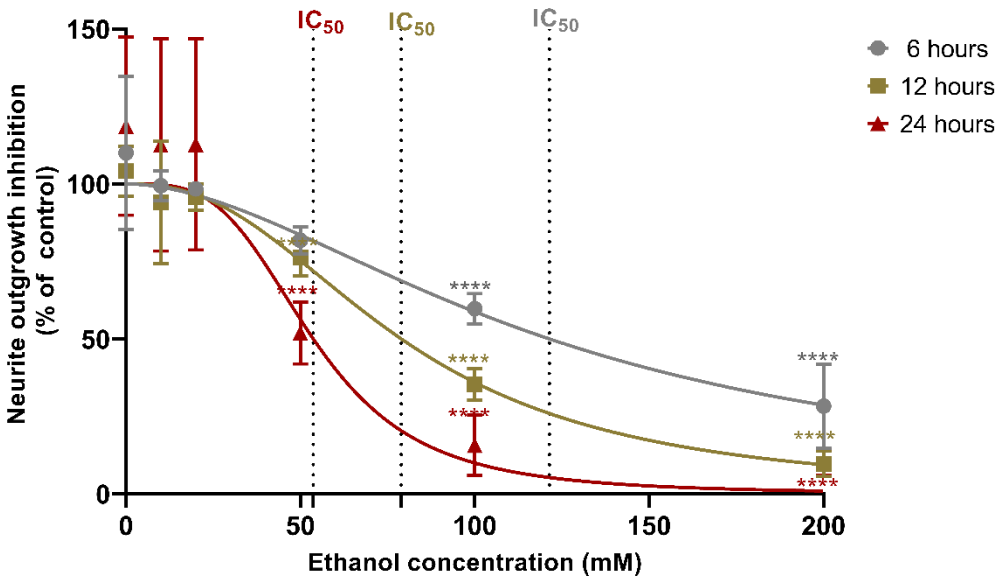
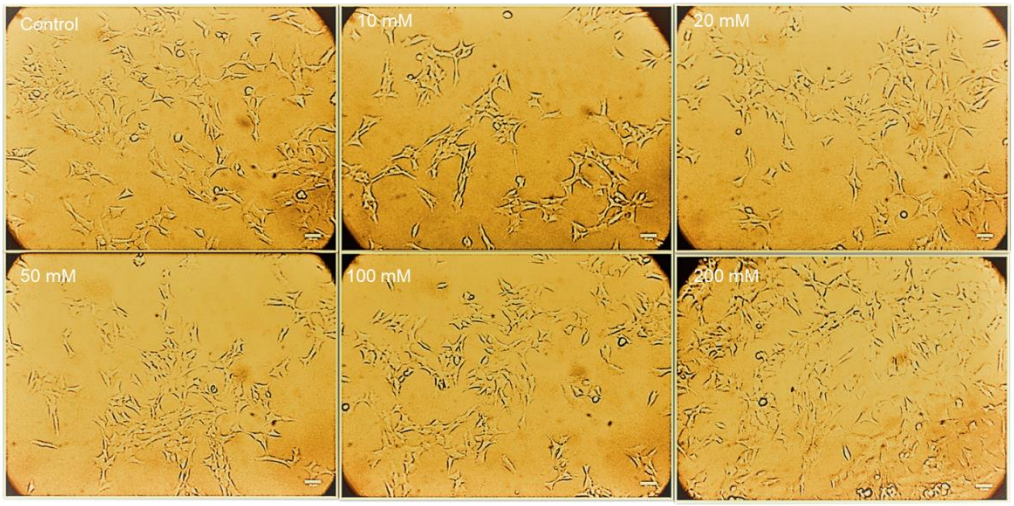
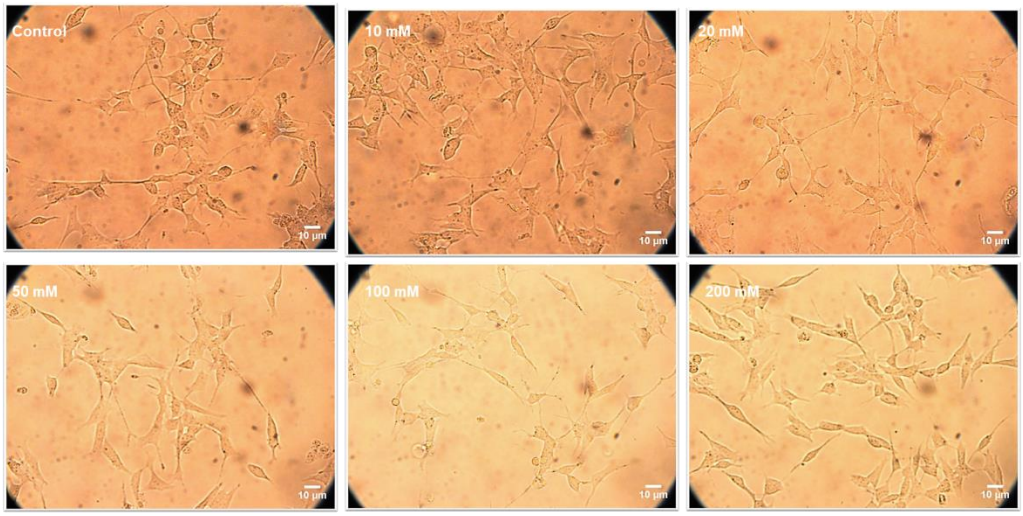


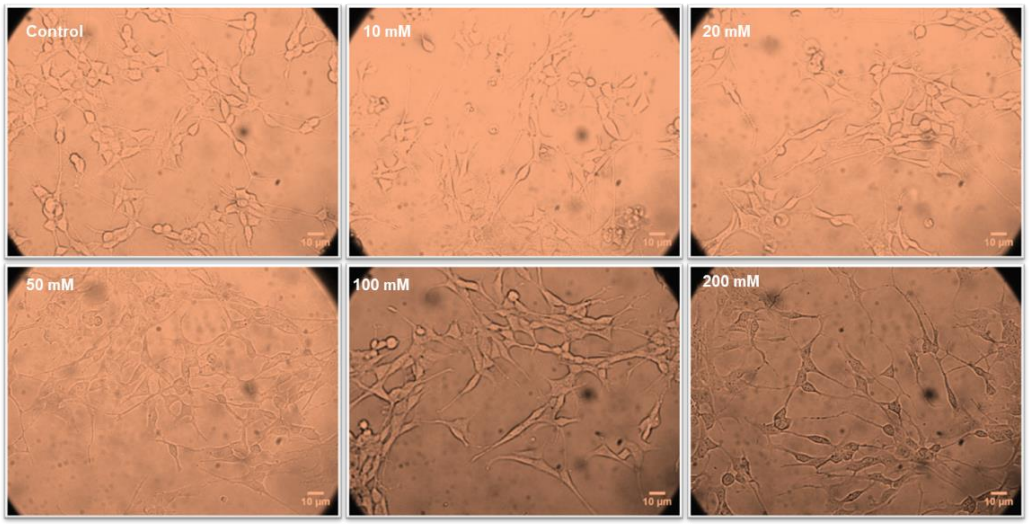
Figure 6-6: Effect of ethanol on neurite outgrowth of differentiating SH-SY5Y cells.
SH-SY5Y cells were induced to differentiate for 6, 12 and 24 h in the presence of 0 - 200 mM concentrations of ethanol. Images were captured from phase contrast microscope and neurite lengths were quantified using the neurite tracer tool in ImageJ. Data are expressed as mean lengths per 200 cells and were normalised to the lengths of control treatments and expressed as percentage to the controls of five independent experiments with three replicates in each treatment (n=5). Results analysed using one-way ANOVA with Turkey's multiple comparison and expressed as the mean ± standard error of the mean (SEM), when SEM bar is not apparent, this means that error is smaller than the symbol size. For significance; ****p<0.0001.


Control
10 mM
20 mM
50 mM
100 mM
200 mM

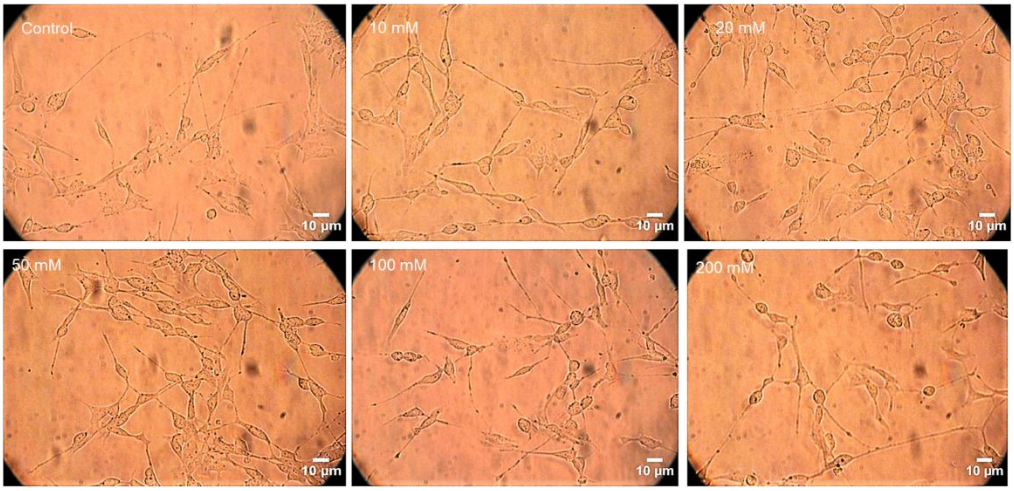
A


Control
10 mM
20 mM
50 mM
100 mM
200 mM

B


Control
10 mM
20 mM
50 mM
100 mM
200 mM

C



D

Figure 6-7: Effect of ethanol for differentiating SH-SY5Y cells.
SH-SY5Y cells were induced to differentiate for 3 h (A) 6 h (B),12 h (C) and 24 h (D) in the presence of 0 - 200 mM concentrations of ethanol. Images were captured from phase contrast microscope. Scale bar: 10 µm.

Figure 6-7 showed that the control treatment at 6, 12 and 24h had typical outgrowth of neurites for differentiating cells, and that ethanol exposure affected the neurite outgrowth in a concentration and exposure-dependent manner. There was no quantifiable neurite growth apparent at 3 h post-exposure (Figure 6-7 A). There was a dramatic increase in neurite outgrowth inhibition compared to control treatments when the ethanol concentration continues to increase. These findings were further confirmed by quantitative analysis of effects of alcohol on neurite outgrowth as depicted in Figure 6.6, which shows a significant reduction of neurite outgrowth of pre-differentiated cells in a concentration-dependent manner with ethanol exposure. However, there was no significant neurite length outgrowth inhibition at 10 mM alcohol treatments at 6 h (p= 0.1927), 12 h (p=0.0916) and 24 h (p=0.9698), showing 10.5%, 10.5% and 6.7%, respectively, compared to control treatments. Neurite length retraction was not significant at 20 mM concentrations at all time points compared to the corresponding controls; showing a percentage of 11.5% at 6 h (p=0.1312), 10% at 12 h (p=0.2070), and 6% at 24 h (p=0.9727) inhibition compared to control treatments. Interestingly, there was no significant difference in inhibition of

neurite outgrowth at 20 mM compared to all other time points (Table 6-3). After 20 mM, the dose-response curves got steeper when the ethanol concentration continued to increase, indicating higher concentration effects on differentiation of the cells. There was a strong effect apparent at 200 mM treatment for 6,12 and 24 h exposures and a significant reduction of neurite lengths in remaining cells exposed to 200 mM treatment compared to control treatments. These results suggest that 20 mM is the threshold concentration that induced neurite inhibition at all time points. In line with the microscopic observations, neuronal cells lost their contacts before losing their viability when undergoing differentiation upon alcohol exposure. Also, the rate of inhibiting neurite outgrowth in differentiating cells was significantly different from control treatments at 6, 12, and 24 h exposed at the 10 - 200 mM concentration range, hence 50% neurite inhibition concentrations for 24 h was lower than that of the 6 h and 12 h (Table 6-3 and Table 6-9).

Table 6-3: Comparison of effect of ethanol on neurite outgrowth with exposure duration.

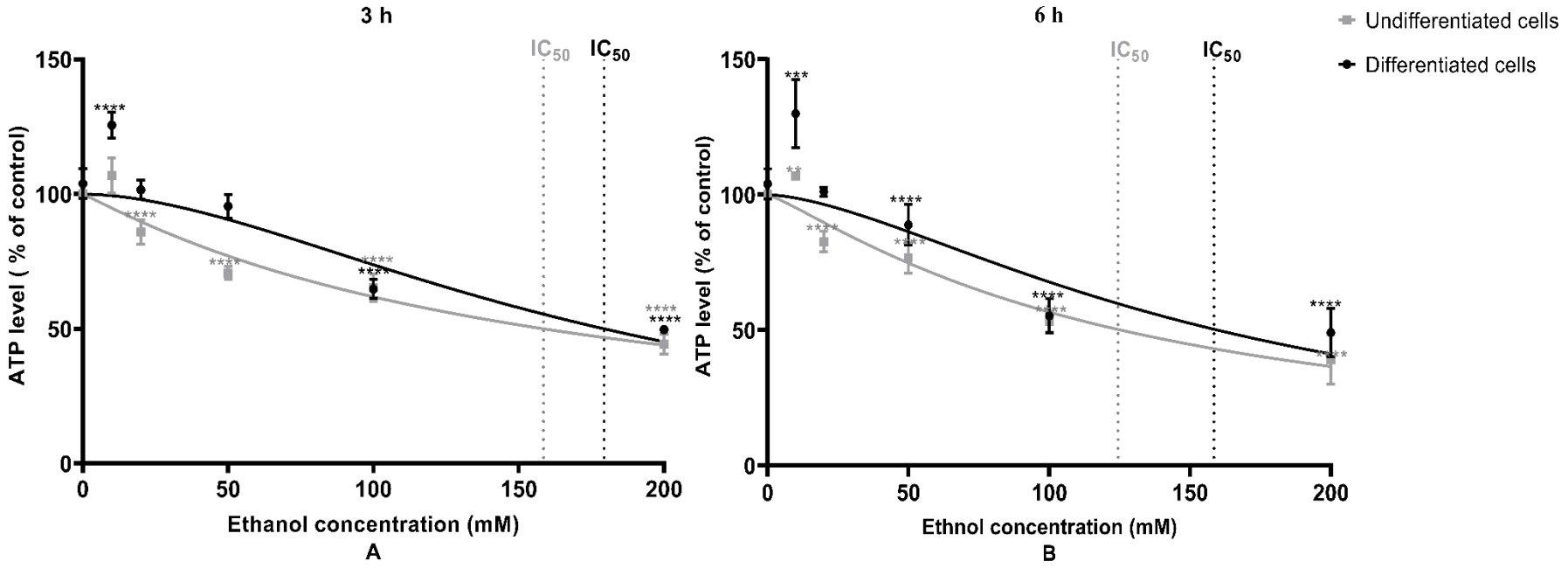
Treatments (mM)	6 h vs 12 h	6 h vs 24 h	12 h vs 24 h
10	NS	NS	0.0331
20	NS	NS	NS
50	NS	0.0002	0.0031
100	0.0030	<0.0001	0.0227
200	0.0386	0.0446	NS

NS- Not significant, $p<0.05$

6.3.3 Alcohol affected energy levels of SH-SY5Y cells in a concentration and time dependent manner.

Next, ATP levels of the ethanol exposed cells were quantified using an ATP assay. The effect of ethanol upon cellular ATP levels for undifferentiated and differentiated cells mirrored the MTT dose-response curves (Figure 6-8). ATP levels decreased with increasing concentration and with increasing the exposure duration of ethanol to cells. Interestingly, 10 mM concentration increased cellular ATP levels by 6% at 3 and 6 h exposures for undifferentiated cells and 11-15% at 12 and 24 h. Differentiated cells had boosted cellular ATP levels by 20-22% at all time points for 10 mM exposures. ATP levels start to decline significantly at concentrations above 20 mM in all time points. At 200 mM exposure for both undifferentiated and differentiated cells, there was a dramatic decline in ATP levels mirroring the MTT cell metabolic activity and viability concentration-response curves. Both 3 and 6 h concentration-responses exhibited a linear relationship with ATP levels and concentration of ethanol for both phenotypes. A significant decline of ATP levels was observed from 20 - 200 mM for undifferentiated cells compare to controls, while differentiated cells showed significant ATP level decline at 100 and 200 mM at 3 h, and 50 - 200 mM at 6 h exposure (Figure 6-9 A and B).

12 h and 24 h exposures showed the greatest effects of ethanol in the range of 20 - 200 mM concentration, as a significant drop in ATP levels in both phenotypes. The rate of ATP decline compared to the control showed a significant difference for differentiated vs undifferentiated cells (Table 6-8). 100 mM concentration of ethanol showed a significant effect on cellular ATP levels for undifferentiated cells at all time points, while 50 mM and 100 mM showed a significant effect on both cell phenotypes at 6,12 and 24 h exposures (Table 6-4).


3 h
6 h
Undifferentiated cells
Differentiated cells
IC50
IC50
ATP level (% of control)
ATP level (% of control)
Ethanol concentration (mM)
Ethnol concentration (mM)
A
B

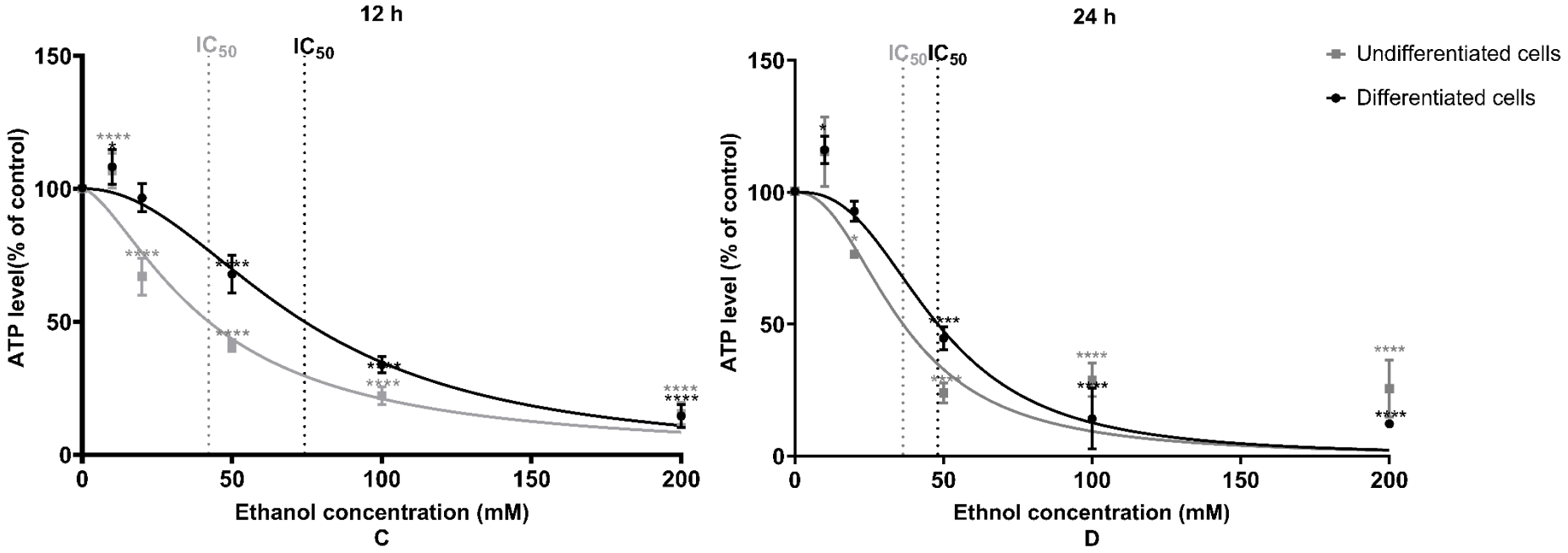


Figure 6-8: Effect of ethanol on cellular ATP levels in SH-SY5Y cells.
Undifferentiated and differentiated cells were challenged with 0 - 200 mM ethanol for durations of 3 h (A), 6 h (B), 12 h (C) and 24 h (D). Cellular ATP levels were assessed using ATP luminescence assay. Readings were normalized to the ATP level of control, providing ATP levels percentages, as a percentage value to the control. Control and treatments were performed as triplicates in 5 independent experiments (n=5). Results were analysed using one-way ANOVA with Dunnett's multiple comparison and expressed as the mean ± standard error of the mean (SEM), when SEM bar is not apparent, this means that error is smaller than the symbol size. For significance; **p*<0.05, ***p*<0.01, ****p*<0.001, *****p*<0.0001.

Table 6-4: Comparison of ethanol toxicity in different time points in undifferentiated and differentiated SH-SY5Y cells measured by ATP assay.

Cell type	Treatments (mM)	3h vs 6 h	3h vs 12 h	3 h vs 24 h	6 h vs 12 h	6 h vs 24 h	12 h vs 24 h
Undifferentiated	10	NS	NS	NS	NS	NS	NS
	20	NS	0.0004	NS	0.0039	NS	NS
	50	NS	<0.0001	<0.0001	<0.0001	<0.0001	0.0013
	100	0.0381	<0.0001	<0.0001	<0.0001	<0.0001	0.5266
	200	NS	<0.0001	0.0019	<0.0001	0.0334	NS
Differentiated	10	NS	0.0035	NS	0.0002	NS	NS
	20	NS	NS	NS	NS	NS	NS
	50	NS	<0.0001	<0.0001	0.0003	<0.0001	<0.0001
	100	NS	<0.0001	<0.0001	<0.0001	<0.0001	0.0008
	200	NS	<0.0001	<0.0001	<0.0001	<0.0001	NS

NS- Not significant, $p<0.05$.

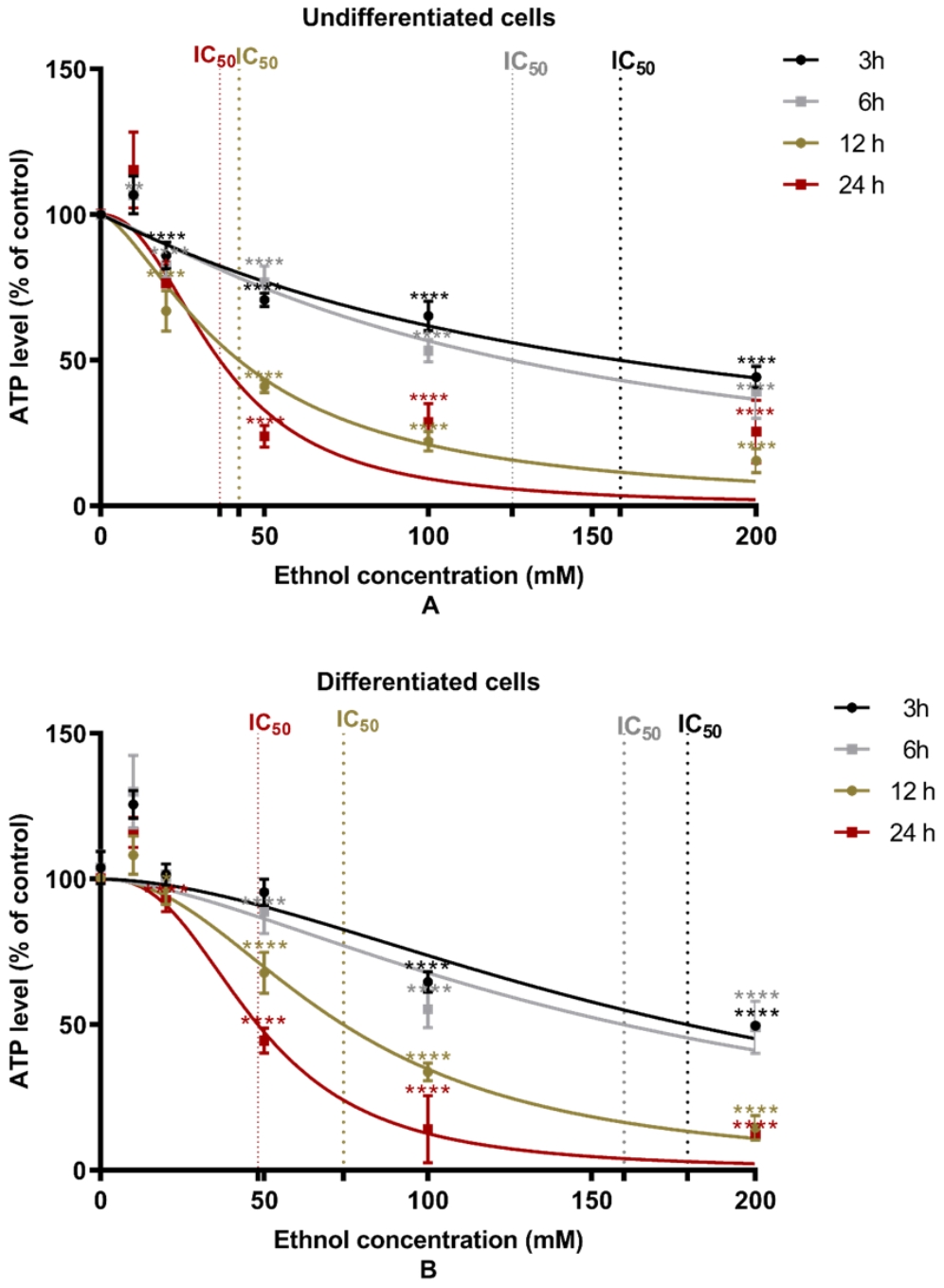


Figure 6-9: Effect of ethanol on cellular ATP levels of undifferentiated and differentiated SH-SY5Y cells.

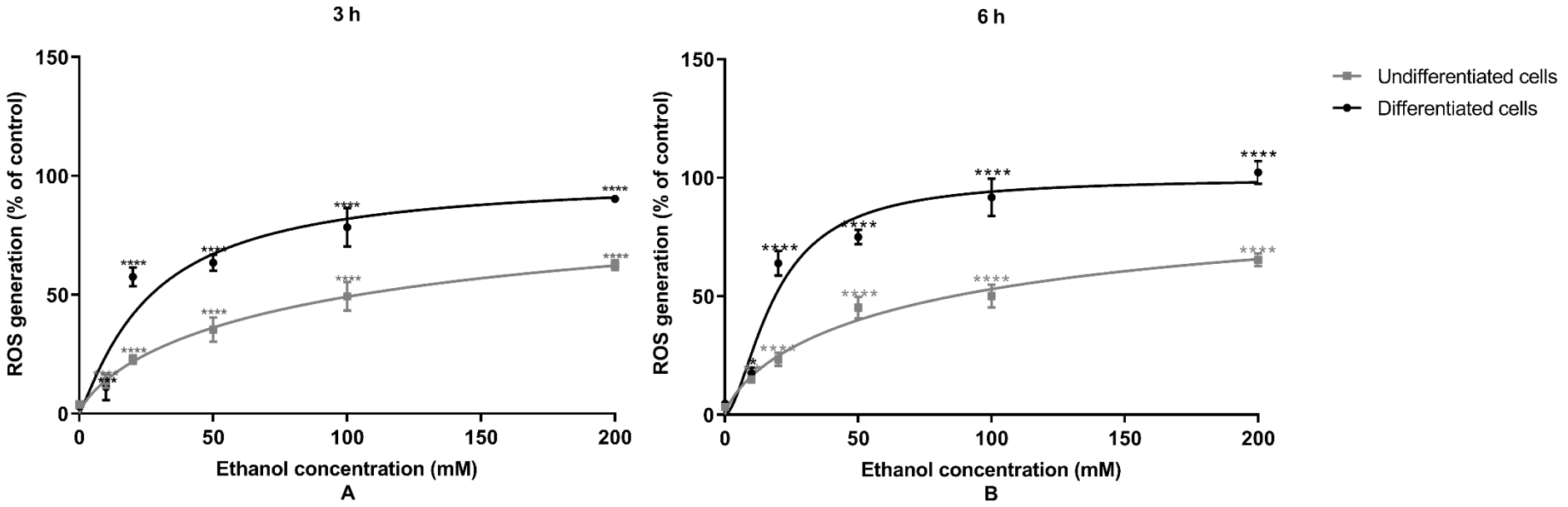
A- undifferentiated and B- differentiated cells were challenged with 0 - 200 mM for durations of 3, 6, 12and 24 h. Cellular ATP levels was assessed using an ATP luminescence assay. Readings were normalized to the ATP level of control, providing ATP levels as a percentage of the control. Control and treatments were performed as triplicates in 5 independent experiments (n=5). Results were analysed using one-way ANOVA with Dunnett's multiple comparison and expressed as the mean ± standard error of the mean (SEM), when SEM bar is not apparent, this means that error is smaller than the symbol size. For significance; *p<0.05, **p<0.01, ***p<0.001, ****p<0.0001.

6.3.4 Alcohol induced ROS generation in SH-SY5Y cells.

The levels of ROS generation in response to alcohol exposure were quantified by DCDFA assay. Figure 6-10 showed that the ROS generation occurs after ethanol exposure to undifferentiated and differentiated SH-SY5Y cells in a concentration- and time-dependent manner. Ethanol exposure significantly induced ROS production compared to the control treatments in all time points and in a concentration-dependent manner. The level of ROS was highest at 6 h exposure and reached levels that plateaued at 50 - 200 mM ethanol (Figure 6-10), while 3 h exposure showed the highest levels of ROS generation compared to 12 and 24 h (Table 6-5; Figure 6-10). Differentiated cells generated more ROS than undifferentiated cells at 3 and 6 h exposures, while 12 and 24 h undifferentiated cells generated more ROS than differentiated cells.

A comparison of undifferentiated and differentiated cells at 3 h showed that at 10 mM the ROS induced by ethanol in both cells was without marked difference compared to the corresponding controls, but 20 - 200 mM showed significant differences between ROS generation for undifferentiated and differentiated cells; with differentiated cells more susceptible to ROS damage than undifferentiated cells. Herein, 100 and 200 mM ethanol concentrations induced ROS in undifferentiated and differentiated cells at 12 and 24 h with significant differences, such that there was higher ROS production in undifferentiated cells than in differentiated cells at the longer exposure durations (Table 6-5). Furthermore, 20 and 50 mM ethanol induced significant ROS in undifferentiated cells than in differentiated cells at 12 and 24 h compared to 3 and 6 h exposure durations (Figure 6-11). Collectively, the results suggest that alcohol induces oxidative stress in both undifferentiated and differentiated cells in a concentration and time-dependent fashion, but at 12 and 24 hours there was a

stronger oxidative stress response by undifferentiated cells compared with differentiated cells.


3 h
6 h
ROS generation (% of control)
Ethanol concentration (mM)
A
B
Undifferentiated cells
Differentiated cells

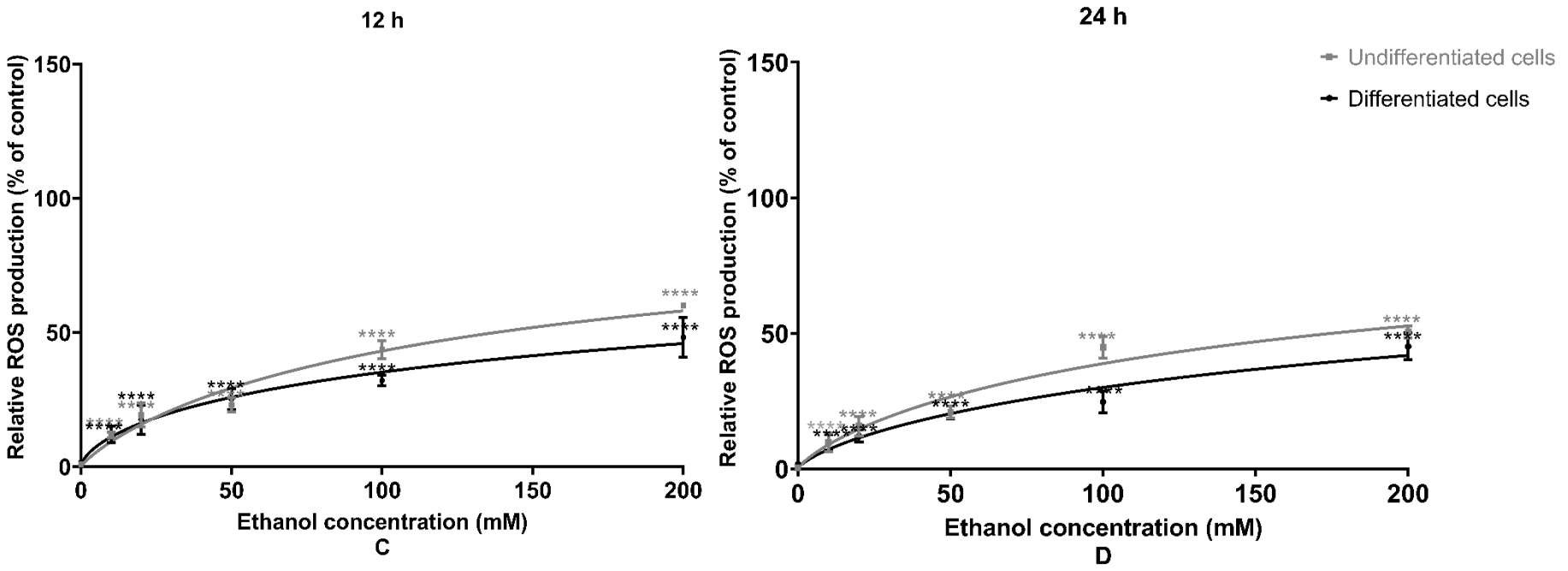


Figure 6-10: Effect of ethanol on cellular ROS generation in SH-SY5Y cells.
Undifferentiated and differentiated cells were challenged with 0 - 200 mM for durations of 3 h (A), 6 h (B), 12 h (C) and 24 h (D). Cellular ROS generation was assessed using DCFDA assay. Readings were normalized to controls by keeping 0.5 mM H_2O_2 treatments as 100%, providing a ROS generation percentage, as a percentage value to the control. Control and treatments were performed as triplicates in 5 independent experiments (n=5). Results were analysed using one-way ANOVA with Dunnett's multiple comparison and expressed as the mean ± standard error of the mean (SEM), when SEM bar is not apparent, this means that error is smaller than the symbol size. For significance; *p<0.05, **p<0.01, ***p<0.001, ****p<0.0001.

Table 6-5: Comparison of ethanol induced ROS generation at different time points in undifferentiated and differentiated SH-SY5Y cells measured by DCFDA assay.

Cell type	Treatments (mM)	3h vs 6 h	3h vs 12 h	3 h vs 24 h	6 h vs 12 h	6 h vs 24 h	12 h vs 24 h
Undifferentiated	10	NS	NS	NS	NS	NS	NS
	20	NS	NS	NS	NS	NS	NS
	50	0.0297	0.0038	0.0006	<0.0001	<0.0001	NS
	100	NS	NS	NS	NS	NS	NS
	200	NS	NS	0.0058	NS	0.0004	0.0386
Differentiated	10	NS	NS	NS	NS	NS	NS
	20	<0.0001	<0.0001	NS	NS	<0.0001	<0.0001
	50	<0.0001	<0.0001	0.0160	NS	<0.0001	<0.0001
	100	<0.0001	<0.0001	0.0039	NS	<0.0001	0.0008
	200	<0.0001	<0.0001	0.0111	NS	<0.0001	<0.0001

NS- Not significant; $p<0.05$.

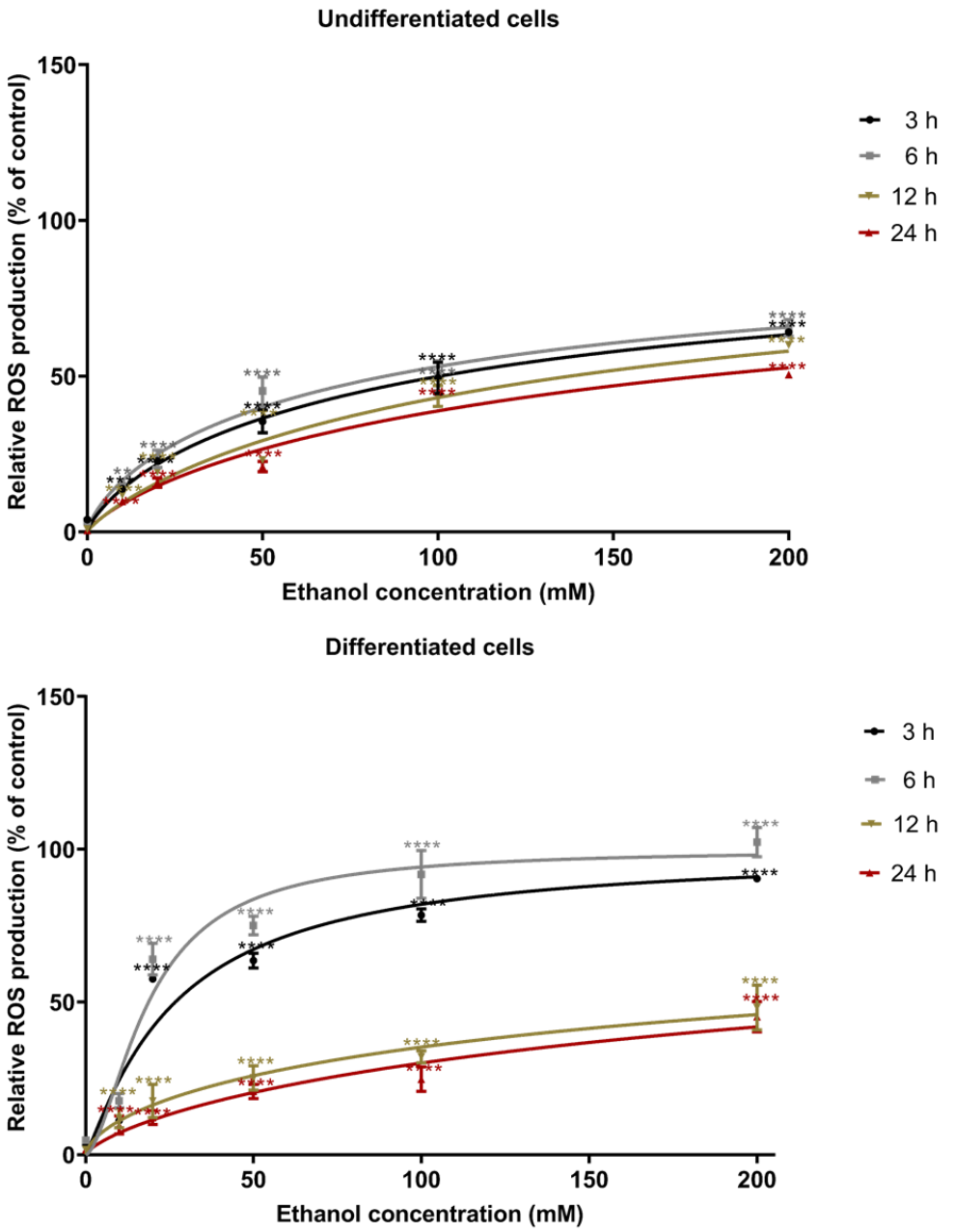


Figure 6-11: Effect of ethanol on ROS generation of undifferentiated and differentiated SH-SY5Y cells.

A- undifferentiated and B- differentiated cells were challenged with 0 - 200 mM for durations of 3, 6, 12 and 24 h. Cellular ROS generation was assessed using a DCFDA assay. Readings were normalized to controls, providing ROS generation as a percentage value to the control. Control and treatments were performed as triplicates in 5 independent experiments (n=5). Results were analysed using one-way ANOVA with Dunnett's multiple comparison and expressed as the mean ± standard error of the mean (SEM), when SEM bar is not apparent, this means that error is smaller than the symbol size. For significance; *p<0.05, **p<0.01, ***p<0.001, ****p<0.0001.

6.3.5 Alcohol-induced oxidative damage to proteins

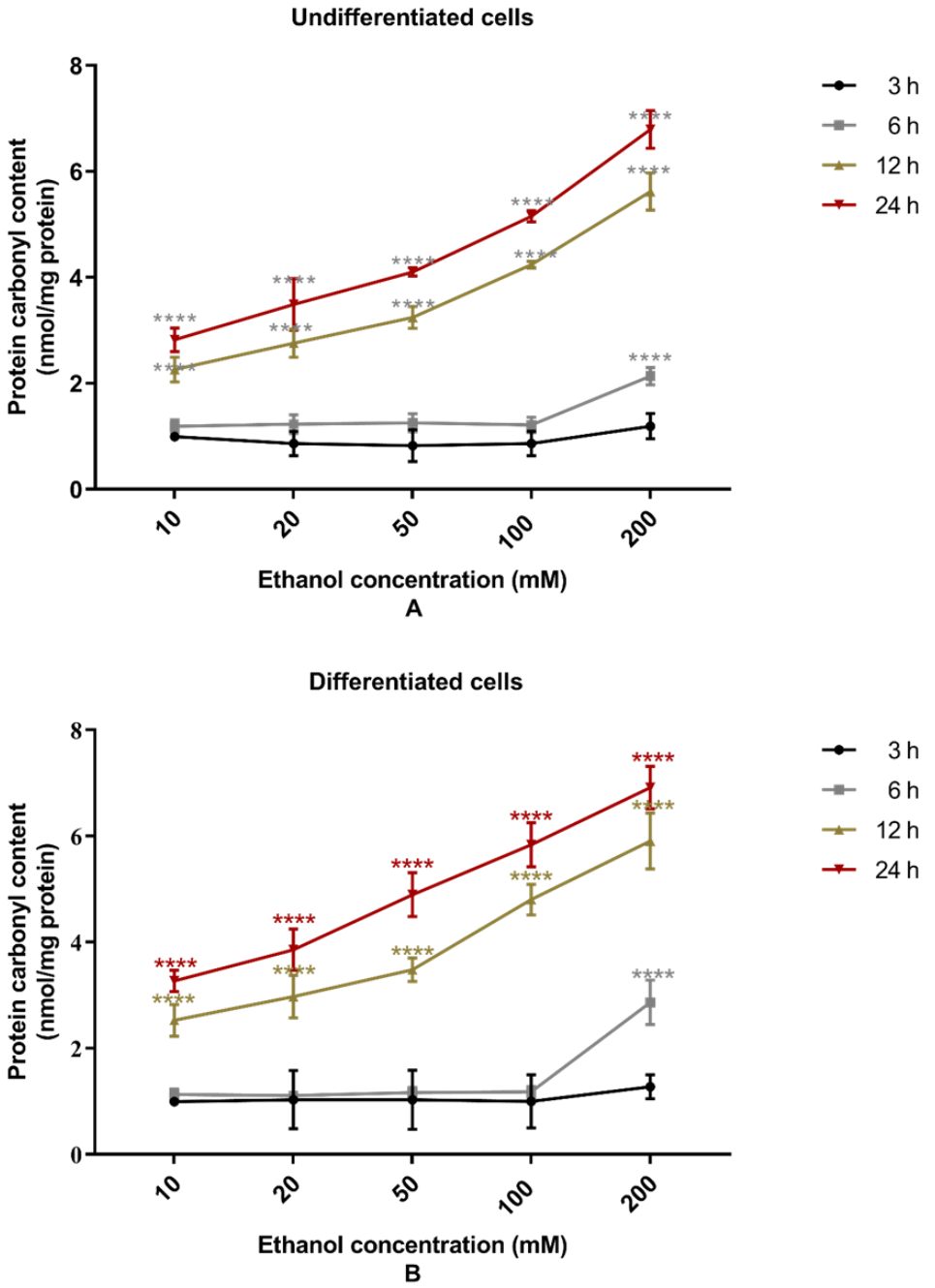


Figure 6-12: Quantitation of oxidatively damaged proteins as protein carbonyl content.
A- undifferentiated and B- differentiated SH-SY5Y cells were exposed to alcohol (10 - 200 mM) for duration of 3, 6, 12 and 24 h, and the protein carbonyl content quantified in crude cytosolic fractions by spectrophotometric protein carbonyl determination assay. Each data point represents the mean of at least 5 individual experiments. Results were analysed using one-way ANOVA with Dunnett's multiple comparison and expressed as the mean ± standard error of the mean (SEM), when SEM bar is not apparent, this means that error is smaller than the symbol size. For significance: ****p<0.0001.

Figure 6-12 illustrates the oxidative damage to cytosolic proteins in undifferentiated and differentiated cells quantified as a measure of protein carbonylation at 3, 6, 12 and 24 h exposures. Protein carbonyl content increased with increasing ethanol concentration as shown in Figure 6-12. However, 1 - 100 mM concentrations showed similar levels of protein carbonyls for 3 and 6 h exposures, whereas 200 mM showed a significant increase compared to the other concentrations of ethanol for both phenotypes at 6 h. Significant levels of protein carbonyls were observed at 12 and 24 hours compared to the controls. Interestingly, 10 and 20 mM concentrations also induced significant protein carbonylation, with both phenotypes showing a positive correlation with ROS generation (Table 6-6). Alcoholic and control brain samples also analysed by protein carbonyl content assay to compare the protein carbonyl levels. The endogenous levels of carbonylation in alcoholic brain were similar to those for a high (toxic) exposure of 100 - 200 mM alcohol to cells. Control and alcoholic brain tissue had the same pattern of oxidatively-damaged proteins, but levels were significantly increased 1.8-fold in alcoholic subjects (Figure 6-13).

Differentiated cells showed more tendency for cytosolic protein carbonylation compared to the undifferentiated cells and there is significant difference between the 12 and 24 h exposures of ethanol in protein carbonylation (Table 6-7). Correlation analysis of levels of protein carbonyl content and ROS generation showed a significant positive correlation between ROS and PCC at each concentration tested, suggesting increasing ROS levels increased the protein carbonylation in undifferentiated and differentiated cells after 12 and 24 h (Table 6-6). Interestingly, cellular ATP levels showed, there is a significant negative correlation that exists only at 12 and 24 h alcohol exposed differentiated cells with PCC. Results of protein carbonyl analysis showed that

the differentiated cells induced significant levels of protein carbonylation after 24 h exposure and were susceptible to more oxidative damage than undifferentiated cells. Differentiated cells are a more relevant model to mimic the human neuronal cells, and hence differentiated cells exposed to 0 - 200 mM were used to visualize oxidatively damage proteins (Figure 6-14). At the same time, alcoholic and control brain sample were also resolved by gel electrophoresis and immunoblotted to visualize the oxidatively damage protein in alcoholic and control human brains to compare *in vivo* conditions. Application of 10 mM ethanol was without detectable effects, but 20 - 200 mM induced a progressive increase in the levels of carbonylated proteins revealed by oxyblot.

The major proteins modified were characterized by their denatured approximate molecular weights proteins was observed for human brain extract as that for alcohol-treated cells (Figure 6-13), indicative of overlapping target proteins of 120, 110, 90, and 50 kDa.

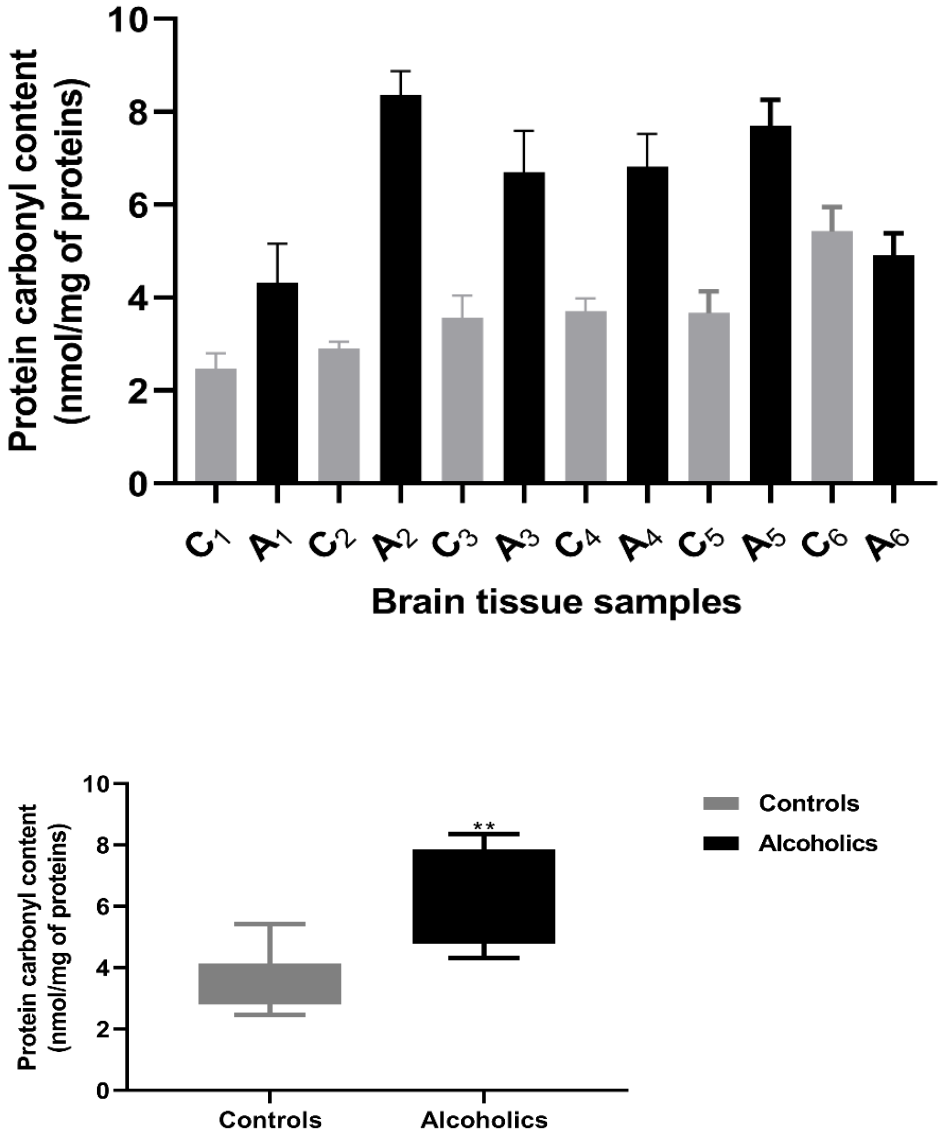


Figure 6-13: Protein carbonyl contents of alcoholic and control brain samples.

Crude cytosolic fractions of control (C) and alcoholic (A) brains protein carbonyl content quantified by spectrophotometric protein carbonyl determination assay. Each data point represents the mean of at least 5 individual experiments. Results were analysed using one-way ANOVA with Dunnett's multiple comparison and expressed as the mean ± standard error of the mean (SEM), when SEM bar is not apparent, this means that error is smaller than the symbol size For significance: ** $p<0.01$.

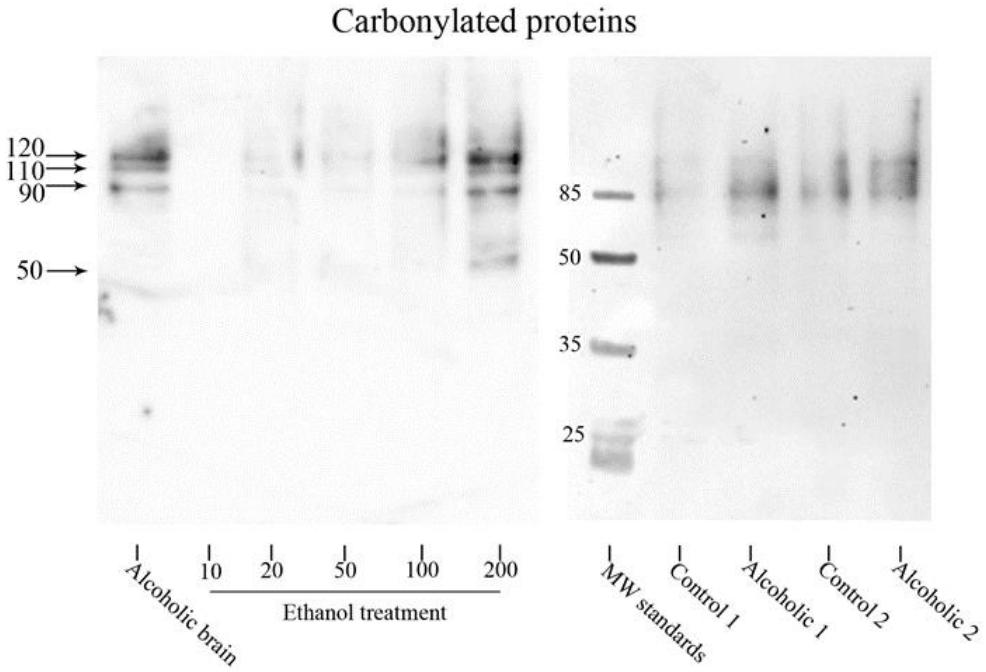


Figure 6-14: Cytosolic protein carbonylation of differentiated cells, alcoholic and control brain samples.
Differentiated cells were exposed to 10, 20, 50, 100 and 200 mM concentrations ethanol for 24 h. Crude cytosolic fractions of treated cells, alcoholic and control brains were DNPH derivatized, resolved by gel electrophoresis and immunoblotted with anti-DNPH antibody to identify the specific protein targets of protein carbonylation of ethanol exposure. Each experiment was conducted as 3 independent experiments with three replicates.

Table 6-6: Correlation between the ROS generation and protein carbonyl content / ATP production in SH-SY5Y cells.

Cell Type	Treatment duration (hours)	ROS vs PCC			ROS vs ATP		
		r	**R^2**	***P* value**	***r***	**R^2**	***P* value**
Undifferentiated	3	0.4874	0.2375	NS	-0.4018	0.1615	NS
Differentiated		0.5758	0.3315	NS	-0.6853	0.4696	NS
Undifferentiated	6	0.7193	0.5175	NS	-0.8574	0.7352	NS
Differentiated		0.8584	0.7369	NS	-0.6508	0.4235	NS
Undifferentiated	12	0.9940	0.9881	0.0006	-0.8882	0.7890	0.0441
Differentiated		0.8624	0.7437	NS	-0.9724	0.9455	0.0055
Undifferentiated	24	0.9592	0.9200	0.0098	-0.7724	0.5966	NS
Differentiated		0.9579	0.9175	0.0103	-0.9566	0.9151	0.0108

r- Pearson's correlation coefficient; NS- Not significant; $p<0.005$

Table 6-7: Comparison of ethanol toxicity at different time points in undifferentiated and differentiated SH-SY5Y cells for protein carbonyl content.

Cell type	Treatments (mM)	3h vs 6 h	3h vs 12 h	3 h vs 24 h	6 h vs 12 h	6 h vs 24 h	12 h vs 24 h
Undifferentiated	10	NS	<0.0001	<0.0001	<0.0001	<0.0001	0.0271
	20	NS	<0.0001	<0.0001	<0.0001	<0.0001	0.0024
	50	NS	<0.0001	<0.0001	<0.0001	<0.0001	0.0004
	100	NS	<0.0001	<0.0001	<0.0001	<0.0001	0.0001
	200	<0.0001	<0.0001	<0.0001	<0.0001	<0.0001	<0.0001
Differentiated	10	NS	<0.0001	<0.0001	0.0001	<0.0001	NS
	20	NS	<0.0001	<0.0001	<0.0001	<0.0001	0.0188
	50	NS	<0.0001	<0.0001	<0.0001	<0.0001	<0.0001
	100	NS	<0.0001	<0.0001	<0.0001	<0.0001	<0.0001
	200	<0.0001	<0.0001	<0.0001	<0.0001	<0.0001	0.0059

NS- Not significant; $p<0.05$.

Table 6-8: Comparison of the cytotoxicity of alcohol to undifferentiated vs differentiated SH-SY5Y cells.

		Undifferentiated vs differentiated SH-SY5Y cells				
Alcohol treatment (mM)	**Exposure time point (hrs)**	**MTT assay**	**ATP assay**	**LDH assay**	**ROS assay**	**PCC assay**
10	3 6 12 24	0.0075 NS NS 0.0161	<0.0001 <0.0001 0.0004 NS	NS NS NS NS	NS NS NS NS	NS NS <0.0001 NS
20	3 6 12 24	NS NS NS <0.0001	<0.0001 0.0002 <0.0001 NS	NS NS 0.0026 <0.0001	<0.0001 <0.0001 NS 0.0016	NS NS NS NS
50	3 6 12 24	NS NS <0.0001 0.0002	<0.0001 0.0138 <0.0001 0.0098	0.0001 NS <0.0001 <0.0001	<0.0001 <0.0001 NS NS	NS NS 0.0035 0.0004
100	3 6 12 24	NS 0.0493 <0.0001 <0.0001	NS NS <0.0001 NS	<0.0001 <0.0001 0.0070 0.0278	<0.0001 <0.0001 <0.0001 <0.0001	NS NS <0.0001 0.0028
200	3 6 12 24	NS 0.0120 NS NS	NS NS NS NS	0.0342 NS NS NS	<0.0001 <0.0001 <0.0001 <0.0001	NS <0.0001 NS 0.0391

NS- Not significant*; p* value 0.05, MTT- (4,5-dimethylthiazol-2-yl)-2,5-diphenyltetrazolium bromide, LDH- Lactose dehydrogenase, ATP- Adenosine triphosphate.

Table 6-9: Toxicity of alcohol to undifferentiated or differentiated SH-SY5Y cells.

Cell Type	Treatment duration (h)	MTT assay		ATP assay		LDH assay		Neurite reduction	
		IC_{50}	R^2	IC_{50}	R^2	IC_{50}	R^2	IC_{50}	R^2
Undifferentiated	3	149.8 ± 18.6	0.8800	158.5 ± 17.3	0.9149	110.6 ± 3.1	0.9878	N/A	N/A
Differentiated		160.5 ± 25.8	0.7969	179.4 ± 26.3	0.7732	172.5 ± 3.4	0.9863	Non observable	-
Undifferentiated	6	111.5 ± 7.6	0.9453	124.4 ± 10.6	0.9430	107.2 ± 4.6	0.9722	N/A	N/A
Differentiated		124.4 ± 14.7	0.8573	158.2 ± 29.2	0.7196	136.1 ± 5.9	0.9507	121.4 ± 7.6	0.8383
Undifferentiated	12	46.7 ± 3.1	0.9648	42.2 ± 3.9	0.9445	46.9 ± 3.1	0.9743	N/A	N/A
Differentiated		75.25 ± 7.0	0.9268	74.4 ± 3.7	0.9745	75.8 ± 4.5	0.9551	79.0 ± 3.2	0.9272
Undifferentiated	24	23.3 ± 2.1	0.9372	35.97 ± 0.6	0.8476	24.9 ± 2.3	0.9371	N/A	N/A
Differentiated		54.83 ± 6.5	0.9016	48.08 ± 3.4	0.9551	59.10 ± 2.3	0.9391	53.72 ± 7.5	0.8383

IC_{50}- 50% inhibition concentration; MTT- (4,5-dimethylthiazol-2-yl)-2,5-diphenyltetrazolium bromide, LDH- Lactose dehydrogenase, ATP- Adenosine triphosphate.

6.4 Discussion

Alcohol is a well-known cytotoxic agent that induces a number of responses within neuronal cells. In spite of several published studies, the mechanism of alcohol-induced cytotoxicity remains unclear. However, drinking pattern is associated with risk of alcohol and related pathologies, but little is known about the effects of binge drinking on neuronal cells and the mechanism of inducing cytotoxic responses of neuronal cells. Herein, human neuroblastoma cells were exposed to low and high concentrations of alcohol, and this demonstrated that neurons can be killed at exposures relevant to binge drinking, and alcohol had effects on neuronal differentiation, and that surviving neurons experienced damage through redox stress and protein carbonylation.

The toxicity of alcohol to both undifferentiated and differentiated cells was assessed by MTT, LDH and ATP assays, and this showed that alcohol induced a concentration and time-dependent reduction of cell viability loss and cell death in both undifferentiated and differentiated cells. Three independent assays confirmed that alcohol induced minimal toxicity until a 10 mM concentration was reached for both phenotypes at all time points. Cell viability and cell death was significantly reduced over the concentration range of 20 - 200 mM. Interestingly, differentiated cells were more resistant to alcohol exposure according to this study. A concentration-dependent decrease in cell viability had been observed by Liu et al. (2014) showing that 0 - 500 mM ethanol reduced cell viability of human neuroblastoma SH-SY5Y cells. Significant viability loss was demonstrated at 100 mM, as assessed by MTS assay, while ATP assay also indicated similar results. In line with the current study, Liu et al. (2014) showed that LDH release increased in a concentration-dependent manner. In contrast, the current study used both undifferentiated and differentiated cells, while Liu et al. (2014) only considered effects in undifferentiated cells. This consideration is

consistent with the current study there was a concentration-dependent decrease in cell viability recorded in human neuroblastoma cells such as SH-SY5Y, SH-N-SK and IMR32 (Luo and Miller, 1997). However, a number of studies have demonstrated that retinoic acid differentiated cells were less susceptible to alcohol-induced cell damage (Pantazis et al., 1992, Saunders et al., 1995, Serio et al., 2019). Saunders et al. (1995) showed that retinoic acid ameliorates the inhibition of neuronal differentiation by alcohol with coordinated effects on neurite extension in LAN-5 human cultured neuronal cells. Differentiated cells also showed resistance to neurotoxic compounds such as MPP^+ with biogenetic changes in differentiation to cholinergic phenotypes (Cheung et al., 2009, Shipley et al., 2016).

Interestingly, mild positive effects on neuronal cell metabolic activity were observed after application of 10 mM alcohol to both phenotypes of SH-SY5Y cells at all time points tested. This may reflect increased cell metabolic activity and proliferation of cells. A blood alcohol concentration (BAC) of 10 mM can be achieved through consumption of a single measure of fortified spirit or pint of strong beer. Regular intake of alcohol to a BAC of 10 mM would represent low or possibly 'moderate' alcohol consumption (Eckardt et al., 1998), a level proposed to provide neuro- or cardio-protective effects, with a relative health risk that adheres to a 'J-curve' (Anstey et al., 2009, Rehm et al., 2003, Rehm et al., 2017b). It is therefore interesting to note that the direct effects of alcohol to neurons also produces a 'J-curve' for cell viability.

The 20 - 200 mM alcohol range showed significant effects on neuronal cells mirroring the consumption of several drinks in a period of a few hours. A 6 h exposure showed that 20 and 50 mM have moderate effects on SH-SY5Y cell viability, however, 100 to 200 mM showed a significant loss of neurones. This showed heavy drinking sessions through consumption of more than 60 g of pure

alcohol kills neuronal cells even at 6 h exposure. A 100 - 200 mM BAC resulted in a substantial decline of neuronal viability even at a 3 h exposure. In line with this, 100 mM alcohol can significantly influence human neurogenesis (Louis et al., 2018).

An effect of alcohol on the cell differentiation process was observed using neurite outgrowth inhibition, which is a morphological marker of neuronal differentiation. Neurite inhibition at 10 and 20 mM ethanol was not significant, but after 20 mM, significant neurite outgrowth inhibition was observed. A similar observation was recorded in rat cerebellar neuronal cells that 1 - 100 mM ethanol exposure, as this reduced neurite outgrowth in a concentration and time-dependent manner (Bearer et al., 1999). However, the IC_{50} concentration for neurite outgrowth inhibition was 400 mM which is a significantly higher value than that of the current study. This could reflect a difference between rat cell models and their sensitivity to ethanol is different than that of human neuronal cells. In support to this, a study demonstrated decreased neurite outgrowth of LA-N-5 human neuroblastoma cells treated with 109 mM ethanol with different concentrations of retinoic acid in a time-dependent manner (Saunders et al., 1995). Therefore, the ethanol effects on cell differentiation in SH-SY5Y cells were over a concentration range of 20 - 200 mM. The current study suggests that ethanol effects on neurite outgrowth in differentiating cells, and this could lead to neuronal cell contact loss where it effects nerve impulse transmission and synaptic performance. Hence, reduction of cognitive capacities experienced with moderate to heavy drinkers (Sabia et al., 2014, Topiwala and Ebmeier, 2018) could reflect both reduced cell number and a loss of functional neuronal contacts. This has been further examined in a study with cerebellar granule neuronal cells, that the ethanol effect on cell adhesion molecules and

induced neurodevelopmental cell pathologies was observed in developing brains due to alcohol exposure (Bearer et al., 1999).

Ethanol induced oxidative stress in both undifferentiated cells and differentiated cells. This finding is consistent with the other studies that ROS increased in a concentration-dependent manner (Haorah et al. 2008, Wang et al. 2012). Peak ROS levels were observed at 6 h exposure while 3 h exposure still induced a considerable level of ROS, when compared to that at 12 h and 24 h. This could be due to 12 and 24 hour exposure evident more cell death than in 3 and 6 h exposure. Therefore, ROS generation in remaining cells could be lower than that of the 3 and 6 h exposures. Interestingly, alcohol-induced significant levels of ROS even at 10 mM: a concentration that did not compromise cell viability. Relatively low levels of ROS may not be detrimental to cell health, but influence cellular signalling, and may also be mitigated by cellular (antioxidant) defence and repair mechanisms (Boonstra and Post, 2004). Nevertheless, a threshold is reached beyond which ROS are able to bind to and damage cellular components including proteins, lipids, as well as contributing to genotoxicity via direct or indirect DNA damage. These relatively high levels of ROS are often deleterious to the cell and contribute to the induction of apoptosis (Simon et al., 2000, Li et al., 2016). Interestingly, undifferentiated cells generate more ROS at 12 and 24 h in the current study. It has been shown that differentiated SH-SY5Y cells were more resistant to ROS damages than undifferentiated cells due to their mitochondrial bioenergetic changes during differentiation with retinoic acid (Schneider et al., 2011).

A time course of production of oxidatively-damaged proteins was considered via protein carbonyl content (PCC) in response to alcohol exposures. Cellular oxidative stress triggers increased protein carbonyl content via formation of aldehydes and ketones, and this is usually irreversible and may impair normal

protein structure and function. Interestingly, alcohol-induced elevation of PCC lagged the 6 h peak of ROS, with highest levels of PCC detected at 12 and 24 hours. The process of protein carbonylation is gradual after ROS production as observed in this study, but the rationale for this temporal delay will need to be investigated further. However, correlation analysis showed there was a negative correlation with ATP levels in cells. This suggested that increase ROS levels induced mitochondrial dysfunction and a drop in ATP levels, consistent with reduced cell function and viability. However, consistent with all cell viability assays, 10 mM ethanol concentration induced moderate protein carbonylation compared to higher concentrations, even though this ethanol concentration does not induce cell death. Noteworthy, was that the endogenous levels of oxidative damage in alcoholic brain were similar to those from the highest induction of cellular toxicity at the higher ethanol concentrations such as 100 and 200 mM. The identity of the proteins susceptible to alcohol-induced oxidative damage, and how this damage could impinge upon protein function will be addressed in future studies.

In conclusion, ethanol exposure caused viability loss and induced oxidative stress in both undifferentiated and differentiated cells with limited impact at 10 mM concentration on both phenotypes, suggesting a possible mechanism by which alcohol exposure exerts detrimental deficits in the brain. In addition, oxidative stress damages proteins which alters the integrity of cells, and this might be underlying mechanism of increased severity of cytotoxic responses of neuronal cells to the toxic effects of alcohol.

7 NEUROTOXICITY EVALUATION OF ALCOHOL USING HUMAN PROGENITOR NEURONAL STEM CELLS

7.1 Introduction

Alcohol is considered as a teratogen and its consumption during pregnancy can cause adverse effects on the developing foetus (Brocardo et al., 2011, Zhang et al., 2018). However, there is no safe amount and safe time during pregnancy to consume alcohol. Even mild and moderate exposures to alcohol are associated with the alteration of the developing brain and its functions (Zhang et al., 2018). It has been proven that the degree of CNS dysfunctions depends on quantity of alcohol consumed, pattern of consumption, and the time of consumption during pregnancy (Brocardo et al., 2011, Zhang et al., 2018).

In general, alcohol exposure causes functional changes and induced neuronal death by apoptosis (Goodlett and Horn, 2001, Goodlett et al., 2005). The mechanism by which alcohol hinders the neuronal cell function as well as causes cell death during pregnancy are still in debate. Binge-like alcohol exposures during pregnancy induce considerable number of neuronal cell death through apoptosis in the brain, as shown using rodent models (Brocardo et al., 2011). Increase of expression of pro-apoptotic proteins, mitochondrial damage and induced caspase cascade have been shown as mechanisms of neurodegeneration in neonatal brain in rodents and in humans due to ethanol exposure (Dikranian et al., 2005, Harper and Matsumoto, 2005, Crews et al., 2006, Cole et al., 2012).

There is an increasing body of literature implicating that prenatal alcohol exposure causes oxidative stress in developing organs including brain, even at very low exposures (Brocardo et al., 2007). Apart from that, growing lines of evidences have shown a role of oxidative stress in FASD development directly

in mouse models, but very few studies demonstrated ROS generation in animals exposed to alcohol during pregnancy (Heaton et al., 2002, Heaton et al., 2003, Kane et al., 2008, Dong et al., 2010). However, all these findings have suggested multiple mechanisms that are interconnected to induce toxicological consequences to neuronal cells spontaneously that sequentially lead to cell death.

The previous chapter of this thesis showed that alcohol induced oxidative stress damage and cell death in neuronal cells. However, the complexity of human brain and presence of other cell lineages could affect toxicological responses of neuronal cells to alcohol. For example, it has been shown that alcohol inhibits astrocyte proliferation, reduces release of factors promoting neurite outgrowth, triggers glutathione depletion and reduces progenitor cell survival (Guizzetti et al., 2003, Zhang et al., 2018). Alcohol effects on oligodendrocytes have been reported in the literature showing an effect on myelination, and biochemical alteration of myelin (Zhang et al., 2018). These findings suggest that there is a direct effect of alcohol on neuronal cells that can be mediated by other glial cells, and this may contribute to a reduced severity of responses. This is very important to consider in developmental neurotoxicity studies as critical developmental events in the nervous system are precisely temporarily and spatially coordinated (Cowan, 1998, Sanes et al., 2000) with other glial cells (Bal-Price et al., 2010). Human progenitor cortical neuronal stem cells closely resemble the complexity of CNS including astrocytes, and oligodendrocytes upon mitogen withdrawal from the growing media, and when grown in monolayer culture, could differentiate into three cell lineages of the CNS (Donato et al., 2007). An effect on critical events of neurogenesis can be observed upon alcohol in these cells such as proliferation, migration, differentiation, and apoptosis.

Therefore, the purpose of this study was to examine the direct toxicity of alcohol on human progenitor cortical neuronal cells, including cellular cytotoxicity, energy levels and whether alcohol inflicts cellular cytotoxicity via oxidative stress. Oxidative stress damages to cellular proteins were also evaluated.

7.2 Results

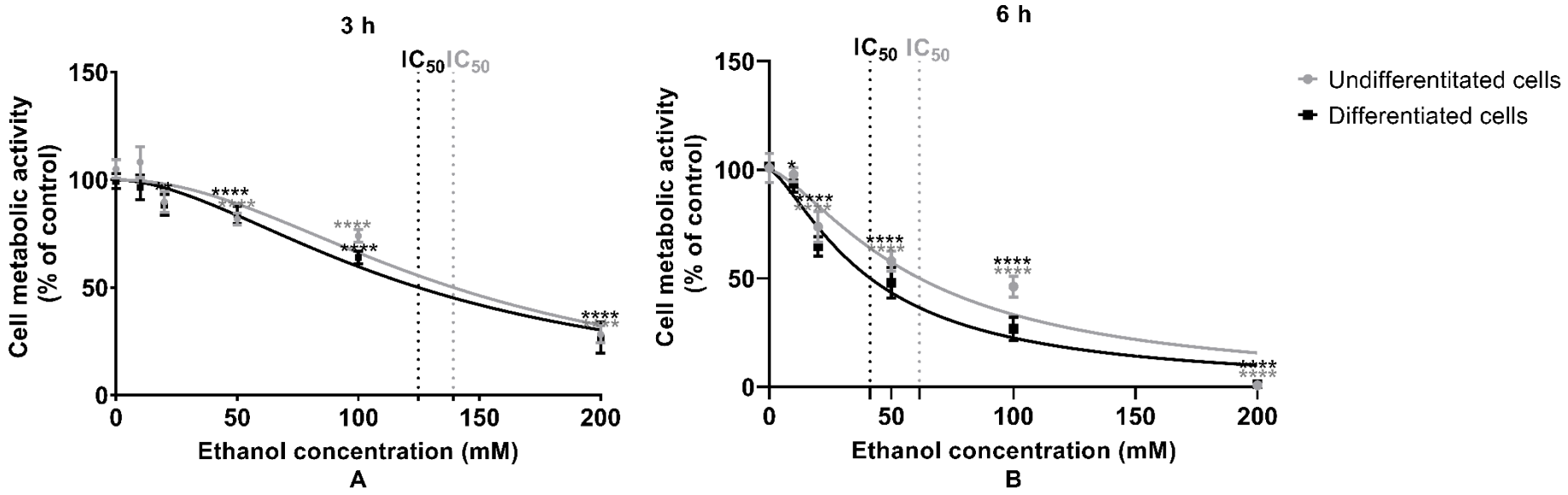
7.2.1 Alcohol reduced cell metabolic activity and cell viability in hNPCs.

The impact of ethanol on cell metabolic activity and cell viability was measured in undifferentiated and undifferentiated cells at 3, 6, 12 and 24 h post exposure. Cells were exposed to ethanol at 0, 10, 20, 50, 100, and 200 mM concentrations and metabolic activities in cultured cells measured using a MTT cell viability assay. Functional cell survival against the concentration of ethanol showed a linear relationship (Figure 7-1 A) in both phenotypes of ReNcell CX at 3 h exposure, but 6, 12 and 24 h (Figure 7-1 B-D) exposures exhibited classical dose-response relationships with increasing ethanol concentration, in both ReNcell CX cell phenotypes. This suggested ethanol reduced cell metabolic activity and cell viability of undifferentiated and differentiated cells in a concentration and exposure duration manner.

As shown in Figure 7-1, the cell viability responses of undifferentiated and differentiated ReNcell CX were highly sensitive to ethanol as early as 3 h post-exposure at 20 mM and higher concentrations. The effect was dramatic at 50, 100 and 200 mM at all time points tested. Both undifferentiated and differentiated cells exhibited significant reductions of cell metabolic activity and viability loss at 20, 50,100 and 200 mM for all time points. More than 70% cell viability loss was apparent at 200 mM ethanol with both cell phenotypes at 3 h exposures, while 6 h, 12 h and 24 h showed more than 95% cell viability loss compare to controls. The dramatic effect of ethanol on both cell phenotypes of ReNcell CX was apparent at 20 - 200 mM at 6 h, 12 h and 24 h suggesting the levels of cell viability decreased with increasing exposure duration (Figure 7-2). 10 mM concentration did not induce significant reduction of cell viability at 3 h

compared to controls for both phenotypes whereas, when the incubation time increased, the 10 mM concentration did influence cell viability compared to controls. The effect became dramatic at 24 h exposure compared to controls (p<0.0001). However, 10 and 20 mM concentrations showed moderately significant cell metabolic activity and cell viability reduction at 6 h and 12 h, but the 24 h effect of 10 or 20 mM was dramatic compared to the control treatments for both undifferentiated and differentiated cells. This suggested that ethanol concentrations up to 10 mM do not significantly effect cell metabolic activity of both phenotypes up to 6 h.

At 50 mM, undifferentiated cells showed significant differences in cell metabolic activity and cell viability loss at the tested time points (Table 7-1) in both phenotypes. Comparison of undifferentiated vs differentiated cell responses to ethanol exposure indicated that 20 mM concentration induced significantly different responses in undifferentiated and differentiated cells at 6 h exposure while, 50 - 200 mM concentration induced toxicity in cells without marked difference at every tested time points (Table 7-7). Interestingly, undifferentiated cells exhibited more resistance to ethanol exposure and toxicity than differentiated cells. Hence, 50% inhibition concentrations (IC_{50}) values were higher than that of the differentiated cells (Table 7.8). MTT assay results suggested that the difference in metabolic activity and cellular viability reduction induced by ethanol in ReNcell CX was quite significant between undifferentiated and differentiated cells, and reduction of cell viability loss in undifferentiated cells was not significantly different from undifferentiated cells exposed to 20 - 200 mM up to 24 h. MTT assays measured cytotoxic activity of alcohol exposed cells, but it can potentially suggest cytostatic responses to ethanol as well. Therefore, cell viability loss was further validated by LDH assay to confirm ethanol induced cell death in hNPCs.


3 h
6 h
IC50
IC50
Cell metabolic activity (% of control)
Ethanol concentration (mM)
A
B
Undifferentitated cells
Differentiated cells

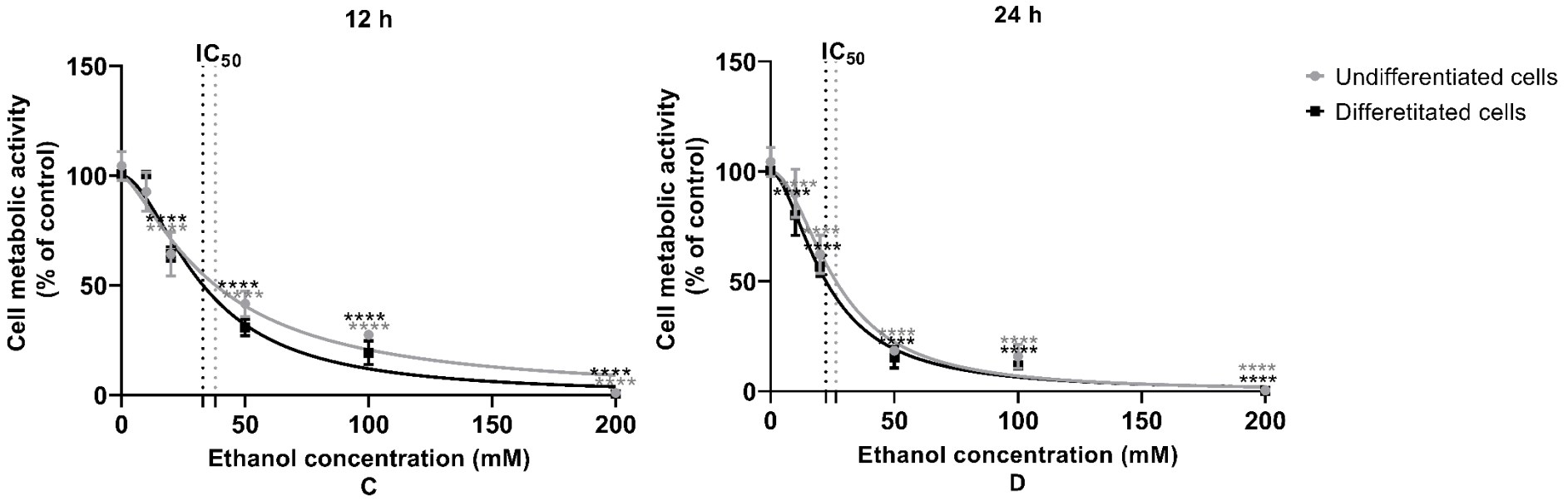


Figure 7-1: Cell metabolic and cell viability responses to alcohol by hNPCs.
Undifferentiated and differentiated cells were challenged with 0 - 200 mM for durations of 3 h (A), 6 h (B), 12 h (C) and 24 h (D). Viability was assessed using MTT assay. Readings were normalized to the viability of control, providing cell viability percentage, as a percentage value to the control. Control and treatments were performed as triplicates in 5 independent experiments (n=5). Results were analysed using one-way ANOVA with Dunnett's multiple comparison and expressed as the mean ± standard error of the mean (SEM), when SEM bar is not apparent, this means that error is smaller than the symbol size. For significance; ***p*<0.01, ****p*<0.01, *****p*<0.0001.

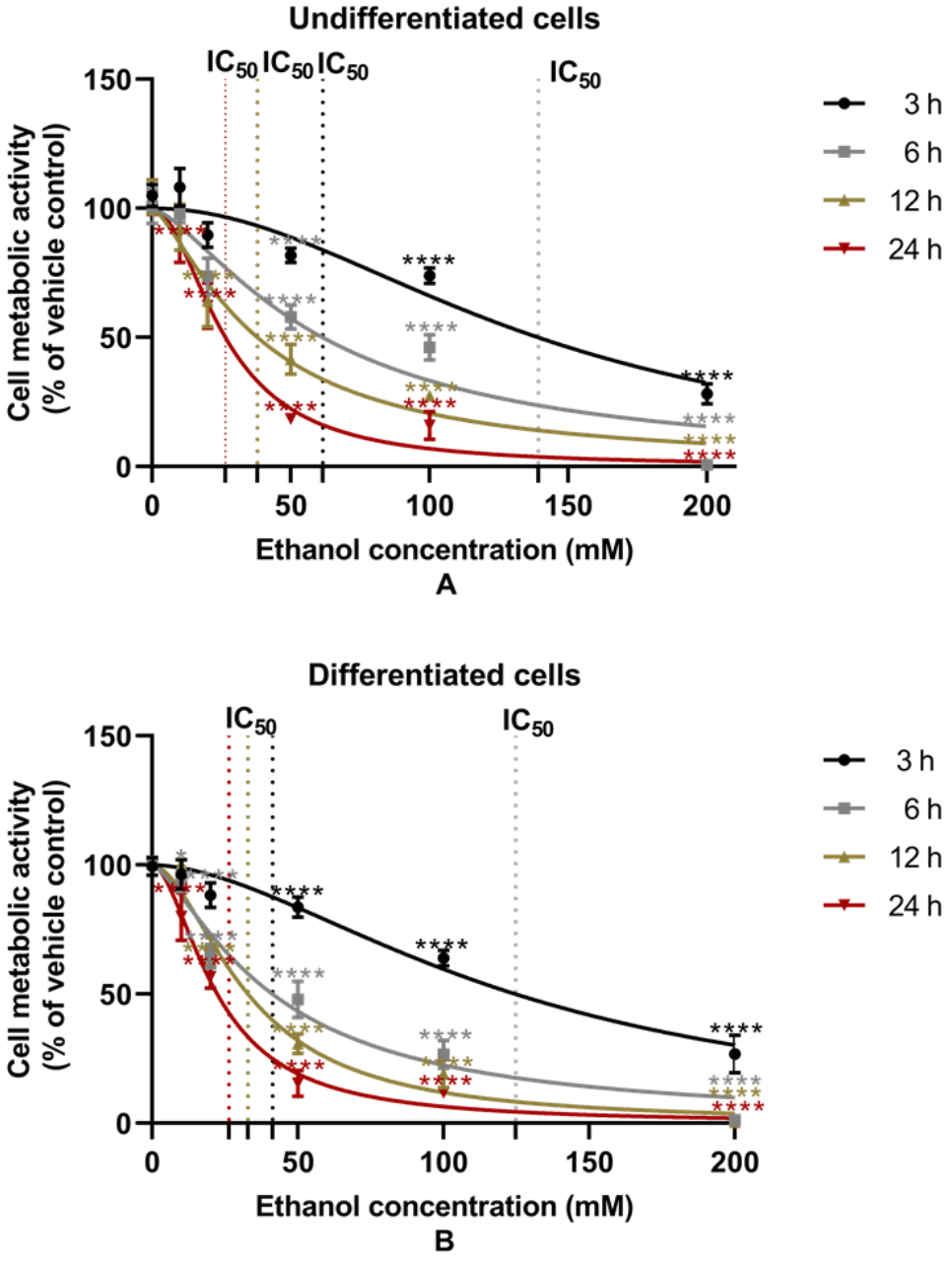


Figure 7-2: Effect of ethanol on undifferentiated and differentiated hNPCs.

A- undifferentiated and B- differentiated cells were challenged with 0 - 200 mM for durations of 3, 6, 12 and 24 h. Viability was assessed using MTT assay. Readings were normalized to the viability of control, providing cell viability percentage, as a percentage value to the control. Control and treatments were performed as triplicates in 5 independent experiments (n=5). Results were analysed using one-way ANOVA with Dunnett's multiple comparison and expressed as the mean ± standard error of the mean (SEM), when SEM bar is not apparent, this means that error is smaller than the symbol size. For significance; **p<0.01, ***p<0.01, ****p<0.0001.

Table 7-1: Comparison of ethanol toxicity in different time points in undifferentiated and differentiated hNPCs measured by MTT assay.

Cell type	Treatments (mM)	3h vs 6 h	3h vs 12 h	3 h vs 24 h	6 h vs 12 h	6 h vs 24 h	12 h vs 24 h
Undifferentiated	10	NS	0.0100	0.0020	NS	NS	NS
	20	0.0081	<0.0001	<0.0001	NS	NS	NS
	50	<0.0001	<0.0001	<0.0001	0.0062	<0.0001	<0.0001
	100	<0.0001	<0.0001	<0.0001	0.0014	<0.0001	NS
	200	<0.0001	<0.0001	0.0007	NS	NS	NS
Differentiated	10	NS	NS	0.0002	NS	0.0019	<0.0001
	20	NS	NS	NS	<0.0001	<0.0001	<0.0001
	50	<0.0001	<0.0001	<0.0001	<0.0001	<0.0001	0.0004
	100	<0.0001	<0.0001	<0.0001	NS	0.0006	NS
	200	<0.0001	<0.0001	<0.0001	NS	NS	NS

NS- Not significant, $p<0.05$.

7.2.2 Alcohol induced cell death in hNPCs in a concentration and time-dependent manner.

To gain insight into ethanol mediated cytotoxicity in undifferentiated and differentiated cells, an LDH assay was done for both undifferentiated and differentiated cells exposed for 3, 6, 12, and 24 h. Similar to MTT assays, ethanol induced LDH activity in both undifferentiated and differentiated cells in a concentration and time-dependent manner.

Measurement of LDH activity against the concentration of alcohol at 3 h post exposure showed a linear relationship similar to MTT assays (Figure 7-3 A). However, 20 mM concentration showed significant LDH production compared to the control treatment, which contrasts the MTT assay in both undifferentiated and differentiated cells. A dramatic effect of ethanol was apparent at 200 mM in both phenotypes which was observed similarly in MTT assays for 3 h exposure. The cell viability loss percentage at 3 h exposure in undifferentiated cells was 64% while it was 74% for differentiated cells compared to controls.

However, 6 h exposure showed classical dose-response curves of inhibition of cell viability by increasing LDH leakage, with pronounced cell death observed at 20 - 200 mM compared to control treatment in both phenotypes. 10 mM concentration did not induce significant LDH production compared to controls in both phenotypes (Figure 7-4 B). This is in contrast to the MTT assays that showed significant viability loss starts at 10 mM in differentiated cells. At 20 mM concentration, there was a 20.8% difference in cell death at 6 h compared with 3 h, with a marked difference at 50 mM concentration, with induction of 25.7% cell death compared to 3 h exposure in undifferentiated cells (Figure 7-4; Table 7-2). At 20 mM, differentiated cells showed 33% mean difference in LDH production compared to the 3 h exposure, while at 50 mM concentration there

was 30% cell death compared to the 3 h (Figure 7-4; Table 7-2). 10 mM concentration induced significant LDH production at 12 h and 24 h as in MTT assays indicating the exposure duration effect on cell death (Figure 7-3 C, D). 200 mM induced more than 90% cell death in both phenotypes at 12 and 24 h exposure. Comparison of 12 h and 24 h exposure of ethanol in both phenotypes showed that at 50 mM induced significant LDH production in both phenotypes compared to the controls in each time points (Table 7-2).

The results of the LDH assay suggested that differentiated cells were highly susceptible to the toxicity of ethanol at every time point tested, and thereby confirmed the MTT results. Hence, IC_{50} values for LDH activity was higher in undifferentiated cells than differentiated cells (Table 7-7). Also, the results proved that difference in LDH activity induced by ethanol in ReNcell CX was quite significant between undifferentiated and differentiated cells, but the increased cell cytotoxicity to undifferentiated cells was not significantly different from differentiated cells cultures at exposures of 20 - 200 mM up to 24 h (Table 7-7).

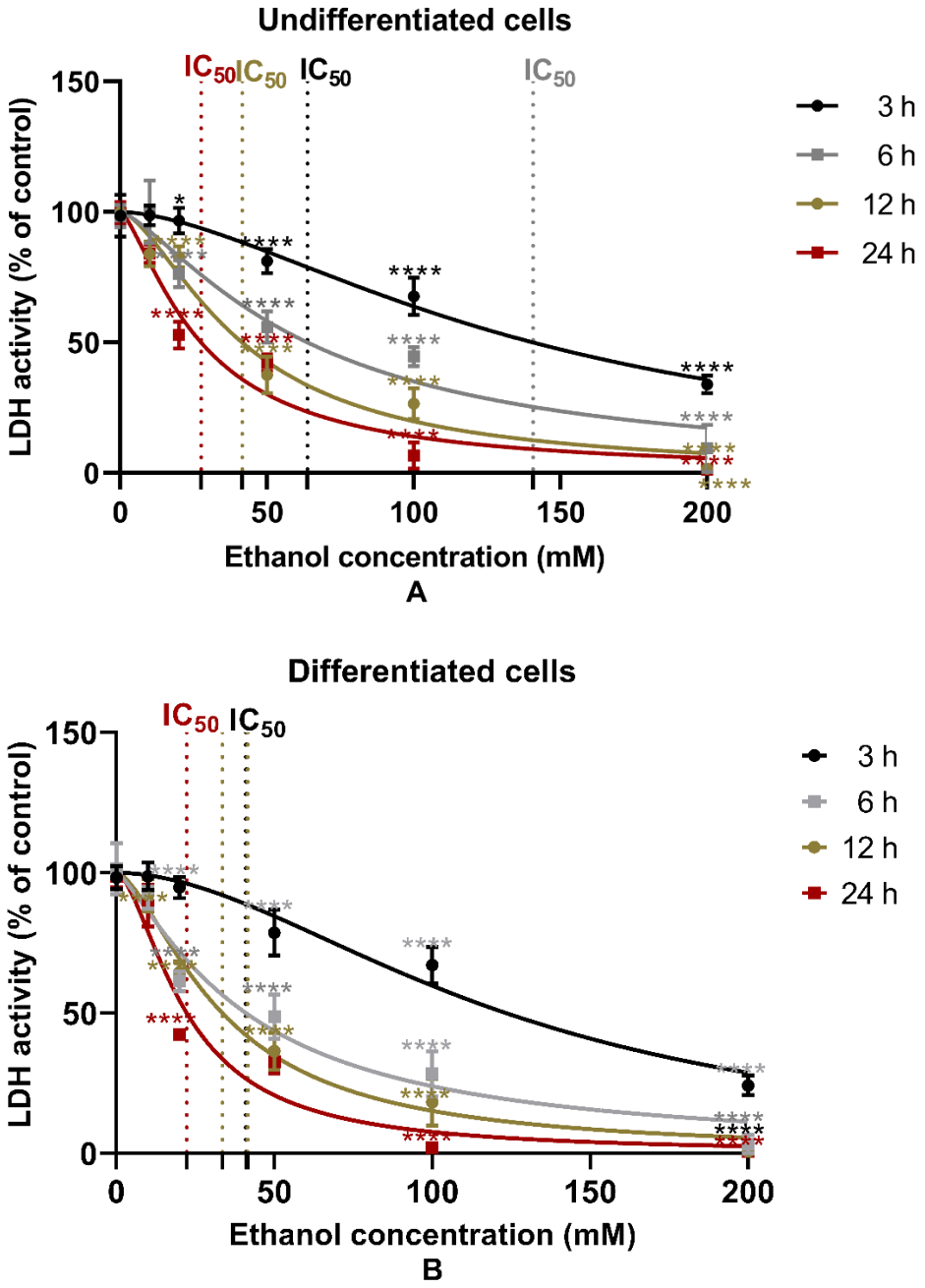
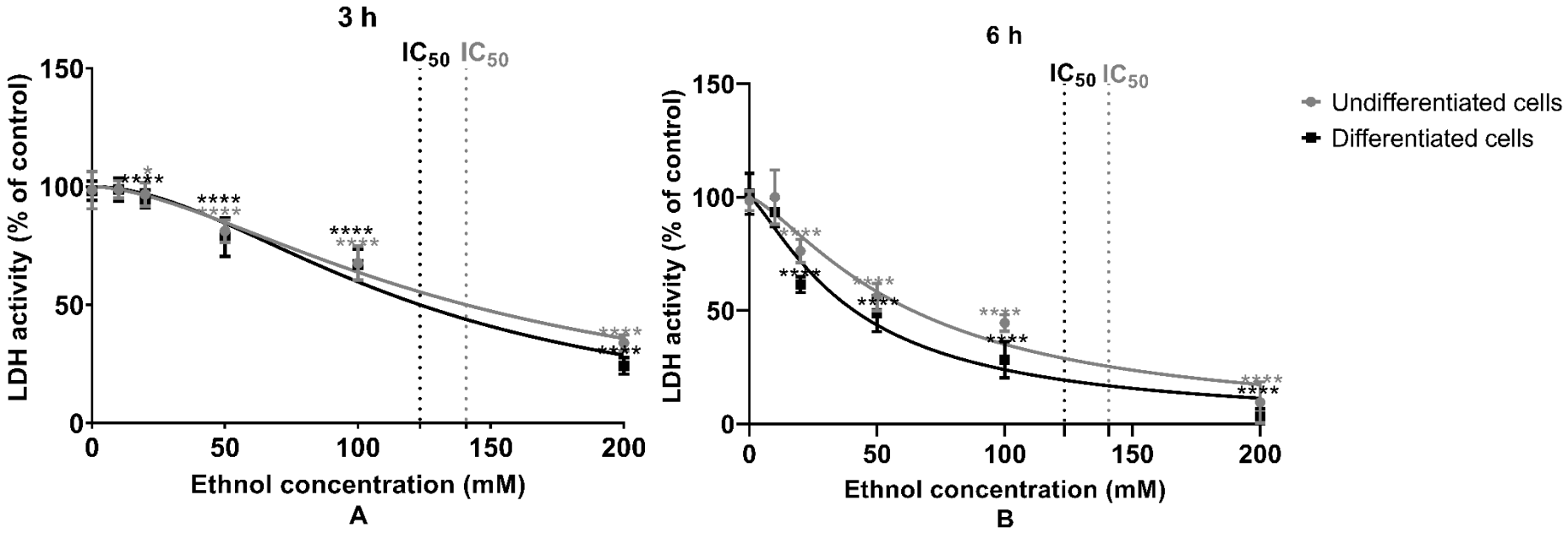


Figure 7-3: LDH activity of undifferentiated and differentiated hNPCs.
A- undifferentiated and B- differentiated cells were challenged with 0 - 200 mM for durations of 3, 6, 12 and 24 h. Viability was assessed using LDH assay. Readings were normalized to the LDH activity of control, providing LDH activity percentage, as a percentage value to the control. Control and treatments were performed as triplicates in 5 independent experiments (n=5). Results were analysed using one-way ANOVA with Dunnett's multiple comparison and expressed as the mean ± standard error of the mean (SEM), when SEM bar is not apparent, this means that error is smaller than the symbol size. For significance; *p<0.05, **p<0.01, ***p<0.001, ****p<0.0001.


3 h
6 h
IC50
IC50
LDH activity (% of control)
Ethnol concentration (mM)
A
B
Undifferentiated cells
Differentiated cells

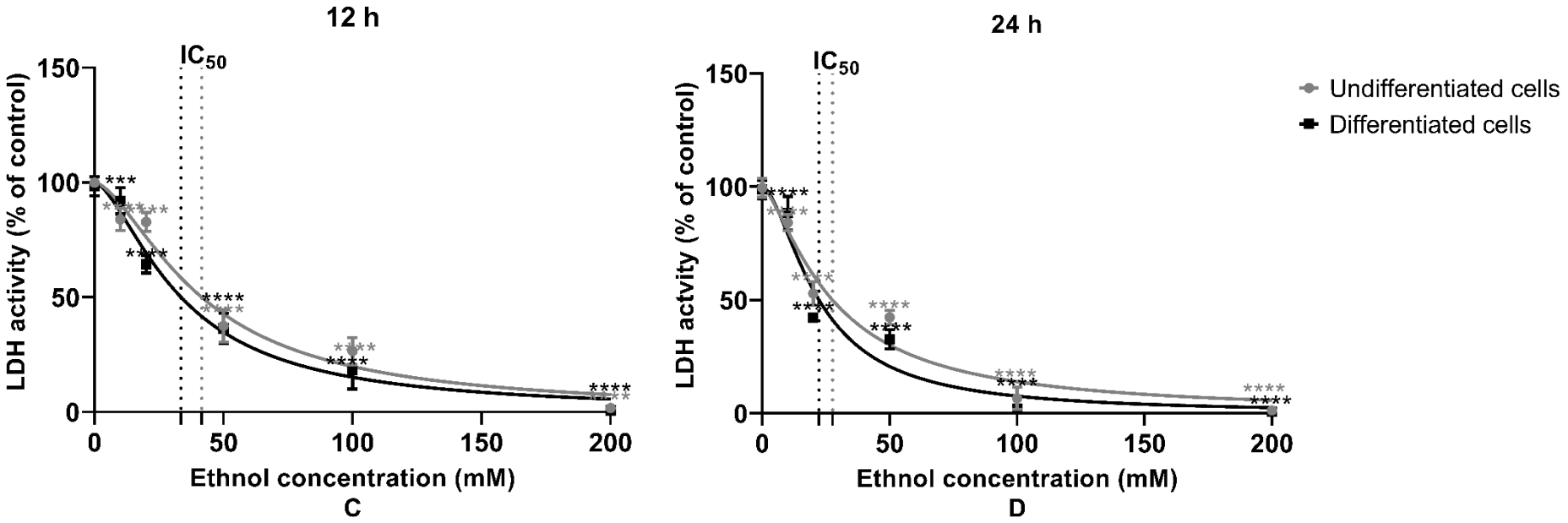


Figure 7-4: LDH activity of alcohol exposed hNPCs.
Undifferentiated and differentiated cells were challenged with 0 - 200 mM for durations of 3 h (A), 6 h (B), 12 h (C) and 24 h (D). Viability was assessed using LDH assay. Readings were normalized to the LDH activity of control, providing LDH activity percentage, as a percentage value to the control. Control and treatments were performed as triplicates in 5 independent experiments (n=5). Results were analysed using one-way ANOVA with Dunnett's multiple comparison and expressed as the mean ± standard error of the mean (SEM), when SEM bar is not apparent, this means that error is smaller than the symbol size. For significance; **p*<0.05, ***p*<0.01, ****p*<0.001, *****p*<0.0001.

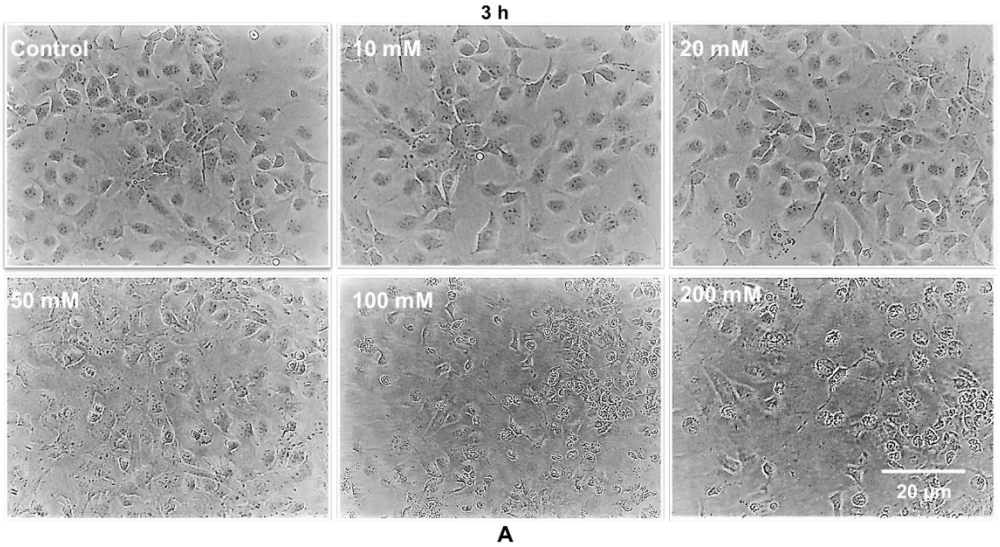
Table 7-2: Comparison of ethanol toxicity in different time points in undifferentiated and differentiated hNPCs measured by LDH assay.

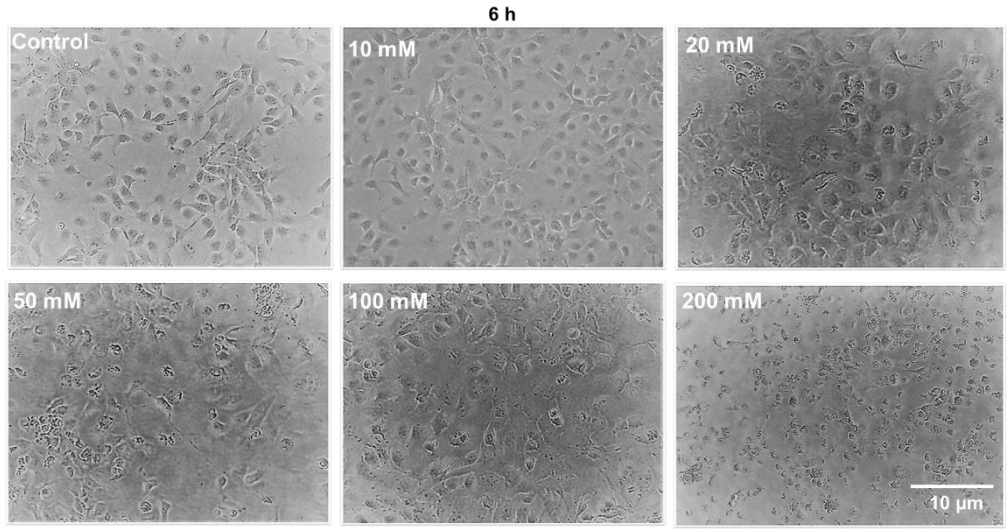
Cell type	Treatments (mM)	3h vs 6 h	3h vs 12 h	3 h vs 24 h	6 h vs 12 h	6 h vs 24 h	12 h vs 24 h
Undifferentiated	10	NS	0.0096	0.0109	0.0042	0.0048	NS
	20	0.0002	0.0163	<0.0001	NS	<0.0001	<0.0001
	50	<0.0001	<0.0001	<0.0001	0.0009	0.0207	<0.0001
	100	<0.0001	<0.0001	<0.0001	0.0012	<0.0001	0.0003
	200	<0.0001	<0.0001	0.0007	NS	NS	NS
Differentiated	10	NS	NS	NS	NS	NS	NS
	20	<0.0001	<0.0001	<0.0001	NS	0.0006	<0.0001
	50	<0.0001	<0.0001	<0.0001	0.0423	0.0045	NS
	100	<0.0001	<0.0001	<0.0001	NS	<0.0001	0.0036
	200	0.0002	<0.0001	<0.0001	NS	NS	NS

NS- Not significant, $p<0.05$.

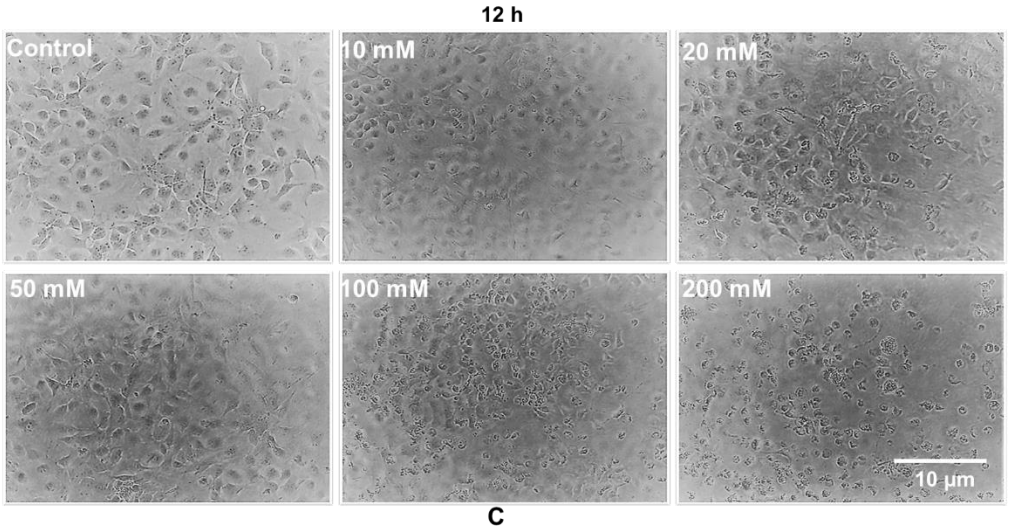
7.2.3 Alcohol-induced morphological alterations to hNPCs

Undifferentiated and differentiated cells treated with ethanol for 3, 6, 12 or 24 h were observed under the phase contrast microscope and images captured to evaluate the morphological changes that arose from ethanol exposure. In line with the MTT and LDH assay results, images verified that the increasing concentration of ethanol influenced cell viability and induced cell death in both phenotypes of ReNcell CX as shown in Figure 7-5, and in a concentration and time dependent manner. Higher concentrations of 100, and 200 mM ethanol showed dramatic cell death, and cell shrinkage in the remaining cells. Also, at 200 mM for 3 h exposures, both undifferentiated and differentiated cells showed a loss of viable cells compared to control treatments. In differentiated cells, the loss of cellular projections was observed with increasing ethanol concentrations.

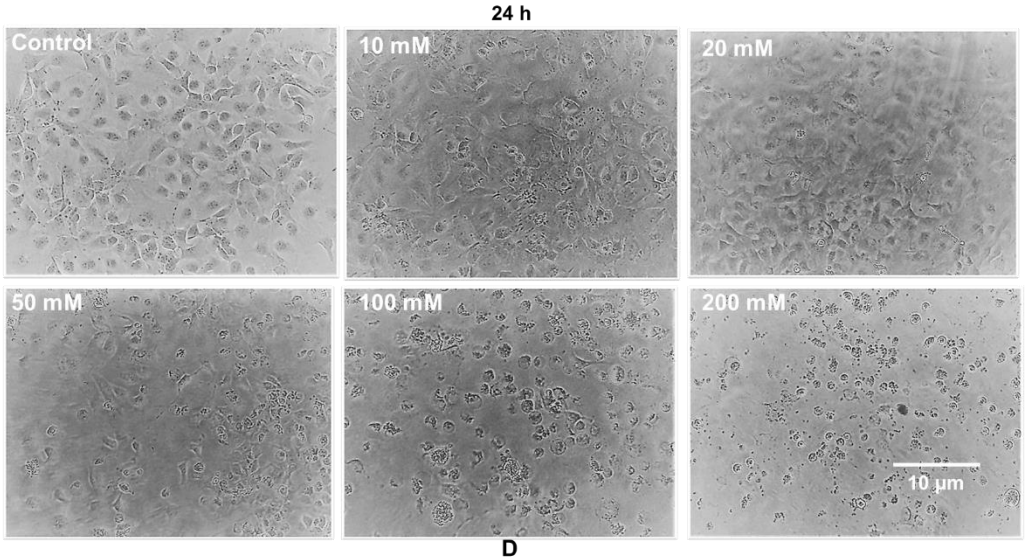



6 h
Control
10 mM
20 mM
50 mM
100 mM
200 mM
10 µm

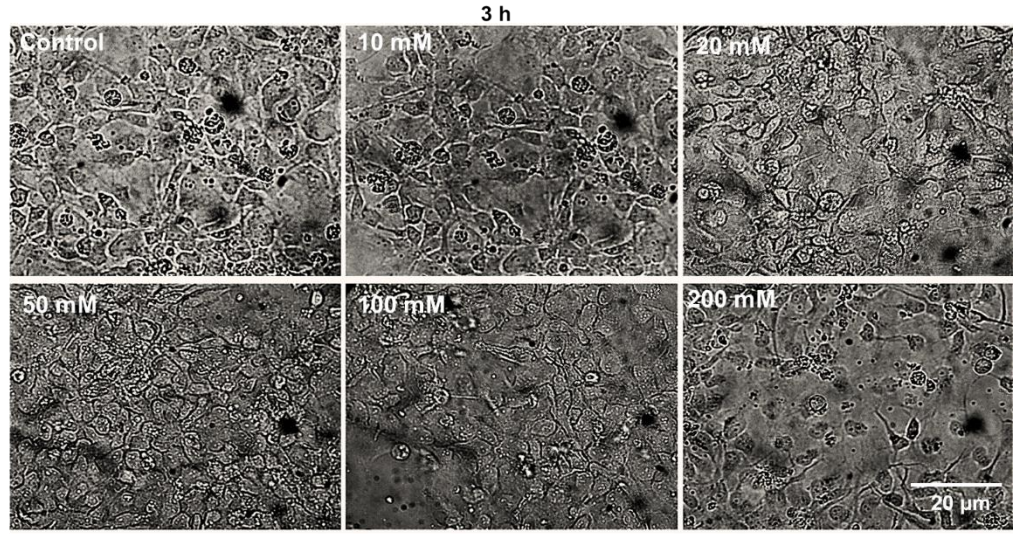
B


12 h
Control
10 mM
20 mM
50 mM
100 mM
200 mM
10 µm

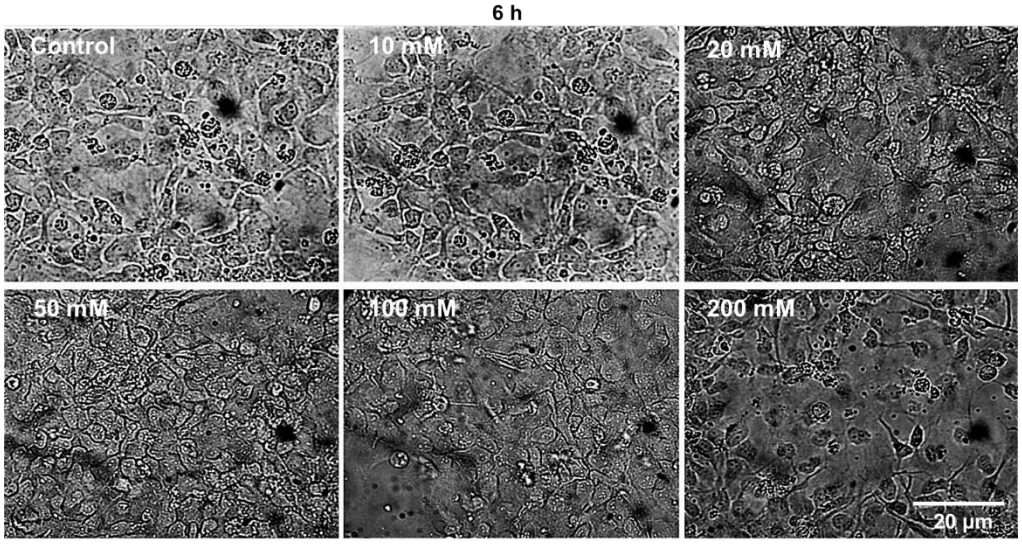
C


24 h
Control
10 mM
20 mM
50 mM
100 mM
200 mM
10 µm

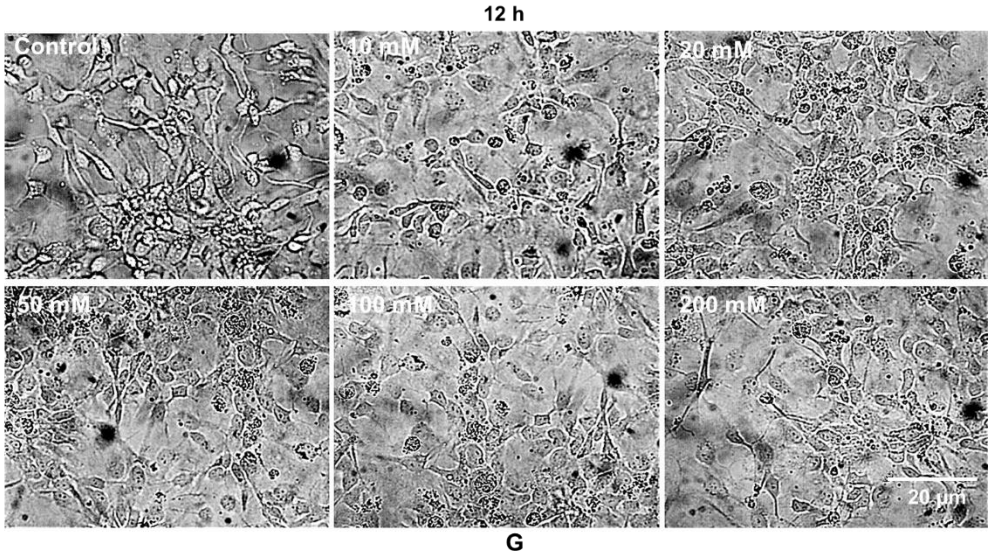
D


3 h
Control
10 mM
20 mM
50 mM
100 mM
200 mM
20 µm

E


6 h
Control
10 mM
20 mM
50 mM
100 mM
200 mM
20 µm

F


12 h
Control
10 mM
20 mM
50 mM
100 mM
200 mM
20 µm

G

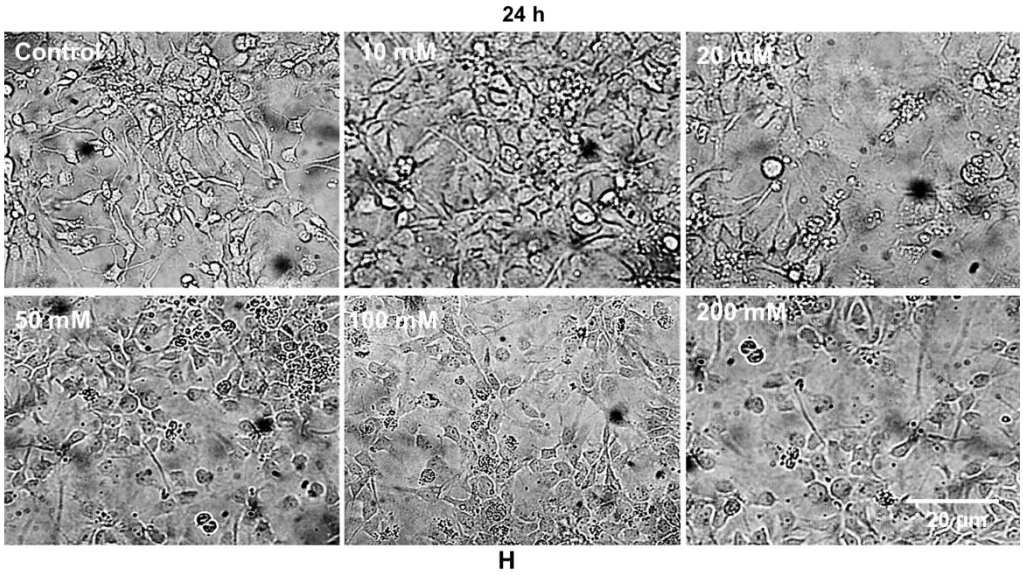


Figure 7-5: Effect of ethanol on undifferentiated and differentiated hNPCs. Undifferentiated cells A- 3 h; B- 6 h; C-12 h and D- 24 h. Differentiated cells E- 3 h; F- 6 h; G- 12 h and H- 24 h. Images were captured using a phase contrast microscope with magnification of 40X.

7.2.4 Alcohol effect on cellular ATP production in hNPCs.

MTT assays confirmed that ethanol showed an impact on cell metabolic activities of both undifferentiated and differentiated cells. Hence, to gain a further insight into the possible impact of ethanol on cellular energy levels, ATP levels were assayed. The cultures of undifferentiated cells and differentiated cells of hNPCs were exposed to ethanol for 3, 6, 12 and 24 h, and ATP levels quantified using an ATP luminescence assay according to the manufacturer's instructions. Interestingly, consistent with cell viability and LDH assays, undifferentiated and differentiated cells reduced ATP levels with an increasing ethanol concentration and duration of exposure (Figure 7.6).

After 3 h of ethanol exposure, the dose-response curves exhibited a linear relationship with cellular ATP levels, mirroring the MTT viability dose response-curves in both phenotypes of hNPCs. At 6, 12 and 24 h exposures, there were typical dose-response relationships for both undifferentiated and differentiated cells similar to the MTT viability curves. Remarkably, 10 mM concentration did

not significantly affect cellular ATP levels at 3 h in undifferentiated cells and differentiated cells compared to controls treatments. Significant ATP level decline at 10 mM was observed at 6, 12 and 24 h post exposures compared to the controls. Differentiated cells reduced cellular ATP levels by 14 - 22% in all time points at 10 mM, while undifferentiated cells showed 11 - 16% compared to control treatments. ATP started to decline at concentrations above 20 mM significantly in all time points compared to controls. Significant decline of ATP levels was observed from 20 - 200 mM for differentiated cells compare to controls, while undifferentiated cells showed significant ATP level decline at 100 and 200 mM at 3 h and 50 - 200 mM at 6 h exposures (Figure 7-6 A and B). At 200 mM exposure, both undifferentiated and differentiated cells showed a dramatic decline in ATP levels, mirroring the MTT cell metabolic activity and viability dose-response curves in all time points.

12 and 24 h exposure to ethanol showed a greater impact in the range of 20-200 mM concentration, with a significant drop in ATP levels in both phenotypes. The rate of ATP decline compared to the control showed a significant difference in differentiated and undifferentiated cells (Table 7-8). At a 50 mM concentration of ethanol there was a significant effect upon cellular ATP levels of differentiated cells at all time points, while 50 mM and 100 mM showed a significant effect on undifferentiated cells at 6, 12 and 24 h exposures (Table 7-3). Differentiated cells showed a significant ATP decline compared to controls in all time points tested (Figure 7-6) upon toxic insult of ethanol. The results suggested that the ATP decline in cells occurs in line with the cell viability loss in both undifferentiated and differentiated hNPCs, and the ATP decline was sometimes significant between undifferentiated and differentiated cells. The reduction rate of ATP levels in undifferentiated cells by ethanol was not significantly different

than those of differentiated cells at 50, 100, and 200 mM concentrations up to 24 h post exposures (Table 7-7).

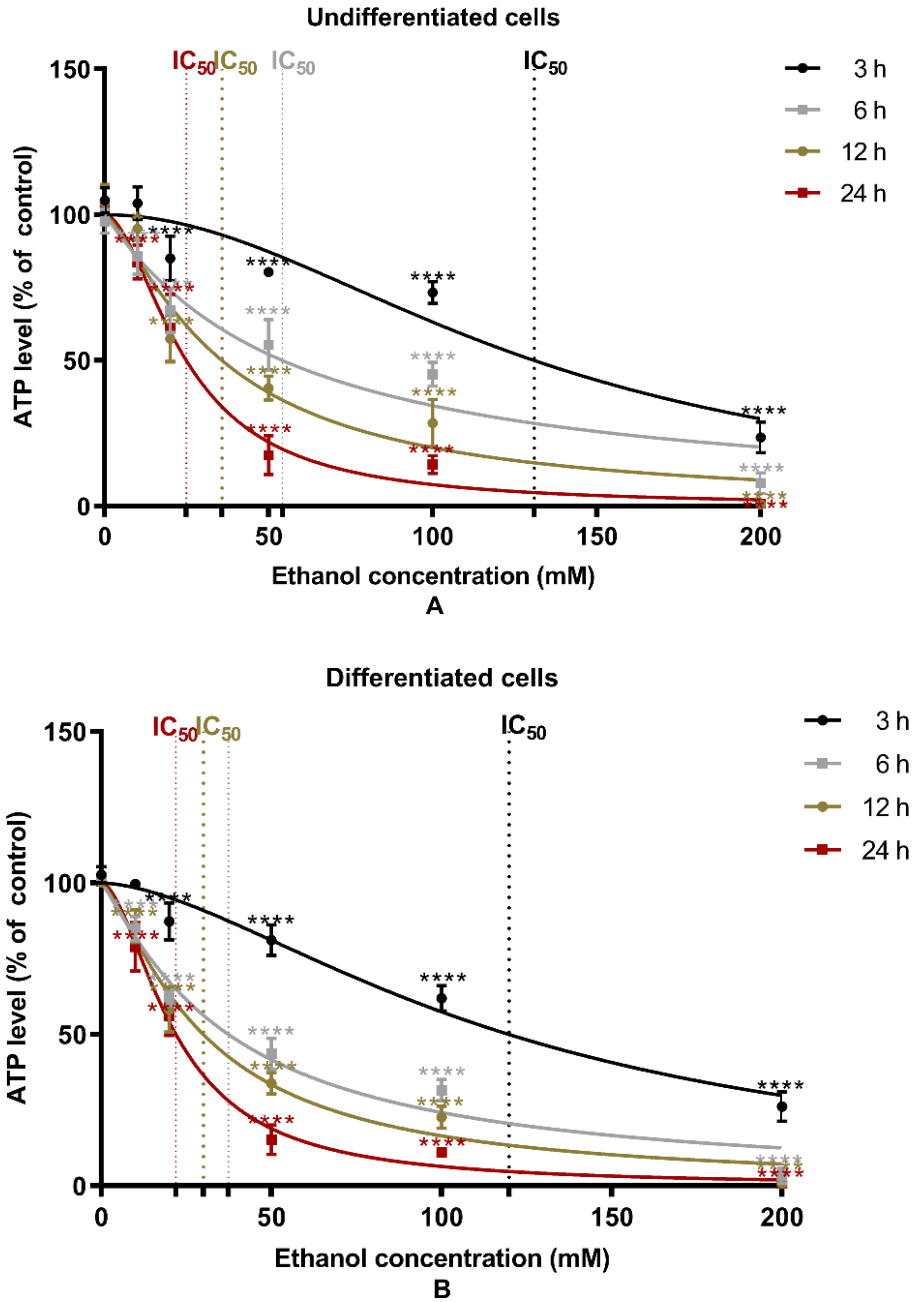
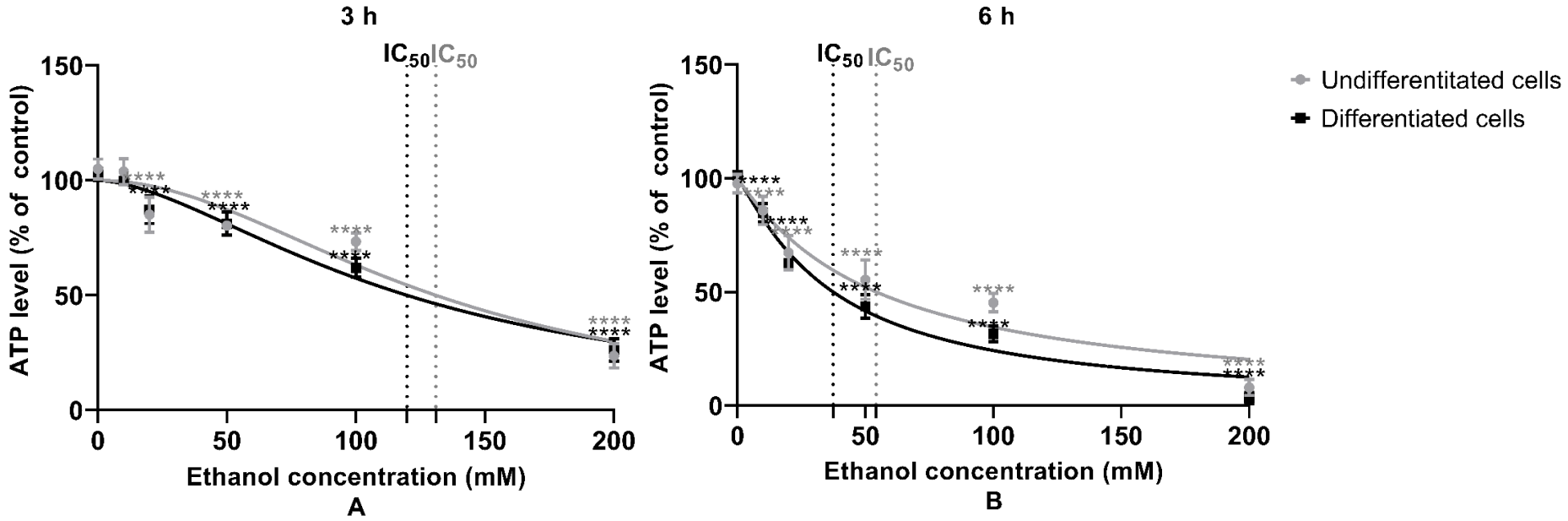


Figure 7-6: Effect of ethanol on cellular ATP levels of undifferentiated and differentiated hNPCs.

A- undifferentiated and B- differentiated cells were challenged with 0 - 200 mM for durations of 3, 6, 12 and 24 h. Cellular ATP levels was assessed using ATP luminescence assay. Readings were normalized to the ATP level of control, providing ATP level as percentage, to the control. Control and treatments were performed as triplicates in 5 independent experiments (n=5). Results were analysed using one-way ANOVA with Dunnett's multiple comparison and expressed as the mean ± standard error of the mean (SEM), when SEM bar is not apparent, this means that error is smaller than the symbol size. For significance; *p<0.05, ***p<0.001, ****p<0.0001.


3 h
6 h
IC50
IC50
ATP level (% of control)
Ethanol concentration (mM)
A
B
Undifferentitated cells
Differentiated cells

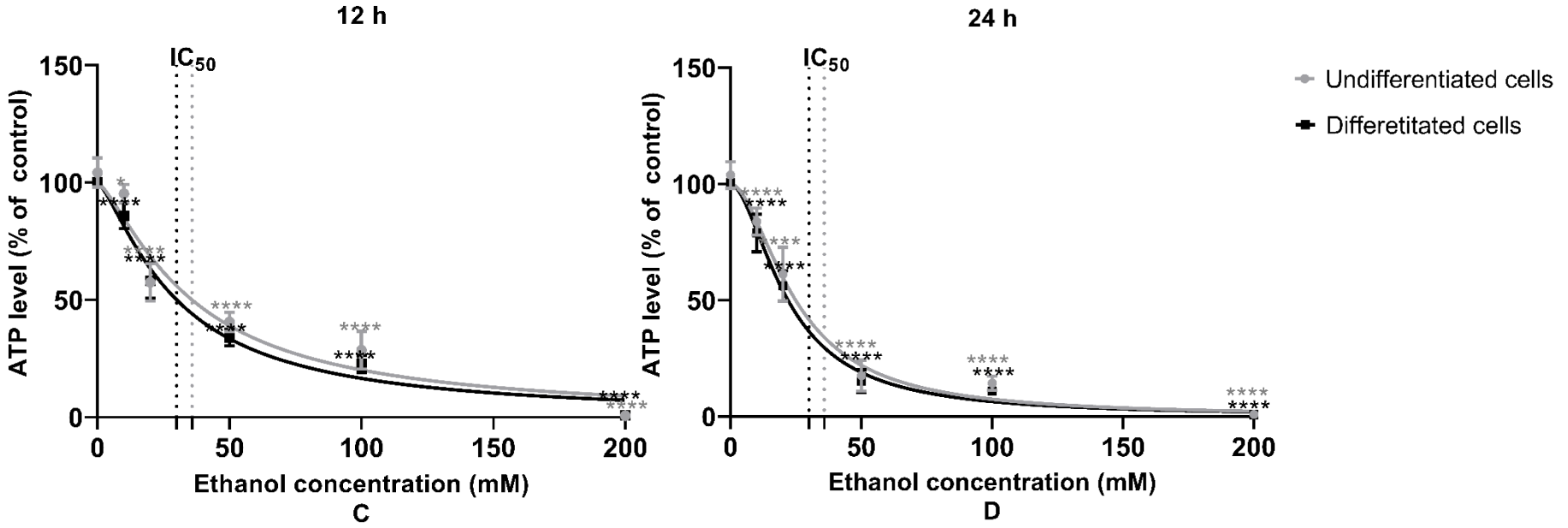


Figure 7-7: Effect of ethanol on cellular ATP levels in hNPCs.
Undifferentiated and differentiated cells were challenged with 0 - 200 mM for durations of 3 h (A), 6 h (B), 12 h (C) and 24 h (D). Cellular ATP levels was assessed using ATP luminescence assay. Readings were normalized to the ATP level of control, providing ATP levels percentages, as a percentage value to the control. Control and treatments were performed as triplicates in 5 independent experiments (n=5). Results were analysed using one-way ANOVA with Dunnett's multiple comparison and expressed as the mean ± standard error of the mean (SEM), when SEM bar is not apparent, this means that error is smaller than the symbol size. For significance; *p<0.05, ***p<0.001, ****p<0.0001.

Table 7-3: Comparison of ethanol toxicity at different time points in undifferentiated and differentiated hNPCs measured by ATP assay.

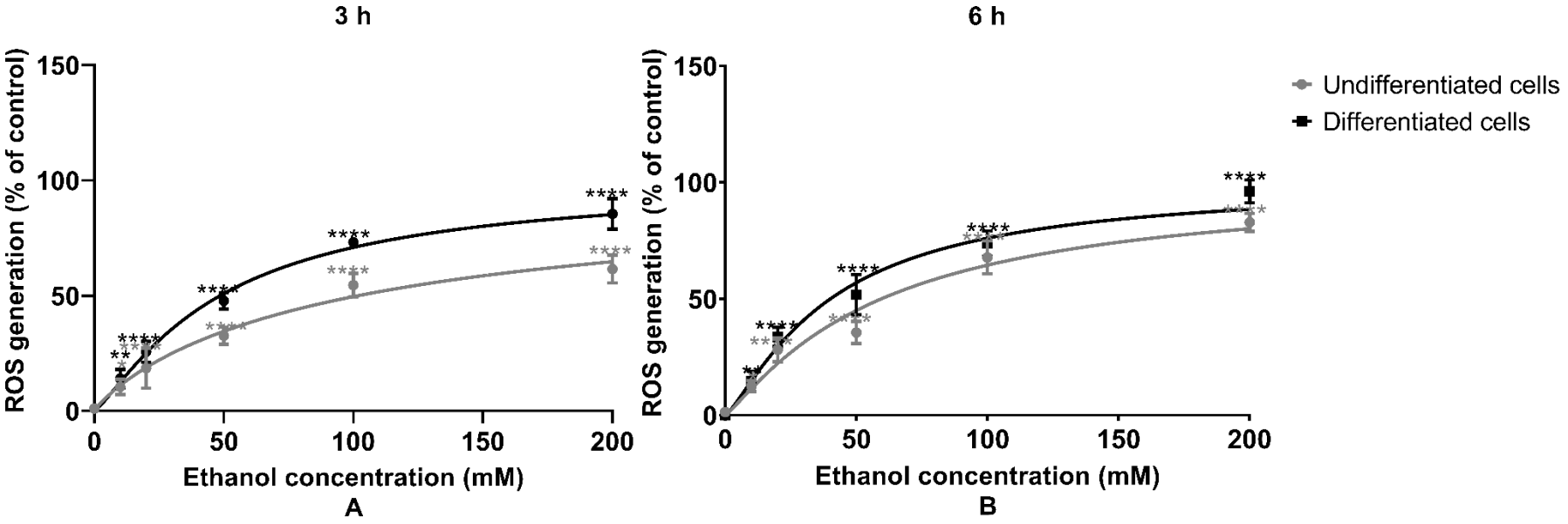
Cell type	Treatments (mM)	3h vs 6 h	3h vs 12 h	3 h vs 24 h	6 h vs 12 h	6 h vs 24 h	12 h vs 24 h
Undifferentiated	10	0.0024	NS	0.0007	NS	NS	NS
	20	0.0028	<0.0001	<0.0001	NS	NS	NS
	50	<0.0001	<0.0001	<0.0001	0.0164	<0.0001	<0.0001
	100	<0.0001	<0.0001	<0.0001	0.0055	<0.0001	0.0225
	200	0.0100	<0.0001	0.0001	NS	NS	NS
Differentiated	10	0.0005	0.0011	<0.0001	NS	NS	NS
	20	<0.0001	<0.0001	<0.0001	NS	NS	NS
	50	<0.0001	<0.0001	<0.0001	0.0352	<0.0001	<0.0001
	100	<0.0001	<0.0001	<0.0001	NS	<0.0001	0.0071
	200	<0.0001	<0.0001	<0.0001	NS	NS	NS

NS- Not significant, $p<0.05$.

7.2.5 Alcohol-induced oxidative stress in hNPCs.

Since ethanol exposure could involve oxidative stress, a DCFDA assay was used to detect the ROS level within undifferentiated and differentiated cells exposed to ethanol in hNPCs. Both phenotypes of hNPCs induced ROS upon ethanol exposure in a concentration-dependent manner. The mean ROS production in both phenotypes were higher at the 3 and 6 h exposures and peaked at 6h. ROS production increased progressively with increasing concentration and diminished significantly by 12 and 24 h exposures (Figure 7-8).

A comparison of undifferentiated and differentiated cells at 3 h showed that at 10 mM, the ROS induced by ethanol in both cells was significantly different compared to the corresponding controls, but 20 - 200 mM showed significant differences between ROS generation in undifferentiated and differentiated cells, suggesting differentiated cells were more susceptible to ROS damage than undifferentiated cells. At 100 and 200 mM concentrations, ethanol induced ROS in undifferentiated and differentiated cells, and for 12 and 24 h exposures, there was a significant difference such that there was higher ROS production in differentiated cells than in undifferentiated cells at these longer exposures (Table 7-4, Figure 7-9). However, 10 and 20 mM ethanol induced significantly more ROS in undifferentiated cells than in differentiated cells at 12 and 24 h compared to 3 and 6 h exposure durations (Table 7-7). The results of the DCFDA suggested alcohol induced oxidative stress in both undifferentiated and differentiated cells in a concentration and time-dependent fashion, while 12 and 24 hours showed severe oxidative stress responses by both phenotypes. At lower concentrations up to 10 mM, ethanol induced a significant level of ROS in both phenotypes of hNPCs cells at 12 and 24 h exposures (Table 7-4).


3 h
6 h
ROS generation (% of control)
150
100
50
0
0
50
100
150
200
Ethanol concentration (mM)
A
B
Undifferentiated cells
Differentiated cells

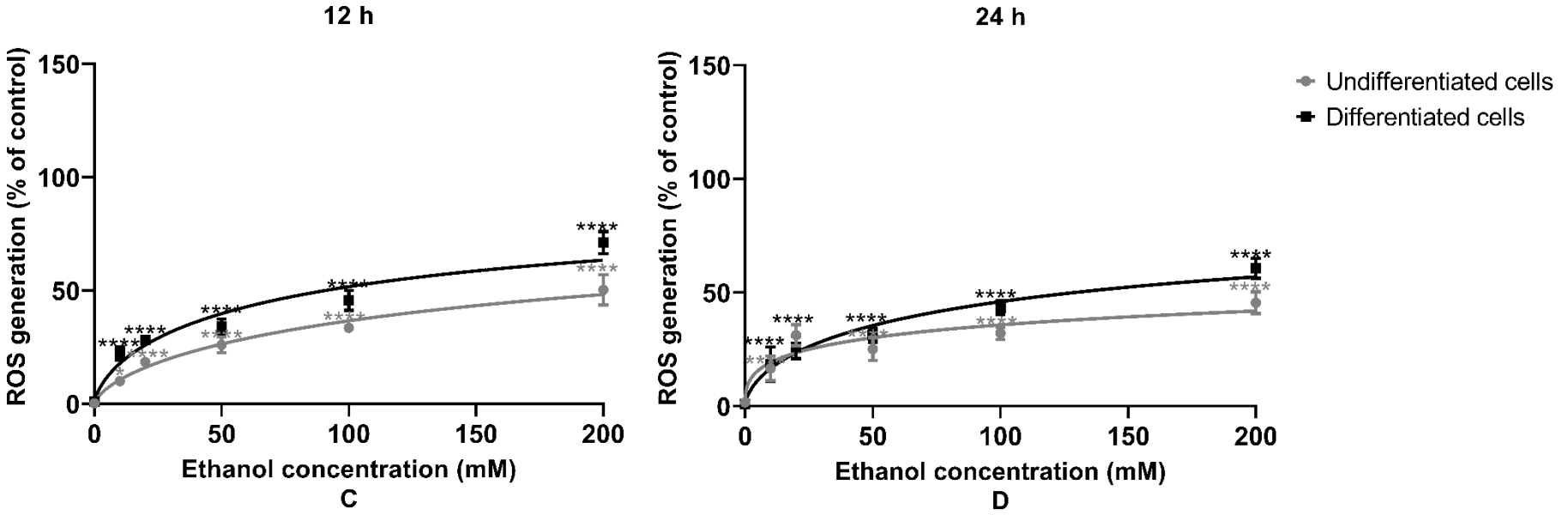


Figure 7-8: Effect of ethanol on ROS generation in hNPCs.
Undifferentiated and differentiated cells were challenged with 0 - 200 mM for durations of 3 h (A), 6 h (B), 12 h (C) and 24 h (D). Cellular ROS generation was assessed using DCFDA assay. Readings were normalized to the viability of control by keeping 0.5 mM H_2O_2 as 100 %, providing ROS generation percentage, as a percentage value to the control. Control and treatments were performed as triplicates in 5 independent experiments (n=5). Results were analysed using one-way ANOVA with Dunnett's multiple comparison and expressed as the mean ± standard error of the mean (SEM), when SEM bar is not apparent, this means that error is smaller than the symbol size. For significance; *p<0.05, **p<0.01, ****p<0.0001.

Table 7-4: Comparison of ethanol induced ROS generation at different time points in undifferentiated and differentiated hNPCs cells measured by DCFDA assay.

Cell type	Treatments (mM)	3h vs 6 h	3h vs 12 h	3 h vs 24 h	6 h vs 12 h	6 h vs 24 h	12 h vs 24 h
Undifferentiated	10	NS	NS	NS	NS	NS	NS
	20	0.0463	NS	0.0044	0.0450	NS	0.0042
	50	NS	NS	NS	0.0478	0.0259	NS
	100	0.0030	<0.0001	<0.0001	<0.0001	<0.0001	NS
	200	<0.0001	0.0139	0.0002	<0.0001	<0.0001	NS
Differentiated	10	NS	NS	NS	NS	NS	NS
	20	NS	NS	NS	NS	NS	NS
	50	NS	0.0020	0.0001	<0.0001	<0.0001	NS
	100	NS	<0.0001	<0.0001	<0.0001	<0.0001	NS
	200	0.0198	0.0009	<0.0001	<0.0001	<0.0001	0.0221

NS- Not significant; $p<0.05$.

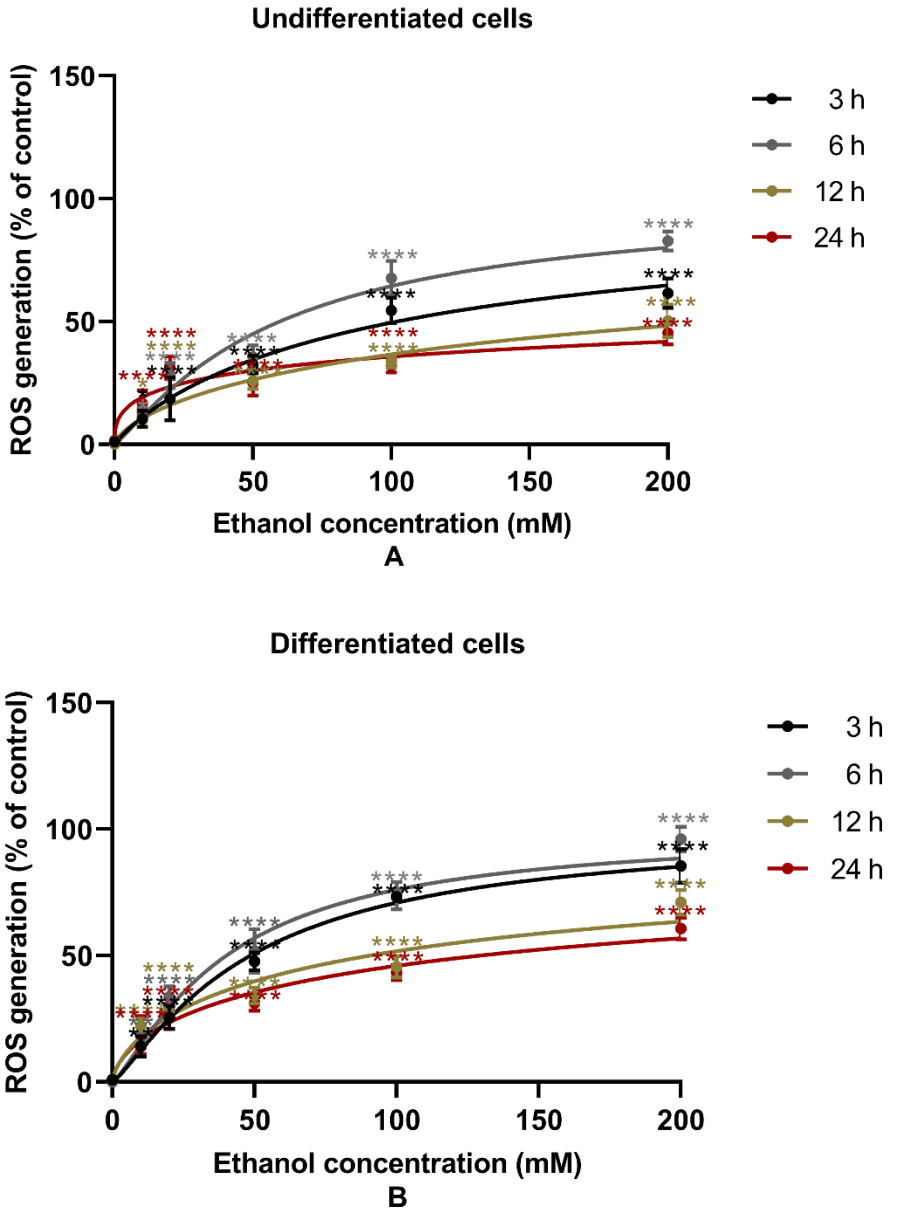


Figure 7-9: Effect of ethanol on ROS generation in undifferentiated and differentiated hNPCs.

A- undifferentiated and B- differentiated cells were challenged with 0 - 200 mM for durations of 3, 6, 12 and 24 h. Cellular ROS generation was assessed using DCFDA assay. Readings were normalized to the viability of control keeping 0.5 mM H_2O_2 as 100 %, providing ROS generation percentage, as a percentage value to the control. Control and treatments were performed as triplicates in 5 independent experiments (n=5). Results were analysed using one-way ANOVA with Dunnett's multiple comparison and expressed as the mean ± standard error of the mean (SEM), when SEM bar is not apparent, this means that error is smaller than the symbol size. For significance; *p<0.05, **p<0.01, ***p<0.001, ****p<0.0001.

7.2.6 Alcohol induced oxidative stress damage to proteins and associated elevation of ROS.

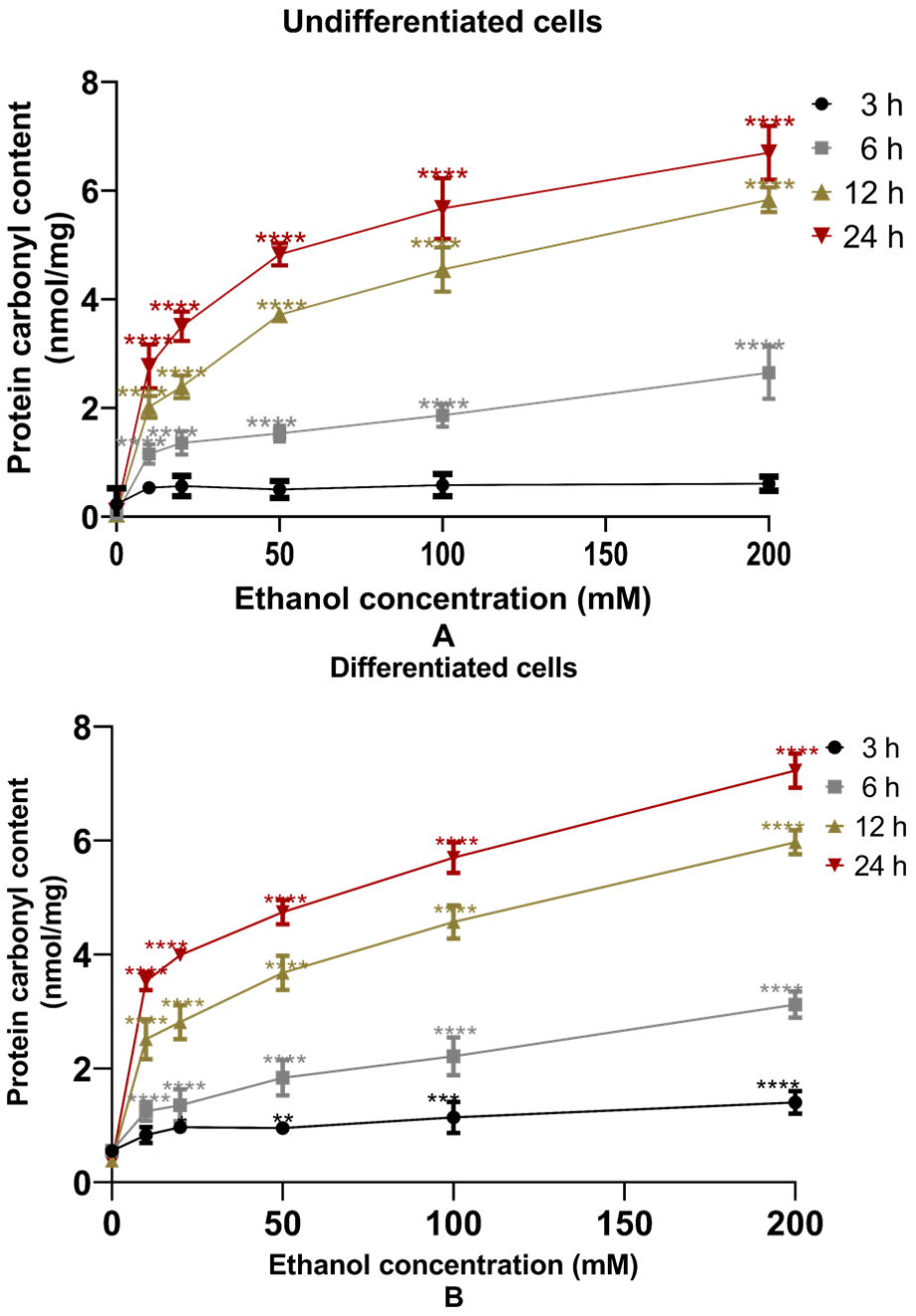


Figure 7-10: Cytosolic protein carbonylation of undifferentiated and differentiated hNPCs exposed to ethanol.
A- undifferentiated or B- differentiated (B) ReNcell CX cells were exposed to alcohol (10 - 200 mM) for duration of 3, 6, 12, or 24 h, and the protein carbonyl content quantified in crude cytosolic fractions by spectrophotometric protein carbonyl determination assay. Each data point represents the mean of at least 5 individual experiments. Results were analysed using one-way ANOVA with Dunnett's multiple comparison and expressed as the mean ± standard error of the mean (SEM), when SEM bar is not apparent, this means that error is smaller than the symbol size. For significance: ***p<0.001, ****p<0.0001.

The DCFDA assay showed that there was a concentration-dependent involvement of ethanol in induced oxidative stress to hNPCs. Then, to gain insight into cytosolic protein oxidation due to oxidative stress, protein carbonyl content (PCC) was estimated by spectrophotometric PCC assay. Both undifferentiated and differentiated cells exposed to ethanol showed a concentration and time dependent increase in PCC. However, 3 h exposure did not induce significant PCC in undifferentiated cells, while differentiated cell showed significant PCC at 50 - 200 mM compared to control treatments (Figure 7-10). A 6 h exposure showed significant PCC in both undifferentiated and differentiated cells compared to controls at concentrations of 10 - 200 mM. There was a progressive increase of PCC in both phenotypes that was observed at 12 and 24 h. Interestingly, even 10 mM ethanol induced PCC in both phenotypes at 6, 12 and 24 h exposures. A comparison of each of the time points for protein carbonyls in cells showed significant differences at 20 - 200 mM range in both phenotypes (Table 7-5), and undifferentiated vs differentiated cells showed significant protein oxidation responses across the concentration range of 10 - 200 mM (Table 7-7). Differentiated cells showed significantly more PCC levels compared to undifferentiated cells. A correlation analysis of levels of protein carbonyl content and ROS generation showed a positive correlation between ROS and PCC in each concentration tested; suggesting that the increase of protein carbonylation corresponded to the ROS generation increases in undifferentiated and differentiated cells (Table 7-6), and this was negatively correlated with ATP levels in cells (Table 7-6). However, there was not a significant correlation observed at 3 h exposure between PCC and ROS level and PCC and ATP levels.

Since 12 h and 24 h induced significant PCC in both undifferentiated and differentiated cells, crude cytosolic fractions from undifferentiated and

differentiated cells after treatment with ethanol were oxyblotted to visualize the carbonylated proteins. The major proteins modified were characterized by their denatured approximate molecular weights and compared with those present in a human brain extract from an alcoholic patient (Figure 7-10). Overlap of protein targets was evident at denatured molecular weights of 120, 110, 90 kDa. Interestingly, both 12 and 24 h exposures induced oxidative damage to the same protein targets, but with different severity levels. Figure 7-11 indicates that 10 mM ethanol induced a significant level of protein carbonylation compared to the corresponding control treatments in both phenotypes at 12 and 24 h. In turn this result further proved that protein carbonyls were induced by oxidative stress are not eliminated until 24 h from both undifferentiated and differentiated cells upon alcohol exposure even at 10 mM concentration.

Table 7-5: Comparison of ethanol toxicity in different time points in undifferentiated and differentiated hNPCs for protein carbonyl content

Cell type	Treatments (mM)	3h vs 6 h	3h vs 12 h	3 h vs 24 h	6 h vs 12 h	6 h vs 24 h	12 h vs 24 h
Undifferentiated	10	0.0192	<0.0001	<0.0001	0.0006	<0.0001	0.0033
	20	0.0017	<0.0001	<0.0001	<0.0001	<0.0001	<0.0001
	50	<0.0001	<0.0001	<0.0001	<0.0001	<0.0001	<0.0001
	100	<0.0001	<0.0001	<0.0001	<0.0001	<0.0001	<0.0001
	200	<0.0001	<0.0001	<0.0001	<0.0001	<0.0001	0.0006
Differentiated	10	NS	<0.0001	<0.0001	<0.0001	<0.0001	<0.0001
	20	<0.0001	<0.0001	<0.0001	<0.0001	<0.0001	<0.0001
	50	<0.0001	<0.0001	0.0001	<0.0001	<0.0001	<0.0001
	100	<0.0001	<0.0001	<0.0001	<0.0001	<0.0001	<0.0001
	200	<0.0001	<0.0001	<0.0001	<0.0001	<0.0001	<0.0001

NS- Not significant; $p<0.05$.

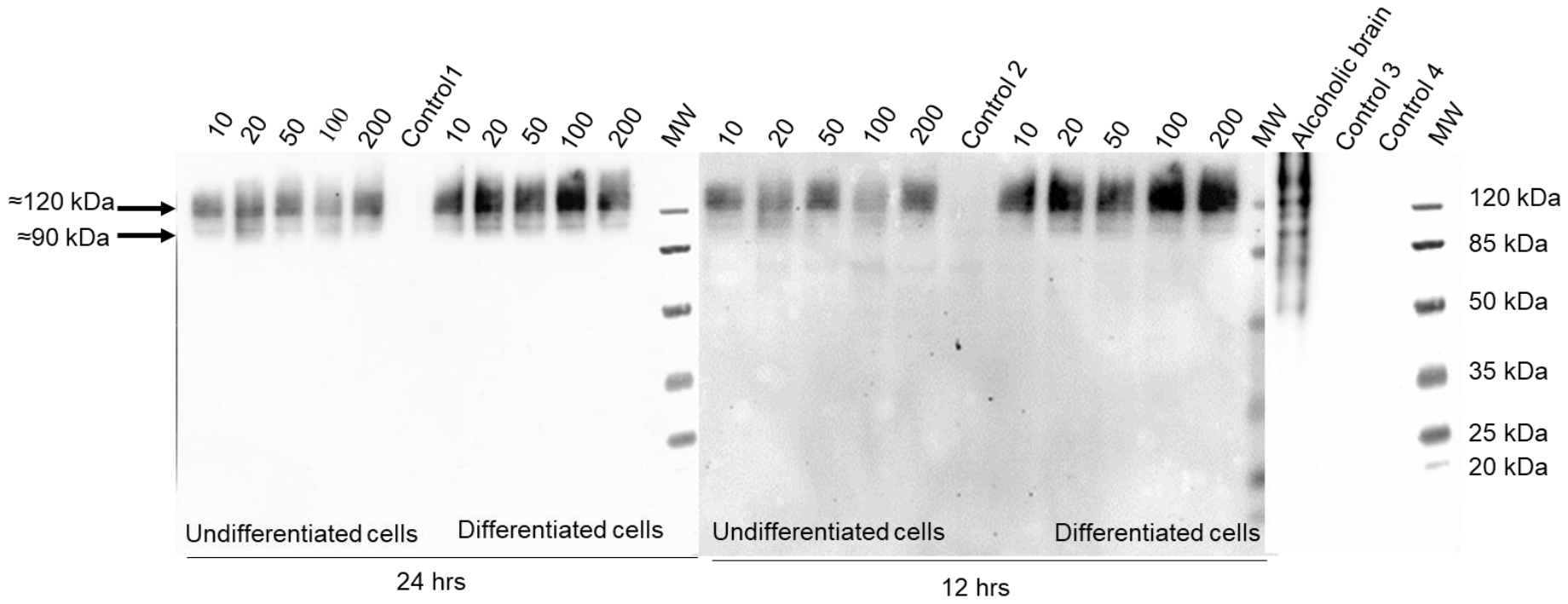


Figure 7-11: Cytosolic protein carbonylation of alcohol treated undifferentiated and differentiated hNPCs.
Undifferentiated and differentiated cells were exposed to 10, 20 ,50,100 and 200 mM concentrations ethanol for 12 and 24 h. Crude cytosolic fractions of treated cells alcoholic brains were DNPH derivatized, resolved by gel electrophoresis and immunoblotted with anti-DNPH antibody to identify the specific protein targets of protein carbonylation of ethanol exposure. Each experiment was conducted as 3 independent experiments with three replicates.
Control 1- untreated (0 mM) undifferentiated cells for 12 h, Control 2- untreated (0 mM) undifferentiated cells for 24 h, Control 3- untreated (0 mM) differentiated cells for 12 h, Control 4- untreated (0 mM) differentiated cells for 24 h.

Table 7-6: Correlation between the ROS generation and protein carbonyl content / ROS generation or ATP production in hNPCs.

Cell Type	Treatment duration (hours)	ROS vs PCC			ROS vs ATP		
		r	**R^2**	***P* value**	***r***	**R^2**	***P* value**
Undifferentiated	3	0.7035	0.4950	0.1188*	-0.5939	0.3527	0.2139*
Differentiated		0.9395	0.8826	0.0054	-0.9389	0.8815	0.0055
Undifferentiated	6	0.9285	0.8622	0.0075	-0.9512	0.9048	0.0035
Differentiated		0.9785	0.9575	0.0007	-0.9815	0.9634	0.0005
Undifferentiated	12	0.9837	0.9676	0.0004	-0.9618	0.9250	0.0022
Differentiated		0.9853	0.9707	0.0003	-0.9532	0.9087	0.0032
Undifferentiated	24	0.9390	0.8817	0.0055	-0.9592	0.9201	0.0025
Differentiated		0.9791	0.9586	0.0007	-0.9264	0.8582	0.0079

r- Pearson's correlation coefficient; *- Not significant; $p<0.05$

Table 7-7: Comparison of the cytotoxicity of alcohol to undifferentiated vs differentiated hNPCs.

		Undifferentiated vs differentiated hNPCs				
Alcohol treatment (mM)	Exposure time point (hrs)	MTT assay	ATP assay	LDH assay	ROS assay	PCC assay
10	3	0.0006	NS	NS	NS	NS
	6	NS	NS	NS	NS	NS
	12	NS	0.0058	<0.0001	0.0006	0.0010
	24	NS	0.0214	0.0035	NS	NS
20	3	NS	NS	0.0055	NS	0.0169
	6	0.0015	NS	<0.0001	NS	NS
	12	NS	NS	<0.0001	0.0068	0.0034
	24	NS	0.0180	<0.0001	0.0016	NS
50	3	NS	NS	0.0003	<0.0001	0.0063
	6	0.0007	<0.0001	0.0033	<0.0001	NS
	12	NS	NS	NS	0.0264	NS
	24	NS	NS	<0.0001	NS	0.0002
100	3	0.0036	0.0009	NS	<0.0001	0.0007
	6	<0.0001	<0.0001	<0.0001	NS	NS
	12	NS	NS	<0.0001	0.0007	NS
	24	NS	NS	0.0008	0.0003	0.0010
200	3	NS	NS	<0.0001	<0.0001	<0.0001
	6	0.0120	NS	0.0141	0.0004	0.0345
	12	NS	NS	NS	<0.0001	NS
	24	NS	NS	NS	<0.0001	0.0208

NS- Not significant, $p<0.05$, MTT- (4,5-dimethylthiazol-2-yl)-2,5-diphenyltetrazolium bromide, LDH- Lactose dehydrogenase, ATP- Adenosine triphosphate.

Table 7-8: Toxicity of alcohol to undifferentiated or differentiated hNPCs.

Cell Type	Treatment duration (hours)	MTT assay		ATP assay		LDH assay	
		IC_{50} (µM)	R^2	IC_{50} (µM)	R^2	IC_{50} (µM)	R^2
Undifferentiated	3	139.2 ± 9.900	0.9193	131.0 ± 10.540	0.9000	140.7 ± 3.748	0.9890
Differentiated		124.8 ± 5.822	0.9657	119.8 ± 5.825	0.9682	123.4 ± 5.269	0.9713
Undifferentiated	6	60.92 ± 6.260	0.9256	54.24 ± 5.584	0.9304	63.06 ± 4.516	0.9605
Differentiated		41.52 ± 2.983	0.9681	37.58 ± 2.647	0.9712	41.04 ± 3.439	0.9560
Undifferentiated	12	37.97 ± 3.417	0.9536	35.67 ± 3.634	0.9431	39.06 ± 1.896	0.9833
Differentiated		32.94 ± 2.247	0.9706	30.00 ± 1.731	0.9804	35.85 ± 2.243	0.9753
Undifferentiated	24	26.01 ± 1.492	0.9787	24.88 ± 0.976	0.9895	27.47 ± 2.308	0.9599
Differentiated		22.38 ± 0.665	0.9939	21.96 ± 0.664	0.9937	22.30 ± 1.963	0.9525

IC_{50}- 50% inhibition concentration; MTT- (4,5-dimethylthiazol-2-yl)-2,5-diphenyltetrazolium bromide, LDH- Lactate dehydrogenase, ATP- Adenosine triphosphate.

7.3 Discussion

Ethanol is considered as one of the most widely used recreational drugs worldwide and causes 4% of the global burden of disease. The ethanol content in alcoholic beverages usually varies between 3% and 50% alcohol by volume, and in some cases can be higher (Rajendram et al., 2016). Consumption of ethanol beverages increase the blood alcohol concentration depending on the quality, quantity, and pattern of consumption. Prenatal alcohol exposure is linked with FASD development and the consequences of this may vary with the pattern of alcohol consumption, exposure duration, and age of the foetus (Brocardo et al., 2011, Zhang et al., 2018). Many acute effects of ethanol exposure correlate with the peak blood ethanol concentrations. It has been showed that the foetal blood alcohol concentrations (BACs) reach levels nearly comparable to maternal levels 2 h after maternal consumption of alcohol (Burd et al., 2012). Hence this study evaluated the toxic effects of alcohol in human progenitor cortical neuronal cells to model an episode of drinking using low/moderate and high BACs.

The vulnerability of hNPCs was first accessed by cell viability assays to evaluate the effect of direct alcohol exposure on their metabolic activities and cell death and determine the safe levels. MTT, LDH and ATP assays showed that until 3 h, all concentrations except 200 mM induced moderate toxicity on both undifferentiated and differentiated cells. However, extending the exposure time induced robust cytotoxicity. Interestingly, up to 10 mM concentration cells showed tolerance in both phenotypes indicating minimal toxic insult until 10 mM for 3 h exposure. Although the 6 h exposure period showed vulnerability of cells to all concentrations in both undifferentiated and differentiated cells, inconsistent with the previous study on neurotoxicity evaluation of alcohol exposure to human neuroblastoma cells (Chapter VI). In contrast to the previous

study, the current study showed that differentiated cells were more susceptible to the toxic insult of alcohol than the undifferentiated cells. This suggested alcohol toxicity was stage and cell specific. In line with the current findings, Donadoni et al. (2019) showed that primary human foetal derived neuronal cultures of immature and mature neurones were highly sensitive to ethanol at 25 mM after 6 h, and that the effects were more dramatic at 24 h exposure. The study also confirmed that the stage of differentiation was affected by ethanol exposure by exposing 1 week and 4 week differentiated cells. Consistent with the current study, measurements of cell viability and cell death assays by Donadoni et al. (2019) confirmed that immature and mature hNPCs showed significant toxicity responses at 50 mM and 75 mM for 6 and 24 h post exposures. Opposed to the current study, Donadoni et al. (2019) showed that mature neurones were more resistant to toxic insult of ethanol than immature neurones. This can be due to differences in experimental condition and the cell models used for the evaluation. However, these observations are in line with studies in which the toxic effects of ethanol were evalutated on neural stem cells and progenitors during adult neurogenesis using *in vitro* cell culture and *in vivo* animal exposures (Vangipuram and Lyman, 2010, Campbell et al., 2014). However, 72 mM of ethanol in blood showed decreased neurogenesis in rats as well as 80 mM blood alcohol concentration reported FASD in new-borns (Kvigne et al., 2012). 100 mM ethanol has severe effects on human neurogenesis (Louis et al., 2018). These findings were further justified by the current study that more than 50 mM acute ethanol exposure significantly affected cell metabolic activity and cell viability loss in hNPCs (Kashem et al., 2018).

In the hNPCs cell culture model, alcohol toxicity assessment by ATP assay showed a robust toxicity in hNPCs by diminishing cellular ATP levels. In turn,

this suggested malfunctioning of cellular mitochondria. The effect was significant at the highest ethanol concentrations and increasing exposure durations. Ethanol effects on human neuronal cells showed concentration-dependent decreases in ATP levels as observed in the current study (Liu et al., 2014). Similar observations were demonstrated in the previous study with human neuroblastoma cells (Chapter VI), whereas, undifferentiated cells showed a more significant drop in ATP levels than differentiated cells. Herein, differentiated cells showed significant ATP reduction compared to undifferentiated cells upon ethanol exposure in all tested time points. Moreover, this suggests that hNPCs differentiated cells were more susceptible to ethanol toxicity showing cell and stage specific effects. Ethanol can induce mitochondrial dysfunction via altering mitochondrial biogenesis and functions, and also mitochondrial transcriptional factor changes that influence the energy metabolism process have been reported (Liu et al., 2014), leading to ATP depletion in neuronal cells.

Mitochondrial dysfunction exhibited by ATP depletion in hNPCs upon ethanol exposure was further explained by an association with redox imbalance induced by ethanol (Liu et al., 2014). Mitochondria are a major source of ROS generation in neuronal cells (Haorah et al., 2008, Wang et al., 2015b). hNPCs exposed to various concentrations of ethanol showed generation of ROS in a concentration-dependent manner with highest levels observed after 6 h exposure in the study. This can be due to different uptake mechanisms of cells and time taken to affect the oxidation status of the cells by depleting the cellular antioxidant system (Kohen and Nyska, 2002). Moreover, 12 and 24 h showed that ROS generation levels were diminished compared to 3 and 6 h while generation was concordant with a concentration-dependent manner observed at 3 and 6 h exposures. This can be supported by the LDH assay results in which increasing time duration of

ethanol exposure of both undifferentiated and differentiated cells resulted in significant cell death. Therefore, ROS generation of existing cells could be lower than that of 3 and 6 h exposure where there is significantly lower cell death observed than that observed at 12 and 24 h exposures. Furthermore, ROS have a short half-life and can undergo various types of oxidation and adduction reactions with cellular macromolecules such as lipids in cells. To support this notion, ethanol-induced lipid peroxidation was demonstrated after a 24 h exposure in human neuroblastoma cells by Saito et al. (2005). ROS generation in ethanol exposed cells has also been observed in human derived cell models *in vitro* (Haorah et al., 2008). However, a comparison of levels of ROS generation upon ethanol exposure with existing studies was impossible due to unevenness of experimental conditions. Therefore, ethanol induced cytotoxic responses of undifferentiated and differentiated cells of hNPCs occurs via oxidative stress, induced mitochondrial dysfunction and ATP depletion, according to the current study. Moreover, results suggest that the exposure of hNPCs to moderate to high BAC alcohol levels (20-200mM) for 24 h was sufficient to trigger obvious progenitor cell death due to oxidative stress.

The time course production of oxidatively-damaged proteins in both phenotypes of hNPCs was measured by PCC determination assay, and this showed that there was a considerable increase of PCC levels after 12 and 24 h exposures in both cells, but a moderate increase at 6 h exposures. The correlation analysis showed a direct positive correlation of ROS generation and PCC levels in cells. This suggests that cellular oxidative stress triggers protein carbonylation in both undifferentiated and differentiated cells. However, comparison with the previous study with human neuroblastoma SH-SY5Y cells, hNPCs showed significant levels of protein carbonyls at 6 h exposure, but progressive levels at 12 and 24 h exposures, with a peak at 24 h. However, this result suggests that protein

carbonylation after exposure to ethanol in hNPCs is gradual after the ROS production. After 12 and 24 h exposures, there was significant protein carbonylation of proteins, with increased levels at the same protein profile at 24 h, suggesting increased accumulation after 24 hours. Protein carbonyls are removed or repaired by proteolytic degradation in cells (Divald and Powell, 2006). In cells most of the oxidised proteins are degraded by the 20S proteasome (Divald and Powell, 2006). However, excessive carbonylated proteins can be resistant to degradation and accumulate in cells. Active sites of the proteins can be oxidised and, proteins undergo further structural and functional changes (Ding and Keller, 2001). Cytoskeleton protein carbonylation may cause changes in cytoskeleton integrity of neuronal cells and interfere with signal transmission (Flaskos 2014). For instance, ethanol-induced oxidation of tubulin disrupts the microtubule cytoskeleton and injures the functional and structural integrity of the intestinal mucosa (Banan et al., 1999, Banan et al., 2000). The accumulation of certain higher molecular weight proteins proved to be toxic to the cell and subsequent cell viability loss has been observed (Dasgupta et al., 2012). Thus, in the current study, a higher ethanol concentration induced significant protein carbonyls and these accumulated in cells. Hence protein carbonylation will likely have induced structural and functional changes in cells. The cellular responses arose from the ethanol exposure even at the lower concentrations, without changes in metabolic activity and viability loss, so functional changes of proteins by carbonylation are below the threshold of cell death. Therefore, cytotoxic responses arose from the ethanol induced oxidative stress in undifferentiated and differentiated cells of hNPCs cause functional and structural changes in cells, and these may cause functional changes associated with ethanol related pathophysiological damage.

In conclusion this chapter of the study focused on the direct effect of ethanol on undifferentiated and differentiated HNPCs. Herein, the threshold alcohol concentration that was able to cause cell damage and cell death in hNPCs is 10 mM and 3 h duration of exposure. Interestingly, it has been shown that foetal BAC can be found within 1 minute after the rise in maternal BAC during alcohol consumption (Burd et al., 2012). Epidemiological study has suggested that ~9 - 11 mM BAC was present in the foetus at the delivery, when the maternal BAC was ~17 mM before delivery (Kvigne et al., 2012). The results of this study suggest that 10 mM is the threshold level that can still induce neuronal cell damage, which is a BACs of 0.04-0.05% (≈9 - 11 mM). The aforemetioned study further showed that 80 mM BAC in the mother caused FAS related characteristics in newborns (Kvigne et al., 2012). The current study showed that 50 - 200 mM induced severe cytotoxic responses in hNPCs. Interestingly, it appears that even 10 mM alcohol exposure causes oxidative stress and protein carbonylation in hNPCs, levels that could arise from a single drink. The cytoskeleton is a potential target of oxidative stress damages induced by alcohol exposure. Thefore, the study suggests that cellular pathology can arise from prenatal alcohol exposure, and from functional changes to the remaining cells even after mild alcohol exposures.

8 EFFECT OF PESTICIDES AND ETHANOL CO-EXPOSURES ON HUMAN NEUROBLASTOMA SH-SY5Y CELLS

8.1 Introduction

Many environmental pollutants have been shown to significantly alter the functioning of the CNS. Chlorpyrifos, Azamethiphos, Aldicarb are three commonly used pesticides, and Chapters IV and V proved that these three pesticides can disrupt neuronal functions via oxidative stress. Additive/synergistic toxicity of pesticide mixtures is also evident from *in vivo* and *in vitro* studies (Moretto and Colosio, 2011, Singh et al., 2017, Fu et al., 2019). The metabolism of pesticides in the human body can be modified by social habits. Workers occupationally exposed to agrochemicals may take alcoholic beverages occasionally or habitually. However, the underlying mechanism of altering the general neuronal cell functioning due to ethanol exposure is also similar to the organophosphate and carbamate pesticides tested in this study (Chapter VI and VII), but the cytotoxic responses are different according to the study of ethanol exposure to human neuroblastoma cells (Chapter VI). In turn, both tested pesticides and ethanol have been shown to alter the oxidative status of human neuroblastoma SH-SY5Y cells, and ROS generation recognized as the route of inducing cytotoxicity.

Co-exposure of ethanol with insecticides or herbicide has been studied on rat models and demonstrated synergistic or antagonistic effects on cellular functions (Abarikwu et al., 2017, Owumi and Najophe, 2019). However, direct interactive effects of ethanol and organophosphate or carbamate pesticides on human neuronal cell models have not been studied yet. With the opinion that human exposure to the pesticides and habitual consumption of alcohol could adversely affect the CNS, this study was designed to investigate the oxidative

status of the neuronal cells and their cytotoxic responses to simultaneous exposure of low pesticides doses and ethanol.

8.2 Results

8.2.1 Effect of co-exposure of ethanol with low doses of OP and carbamate pesticides on cell metabolic activity and cell viability of SH-SY5Y cells.

Undifferentiated and differentiated SH-SY5Y cells were treated with both ethanol and CPO, AZO, and Aldicarb to evaluate the interactive effects on cells. Cell metabolic activity and cell viability were evaluated by MTT assays. Alcohol was used in the concentration range of 10, 20, 50, 100, and 200 mM and pesticide concentrations of IC_5, IC_{10}, $IC_{20,}$ and IC_{50} which were interpolated from there corresponding cell viability curves (Chapter IV).

8.2.1.1 *CPO and ethanol*

According to Figure 8-1 A, co-exposure of alcohol and CPO exposure on cell metabolic activity and cell viability of undifferentiated SH-SY5Y cells showed various responses compared to control treatments. Interestingly, IC_5 and IC_{50} of CPO treatment showed a concentration-dependent decrease in cell viability of undifferentiated cells over the range of 10 - 200 mM alcohol exposure. However, IC_5 pairing with 10 and 20 mM ethanol did not show significant cell metabolic activity and cell viability loss (p>0.05) in undifferentiated SH-SY5Y cells for 24 h exposure (6% and 7%, respectively). Contrastingly, the pairing of IC_{50} of CPO with 10 and 20 mM concentration showed a significant drop (p<0.0001) in cell metabolic activity and cell viability of undifferentiated cells compared to control treatments. The pairing of ethanol showed a non-monotonically decrease in cell viability with IC_{10} and IC_{20} concentration of CPO on undifferentiated cells compared to control treatments (Table 8-1).

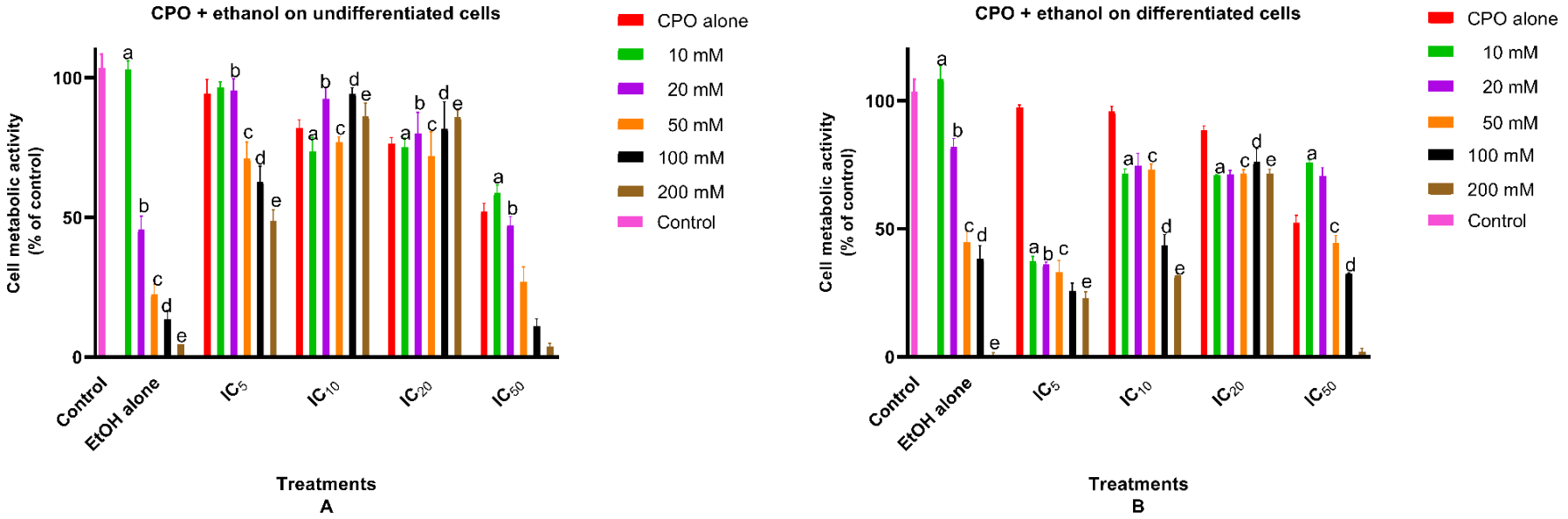


Figure 8-1: Co-exposure to ethanol and CPO SH-SY5Y cells for 24 h.

A- undifferentiated cells and B- differentiated cells were treated with CPO and ethanol for 24 h. Viability was assessed using MTT assay. Readings were normalized to the viability of control, providing cell viability percentage, as a percentage value to the control. Control and treatments were performed as triplicates in 5 individual experiments (n=5). Results were analysed using two-way ANOVA with Tukey's multiple comparison and expressed as the mean ± standard error of the mean (SEM), when SEM bar is not apparent, this means that error is smaller than the symbol size. Comparison of treatments with non-treated control are indicated in Table 8-1. **a** – significant difference with 10 mM ethanol, **b** - significant difference with 20 mM ethanol, **c** - significant difference with 50 mM ethanol, **d** - significant difference with 100 mM ethanol**, e** - significant difference with 200 mM ethanol.

Table 8-1: Comparison of treatment combinations of ethanol and CPO with their corresponding non-treated controls. Results were analysed by two-way ANOVA and means comparison was done by Tukey's multiple comparison tests.

Treatments		Undifferentiated cells	Differentiated cells
IC_5	10	NS	<0.0001
	20	NS	<0.0001
	50	<0.0001	<0.0001
	100	<0.0001	<0.0001
	200	<0.0001	<0.0001
IC_{10}	10	<0.0001	<0.0001
	20	NS	<0.0001
	50	<0.0001	<0.0001
	100	NS	<0.0001
	200	0.0008	<0.0001
IC_{20}	10	<0.0001	<0.0001
	20	<0.0001	<0.0001
	50	<0.0001	<0.0001
	100	<0.0001	<0.0001
	200	<0.0001	<0.0001
IC_{50}	10	<0.0001	<0.0001
	20	<0.0001	<0.0001
	50	<0.0001	<0.0001
	100	<0.0001	<0.0001
	200	<0.0001	<0.0001
IC_5		NS	NS
IC_{10}		<0.0001	NS
IC_{20}		<0.0001	<0.0001
IC_{50}		<0.0001	<0.0001
10 mM		NS	NS
20 mM		<0.0001	<0.0001
50 mM		<0.0001	<0.0001
100 mM		<0.0001	<0.0001
200 mm		<0.0001	<0.0001

NS- Not significant

At IC_{10} paired with 10 (26%) and 50 mM (22.6%) ethanol concentrations reduced cellular metabolic activity and cell viability significantly, while IC_{10} paired with 20 (10%) and 100 mM (5%) decreased cell metabolic activities and cell viability slightly, but not statistically significant compared to the controls in undifferentiated cells (IC_{10}+20mM p=0.1432; IC_{10}+100 mM p=0.3529). However, IC_{10} pairing with 200 mM ethanol decreased cell viability significantly compared to the controls (p=0.0015). 10 and 50 mM (26% and 36%) ethanol paired with IC_{20} and at 20 (22%),100 (18%) and 200 mM (19%) paired with IC_{20} of CPO, induced cell metabolic activity and cell viability loss in undifferentiated

cells non-monotonically with increasing ethanol concentrations compared to non-treated controls.

Comparison with single treatments of CPO (red bar) showed that IC_5 coupled with 50 - 200 mM ethanol treatments were significantly reduced cell viability than IC_5 of CPO alone, while IC_{50} coupled with 10 mM ethanol reduced cell viability less than single pesticide treatments, and IC_{50} paired with 20 - 200 reduced cell viability significantly compared to single IC_{50} of CPO.

Similar to the undifferentiated cell responses for the joint toxicity of CPO and ethanol, differentiated cells exhibited concentration-dependent decreased cell metabolic activity and cell viability only for IC_5 and IC_{50} paired with 10 - 200 mM ethanol compared to the control treatments (Figure 8-1 B). However, the pairing of IC_{10} and IC_{20} of CPO paired with 10 - 200 mM ethanol did not exhibit a concentration-dependent decrease in cell viability in differentiated cells compared to control treatment. Interestingly, IC_{10} of CPO paired with 10 mM ethanol induced a significant (32%) (p<0.0001) cell metabolic activity and cell viability decrease, and were lower than either pairing with 20 mM (2.9%) or 5 mM (1.5%) ethanol compared to the controls in differentiated cells. A concentration-dependent decrease in cell viability was apparent for 10, 50, 100, and 200 mM compared to control treatments coupled with IC_{10} of CPO. Interestingly, joint toxicity of IC_{10} and IC_{20} of CPO induced cell metabolic activity and cell viability loss in differentiated cells to a slightly lower level compared to lower doses like IC_5 and IC_{50} pairing with ethanol compared to their controls.

Interestingly, IC_5 with 10 - 200mM ethanol significantly reduced cell viability of differentiated cells compared to IC_5 of CPO alone treatment. According to Figure 8-1 B, all treatment combinations exhibited a significant effect on cell viability compared to the corresponding CPO alone treatment (red bar).

The single treatments of CPO, IC_5, IC_{10}, IC_{20} and IC_{50} on both phenotypes when compared with joint toxicities of CPO and ethanol are shown in Table 8-2. According to Table 8-2, low doses of CPO+10 - 200 mM ethanol induced synergistic or antagonistic effects on both phenotypes.

A comparison between undifferentiated and differentiated cells for the joint toxicity of CPO and ethanol, showed significant interaction and IC_5 concentration paired with ethanol concentrations showed greater cell viability loss in differentiated cells than in undifferentiated cells (Table 8-22).

Table 8-2: Synergistic and antagonistic effect of joint toxicity of CPO and alcohol in SH-SY5Y cells.

Treatments		Undifferentiated cells	Differentiated cells
IC_5	10	4.00	0.17
	20	0.46	0.29
	50	3.17	0.60
	100	4.69	0.90
	200	4.13	1.50
IC_{10}	10	1.19	0.64
	20	3.43	1.08
	50	3.22	2.11
	100	6.06	1.66
	200	6.54	2.24
IC_{20}	10	1.16	0.91
	20	2.17	1.26
	50	2.22	2.31
	100	3.17	4.70
	200	4.81	7.46
IC_{50}	10	1.10	2.15
	20	1.24	2.11
	50	1.13	0.90
	100	0.75	1.49
	200	0.39	0.03

Combination index (CI) was calculated using the CompuSyn software and Chou-Talalay method provide quantitative definition for an additive (CI=1), synergistic (CI<1) or antagonistic (CI>1) effect of ethanol and CPO combinations for both phenotypes.

8.2.1.2 *AZO and ethanol*

Joint toxicity of AZO and ethanol in undifferentiated cells showed a concentration-dependent decrease in cell metabolic activity and cell viability loss with increasing ethanol concentrations with pairings of low doses of AZO (Figure 8-2 A).

However, IC_{10} coupled with 10, 20, 50,100 and 200 mM ethanol showed a non-monotonical response in cell viability showing that the pairing of IC_{10} with 100 mM (35.5%) ethanol decreased cell metabolic activity and cell viability significantly compared to the 50 (35%) and 200 (28%) mM coupled with IC_{10} (Figure 8-2 A).

All tested low doses of AZO pairing with ethanol showed a significant difference with their corresponding single AZO treatments (red bar), while IC_{20} of AZO paired with 10 mM ethanol and IC_{50} paired with 20 mM ethanol, did not exhibit significance differences between their corresponding individual treatments (IC_{20}+20 mM p=0.9863; IC_{50}+20 mM (p=0.2471) in undifferentiated cells (Figure 8-2 A).

When considering the single ethanol treatment on undifferentiated cells, IC_5, IC_{10} and IC_{20} pairing with 10 - 200 mM ethanol treatments exhibited significant cell viability changes compared to their corresponding single treatments of ethanol (letters indicated in the graph).

Cell survival for the pairing of low doses of AZO with alcohol in differentiated cells showed a concentration-dependent decrease in cell viability compared to their controls for the pairing of IC_5, $IC_{10,}$ and IC_{50}. Interestingly, joint toxicity induced by pairing of IC_{20} with 20 mM (47.5%; p<0.0001) ethanol showed the greatest cell metabolic activity decrease and cell viability loss, than pairing with other concentrations of ethanol. The strong effect on cell viability loss was apparent at IC_{20} pairing with 200 mM ethanol for 24 h (67.5%) compared to controls (Figure 8-2 B). IC_{20} coupled with 50 and 100 mM ethanol showed 34.4% and 15% decreases of cell metabolic activity and cell viability in differentiated cells compared to controls, respectively. The cell metabolic activity and cell viability decrease in IC_{20}+50 mM pairing was significantly different from other pairings with IC_{20} of AZO (IC_{20}+10 mM =24%; IC_{20}+20 mM =13.05%; IC_{20}+100

mM=19.05% and IC_{20}+200 mM=33.05%). IC_{20} pairing with 100 mM ethanol in differentiated cells showed significant difference between IC_{20} paired with 20 (32.5% increase), 50 (19.48% increase) and 200 mM (52.5% increase) ethanol. Significant decreases in cell viability and cell metabolic activity were apparent at IC_5 paired with 100 and 200 mM (81% and 80% respectively) ethanol, and IC_{50} paired with 200 mM (97%) ethanol than other low dose pairings.

All IC_5 pairings with ethanol showed significant viability decrease compared to the single treatment of IC_5 AZO for differentiated cells. IC_{50} paired with 50 mM ethanol did not exhibit significant differences compared to single treatment of IC_{50} of AZO, while other 10, 20, 100 and 200 mM treatment combinations significantly influenced viability for differentiated cells compared to AZO alone treatment (red bar). Contrastingly, 20 and 200 mM paired with IC_{10} and 100 and 200 mM paired with IC_{20}, displayed a significant influence on cell viability compared to single treatments of IC_{10} and IC_{20} of AZO.

When considering the single treatments of ethanol, all treatment combinations induced significant changes in cell viability in differentiated cells compared to corresponding single treatments, except IC_{50} combined with 50, 100 and 200 mM ethanol treatments (p>0.005) (50 mM; letter: c). Synergistic /antagonistic effects of joint toxicity of AZO and ethanol for SH-SY5Y cells are shown in Table 8-4.

A comparison of undifferentiated and differentiated cells for their metabolic activity and viability loss showed a significant interaction, and a significant difference was apparent at IC_5 of AZO pairing along with different concentrations of ethanol for 24 h exposures (Table 8-22).

Table 8-3: Comparison of treatment combinations of ethanol and AZO with their corresponding non-treated control. Results were analysed by two-way ANOVA and means comparison was done by Tukey's multiple comparison tests.

Treatments		Undifferentiated cells	Differentiated cells
IC_5	10	<0.0001	<0.0001
	20	<0.0001	<0.0001
	50	<0.0001	<0.0001
	100	<0.0001	<0.0001
	200	<0.0001	<0.0001
IC_{10}	10	<0.0001	NS
	20	<0.0001	<0.0001
	50	<0.0001	<0.0001
	100	<0.0001	<0.0001
	200	<0.0001	<0.0001
IC_{20}	10	<0.0001	0.0107
	20	<0.0001	<0.0001
	50	<0.0001	<0.0001
	100	<0.0001	<0.0001
	200	<0.0001	<0.0001
IC_{50}	10	NS	<0.0001
	20	<0.0001	<0.0001
	50	<0.0001	<0.0001
	100	<0.0001	<0.0001
	200	<0.0001	<0.0001
IC_5 IC_{10} IC_{20} IC_{50}		NS 0.0082 <0.0001 <0.0001	NS 0.0163 <0.0001 <0.0001
10 mM 20 mM 50 mM 100 mM 200 mm		NS <0.0001 <0.0001 <0.0001 <0.0001	NS <0.0001 <0.0001 <0.0001 <0.0001

NS- Not significant

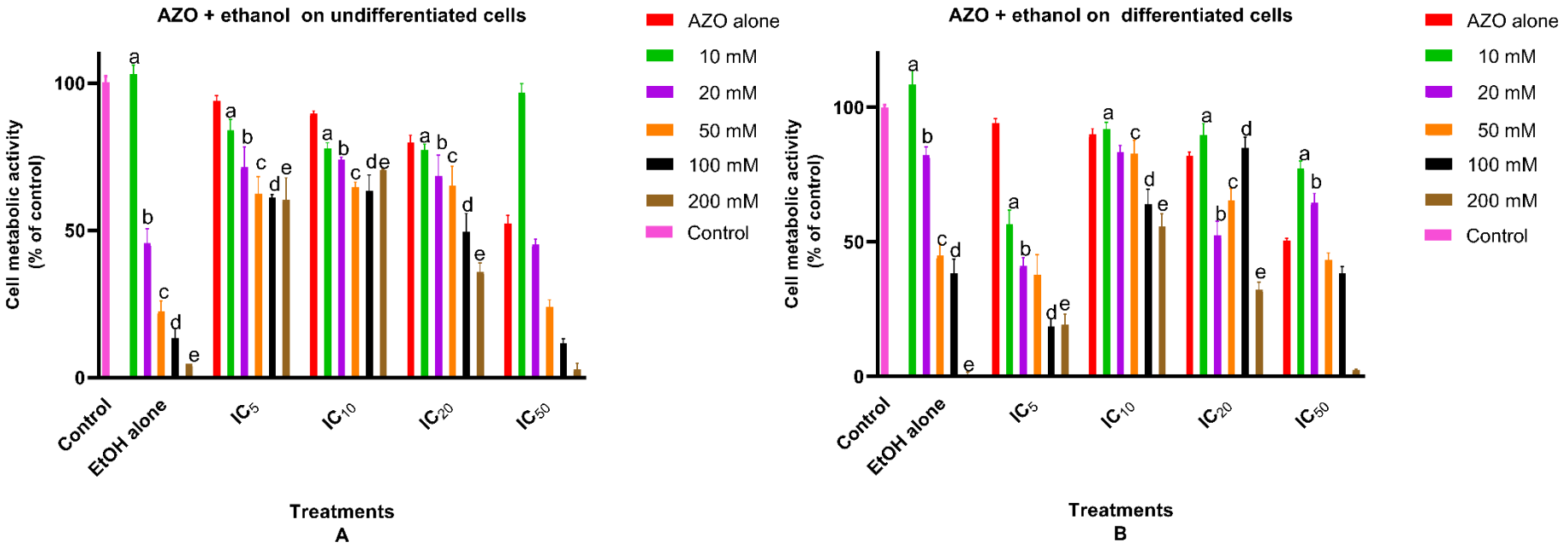


Figure 8-2: Co-exposure to ethanol and AZO for SH-SY5Y cells for 24 h.

A- undifferentiated cells and B- differentiated cells were treated with AZO and ethanol for 24 h. Viability was assessed using MTT assay. Readings were normalized to the viability of control, providing cell viability percentage, as a percentage value to the control. Control and treatments were performed as triplicates in 5 individual experiments (n=5). Results were analysed using two-way ANOVA with Tukey's multiple comparison and expressed as the mean ± standard error of the mean (SEM), when SEM bar is not apparent, this means that error is smaller than the symbol size. Comparison of treatments with non-treated control are indicated in Table 8-3. **a** - significance difference with 10 mM ethanol, **b** - significance difference with 20 mM ethanol, **c** - significance difference with 50 mM ethanol, **d** - significance difference with 100 mM ethanol, **e** - significance difference with 200 mM ethanol.

Table 8-4: Synergistic and antagonistic effect of joint toxicity of AZO and alcohol in SH-SY5Y cells.

Treatments		Undifferentiated cells	Differentiated cells
IC_5	10	1.39	0.35
	20	1.44	0.38
	50	2.48	0.79
	100	4.60	0.79
	200	6.70	1.60
IC_{10}	10	1.28	2.50
	20	1.77	1.92
	50	2.79	3.72
	100	5.13	3.35
	200	6.50	5.08
IC_{20}	10	1.73	3.12
	20	1.78	0.82
	50	3.12	2.20
	100	3.57	6.59
	200	4.57	2.70
IC_{50}	10	6.87	2.91
	20	1.29	2.06
	50	1.04	1.56
	100	0.92	2.09
	200	0.53	0.41

Combination index (CI) was calculated using the CompuSyn software and Chou-Talalay method provide quantitative definition for an additive (CI=1), synergistic (CI<1) or antagonistic (CI>1) effect of ethanol and CPO combinations for both phenotypes.

8.2.1.3 ***Aldicarb with ethanol***

Joint toxicity of Aldicarb and ethanol on cell metabolic activity and cell viability loss in SH-SY5Y cells is depicted in Figures 8-3. A similar line of cytotoxicity responses to CPO and AZO was observed compared to control treatments with an interactive effect with Aldicarb and ethanol on SH-SY5Y cells. Both undifferentiated and differentiated cells reduced cell viability in a concentration-dependent manner with an interactive effect of Aldicarb and ethanol exposure in all pairings according to Figure 8-3.

The IC_5 pairing with 10, 20 and 50 mM ethanol did not induce significant cell metabolic activity and cell viability loss in undifferentiated cells (p=0.9990; p=0.8304; p>0.05, respectively). Also, IC_{10} of Aldicarb pairing with 10 and 20 mM ethanol and IC_{50} of AZO with 10 mM ethanol was not significantly different from non-treated controls.

IC_5+10 mM, IC_5+20 mM, IC_{10}+10 mM and IC_{10}+20 mM did not exhibit significantly different values compared to individual treatments of IC_5 and IC_{10} of Aldicarb for undifferentiated cells (red bar). All combinations of IC_5, IC_{10} and IC_{20} showed a significant effect on cell viability compared to the corresponding ethanol treatments, while there was no significant difference between single treatment of ethanol and the combination of IC_{50} with 100 and 200 mM ethanol treatments (letters a, b, c, d, and e) for undifferentiated cells.

The effect of co-exposure of Aldicard and ethanol on differentiated cells was depicted in Figure 8-3 B. Remarkably, IC_5+10 mM (1%) and IC_5+20 mM (3%) ethanol, IC_{10}+10 mM (3%) and IC_{10}+20 mM (4%) ethanol and IC_{20}+20 mM (9%) ethanol did not affect cell metabolic activity and cell viability loss (p>0.05), compared to non-treated controls in differentiated cells for Aldicarb and ethanol treatments. All pairings of IC_{50} of Aldicarb significantly reduced the cell viability in undifferentiated cells greater than other combinations (Table 8-5).

IC_5+100mM and IC_5+200 mM (p<0.0001) showed significant differences in cell viability compared to single IC_5 treatments, while IC_{10} paired with 50,100 and 200 mM ethanol, IC_{20} and IC_{50} paired with 10 and 20 mM ethanol, also exhibited significant influences on cell viability in differentiated cells compared with IC_{10}, IC_{20} and IC_{50} as single pesticide treatments.

IC_5,IC_{10},IC_{20} and IC_{50} treatment combinations showed significant differences compared with individual ethanol treatments except IC_{50} with 50, 100, or 200 mM ethanol treatments (letters indicated as c,d,e) in differentiated cells Synergitic /antigonistic effects of jthe oint toxicity of Aldicarb and ethanol for SH-SY5Y cell are indicated in Table 8-6.

A comparison of undifferentiated cells vs differentiated cells showed a significant interaction on cell viability responses for low doses of Aldicarb and ethanol (Table 8-22).

Table 8-5: Comparison of treatment combinations of ethanol and Aldicarb with their corresponding non-treated controls. Results were analysed by two-way ANOVA and means comparison was done by Tukey's multiple comparison tests.

Treatments		Undifferentiated cells	Differentiated cells
IC_5	10	NS	NS
	20	NS	NS
	50	NS	NS
	100	<0.0001	<0.0001
	200	<0.0001	<0.0001
IC_{10}	10	NS	NS
	20	NS	NS
	50	<0.0001	0.0001
	100	<0.0001	<0.0001
	200	<0.0001	<0.0001
IC_{20}	10	<0.0001	0.0031
	20	0.0001	NS
	50	<0.0001	<0.0001
	100	<0.0001	<0.0001
	200	<0.0001	<0.0001
IC_{50}	10	NS	0.0006
	20	<0.0001	<0.0001
	50	<0.0001	<0.0001
	100	<0.0001	<0.0001
	200	<0.0001	<0.0001
IC_5		NS	NS
IC_{10}		0.0056	NS
IC_{20}		<0.0001	<0.0001
IC_{50}		<0.0001	<0.0001
10 mM		NS	NS
20 mM		<0.0001	<0.0001
50 mM		<0.0001	<0.0001
100 mM		<0.0001	<0.0001
200 mm		<0.0001	<0.0001

NS- Not significant

Table 8-6: Synergistic and antagonistic effects of joint toxicity of Aldicarb and alcohol for SH-SY5Y cells.

Treatments		Undifferentiated cells	Differentiated cells
IC_5	10	9.01	1.17
	20	7.58.	1.12
	50	9.00	7.49
	100	6.31	4.68
	200	4.53	4.55
IC_{10}	10	3.42	6.00
	20	3.61	4.26
	50	4.63	3.29
	100	6.76	3.24
	200	6.23	4.68
IC_{20}	10	2.23	5.06
	20	4.17	8.38
	50	4.22	5.45
	100	5.17	8.03
	200	6.81	8.50
IC_{50}	10	4.10	7.04
	20	0.90	4.75
	50	0.74	2.23
	100	0.94	2.39
	200	0.82	0.53

Combination index (CI) was calculated using the CompuSyn software and Chou-Talalay method provide quantitative definition for an additive (CI=1), synergistic (CI<1) or antagonistic (CI>1) effect of ethanol and CPO combinations for both phenotypes.

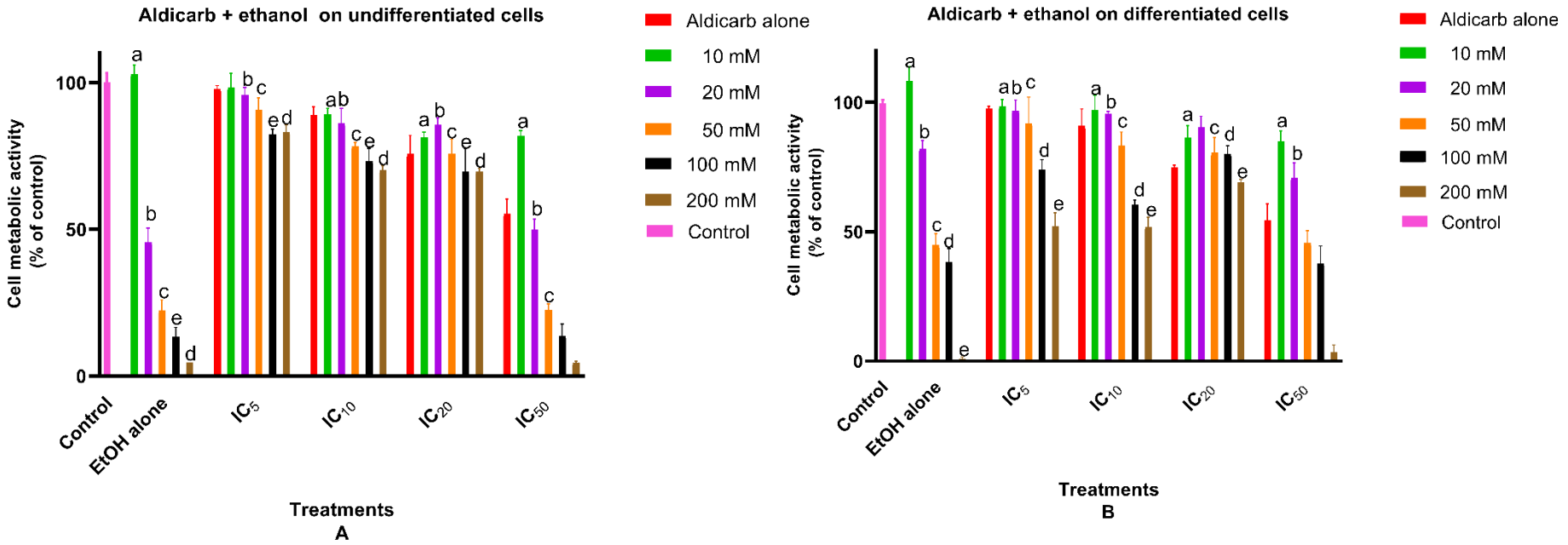


Figure 8-3: Co-exposure to ethanol and Aldicarb SH-SY5Y cells for 24 h.

A- undifferentiated cells and B- differentiated cells were treated with Aldicarb and ethanol for 24 h. Viability was assessed using MTT assay. Readings were normalized to the viability of control, providing cell viability percentage, as a percentage value to the control. Control and treatments were performed as triplicates in 5 individual experiments (n=5). Results were analysed using two-way ANOVA with Tukey's multiple comparison and expressed as the mean ± standard error of the mean (SEM), when SEM bar is not apparent, this means that error is smaller than the symbol size. Comparison of treatments with non-treated control are indicated in Table 8-3. **a** - significance difference with 10 mM ethanol, **b** - significance difference with 20 mM ethanol, **c** - significance difference with 50 mM ethanol, **d** - significance difference with 100 mM ethanol, **e** - significance difference with 200 mM ethanol.

8.2.2 Interactive effect of ethanol and low doses of OP and carbamate pesticide on cell death of SH-SY5Y cells.

MTT assay could suggest a cytostatic effect on cells to co-exposure of pesticides and ethanol, hence viability loss was further validated by LDH assay. The interactive effect of IC_5, IC_{10}, $IC_{20,}$ and IC_{50} of CPO, AZO, and Aldicarb paired with ethanol 10-200 mM on SH-SY5Y cell death was evaluated using a LDH assay.

8.2.2.1 *CPO and ethanol*

Undifferentiated SH-SY5Y cells exposed to CPO and ethanol showed a concentration-dependent increase in LDH production compared to controls in treatments coupled with IC_5 and IC_{50} of CPO with 10 - 200 mM ethanol. In line with the MTT assays, IC_{10} and IC_{20} concentrations of CPO with ethanol showed non-monotonical responses. In both IC_{10} and IC_{20} there was significant LDH production at 50 mM (39.8% and 34%) than other concentrations of ethanol, when compared to IC_{10} of CPO and IC_{20} of CPO, similar to the MTT assays (Figure 8-4 A).

Two-way ANOVA and multiple comparisons with Tukey's test indicated that the treatment combinations of CPO and ethanol were significantly different from their individual treatments at low CPO doses in undifferentiated cells (red bar in each graph in treatment group), except IC_5+10 or 20 mM, IC_{10}+20, 100, or 200 mM, IC_{20}+10, 20, 100, or 200 mM, and IC_{50}+10 or 20 mM ethanol. All combinations of IC_{20} showed significant difference compared to their single treatments of ethanol (indicated by letters) in undifferentiated cells.

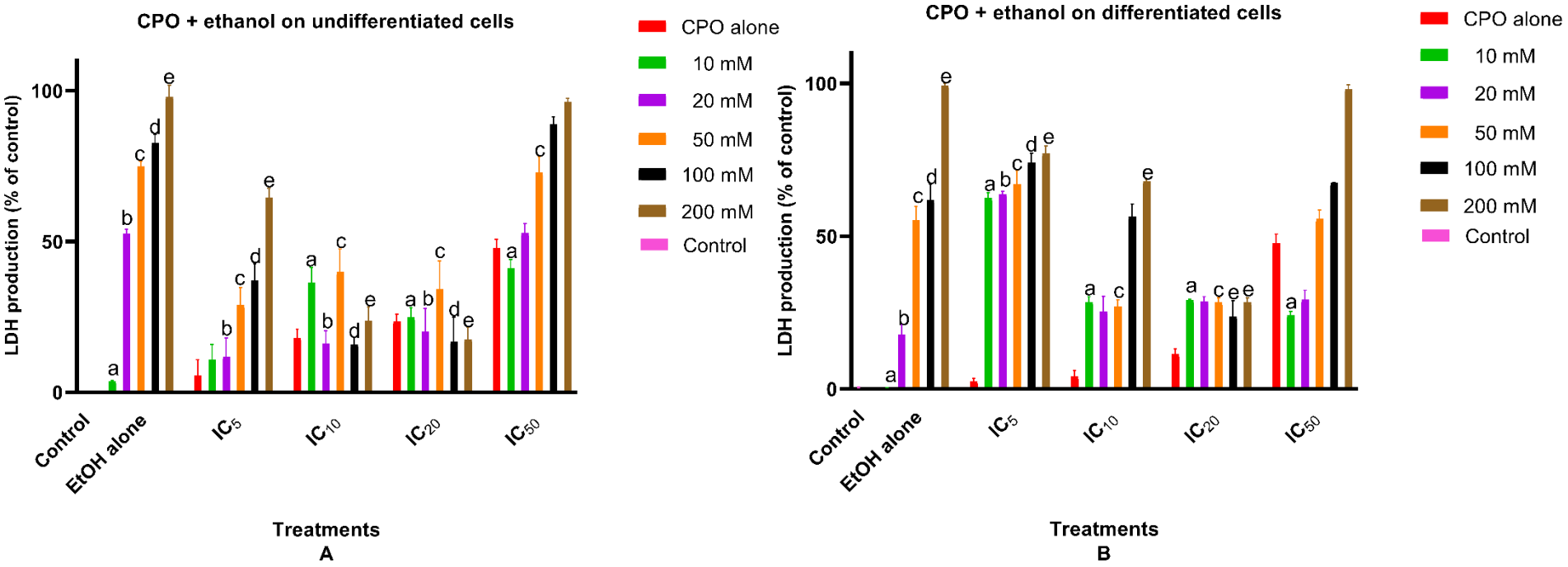


Figure 8-4: Co-exposure to ethanol and CPO and LDH production in differentiated SH-SY5Y cells after 24 h.
A- undifferentiated cells and B- differentiated cells were treated with CPO and ethanol for 24 h. Cell death was assessed using LDH assay. Readings were normalized to the LDH production of control, providing LDH production percentage, as a percentage value to the control. Control and treatments were performed as triplicates in 5 individual experiments (n=5). Results were analysed using two-way ANOVA with Tukey's multiple comparison and expressed as the mean ± standard error of the mean (SEM), when SEM bar is not apparent, this means that error is smaller than the symbol size. Comparison of treatments with non-treated control are indicated in Table 8-7. **a** – significant difference with 10 mM ethanol, **b** - significant difference with 20 mM ethanol, **c** - significant difference with 50 mM ethanol, **d** - significant difference with 100 mM ethanol**, e** - significant difference with 200 mM ethanol.

Table 8-7: Comparison of treatment combinations of ethanol and CPO with their corresponding non-treated controls. Results were analysed by two-way ANOVA and means comparison was done by Tukey's multiple comparison tests.

Treatments		Undifferentiated cells	Differentiated cells
IC_5	10	NS	NS
	20	NS	NS
	50	NS	NS
	100	<0.0001	<0.0001
	200	<0.0001	<0.0001
IC_{10}	10	NS	NS
	20	NS	NS
	50	<0.0001	0.0001
	100	<0.0001	<0.0001
	200	<0.0001	<0.0001
IC_{20}	10	<0.0001	0.0031
	20	0.0001	NS
	50	<0.0001	<0.0001
	100	<0.0001	<0.0001
	200	<0.0001	<0.0001
IC_{50}	10	NS	0.0006
	20	<0.0001	<0.0001
	50	<0.0001	<0.0001
	100	<0.0001	<0.0001
	200	<0.0001	<0.0001
IC_5 IC_{10} IC_{20} IC_{50}		NS 0.0056 <0.0001 <0.0001	NS NS <0.0001 <0.0001
10 mM 20 mM 50 mM 100 mM 200 mm		NS <0.0001 <0.0001 <0.0001 <0.0001	NS <0.0001 <0.0001 <0.0001 <0.0001

NS- Not significant

Joint toxicity of ethanol with CPO induced a concentration-dependent increase in LDH production at IC_5 when coupled with ethanol, and IC_{10} when coupled with ethanol with increasing concentration of ethanol at 24 h exposure for differentiated cells (Figure 8-4 B). LDH production in the pairing of IC_5 of CPO with 10 - 200 mM ethanol were significantly higher than other low doses coupled with ethanol, compared with their corresponding controls. In line with the MTT assay, joint toxicity of IC_5 of CPO concentration with different concentrations of ethanol-induced a synergistic response on LDH production in differentiated SH-SY5Y cells. Non-monotonical dose responses can be observed with differentiated cells for LDH production at IC_{10}, IC_{20} and IC_{50} for CPO

concentrations coupled with different concentrations of ethanol. IC_{20} paired with 100 mM (28%) ethanol showed significant LDH production compared to control treatments, but lower than the other concentrations when paired with IC_{20} of CPO in differentiated cells. IC_{50} paired with 10 and 200 mM (36% and 33%) ethanol treatments caused significant LDH production in differentiated cells and higher than that of 20, 50 and 100 mM treatments (28%,28%, and 30%) (Figure 8-4 B).

All treatment combinations of CPO showed a significant difference with their corresponding single low doses CPO treatment except IC_{50}+50 mM (p<0.05). When considering the single exposures of 10 - 200 mM ethanol on differentiated cells, treatment combinations of IC_{50} demonstrated a similar response except IC_{50}+10 mM (“a” indicated in the graph).

A comparison of the joint toxicity of CPO and ethanol in undifferentiated and differentiated cells showed significant differences at each exposure concentration (Table 8-22).

8.2.2.2 ***AZO and ethanol***

Co-exposure of low doses of AZO and ethanol is depicted in Figure 8-5 A for undifferentiated SH-SY5Y cells. IC_5, IC_{20} and IC_{50} pairing with ethanol at 10, 20, 50, 100 and 200 mM showed a concentration-dependent increase in LDH production in undifferentiated SH-SY5Y cells, while IC_{10} coupled with different concentrations of ethanol showed a non-monotonical increase of LDH production in undifferentiated SH-SY5Y cells compared to corresponding control treatments. According to Figure 8-5 A, IC_{50} paired with 10 mM, ethanol-induced a non-significant LDH production compared to controls (3%; p=0.9440), but this was significant for IC_{50} of AZO with 20 (34%), 50 (35%), 100 (58%) and 200 mM (72%) ethanol in undifferentiated cells. Remarkably, IC_{10} of AZO pairing with 100 mM (36.1%) induced higher LDH production than that induced by

pairing with 200 mM (29%) in undifferentiated cells, but not statistically significant compared to 200 mM pairing. But it was significant compared to 20 mM (p=0.0321) pairing with IC_{10} of AZO in undifferentiated cells.

The joint toxicity of AZO with ethanol in all treatments were significantly different from their corresponding AZO alone treatments, except IC_{20}+10 mM (p=0.9765) and IC_{50}+20 mM (p=0.9765) treatment for undifferentiated cells.

When consider comparison with the single ethanol exposure of 10 - 200 mM and IC_{50} of AZO pairings of 10 - 200 mM ethanol, IC_{50} combination exhibited a similar effect on undifferentiated cells with combination with IC_{50} of AZO (letters indicated in graph).

Differentiated cells showed similar responses to joint toxicity of AZO at low doses with ethanol exposure for 24 h to those from the MTT assay (Figure 8-5 B). LDH production increases with increasing ethanol concentrations with the coupling of IC_5, $IC_{10,}$ and IC_{50} with 10 - 200 mM of ethanol. But IC_{20} of AZO paired with ethanol showed non-monotonical responses for LDH production in differentiated cells. 100 mM ethanol showed significantly lower production of LDH in differentiated cells when coupled with IC_{20} of AZO in differentiated cells (14%) compared to control. IC_{20} coupled with 20 mM ethanol showed a 47% increase in LDH production compared to controls. Compared to ethanol when coupled with IC_{10}, IC_{20} and IC_{50} concentrations of AZO, IC_5 of AZO when paired with ethanol induced significant LDH production in differentiated cells. 200 mM induced significant LDH production in all combinations compared to controls.

In differentiated cells, IC_{10} paired with 10, 20, 50 mM ethanol was not significantly different from IC_{10} treatment alone while, IC_{20} paired with 10 mM and 100 mM treatments were also not significantly different from IC_{20} treatment

alone. Only IC_{50} when paired with 50 mM ethanol treatment was not significantly different from IC_{50} AZO (p=0.1306) treatments in differentiated cells.

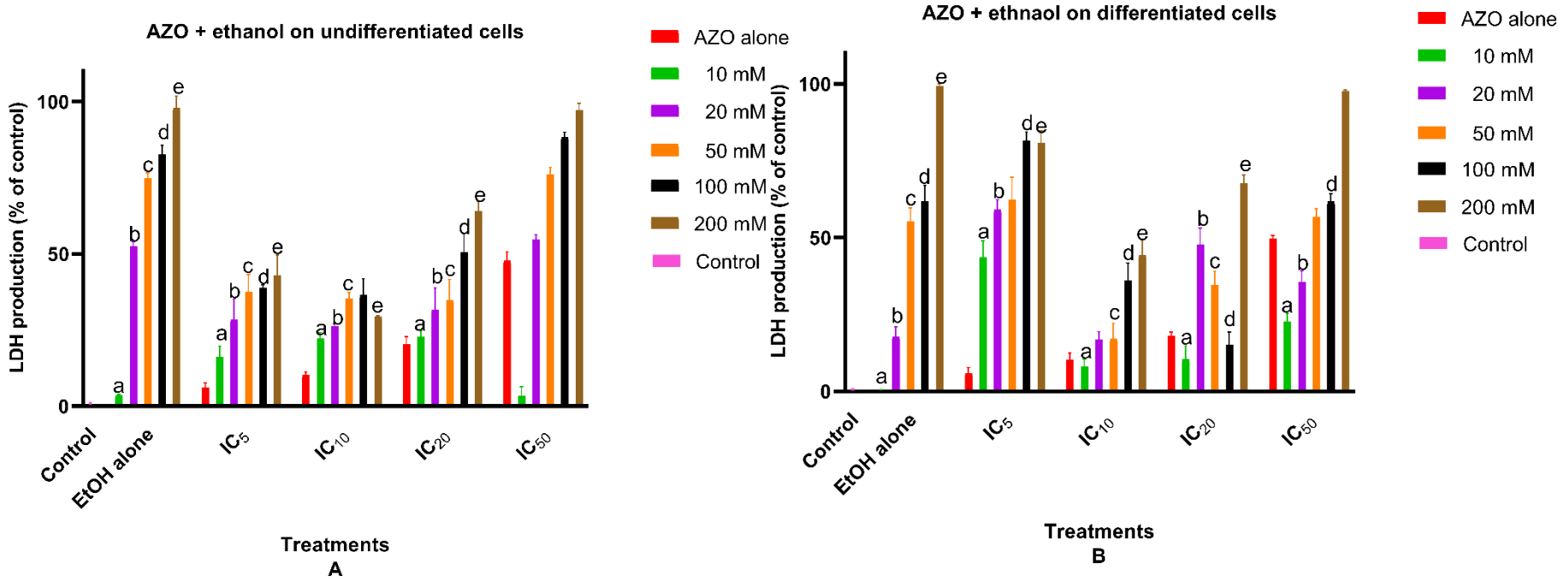


Figure 8-5: Co-exposure to ethanol and AZO and LDH production for undifferentiated SH-SY5Y cells for a 24 h exposure.
A- undifferentiated cells and B- differentiated cells were treated with AZO and ethanol for 24 h. Cell death was assessed using LDH assay. Readings were normalized to the LDH production of control, providing LDH production percentage, as a percentage value to the control. Control and treatments were performed as triplicates in 5 individual experiments (n=5). Results were analysed using two-way ANOVA with Tukey's multiple comparison and expressed as the mean ± standard error of the mean (SEM), when SEM bar is not apparent, this means that error is smaller than the symbol size. Comparison of treatments with non-treated control are indicated in Table 8-8. **a** – significant difference with 10 mM ethanol, **b** - significant difference with 20 mM ethanol, **c** - significant difference with 50 mM ethanol, **d** - significant difference with 100 mM ethanol**, e** - significant difference with 200 mM ethanol.

Table 8-8: Comparison of treatment combinations of ethanol and AZO with their corresponding non-treated controls. Results were analysed by two-way ANOVA and means comparison was done by Tukey's multiple comparison tests.

Treatments		Undifferentiated cells	Differentiated cells
IC_5	10	<0.0001	<0.0001
	20	<0.0001	<0.0001
	50	<0.0001	<0.0001
	100	<0.0001	<0.0001
	200	<0.0001	<0.0001
IC_{10}	10	<0.0001	NS
	20	<0.0001	<0.0001
	50	<0.0001	<0.0001
	100	<0.0001	<0.0001
	200	<0.0001	<0.0001
IC_{20}	10	<0.0001	0.0107
	20	<0.0001	<0.0001
	50	<0.0001	<0.0001
	100	<0.0001	<0.0001
	200	<0.0001	<0.0001
IC_{50}	10	NS	<0.0001
	20	<0.0001	<0.0001
	50	<0.0001	<0.0001
	100	<0.0001	<0.0001
	200	<0.0001	<0.0001
IC_5		NS	NS
IC_{10}		0.0082	0.0163
IC_{20}		<0.0001	<0.0001
IC_{50}		<0.0001	<0.0001
10 mM		NS	NS
20 mM		<0.0001	<0.0001
50 mM		<0.0001	<0.0001
100 mM		<0.0001	<0.0001
200 mm		<0.0001	<0.0001

NS- Not significant

Except IC_{10}+20 mM and IC_{50} paired with 50, 100 and 200 mM, all combinations produced significant levels of LDH compared to treatments with ethanol alone.

A comparison of undifferentiated vs differentiated cells in response to LDH production exposed to low doses of AZO and ethanol, showed a significant difference between the two phenotypes (Table 8-22).

8.2.2.3 ***Aldicarb and ethanol***

Co-exposure of Aldicarb and ethanol induced a concentration-dependent LDH production with a pairing of IC_5, $IC_{10,}$ and IC_{50} with increasing ethanol concentrations in undifferentiated cells (Figure 8-6 A). However, IC_{20} coupled with ethanol at 20 mM showed significant LDH production (13%) compared to control, but lower than IC_{20} coupled with 10 (18%), 50 (23%), 100 (29%) and 200 (30%) mM concentrations. Interestingly, in line with MTT assays, 10 and 20 mM of ethanol paired with IC_5 concentration of Aldicarb did not induce significant LDH production in undifferentiated cells (p=0.9002 and p=0.6839).

50 - 200 mM ethanol coupled with all Aldicarb concentrations induced significantly higher LDH levels than ethanol alone in undifferentiated cells. When compared with the Aldicarb alone, IC_5+10 or 20 mM, IC_{10}+10 or 20 mM, IC_{20}+10, 50, 100, or 200 mM, and IC_{50}+100 mM treatments showed non-significant LDH production compared to their corresponding single Aldicarb treatments.

Similar to undifferentiated cells, differentiated SH-SY5Y cells exposed to the Aldicarb at low doses and ethanol, induced a concentration-dependent LDH production at IC_5, $IC_{10,}$ and IC_{50} exposures with increasing concentrations of ethanol. IC_{20} of Aldicarb when paired with 20 mM ethanol did not induce significant (9%) (p= 0.1209) levels of LDH (Figure 8-6 B).

IC_5 coupled with 10, 20 or 50 mM ethanol resulted in non-significant LDH production compared to single IC_5 Aldicarb treatment. The combination of 10, 20, or 50 mM ethanol with IC_{10} showed non-significant LDH production compared to IC_{10} treatment alone. 10 and 20 mM ethanol coupled with IC_{20} and IC_{50}+50,100, or 200 mM treatments also exhibited non-significant LDH levels compared to their corresponding individual treatments.

All treatment combinations of Aldicarb and ethanol exhibited significance differences compared to their corresponding single ethanol treatments for differentiated cells.

Table 8-9: Comparison of treatment combinations of Aldicarb with ethanol and their corresponding non-treated controls. Results were analysed by two-way ANOVA and means comparison by Tukey's multiple comparison tests.

Treatments		Undifferentiated cells	Differentiated cells
IC_5	10	NS	NS
	20	NS	NS
	50	NS	NS
	100	<0.0001	<0.0001
	200	<0.0001	<0.0001
IC_{10}	10	NS	NS
	20	NS	NS
	50	<0.0001	0.0001
	100	<0.0001	<0.0001
	200	<0.0001	<0.0001
IC_{20}	10	<0.0001	0.0031
	20	0.0001	NS
	50	<0.0001	<0.0001
	100	<0.0001	<0.0001
	200	<0.0001	<0.0001
IC_{50}	10	NS	0.0006
	20	<0.0001	<0.0001
	50	<0.0001	<0.0001
	100	<0.0001	<0.0001
	200	<0.0001	<0.0001
IC_5		NS	NS
IC_{10}		0.0056	NS
IC_{20}		<0.0001	<0.0001
IC_{50}		<0.0001	<0.0001
10 mM		NS	NS
20 mM		<0.0001	<0.0001
50 mM		<0.0001	<0.0001
100 mM		<0.0001	<0.0001
200 mm		<0.0001	<0.0001

NS- Not significant

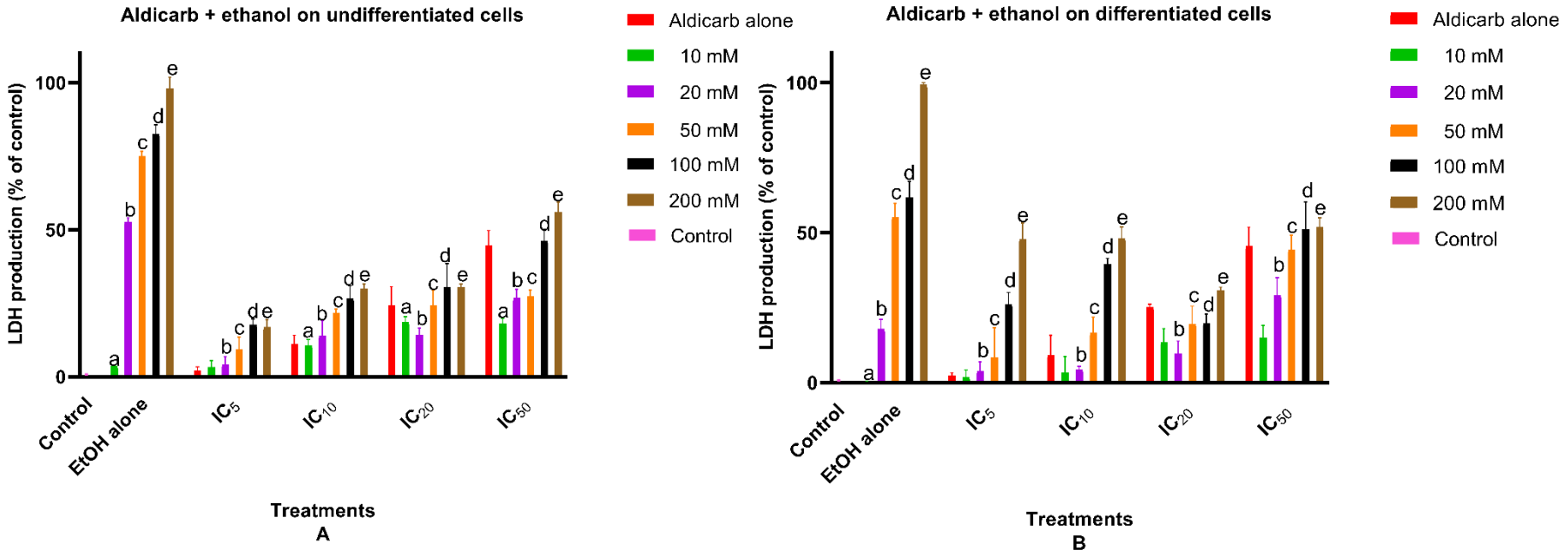
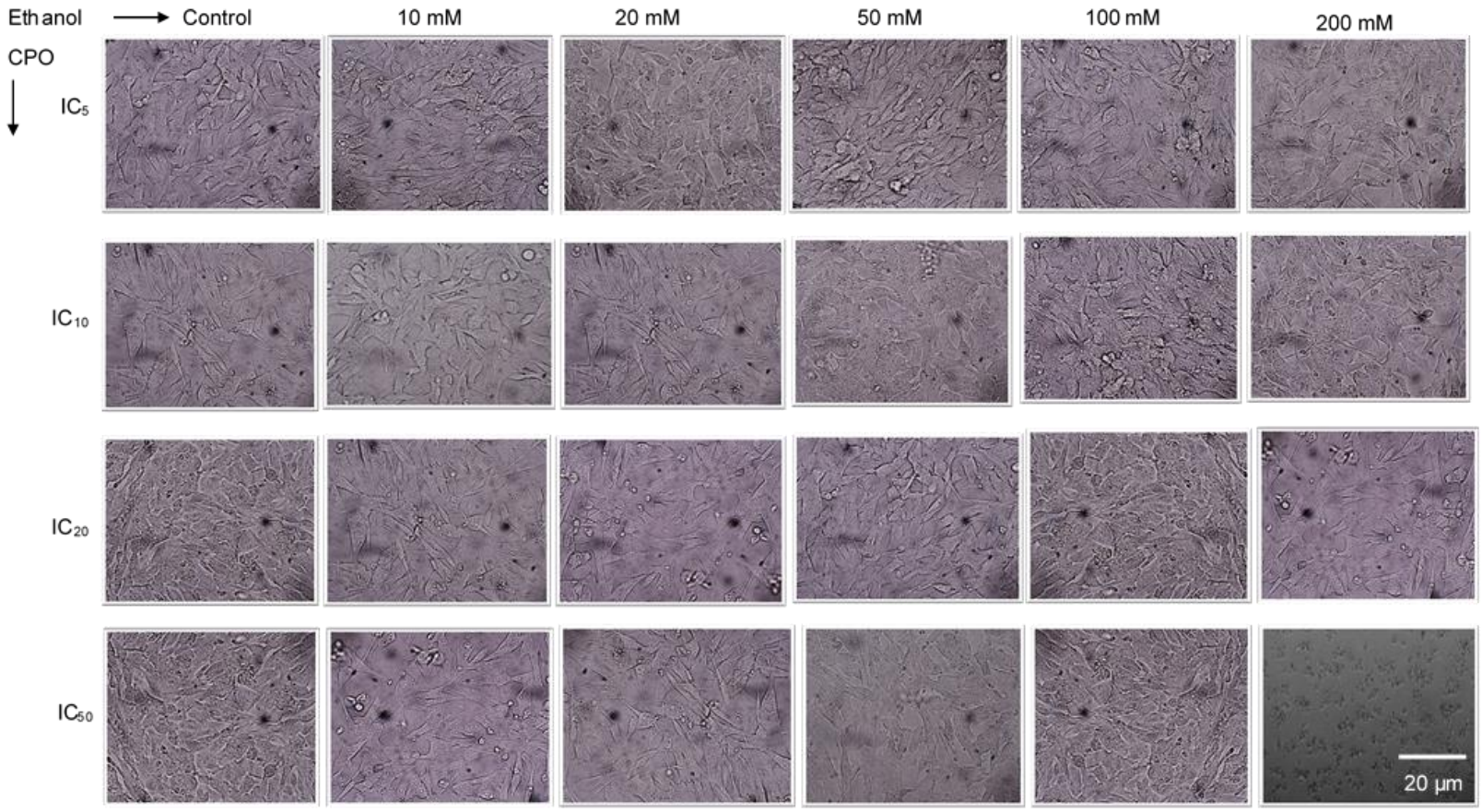


Figure 8-6: Co-exposure to Aldicarb and ethanol and LDH production for differentiated SH-SY5Y cells after 24 h exposure.
A- undifferentiated cells and B- differentiated cells were treated with Aldicarb and ethanol for 24 h. Cell death was assessed using LDH assay. Readings were normalized to the LDH production of control, providing LDH production percentage, as a percentage value to the control. Control and treatments were performed as triplicates in 5 individual experiments (n=5). Results were analysed using two-way ANOVA with Tukey's multiple comparison and expressed as the mean ± standard error of the mean (SEM), when SEM bar is not apparent, this means that error is smaller than the symbol size. Comparison of treatments with non-treated control are indicated in Table 8-9. **a** – significant difference with 10 mM ethanol, **b** - significant difference with 20 mM ethanol, **c** - significant difference with 50 mM ethanol, **d** - significant difference with 100 mM ethanol**, e** - significant difference with 200 mM ethanol.

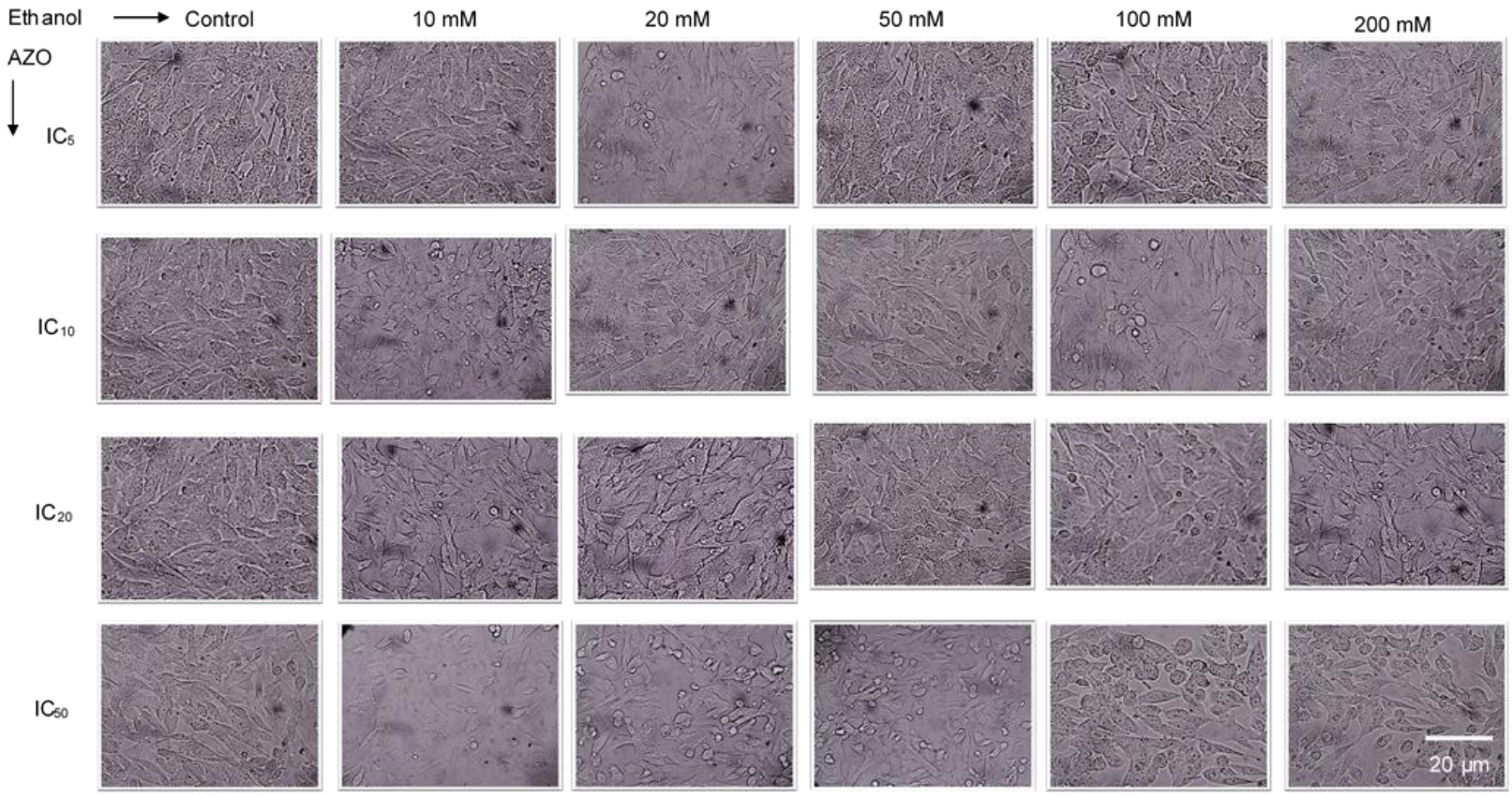
A comparison of undifferentiated cells vs differentiated cells showed significant differences in their toxic responses and LDH production after the joint exposure to Aldicarb and ethanol (Table 8-22).

8.2.3 Co-exposure of ethanol with low doses of OP and carbamate pesticide causes morphological impairments of SH-SY5Y cells.

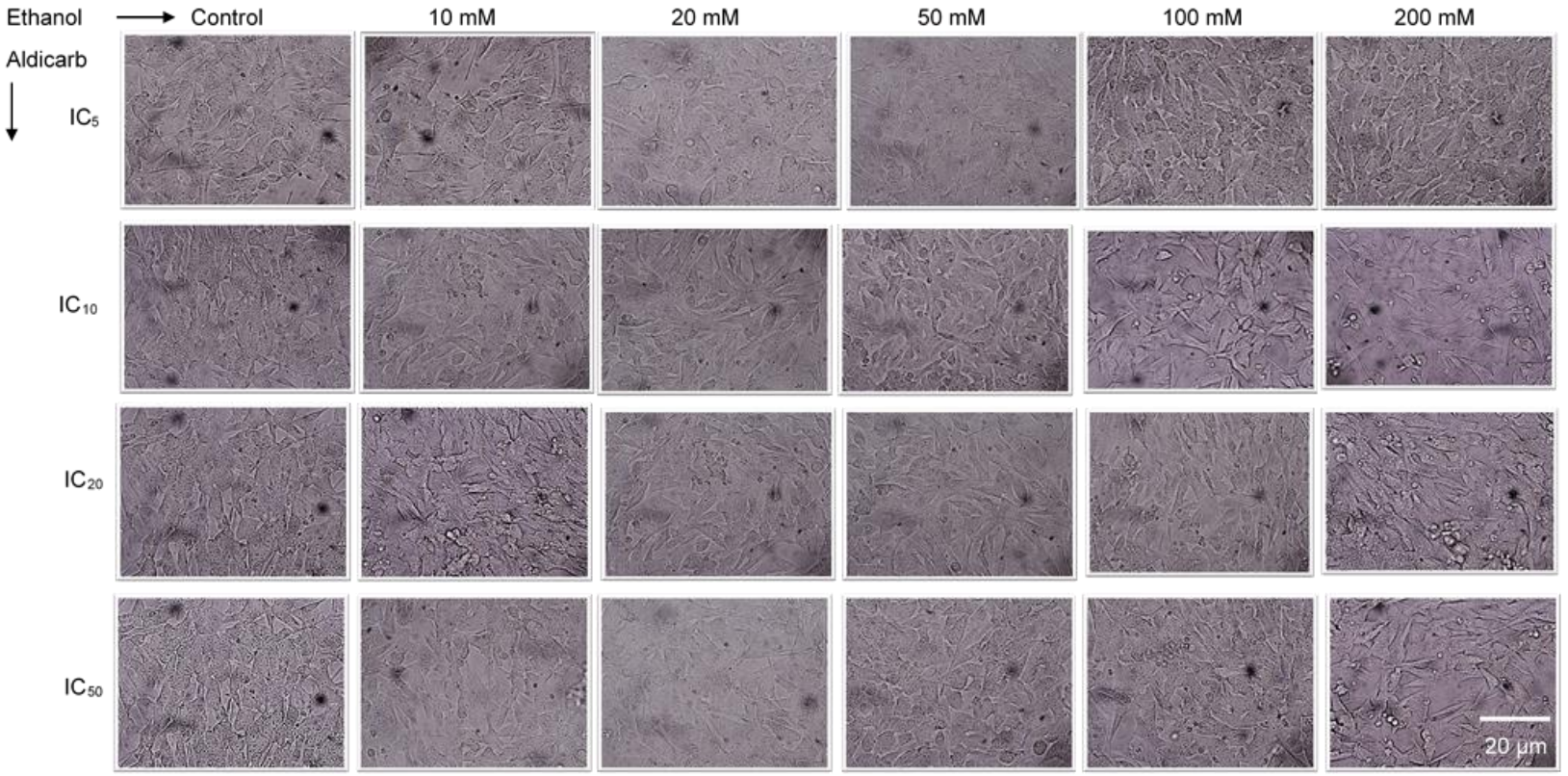
Morphological changes were apparent with low doses of CPO, AZO, and Aldicarb when paired with 10 - 200 mM ethanol concentrations for both phenotypes of SH-SY5Y cells as captured by phase-contrast microscopy. According to the images, low doses of CPO, AZO, and ethanol coupled with 10 - 200 mM ethanol showed variable responses, with cell shrinkage, blunting of neurites, and cell death at higher concentrations of ethanol with pesticides. However, images indicated that IC_{20} doses of the three tested pesticides coupled with ethanol showed a non-monotonical decrease in cell viability in line with MTT and LDH assays (Figure 8-7).


Ethanol
Control
10 mM
20 mM
50 mM
100 mM
200 mM
CPO
IC5
IC10
IC20
IC50
20 µm

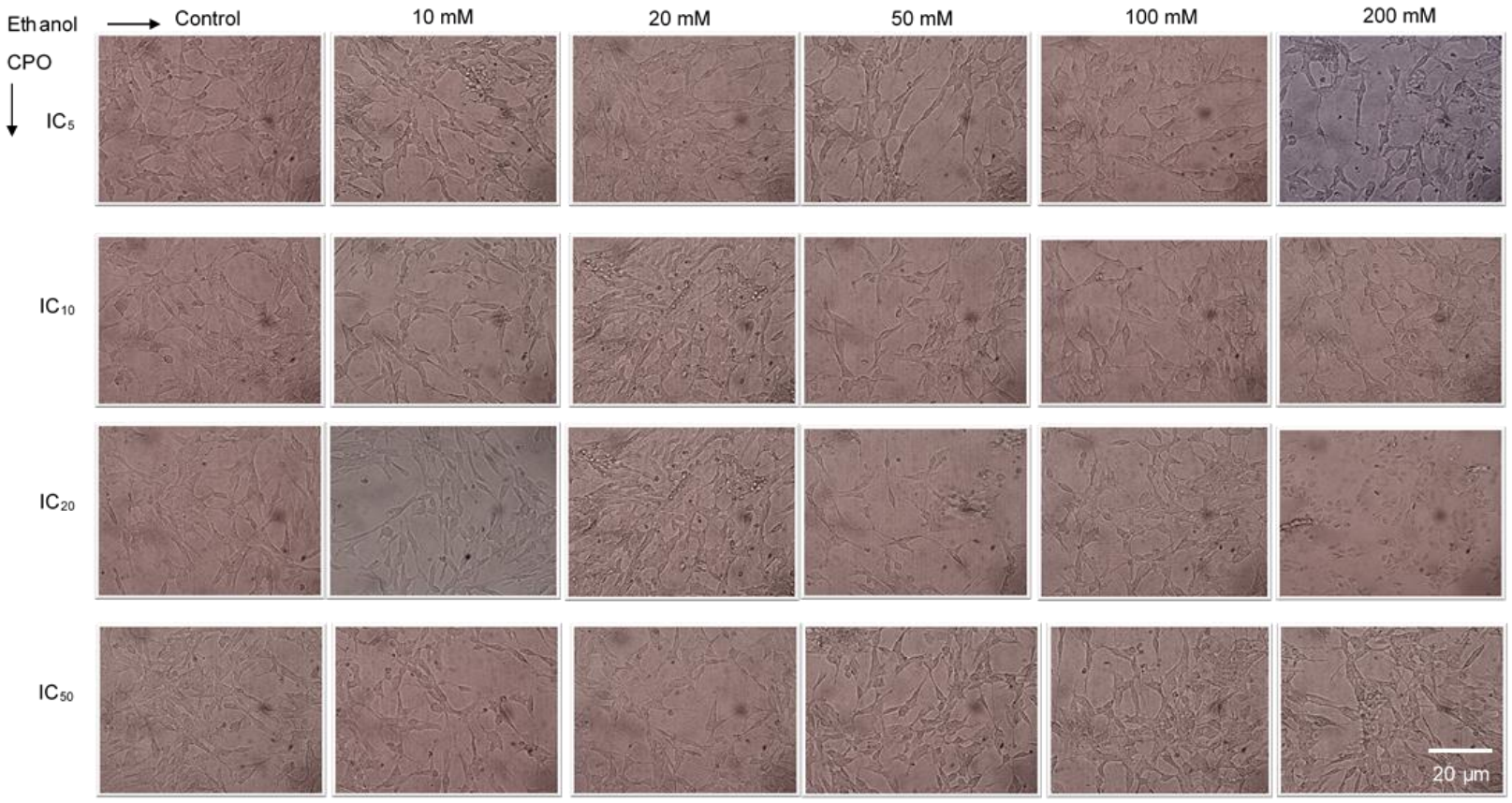
A


Ethanol
Control
10 mM
20 mM
50 mM
100 mM
200 mM
AZO
IC5
IC10
IC20
IC50
20 µm

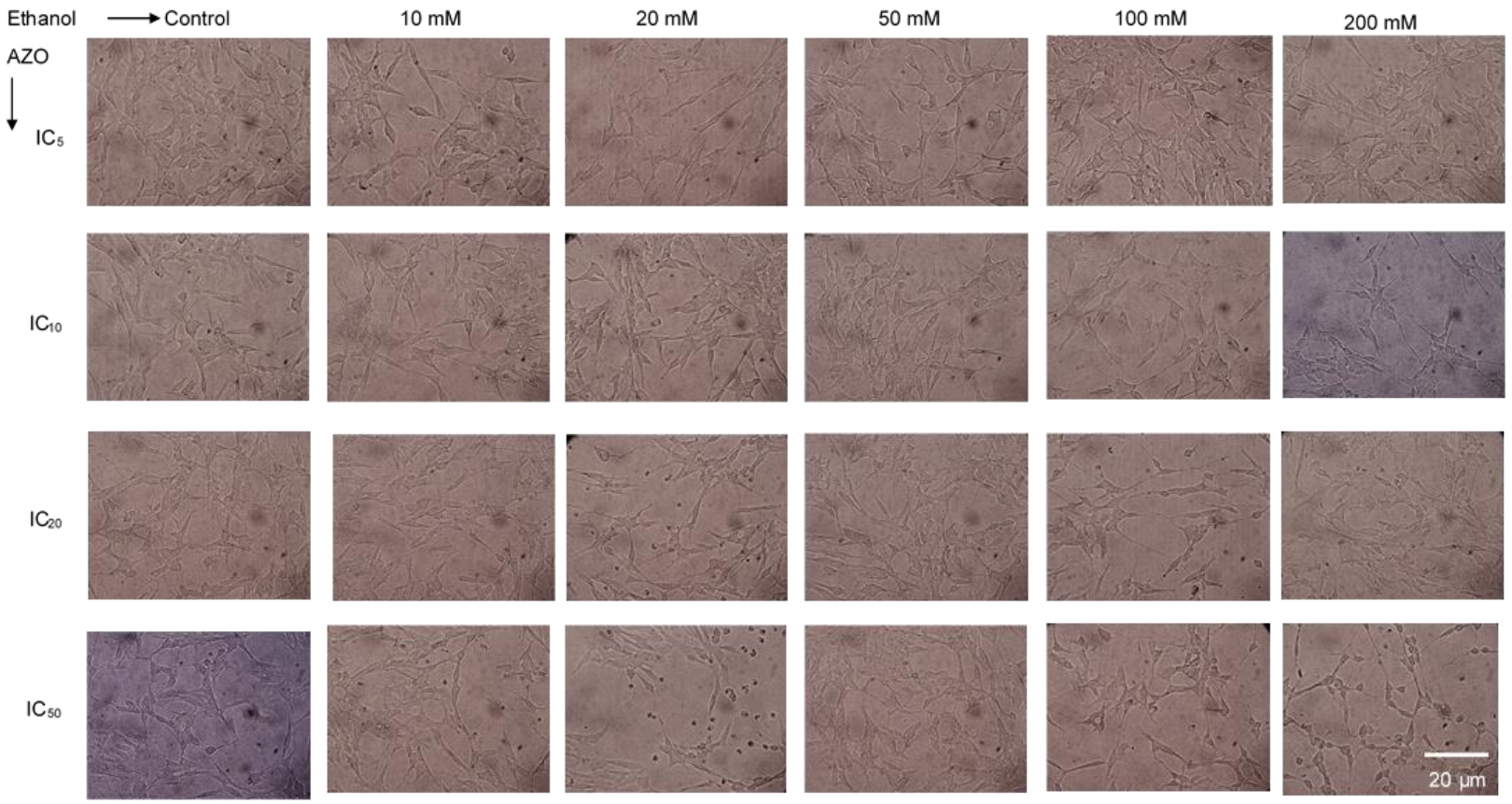
B


Ethanol
Control
10 mM
20 mM
50 mM
100 mM
200 mM
Aldicarb
IC5
IC10
IC20
IC50
20 µm

C


Ethanol
CPO
Control
10 mM
20 mM
50 mM
100 mM
200 mM
IC5
IC10
IC20
IC50
20 µm

D


Ethanol
Control
10 mM
20 mM
50 mM
100 mM
200 mM
AZO
IC5
IC10
IC20
IC50
20 µm

E

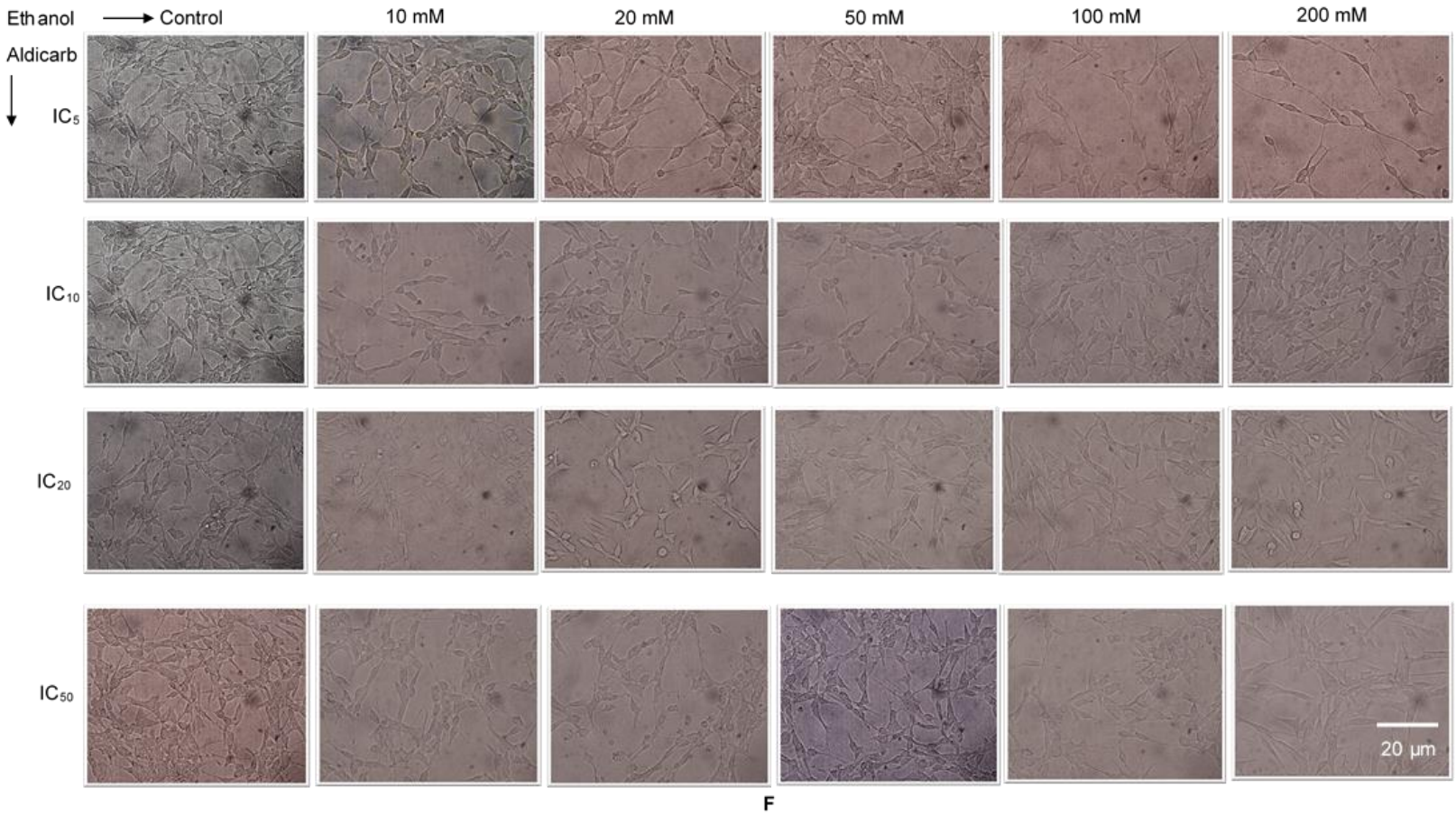


Figure 8-7: Co-exposure of CPO, AZO and Aldicarb with ethanol on SH-SY5Y cells for 24 h.
Undifferentiated cells A; B; C; Differentiated cells D, E, and F exposed to IC_5, IC_{10}, IC_{20} and IC_{50} of CPO, AZO and Aldicarb with ethanol over the concentration range of 10, 20, 50,100 and 200 mM. Images are captures from the phase contrast microscope with magnification of 40X.

8.2.4 Impact of co-exposure of ethanol with low doses of OP and carbamate pesticide on energy levels of SH-SY5Y cells.

Co-exposure of CPO, AZO, and Aldicarb on cellular ATP production were evaluated by using an ATP assay. Undifferentiated and differentiated cells were exposed to a combination of CPO, AZO, and Aldicarb low doses with 10 - 200 mM ethanol for 24 h.

8.2.4.1 *CPO and ethanol*

Joint toxicity of IC_5, IC_{10}, $IC_{20,}$ and IC_{50} of CPO with 10 - 200 mM ethanol for undifferentiated cells is depicted in Figure 8-8 A. Cellular ATP levels displayed a concentration-dependent decrease for joint toxicity of IC_5 and IC_{50} with ethanol when ethanol concentration continues to increase, mirroring the MTT dose responses. However, IC_{10} and IC_{20} with ethanol showed a non-monotonical decrease in cellular ATP levels compared with controls when the ethanol concentration increased. Joint toxicity of IC_{10} with 20 (12%) and 100 mM (4.7%) ethanol showed a non-significant decrease in cellular ATP levels in undifferentiated cells (p=0.1594; p=0.9465) compared to controls. However, 20 (17%) and 100 (14%) mM paired with IC_{20} of CPO showed a significant decrease in cellular ATP levels, but lower than that of 10 (22%) and 50 mM (31%) treatments.

All treatment combinations of CPO and ethanol in undifferentiated cells showed a significant influence on cellular ATP levels in undifferentiated cells than single treatments. All combinations of IC_{20} and IC_{50} treatment groups showed significant differences compared to their CPO alone treatments (red bar) while IC_5+50, 100, or 200 mM ethanol and IC_{10}+10 and 50 mM ethanol showed significance differences in ATP levels compared to their single treatments of CPO. All combinations induced significant levels of ATP depletion compared to

their corresponding ethanol treatments in each treatment groups (indicated by letters in graphs).

Differentiated SH-SY5Y cells exposed to CPO at low doses and ethanol showed similar behaviour observed in MTT assays (Figure 8.8 B). Cellular ATP levels of differentiated cells exposed to IC_5 and IC_{50} decreased in a concentration-dependent manner compared to their untreated controls. However, IC_{10} and IC_{20} treatments showed a non-monotonical decrease in ATP levels with increasing ethanol concertation. IC_{10} pairing with 20 mM (32%) ethanol treatment and IC_{20} treatment paring with 100 mM (27%) treatment showed slightly lower ATP drop compared to their non-treated controls. Interestingly, results showed that the combination of ethanol with IC_5 of CPO had a dramatic effect on cellular ATP levels compared to other treatment combination for differentiated cells.

IC_5 with different combinations of ethanol showed significant differences in cellular ATP levels than IC_5 of CPO treated alone, while IC_{50} combinations exhibited a significant difference in depletion of ATP levels with 10 - 200 mM ethanol than that of IC_{50} treated alone. Similarly, IC_{10} and IC_{20} combinations also displayed significant influence on ATP levels of differentiated cells than when treated alone. However, all combinations showed a significant drop in ATP levels compared to ethanol treatments than ethanol treated alone over the range of 10 - 200 mM for differentiated cells.

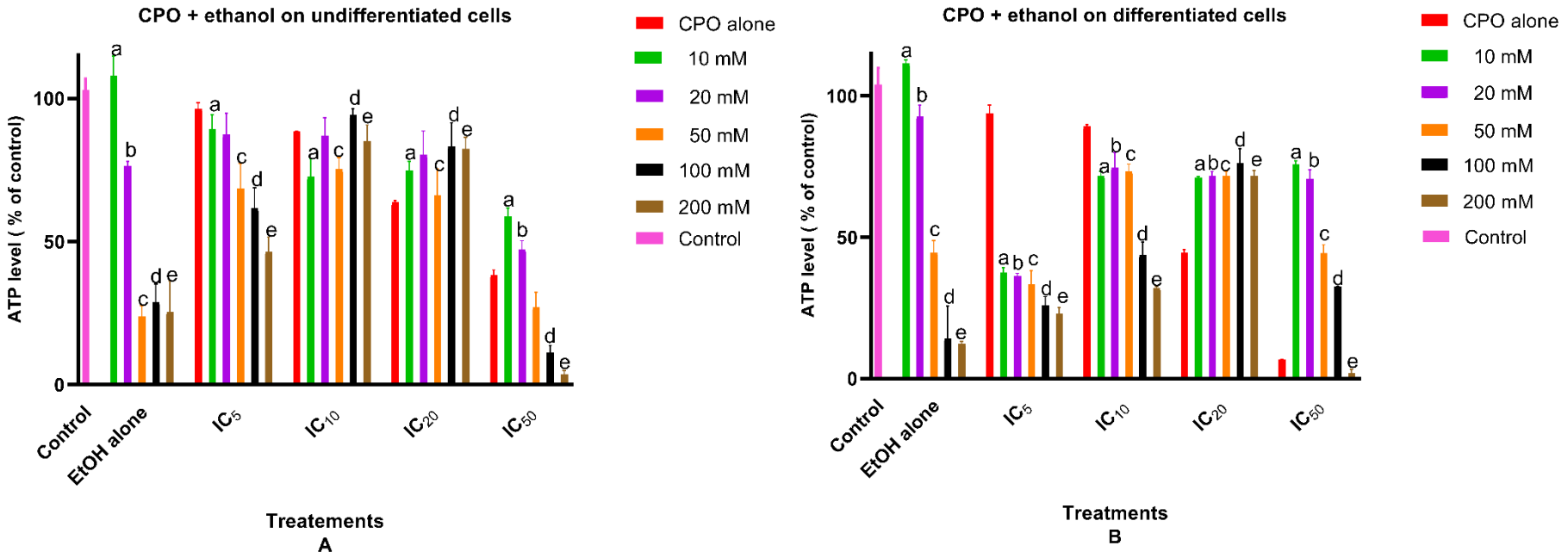


Figure 8-8: Co-exposure to ethanol and CPO and cellular ATP production in differentiated SH-SY5Y cells for 24 h.
A- undifferentiated cells and B- differentiated cells were treated with CPO and ethanol for 24 h. Cellular ATP levels were assessed using ATP assay. Readings were normalized to the ATP level of control, providing ATP level percentage, as a percentage value to the control. Control and treatments were performed as triplicates in 5 individual experiments (n=5). Results were analysed using two-way ANOVA with Tukey's multiple comparison and expressed as the mean ± standard error of the mean (SEM), when SEM bar is not apparent, this means that error is smaller than the symbol size. Comparison of treatments with non-treated control are indicated in Table 8-10; **a** - significance difference with 10 mM ethanol, **b** - significance difference with 20 mM ethanol, **c**- significance difference with 50 mM ethanol, **d** - significance difference with 100 mM ethanol, **e** - significance difference with 200 mM ethanol.

Table 8-10: Comparison of treatment combinations of ethanol and CPO with their corresponding non-treated controls. Results were analysed by two-way ANOVA and means comparison was done by Tukey's multiple comparison tests.

Treatments		Undifferentiated cells	Differentiated cells
IC_5	10	NS	<0.0001
	20	0.0116	<0.0001
	50	<0.0001	<0.0001
	100	<0.0001	<0.0001
	200	<0.0001	<0.0001
IC_{10}	10	<0.0001	<0.0001
	20	NS	<0.0001
	50	<0.0001	<0.0001
	100	NS	<0.0001
	200	NS	<0.0001
IC_{20}	10	<0.0001	<0.0001
	20	0.0004	<0.0001
	50	<0.0001	<0.0001
	100	0.0054	<0.0001
	200	0.0025	<0.0001
IC_{50}	10	<0.0001	<0.0001
	20	<0.0001	<0.0001
	50	<0.0001	<0.0001
	100	<0.0001	<0.0001
	200	<0.0001	<0.0001
IC_5		NS	0.0280
IC_{10}		<0.0001	<0.0001
IC_{20}		<0.0001	<0.0001
IC_{50}		<0.0001	<0.0001
10 mM		NS	NS
20 mM		<0.0001	0.0114
50 mM		<0.0001	<0.0001
100 mM		<0.0001	<0.0001
200 mm		<0.0001	<0.0001

NS- Not significant

8.2.4.2 *AZO and ethanol*

Undifferentiated SH-SY5Y cells exposed to AZO and ethanol showed ATP level decreases in IC_5, $IC_{20,}$ and IC_{50} coupled with ethanol in a concentration-dependent fashion along with increasing ethanol concentrations, suggesting higher concentrations caused a dramatic effect on cells compared to controls (Figure 8-9 A). A similar observation was apparent with the MTT assays and IC_{50} combination with different ethanol concentrations as these showed a dramatic effect on cellular metabolic activity and cell viability of undifferentiated cells (Figure 8-1 A). Interestingly, IC_{10} paired with 200 mM (29%) ethanol showed a moderate effect on cellular ATP levels of undifferentiated cells

compared to other treatment combinations with IC_{10}. Combination of 100 mM (36%) ethanol and IC_{10} of AZO on undifferentiated cells induced a slight drop in ATP levels when compared to that of 200 mM with IC_{10}.

IC_5 and IC_{10} of AZO combinations with ethanol over the 10 - 200 mM concentration range showed a significant drop in ATP than when treated alone, and IC_{20}+10, 100 and 200 mM ethanol showed a significant level of ATP changes compared with single IC_{20} treatment for undifferentiated cells. Interestingly, all combinations showed substantial ATP level decreases compared to single IC_{50} of AZO treatment in undifferentiated cells. However, all combinations showed significant ATP drop compared to single ethanol treatments in undifferentiated cells except IC_{50} when coupled with 100 and 200 mM ethanol treatments.

Differentiated cells exhibited a pesticide and ethanol induced concentration-dependent decrease in ATP levels compared to controls except for IC_{20} of AZO pairing with ethanol for increasing ethanol concentrations (Figure 8-9 B). IC_{20} paired with 100 mM (14.9%) treatment showed less ATP drop compared to other treatment combinations. A significant ATP level drop in differentiated cells in the same treatment group was observed for the joint toxicity of IC_{20} of AZO and 20 mM (48%) ethanol, compared to other higher concentrations of ethanol in combination with IC_{20} of AZO (Figure 8-9 B).

However, comparison of a single exposure of IC_5 of AZO showed a significant difference with all treatment combinations of IC_5 with ethanol. IC_{10}+10 mM and IC_{10}+20 mM, IC_{10}+50 mM ethanol exhibited similar levels of ATP drop compared with single exposures of IC_{10} of AZO for differentiated cells. On the other hand, IC_{20} with 10, 20, 50 and 200 mM ethanol showed significance differences in ATP level depletion compared with single exposures of IC_{20}. All treatment combinations with low doses of AZO and ethanol showed significant effects on

ATP levels compared to single exposures of ethanol over 10 - 200 mM concentration, except IC_5+200 mM and IC_{50}+200 mM treatments.

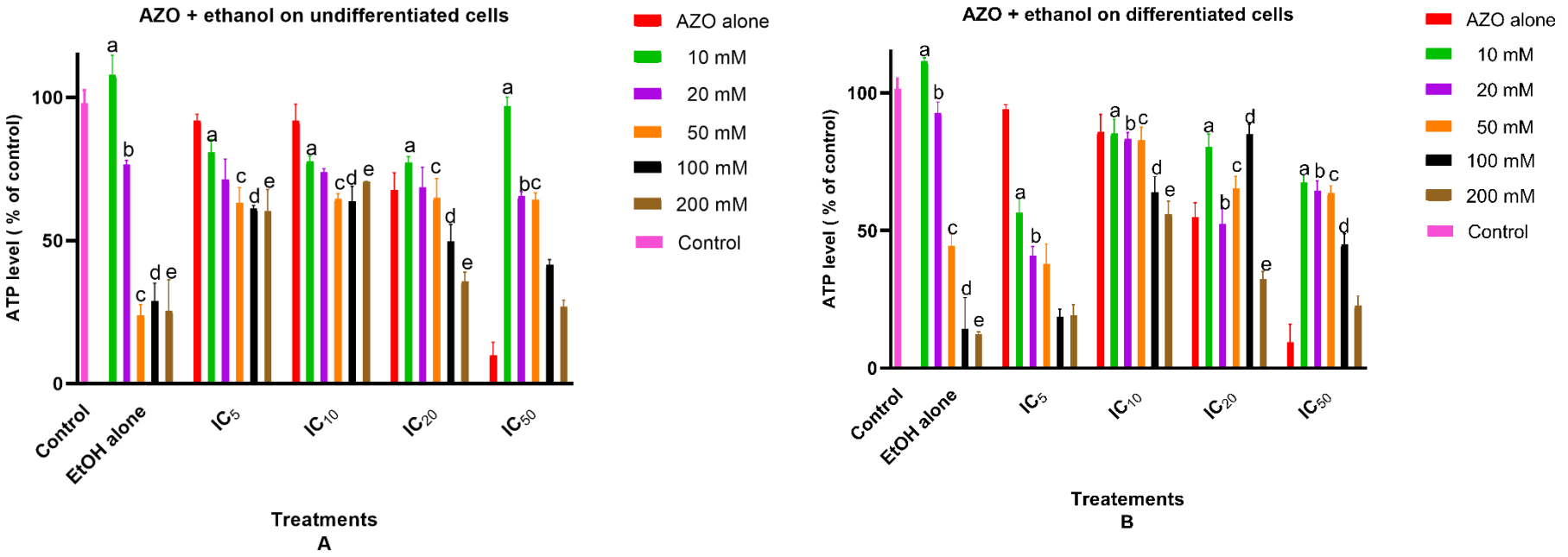


Figure 8-9: Co-exposure to ethanol and AZO and cellular ATP production in differentiated SH-SY5Y cells after 24 h.
A- undifferentiated cells and B- differentiated cells were treated with AZO and ethanol for 24 h. Cellular ATP levels were assessed using ATP assay. Readings were normalized to the ATP level of control, providing ATP level percentage, as a percentage value to the control. Control and treatments were performed as triplicates in 5 individual experiments (n=5). Results were analysed using two-way ANOVA with Tukey's multiple comparison and expressed as the mean ± standard error of the mean (SEM), when SEM bar is not apparent, this means that error is smaller than the symbol size. Comparison of treatments with non-treated control are indicated in Table 8-11; **a** - significance difference with 10 mM ethanol, **b** - significance difference with 20 mM ethanol, **c**- significance difference with 50 mM ethanol, **d** - significance difference with 100 mM ethanol, **e** - significance difference with 200 mM ethanol.

Table 8-11: Comparison of treatment combinations of ethanol and AZO with their corresponding non-treated controls. Results were analysed by two-way ANOVA and means comparison was done by Tukey's multiple comparison tests.

Treatments		Undifferentiated cells	Differentiated cells
IC_5	10	0.0002	<0.0001
	20	<0.0001	<0.0001
	50	<0.0001	<0.0001
	100	<0.0001	<0.0001
	200	<0.0001	<0.0001
IC_{10}	10	<0.0001	0.0005
	20	<0.0001	<0.0001
	50	<0.0001	<0.0001
	100	<0.0001	<0.0001
	200	<0.0001	<0.0001
IC_{20}	10	<0.0001	<0.0001
	20	<0.0001	<0.0001
	50	<0.0001	<0.0001
	100	<0.0001	<0.0001
	200	<0.0001	<0.0001
IC_{50}	10	NS	<0.0001
	20	<0.0001	<0.0001
	50	<0.0001	<0.0001
	100	<0.0001	<0.0001
	200	<0.0001	<0.0001
IC_5		NS	0.0280
IC_{10}		<0.0001	<0.0001
IC_{20}		<0.0001	<0.0001
IC_{50}		<0.0001	<0.0001
10 mM		NS	NS
20 mM		<0.0001	0.0114
50 mM		<0.0001	<0.0001
100 mM		<0.0001	<0.0001
200 mm		<0.0001	<0.0001

NS- Not significant

8.2.4.3 *Aldicarb and ethanol*

The combined effect of Aldicarb and ethanol is depicted in Figure 8-10. According to the graph, Aldicarb induced a significant ATP level drop in undifferentiated SH-SY5Y cells in a concentration-dependent fashion along with increasing ethanol concentration at each pesticide combination (Figure 8-10 A). Interestingly, IC_{20} pairing with 20 mM (13%) showed less ATP drop compared to IC_{20} paired with 10 mM ethanol (18%) but without a significant difference between the two treatments.

IC_5 treatment combinations with 10 and 20 mM ethanol showed a non-significant drop of ATP levels compared to single exposures, while IC_{10}+10 mM

and IC_{20}+10 or 20 mM, and IC_{50}+100 mM, also induced similar level of ATP production compared to their corresponding single exposures of Aldicarb. When considering the single exposure of ethanol, all treatment combinations with Aldicarb induced a significant level of ATP drop in undifferentiated cells (Figure 8-10 A).

Differentiated SH-SY5Y cells exposed to the joint toxicity of Aldicarb and ethanol exhibited a concentration-dependent decrease in each combination, showing a dramatic effect with Aldicarb and 200 mM ethanol in each combination at IC_5, $IC_{10,}$ and IC_{20}. However, IC_{50} paired with 200 mM ethanol showed a significant ATP decrease (58%), but it was greater (10%; p=0.0213) than that of the pairing with IC_{50} with 100 mM (48%) ethanol compared to controls for differentiated cells.

IC_5 paired with 10 mM ethanol did not induce significant energy level (ATP) drop in cells compared to the single IC_5 treatment, but all other combinations showed significant differences compared to single exposures, while all treatment combinations of IC_{10} and IC_{20} induced a significant effect on cellular ATP levels compared to the single treatment of Aldicarb (red bar). Interestingly, when compared with the single exposure of IC_{50} of Aldicarb, IC_{50}+10 - 200 mM ethanol induced significant decreases in energy levels depletion in differentiated cells However, all treatment combinations showed significant ATP level changes when compared with single exposures of 10 - 200 mM ethanol.

A comparison of undifferentiated cells vs differentiated cells with regard to the joint toxicity of CPO, AZO, and Aldicarb at low doses with ethanol over the concentration range of 0 - 200 mM, showed significant differences suggesting each combination has a selective effect on phenotypes in SH-SY5Y cells (Table 8-22).

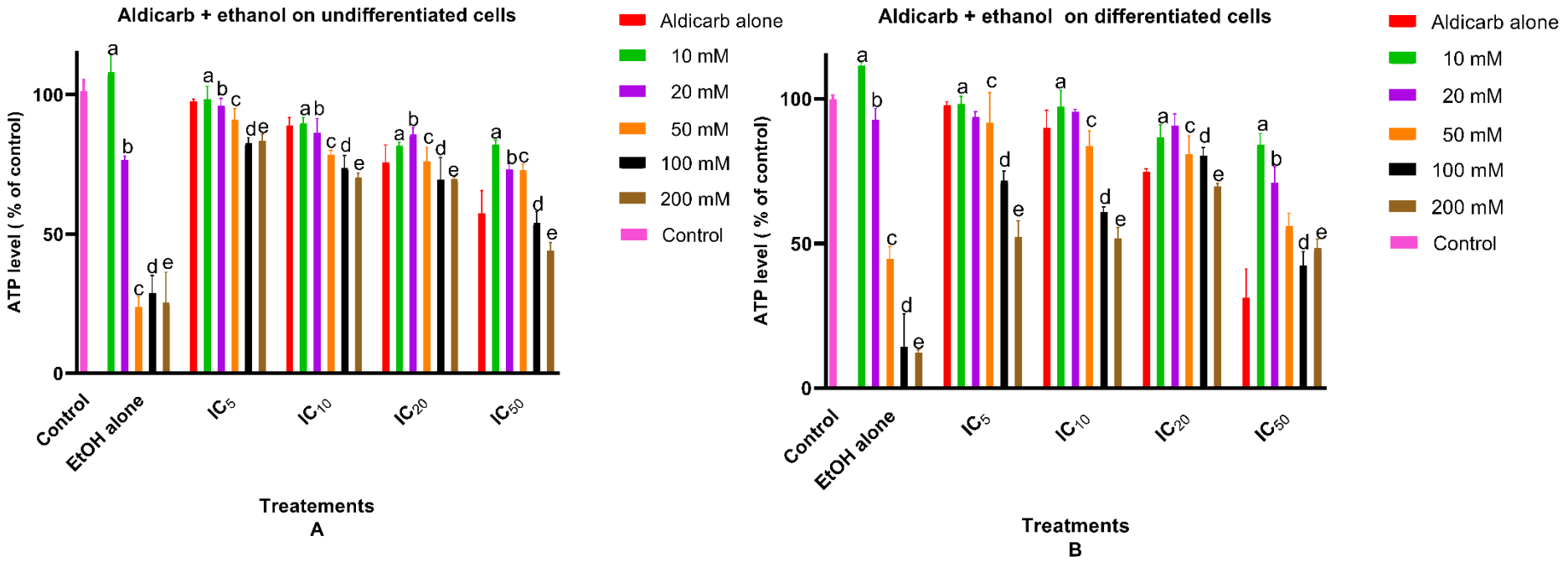


Figure 8-10: Co-exposure to ethanol and Aldicarb and effect on cellular ATP production in differentiated SH-SY5Y cells after 24 h.
A- undifferentiated cells and B- differentiated cells were treated with Aldicarb and ethanol for 24 h. Cellular ATP levels were assessed using ATP assay. Readings were normalized to the ATP level of control, providing ATP level percentage, as a percentage value to the control. Control and treatments were performed as triplicates in 5 individual experiments (n=5). Results were analysed using two-way ANOVA with Tukey's multiple comparison and expressed as the mean ± standard error of the mean (SEM), when SEM bar is not apparent, this means that error is smaller than the symbol size. Comparison of treatments with non-treated control are indicated in Table 8-12; **a** - significance difference with 10 mM ethanol, **b** - significance difference with 20 mM ethanol, **c**- significance difference with 50 mM ethanol, **d** - significance difference with 100 mM ethanol, **e** - significance difference with 200 mM ethanol.

Table 8-12: Comparison of treatment combinations of ethanol and Aldicarb with their corresponding non-treated controls. Results were analysed by two-way ANOVA and means comparison was done by Tukey's multiple comparison tests.

Treatments		Undifferentiated cells	Differentiated cells
IC_5	10	0.0002	<0.0001
	20	<0.0001	<0.0001
	50	<0.0001	<0.0001
	100	<0.0001	<0.0001
	200	<0.0001	<0.0001
IC_{10}	10	<0.0001	0.0005
	20	<0.0001	<0.0001
	50	<0.0001	<0.0001
	100	<0.0001	<0.0001
	200	<0.0001	<0.0001
IC_{20}	10	<0.0001	<0.0001
	20	<0.0001	<0.0001
	50	<0.0001	<0.0001
	100	<0.0001	<0.0001
	200	<0.0001	<0.0001
IC_{50}	10	NS	<0.0001
	20	<0.0001	<0.0001
	50	<0.0001	<0.0001
	100	<0.0001	<0.0001
	200	<0.0001	<0.0001
IC_5		NS	0.0280
IC_{10}		<0.0001	<0.0001
IC_{20}		<0.0001	<0.0001
IC_{50}		<0.0001	<0.0001
10 mM		NS	NS
20 mM		<0.0001	0.0114
50 mM		<0.0001	<0.0001
100 mM		<0.0001	<0.0001
200 mm		<0.0001	<0.0001

NS- Not significant

8.2.5 Co-exposure of ethanol with low doses of OP and carbamate pesticide, effects on SH-SY5Y cell differentiation.

The effect of co-exposures of CPO, AZO, and Aldicarb with ethanol at 10 - 200 mM on cell differentiation of SH-SY5Y cells were evaluated using neurite outgrowth inhibition. Cells were co-exposed to treatments (pesticide + ethanol) to differentiating cells and images were captured after 24 h.

8.2.5.1 *CPO and ethanol*

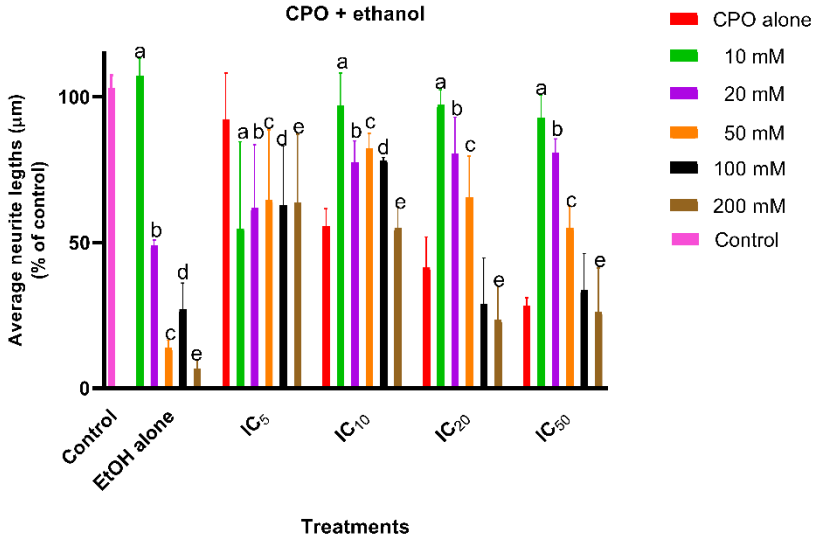


Figure 8-11: Effect of co-exposure of ethanol and CPO on neurite outgrowth of differentiating SH-SY5Y cells.
Differentiating cells were treated with CPO and ethanol for 24 h. Neurite lengths were measured using the neurite tracer tool in ImageJ using images captured from the phase contrast microscope. Measurements were normalized to the control, providing average neurite lengths as a percentage value to the control. Control and treatments were performed as triplicates in 5 individual experiments (n=5). Results were analysed using two-way ANOVA with Tukey's multiple comparison and expressed as the mean ± standard error of the mean (SEM). Comparison of treatments with non-treated control are indicated in Table 8-13; **a** - significance difference with 10 mM ethanol, **b** - significance difference with 20 mM ethanol, **c**- significance difference with 50 mM ethanol, **d** - significance difference with 100 mM ethanol, **e** - significance difference with 200 mM ethanol.

Co-exposure of CPO and ethanol decreased the neurite lengths in differentiating neurons in a concentration-dependent fashion, when increasing the concentration of ethanol for IC_{20} and IC_{50} paired with ethanol (Figure 8-11). However, IC_5 coupled with 10 mM significantly reduced neurite lengths (48%) compared to controls and with a 7 - 8% decrease compared to that of the IC_5 pairing with 20, 50, 100, and 200 mM ethanol. IC_{10} coupling with 10, 20, 50 and 100 mM did not show a significant effect on neurite initiation in differentiating cells, while IC_{10} pairing with 200 mM significantly (p<0.0002) reduced neurite lengths in differentiating cells compared to control treatments. IC_{20} and IC_{50} paired with 10 and 20 mM of ethanol did not show significant effects on neurite outgrowth compared to controls, while IC_{20} and IC_{50} coupled with 50, 100 and

200 mM (p<0.05) showed a significant decrease in neurite lengths compared to controls (Figure 8-14 A).

When compared with single exposures of IC_5, IC_{10}, IC_{20} and IC_{50} only IC_5 treatment combinations of ethanol with 10 - 200mM reduced the neurite outgrowth significantly, while IC_{10} combinations increased neurite outgrowth significantly compared to the single treatment of IC_{10}. All treatment combinations of IC_{20} were significantly different from single exposures, whereas IC_{20} combined with 10 (55%), 20 (39%) and 50 mM (24%) ethanol increased neurite outgrowth relative to the IC_{20} single exposure, and 100 (12%) and 200 (17%) mM significantly reduced neurite outgrowth.

All combinations increased neurite length significantly compared to 20 - 200 mM single exposures of ethanol except the 10 mM ethanol single exposure.

8.2.5.2 ***AZO and ethanol***

The effect of joint toxicity of AZO and 10 - 200 mM ethanol was depicted in Figure 8-12. IC_5, IC_{10}, IC_{20}, and IC_{50} of AZO paired with ethanol at 10 mM did not influence neurite outgrowth significantly, and IC_5, IC_{10}, and IC_{50} of AZO paired with 20 mM did not exhibit a significant reduction in neurite outgrowth in differentiating cells. 50 - 200 mM ethanol coupled with all low doses of AZO exhibited significant effects on neurite outgrowth in differentiating cells. Remarkably, IC_{20} of AZO paired with 20 and 50 mM ethanol showed a significant decrease in neurite outgrowth for differentiating SH-SY5Y cells compared to controls (90 and 92%, respectively) (p<0.0001), suggesting a synergistic effect of IC_{20} of AZO and 20 and 50 mM ethanol on differentiating cells.

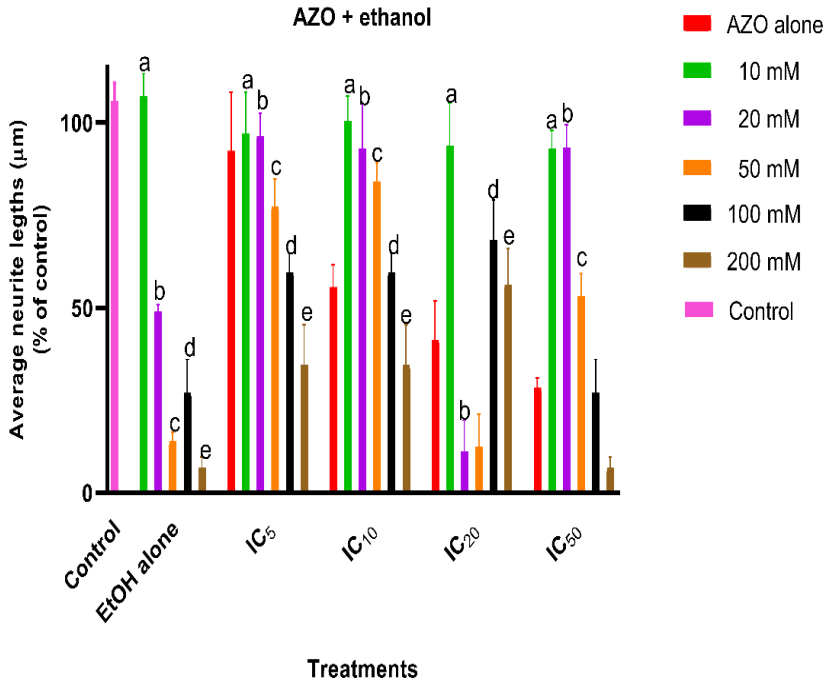


Figure 8-12: Effect of co-exposure of ethanol and AZO on neurite outgrowth of differentiating SH-SY5Y cells.
Differentiating cells were treated with AZO and ethanol for 24 h. Neurite lengths were measured using the neurite tracer tool in imageJ using images captured from phase contrast microscope. Measurements were normalized to the control, providing average neurite lengths as a percentage value to the control. Control and treatments were performed as triplicates in 5 individual experiments (n=5). Results were analysed using two-way ANOVA with Tukey's multiple comparison and expressed as the mean ± standard error of the mean (SEM). Comparison of treatments with non-treated control are indicated in Table 8-13; **a** - significance difference with 10 mM ethanol, **b** - significance difference with 20 mM ethanol, **c**- significance difference with 50 mM ethanol, **d** - significance difference with 100 mM ethanol, **e** - significance difference with 200 mM ethanol.

However, when comparing the main effects of IC_5, IC_{10}, $IC_{20,}$ and IC_{50} of AZO and ethanol at 10 - 200 mM concentrations, IC_{50} paired with 10 - 200 mM greatly influenced the neurite outgrowth of differentiating SH-SY5Y cells. IC_{50} of AZO paired with 200 mM ethanol showed a dramatic effect on neurite outgrowth by inhibiting neurite outgrowth by 96% compared to control treatments.

When considering the difference between single exposure of AZO on differentiating cells, IC_5 combined with 50 - 200 mM significantly reduced the outgrowth of neurites compared to a single exposure of IC_5. IC_{10} paired with 10 -100 mM increased neurite outgrowth significantly compared to single

exposures, although IC_{10} paired with 200 mM showed significantly decreased neurite lengths compared to a single exposure of IC_{10} of AZO. Interestingly, IC_{20} paired with 20 and 50 mM reduced the neurite outgrowth significantly compared to a single exposure of IC_{20} and with the other treatment combinations of IC_{20} (Figure 8-14 B, white arrows). IC_{50} remarkably reduced neurite outgrowth compared to a single exposure when in combination with 200 mM ethanol in differentiating cells.

8.2.5.3 *Aldicarb and ethanol*

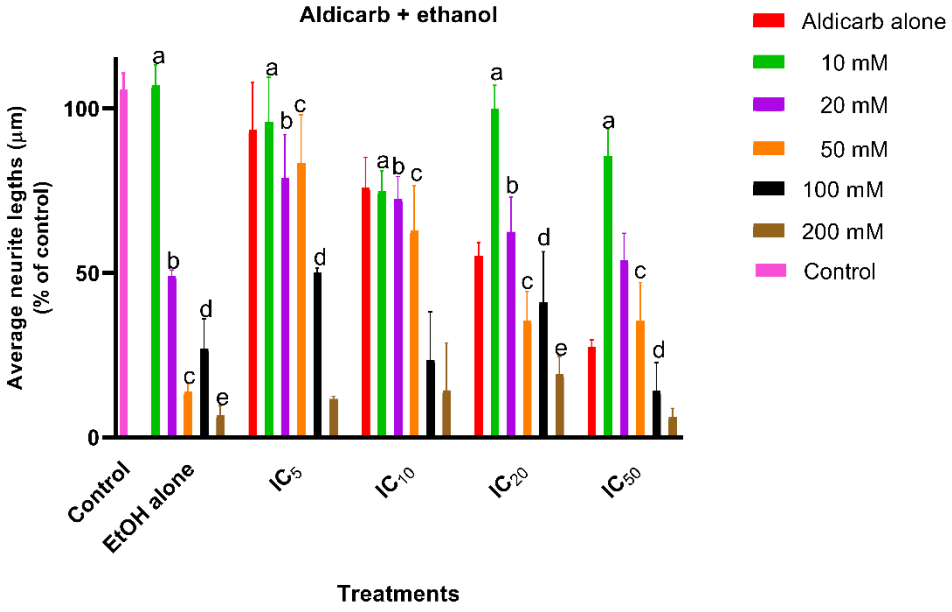


Figure 8-13: Effect of co-exposure of ethanol and Aldicarb on neurite outgrowth of differentiating SH-SY5Y cells.
Differentiating cells were treated with Aldicarb and ethanol for 24 h. Neurite lengths were measured using the neurite tracer tool in ImageJ using images captured from phase contrast microscope. Measurements were normalized to the control, providing average neurite lengths as percentage value to the control. Control and treatments were performed as triplicates in 5 individual experiments (n=5). Results were analysed using two-way ANOVA with Tukey's multiple comparison and expressed as the mean ± standard error of the mean (SEM). Comparison of treatments with non-treated control are indicated in Table 8-13; **a** - significance difference with 10 mM ethanol, **b** - significance difference with 20 mM ethanol, **c**- significance difference with 50 mM ethanol, **d** - significance difference with 100 mM ethanol, **e** - significance difference with 200 mM ethanol.

According to Figure 8-13, all Aldicarb and ethanol combinations showed a concentration-dependent decrease in neurite lengths in differentiating cells

compared to controls with increasing ethanol concentrations. IC_5 and IC_{20} of Aldicarb combined with ethanol at 10 mM did not induce significant neurite inhibition compared to controls. 20 mM ethanol concentration paired with IC_5, IC_{10} and IC_{20} of Aldicarb induced significant inhibition of neurite outgrowth in differentiating cells compared to controls (by 24%, 33%, and 40%, respectively). IC_{50} of Aldicarb paired with 20 mM (49%) ethanol dramatically reduced the neurite outgrowth compared to controls in differentiating cells. IC_5 combined with 50 mM ethanol induced neurite outgrowth inhibition, but this was not statistically significant (p=0.0811) compared to controls. IC_5, IC_{10}, $IC_{20,}$ and IC_{50} of Aldicarb combined with 200 mM ethanol showed a dramatic effect on neurite outgrowth inhibition in differentiating cells and the effect was strongest with high pesticide and ethanol concentrations compared to control treatments (IC_{50}+200 mM ethanol = 96% inhibition) (Figure 8-13).

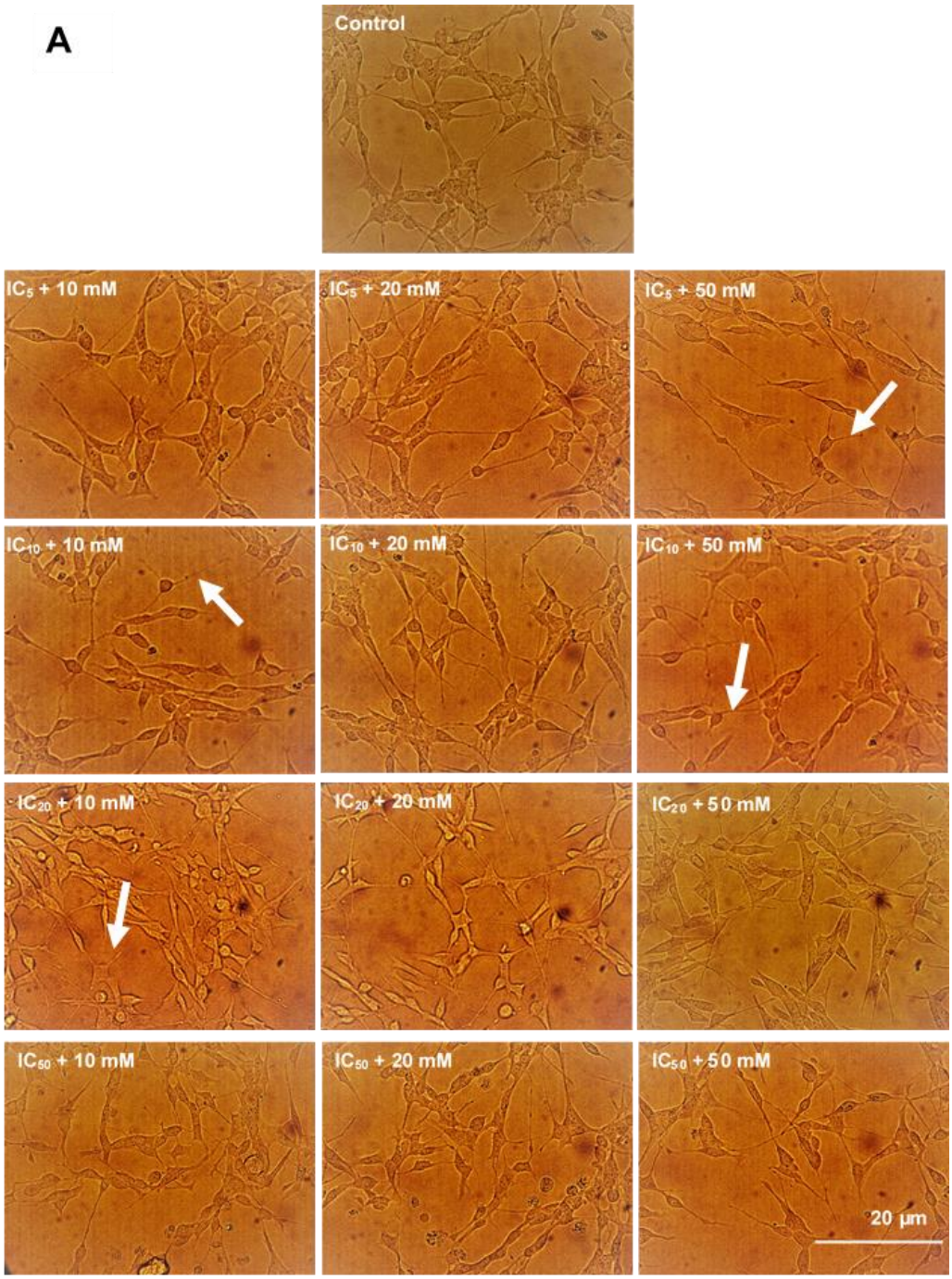
All combinations showed a significant difference between the single exposures of Aldicarb and ethanol except IC_5+50 mM, IC_{10}+10 mM and IC_{50}+200 mM with their corresponding Aldicarb single exposures.

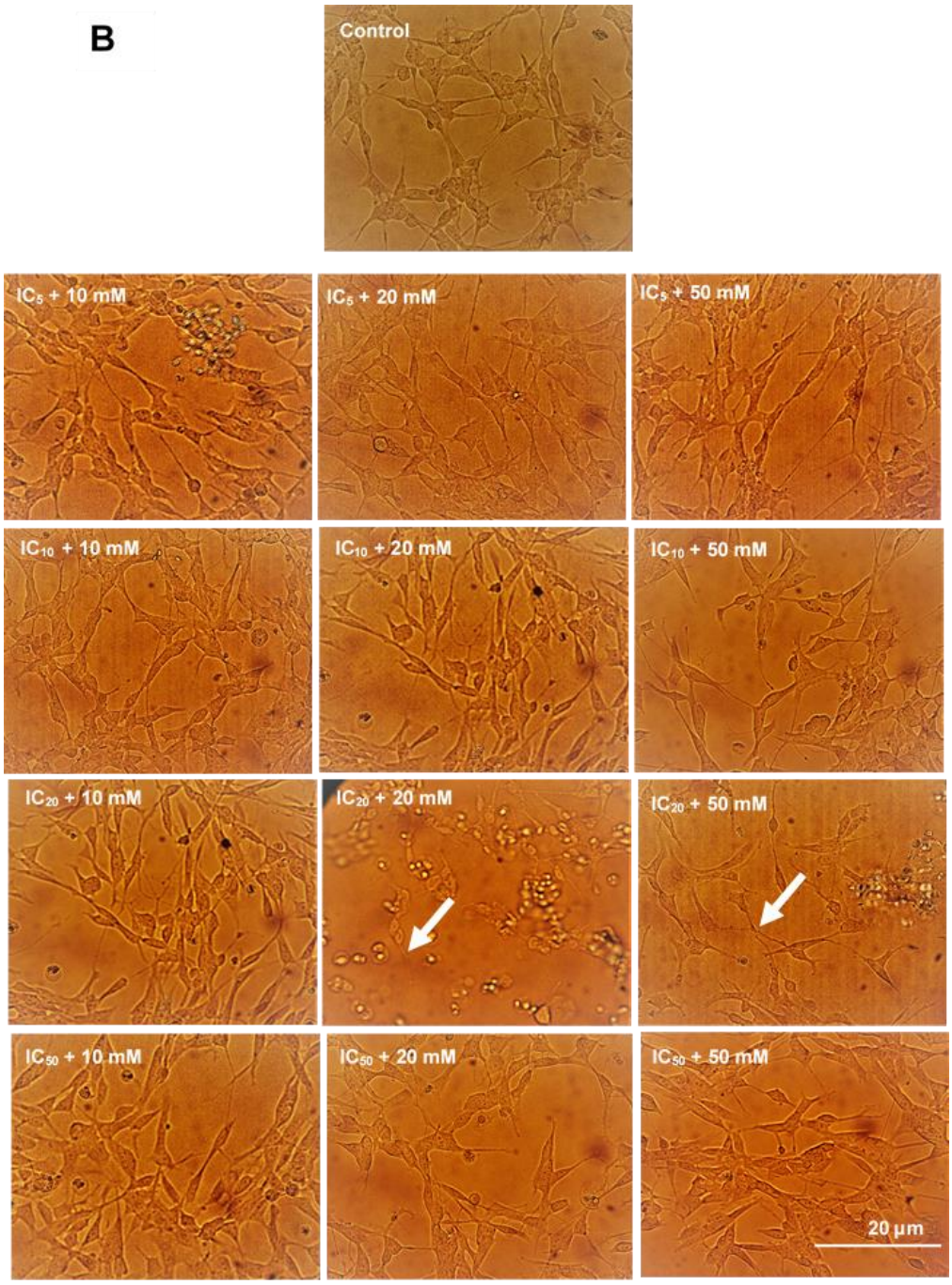
The quantification of neurite outgrowth inhibitions was further assessed with microscopic images. The images showed that in the absence of pesticides, cells had typical cellular morphology of pre-differentiated cells, with cell body and long extending processes. After exposure to different concentrations of CPO, AZO, and Aldicarb in combination with different concentrations of ethanol, inhibition of neurite outgrowth was apparent compared to the controls when concentrations continued to increase (Figure 8-14).

Table 8-13: Comparison of treatment combinations of ethanol and pesticides with their corresponding non-treated controls. Results were analysed by two-way ANOVA and means comparison was done by Tukey's multiple comparison tests.

Treatments		CPO	AZO	Aldicarb
IC_5	10	<0.0001	NS	NS
	20	0.0007	NS	0.0133
	50	0.0021	0.0012	NS
	100	0.0010	<0.0001	<0.0001
	200	0.0014	<0.0001	<0.0001
IC_{10}	10	NS	NS	0.0005
	20	0.0620	NS	0.0001
	50	NS	0.0404	<0.0001
	100	NS	<0.0001	<0.0001
	200	<0.0001	<0.0001	<0.0001
IC_{20}	10	NS	NS	NS
	20	NS	<0.0001	<0.0001
	50	0.0028	<0.0001	<0.0001
	100	<0.0001	<0.0001	<0.0001
	200	<0.0001	<0.0001	<0.0001
IC_{50}	10	NS	NS	NS
	20	NS	NS	<0.0001
	50	<0.0001	<0.0001	<0.0001
	100	<0.0001	<0.0001	<0.0001
	200	<0.0001	<0.0001	<0.0001
IC_5		NS	NS	NS
IC_{10}		<0.0001	<0.0001	0.0009
IC_{20}		<0.0001	<0.0001	<0.0001
IC_{50}		<0.0001	<0.0001	<0.0001
10 mM		NS	NS	NS
20 mM		<0.0001	<0.0001	<0.0001
50 mM		<0.0001	<0.0001	<0.0001
100 mM		<0.0001	<0.0001	<0.0001
200 mm		<0.0001	<0.0001	<0.0001

NS- Not significant


A
Control
IC5 + 10 mM
IC5 + 20 mM
IC5 + 50 mM
IC10 + 10 mM
IC10 + 20 mM
IC10 + 50 mM
IC20 + 10 mM
IC20 + 20 mM
IC20 + 50 mM
IC50 + 10 mM
IC50 + 20 mM
IC50 + 50 mM
20 µm


B
Control
IC5 + 10 mM
IC5 + 20 mM
IC5 + 50 mM
IC10 + 10 mM
IC10 + 20 mM
IC10 + 50 mM
IC20 + 10 mM
IC20 + 20 mM
IC20 + 50 mM
IC50 + 10 mM
IC50 + 20 mM
IC50 + 50 mM
20 µm

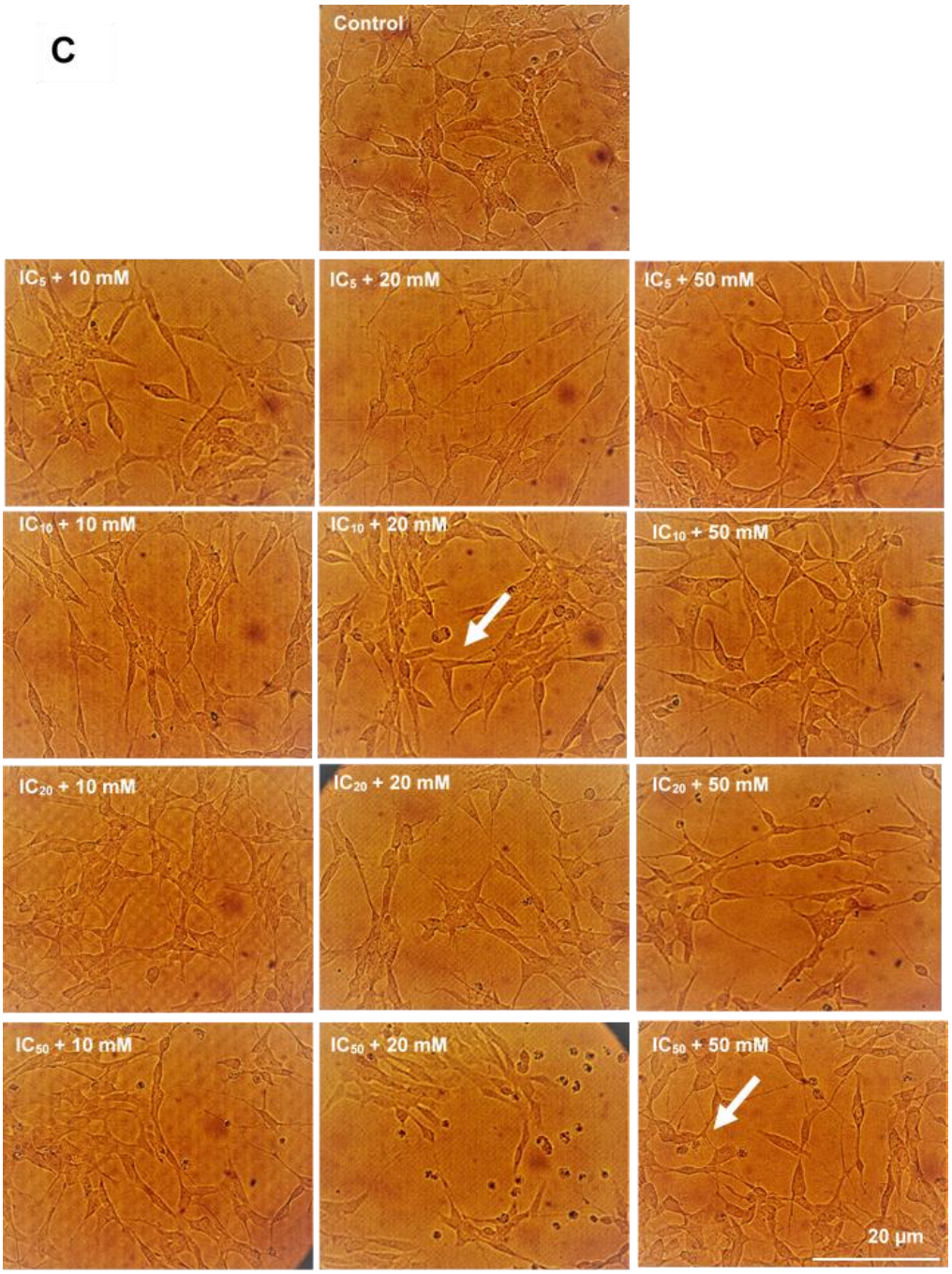


Figure 8-14: Effect of joint toxicity of CPO, AZO and Aldicarb on differentiating SH-SY5Y cells.

Significant changes in neurite out growth in differentiating cells co-exposed to IC_5, IC_{10}, IC_{20} and IC_{50} of CPO (A), AZO (B) and Aldicarb (C) with ethanol over the range of 10, 20, 50,100 and 200 mM. Images are captures from phase contrast microscope with magnification of 40X. White arrows indicate the reduced neurite lengths in differentiating cells.

8.2.6 Co-exposure of ethanol with low doses of OP and carbamate pesticide on induction of oxidative stress in SH-SY5Y.

Next, to gain insight into the oxidative stress induced by co-exposure of CPO, AZO, and Aldicarb with ethanol on undifferentiated and differentiated SH-SY5Y cells, cellular ROS levels were quantified using a DCDFA assay.

8.2.6.1 *CPO and ethanol*

According to Figure 8-15 A, CPO exposed undifferentiated cells generated significant levels of ROS compared to control in each combination of treatment with CPO and ethanol for 24 h exposures. 200 mM ethanol induced the highest levels of ROS in each combination group compared to controls. IC_5 paired with 10 mM (16 %) and 50 mM (30%) generated comparatively low levels of ROS to those from 20, 100, and 200 mM ethanol (p<0.0001) for the same group of combinations. A similar pattern of ROS generation was apparent at IC_{50} of CPO with 10 and 50 mM ethanol, where other combinations of ethanol and CPO in the same group generated more ROS when compared to controls. Interestingly, IC_{20} combined with 10 and 100 mM ethanol showed a slightly lower ROS production compared to the 20, 50 and 200 mM ethanol paired with CPO IC_{20}.

IC_{10} of CPO combined with ethanol showed similar levels of ROS generation in each concentration of ethanol suggesting all concentration combinations of that group induced a significant level of ROS in undifferentiated cells.

Graph 8-15 A indicates all treatment combinations induced statistically significant levels of ROS compared to their corresponding CPO or ethanol single treatments in undifferentiated cells.

Differentiated cells co-exposed to CPO and ethanol showed significant levels of ROS generation compared with controls in all treatment combinations (Figure 8-15 B). 200 mM joined with IC_5, IC_{10}, $IC_{20,}$ and IC_{50} of CPO induced significantly

higher levels of ROS (>80%) compared to controls than other treatment combinations within each group of treatments, as depicted in Figure 8-15 B., IC_{10} combined with 20 and 50 mM ethanol also produced more ROS (93% and 74%, respectively) than other combinations with IC_{20} within the IC_{10} groups of treatments. Similarly, IC_{20} paired with 10 and 50 mM ethanol induced significant levels of ROS in differentiated cells compared to controls, and other treatment combinations within the group. These results suggest that higher concentrations of ethanol induce ROS in differentiated cells in a concentration dependent manner with CPO (Figure 8-15 B).

IC_5 combined with 10, 20, 50 and 200 mM ethanol showed significant ROS generation compared to the single IC_5 treatment on differentiated cells, while 20, 50, 200 mM with IC_{10} and 10, 50 and 200 mM with IC_{20} showed significant levels of ROS generation, compared to their single treatments of CPO for differentiated cells. 100 mM ethanol did not exhibit significant ROS generation compared to the single ethanol treatment in differentiated cells.

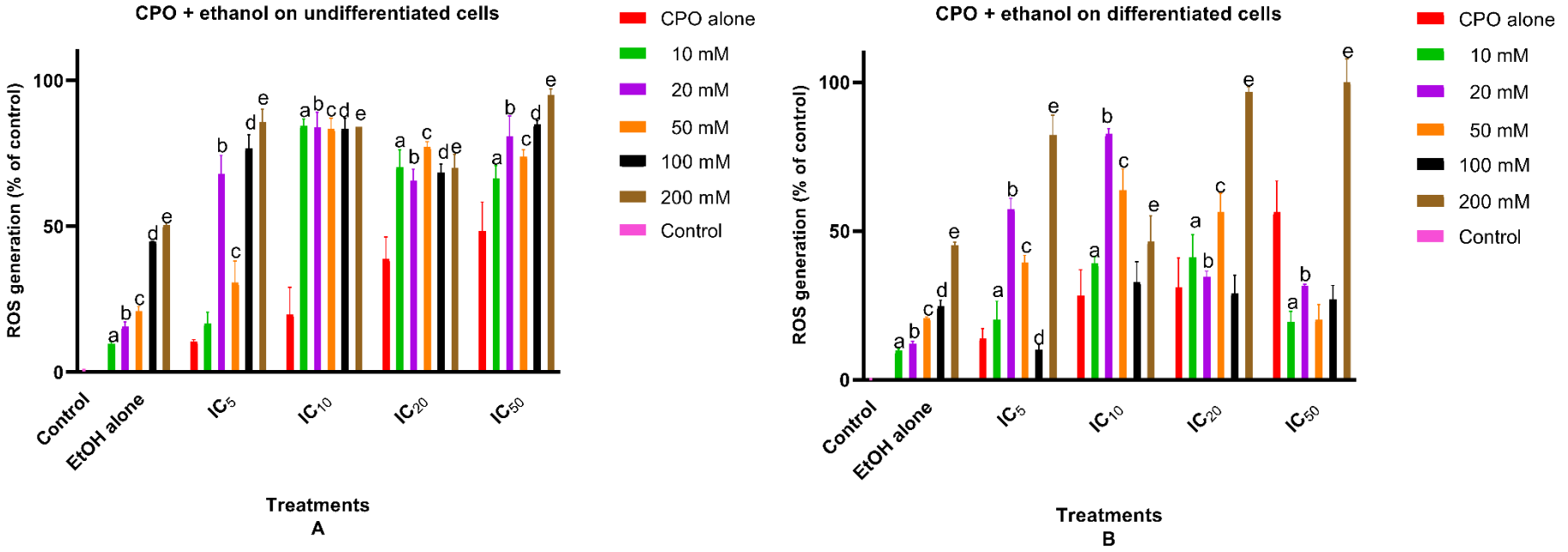


Figure 8-15: Effect of co-exposure to ethanol and CPO on ROS generation in undifferentiated and differentiated SH-SY5Y cells after 24 h.

A- undifferentiated cells and B- differentiated were treated with CPO and ethanol for 24 h. Cellular ROS levels were assessed using DCFDA assay. Readings were normalized to the ROS level of control, providing ROS level in percentage, as a percentage value to the control. Control and treatments were performed as triplicates in 5 individual experiments (n=5). Results were analysed using two-way ANOVA with Tukey's multiple comparison and expressed as the mean ± standard error of the mean (SEM), when SEM bar is not apparent, this means that error is smaller than the symbol size. Comparison of treatments with non-treated control are indicated in Table 8-14; **a** - significance difference with 10 mM ethanol, **b** - significance difference with 20 mM ethanol, **c**- significance difference with 50 mM ethanol, **d** - significance difference with 100 mM ethanol, **e** - significance difference with 200 mM ethanol.

Table 8-14: Comparison of treatment combinations of ethanol and CPO with their corresponding non-treated controls. Results were analysed by two-way ANOVA and means comparison was done by Tukey's multiple comparison tests.

Treatments		Undifferentiated cells	Differentiated cells
IC_5	10	<0.0001	<0.0001
	20	<0.0001	<0.0001
	50	<0.0001	<0.0001
	100	<0.0001	NS
	200	<0.0001	<0.0001
IC_{10}	10	<0.0001	<0.0001
	20	<0.0001	<0.0001
	50	<0.0001	<0.0001
	100	<0.0001	<0.0001
	200	<0.0001	<0.0001
IC_{20}	10	<0.0001	<0.0001
	20	<0.0001	<0.0001
	50	<0.0001	<0.0001
	100	<0.0001	<0.0001
	200	<0.0001	<0.0001
IC_{50}	10	<0.0001	0.0009
	20	<0.0001	<0.0001
	50	<0.0001	0.0004
	100	<0.0001	<0.0001
	200	<0.0001	<0.0001
IC_5		0.0436	0.0162
IC_{10}		<0.0001	<0.0001
IC_{20}		<0.0001	<0.0001
IC_{50}		<0.0001	<0.0001
10 mM		<0.0001	<0.0001
20 mM		<0.0001	<0.0001
50 mM		<0.0001	<0.0001
100 mM		<0.0001	<0.0001
200 mm		<0.0001	<0.0001

NS- Not significant

8.2.6.2 *AZO and ethanol*

The joint toxicity of AZO and ethanol on ROS generation in undifferentiated cells was depicted in Figure 8-16 A. According to the graph, IC_{10} and IC_{50} concentrations of AZO showed a concentration-dependent increase in ROS levels compared to controls with increasing ethanol concentration. IC_5 of AZO combined with 20, 100 and 200 mM ethanol generated similar levels of ROS (~86%) compared to controls, while 10, 50, and 200 mM ethanol combined with IC_{20} of AZO generated a concentration-dependent ROS production in undifferentiated cells (10 mM - 75%; 50 mM: 80% and 200 mM: 85%). 20 mM

and 100 mM when paired with IC_{20} showed a decrease (69% and 58%, respectively), in the levels of ROS compared to 10, 50, and 100 mM paired with IC_{20} of AZO for undifferentiated cells. IC_{50} of AZO paired with 10, 20, 50, 100 and 200 mM ethanol generated the highest levels of ROS in every combination when compared to the other combinations of AZO and ethanol for undifferentiated cells. All combinations generated significantly higher levels of ROS compared to their single treatments of ethanol for 10 - 200 mM ethanol, while at IC_5, IC_{10} and IC_{20} all combinations induced significant level of ROS relative to their single treatments for AZO in differentiated cells.

Figure 8-16 B shows the interactive effect of AZO and ethanol on ROS generation in differentiated SH-SY5Y after a 24 h exposure. IC_5 and IC_{10} of AZO combination with 10, 20, 50, 100 and 200 mM ethanol showed a concentration-dependent increase in ROS levels in differentiated cells compared to controls, over the range of 10 - 200 mM ethanol. IC_5 paired with 20 and 50 mM ethanol generated similar levels of ROS in differentiated cells compared to controls (36%). The interactive effect of IC_{10} of AZO paired with 10 and 20 mM ethanol generated similar levels of ROS in undifferentiated cells at 24 h exposure. However, IC_{20} and IC_{50} of AZO produced a non-monotonical increase in ROS levels compared to their controls over the range of 10 - 200 mM ethanol. IC_{20} of AZO paired with 20 and 100 mM ethanol generated a lower level of ROS compared to 10, 50 and 200 mM, while IC_{50} combined with 10 and 20 mM ethanol generated low levels of ROS compared with other group combinations of AZO and ethanol for differentiated cells. IC_{50} of AZO paired with 10 mM ethanol generated significantly lower ($p<0.05$) levels of ROS when compared to IC_{50} combined with 50, 100, and 200 mM ethanol for differentiated cells. All combinations showed significant differences in ROS generation compared to their corresponding single treatments with ethanol, whereas IC_{10} and IC_{20} paired

with 10 and 50, and 20 and 100 mM ethanol, respectively, did not induce significant ROS levels compared to IC_{10} and IC_{20} single treatments of AZO.

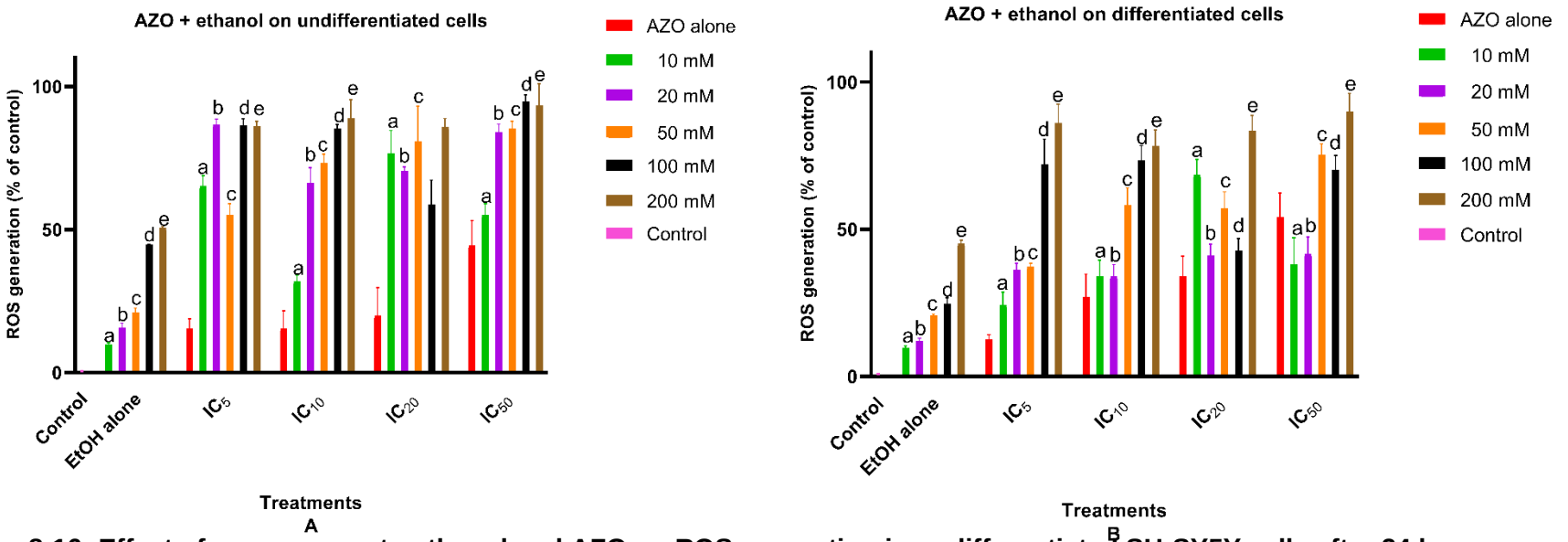


Figure 8-16: Effect of co-exposure to ethanol and AZO on ROS generation in undifferentiated SH-SY5Y cells after 24 h.
A- undifferentiated cells and B- differentiated were treated with AZO and ethanol for 24 h. Cellular ROS levels were assessed using DCFDA assay. Readings were normalized to the ROS level of control, providing ROS level in percentage, as a percentage value to the control. Control and treatments were performed as triplicates in 5 individual experiments (n=5). Results were analysed using two-way ANOVA with Tukey's multiple comparison and expressed as the mean ± standard error of the mean (SEM), when SEM bar is not apparent, this means that error is smaller than the symbol size. Comparison of treatments with non-treated control are indicated in Table 8-15; **a** - significance difference with 10 mM ethanol, **b** - significance difference with 20 mM ethanol, **c**- significance difference with 50 mM ethanol, **d** - significance difference with 100 mM ethanol, **e** - significance difference with 200 mM ethanol.

Table 8-15: Comparison of treatment combinations of ethanol and AZO with their corresponding non-treated controls. Results were analysed by two-way ANOVA and means comparison was done by Tukey's multiple comparison tests.

Treatments		Undifferentiated cells	Differentiated cells
IC_5	10	<0.0001	<0.0001
	20	<0.0001	<0.0001
	50	<0.0001	<0.0001
	100	<0.0001	<0.0001
	200	<0.0001	<0.0001
IC_{10}	10	<0.0001	<0.0001
	20	<0.0001	<0.0001
	50	<0.0001	<0.0001
	100	<0.0001	<0.0001
	200	<0.0001	<0.0001
IC_{20}	10	<0.0001	<0.0001
	20	<0.0001	<0.0001
	50	<0.0001	<0.0001
	100	<0.0001	<0.0001
	200	<0.0001	<0.0001
IC_{50}	10	NS	<0.0001
	20	<0.0001	<0.0001
	50	<0.0001	<0.0001
	100	<0.0001	<0.0001
	200	<0.0001	<0.0001
IC_5		0.0015	0.0206
IC_{10}		0.0020	<0.0001
IC_{20}		<0.0001	<0.0001
IC_{50}		<0.0001	<0.0001
10 mM		<0.0001	<0.0001
20 mM		<0.0001	<0.0001
50 mM		<0.0001	<0.0001
100 mM		<0.0001	<0.0001
200 mm		<0.0001	<0.0001

NS- Not significant

8.2.6.3 *Aldicarb and ethanol*

In undifferentiated cells, joint toxicity of Aldicarb and ethanol induced ROS generation compared to controls as depicted in Figure 8-17 A. The highest level of ROS generation was observed in IC_{10} of Aldicarb paired with 50 mM (96%) ethanol, while the lowest was recorded for IC_{50} of Aldicarb combined with 10 mM (4%) ethanol in undifferentiated cells compared to the control treatments. However, the pairing of IC_5 of Aldicarb produced a concentration-dependent ROS generation along with increasing ethanol concentration. IC_{50} of Aldicarb paired with 100 and 200 mM (86%) ethanol generated similar levels of ROS

compared to controls, while IC_{20} combined with 50 mM ethanol generated the highest levels of ROS in that group for undifferentiated cells.

All treatment combinations of Aldicarb and ethanol induced significant levels of ROS compared to their corresponding single treatments of Aldicarb and ethanol alone.

All combination groups of Aldicarb and ethanol showed a non-monotonical increase in ROS levels for differentiated cells treated for a 24 h exposure. IC_5, IC_{10}, $IC_{20,}$ and IC_{50} of Aldicarb paired with 200 mM generated the highest levels of ROS in all combination groups. IC_{20} of Aldicarb paired with 100 mM ethanol generated a slightly higher level of ROS compared to that of IC_{20} with 200 mM (3.5%). IC_{10} paired with 20 (60%) and 200 (86%) mM ethanol generated significantly higher ROS than other treatment combinations with IC_{10}. IC_{50} induced a concentration-dependent increase of ROS generation over the range of 10 - 200 mM ethanol.

All combinations induced significant ROS in differentiated cells than those generated for ethanol alone treatments. Interestingly, IC_{20} did not induce a significant level of ROS with 10 and 20 mM ethanol combinations relative to single treatments (Figure 8-17 B; red bar).

A comparison of undifferentiated cells vs differentiated cells showed a significant interaction between each treatment group for the toxicity of Aldicarb and ethanol (Table 8-22).

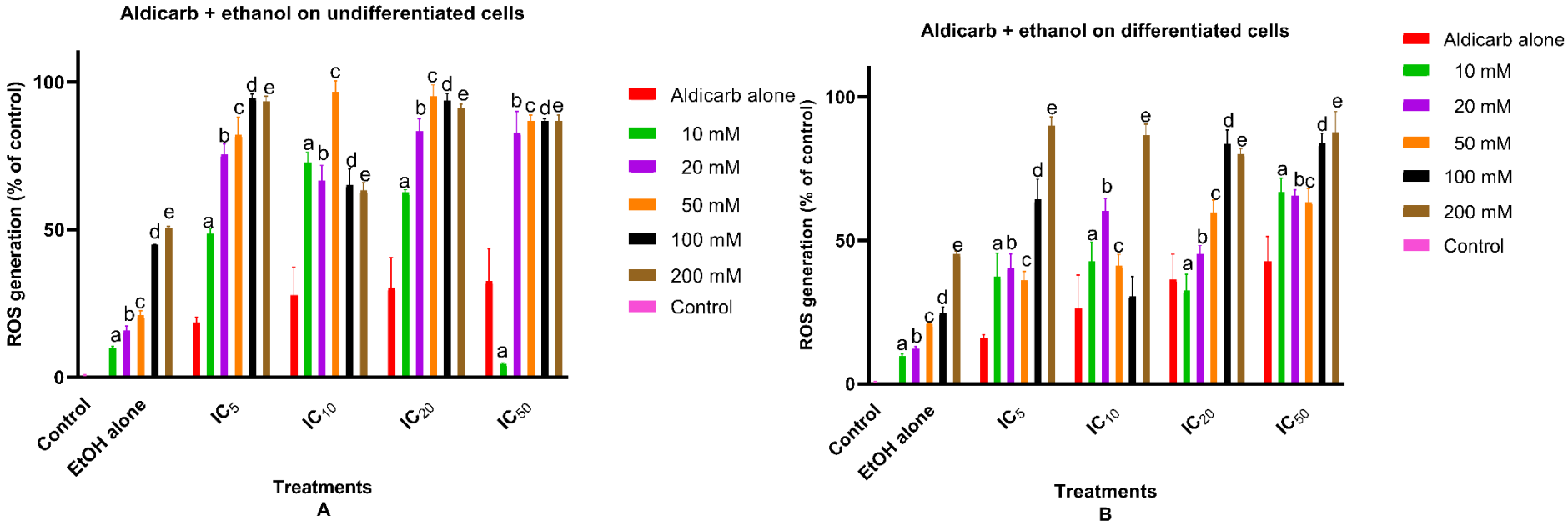


Figure 8-17: Effect of co-exposure to ethanol and Aldicarb on ROS generation in undifferentiated SH-SY5Y cells after 24 h.
A- undifferentiated cells and B- differentiated were treated with Aldicarb and ethanol for 24 h. Cellular ROS levels were assessed using DCFDA assay. Readings were normalized to the ROS level of control, providing ROS level in percentage, as a percentage value to the control. Control and treatments were performed as triplicates in 5 individual experiments (n=5). Results were analysed using two-way ANOVA with Tukey's multiple comparison and expressed as the mean ± standard error of the mean (SEM), when SEM bar is not apparent, this means that error is smaller than the symbol size. Comparison of treatments with non-treated control are indicated in Table 8-16; **a** - significance difference with 10 mM ethanol, **b** - significance difference with 20 mM ethanol, **c**- significance difference with 50 mM ethanol, **d** - significance difference with 100 mM ethanol, **e** - significance difference with 200 mM ethanol.

Table 8-16: Comparison of treatment combinations of ethanol and Aldicarb with their corresponding non-treated controls. Results were analysed by two-way ANOVA and means comparison was done by Tukey's multiple comparison tests.

Treatments		Undifferentiated cells	Differentiated cells
IC_5	10	0.0002	<0.0001
	20	<0.0001	<0.0001
	50	<0.0001	<0.0001
	100	<0.0001	<0.0001
	200	<0.0001	<0.0001
IC_{10}	10	<0.0001	<0.0001
	20	<0.0001	<0.0001
	50	<0.0001	<0.0001
	100	<0.0001	<0.0001
	200	<0.0001	<0.0001
IC_{20}	10	<0.0001	<0.0001
	20	<0.0001	<0.0001
	50	<0.0001	<0.0001
	100	<0.0001	<0.0001
	200	<0.0001	<0.0001
IC_{50}	10	NS	<0.0001
	20	<0.0001	<0.0001
	50	<0.0001	<0.0001
	100	<0.0001	<0.0001
	200	<0.0001	<0.0001
IC_5		<0.0001	0.0017
IC_{10}		<0.0001	<0.0001
IC_{20}		<0.0001	<0.0001
IC_{50}		<0.0001	<0.0001
10 mM		<0.0001	<0.0001
20 mM		<0.0001	<0.0001
50 mM		<0.0001	<0.0001
100 mM		<0.0001	<0.0001
200 mm		<0.0001	<0.0001

NS- Not significant

Table 8-17: Synergistic and antagonistic effect of joint toxicity of CPO and alcohol on ROS generation in SH-SY5Y cells

Treatments		CPO		AZO		Aldicarb	
		Undifferentiated	Differentiated	Undifferentiated	Differentiated	Undifferentiated	Differentiated
IC_5	10	1.07	0.82	0.04	0.98	0.07	0.23
	20	0.90	0.12	0.01	0.98	0.02	0.23
	50	1.03	0.45	0.24	2.29	0.03	0.49
	100	0.15	0.01	0.05	0.86	0.01	0.14
	200	0.13	0.80	0.11	0.65	0.04	0.25
IC_{10}	10	0.04	0.47	0.4	0.59	0.01	0.28
	20	0.05	0.40	0.08	1.11	0.04	0.10
	50	0.07	0.18	0.98	0.87	0.00	0.48
	100	0.11	1.31	0.06	0.79	0.25	1.43
	200	0.17	0.93	0.08	1.16	0.55	0.04
IC_{20}	10	0.19	0.81	0.04	0.12	0.03	1.09
	20	0.27	1.20	0.07	0.85	0.14	0.48
	50	0.18	0.46	0.06	0.95	0.00	0.23
	100	0.40	2.39	0.46	3.62	0.01	0.04
	200	0.55	0.01	0.12	0.82	0.06	0.10
IC_{50}	10	0.56	4.12	0.39	0.69	0.41	0.24
	20	0.26	3.12	0.05	0.93	0.01	0.27
	50	0.44	4.34	0.06	0.37	0.02	0.36
	100	0.24	2.17	0.02	0.98	0.05	0.07
	200	0.08	0.00	0.04	0.41	0.10	0.06

Combination index (CI) was calculated using the CompuSyn software and Chou-Talalay method provide quantitative definition for an additive (CI=1), synergistic (CI<1) or antagonistic (CI>1) effect of ethanol and CPO combinations for both phenotypes.

8.2.7 **Oxidative stress-induced protein damage in SH-SY5Y cells by the co-exposure of ethanol with low doses of OP and carbamate pesticides**.

Next, to gain insight into oxidative protein damages in SH-SY5Y cells induced as a response to CPO, AZO, Aldicarb, and ethanol co-exposure, protein carbonylation levels were quantified using a spectrophotometric protein carbonylation assay as detailed by Colombo et al. (2016).

8.2.7.1 ***CPO and ethanol***

Joint toxicity of CPO and ethanol-induced PCC levels increased ROS levels in undifferentiated cells (Figure 8-18 A). IC_5, IC_{10}, $IC_{20,}$ and IC_{50} of CPO paired with 200 mM ethanol-induced the highest levels of PCC in undifferentiated cells compared to controls. IC_{20} of CPO coupled with 10 - 200 mM ethanol, induced comparatively higher levels of PCC in the undifferentiated cells, when compared with the other concentration combination groups in undifferentiated cells upon CPO exposure.

200 mM paired with IC_{20} and IC_{50} of CPO did not induce a significant level of PCC in undifferentiated cells compared to the single treatments of CPO and ethanol. Also, IC_5 coupled with 10 mM ethanol induced a similar level of PCC in undifferentiated cells compared to the IC_5 single treatment of CPO. All other combinations induced significant levels of PCC in undifferentiated cells compared to their corresponding CPO alone treatments. However, IC_{20} and IC_{50} of CPO coupled with 10 - 100 mM ethanol showed lower levels of PCC than those induced by single treatments of IC_{20} and IC_{50}.

200 mM paired with all tested low doses did not induce significant levels of PCC in undifferentiated cells compared to a single 200 mM ethanol treatment (letter e indicates the significance difference between 200 mM ethanol).

Differentiated cells showed uneven production of protein carbonyls due to the exposure of CPO and ethanol in each combination group of IC_5, IC_{10}, $IC_{20,}$ and IC_{50} of CPO and ethanol compared to controls (Figure 8-18 B). However, the highest concentration of ethanol coupled with low doses of CPO induced more protein carbonyls in differentiated cells. IC_{20} paired with 10 mM and IC_{50} paired with 10 mM ethanol induced higher levels of PCC compared to the other treatment combinations for the same group in differentiated cells.

However, IC_{50} combined with 200 mM did not induce significant levels of PCC in differentiated cells compared to a single treatment at IC_{50}. IC_{20} and IC_{50} coupled with 10 mM ethanol induced similar levels of ROS without a significant difference for differentiated cells compared to their single treatments. All treatment combinations of IC_5 induced significantly higher levels of PCC in differentiated cells than treatments with IC_5 alone.

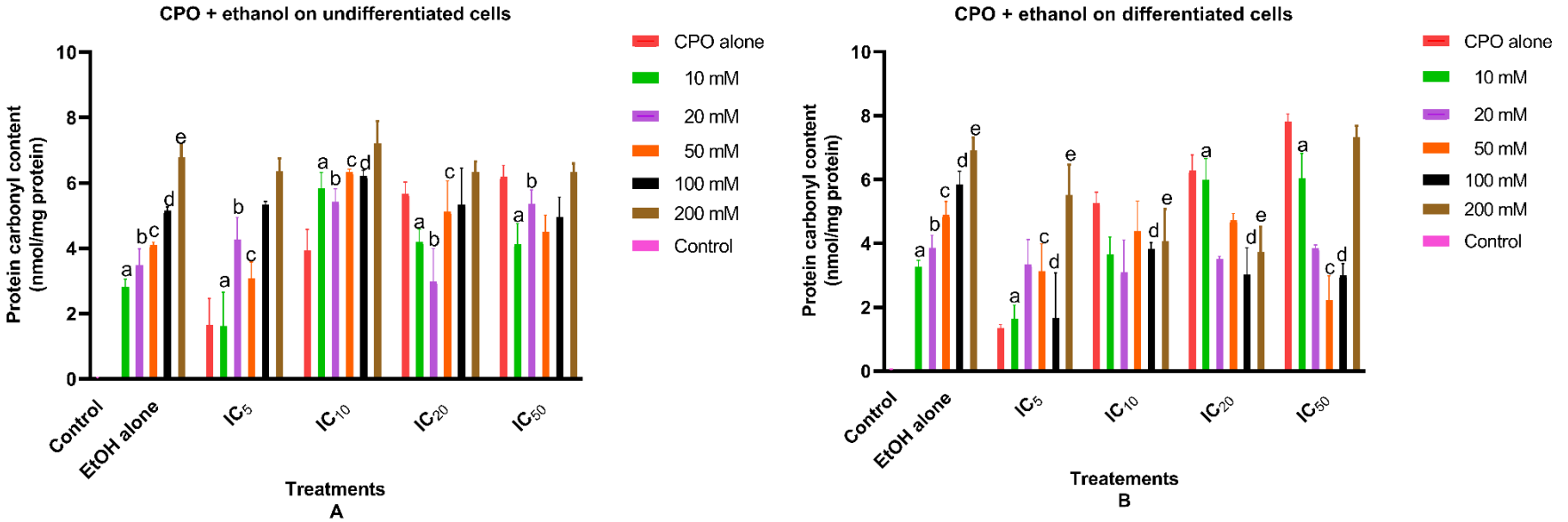


Figure 8-18: Effect of co-exposure to ethanol and CPO on cellular protein carbonyl levels of undifferentiated SH-SY5Y cells for 24 h.
A- undifferentiated cells and B- differentiated cells were treated with CPO and ethanol for 24 h. Cellular protein carbonyl levels were assessed using protein carbonyl content assay. Control and treatments were performed as triplicates in 5 individual experiments (n=5). Results were analysed using two-way ANOVA with Tukey's multiple comparison and expressed as the mean ± standard error of the mean (SEM), when SEM bar is not apparent, this means that error is smaller than the symbol size. Comparison of treatments with non-treated control are indicated in Table 8-18; **a** - significance difference with 10 mM ethanol, **b** - significance difference with 20 mM ethanol, **c**- significance difference with 50 mM ethanol, **d** - significance difference with 100 mM ethanol, **e** - significance difference with 200 mM ethanol.

Table 8-18: Comparison of treatment combinations of ethanol and CPO with their corresponding non-treated controls. Results were analysed by two-way ANOVA and means comparison was done by Tukey's multiple comparison tests.

Treatments		Undifferentiated cells	Differentiated cells
IC_5	10	0.0024	0.0126
	20	<0.0001	<0.0001
	50	<0.0001	<0.0001
	100	<0.0001	0.0103
	200	<0.0001	<0.0001
IC_{10}	10	<0.0001	<0.0001
	20	<0.0001	<0.0001
	50	<0.0001	<0.0001
	100	<0.0001	<0.0001
	200	<0.0001	<0.0001
IC_{20}	10	<0.0001	<0.0001
	20	<0.0001	<0.0001
	50	<0.0001	<0.0001
	100	<0.0001	<0.0001
	200	<0.0001	<0.0001
IC_{50}	10	<0.0001	<0.0001
	20	<0.0001	<0.0001
	50	<0.0001	0.0001
	100	<0.0001	<0.0001
	200	<0.0001	<0.0001
IC_5		0.0018	0.0792
IC_{10}		<0.0001	<0.0001
IC_{20}		<0.0001	<0.0001
IC_{50}		<0.0001	<0.0001
10 mM		<0.0001	<0.0001
20 mM		<0.0001	<0.0001
50 mM		<0.0001	<0.0001
100 mM		<0.0001	<0.0001
200 mm		<0.0001	<0.0001

NS- Not significant

8.2.7.2 *AZO and ethanol*

Joint toxicity of low doses of AZO and ethanol exposure on undifferentiated SH-SY5Y cells on cellular protein carbonylation is depicted in Figure 8-19 A. According to the results, IC_5 and IC_{20} of AZO combined with 10, 20, 50, 100 and 200 mM ethanol showed a concentration-dependent increase in PCC levels in undifferentiated cells compared to control treatments. Interestingly, IC_{50} paired with 200 mM induced a similar level of PCC in undifferentiated cells without showing a significance difference when treated alone. However, 20 - 200 mM ethanol and IC_5 of AZO increased the PCC in cells compared to a single IC_5 treatment. All treatment combinations induced PCC in undifferentiated cells and

showed significant decreases or increases compared to the single ethanol treatments.

According to Figure 8-19 B, all combinations of AZO and ethanol induced protein carbonylation in differentiated cells. The highest concentration (200 mM) of ethanol induced significantly higher PCC levels for IC_5, IC_{10} IC_{20}, and IC_{50} of AZO. 100 mM ethanol induced significantly higher levels of PCC in combination with IC_{10} of AZO. Notably, I0 mM ethanol combined with IC_{10} of AZO induced a significant level of PCC compared to controls. IC_{10} combined with ethanol induced a concentration-dependent increase of PCC in differentiated cells with increasing ethanol concentrations.

However, when compared with the single doses of AZO on differentiated cells, all treatment combinations did not exceed the PCC level that was induced by IC_{50} alone. Ethanol single treatments induced significantly lower PCC in IC_5 with 10, 50 and 100 mM ethanol pairings.

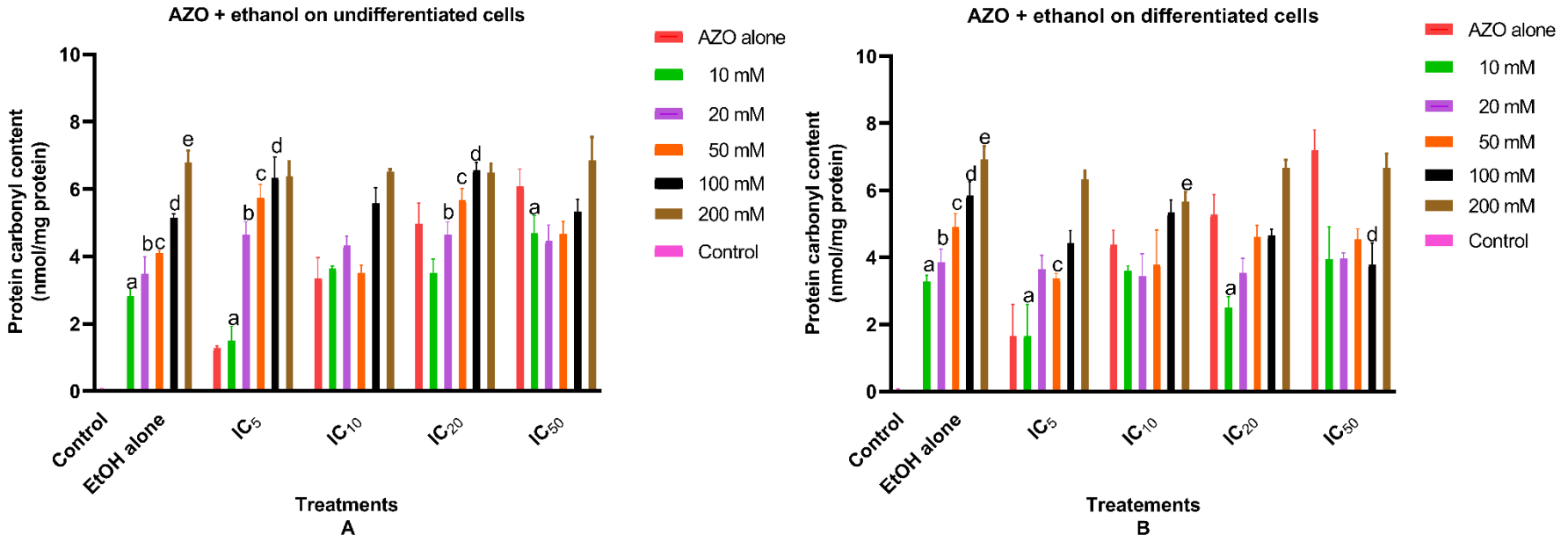


Figure 8-19: Effect of co-exposure to ethanol and AZO on cellular protein carbonyl levels of undifferentiated SH-SY5Y cells for 24 h.
A- undifferentiated cells and B- differentiated cells were treated with AZO and ethanol for 24 h. Cellular protein carbonyl levels were assessed using protein carbonyl content assay. Control and treatments were performed as triplicates in 5 individual experiments (n=5). Results were analysed using two-way ANOVA with Tukey's multiple comparison and expressed as the mean ± standard error of the mean (SEM), when SEM bar is not apparent, this means that error is smaller than the symbol size. Comparison of treatments with non-treated control are indicated in Table 8-19; **a** - significance difference with 10 mM ethanol, **b** - significance difference with 20 mM ethanol, **c**- significance difference with 50 mM ethanol, **d** - significance difference with 100 mM ethanol, **e** - significance difference with 200 mM ethanol.

Table 8-19: Comparison of treatment combinations of ethanol and AZO with their corresponding non-treated controls. Results were analysed by two-way ANOVA and means comparison was done by Tukey's multiple comparison tests.

Treatments		Undifferentiated cells	Differentiated cells
IC_5	10	0.0006	<0.0001
	20	<0.0001	<0.0001
	50	<0.0001	<0.0001
	100	<0.0001	<0.0001
	200	<0.0001	<0.0001
IC_{10}	10	<0.0001	0.0005
	20	<0.0001	<0.0001
	50	<0.0001	<0.0001
	100	<0.0001	<0.0001
	200	<0.0001	<0.0001
IC_{20}	10	<0.0001	<0.0001
	20	<0.0001	<0.0001
	50	<0.0001	<0.0001
	100	<0.0001	<0.0001
	200	<0.0001	<0.0001
IC_{50}	10	<0.0001	<0.0001
	20	<0.0001	<0.0001
	50	<0.0001	<0.0001
	100	<0.0001	<0.0001
	200	<0.0001	<0.0001
IC_5		0.0008	0.0280
IC_{10}		<0.0001	<0.0001
IC_{20}		<0.0001	<0.0001
IC_{50}		<0.0001	<0.0001
10 mM		<0.0001	<0.0001
20 mM		<0.0001	<0.0001
50 mM		<0.0001	<0.0001
100 mM		<0.0001	<0.0001
200 mm		<0.0001	<0.0001

NS- Not significant

8.2.7.3 *Aldicarb and ethanol*

Undifferentiated cells exposed to Aldicarb and ethanol showed a concentration-dependent increase in PCC levels for IC_5, IC_{10}, and IC_{20} of Aldicarb with 10-200 mM ethanol compared to control treatments as shown in Figure 8-20 A. A similar pattern was observed for ROS generation in Aldicarb exposed undifferentiated cells. Although, IC_{50} combined with 10 - 200 mM showed a non-monotonical increase in PCC compared to controls.

IC_5 paired with 20 - 200 mM ethanol showed significant PCC in undifferentiated cells compared to IC_5 treated alone. IC_{10} paired with 10, 20, 50 and 200 mM exhibited significant PCC levels compared to IC_{10} treated alone. IC_{20} and IC_{50}

showed significant PCC levels in cells compared to single exposures when paired with 20 - 200 mM and 10 - 200 mM ethanol, respectively.

Except IC_{20} and IC_{50} with 200 mM ethanol, all treatment combinations showed a significant influence on PCC levels in undifferentiated cells when compared to their single ethanol treatments.

Differentiated cells exposed to Aldicarb and ethanol exhibited significantly increased PCC with increasing pesticide concentrations in a non-monotonical fashion. However, a concentration-dependent increase was observed at IC_5, IC_{20}, and IC_{50} of Aldicarb and ethanol over the concentration range of 10 - 200 mM compared to controls. Consistent with ROS generation upon co-exposure of Aldicarb and ethanol, IC_5, IC_{10}, IC_{20}, IC_{50} with 200 mM ethanol induced higher protein carbonyl levels in differentiated cells.

IC_5 paired with 20 - 200 mM showed significantly different PCC levels compared with IC_5 alone. IC_{10} paired with 10, 20, 50 and 200 mM ethanol induced significant levels of PCC in differentiated cells compared to IC_{10} alone. IC_{50} paired with 10, 50, 100 and 200 mM ethanol induced significant levels of PCC in differentiated cells compared to IC_{50} alone.

Comparison of undifferentiated vs differentiated cells at inducing protein carbonylation for each treatment combination showed significant differences as tabulated in Table 8-22. Crude cytosolic fractions of differentiated cells treated with CPO+ethanol, AZO+ethanol and Aldicarb+ethanol were oxyblotted to visualize the carbonylated proteins. The major proteins modified were characterised by their approximate denatured molecular weights. Overlapping protein targets were evident at denatured molecular weights of ~120, 110, 85 and 55 kD in all three pesticide and ethanol combinations (Figure 8-21).

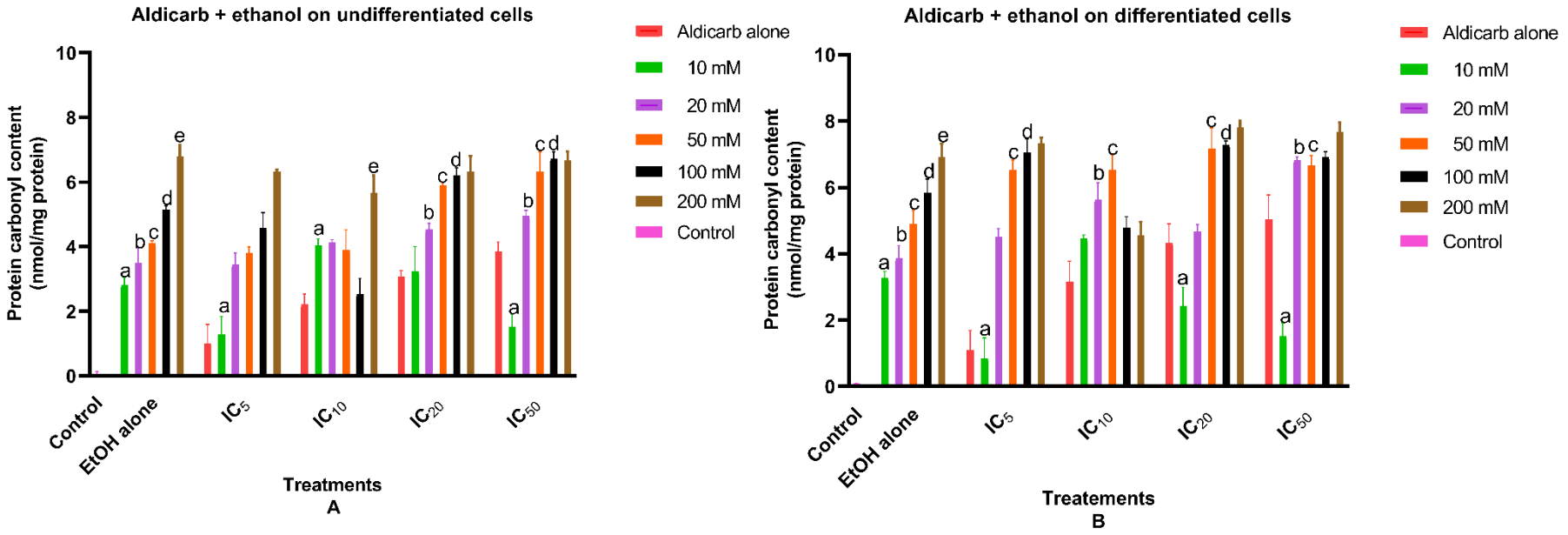


Figure 8-20: Effect of co-exposure to ethanol and Aldicarb on cellular protein carbonyl levels of undifferentiated SH-SY5Y cells for 24 h.

A- undifferentiated cells and B- differentiated cells were treated with Aldicarb and ethanol for 24 h. Cellular protein carbonyl levels were assessed using protein carbonyl content assay. Control and treatments were performed as triplicates in 5 individual experiments (n=5). Results were analysed using two-way ANOVA with Tukey's multiple comparison and expressed as the mean ± standard error of the mean (SEM), when SEM bar is not apparent, this means that error is smaller than the symbol size. Comparison of treatments with non-treated control are indicated in Table 8-20; **a** - significance difference with 10 mM ethanol, **b** - significance difference with 20 mM ethanol, **c**- significance difference with 50 mM ethanol, **d** - significance difference with 100 mM ethanol, **e** - significance difference with 200 mM ethanol.

Table 8-20: Comparison of treatment combinations of ethanol and Aldicarb with their corresponding non-treated controls. Results were analysed by two-way ANOVA and means comparison was done by Tukey's multiple comparison tests.

Treatments		Undifferentiated cells	Differentiated cells
IC_5	10	NS	<0.0001
	20	<0.0001	<0.0001
	50	<0.0001	<0.0001
	100	<0.0001	<0.0001
	200	<0.0001	<0.0001
IC_{10}	10	<0.0001	<0.0001
	20	<0.0001	<0.0001
	50	<0.0001	<0.0001
	100	<0.0001	<0.0001
	200	<0.0001	<0.0001
IC_{20}	10	<0.0001	<0.0001
	20	<0.0001	<0.0001
	50	<0.0001	<0.0001
	100	<0.0001	<0.0001
	200	<0.0001	<0.0001
IC_{50}	10	<0.0001	<0.0001
	20	<0.0001	<0.0001
	50	<0.0001	<0.0001
	100	<0.0001	<0.0001
	200	<0.0001	<0.0001
IC_5		0.0128	0.0070
IC_{10}		<0.0001	<0.0001
IC_{20}		<0.0001	<0.0001
IC_{50}		<0.0001	<0.0001
10 mM		<0.0001	<0.0001
20 mM		<0.0001	0.0114
50 mM		<0.0001	<0.0001
100 mM		<0.0001	<0.0001
200 mm		<0.0001	<0.0001

NS- Not significant

Table 8-21: Synergistic and antagonistic effect of joint toxicity of CPO and alcohol on PCC in SH-SY5Y cells

Treatments		CPO		AZO		Aldicarb	
		Undifferentiated	Differentiated	Undifferentiated	Differentiated	Undifferentiated	Differentiated
IC_5	10	2.14	5.27	1.766	8.39	6.82	4.60
	20	0.49	2.57	0.39	1.87	0.69	0.33
	50	1.43	4.46	0.48	5.77	1.92	0.33
	100	0.93	5.87	0.69	3.27	1.97	0.41
	200	1.25	2.32	1.25	1.29	1.25	0.63
IC_{10}	10	0.38	1.50	0.78	1.60	0.49	5.18
	20	0.50	3.84	0.67	2.80	0.43	4.32
	50	1.40	2.09	1.39	3.78	1.89	5.25
	100	0.86	5.16	1.09	1.68	5.34	3.24
	200	1.11	4.77	1.32	1.87	1.89	3.98
IC_{20}	10	1.31	0.94	1.42	6.98	1.36	4.62
	20	2.65	1.19	1.01	3.31	0.68	1.10
	50	1.23	1.04	0.94	2.29	0.54	0.47
	100	1.53	1.39	1.01	3.40	0.79	0.60
	200	1.70	1.23	1.58	1.46	1.35	0.70
IC_{50}	10	3.17	4.03	2.10	3.99	7.15	4.47
	20	2.03	2.74	2.38	4.44	0.87	0.92
	50	3.01	4.55	2.50	4.04	0.61	1.10
	100	3.03	4.54	2.41	7.60	0.77	1.20
	200	2.50	3.06	2.11	2.73	1.69	1.15

Combination index (CI) was calculated using the CompuSyn software and Chou-Talalay method provide quantitative definition for an additive (CI=1), synergistic (CI<1) or antagonistic (CI>1) effect of ethanol and CPO combinations for both phenotypes.

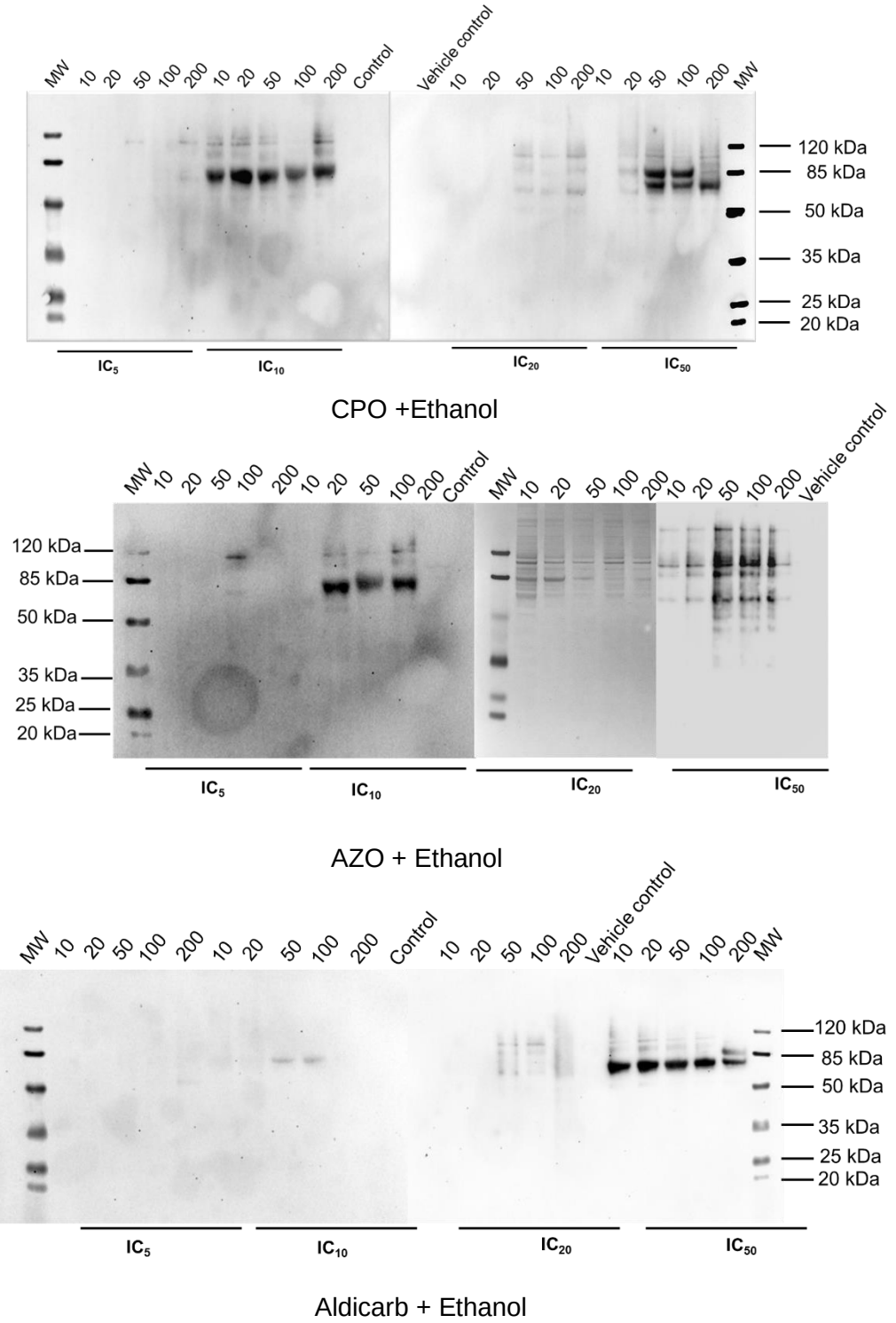


Figure 8-21: Cytosolic protein carbonylation of joint toxicity of CPO or AZO or Aldicarb treated differentiated SH-SY5Y cells with ethanol.
Differentiated cells were co-incubated with CPO + ethanol, AZO + ethanol, Aldicarb + ethanol for 24 h. Crude cytosolic fractions were DNPH derivatised, resolved by gel electrophoresis and immunoblotted with anti-DNPH antibody to identify the specific protein targets of protein carbonylation of ethanol exposure. Each experiment was conducted as three independent experiments with three replicates.

Table 8-22: Joint toxicity of CPO, AZO, and Aldicarb with alcohol on undifferentiated vs differentiated cells.

Pesticides	Treatment		Undifferentiated vs Differentiated				
			MTT	LDH	ATP	ROS	PCC
CPO	IC_5	10	<0.0001	<0.0001	<0.0001	NS	NS
		20	<0.0001	<0.0001	<0.0001	0.0348	NS
		50	<0.0001	<0.0001	<0.0001	NS	NS
		100	<0.0001	<0.0001	<0.0001	<0.0001	<0.0001
		200	<0.0001	0.0014	<0.0001	NS	NS
	IC_{10}	10	NS	NS	NS	<0.0001	0.0002
		20	NS	0.0266	0.0146	NS	<0.0001
		50	NS	0.0010	NS	<0.0001	0.0010
		100	<0.0001	<0.0001	<0.0001	<0.0001	<0.0001
		200	<0.0001	<0.0001	<0.0001	<0.0001	<0.0001
	IC_{20}	10	NS	NS	NS	<0.0001	0.0079
		20	NS	NS	NS	<0.0001	NS
		50	NS	NS	NS	<0.0001	NS
		100	<0.0001	NS	NS	<0.0001	0.0005
		200	<0.0001	0.0405	NS	<0.0001	0.0001
	IC_{50}	10	NS	0.0022	NS	<0.0001	<0.0001
		20	NS	NS	NS	<0.0001	0.0021
		50	NS	NS	NS	<0.0001	<0.0001
		100	0.0019	0.0005	0.0020	<0.0001	<0.0001
		200	<0.0001	<0.0001	<0.0001	NS	NS
AZO	IC_5	10	<0.0001	<0.0001	<0.0001	<0.0001	0.0015
		20	<0.0001	<0.0001	<0.0001	<0.0001	0.0081
		50	<0.0001	<0.0001	<0.0001	<0.0001	<0.0001
		100	<0.0001	<0.0001	<0.0001	0.0003	<0.0001
		200	<0.0001	<0.0001	<0.0001	NS	NS
	IC_{10}	10	0.0004	<0.0001	NS	NS	NS
		20	0.0278	0.0056	0.0361	<0.0001	NS
		50	<0.0001	<0.0001	<0.0001	0.0005	NS
		100	NS	NS	NS	0.0071	NS
		200	0.0002	<0.0001	0.0003	0.0218	NS
	IC_{20}	10	0.0194	0.0074	NS	NS	0.0008
		20	0.0015	0.0004	0.0014	<0.0001	0.0003
		50	NS	NS	NS	<0.0001	0.0005
		100	<0.0001	<0.0001	<0.0001	0.0093	<0.0001
		200	NS	NS	NS	NS	NS
	IC_{50}	10	<0.0001	<0.0001	<0.0001	0.0005	NS
		20	NS	NS	NS	<0.0001	NS
		50	NS	NS	NS	NS	NS
		100	NS	NS	NS	<0.0001	0.0021
		200	NS	NS	NS	NS	NS
Aldicarb	IC_5	10	NS	NS	NS	0.0112	<0.0001
		20	NS	NS	NS	<0.0001	<0.0001
		50	NS	NS	NS	<0.0001	<0.0001
		100	NS	NS	0.0219	<0.0001	<0.0001
		200	<0.0001	<0.0001	<0.0001	NS	<0.0001
	IC_{10}	10	NS	0.0379	NS	<0.0001	NS
		20	0.0134	0.0041	0.0207	NS	0.0001
		50	NS	NS	NS	<0.0001	<0.0001
		100	0.0005	<0.0001	0.0006	<0.0001	<0.0001
		200	<0.0001	<0.0001	<0.0001	<0.0001	0.0039
	IC_{20}	10	NS	NS	NS	<0.0001	NS
		20	NS	NS	NS	<0.0001	NS
		50	NS	NS	NS	<0.0001	0.0010

		100	0.0276	0.0096	0.0263	0.0024	0.0056
		200	NS	NS	NS	0.0008	0.0001
	IC_{50}	10	NS	NS	NS	<0.0001	NS
		20	0.0016	NS	NS	<0.0001	<0.0001
		50	0.0052	<0.0001	<0.0001	<0.0001	NS
		100	0.0134	NS	0.0029	NS	NS
		200	NS	NS	NS	NS	0.0008

MTT- (4,5-dimethylthiazol-2-yl)-2,5-diphenyltetrazolium bromide, LDH- Lactate dehydrogenase, ATP- Adenosine triphosphate, NS- Not significant

8.3 Discussion

Co-exposure of the organophosphate pesticides: Chlorpyrifos-oxon, Azamethiphos-oxon and carbamate pesticide, Aldicarb, with ethanol indicates that a main route of cytotoxicity is via ROS generation and with a change in oxidative stress that relates to exposure concentration in human neuroblastoma SH-SY5Y cells, according to this study. Low doses of CPO, AZO, and Aldicarb when coupled with 10 - 200 mM ethanol induced cytotoxic responses in both undifferentiated and differentiated cells that increased with increasing alcohol concentrations.

Ethanol co-incubation with pesticides particularly draws attention to research that has considered the combined effect of ethanol and pesticides, that can worsen the outcome of occupational and intentional poisoning of pesticides (van der Hoek and Konradsen, 2005, Eddleston et al., 2006). Epidemiological studies have pointed out that patients, particularly men, that ingested alcohol around the time of poisoning may have induced coma and respiratory failure (Eddleston et al., 2009). Clinical manifestations of the joint toxicity of ethanol and OP or carbamate poisoning was said to be worse than the clinical manifestation occurred due to single poisonings according to these studies (Eddleston, 2019). Apart from this, the mechanism of single poisoning of OP or carbamate pesticides and ethanol has been widely studied, the mechanism of joint toxicity of OP or carbamate with ethanol remains unclear. Although, *in vitro* studies have suggested a synergistic effect of pesticide mixtures of OP or carbamate pesticides in the literature (Segal and Fedoroff, 1989, Fu et al., 2019), joint toxicity of ethanol and OP or carbamate pesticides were not recorded as *in vitro* studies.

In this study, co-exposure of CPO, AZO, and Aldicarb with ethanol influenced cell metabolic activity and cell viability of both phenotypes of SH-SY5Y cells.

However, exposure of CPO to differentiated cells were notably susceptible at IC_5 when coupled with 10 - 100 mM, more than other combinations showing antagonistic effects. According to Chapter IV, differentiated cells were more susceptible to pesticide toxicity than undifferentiated cells. Compared to the individual effects of 10 - 200 mM ethanol for 24 h exposure (Chapter VI,) 200 mM showed a dramatic effect on cell viability causing 90% cell loss compared to controls as revealed by MTT assays. However, IC_5 paired with 200 mM showed 81% cell loss compared to non-treated controls in differentiated cells. Similar to the CPO and ethanol effects on differentiated SH-SY5Y cells, AZO and ethanol produced a dramatic effect on cell viability of differentiated cells with pairing over the concentration range of 10 - 200 mM. IC_5 paired with 200 mM ethanol showed 80% cell loss compared to control. Compared to the tested OPs, the carbamate pesticide, Aldicarb, showed a moderate effect on differentiated cells. Low doses of Aldicarb induced cell viability and metabolic activity decreases in a concentration-dependent manner in all groups (IC_5; IC_{10}; IC_{20} and IC_{50}). However, all combinations with 200 mM ethanol influenced cell metabolic activity and cell viability more than other combinations. These subtle changes in cell viability observed in the MTT assays with co-exposure of alcohol and OP and carbamate could be due to experimental variations, and further experimentation would be required to validate the cell metabolic activity and cell viability loss with co-incubation of OP and carbamate pesticides with ethanol.

A retrospective study undertaken with OP insecticide poisoned patients (135) that had also ingested alcohol, showed a worse outcome than patients that had ingested alcohol only, and also, the outcome worsened with higher BAC and higher doses of OP pesticides (Lee et al., 2017). This study further demonstrated that the BAC is correlated with the ingested volume of OP pesticides. Furthermore, the volume and strength of alcohol ingested at the

time of poisoning was a factor such that higher than ~37 mM BAC was a risk factor for OP-induced mortality. In line with this, all concentrations above 10 mM paired with IC_5, IC_{10}, IC_{20}, and IC_{50} induced significant viability loss in differentiated cells in the current study.

In line with the MTT assays, LDH and ATP assays showed that there was a considerable effect of joint toxicity of CPO, AZO, and Aldicarb on undifferentiated and differentiated cells. Joint toxicity of CPO, AZO and Aldicarb induced neuronal cell death by reducing cellular ATP levels. This is consistent with the previous studies done with three pesticides undertaken in Chapter IV and VI with human neuroblastoma SH-SY5Y cells and ethanol on the same cell line. However, the subtle changes observed in IC_{10} and IC_{20} pairing with ethanol, need to be further evaluated with an increased number of repeated experiments to validate the influence of joint exposures to both phenotypes.

However, joint toxicity of OP or carbamate toxicity tested in this study with ethanol showed an effect on cell differentiation, as detected by the neurite outgrowth assay. All combinations affected the differentiation of SH-SY5Y cells indicating ethanol with OP or carbamate pesticide affected neuronal cell differentiation. Nevertheless, some combinations showed an effect on differentiation, but not a significant effect compared with the controls, implying a limited affect or possibly an antagonistic effect between the agents on neurite outgrowth. These experiments were repeated only 5 times and need more validation experiments and the variability could be reduced by more experimental numbers.

Lastly, co-exposure of OP or carbamate pesticide with ethanol was evaluated with cellular oxidative stress markers, ROS and protein carbonylation content (PCC). All treatment combinations of CPO, AZO, and Aldicarb with ethanol induced ROS and protein carbonyls in both undifferentiated and differentiated

cells. The comparison of the oxidatively damaged proteins observed with the ethanol and pesticide co-treatment with those characterised by individual treatments showed that the cabonylation of 50/55 kDa is strong in either alcohol or pesticide treatments, Furthermore, high intensity apparent when alcohol is combined with pesticide compared to single alcohol treatments. This suggested that 50/55 kDa is a common site that could be “saturated”, with redox damage when alone or when the agents are combined. This suggests that both ethanol and the tested pesticides can alter redox status in cells by the route of ROS generation. The cellular cytotoxic responses arose from the co-exposure of tested pesticides with ethanol on both undifferentiated and differentiated cells and correlated with elevated levels of ROS. CPO, AZO, and Aldicarb vary with their lipid solubility, which will affect their cell take-up and associated toxicity. Hence, lipophilicity of pesticide markedly influences the acuteness of toxicity (Eddleston et al., 2009), and this could be affected by the concentration of ethanol. When comparing the three pesticides with alcohol co-exposure, CPO showed a stronger effect on undifferentiated cells and differentiated cells than AZO and Aldicarb. However, differentiated cells showed more susceptibility to the combination effect than undifferentiated cells. According to the results of this study, even at the IC_5 concentration of the three pesticides, there was ROS generation and protein carbonylation in cellular cytosolic proteins in both undifferentiated and differentiated cells. 200 mM ethanol combined with IC_5, IC_{10}, IC_{20}, and IC_{50} concentrations of CPO, AZO, and Aldicarb induced a significant level of ROS and protein carbonyls. These remarkable changes in the oxidative status of the undifferentiated and differentiated cells co-exposed to ethanol with pesticides were associated with cellular morphological changes and a cytotoxic response that diminished energy levels. Hence this study demonstrates that the cytotoxic effects of co-exposure can be due to either ethanol or pesticides or both in undifferentiated and differentiated cells. For

instance, IC_{50} AZO with ethanol over the range of 10 - 200 mM showed non-significant cell metabolic and viability loss in undifferentiated cells, compared to single ethanol exposures of 10 – 200 mM, and this was significantly different from the single exposure of IC_{50} of AZO. Therefore, this points out the effect is due to ethanol (Figure 8-2 A). It has been demonstrated that ethanol can enhance the solubility of pesticides (Otero-Diaz, 2017). The interaction of CPO, AZO, and Aldicarb induced a number of synergistic or antagonistic effects (Table 8-2, 8-4 and 8-6) when in certain combinations, and this might in part reflect alteration of the solubility of the pesticides at that concentration of alcohol.

A prospective study of ingestion of the OP hydrophilic pesticide, dimethyl insecticide, dimethoateEC40, showed that ingestion of the pesticide and alcohol increased the risk of mortality. Further, the study concluded that the higher BAC is independent from the plasma dimethoate concentration and also was not linked with the outcome of the exposure (Eddleston et al., 2009). Another prospective study done in Sri Lanka showed that the lipophilic S-alkyl OP insecticide, profenofos, when co-ingested with alcohol by a 64 men cohort, that 10 of men died due to coingestion of profenofos and alcohol (Dhanarisi et al., 2018). These two studies suggest that co-ingestion of alcohol with OP is associated with increased risk of death after pesticide poisoning. Furthermore, the relationship between alcohol coingestion and outcome in profenofos self-poisoning study showed that the coingested patients were chronic alcohol users consuming alcohol daily (54.7% of cohort). The patients with alcohol and pesticide co-ingestion needed longer hospital stays than non-alcoholics with profenofos poisoning according to the study (Dhanarisi et al., 2018). This study illustrated that the effect of outcome was due to larger ingestions of pesticide or due to an interaction of profenofos with ethanol (Dhanarisi et al., 2018).

According to the current study, the interaction of OP and carbamate pesticide with alcohol on cytotoxic responses to neuronal cells can be due to elevated ROS levels and protein carbonylation which likely lead to altered general cell functioning. Combinations of low doses of OP and carbamate pesticide with alcohol induced synergistic or antagonistic effects on cytotoxic responses of neuronal cells, and perhaps clinical manifestations that arose from the co-ingestion might be related to this synergistic or antagonistic effects as revealed by the current study. However, Dhanarisi et al. (2018) showed variations in AChE inhibition levels of alcoholic and non-alcoholic pesticide poisoned patients, and these authors further reported an association of AChE inhibition should be further investigated with the concentration of profenofos ingested. It is important to evaluate the AChE inhibition in cells co-exposed to three tested pesticides and alcohol to gain insight into the association of AChE inhibition and cellular metabolic activities. Although Lee et al. (2017) reported that higher doses of dimethoate were associated with effects of ethanol, but not the ethanol itself, when inducing the clinical manifestations that arose from the exposures. According to the current study, IC_{50} concentration induced strong cytotoxic responses with ethanol interaction compared to the other concentrations of these three pesticides, in agreement with this study. However, the aformentioned studies with OP pesticides and alcohol coingesion have not measured the OP concentrations in the blood or plasma in the selected cohort, thus association of ethanol and OP pesticides cannot be predictive with outcome relative to the doses ingested.

According to the previous retrospective studies and the current study, there is an association with the pesticides and ethanol in inducing cytotoxic repsonses in neuronal cells. The current study proved that these responses are stage specific. ROS generation is a route of induction of cellular responses. This

provides an insight into the understanding of the impact of coingested alcohol and OP or carbamate, and the severity of response that might ensue, and how this may guide future integrated policy to improve the management of OP poisoning and to reduce overall mortality after coingestion. Furthermore, this may be important for determining future therapeutics for management of alcohol and pesticide poisoned patients, for example, by the use of antioxidants to combat the excessive redox stress.

In conclusion, joint toxicities of CPO, AZO, and Aldicarb with ethanol-induced cytotoxicity in undifferentiated and differentiated SH-SY5Y cells resulted in alteration of the oxidative status of cells. Increased protein carbonylation damage was observed as a response to this elevated ROS. The joint toxicity of pesticide and alcohol had a notable effect on cell toxicity and cell differentiation of SH-SY5Y cells.

9 GENERAL DISCUSSION

9.1 Summary of findings

This thesis focused on the neurotoxicity evaluation of pesticides and alcohol using human neuroblastoma SH-SY5Y cells and human cortical progenitor neural stem cells (ReNcell CX/ hNPCs). Evaluation of pesticide neurotoxicity has been done using commonly used oxon metabolites of two organophosphorus pesticides, Chlorphyrifos and Azamethiphos and carbamate pesticide, Aldicarb. Chlorpyrifos is currently banned in several countries around the world, but still used in Asian countries where organophosphate insecticides are widely available for agriculture as well as for non-agricultural purposes. Azamethiphos is also used in several insecticide formulations in households and for salmon farming. Aldicarb is a commonly used carbamate pesticide and use as a soil applicant. Intentional and occupational poisoning of these pesticides in humans is one of the social and economic burdens in developed and developing countries in the world. The effect of these pesticides on the developing brain is gaining attention due to its vulnerability and potential to cause health consequences in the long term. On the other hand, although alcohol consumption is part of the social fabric in many countries there is a health risk associated with alcohol consumption that is extensive.

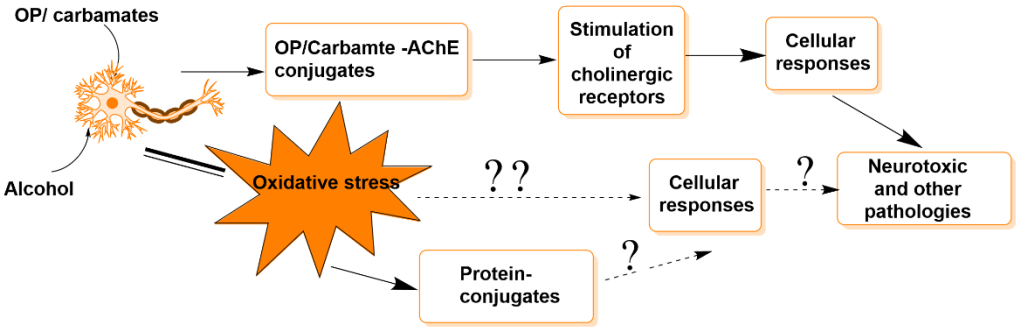


Figure 9-1: Possible pathways of oxidative stress and other protein adducts resulting in cellular toxic responses after alcohol and pesticides exposure in neuronal cells.

However, oxidative stress and the association of neurotoxic pathologies were suggested with OP/carbamate and alcohol exposure, and oxidative stress mediated protein targets and their relation to cellular responses were rarely touched upon in the literature (Figure 9-1). In light of these uncertainties, human risk assessment of acute exposure to OP/carbamate pesticides and alcohol and their underlying mechanisms of toxicity are important to study, to clarify the doses currently considered are safe for the general population and occupationally exposed workers. One of the major challenge with the neurotoxicity evalauation of above mentioned pesticides and alcohol is the outcome of the exposure depends not only on the dose and duration of the exposure, but also on the neurodevelopment stages. Therefore, this study focused on the toxicological consequences of both these neurotoxicants on human neuronal cells and their underlying mechanism of toxicity at the cellular level, which will assist with determination of safety levels of each neurotoxicants to human neurones.

Chapter IV and V focus on the effect of selected OP and carbamate pesticides on human neuroblastoma and human cortical progenitor neural stem cells using both undifferentiated and differentiated cells. Chapter IV and V conclude that the three pesticides induced cytotoxicity in both undifferentiated and differentiated cells and that AChE inhibition and ROS generation are main sources of inducing cytotoxicity to cells. Furthermore, the current studies showed that differentiated cells in both cell lines were more susceptible to the toxicity of pesticides than undifferentiated cells at 24 h exposures. Therefore, these studies of pesticides demonstrated that cytotoxicity to CPO, AZO and Aldicarb is cell type and stage-specific. CPO exerted potent toxicity compared to AZO and Aldicarb on differentiated cells in both cell lines while AZO showed potent toxicity in undifferentiated cells in both cell lines. Aldicarb exerted more

potent toxicity on differentiated cells than undifferentiated cells as revealed by three independent asays (MTT, LDH and ATP assays). The IC_{50} generated from their corresponding concentration-response curves confirmed that the hNPCs were more sensitive to CPO, AZO, and Aldicarb than the human neuroblastoma SH-SY5Y cells. The findings of CPO, AZO, and Aldicarb on hNPCs suggested that cytotoxicity was induced at a range of 1 - 20 µM while 4 - 40 µM was required for toxicity to human neuroblastoma SH-SY5Y cells. Interestingly, AChE inhibition in hNPCs occurred at lower concentration ranges than in human neuroblastoma SH-SY5Y cells. That implyies susceptibility of hNPCs to all three pesticides than that of human neuroblastoma SH-SY5Y cells via AChE inhiibition. However, both cell lines showed that AChE inhibition was not the sole mechanism of pesticide-induced cytotoxicity, but AChE inhibition by CPO, AZO, and Aldicarb was associated with cell viability. CPO, AZO, and Aldicarb's effects on cell differentiation of SH-SY5Y cells showed that all three pesticides exerted a significant effect on cell differentiation, suggesting specific neuronal development events were potentially disrupted by CPO, AZO and Aldicarb exposures. Remarkably, lower concentrations than those required to significantly reduce cell metabolic activity or cell viability were still able to induce ROS generation in cells. This elevated ROS, even at low doses of the three tested pesticides, influenced cytosolic protein carbonylation in both undifferentiated and differentiating cells, suggesting there were a number of proteins that were major targets of pesticide-induced oxidative stress in both human neuroblastoma SH-SY5Y cells and hNPCs. Even at very low doses, such as IC_{10}, a significant level of protein carbonylation was induced. Interestingly, a protein of ~50kDa was a major target of ROS, as revealed by the studies undertaken in both human neuroblastoma and hNPCs upon CPO, AZO and Aldicarb exposures.

Chapter VI and VII conclude that acute exposure to alcohol induces cytotoxicity in a concentration- and time-dependent manner in both human neuroblastoma cells and hNPCs, mimicking exposure durations of episodic binge drinking. Undifferentiated SH-SY5Y cells were more susceptible to alcohol-induced cytotoxicity than differentiated SH-SY5Y cells. However, the study results revealed that differentiated hNPCs were more susceptible to concentration and time-dependent effects of alcohol than undifferentiated cells by MTT, LDH, and ATP assays. The time durations selected for the study represented binge-like episode drinking of 3 and 6 h exposures, which for human neuroblastoma cells produced a linear relationship between alcohol concentration and cell survival. By comparison, hNPCs only showed a linear relationship with cell survival for a 3 h exposure. At 12 and 24 h exposures to alcohol for both undifferentiated and differentiated cells, a cytotoxic response was induced without a marked difference between both cell lines. Notably, all low and high concentrations of alcohol-induced ROS generation in both human neuroblastoma and hNPCs at 3, 6, 12, and 24 h exposures, while the shorter exposures of 3 and 6 h showed peak ROS production in both cell lines. Interestingly, the alcohol-induced elevation of PCC lagged the 6 h peak of ROS, with the highest levels of PCC detected at 12 and 24 hours in human neuroblastoma cells. However, hNPCs showed a gradual increase in PCC in both differentiated and undifferentiated cells after 6 h exposure. Also notable was the range of protein carbonylations in hNPCs that differed from those in human neuroblastoma SH-SY5Y cells, as revealed by oxyblots. Protein bands at ~85 - 250 kDa were carbonylated in hNPCs whereas ~50 - 120 kDa protein carbonylations predominated in SH-SY5Y cells. This difference could be due to the fact that SH-SY5Y cells represent only a neuronal cell population, while hNPCs represent three cell linages. This brings forward the differential effect of alcohol on pure cell populations or their intracellular interactions. The process of protein

carbonylation is gradual after ROS production as observed in this study in both cell lines upon alcohol exposure, but the rationale for this temporal delay will need to be investigated further.

The next part of the thesis focused on the influence of co-exposure of pesticides and alcohol upon cytotoxicity responses in both undifferentiated and differentiated cells. This study showed a co-exposure effect on inducing cytotoxicity to undifferentiated and differentiated human neuroblastoma cells. The effects were mediated via ROS generation and protein carbonylation, and ATP depletion. This study concluded that the severity of cytotoxic responses has an association with the interaction of both neurotoxicants, and that particularly higher doses of the three tested pesticides with different combinations of ethanol, induced concentration dependent increases in cytotoxic responses for both phenotypes. Some low doses of pesticide combinations with alcohol induced synergistic effects on cells. Interestingly, the interactive effect of low doses of pesticides and alcohol induced cellular cytosolic protein damages in association with ROS generation in both undifferentiated and differentiated cells. The PCC levels were similar to the individual pesticide and ethanol-induced PCC levels observed for 24 h exposure as in Chapter IV and VI with human neuroblastoma cells. These disturbances in cellular cytosolic proteins could influence the neurite outgrowth inhibition/neurite degradation observed in morphological impairments apparent for differentiated cells compared to the non-treated controls.

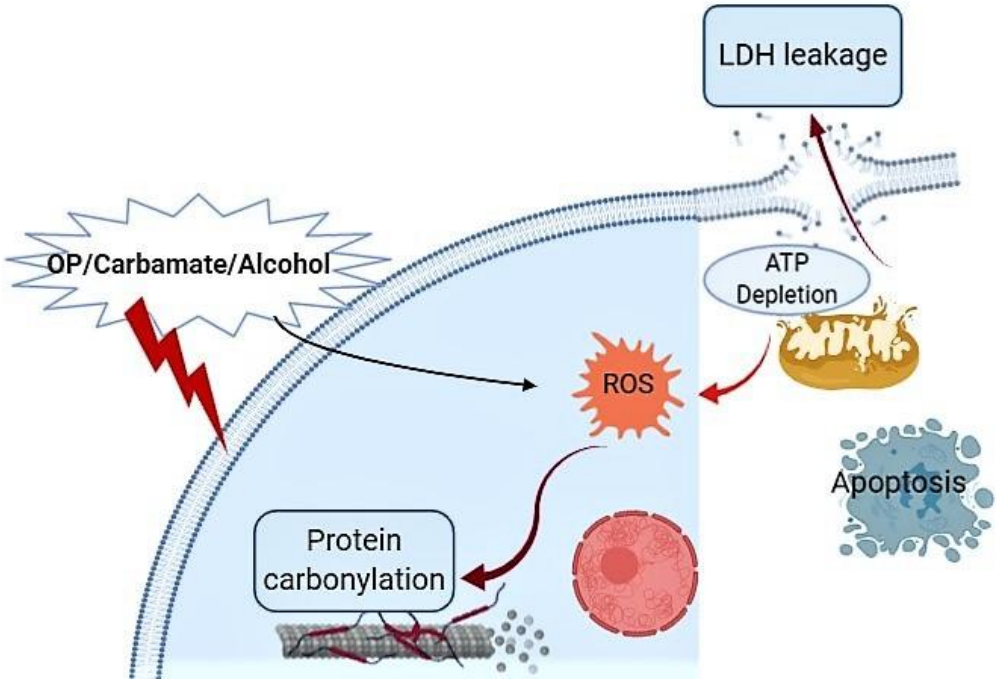


Figure 9-3: Schematic diagram of common mechanisms underlying the cytotoxicity of exposure to CPO, AZO, Aldicarb and alcohol in human neuroblastoma SH-SY5Y cells and human cortical progenitor neuronal cells.

Figure 9-2 represents the common mechanism underlying the CPO, AZO, Aldicarb, and alcohol-induced cytotoxicity of both phenotypes of human neuroblastoma SH-SY5Y cells and human cortical progenitor neuronal stem cells, according to the current study. Cytotoxicity of CPO, AZO, Aldicarb, and alcohol is cell type and stage-specific. Cell metabolic activity and cell viability of both cell lines decreased when concentrations of pesticides and alcohol continue to increase. Herein, pesticides and alcohol exposure results in cellular ATP level depletion in a concentration-dependent manner. This study has emphasised that ATP levels in both cell lines have a critical effect on cell metabolic activities and cell viability of human neuronal cells, and whether the neurotoxicant induced cell death is strongly dependent on the cellular ATP level depletion. The study confirm ATP level depletion in human neuronal cells is one route of cytotoxicity.

The mechanism of neurotoxicity of direct oxon metabolites of OP, carbamate and alcohol exposure is oxidative stress due to generation of ROS in human neuronal cells according to the current study. Elevated ROS levels in neuronal cells upon exposure of tested neurotoxicants, or through the combination of the neurotoxicants, significantly affected cellular reducing power capabilities, and resulted in protein redox damage. Collectively, the neurotoxic responses were effects on cellular metabolism, attenuation of ATP supply and functions of cellular proteins.

According to the current study, cytoskeleton proteins are a potential target of oxidative stress induced by OP/carbamate pesticides and alcohol exposures. The neuronal cytoskeleton plays a vital role in cellular morphological structure, maintaining and controlling the developmental process in the nervous system. These processes include cell proliferation, migration, differentiation, morphogenesis, neurite outgrowth, elongation of axons, branching of dendrites, steering of growth cones, and apoptosis (Flaskos, 2014). Perturbations of the neuronal cytoskeleton influence these neuronal development stages (Flaskos 2014). The neuronal cytoskeleton is a fibrous network composed of three groups of proteins: microtubules, intermediate filaments, and microfilaments. All of these maintain cell structural rigidity and play important roles in neurite extensions and axonal growth. Microtubules have an important role in neuron growth, physiology, and regulation of neuronal morphology, intracellular transport and outgrowth of neurite and axons. Microtubules are a collection of two heterodimers of α and β tubulins and microtubule-associated proteins (MAPs). During cell division, microtubules undergo polymerization and depolymerisation reactions. The main protein associated with microtubules is α and β tubulins which are approximately 55 kDa in molecular weight. They consist of several isoforms, β tubulin isoforms have specific roles in neuronal

development. β III tubulin isoform is present in neuronal cells and expressed upon neuronal differentiation and plays a vital role in neurite outgrowth (Radio and Mundy, 2008). Neurofilament protein present in the intermediate filaments are expressed in neuronal cells and widely studied about phosphorylation after CPF and CPO exposure. Microfilaments are another group of proteins present in the neuronal cytoskeletal network and composed of actin proteins of approximately 43 kDa in molecular weight. Microfilaments are rich in dendritic processes and growth cones of neuronal cells. Intermediate filaments are slightly smaller than microtubules and provide structural support to cells. All of these three cytoskeletal proteins are interlinked to form the cytoskeleton network in neuronal cells (Butterfield, 2017). Alyamani (2018) showed that neurite inhibitaory effects induced by CPO in differentiating N2a cells was associated with reduced cytoskeleton protein expression levels in axons and dentrites. The disruption of cytoskeletal gene expression was associated with altered cytoskeletal protein expression levels of N2a upon sublethal CPO exposure. The study further confirmed that β III expression levels with mRNA expression of *TUBB3* in human progenitor neuronal stem cells significantly changed upon 3 and 10 µM CPO exposure.

CPO, AZO, Aldicarb, and alcohol exposure induced carbonylation of ~50 kDa protein as revealed by the Oxyblots. β II tubulin and α-tubulin changes were also observed in pesticide and alcohol exposure in human neuroblastoma cells while β III tubulin expression changes were observed in differentiated hNPCs upon pesticide exposure (Annexure 1; Figure 2 and 4). These cytoskeleton proteins could be one of the major targets of oxidative stress due to their higher abundancy compared to other macromolecules in neuronal cells (Gardiner et al., 2013, Davies, 2016). Neurotoxicant exposure induced oxidative stress could cause changes in their protein expression and/or post-translational

modification. Some oxidative stress effects on cytoskeleton proteins could act as protective responses, while others are likely detrimental to the cells. For instance, irreversible post-translational protein changes and aggregation of higher molecular weight proteins are toxic to the cells, while reversible changes act as cellular responses to oxidative stress and can mediate after-effects (Gardiner et al. 2013, Cai and Yan 2013). Therefore, neurite outgrowth inhibition and neurite degradation in differentiated cells could relate to protein carbonylation of cytoskeleton proteins and further investigation would be important to delineate this potential association between protein carbonylation and neurite outgrowth inhibition of neuronal cells after pesticides and alcohol exposures.

When conducting experiments with neurotoxicants in animal-free *in vitro* systems, selection of concentrations related to actual human exposure is difficult but crucial to attempt to mimic the relevant pathways activated during *in vivo* conditions. For the pesticide study with human neuroblastoma SH-SY5Y cells and hNPCs, concentration ranges were selected from prior experiments to determine the effective range. Then further validation and other neurotoxic endpoints except initial viability testing were done using low and high doses of three selected pesticides to determine the underlying mechanism of cytotoxicity (Bal-Price et al., 2010). A general functional endpoint of neurotoxicants after *in vivo* exposure was mimicked through the evaluation of a critical process which was the *in vitro* morphological biomarker change associated with neurite outgrowth and its inhibition. The use of oxon metabolites of two OP pesticides and Aldicarb were assessed for their acute toxicity evaluation, and this will minimize any bioactivation of the parent insecticides. However, it is difficult to unequivocably establish correlation between *in vivo* human exposures and the experimental concentrations used in the current work. Concerning CPO

exposure to human neuronal cells, previous studies have indicated that CPO-inhibited neurite outgrowth and reduced cytoskeletal protein expression levels at similar concentrations (1-10 µM) to those used in this study, which is clinically relevant to human developmental neurotoxicity (Flaskos, 2011, Flaskos, 2012). As observed in the current studies with CPO, protein carbonylation was observed even at IC_{10} concentrations for the three pesticides including CPO. IC_{10} of CPO for differentiated SH-SY5Y cells was calculated as 3 µM and for hNPCs as 0.4 µM. It has been suggested that low micromolar concentrations of CPO are attainable in developing organisms since micromolar levels of CPF (22.8 µM) were detectable in the meconium samples of new-born children (Ostrea et al., 2002). In regions of agriculture-based farming which used CPF, 70% of pregnant women had detectable levels of CPF in their blood circulation. CPF ranged from 3.95 µM in pregnant mothers and 4.92 µM in new borns (Huen et al., 2012). In patients with acute poisoning with CPF the blood concentration reached 12 µM. It is well established that the CPO is more water-soluble than CPF, which might reduce the ability to pass across the placenta. However, there was detection of a significant amount of AChE inhibition in mammalian foetus following *in vivo* exposure of pregnant animals to CPF and other OPs (Gupta et al., 2018), further supporting the above notion that foetal exposure to CPO can occur (Flaskos, 2011). There is no human exposure data available for Azamethiphos or Azamethiphos-oxon. Aldicarb exposure in humans has been reported in low doses and shows an association with developmental neurotoxicity in humans (Blacker et al., 2010). A study of voluntary exposure of humans to Aldicarb showed increasing blood AChE inhibition at 1 and 2 h post exposures where 0.025, 0.05 or 0.1 mg/kg acute exposure had occurred (Baron, 1994). However, these *in vivo* doses could not be compared directly with *in vitro* concentrations or doses to cells, as different tissues interact with each other

physiologically to exhibit toxicological consequences of pesticides, and *in vitro* mimickry of biotransformation and metabolism is invariably not feasible.

Acute OP poisoning and induced oxidative stress and the association of intermediate syndrome has been documented (Dandapani et al., 2003). The acute exposure of OP showed enhancement of erythrocyte membrane lipid peroxidation than the non-exposed group for OP exposed patients (Dandapani et al., 2003). This study further mentioned that AChE inhibition triggers oxidative stress in the body and was associated with muscle dysfunction. Another study showed acutely OP intoxicated patients showed elevated levels of MDA and SOD, and decreased AChE activity in erythrocytes (Vidyasagar, 2004). These parameters were not reached to the normal levels even after classic treatments used for OP poisoning in humans. This suggests currently used treatments not effective for acute poisoning of OP induced severe oxidative stress in humans (Vidyasagar et al., 2004). Rajnbar et al. (2005) reported that OP poisoned patients had thiobarbituric acid reactive substances (TBARS) (a marker of lipid peroxidation) and reduced plasma total antioxidant capacity (Ranjbar et al., 2005). This suggests that an organism cannot mediate the effect of a sudden increase of ROS after acute OP poisoning, and it has cellular consequences. Proposcur, a carbamate insecticide, produced enhanced levels of lipid peroxidation and decreased GSH levels, implying carbamates trigger oxidative stress in humans upon acute exposure (Banerjee et al., 1999).

The impact of alcohol on health relates to both the volume of alcohol consumed and the pattern of drinking, including the number of heavy drinking sessions (Rehm et al., 2017b). Exposure to neurons of 20 or 50 mM alcohol corresponds to BACs that typify consumption of several drinks in a period of a few hours; a binge drinking session that will result in intoxication for susceptible individuals (Eckardt et al., 1998). The 6 h exposure to 20 or 50 mM alcohol was used to

model a heavy drinking session from evening to early morning, and this did induce significant loss of neurons. A BAC of 20 - 50 mM can easily be achieved in a single heavy drinking session through consumption of 60+ grams of pure alcohol, from, for example, the consumption of 5 or more pints of beer each containing ≈12 g of alcohol. Thus heavy drinking on one or more evenings at a weekend will easily reach or surpass the guidelines for weekly alcohol intake; with potentially more detriment to health (Eckardt et al., 1998, Rehm et al., 2003). It has been estimated that ≈20% of adults globally within the age range of 18 - 24 are heavy episodic drinkers, a percentage predicted to increase over the coming decade (CDC, 2019, Manthey et al., 2019).

Alcohol exposures of 100 or 200 mM to neurons induced substantive declines in neuronal viability even for the shortest time point (3 h). For susceptible individuals, BACs of 100 - 200 mM will induce a loss of consciousness, coma, or even death. Nevertheless, individuals used to chronic alcohol exposures, such as patients with alcohol use disorders (AUDs), develop tolerance to alcohol's CNS effects as well as displaying heightened alcohol metabolism enabling them to withstand high systemic BACs. Although a 24 h alcohol exposure would be considered uncommon for most weekend binge drinkers, sustained intoxication may be experienced by individuals with AUDs. The study results suggest that exposure to neurons of moderate to high BACs (20 or 50 mM) for 24 h is still sufficient to trigger substantive neuronal death; approaching 24 h IC_{50} values for differentiated cells. The current study with alcohol on both human neuroblastoma and hNPCs showed that the primary source of cytotoxicity is oxidative stress. Results from human alcoholics showed alcohol and its metabolites induced oxidative stress. As a secondary effect of alcohol exposure, acetaldehyde and aldehydic products of lipid peroxidation were formed, that can bind to proteins forming stable adducts. The protein structure

and functional changes that arise from oxidation reactions are associated with cellular pathologies. The aforementioned study points out damaged proteins in the centrilobular region of the liver in alcohol abusers with an early phase of histological liver damage (Niemelä, 1999). It is well documented that loss of cytosolic α- and β-tubulin is a major pathological hallmark in alcoholic brains compared to control brains (Labisso et al., 2018b). According to the current study, carbonylation of cytosolic protein may be linked with the brain volume shrinkage and volume loss due to the disruption of the cytoskeleton network.

Co-exposure of ethanol and pesticides are common in developing countries among occupational workers (Eddleston et al., 2009). Depending upon the chemical nature of the pesticide coingested with alcohol, the clinical manifestations that arise maybe worse than just the pesticide alone. However, clinical management of the poisoning of coingestion of ethanol and pesticides were not worked with the current treatments used for pesticide poisoning management in hospitals such as oxime treatment (Eddleston et al., 2009). The chapter IX of thesis is a study focussed upon co-exposures is an insight into understanding the pathology of poisoning, including solvents and consideration of novel treatments for coingestion of ethanol and pesticide poisonings.

9.2 Limitations of the study and future work

The study used relatively high throughput assays to determine the IC_{50} values of each neurotixicant used as this provided an opportunity to evaluate the neurotoxicity of each of the compounds in a cost and time effective manner in two different cell lines. Human neuroblastoma SH-SY5Y cells only represent a single (albeit homogeneous) neuronal cell population from the CNS, which may not represent the response from a mixed cellular population/or their intercellular interactions. Furthermore, it has been stated that neuroblastoma cell line

express tumor growth-related genes that may effect cell responses upon chemical exposure. However, by comparing data with that derived from the use of human progenitor cortical neural stem cells, there was an opportunity to evaluate the neurotoxicity of these compounds using a system more closely resembling that of the complexicity of the CNS and representation of three cell lineages.

One major limitation of this study, which is often been criticized as problem with *in vitro* pesticide studies, is the lack of metabolic competence. However, current studies targeted the evaluation of direct effects of OP and carbamate or alcohol to neuronal cells. The use of active metabolites for the current studies minimizes any influence of species differences in the bioactivation of the parent insecticides. In order to compensate for the lack of metabolic competencies addition of S9-mix, hepatocyte-conditioned media with treatments or direct co-culture could be considered in future studies. For the case of biotransformation of enzymes in the brain and their role in toxicity, there is a dependency on the systemic biotransformation of parental compound after entry to the body. Thus, the impact of metabolic effects can be different depending on the type and route of exposure. The Integrated European project of acute systemic Toxicity ("A-cute-TOX"- Optimization and pre-validation of an *in vitro* test strategy for predicting human acute toxicity) demonstrated that the acute systemic toxicity of pesticides seems to be less dependent on expression of biotrasformation enzymes, than their role of toxicity and the type of exposure (Bal-Price et al., 2010).

Nevertheless, OP and carbamate pesticides studies in both cell lines cannot be completely correlated to human conditions due to the complexity of the CNS and it is not possible to cover all of these mechanisms with these two cell models and a finite number of measured endpoints. So there is an unmet need to

consider validation of the current data with more human primary cell lines, and 3D neuronal cell models, or from using chip technology to get a more relevant predictive observations of the behaviour and responses to these pesticides in humans.

The lower doses of pesticide like IC_5 and IC_{10} can induce ROS generation and protein carbonylation in cells which equates to low micromolar/nanomolar concentrations for SH-SY5Y and hNPCs and perturbs cells without affecting cell viability. This concentration range even stimulated oxidative stress at lower concentrations in hNPCs. It will be important to evaluate the oxidative damages to RNA/DNA under these concentrations to delineate further the molecular-level mechanisms of CPO, AZO, and Aldicarb neurotoxicity.

The current study showed cytosolic proteins are a potential target of the ROS generated by the pesticide and alcohol exposure. An ~50 kDa protein was a major target for carbonylation by both alcohol and pesticide which was also observed in cytosolic fractions of alcoholic brains in humans (Chapter VI). Therefore, it important to identify the exact proteins and their isoforms which are carbonylated due to oxidative stress in both SH-SY5Y cells and hNPCs by the CPO, AZO, Aldicarb and alcohol exposure, to delineate the association between cytotoxicity and cellular morphological impairments that arose from these exposures (Annexure 1; Identification of major proteins by two-dimensional oxyblot). Further, it is interesting to find out the possible interactions among carbonylated proteins that arose from the exposures to gain insight into the biological interactions of cellular metabolic pathways in SH-SY5Y cells and hNPCs. Protein aggregation assays could be performed to evaluate the effect of carbonylation on the aggregation process and examine the presence/levels of high molecular weight proteins that are resistant to proteolytic degradation. Proteomic studies could be carried out to find the possible cross-links within

tubulins as documented for CPO that can cause isopeptide crosslinking and promote tubulin aggregations (Schopfer and Lockridge, 2018). The study could be undertaken with tubulins exposed to CPO directly, but it is also important to carry out the study with *in vitro* treated cells such as hNPCs which is a more relevant model to represent the human CNS.

Reduced cellular ATP levels were observed in all tested low and high concentrations of the CPO, AZO, Aldicarb, and alcohol in both SH-SY5Y cells and hNPCs. This suggested cellular mitochondria are a major target of three pesticides and alcohol in both undifferentiated and differentiated cells. Therefore, the study could be further expanded to study mitochondrial bioenergetics related to pesticide and alcohol exposure in future studies.

A major limitation of the alcohol studies with SH-SY5Y and hNPCs is that ethyl alcohol (ethanol) was diluted in media and applied the mixture directly to plated neuronal cells. Hence the concentration of alcohol experienced by both cells is sustained and will only be reduced if the ethanol applied undergoes oxidative metabolism. By contrast, BACs will drop with ongoing alcohol metabolism, principally via the action of alcohol dehydrogenase in the liver parenchyma to form acetaldehyde. The acetaldehyde produced is short-lived, and subsequently converted to acetate by the action of acetaldehyde dehydrogenase (Osna et al., 2017). Additionally, cytochrome P450 enzymes and catalase can provide subsidiary ethanol metabolism, more often for excessive and chronic alcohol users. Hence, the alcohol concentrations the current studies with SH-SY5Y and hNPCs have investigated more appropriately model fixed BACs (for the durations examined) if negligible alcohol metabolism by both cells lines is assumed. Nonetheless, in favour of the currently used approach in study, binge drinking behavior typically involves a repeat purchase

of alcohol after each drink has been consumed, so BACs may certainly be sustained during an acute drinking session.

A second *caveat* of the current studies with alcohol was that pure alcohol was used for experimentation. Although this ensured that the observed (toxic) effects on cells were solely due to alcohol (and not other chemical impurities), alcoholic drinks generally contain a multitude of chemicals. Indeed, the purported cardio-protective effects of low to moderate alcohol consumption, particularly with wine and beer have been, at least in part, postulated to result from the antioxidant properties of polyphenolic compounds such as resveratrol (Hung et al., 2000, Wu and Hsieh, 2011). However, worldwide, ≈45% of total recorded alcohol consumption is in the form of spirits, beer at ≈34%, and wine only constituting ≈12% of consumption. Likewise, spirts are the preferential alcohol purchase, by volume, in England and Wales (Burton et al., 2017). Therefore, consideration of pure alcohol, for which spirits (typically 72-100 proof (36-50% alcohol by volume) are the closest purchasable equivalent, is in keeping with the modelling experiments undertaken.

Current studies have only considered a single, acute alcohol exposure to neurons and cannot provide insight into the neurobiological and neuropathological changes that arise as a consequence of multiple alcohol exposures, or indeed the gene expression changes associated with adaptation and dependence experienced by chronic, excessive alcohol users (Erdozain and Callado, 2014). Furthermore, neuronal loss and cognitive defects sustained from acute or subacute alcohol exposure may be balanced by tissue recovery and neurogenesis during periods of abstinence (Obernier et al., 2002a, Obernier et al., 2002b, Crews and Nixon, 2009).

The joint exposure of OP/carbamate pesticides with alcohol resulted in subtle changes in cell viability at certain exposures. The observed

synergistic/antagosistic effects observed in certain combinations could be due to experimental variations, and further validation would be important from a technical viewpoint. More experimental validation could aleviate these subtle changes and more uniform dose-repsonses could be observed. One other main characteristic of this study was that, only a single cell type was considered, hence the analyses could be repeated with ReNcell Cx cells.

The co-exposure of pesticide and alcohol suggested that the inclusion of alcohol as a solvent had a significant influence on inducing cytotoxicity at low doses of pesticides. Herein, pesticide studies were done with pure oxon metabolites of CPO AZO and Aldicarb to prevent the influence of species differences in the bioactivation of the parent insecticides. However, a person who drinks OP or carbamate pesticides ingests not only the active OP ingredient but also the surfactant which uses a range of formulations. The co-exposure study suggested that that solvent effects should also be considered when determining the safety levels of pesticides in future studies. This study could be repeated with hNPCs to use a more representative model of the human CNS. Furthermore, the exposure time and doses, not reflect the effect co-exposure associated with chronic exposure. This fact is particularly relevant for lower concentrations of pesticides associated with developmental neurotoxicity that may exert an influence after extended exposure durations.

The studies in this thesis conclude that acute exposure of OP/carbamate and alcohol induced oxidative stress and this is one of the mechanisms of cytotoxicity. As revealed by the ROS assays undertaken in the presence of N-acetylcystine (NAC), there was a reduced ROS level even when combined with the highest concentrations tested (IC_{80} + NAC with CPO, AZO and Aldicarb or 200 mM + NAC for ethanol treatments (Annexure 1; Figure 1,3,6,8). NAC has been tested for its anti-oxidative properties in OP poisonings (Cankayali et al.,

2005, Shadnia et al., 2007, Yurumez et al., 2007, Mahmoud et al., 2019). NAC provides sulfydryl groups to an organism or through metabolism can lead to increased GSH levels (Rice-Evans and Diplock, 1993, Firuzi et al., 2011), and reduce ROS levels (Rice-Evans and Diplock, 1993). It has a broad therapeutic index and is considered therapeutically safe (Rice-Evans and Diplock, 1993, Vendemiale et al., 1999). NAC can play a prophylactic as well as therapeutic function in OP toxicity (Yurumez et al., 2007). The co-exposure of pesticides and ethanol showed synergistic/antagonistic effects on ROS generation levels in SH-SY5Y cells so there is a potential to use antioxidant compounds to combat the oxidative damage. Other than NAC, Vitamin E and C have been reported as antioxidants used to minimize the MDA and ROS levels in pesticide toxicity studies using animal models (Güney et al., 2007). Melatonin was also shown as an endogenous antioxidant in acute poisoning of OP pesticides (Buyukokuroglu et al., 2008). Therefore, greater effort is required to elucidate potential antioxidants for reduction of ROS levels to provide therapeutic avenues for alcohol and pesticide poisonings.

9.3 Conclusions

In conclusion, the present studies used several morphological and biochemical approaches to study the neurotoxic effects of CPO, AZO, Aldircarb and alcohol using human neuroblastoma SH-SY5Y cells and human cortical progenitor neural stem cells. The data of the current study with the above nerotoxicants established that:

- CPO, AZO and Aldicarb and alcohol induced concentration and time dependent decreased cell metabolic activity and cell viability loss in both human neuroblastoma SH-SY5Y cells and hNPCs.

- The IC_{50} values of CPO, AZO and Aldicarb confirm that 4 - 40 µM is the effective concentration range for SH-SY5Y cells while a concentration range of 1 - 20 µM was effective for hNPCs for inducing cytotoxicity. Alcohol concentrations even at 10 mM were not effective at reducing cell metabolic activity or cell viability of SH-SY5Y cells, whereas hNPCs showed sensitivity to alcohol exposure at 10 mM.
- AChE inhibition by the three pesticides increased the severity of cytotoxic responses in both SH-SY5Y and hNPCs cells after exposure to CPO, AZO or Aldicarb.
- ROS was one means by which cytotoxicity was induced by CPO, AZO, Aldicarb or Alcohol in human neuronal cells. However, the concentrations below that effected cell metabolic functions were still able to induce ROS in both SH-SY5Y cells and hNPCs. ATP depletion was linked to elvated ROS levels in cells, and ATP levels declined consistent with the fate (death) of human neuronal cells in response to CPO, AZO, Aldicarb or alcohol exposure.
- Cytosolic proteins are potential targets of CPO, AZO, Aldicarb and alcohol induced oxidative stress and oxidative stress mediated protein carbonylation, and this could impact upon the general cell functions of SH-SY5Y and hNPCs (Figure 9-2).

The current study proved human neuroblastoma SH-SY5Y provide a mono-culture cell model for modelling neurotoxicity of pesticides and alcohol while human cortical progenitor neural stem cells reduced the levels of uncertainty associated with mono-culture cell model results. This highlights both these cell models can be used for toxicity testing and guide chemical prioritization studies for further testing in a rapid and cost-effective manner.

REFERENCES

ABARIKWU, S. O., DURU, Q. C., NJOKU, R.-C. C., AMADI, B. A., TAMUNOIBUOMIE, A. & KEBOH, E. 2017. Effects of co-exposure to atrazine and ethanol on the oxidative damage of kidney and liver in Wistar rats. *Renal failure,* 39**,** 588-596.

ABDEL-SALAM, O. M. E., YOUNESS, E. R., ESMAIL, R. S. E., MOHAMMED, N. A., KHADRAWY, Y. A., SLEEM, A. A. & ABDULAZIZ, A. M. 2018. Protection by Neostigmine and Atropine Against Brain and Liver Injury Induced by Acute Malathion Exposure. *Journal of Nanoscience and Nanotechnology,* 18**,** 510-521.

ABEL, E. L. & HANNIGAN, J. H. 1995. Maternal risk factors in fetal alcohol syndrome: Provocative and permissive influences. *Neurotoxicology and Teratology,* 17**,** 445-462.

ALDINI, G., DALLE-DONNE, I., VISTOLI, G., MAFFEI FACINO, R. & CARINI, M. 2005. Covalent modification of actin by 4-hydroxy-trans-2-nonenal (HNE): LC-ESI-MS/MS evidence for Cys374 Michael adduction. *J Mass Spectrom,* 40**,** 946-54.

ALLEN, N. J. & BARRES, B. A. 2009. Glia — more than just brain glue. *Nature,* 457**,** 675-677.

ALYAMANI, N. 2018. Molecular-genetics studies of organophosphate induced neurodegenration in differetiating mamalian cell lines and human neuralprogenitor stem cells. *PhD theis*.

ANDERSON, C. C., AIVAZIDIS, S., KUZYK, C. L., JAIN, A. & ROEDE, J. R. 2018. Acute Maneb Exposure Significantly Alters Both Glycolysis and Mitochondrial Function in Neuroblastoma Cells. *Toxicological Sciences,* 165**,** 61-73.

ANSTEY, K. J., MACK, H. A. & CHERBUIN, N. 2009. Alcohol Consumption as a Risk Factor for Dementia and Cognitive Decline: Meta-Analysis of Prospective Studies. *The American Journal of Geriatric Psychiatry,* 17**,** 542-555.

AUTHORITY, E. F. S. 2019. The 2017 European Union report on pesticide residues in food. *EFSA Journal,* 17**,** e05743.

BAL-PRICE, A. K., HOGBERG, H. T., BUZANSKA, L. & COECKE, S. 2010. Relevance of in vitro neurotoxicity testing for regulatory requirements: Challenges to be considered. *Neurotoxicology and Teratology,* 32**,** 36-41.

BALASZCZUK, V., BENDER, C., PERENO, G. L. & BELTRAMINO, C. A. 2011. Alcohol-induced neuronal death in central extended amygdala and pyriform cortex during the postnatal period of the rat. *Int J Dev Neurosci,* 29**,** 733-42.

BANAN, A., CHOUDHARY, S., ZHANG, Y., FIELDS, J. Z. & KESHAVARZIAN, A. 1999. Ethanol-Induced Barrier Dysfunction and Its Prevention by

Growth Factors in Human Intestinal Monolayers: Evidence for Oxidative and Cytoskeletal Mechanisms. *Journal of Pharmacology and Experimental Therapeutics,* 291**,** 1075.

BANAN, A., FIELDS, J. Z., DECKER, H., ZHANG, Y. & KESHAVARZIAN, A. 2000. Nitric Oxide and Its Metabolites Mediate Ethanol-Induced Microtubule Disruption and Intestinal Barrier Dysfunction. *Journal of Pharmacology and Experimental Therapeutics,* 294**,** 997.

BANERJEE, B. D., SETH, V., BHATTACHARYA, A., PASHA, S. T. & CHAKRABORTY, A. K. 1999. Biochemical effects of some pesticides on lipid peroxidation and free-radical scavengers. *Toxicology Letters,* 107**,** 33-47.

BARON, R. L. 1994. A carbamate insecticide: a case study of aldicarb. *Environmental health perspectives,* 102 Suppl 11**,** 23-27.

BARONE, S., JR., DAS, K. P., LASSITER, T. L. & WHITE, L. D. 2000. Vulnerable processes of nervous system development: a review of markers and methods. *Neurotoxicology,* 21**,** 15-36.

BARR, D. B. & BUCKLEY, B. 2011. Chapter 20 - In vivo biomarkers and biomonitoring in reproductive and developmental toxicity. *In:* GUPTA, R. C. (ed.) *Reproductive and Developmental Toxicology.* San Diego: Academic Press.

BARRES, B. A. & BARDE, Y.-A. 2000. Neuronal and glial cell biology. *Current Opinion in Neurobiology,* 10**,** 642-648.

BASIRI, S., ESMAILY, H., VOSOUGH-GHANBARI, S., MOHAMMADIRAD, A., YASA, N. & ABDOLLAHI, M. 2007. Improvement by Satureja khuzestanica essential oil of malathion-induced red blood cells acetylcholinesterase inhibition and altered hepatic mitochondrial glycogen phosphorylase and phosphoenolpyruvate carboxykinase activities. *Pesticide Biochemistry and Physiology,* 89**,** 124-129.

BEARER, C. F., SWICK, A. R., O'RIORDAN, M. A. & CHENG, G. 1999. Ethanol inhibits L1-mediated neurite outgrowth in postnatal rat cerebellar granule cells. *The Journal of biological chemistry,* 274**,** 13264-13270.

BERMAN, R. F. & HANNIGAN, J. H. 2000. Effects of prenatal alcohol exposure on the hippocampus: spatial behavior, electrophysiology, and neuroanatomy. *Hippocampus,* 10**,** 94-110.

BETANCOURT, A. M. & CARR, R. L. 2004. The Effect of Chlorpyrifos and Chlorpyrifos-Oxon on Brain Cholinesterase, Muscarinic Receptor Binding, and Neurotrophin Levels in Rats Following Early Postnatal Exposure. *Toxicological Sciences,* 77**,** 63-71.

BIEDLER, J. L., ROFFLER-TARLOV, S., SCHACHNER, M. & FREEDMAN, L. S. 1978. Multiple neurotransmitter synthesis by human neuroblastoma cell lines and clones. *Cancer Res,* 38**,** 3751-7.

BJØRLING-POULSEN, M., ANDERSEN, H. R. & GRANDJEAN, P. 2008a. Potential developmental neurotoxicity of pesticides used in Europe. *Environmental Health,* 7**,** 50.

BJØRLING-POULSEN, M., ANDERSEN, H. R. & GRANDJEAN, P. 2008b. Potential developmental neurotoxicity of pesticides used in Europe. *Environmental health : a global access science source,* 7**,** 50-50.

BLACKER, A. M., KELLY, I. D., LANTZ, J. L., MIHLAN, G. J., JONES, R. L. & YOUNG, B. M. 2010. Chapter 75 - Aldicarb: Toxicity, Exposure and Risks to Humans. *In:* KRIEGER, R. (ed.) *Hayes' Handbook of Pesticide Toxicology (Third Edition).* New York: Academic Press.

BOONSTRA, J. & POST, J. A. 2004. Molecular events associated with reactive oxygen species and cell cycle progression in mammalian cells. *Gene,* 337**,** 1-13.

BOUCAUD-MAITRE, D., RAMBOURG, M. O., SINNO-TELLIER, S., PUSKARCZYK, E., PINEAU, X., KAMMERER, M., BLOCH, J. & LANGRAND, J. 2019. Human exposure to banned pesticides reported to the French Poison Control Centers: 2012-2016. *Environ Toxicol Pharmacol,* 69**,** 51-56.

BOULTON, S., ANDERSON, A., SWALWELL, H., HENDERSON, J. R., MANNING, P. & BIRCH-MACHIN, M. A. 2011. Implications of using the fluorescent probes, dihydrorhodamine 123 and 2',7'-dichlorodihydrofluorescein diacetate, for the detection of UVA-induced reactive oxygen species. *Free Radic Res,* 45**,** 139-46.

BRADY, K. T. 2014. Chapter Nine - The Effects of Alcohol on the Human Nervous System. *In:* MADRAS, B. & KUHAR, M. (eds.) *The Effects of Drug Abuse on the Human Nervous System.* Boston: Academic Press.

BROCARDO, P. S., GIL-MOHAPEL, J. & CHRISTIE, B. R. 2011. The role of oxidative stress in fetal alcohol spectrum disorders. *Brain Research Reviews,* 67**,** 209-225.

BRUST, J. C. M. 2010. Ethanol and cognition: indirect effects, neurotoxicity and neuroprotection: a review. *International journal of environmental research and public health,* 7**,** 1540-1557.

BURD, L., BLAIR, J. & DROPPS, K. 2012. Prenatal alcohol exposure, blood alcohol concentrations and alcohol elimination rates for the mother, fetus and newborn. *J Perinatol,* 32**,** 652-9.

BURD, L. & MARTSOLF, J. T. 1989. Fetal alcohol syndrome: Diagnosis and syndromal variability. *Physiology & Behavior,* 46**,** 39-43.

BURKE, R. D., TODD, S. W., LUMSDEN, E., MULLINS, R. J., MAMCZARZ, J., FAWCETT, W. P., GULLAPALLI, R. P., RANDALL, W. R., PEREIRA, E. F. R. & ALBUQUERQUE, E. X. 2017. Developmental neurotoxicity of the organophosphorus insecticide chlorpyrifos: from clinical findings to preclinical models and potential mechanisms. *J Neurochem,* 142 Suppl 2**,** 162-177.

BURTON, R., HENN, C., LAVOIE, D., O'CONNOR, R., PERKINS, C., SWEENEY, K., GREAVES, F., FERGUSON, B., BEYNON, C., BELLONI, A., MUSTO, V., MARSDEN, J. & SHERON, N. 2017. A rapid evidence review of the effectiveness and cost-effectiveness of alcohol control policies: an English perspective. *Lancet,* 389**,** 1558-1580.

BUTTERFIELD, D. A. & PERLUIGI, M. 2017. Redox Proteomics: A Key Tool for New Insights into Protein Modification with Relevance to Disease. *Antioxid Redox Signal,* 26**,** 277-279.

BUTTERFIELD, D. A. & STADTMAN, E. R. 1997. Chapter 7 Protein Oxidation Processes in Aging Brain. *In:* TIMIRAS, P. S. & BITTAR, E. E. (eds.) *Advances in Cell Aging and Gerontology.* Elsevier.

BUTTERFIELD, D. A. P., M. 2017. Redox Proteomics: A Key Tool for New Insights into Protein Modification with Relevance to Disease. *Antioxidants & Redox Signaling,* 26**,** 277-279.

BUYUKOKUROGLU, M. E., CEMEK, M., YURUMEZ, Y., YAVUZ, Y. & ASLAN, A. 2008. Antioxidative role of melatonin in organophosphate toxicity in rats. *Cell Biology and Toxicology,* 24**,** 151-158.

CAI, Z. & YAN, L.-J. 2013. Protein Oxidative Modifications: Beneficial Roles in Disease and Health. *Journal of biochemical and pharmacological research,* 1**,** 15-26.

CALVIELLO, G., PICCIONI, E., BONINSEGNA, A., TEDESCO, B., MAGGIANO, N., SERINI, S., WOLF, F. I. & PALOZZA, P. 2006. DNA damage and apoptosis induction by the pesticide Mancozeb in rat cells: Involvement of the oxidative mechanism. *Toxicology and Applied Pharmacology,* 211**,** 87-96.

CAMPBELL, J. C., STIPCEVIC, T., FLORES, R. E., PERRY, C. & KIPPIN, T. E. 2014. Alcohol exposure inhibits adult neural stem cell proliferation. *Exp Brain Res,* 232**,** 2775-84.

CANKAYALI, L., DEMIRAG, K., ERIS, O., ERSOZ, B. & MORAL, A. R. 2005. The effects ofN-acetylcysteine on oxidative stress in organophosphate poisoning model. *Advances in Therapy,* 22**,** 107-116.

CARLSON, K. & EHRICH, M. 1999. Organophosphorus Compound-Induced Modification of SH-SY5Y Human Neuroblastoma Mitochondrial Transmembrane Potential. *Toxicology and Applied Pharmacology,* 160**,** 33-42.

CARLSON, K., JORTNER, B. S. & EHRICH, M. 2000. Organophosphorus Compound-Induced Apoptosis in SH-SY5Y Human Neuroblastoma Cells. *Toxicology and Applied Pharmacology,* 168**,** 102-113.

CARR, R. L., ALUGUBELLY, N. & MOHAMMED, A. N. 2018. Chapter Five - Possible Mechanisms of Developmental Neurotoxicity of Organophosphate Insecticides. *In:* ASCHNER, M. & COSTA, L. G. (eds.) *Advances in Neurotoxicology.* Academic Press.

CDC 2019. Alcohol and Public Health. *Centres for Disease Control and Prevention, Binge Drinking Fact Sheets*

CHALMERS-REDMAN, R. M., PRIESTLEY, T., KEMP, J. A. & FINE, A. 1997. In vitro propagation and inducible differentiation of multipotential progenitor cells from human fetal brain. *Neuroscience,* 76**,** 1121-8.

CHAMBERS, J. E. & CHAMBERS, H. W. 1989. Oxidative desulfuration of chlorpyrifos, chlorpyrifos-methyl, and leptophos by rat brain and liver. *Journal of Biochemical Toxicology,* 4**,** 201-203.

CHAMBERS, J. E., MEEK, E. C. & CHAMBERS, H. W. 2010. Chapter 65 - The Metabolism of Organophosphorus Insecticides. *In:* KRIEGER, R. (ed.) *Hayes' Handbook of Pesticide Toxicology (Third Edition).* New York: Academic Press.

CHANG, C. H., YU, C. J., DU, J. C., CHIOU, H. C., CHEN, H. C., YANG, W., CHUNG, M. Y., CHEN, Y. S., HWANG, B., MAO, I. F. & CHEN, M. L. 2018. The interactions among organophosphate pesticide exposure, oxidative stress, and genetic polymorphisms of dopamine receptor D4 increase the risk of attention deficit/hyperactivity disorder in children. *Environ Res,* 160**,** 339-346.

CHANG, X., LU, W., DOU, T., WANG, X., LOU, D., SUN, X. & ZHOU, Z. 2013. Paraquat inhibits cell viability via enhanced oxidative stress and apoptosis in human neural progenitor cells. *Chemico-Biological Interactions,* 206**,** 248-255.

CHEUNG, Y. T., LAU, W. K., YU, M. S., LAI, C. S., YEUNG, S. C., SO, K. F. & CHANG, R. C. 2009. Effects of all-trans-retinoic acid on human SH-SY5Y neuroblastoma as in vitro model in neurotoxicity research. *Neurotoxicology,* 30**,** 127-35.

CHIARADIA, E., RENZONE, G., SCALONI, A., CAPUTO, M., COSTANZI, E., GAMBELUNGHE, A., MUZI, G., AVELLINI, L., EMILIANI, C. & BURATTA, S. 2019. Protein carbonylation in dopaminergic cells exposed to rotenone. *Toxicol Lett,* 309**,** 20-32.

CHO, T. & TIFFANY-CASTIGLIONI, E. 2004. Neurofilament 200 as an indicator of differences between mipafox and paraoxon sensitivity in Sy5Y neuroblastoma cells. *J Toxicol Environ Health A,* 67**,** 987-1000.

CHU, J., TONG, M. & DE LA MONTE, S. M. 2007. Chronic ethanol exposure causes mitochondrial dysfunction and oxidative stress in immature central nervous system neurons. *Acta Neuropathologica,* 113**,** 659-673.

COLE, G. J., ZHANG, C., OJIAKU, P., BELL, V., DEVKOTA, S. & MUKHOPADHYAY, S. 2012. Chapter Seven - Effects of Ethanol Exposure on Nervous System Development in Zebrafish. *In:* JEON, K. W. (ed.) *International Review of Cell and Molecular Biology.* Academic Press.

COLOMBO, G., CLERICI, M., GARAVAGLIA, M. E., GIUSTARINI, D., ROSSI, R., MILZANI, A. & DALLE-DONNE, I. 2016. A step-by-step protocol for assaying protein carbonylation in biological samples. *J Chromatogr B Analyt Technol Biomed Life Sci,* 1019**,** 178-90.

COMPSTON, A., ZAJICEK, J., SUSSMAN, J., WEBB, A., HALL, G., MUIR, D., SHAW, C., WOOD, A. & SCOLDING, N. 1997. Glial lineages and myelination in the central nervous system. *Journal of anatomy,* 190 (Pt 2)**,** 161-200.

COSTA, L. G. 1998. Neurotoxicity testing: a discussion of in vitro alternatives. *Environmental Health Perspectives,* 106**,** 505-510.

COSTA, L. G. 2006. Current issues in organophosphate toxicology. *Clinica Chimica Acta,* 366**,** 1-13.

COSTA, L. G., GIORDANO, G., COLE, T. B., MARSILLACH, J. & FURLONG, C. E. 2013. Paraoxonase 1 (PON1) as a genetic determinant of susceptibility to organophosphate toxicity. *Toxicology,* 307**,** 115-122.

COWAN, W., JESSELL, T., & ZIPURSKY, S. (EDS.) 1998. Molecular and Cellular Approaches to Neural Development.

COX, C. 1994. Chlorpyrifos, Part I (Toxicology). *Journal of pesticide reform,* 12**,** 15-20.

CREWS, F., NIXON, K., KIM, D., JOSEPH, J., SHUKITT-HALE, B., QIN, L. & ZOU, J. 2006. BHT blocks NF-kappaB activation and ethanol-induced brain damage. *Alcohol Clin Exp Res,* 30**,** 1938-49.

CREWS, F. T. & NIXON, K. 2009. Mechanisms of neurodegeneration and regeneration in alcoholism. *Alcohol and alcoholism (Oxford, Oxfordshire),* 44**,** 115-127.

CROOM, E. L., WALLACE, A. D. & HODGSON, E. 2010. Human variation in CYP-specific chlorpyrifos metabolism. *Toxicology,* 276**,** 184-191.

CURTIS, J. M., HAHN, W. S., LONG, E. K., BURRILL, J. S., ARRIAGA, E. A. & BERNLOHR, D. A. 2012. Protein carbonylation and metabolic control systems. *Trends in endocrinology and metabolism: TEM,* 23**,** 399-406.

DAI, H., DENG, Y., ZHANG, J., HAN, H., ZHAO, M., LI, Y., ZHANG, C., TIAN, J., BING, G. & ZHAO, L. 2015. PINK1/Parkin-mediated mitophagy alleviates chlorpyrifos-induced apoptosis in SH-SY5Y cells. *Toxicology,* 334**,** 72-80.

DALLE-DONNE, I., ALDINI, G., CARINI, M., COLOMBO, R., ROSSI, R. & MILZANI, A. 2006. Protein carbonylation, cellular dysfunction, and disease progression. *Journal of cellular and molecular medicine,* 10**,** 389-406.

DALLE-DONNE, I., ROSSI, R., GIUSTARINI, D., GAGLIANO, N., LUSINI, L., MILZANI, A., DI SIMPLICIO, P. & COLOMBO, R. 2001. Actin carbonylation: from a simple marker of protein oxidation to relevant signs of severe functional impairment. *Free Radic Biol Med,* 31**,** 1075-83.

DAMALAS, C. A. & ELEFTHEROHORINOS, I. G. 2011. Pesticide exposure, safety issues, and risk assessment indicators. *International journal of environmental research and public health,* 8**,** 1402-1419.

DANDAPANI, M., ZACHARIAH, A., KAVITHA, M., JEYASEELAN, L. & OOMMEN, A. 2003. Oxidative damage in intermediate syndrome of acute organophosphorus poisoning. *The Indian journal of medical research,* 117**,** 253-9.

DANG, C. V., RESAR, L. M., EMISON, E., KIM, S., LI, Q., PRESCOTT, J. E., WONSEY, D. & ZELLER, K. 1999. Function of the c-Myc oncogenic transcription factor. *Exp Cell Res,* 253**,** 63-77.

DAS, K. & ROYCHOUDHURY, A. 2014. Reactive oxygen species (ROS) and response of antioxidants as ROS-scavengers during environmental stress in plants. *Frontiers in Environmental Science,* 2.

DAS, S. K., MUKHERJEE, S. & VASUDEVAN, D. M. 2011. Effects of long term ethanol consumption on cell death in liver. *Indian J Clin Biochem,* 26**,** 84-7.

DAS, S. K. & VASUDEVAN, D. M. 2007. Alcohol-induced oxidative stress. *Life Sciences,* 81**,** 177-187.

DASGUPTA, A., ZHENG, J. & BIZZOZERO, O. A. 2012. Protein carbonylation and aggregation precede neuronal apoptosis induced by partial glutathione depletion. *ASN neuro,* 4**,** e00084.

DAVIES, G. 2009. Chronic Organophosphate Exposure: Towards the Definition of a Neuropsychiatric Syndrome. *Journal of Nutritional and Environmental Medicine,* 7**,** 169-176.

DAVIES, M. J. 2016. Protein oxidation and peroxidation. *The Biochemical journal,* 473**,** 805-825.

DAVIES, M. J., BAER, D. J., JUDD, J. T., BROWN, E. D., CAMPBELL, W. S. & TAYLOR, P. R. 2002. Effects of moderate alcohol intake on fasting insulin and glucose concentrations and insulin sensitivity in postmenopausal women: a randomized controlled trial. *Jama,* 287**,** 2559-62.

DAVIS, K. M. & WU, J. Y. 2001. Role of glutamatergic and GABAergic systems in alcoholism. *J Biomed Sci,* 8**,** 7-19.

DE BERTRAND, N. & BARCELÓ, D. 1991. Photodegradation of the carbamate pesticides aldicarb, carbaryl and carbofuran in water. *Analytica Chimica Acta,* 254**,** 235-244.

DE FILIPPIS, L., HALIKERE, A., MCGOWAN, H., MOORE, J. C., TISCHFIELD, J. A., HART, R. P. & PANG, Z. P. 2016. Ethanol-mediated activation of the NLRP3 inflammasome in iPS cells and iPS cells-derived neural progenitor cells. *Molecular brain,* 9**,** 51-51.

DE LA MONTE, S., DERDAK, Z. & WANDS, J. R. 2012. Alcohol, insulin resistance and the liver-brain axis. *Journal of gastroenterology and hepatology,* 27 Suppl 2**,** 33-41.

DE OLIVEIRA, M. R., PERES, A., FERREIRA, G. C., SCHUCK, P. F. & BOSCO, S. M. D. 2016. Carnosic Acid Affords Mitochondrial Protection in Chlorpyrifos-Treated Sh-Sy5y Cells. *Neurotoxicity Research,* 30**,** 367-379.

DETTBARN, W.-D., MILATOVIC, D. & GUPTA, R. C. 2006. CHAPTER 36 - Oxidative Stress in Anticholinesterase-Induced Excitotoxicity. *In:* GUPTA, R. C. (ed.) *Toxicology of Organophosphate & Carbamate Compounds.* Burlington: Academic Press.

DHANARISI, H. K. J., GAWARAMMANA, I. B., MOHAMED, F. & EDDLESTON, M. 2018. Relationship between alcohol co-ingestion and outcome in profenofos self-poisoning - A prospective case series. *PloS one,* 13**,** e0200133-e0200133.

DI ROCCO, G., BALDARI, S., PANI, G. & TOIETTA, G. 2019. Stem cells under the influence of alcohol: effects of ethanol consumption on stem/progenitor cells. *Cellular and Molecular Life Sciences,* 76**,** 231-244.

DIKRANIAN, K., QIN, Y.-Q., LABRUYERE, J., NEMMERS, B. & OLNEY, J. W. 2005. Ethanol-induced neuroapoptosis in the developing rodent cerebellum and related brain stem structures. *Developmental Brain Research,* 155**,** 1-13.

DING, Q. & KELLER, J. N. 2001. Proteasomes and proteasome inhibition in the central nervous system. *Free Radic Biol Med,* 31**,** 574-84.

DIRKSEN, C. L., HOWARD, J. A., CRONIN-GOLOMB, A. & OSCAR-BERMAN, M. 2006. Patterns of prefrontal dysfunction in alcoholics with and without Korsakoff's syndrome, patients with Parkinson's disease, and patients with rupture and repair of the anterior communicating artery. *Neuropsychiatr Dis Treat,* 2**,** 327-39.

DIVALD, A. & POWELL, S. R. 2006. Proteasome mediates removal of proteins oxidized during myocardial ischemia. *Free Radical Biology and Medicine,* 40**,** 156-164.

DONADONI, M., CICALESE, S., SARKAR, D. K., CHANG, S. L. & SARIYER, I. K. 2019. Alcohol exposure alters pre-mRNA splicing of antiapoptotic Mcl-1L isoform and induces apoptosis in neural progenitors and immature neurons. *Cell Death & Disease,* 10**,** 447.

DONATO, R., MILJAN, E. A., HINES, S. J., AOUABDI, S., POLLOCK, K., PATEL, S., EDWARDS, F. A. & SINDEN, J. D. 2007. Differential development of neuronal physiological responsiveness in two human neural stem cell lines. *BMC neuroscience,* 8**,** 36-36.

DONG, J., SULIK, K. K. & CHEN, S.-Y. 2010. The role of NOX enzymes in ethanol-induced oxidative stress and apoptosis in mouse embryos. *Toxicology Letters,* 193**,** 94-100.

EATON, D. L., DAROFF, R. B., AUTRUP, H., BRIDGES, J., BUFFLER, P., COSTA, L. G., COYLE, J., MCKHANN, G., MOBLEY, W. C., NADEL, L., NEUBERT, D., SCHULTE-HERMANN, R. & SPENCER, P. S. 2008.

Review of the toxicology of chlorpyrifos with an emphasis on human exposure and neurodevelopment. *Crit Rev Toxicol,* 38 Suppl 2**,** 1-125.

ECKARDT, M. J., FILE, S. E., GESSA, G. L., GRANT, K. A., GUERRI, C., HOFFMAN, P. L., KALANT, H., KOOB, G. F., LI, T.-K. & TABAKOFF, B. 1998. Effects of Moderate Alcohol Consumption on the Central Nervous System*. *Alcoholism: Clinical and Experimental Research,* 22**,** 998-1040.

EDDLESTON, M. 2019. Novel Clinical Toxicology and Pharmacology of Organophosphorus Insecticide Self-Poisoning. *Annual Review of Pharmacology and Toxicology,* 59**,** 341-360.

EDDLESTON, M., BUCKLEY, N. A., GUNNELL, D., DAWSON, A. H. & KONRADSEN, F. 2006. Identification of strategies to prevent death after pesticide self-poisoning using a Haddon matrix. *Inj Prev,* 12**,** 333-7.

EDDLESTON, M., GUNNELL, D., VON MEYER, L. & EYER, P. 2009. Relationship between blood alcohol concentration on admission and outcome in dimethoate organophosphorus self-poisoning. *Br J Clin Pharmacol,* 68**,** 916-9.

EHRICH, M., VAN TASSELL, R., LI, Y. B., ZHOU, Z. G. & KEPLEY, C. L. 2011. Fullerene antioxidants decrease organophosphate-induced acetylcholinesterase inhibition in vitro. *Toxicology in Vitro,* 25**,** 301-307.

ELMORE, S. 2007. Apoptosis: a review of programmed cell death. *Toxicol Pathol,* 35**,** 495-516.

ENCINAS, M., IGLESIAS, M., LIU, Y., WANG, H., MUHAISEN, A., CEÑA, V., GALLEGO, C. & COMELLA, J. 2000. Sequential Treatment of SH-SY5Y Cells with Retinoic Acid and Brain-Derived Neurotrophic Factor Gives Rise to Fully Differentiated, Neurotrophic Factor-Dependent, Human Neuron-Like Cells. *Journal of neurochemistry,* 75**,** 991-1003.

EPA 1998. Extremely Hazardous Substances (EHS) Chemical Profiles and Emergency First Aid Guides. *U.S. Environmental Protection Agency, Washington, D.C.: U.S. Government Printing Office*.

ERDOZAIN, A. M. & CALLADO, L. F. 2014. Neurobiological alterations in alcohol addiction: a review. *Adicciones,* 26**,** 360-70.

ERDOZAIN, A. M., MORENTIN, B., BEDFORD, L., KING, E., TOOTH, D., BREWER, C., WAYNE, D., JOHNSON, L., GERDES, H. K., WIGMORE, P., CALLADO, L. F. & CARTER, W. G. 2014. Alcohol-related brain damage in humans. *PloS one,* 9**,** e93586-e93586.

ERNST, W., JACKMAN, P., DOE, K., PAGE, F., JULIEN, G., MACKAY, K. & SUTHERLAND, T. 2001. Dispersion and Toxicity to Non-target Aquatic Organisms of Pesticides Used to Treat Sea Lice on Salmon in Net Pen Enclosures. *Marine Pollution Bulletin,* 42**,** 432-443.

ESTEVEZ, J. & VILANOVA, E. 2009. Model equations for the kinetics of covalent irreversible enzyme inhibition and spontaneous reactivation:

Esterases and organophosphorus compounds. *Critical Reviews in Toxicology,* 39**,** 427-448.

FAOSTAT 2019. Food and agriculture data for all FAO regional groupings. In (Vol. 2018).

FARIA, J., BARBOSA, J., QUEIRÓS, O., MOREIRA, R., CARVALHO, F. & DINIS-OLIVEIRA, R. J. 2016. Comparative study of the neurotoxicological effects of tramadol and tapentadol in SH-SY5Y cells. *Toxicology,* 359-360**,** 1-10.

FEIST, E., KEARN, J., GAIHRE, Y., O'CONNOR, V. & HOLDEN-DYE, L. 2020. The distinct profiles of the inhibitory effects of fluensulfone, abamectin, aldicarb and fluopyram on Globodera pallida hatching. *Pesticide Biochemistry and Physiology,* 165**,** 104541.

FERREIRA, C. A., NI, D., ROSENKRANS, Z. T. & CAI, W. 2018. Scavenging of reactive oxygen and nitrogen species with nanomaterials. *Nano Res,* 11**,** 4955-4984.

FIGUEROA, D., ASADUZZAMAN, M. & YOUNG, F. 2018. Real time monitoring and quantification of reactive oxygen species in breast cancer cell line MCF-7 by 2′,7′–dichlorofluorescin diacetate (DCFDA) assay. *Journal of Pharmacological and Toxicological Methods,* 94**,** 26-33.

FILLMORE, K. M., STOCKWELL, T., CHIKRITZHS, T., BOSTROM, A. & KERR, W. 2007. Moderate alcohol use and reduced mortality risk: systematic error in prospective studies and new hypotheses. *Ann Epidemiol,* 17**,** S16-23.

FIRUZI, O., MIRI, R., TAVAKKOLI, M. & SASO, L. 2011. Antioxidant therapy: current status and future prospects. *Curr Med Chem,* 18**,** 3871-88.

FLANAGAN, L. A., REBAZA, L. M., DERZIC, S., SCHWARTZ, P. H. & MONUKI, E. S. 2006. Regulation of human neural precursor cells by laminin and integrins. *Journal of neuroscience research,* 83**,** 845-856.

FLASKOS, J. 2012. The developmental neurotoxicity of organophosphorus insecticides: A direct role for the oxon metabolites. *Toxicology Letters,* 209**,** 86-93.

FLASKOS, J., HARRIS, W., SACHANA, M., MUNOZ, D., TACK, J. & HARGREAVES, A. J. 2007. The effects of diazinon and cypermethrin on the differentiation of neuronal and glial cell lines. *Toxicol Appl Pharmacol,* 219**,** 172-80.

FLASKOS, J. A. S., MAGDALINI 2011. Developmental Neurotoxicity of Anticholinesterase Pesticides. *In:* GUPTA, T. S. R. C. (ed.) *Anticholinesterase Pesticides.* John Wiley & Sons, Inc.

FRANKLIN, S. 2017. Chapter 5 - The Peripheral and Central Nervous System. *In:* CONN, P. M. (ed.) *Conn's Translational Neuroscience.* San Diego: Academic Press.

FU, D.-J., LI, P., SONG, J., ZHANG, S.-Y. & XIE, H.-Z. 2019. Mechanisms of synergistic neurotoxicity induced by two high risk pesticide residues –

Chlorpyrifos and Carbofuran via oxidative stress. *Toxicology in Vitro,* 54**,** 338-344.

FUCCI, L., OLIVER, C. N., COON, M. J. & STADTMAN, E. R. 1983. Inactivation of key metabolic enzymes by mixed-function oxidation reactions: possible implication in protein turnover and ageing. *Proceedings of the National Academy of Sciences of the United States of America,* 80**,** 1521-1525.

FURLONG, C. E., HOLLAND, N., RICHTER, R. J., BRADMAN, A., HO, A. & ESKENAZI, B. 2006. PON1 status of farmworker mothers and children as a predictor of organophosphate sensitivity. *Pharmacogenet Genomics,* 16**,** 183-90.

GAGE, F. H. 2000. Mammalian neural stem cells. *Science,* 287**,** 1433-8.

GARDINER, J., OVERALL, R. & MARC, J. 2013. The Nervous System Cytoskeleton under Oxidative Stress. *Diseases,* 1**,** 36-50.

GAVRILESCU, M., DEMNEROVÁ, K., AAMAND, J., AGATHOS, S. & FAVA, F. 2015. Emerging pollutants in the environment: present and future challenges in biomonitoring, ecological risks and bioremediation. *New Biotechnology,* 32**,** 147-156.

GERARD-MONNIER, D. & CHAUDIERE, J. 1996. [Metabolism and antioxidant function of glutathione]. *Pathol Biol (Paris),* 44**,** 77-85.

GIL-MOHAPEL, J., BOEHME, F., KAINER, L. & CHRISTIE, B. R. 2010. Hippocampal cell loss and neurogenesis after fetal alcohol exposure: Insights from different rodent models. *Brain Research Reviews,* 64**,** 283-303.

GIRI, P., GUPTA, L., NAIDU, S., JOSHI, V., PATEL, N., GIRI, S. & SRINIVAS, N. R. 2018. In Vitro Drug-Drug Interaction Potential of Sulfoxide and/or Sulfone Metabolites of Albendazole, Triclabendazole , Aldicarb, Methiocarb, Montelukast and Ziprasidone. *Drug metabolism letters,* 12**,** 101-116.

GLYNN, P. 2006. A mechanism for organophosphate-induced delayed neuropathy. *Toxicology Letters,* 162**,** 94-97.

GLYNN, P., READ, D. J., LUSH, M. J., LI, Y. & ATKINS, J. 1999. Molecular cloning of neuropathy target esterase (NTE). *Chemico-Biological Interactions,* 119-120**,** 513-517.

GOLDIE, B. J., BARNETT, M. M. & CAIRNS, M. J. 2014. BDNF and the maturation of posttranscriptional regulatory networks in human SH-SY5Y neuroblast differentiation. *Frontiers in cellular neuroscience,* 8**,** 325-325.

GONZÁLEZ-ALZAGA, B., LACASAÑA, M., AGUILAR-GARDUÑO, C., RODRÍGUEZ-BARRANCO, M., BALLESTER, F., REBAGLIATO, M. & HERNÁNDEZ, A. F. 2014. A systematic review of neurodevelopmental effects of prenatal and postnatal organophosphate pesticide exposure. *Toxicology Letters,* 230**,** 104-121.

GONZÁLEZ-BURGOS, I., ALEJANDRE-GÓMEZ, M., OLVERA-CORTÉS, M. E., PÉREZ-VEGA, M. I., EVANS, S. & FERIA-VELASCO, A. 2006. Prenatal-through-postnatal exposure to moderate levels of ethanol leads to damage on the hippocampal CA1 field of juvenile rats: a stereology and Golgi study. *Neurosci Res,* 56**,** 400-8.

GOODLETT, C. R. & HORN, K. H. 2001. Mechanisms of alcohol-induced damage to the developing nervous system. *Alcohol research & health : the journal of the National Institute on Alcohol Abuse and Alcoholism,* 25**,** 175-184.

GOODLETT, C. R., HORN, K. H. & ZHOU, F. C. 2005. Alcohol Teratogenesis: Mechanisms of Damage and Strategies for Intervention. *Experimental Biology and Medicine,* 230**,** 394-406.

GRANDJEAN, P. & LANDRIGAN, P. J. 2014. Neurobehavioural effects of developmental toxicity. *The Lancet. Neurology,* 13**,** 330-338.

GRIGORYAN, H., LI, B., XUE, W., GRIGORYAN, M., SCHOPFER, L. M. & LOCKRIDGE, O. 2009a. Mass spectral characterization of organophosphate-labeled lysine in peptides. *Anal Biochem,* 394**,** 92-100.

GRIGORYAN, H., SCHOPFER, L. M., PEEPLES, E. S., DUYSEN, E. G., GRIGORYAN, M., THOMPSON, C. M. & LOCKRIDGE, O. 2009b. Mass spectrometry identifies multiple organophosphorylated sites on tubulin. *Toxicology and Applied Pharmacology,* 240**,** 149-158.

GRIGORYAN, H., SCHOPFER, L. M., THOMPSON, C. M., TERRY, A. V., MASSON, P. & LOCKRIDGE, O. 2008. Mass spectrometry identifies covalent binding of soman, sarin, chlorpyrifos oxon, diisopropyl fluorophosphate, and FP-biotin to tyrosines on tubulin: a potential mechanism of long term toxicity by organophosphorus agents. *Chem Biol Interact,* 175**,** 180-6.

GRUNE, T., JUNG, T., MERKER, K. & DAVIES, K. J. 2004. Decreased proteolysis caused by protein aggregates, inclusion bodies, plaques, lipofuscin, ceroid, and 'aggresomes' during oxidative stress, aging, and disease. *Int J Biochem Cell Biol,* 36**,** 2519-30.

GUIZZETTI, M., BORDI, F., DIEGUEZ-ACUÑA, F. J., VITALONE, A., MADIA, F., WOODS, J. S. & COSTA, L. G. 2003. Nuclear factor κb activation by muscarinic receptors in astroglial cells: effect of ethanol. *Neuroscience,* 120**,** 941-950.

GUIZZETTI, M., PATHAK, S., GIORDANO, G. & COSTA, L. G. 2005. Effect of organophosphorus insecticides and their metabolites on astroglial cell proliferation. *Toxicology,* 215**,** 182-190.

GÜNEY, M., ORAL, B., DEMIRIN, H., ÖZGÜNER, M., TAKE, G., MUNGAN, T. & ALTUNTAS, I. 2007. Evaluation of caspase-dependent apoptosis during methyl parathion-induced endometrial damage in rats: Ameliorating effect of Vitamins E and C. *Environmental Toxicology and Pharmacology,* 23**,** 221-227.

GUPTA, R. C. 2014. Carbamate Pesticides. *In:* WEXLER, P. (ed.) *Encyclopedia of Toxicology (Third Edition).* Oxford: Academic Press.

GUPTA, R. C. & MILATOVIC, D. 2012. Chapter 45 - Organophosphates and carbamates. *In:* GUPTA, R. C. (ed.) *Veterinary Toxicology (Second Edition).* Boston: Academic Press.

GUPTA, R. C., SACHANA, M., MUKHERJEE, I. M., DOSS, R. B., MALIK, J. K. & MILATOVIC, D. 2018. Chapter 37 - Organophosphates and Carbamates. *In:* GUPTA, R. C. (ed.) *Veterinary Toxicology (Third Edition).* Academic Press.

GWAG, B. J., LOBNER, D., KOH, J. Y., WIE, M. B. & CHOI, D. W. 1995. Blockade of glutamate receptors unmasks neuronal apoptosis after oxygen-glucose deprivation in vitro. *Neuroscience,* 68**,** 615-619.

HALLIWELL, B. & WHITEMAN, M. 2004. Measuring reactive species and oxidative damage in vivo and in cell culture: how should you do it and what do the results mean? *Br J Pharmacol,* 142**,** 231-55.

HAMILTON, D. A., KODITUWAKKU, P., SUTHERLAND, R. J. & SAVAGE, D. D. 2003. Children with Fetal Alcohol Syndrome are impaired at place learning but not cued-navigation in a virtual Morris water task. *Behav Brain Res,* 143**,** 85-94.

HAO, H.-N., PARKER, G., ZHAO, J., BARAMI, K. & LYMAN, W. 2003. Differential Responses of Human Neural and Hematopoietic Stem Cells to Ethanol Exposure. *Journal of hematotherapy & stem cell research,* 12**,** 389-99.

HAORAH, J., RAMIREZ, S. H., FLOREANI, N., GORANTLA, S., MORSEY, B. & PERSIDSKY, Y. 2008. Mechanism of alcohol-induced oxidative stress and neuronal injury. *Free radical biology & medicine,* 45**,** 1542-1550.

HARGREAVES, A. J. 2012. Neurodegenerations induced by organophosphorous compounds. *Adv Exp Med Biol,* 724**,** 189-204.

HARPER, C. 1998. The neuropathology of alcohol-specific brain damage, or does alcohol damage the brain? *J Neuropathol Exp Neurol,* 57**,** 101-10.

HARPER, C. 2007. The neurotoxicity of alcohol. *Hum Exp Toxicol,* 26**,** 251-7.

HARPER, C., KRIL, J. & DALY, J. 1987. Are we drinking our neurones away? *Br Med J (Clin Res Ed),* 294**,** 534-6.

HARPER, C. & MATSUMOTO, I. 2005. Ethanol and brain damage. *Curr Opin Pharmacol,* 5**,** 73-8.

HASSEL, B., BACHELARD, H., JONES, P., FONNUM, F. & SONNEWALD, U. 1997. Trafficking of amino acids between neurons and glia in vivo. Effects of inhibition of glial metabolism by fluoroacetate. *J Cereb Blood Flow Metab,* 17**,** 1230-8.

HE, X. W., GAO, J. W., DONG, T. Y., CHEN, M. J., ZHOU, K., CHANG, C. X., LUO, J., WANG, C., WANG, S. L., CHEN, D. Z., ZHOU, Z. M., TIAN, Y., XIA, Y. K. & WANG, X. R. 2017. Developmental Neurotoxicity of

Methamidophos in the Embryo-Larval Stages of Zebrafish. *International Journal of Environmental Research and Public Health,* 14.

HEATON, M. B., PAIVA, M., MADORSKY, I. & SHAW, G. 2003. Ethanol effects on neonatal rat cortex: comparative analyses of neurotrophic factors, apoptosis-related proteins, and oxidative processes during vulnerable and resistant periods. *Developmental Brain Research,* 145**,** 249-262.

HEATON, M. B., PAIVA, M., MAYER, J. & MILLER, R. 2002. Ethanol-mediated generation of reactive oxygen species in developing rat cerebellum. *Neuroscience Letters,* 334**,** 83-86.

HERNÁNDEZ, J. A., LÓPEZ-SÁNCHEZ, R. C. & RENDÓN-RAMÍREZ, A. 2016. Lipids and Oxidative Stress Associated with Ethanol-Induced Neurological Damage. *Oxidative Medicine and Cellular Longevity,* 2016**,** 1543809.

HEUSINKVELD, H. J. & WESTERINK, R. H. S. 2017. Comparison of different in vitro cell models for the assessment of pesticide-induced dopaminergic neurotoxicity. *Toxicology in Vitro,* 45**,** 81-88.

HORTON, M. K., KAHN, L. G., PERERA, F., BARR, D. B. & RAUH, V. 2012. Does the home environment and the sex of the child modify the adverse effects of prenatal exposure to chlorpyrifos on child working memory? *Neurotoxicol Teratol,* 34**,** 534-41.

HOU, L., HUANG, R., SUN, F., ZHANG, L. & WANG, Q. 2019. NADPH oxidase regulates paraquat and maneb-induced dopaminergic neurodegeneration through ferroptosis. *Toxicology,* 417**,** 64-73.

HOWARD, A. S., BUCELLI, R., JETT, D. A., BRUUN, D., YANG, D. & LEIN, P. J. 2005. Chlorpyrifos exerts opposing effects on axonal and dendritic growth in primary neuronal cultures. *Toxicology and Applied Pharmacology,* 207**,** 112-124.

HUEN, K., BRADMAN, A., HARLEY, K., YOUSEFI, P., BOYD BARR, D., ESKENAZI, B. & HOLLAND, N. 2012. Organophosphate pesticide levels in blood and urine of women and newborns living in an agricultural community. *Environ Res,* 117**,** 8-16.

HUNG, L. M., CHEN, J. K., HUANG, S. S., LEE, R. S. & SU, M. J. 2000. Cardioprotective effect of resveratrol, a natural antioxidant derived from grapes. *Cardiovasc Res,* 47**,** 549-55.

IKONOMIDOU, C., BITTIGAU, P., ISHIMARU, M. J., WOZNIAK, D. F., KOCH, C., GENZ, K., PRICE, M. T., STEFOVSKA, V., HORSTER, F., TENKOVA, T., DIKRANIAN, K. & OLNEY, J. W. 2000. Ethanol-induced apoptotic neurodegeneration and fetal alcohol syndrome. *Science,* 287**,** 1056-60.

INTORRE, L., SOLDANI, G., COGNETTI-VARRIALE, A. M., MONNI, G., MEUCCI, V. & PRETTI, C. 2004. Safety of azamethiphos in eel, seabass and trout. *Pharmacological Research,* 49**,** 171-176.

JESSEN, K. R. & MIRSKY, R. 2005. The origin and development of glial cells in peripheral nerves. *Nat Rev Neurosci,* 6**,** 671-82.

JIA, Z. & MISRA, H. P. 2007. Exposure to mixtures of endosulfan and zineb induces apoptotic and necrotic cell death in SH-SY5Y neuroblastoma cells, in vitro. *Journal of Applied Toxicology,* 27**,** 434-446.

JOHNSON, M. K. 1974. THE PRIMARY BIOCHEMICAL LESION LEADING TO THE DELAYED NEUROTOXIC EFFECTS OF SOME ORGANOPHOSPHORUS ESTERS. *Journal of Neurochemistry,* 23**,** 785-789.

JOKANOVIĆ, M. 2001. Biotransformation of organophosphorus compounds. *Toxicology,* 166**,** 139-160.

JOKANOVIĆ, M. & KOSANOVIĆ, M. 2010. Neurotoxic effects in patients poisoned with organophosphorus pesticides. *Environmental Toxicology and Pharmacology,* 29**,** 195-201.

JOKANOVIĆ, M., KOSANOVIĆ, M., BRKIĆ, D. & VUKOMANOVIĆ, P. 2011. Organophosphate induced delayed polyneuropathy in man: An overview. *Clinical Neurology and Neurosurgery,* 113**,** 7-10.

KAMEL, F. & HOPPIN, J. A. 2004. Association of pesticide exposure with neurologic dysfunction and disease. *Environmental health perspectives,* 112**,** 950-958.

KANE, C. J. M., CHANG, J. Y., ROBERSON, P. K., GARG, T. K. & HAN, L. 2008. Ethanol exposure of neonatal rats does not increase biomarkers of oxidative stress in isolated cerebellar granule neurons. *Alcohol,* 42**,** 29-36.

KARAMI-MOHAJERI, S. & ABDOLLAHI, M. 2013. Mitochondrial dysfunction and organophosphorus compounds. *Toxicology and Applied Pharmacology,* 270**,** 39-44.

KARCZMAR, A. G. 2007. Anticholinesterases and War Gases. *In:* KARCZMAR, A. G. (ed.) *Exploring the Vertebrate Central Cholinergic Nervous System.* Boston, MA: Springer US.

KASHEM, M., SULTANA, N. & BALCAR, V. 2018. Exposure of Rat Neural Stem Cells to Ethanol Affects Cell Numbers and Alters Expression of 28 Proteins. *Neurochemical Research,* 43.

KI, Y.-W., PARK, J. H., LEE, J. E., SHIN, I. C. & KOH, H. C. 2013. JNK and p38 MAPK regulate oxidative stress and the inflammatory response in chlorpyrifos-induced apoptosis. *Toxicology Letters,* 218**,** 235-245.

KOH, J.-Y. & COTMAN, C. W. 1992. Programmed cell death: its possible contribution to neurotoxicity mediated by calcium channel antagonists. *Brain Research,* 587**,** 233-240.

KOHEN, R. & NYSKA, A. 2002. Oxidation of biological systems: oxidative stress phenomena, antioxidants, redox reactions, and methods for their quantification. *Toxicol Pathol,* 30**,** 620-50.

KORYSTOV, Y. N., SHAPOSHNIKOVA, V. V., KORYSTOVA, A. F. & EMEL'YANOV, M. O. 2007. Detection of reactive oxygen species induced by radiation in cells using the dichlorofluorescein assay. *Radiat Res,* 168**,** 226-32.

KOVALEVICH, J. & LANGFORD, D. 2013. Considerations for the use of SH-SY5Y neuroblastoma cells in neurobiology. *Methods in molecular biology (Clifton, N.J.),* 1078**,** 9-21.

KUBOTA, M., NAKAZAKI, S., HIRAI, S., SAEKI, N., YAMAURA, A. & KUSAKA, T. 2001. Alcohol consumption and frontal lobe shrinkage: study of 1432 non-alcoholic subjects. *Journal of Neurology, Neurosurgery & Psychiatry,* 71**,** 104.

KVIGNE, V. L., RANDALL, B., SIMANTON, E. G., BRENNEMAN, G. & WELTY, T. K. 2012. Blood Alcohol Levels for American Indian Mothers and Newborns. *Pediatrics,* 130**,** e1015.

LABISSO, W., RAULIN, A.-C., NWIDU, L., KOCON, A., WAYNE, D., ERDOZAIN, A., MORENTIN, B., SCHWENDENER, D., ALLEN, G., ENTICOTT, J., GERDES, H., JOHNSON, L., GRZESKOWIAK, J., DRIZOU, F., TARBOX, R., OSNA, N., KHARBANDA, K., CALLADO, L. & CARTER, W. 2018a. The Loss of α-and β-Tubulin Proteins Are a Pathological Hallmark of Chronic Alcohol Consumption and Natural Brain Ageing. *Brain Sciences,* 8**,** 175.

LABISSO, W. L., RAULIN, A.-C., NWIDU, L. L., KOCON, A., WAYNE, D., ERDOZAIN, A. M., MORENTIN, B., SCHWENDENER, D., ALLEN, G., ENTICOTT, J., GERDES, H. K., JOHNSON, L., GRZESKOWIAK, J., DRIZOU, F., TARBOX, R., OSNA, N. A., KHARBANDA, K. K., CALLADO, L. F. & CARTER, W. G. 2018b. The Loss of α- and β-Tubulin Proteins Are a Pathological Hallmark of Chronic Alcohol Consumption and Natural Brain Ageing. *Brain Sciences,* 8**,** 175.

LEE, J. E., LIM, M. S., PARK, J. H., PARK, C. H. & KOH, H. C. 2014a. Nuclear NF-kappaB contributes to chlorpyrifos-induced apoptosis through p53 signaling in human neural precursor cells. *Neurotoxicology,* 42**,** 58-70.

LEE, J. E., PARK, J. H., JANG, S. J. & KOH, H. C. 2014b. Rosiglitazone inhibits chlorpyrifos-induced apoptosis via modulation of the oxidative stress and inflammatory response in SH-SY5Y cells. *Toxicology and Applied Pharmacology,* 278**,** 159-171.

LEE, Y. H., OH, Y. T., LEE, W. W., AHN, H. C., SOHN, Y. D., AHN, J. Y., MIN, Y. H., KIM, H., LIM, S. W., LEE, K. J., SHIN, D. H., PARK, S. O. & PARK, S. M. 2017. The association of alcohol consumption with patient survival after organophosphate poisoning: a multicenter retrospective study. *Intern Emerg Med,* 12**,** 519-526.

LEVINE, R. L. 2002. Carbonyl modified proteins in cellular regulation, aging, and disease. *Free Radic Biol Med,* 32**,** 790-6.

LI, J., ZHANG, S. & AMAYA, E. 2016. The cellular and molecular mechanisms of tissue repair and regeneration as revealed by studies in Xenopus. *Regeneration (Oxford, England),* 3**,** 198-208.

LI, T., ZHAO, H., HUNG, G.-C., HAN, J., TSAI, S., LI, B., ZHANG, J., PURI, R. K. & LO, S.-C. 2012. Differentially expressed genes and pathways induced by organophosphates in human neuroblastoma cells. *Experimental Biology and Medicine,* 237**,** 1413-1423.

LIFSHITZ, M., SHAHAK, E., BOLOTIN, A. & SOFER, S. 1997. Carbamate poisoning in early childhood and in adults. *J Toxicol Clin Toxicol,* 35**,** 25-7.

LIFSHITZ, M., SHAHAK, E. & SOFER, S. 1999. Carbamate and organophosphate poisoning in young children. *Pediatr Emerg Care,* 15**,** 102-3.

LIONETTO, M. G., CARICATO, R., CALISI, A., GIORDANO, M. E. & SCHETTINO, T. 2013. Acetylcholinesterase as a biomarker in environmental and occupational medicine: new insights and future perspectives. *BioMed research international,* 2013**,** 321213-321213.

LIU, C.-Y., CHANG, P.-A. & WU, Y.-J. 2009. Trichlorfon induces apoptosis in SH-SY5Y neuroblastoma cells via the endoplasmic reticulum? *Chemico-Biological Interactions,* 181**,** 37-44.

LIU, Z., LIU, Y.-P., GAO, R., LI, H., DUNN, T., WU, P., SMITH, R., SARKAR, P. & FANG, X. 2014. Ethanol Suppresses PGC-1α Expression by Interfering with the cAMP-CREB Pathway in Neuronal Cells. *PloS one,* 9**,** e104247.

LOBNER, D. 2000. Comparison of the LDH and MTT assays for quantifying cell death: validity for neuronal apoptosis? *Journal of Neuroscience Methods,* 96**,** 147-152.

LOPES, F. M., SCHRODER, R., DA FROTA, M. L., JR., ZANOTTO-FILHO, A., MULLER, C. B., PIRES, A. S., MEURER, R. T., COLPO, G. D., GELAIN, D. P., KAPCZINSKI, F., MOREIRA, J. C., FERNANDES MDA, C. & KLAMT, F. 2010. Comparison between proliferative and neuron-like SH-SY5Y cells as an in vitro model for Parkinson disease studies. *Brain Res,* 1337**,** 85-94.

LOTTI, M. & MORETTO, A. 2005. Organophosphate-induced delayed polyneuropathy. *Toxicol Rev,* 24**,** 37-49.

LOU, Y. W., CHEN, Y. Y., HSU, S. F., CHEN, R. K., LEE, C. L., KHOO, K. H., TONKS, N. K. & MENG, T. C. 2008. Redox regulation of the protein tyrosine phosphatase PTP1B in cancer cells. *Febs j,* 275**,** 69-88.

LOUIS, L. K., GOPURAPPILLY, R., SURENDRAN, H., DUTTA, S. & PAL, R. 2018. Transcriptional profiling of human neural precursors post alcohol exposure reveals impaired neurogenesis via dysregulation of ERK signaling and miR-145. *Journal of Neurochemistry,* 146**,** 47-62.

LOWRY, O. H., ROSEBROUGH, N. J., FARR, A. L. & RANDALL, R. J. 1951. Protein measurement with the Folin phenol reagent. *J Biol Chem,* 193**,** 265-75.

LUKASZEWICZ-HUSSAIN, A. 2008. Subchronic intoxication with chlorfenvinphos, an organophosphate insecticide, affects rat brain antioxidative enzymes and glutathione level. *Food and Chemical Toxicology,* 46**,** 82-86.

LUKASZEWICZ-HUSSAIN, A. 2010. Role of oxidative stress in organophosphate insecticide toxicity – Short review. *Pesticide Biochemistry and Physiology,* 98**,** 145-150.

LUKASZEWICZ-HUSSAIN, A. 2013. Involvement of oxidative stress in liver injury after subchronic intoxication with low doses of chlorpyrifos - study on rats. *Central European Journal of Medicine,* 8**,** 132-139.

LUO, J. & MILLER, M. W. 1997. Differential Sensitivity of Human Neuroblastoma Cell Lines to Ethanol: Correlations with Their Proliferative Responses to Mitogenic Growth Factors and Expression of Growth Factor Receptors. *Alcoholism: Clinical and Experimental Research,* 21**,** 1186-1194.

LUQMAN, E. M., SUDIANA, I. K., DARMANTO, W., ACHMAD, A. B. & WIDJIATI 2019. Mouse (Mus Musculus) Embryonic Cerebral Cortex Cell Death Caused by Carbofuran Insecticide Exposure. *Journal of veterinary research,* 63**,** 413-421.

MACINTOSH, D. L., KABIRU, C., ECHOLS, S. L. & RYAN, P. B. 2001. Dietary exposure to chlorpyrifos and levels of 3,5,6-trichloro-2-pyridinol in urine. *Journal of Exposure Science & Environmental Epidemiology,* 11**,** 279-285.

MADIAN, A. G., HINDUPUR, J., HULLEMAN, J. D., DIAZ-MALDONADO, N., MISHRA, V. R., GUIGARD, E., KAY, C. M., ROCHET, J. C. & REGNIER, F. E. 2012. Effect of single amino acid substitution on oxidative modifications of the Parkinson's disease-related protein, DJ-1. *Mol Cell Proteomics,* 11**,** M111.010892.

MAHMOUD, S. M., ABDEL MONEIM, A. E., QAYED, M. M. & EL-YAMANY, N. A. 2019. Potential role of N-acetylcysteine on chlorpyrifos-induced neurotoxicity in rats. *Environ Sci Pollut Res Int,* 26**,** 20731-20741.

MANDAL, C., KIM, S. H., CHAI, J. C., LEE, Y. S., JUNG, K. H. & CHAI, Y. G. 2018. Gene expression signatures after ethanol exposure in differentiating embryoid bodies. *Toxicology in Vitro,* 46**,** 66-76.

MANGAS, I., ESTEVEZ, J., VILANOVA, E. & FRANÇA, T. C. C. 2017. New insights on molecular interactions of organophosphorus pesticides with esterases. *Toxicology,* 376**,** 30-43.

MANTHEY, J., SHIELD, K. D., RYLETT, M., HASAN, O. S. M., PROBST, C. & REHM, J. 2019. Global alcohol exposure between 1990 and 2017 and forecasts until 2030: a modelling study. *The Lancet,* 393**,** 2493-2502.

MARINO, M. D., AKSENOV, M. Y. & KELLY, S. J. 2004. Vitamin E protects against alcohol-induced cell loss and oxidative stress in the neonatal rat hippocampus. *International Journal of Developmental Neuroscience,* 22**,** 363-377.

MASSICOTTE, C., KNIGHT, K., SCHYF, C. J. V. D., JORTNER, B. S. & EHRICH, M. 2005. Effects of organophosphorus compounds on ATP production and mitochondrial integrity in cultured cells. *Neurotoxicity Research,* 7**,** 203-217.

MATÉS, J. M., PÉREZ-GÓMEZ, C. & DE CASTRO, I. N. 1999. Antioxidant enzymes and human diseases. *Clinical Biochemistry,* 32**,** 595-603.

MAXI, J. K., DEAN, M., ZABALETA, J., REISS, K., BAGBY, G. J., NELSON, S., WINSAUER, P. J., PERUZZI, F. & MOLINA, P. E. 2016. Chronic Binge Alcohol Administration Dysregulates Hippocampal Genes Involved in Immunity and Neurogenesis in Simian Immunodeficiency Virus-Infected Macaques. *Biomolecules,* 6.

MAY, P. A., BAETE, A., RUSSO, J., ELLIOTT, A. J., BLANKENSHIP, J., KALBERG, W. O., BUCKLEY, D., BROOKS, M., HASKEN, J., ABDUL-RAHMAN, O., ADAM, M. P., ROBINSON, L. K., MANNING, M. & HOYME, H. E. 2014. Prevalence and Characteristics of Fetal Alcohol Spectrum Disorders. *Pediatrics,* 134**,** 855.

MAY, P. A., GOSSAGE, J. P., KALBERG, W. O., ROBINSON, L. K., BUCKLEY, D., MANNING, M. & HOYME, H. E. 2009. Prevalence and epidemiologic characteristics of FASD from various research methods with an emphasis on recent in-school studies. *Developmental Disabilities Research Reviews,* 15**,** 176-192.

MCGEE, C. L. & RILEY, E. P. 2006. Brain imaging and fetal alcohol spectrum disorders. *Ann Ist Super Sanita,* 42**,** 46-52.

MEARNS, J., DUNN, J. & LEES-HALEY, P. R. 1994. Psychological effects of organophosphate pesticides: a review and call for research by psychologists. *J Clin Psychol,* 50**,** 286-94.

MENSE, S. M., SENGUPTA, A., LAN, C., ZHOU, M., BENTSMAN, G., VOLSKY, D. J., WHYATT, R. M., PERERA, F. P. & ZHANG, L. 2006. The Common Insecticides Cyfluthrin and Chlorpyrifos Alter the Expression of a Subset of Genes with Diverse Functions in Primary Human Astrocytes. *Toxicological Sciences,* 93**,** 125-135.

MICHAEL J. MORGAN, Y.-S. K., AND ZHENGGANG LIU 2007. Lipid Rafts and Oxidative Stress–Induced Cell Death. *Antioxidants & Redox Signaling,* 9**,** 1471-1484.

MIDDLEMORE-RISHER, M.-L., ADAM, B.-L., LAMBERT, N. A. & TERRY, A. V., JR. 2011. Effects of chlorpyrifos and chlorpyrifos-oxon on the dynamics and movement of mitochondria in rat cortical neurons. *The Journal of pharmacology and experimental therapeutics,* 339**,** 341-349.

MILATOVIC, D., GUPTA, R. C. & ASCHNER, M. 2006. Anticholinesterase toxicity and oxidative stress. *Thescientificworldjournal,* 6**,** 295-310.

MILLER, D. B. 1982. Neurotoxicity of the pesticidal carbamates. *Neurobehav Toxicol Teratol,* 4**,** 779-87.

MOON, Y., KWON, Y. & YU, S. 2013. How does ethanol induce apoptotic cell death of SK-N-SH neuroblastoma cells. *Neural regeneration research,* 8**,** 1853-1862.

MORETTO, A. & COLOSIO, C. 2011. Biochemical and toxicological evidence of neurological effects of pesticides: The example of Parkinson's disease. *NeuroToxicology,* 32**,** 383-391.

MOSMANN, T. 1983. Rapid colorimetric assay for cellular growth and survival: application to proliferation and cytotoxicity assays. *J Immunol Methods,* 65**,** 55-63.

MOSTAFALOU, S. & ABDOLLAHI, M. 2018. The link of organophosphorus pesticides with neurodegenerative and neurodevelopmental diseases based on evidence and mechanisms. *Toxicology,* 409**,** 44-52.

MOULTON, C. A., FLEMING, W. J. & PURNELL, C. E. 1996. Effects of two cholinesterase-inhibiting pesticides on freshwater mussels. *Environmental Toxicology & Chemistry $V 15***,** 131-137.

MSHANA, R., TADESSE, G., ABATE, G. & MIÖRNER, H. 1998. Use of 3-(4,5-Dimethylthiazol-2-yl)-2,5-Diphenyl Tetrazolium Bromide for Rapid Detection of Rifampin-ResistantMycobacterium tuberculosis. *Journal of clinical microbiology,* 36**,** 1214-9.

NAUGHTON, S. X. & TERRY, A. V. 2018. Neurotoxicity in acute and repeated organophosphate exposure. *Toxicology,* 408**,** 101-112.

NEELY, M. D., SIDELL, K. R., GRAHAM, D. G. & MONTINE, T. J. 1999. The lipid peroxidation product 4-hydroxynonenal inhibits neurite outgrowth, disrupts neuronal microtubules, and modifies cellular tubulin. *J Neurochem,* 72**,** 2323-33.

NIEMELÄ, O. 1999. Aldehyde-protein adducts in the liver as a result of ethanol-induced oxidative stress. *Frontiers in bioscience : a journal and virtual library* [Online], 4. Available: http://europepmc.org/abstract/MED/10352137

https://doi.org/10.2741/niemela [Accessed 1999/06//].

NIEMELÄ, O., PARKKILA, S., JUVONEN, R. O., VIITALA, K., GELBOIN, H. V. & PASANEN, M. 2000. Cytochromes P450 2A6, 2E1, and 3A and production of protein-aldehyde adducts in the liver of patients with alcoholic and non-alcoholic liver diseases. *Journal of Hepatology,* 33**,** 893-901.

O'HALLORAN, J. & HOGANS, W. E. 1996. First use in North America of azamethiphos to treat Atlantic salmon for sea lice infestation: procedures and efficacy. *Can Vet J,* 37**,** 610-1.

OBERNIER, J. A., BOULDIN, T. W. & CREWS, F. T. 2002a. Binge Ethanol Exposure in Adult Rats Causes Necrotic Cell Death. *Alcoholism: Clinical and Experimental Research,* 26**,** 547-557.

OBERNIER, J. A., WHITE, A. M., SWARTZWELDER, H. S. & CREWS, F. T. 2002b. Cognitive deficits and CNS damage after a 4-day binge ethanol exposure in rats. *Pharmacol Biochem Behav,* 72**,** 521-32.

OSNA, N. A., DONOHUE, T. M., JR. & KHARBANDA, K. K. 2017. Alcoholic Liver Disease: Pathogenesis and Current Management. *Alcohol Res,* 38**,** 147-161.

OSTREA, E. M., MORALES, V., NGOUMGNA, E., PRESCILLA, R., TAN, E., HERNANDEZ, E., RAMIREZ, G. B., CIFRA, H. L. & MANLAPAZ, M. L. 2002. Prevalence of fetal exposure to environmental toxins as determined by meconium analysis. *Neurotoxicology,* 23**,** 329-39.

OTERO-DIAZ, M. 2017. Cosolvent Effects of Ethanol and Dissolved Organic Matter on the Aqueous Solubility and Partitioning of Organochlorine Pesticides. *PhD thesis*.

OU, X.-M., STOCKMEIER, C. A., MELTZER, H. Y., OVERHOLSER, J. C., JURJUS, G. J., DIETER, L., CHEN, K., LU, D., JOHNSON, C., YOUDIM, M. B. H., AUSTIN, M. C., LUO, J., SAWA, A., MAY, W. & SHIH, J. C. 2010. A Novel Role for Glyceraldehyde-3-Phosphate Dehydrogenase and Monoamine Oxidase B Cascade in Ethanol-Induced Cellular Damage. *Biological Psychiatry,* 67**,** 855-863.

OWUMI, S. & NAJOPHE, E. 2019. Dichloromethane and ethanol co-exposure aggravates oxidative stress indices causing hepatic and renal dysfunction in pubertal rats. *Toxicology Research and Application,* 3**,** 239784731985528.

PÅHLMAN, S., RUUSALA, A.-I., ABRAHAMSSON, L., MATTSSON, M. E. K. & ESSCHER, T. 1984. Retinoic acid-induced differentiation of cultured human neuroblastoma cells: a comparison with phorbolester-induced differentiation. *Cell Differentiation,* 14**,** 135-144.

PALMER, J. A., POENITZSCH, A. M., SMITH, S. M., CONARD, K. R., WEST, P. R. & CEZAR, G. G. 2012. Metabolic biomarkers of prenatal alcohol exposure in human embryonic stem cell-derived neural lineages. *Alcoholism, clinical and experimental research,* 36**,** 1314-1324.

PANTAZIS, N. J., DOHRMAN, D. P., LUO, J., GOODLETT, C. R. & WEST, J. R. 1992. Alcohol reduces the number of pheochromocytoma (PC12) cells in culture. *Alcohol,* 9**,** 171-80.

PARK, J. H., KO, J., HWANG, J. & KOH, H. C. 2015. Dynamin-related protein 1 mediates mitochondria-dependent apoptosis in chlorpyrifos-treated SH-SY5Y cells. *NeuroToxicology,* 51**,** 145-157.

PARK, J. H., KO, J., PARK, Y. S., PARK, J., HWANG, J. & KOH, H. C. 2017. Clearance of Damaged Mitochondria Through PINK1 Stabilization by JNK and ERK MAPK Signaling in Chlorpyrifos-Treated Neuroblastoma Cells. *Molecular Neurobiology,* 54**,** 1844-1857.

PERKINS, E. J., EL-ALFY, A. & SCHLENK, D. 1999. In vitro sulfoxidation of aldicarb by hepatic microsomes of channel catfish, Ictalurus punctatus. *Toxicological Sciences,* 48**,** 67-73.

PETRENKO, C. & RILEY, E. 2006. Brain imaging and fetal alcohol spectrum disorders. *Annali dell'Istituto superiore di sanità,* 42**,** 46-52.

PFEFFERBAUM, A., SULLIVAN, E. V., MATHALON, D. H. & LIM, K. O. 1997. Frontal lobe volume loss observed with magnetic resonance imaging in older chronic alcoholics. *Alcohol Clin Exp Res,* 21**,** 521-9.

PHILIPPAT, C., BARKOSKI, J., TANCREDI, D. J., ELMS, B., BARR, D. B., OZONOFF, S., BENNETT, D. H. & HERTZ-PICCIOTTO, I. 2018. Prenatal exposure to organophosphate pesticides and risk of autism spectrum disorders and other non-typical development at 3 years in a high-risk cohort. *International journal of hygiene and environmental health,* 221**,** 548-555.

PIZZURRO, D. M., DAO, K. & COSTA, L. G. 2014. Astrocytes protect against diazinon- and diazoxon-induced inhibition of neurite outgrowth by regulating neuronal glutathione. *Toxicology,* 318**,** 59-68.

POOL, M., THIEMANN, J., BAR-OR, A. & FOURNIER, A. 2008. NeuriteTracer: A novel ImageJ plugin for automated quantification of neurite outgrowth. *Journal of neuroscience methods,* 168**,** 134-9.

POSSAMAI, F. P., FORTUNATO, J. J., FEIER, G., AGOSTINHO, F. R., QUEVEDO, J., WILHELM FILHO, D. & DAL-PIZZOL, F. 2007. Oxidative stress after acute and sub-chronic malathion intoxication in Wistar rats. *Environmental Toxicology and Pharmacology,* 23**,** 198-204.

PRENDERGAST, M. A., SELF, R. L., SMITH, K. J., GHAYOUMI, L., MULLINS, M. M., BUTLER, T. R., BUCCAFUSCO, J. J., GEARHART, D. A. & TERRY, A. V., JR. 2007. Microtubule-associated targets in chlorpyrifos oxon hippocampal neurotoxicity. *Neuroscience,* 146**,** 330-339.

QIAO, D., SEIDLER, F. J. & SLOTKIN, T. A. 2005. Oxidative mechanisms contributing to the developmental neurotoxicity of nicotine and chlorpyrifos. *Toxicology and Applied Pharmacology,* 206**,** 17-26.

RADIO, N. M. & MUNDY, W. R. 2008. Developmental neurotoxicity testing in vitro: models for assessing chemical effects on neurite outgrowth. *Neurotoxicology,* 29**,** 361-76.

RAGHUNATH, M., PATTI, R., BANNERMAN, P., LEE, C. M., BAKER, S., SUTTON, L. N., PHILLIPS, P. C. & DAMODAR REDDY, C. 2000. A novel kinase, AATYK induces and promotes neuronal differentiation in a human neuroblastoma (SH-SY5Y) cell line. *Molecular Brain Research,* 77**,** 151-162.

RAHIMI, R. & ABDOLLAHI, M. 2007. A review on the mechanisms involved in hyperglycemia induced by organophosphorus pesticides. *Pesticide Biochemistry and Physiology,* 88**,** 115-121.

RAJENDRAM, R., RAJENDRAM, R. & PREEDY, V. R. 2016. Chapter 35 - Ethanol Metabolism and Implications for Disease. *In:* PREEDY, V. R. (ed.) *Neuropathology of Drug Addictions and Substance Misuse.* San Diego: Academic Press.

RAMACHANDRAN, V., PEREZ, A., CHEN, J., SENTHIL, D., SCHENKER, S. & HENDERSON, G. I. 2001. In Utero Ethanol Exposure Causes Mitochondrial Dysfunction, Which Can Result in Apoptotic Cell Death in Fetal Brain: A Potential Role for 4-Hydroxynonenal. *Alcoholism: Clinical and Experimental Research,* 25**,** 862-871.

RANJBAR, A., SOLHI, H., MASHAYEKHI, F. J., SUSANABDI, A., REZAIE, A. & ABDOLLAHI, M. 2005. Oxidative stress in acute human poisoning with organophosphorus insecticides; a case control study. *Environmental Toxicology and Pharmacology,* 20**,** 88-91.

RASZEWSKI, G., LEMIESZEK, M. K., ŁUKAWSKI, K., JUSZCZAK, M. & RZESKI, W. 2015. Chlorpyrifos and Cypermethrin Induce Apoptosis in Human Neuroblastoma Cell Line SH-SY5Y. *Basic & Clinical Pharmacology & Toxicology,* 116**,** 158-167.

RAUH, V. A., GARFINKEL, R., PERERA, F. P., ANDREWS, H. F., HOEPNER, L., BARR, D. B., WHITEHEAD, R., TANG, D. & WHYATT, R. W. 2006. Impact of prenatal chlorpyrifos exposure on neurodevelopment in the first 3 years of life among inner-city children. *Pediatrics,* 118**,** e1845-e1859.

RAWN, D., KRAKALOVICH, T., FORSYTH, D. & ROSCOE, V. 2009. Analysis of fin and non-fin fish products for azamethiphos and dichlorvos residues from the Canadian retail market. *International Journal of Food Science & Technology,* 44**,** 1510-1516.

RAY, D. E. & RICHARDS, P. G. 2001. The potential for toxic effects of chronic, low-dose exposure to organophosphates. *Toxicology Letters,* 120**,** 343-351.

REDZA-DUTORDOIR, M. & AVERILL-BATES, D. A. 2016. Activation of apoptosis signalling pathways by reactive oxygen species. *Biochimica et Biophysica Acta (BBA) - Molecular Cell Research,* 1863**,** 2977-2992.

REHM, J., GMEL, G. E., SR., GMEL, G., HASAN, O. S. M., IMTIAZ, S., POPOVA, S., PROBST, C., ROERECKE, M., ROOM, R., SAMOKHVALOV, A. V., SHIELD, K. D. & SHUPER, P. A. 2017a. The relationship between different dimensions of alcohol use and the burden of disease-an update. *Addiction,* 112**,** 968-1001.

REHM, J., GMEL SR, G. E., GMEL, G., HASAN, O. S. M., IMTIAZ, S., POPOVA, S., PROBST, C., ROERECKE, M., ROOM, R., SAMOKHVALOV, A. V., SHIELD, K. D. & SHUPER, P. A. 2017b. The relationship between different dimensions of alcohol use and the burden of disease—an update. *Addiction,* 112**,** 968-1001.

REHM, J., ROOM, R., GRAHAM, K., MONTEIRO, M., GMEL, G. & SEMPOS, C. T. 2003. The relationship of average volume of alcohol consumption and patterns of drinking to burden of disease: an overview. *Addiction,* 98**,** 1209-28.

REISS, R., CHANG, E. T., RICHARDSON, R. J. & GOODMAN, M. 2015. A review of epidemiologic studies of low-level exposures to

organophosphorus insecticides in non-occupational populations. *Critical Reviews in Toxicology,* 45**,** 531-641.

RETH, M. 2002. Hydrogen peroxide as second messenger in lymphocyte activation. *Nat Immunol,* 3**,** 1129-34.

REVIE, C. W., GETTINBY, G., TREASURER, J. W., GRANT, A. N. & REID, S. W. J. 2002. Sea lice infestations on farmed Atlantic salmon in Scotland and the use of ectoparasitic treatments. *Veterinary Record,* 151**,** 753.

REYNA, L., FLORES-MARTÍN, J., RIDANO, M. E., PANZETTA-DUTARI, G. M. & GENTI-RAIMONDI, S. 2017. Chlorpyrifos induces endoplasmic reticulum stress in JEG-3 cells. *Toxicology in Vitro,* 40**,** 88-93.

REYNOLDS, K., LEWIS, B., NOLEN, J. D., KINNEY, G. L., SATHYA, B. & HE, J. 2003. Alcohol consumption and risk of stroke: a meta-analysis. *Jama,* 289**,** 579-88.

RICE-EVANS, C. A. & DIPLOCK, A. T. 1993. Current status of antioxidant therapy. *Free Radical Biology and Medicine,* 15**,** 77-96.

RICHARDSON, J. R. 2014. Azamethiphos. *In:* WEXLER, P. (ed.) *Encyclopedia of Toxicology (Third Edition).* Oxford: Academic Press.

RILEY, E. P. & MCGEE, C. L. 2005. Fetal alcohol spectrum disorders: an overview with emphasis on changes in brain and behavior. *Exp Biol Med (Maywood),* 230**,** 357-65.

RISHER, J. F., MINK, F. L. & STARA, J. F. 1987. The toxicologic effects of the carbamate insecticide aldicarb in mammals: a review. *Environ Health Perspect,* 72**,** 267-81.

RISS, T. L., MORAVEC, R. A., NILES, A. L., DUELLMAN, S., BENINK, H. A., WORZELLA, T. J. & MINOR, L. 2004. Cell Viability Assays. *In:* SITTAMPALAM, G. S., GROSSMAN, A., BRIMACOMBE, K., ARKIN, M., AULD, D., AUSTIN, C. P., BAELL, J., BEJCEK, B., CAAVEIRO, J. M. M., CHUNG, T. D. Y., COUSSENS, N. P., DAHLIN, J. L., DEVANARYAN, V., FOLEY, T. L., GLICKSMAN, M., HALL, M. D., HAAS, J. V., HOARE, S. R. J., INGLESE, J., IVERSEN, P. W., KAHL, S. D., KALES, S. C., KIRSHNER, S., LAL-NAG, M., LI, Z., MCGEE, J., MCMANUS, O., RISS, T., SARADJIAN, P., TRASK, O. J., JR., WEIDNER, J. R., WILDEY, M. J., XIA, M. & XU, X. (eds.) *Assay Guidance Manual.* Bethesda (MD): Eli Lilly & Company and the National Center for Advancing Translational Sciences.

ROEBUCK, T. M., MATTSON, S. N. & RILEY, E. P. 1998. A Review of the Neuroanatomical Findings in Children with Fetal Alcohol Syndrome or Prenatal Exposure to Alcohol. *Alcoholism: Clinical and Experimental Research,* 22**,** 339-344.

ROLDAN-TAPI, L., LEYVA, A., LAYNEZ, F. & SANTED, F. S. 2005. Chronic neuropsychological sequelae of cholinesterase inhibitors in the absence of structural brain damage: two cases of acute poisoning. *Environ Health Perspect,* 113**,** 762-6.

ROLDÁN-TAPIA, L., PARRÓN, T. & SÁNCHEZ-SANTED, F. 2005. Neuropsychological effects of long-term exposure to organophosphate pesticides. *Neurotoxicology and Teratology,* 27**,** 259-266.

ROSS, R. A., SPENGLER, B. A. & BIEDLER, J. L. 1983. Coordinate morphological and biochemical interconversion of human neuroblastoma cells. *J Natl Cancer Inst,* 71**,** 741-7.

ROTH, M., RICHARDS, R. H., DOBSON, D. P. & RAE, G. H. 1996. Field trials on the efficacy of the organophosphorus compound azamethiphos for the control of sea lice (Copepoda: Caligidae) infestations of farmed Atlantic salmon (Salmo salar). *Aquaculture,* 140**,** 217-239.

ROTH, M., RICHARDS, R. H. & SOMMERVILLE, C. 1993. Current practices in the chemotherapeutic control of sea lice infestations in aquaculture: a review. *Journal of Fish Diseases,* 16**,** 1-26.

SABIA, S., ELBAZ, A., BRITTON, A., BELL, S., DUGRAVOT, A., SHIPLEY, M., KIVIMAKI, M. & SINGH-MANOUX, A. 2014. Alcohol consumption and cognitive decline in early old age. *Neurology,* 82**,** 332-9.

SAGARA, J. I., MIURA, K. & BANNAI, S. 1993. Maintenance of neuronal glutathione by glial cells. *J Neurochem,* 61**,** 1672-6.

SAITO, M., SAITO, M., COOPER, T. & VADASZ, C. 2005. Ethanol-Induced Changes in the Content of Triglycerides, Ceramides, and Glucosylceramides in Cultured Neurons. *Alcoholism, clinical and experimental research,* 29**,** 1374-83.

SALMELA, K. S., KESSOVA, I. G., TSYRLOV, I. B. & LIEBER, C. S. 1998. Respective Roles of Human Cytochrome P-4502E1, 1A2, and 3A4 in the Hepatic Microsomal Ethanol Oxidizing System. *Alcoholism: Clinical and Experimental Research,* 22**,** 2125-2132.

SALVI, R. M., LARA, D. R., GHISOLFI, E. S., PORTELA, L. V., DIAS, R. D. & SOUZA, D. O. 2003. Neuropsychiatric Evaluation in Subjects Chronically Exposed to Organophosphate Pesticides. *Toxicological Sciences,* 72**,** 267-271.

SALYHA, Y. 2010. Biological effects assessment of chlorpyrifos and some aspects of its neurotoxicity. *Visnyk of Lviv University. - Biology series***,** 3-14.

SANDOVAL, L., ROSCA, A., ONIGA, A., ZAMBRANO, A., RAMOS, J. J., GONZÁLEZ, M. C., LISTE, I. & MOTAS, M. 2019. Effects of chlorpyrifos on cell death and cellular phenotypic specification of human neural stem cells. *Science of The Total Environment,* 683**,** 445-454.

SANES, D. H., REH, T. A. & HARRIS, W. A. 2000. Development of the nervous system.

SARI, Y., WEEDMAN, J. M. & GE, S. 2012. Activity-dependent neurotrophic factor-derived peptide prevents alcohol-induced apoptosis, in part, through Bcl2 and c-Jun N-terminal kinase signaling pathways in fetal brain of C57BL/6 mouse. *Neuroscience,* 202**,** 465-73.

SARKAR, B., DHIMAN, M., MITTAL, S. & MANTHA, A. K. 2017. Curcumin revitalizes Amyloid beta (25–35)-induced and organophosphate pesticides pestered neurotoxicity in SH-SY5Y and IMR-32 cells via activation of APE1 and Nrf2. *Metabolic Brain Disease,* 32**,** 2045-2061.

SATOH, T. & GUPTA, R. 2011. *Anticholinesterase Pesticides: Metabolism, Neurotoxicity, and Epidemiology*.

SAUNDERS, D. E., HANNIGAN, J. H., ZAJAC, C. S. & WAPPLER, N. L. 1995. Reversal of alcohol's effects on neurite extension and on neuronal GAP43/B50, N-myc, and c-myc protein levels by retinoic acid. *Developmental Brain Research,* 86**,** 16-23.

SAUNDERS, M., MAGNANTI, B. L., CORREIA CARREIRA, S., YANG, A., ALAMO-HERNÁNDEZ, U., RIOJAS-RODRIGUEZ, H., CALAMANDREI, G., KOPPE, J. G., KRAYER VON KRAUSS, M., KEUNE, H. & BARTONOVA, A. 2012. Chlorpyrifos and neurodevelopmental effects: a literature review and expert elicitation on research and policy. *Environmental health : a global access science source,* 11 Suppl 1**,** S5-S5.

SCHNEIDER, L., GIORDANO, S., ZELICKSON, B. R., M, S. J., G, A. B., OUYANG, X., FINEBERG, N., DARLEY-USMAR, V. M. & ZHANG, J. 2011. Differentiation of SH-SY5Y cells to a neuronal phenotype changes cellular bioenergetics and the response to oxidative stress. *Free Radic Biol Med,* 51**,** 2007-17.

SCHOPFER, L. M. & LOCKRIDGE, O. 2018. Chlorpyrifos oxon promotes tubulin aggregation via isopeptide cross-linking between diethoxyphospho-Lys and Glu or Asp: Implications for neurotoxicity. *The Journal of biological chemistry,* 293**,** 13566-13577.

SEGAL, L. M. & FEDOROFF, S. 1989. Cholinesterase inhibition by organophosphorus and carbamate pesticides in aggregate cultures of neural cells from the foetal rat brain: The effects of metabolic activation and pesticide mixtures. *Toxicology in Vitro,* 3**,** 123-128.

SERDARU, M., HAUSSER-HAUW, C., LAPLANE, D., BUGE, A., CASTAIGNE, P., GOULON, M., LHERMITTE, F. & HAUW, J. J. 1988. The clinical spectrum of alcoholic pellagra encephalopathy. A retrospective analysis of 22 cases studied pathologically. *Brain,* 111 (Pt 4)**,** 829-42.

SERIO, R. N., LAURSEN, K. B., URVALEK, A. M., GROSS, S. S. & GUDAS, L. J. 2019. Ethanol promotes differentiation of embryonic stem cells through retinoic acid receptor-γ. *J Biol Chem,* 294**,** 5536-5548.

SHADNIA, S., AZIZI, E., HOSSEINI, R., KHOEI, S., FOULADDEL, S., PAJOUMAND, A., JALALI, N. & ABDOLLAHI, M. 2005. Evaluation of oxidative stress and genotoxicity in organophosphorus insecticide formulators. *Human & Experimental Toxicology,* 24**,** 439-445.

SHADNIA, S., DASGAR, M., TAGHIKHANI, S., MOHAMMADIRAD, A., KHORASANI, R. & ABDOLLAHI, M. 2007. Protective Effects of α-Tocopherol and N-Acetyl-Cysteine on Diazinon-Induced Oxidative

Stress and Acetylcholinesterase Inhibition in Rats. *Toxicology Mechanisms and Methods,* 17**,** 109-115.

SHIEH, P., JAN, C. & LIANG, W. 2019. The protective effects of the antioxidant N-acetylcysteine (NAC) against oxidative stress-associated apoptosis evoked by the organophosphorus insecticide malathion in normal human astrocytes. *Toxicology,* 417**,** 1-14.

SHIELD, K., MANTHEY, J., RYLETT, M., PROBST, C., WETTLAUFER, A., PARRY, C. D. H. & REHM, J. 2020. National, regional, and global burdens of disease from 2000 to 2016 attributable to alcohol use: a comparative risk assessment study. *The Lancet Public Health,* 5**,** e51-e61.

SHIPLEY, M. M., MANGOLD, C. A. & SZPARA, M. L. 2016. Differentiation of the SH-SY5Y Human Neuroblastoma Cell Line. *Journal of visualized experiments : JoVE***,** 53193-53193.

SHIRPOOR, A., SALAMI, S., KHADEM-ANSARI, M. H., MINASSIAN, S. & YEGIAZARIAN, M. 2009. Protective Effect of Vitamin E Against Ethanol-Induced Hyperhomocysteinemia, DNA Damage, and Atrophy in the Developing Male Rat Brain. *Alcoholism: Clinical and Experimental Research,* 33**,** 1181-1186.

SIMON, H. U., HAJ-YEHIA, A. & LEVI-SCHAFFER, F. 2000. Role of reactive oxygen species (ROS) in apoptosis induction. *Apoptosis,* 5**,** 415-418.

SINDI, R. A. 2015. Chlorpyrifos and chlorpyrifos oxon induce neurite retraction and cytoskeletal disruption in mouse N2a cells and human neural progenitor stem cells *A thesis*.

SINGH, N., GUPTA, V. K., KUMAR, A. & SHARMA, B. 2017. Synergistic Effects of Heavy Metals and Pesticides in Living Systems. *Frontiers in Chemistry,* 5.

SINGH, N., LAWANA, V., LUO, J., PHONG, P., ABDALLA, A., PALANISAMY, B., ROKAD, D., SARKAR, S., JIN, H., ANANTHARAM, V., KANTHASAMY, A. G. & KANTHASAMY, A. 2018. Organophosphate pesticide chlorpyrifos impairs STAT1 signaling to induce dopaminergic neurotoxicity: Implications for mitochondria mediated oxidative stress signaling events. *Neurobiology of Disease,* 117**,** 82-113.

SINGH, S. & SHARMA, N. 2000. Neurological syndromes following organophosphate poisoning. *Neurology India,* 48**,** 308-13.

SLATER, T. F., SAWYER, B. & STRÄULI, U. 1963. Studies on succinate-tetrazolium reductase systems: III. Points of coupling of four different tetrazolium salts III. Points of coupling of four different tetrazolium salts. *Biochimica et Biophysica Acta,* 77**,** 383-393.

SLOTKIN, T. A. & SEIDLER, F. J. 2012. Developmental neurotoxicity of organophosphates targets cell cycle and apoptosis, revealed by transcriptional profiles in vivo and in vitro. *Neurotoxicology and teratology,* 34**,** 232-241.

SMERJAC, S. M. & BIZZOZERO, O. A. 2008. Cytoskeletal protein carbonylation and degradation in experimental autoimmune encephalomyelitis. *Journal of neurochemistry,* 105**,** 763-772.

SMITH, D. M. & ATKINSON, R. M. 1995. Alcoholism and dementia. *Int J Addict,* 30**,** 1843-69.

SOGORB, M. & VILANOVA, E. 2011. Detoxication of Anticholinesterase Pesticides.

SOGORB, M. A. & VILANOVA, E. 2002. Enzymes involved in the detoxification of organophosphorus, carbamate and pyrethroid insecticides through hydrolysis. *Toxicology Letters,* 128**,** 215-228.

SPOLARICS, Z. & WU, J.-X. 1997. Role of glutathione and catalase in H2O2detoxification in LPS-activated hepatic endothelial and Kupffer cells. *American Journal of Physiology-Gastrointestinal and Liver Physiology,* 273**,** G1304-G1311.

SRIVASTAVA, A., SINGH, S., RAJPUROHIT, C. S., SRIVASTAVA, P., PANDEY, A., KUMAR, D., KHANNA, V. K. & PANT, A. B. 2018. Secretome of Differentiated PC12 Cells Restores the Monocrotophos-Induced Damages in Human Mesenchymal Stem Cells and SHSY-5Y Cells: Role of Autophagy and Mitochondrial Dynamics. *Neuromolecular Medicine,* 20**,** 233-251.

STADTMAN, E. R. & LEVINE, R. L. 2000. Protein oxidation. *Ann N Y Acad Sci,* 899**,** 191-208.

STEPHENS, R., SPURGEON, A., CALVERT, I. A., BEACH, J., LEVY, L. S., HARRINGTON, J. M. & BERRY, H. 1995. Neuropsychological effects of long-term exposure to organophosphates in sheep dip. *The Lancet,* 345**,** 1135-1139.

STOCKWELL, B. R., FRIEDMANN ANGELI, J. P., BAYIR, H., BUSH, A. I., CONRAD, M., DIXON, S. J., FULDA, S., GASCÓN, S., HATZIOS, S. K., KAGAN, V. E., NOEL, K., JIANG, X., LINKERMANN, A., MURPHY, M. E., OVERHOLTZER, M., OYAGI, A., PAGNUSSAT, G. C., PARK, J., RAN, Q., ROSENFELD, C. S., SALNIKOW, K., TANG, D., TORTI, F. M., TORTI, S. V., TOYOKUNI, S., WOERPEL, K. A. & ZHANG, D. D. 2017. Ferroptosis: A Regulated Cell Death Nexus Linking Metabolism, Redox Biology, and Disease. *Cell,* 171**,** 273-285.

STRUGER, J., GRABUSKI, J., CAGAMPAN, S., SVERKO, E. & MARVIN, C. 2016. Occurrence and Distribution of Carbamate Pesticides and Metalaxyl in Southern Ontario Surface Waters 2007-2010. *Bulletin of environmental contamination and toxicology,* 96**,** 423-431.

SU, L.-J., ZHANG, J.-H., GOMEZ, H., MURUGAN, R., HONG, X., XU, D., JIANG, F. & PENG, Z.-Y. 2019. Reactive Oxygen Species-Induced Lipid Peroxidation in Apoptosis, Autophagy, and Ferroptosis. *Oxidative medicine and cellular longevity,* 2019**,** 5080843-5080843.

SUBRAMANIAM, R., FAN, X. J., SCIVITTARO, V., YANG, J., HA, C. E., PETERSEN, C. E., SUREWICZ, W. K., BHAGAVAN, N. V., WEISS, M.

F. & MONNIER, V. M. 2002. Cellular oxidant stress and advanced glycation endproducts of albumin: caveats of the dichlorofluorescein assay. *Arch Biochem Biophys,* 400**,** 15-25.

SUN, W., CHEN, L., ZHENG, W., WEI, X., WU, W., DUYSEN, E. G. & JIANG, W. 2017. Study of acetylcholinesterase activity and apoptosis in SH-SY5Y cells and mice exposed to ethanol. *Toxicology,* 384**,** 33-39.

TARPEY, M. M. & FRIDOVICH, I. 2001. Methods of Detection of Vascular Reactive Species. *Circulation Research,* 89**,** 224-236.

TAYLOR, J. S. A. A. 2020. Carbamate toxicity. *In: StatPearls [Internet]. Treasure Island*

TERRY, A. V. 2012. Functional consequences of repeated organophosphate exposure: Potential non-cholinergic mechanisms. *Pharmacology & Therapeutics,* 134**,** 355-365.

TESTAI, E., BURATTI, F. M. & DI CONSIGLIO, E. 2010. Chapter 70 - Chlorpyrifos. *In:* KRIEGER, R. (ed.) *Hayes' Handbook of Pesticide Toxicology (Third Edition).* New York: Academic Press.

TETZ, L. M., KAMAU, P. W., CHENG, A. A., MEEKER, J. D. & LOCH-CARUSO, R. 2013. Troubleshooting the dichlorofluorescein assay to avoid artifacts in measurement of toxicant-stimulated cellular production of reactive oxidant species. *Journal of pharmacological and toxicological methods,* 67**,** 56-60.

TODD, E. 2003. CONTAMINATION OF FOOD. *In:* CABALLERO, B. (ed.) *Encyclopedia of Food Sciences and Nutrition (Second Edition).* Oxford: Academic Press.

TOPE, A. M. & PANEMANGALORE, M. 2007. Assessment of oxidative stress due to exposure to pesticides in plasma and urine of traditional limited-resource farm workers: Formation of the DNA-adduct 8-hydroxy-2-deoxy-guanosine (8-OHdG). *Journal of Environmental Science and Health, Part B,* 42**,** 151-155.

TOPIWALA, A. & EBMEIER, K. P. 2018. Effects of drinking on late-life brain and cognition. *Evid Based Ment Health,* 21**,** 12-15.

TRIPATHI, V. K., KUMAR, V., PANDEY, A., VATSA, P., DHASMANA, A., SINGH, R. P., APPIKONDA, S. H. C., HWANG, I. & LOHANI, M. 2017. Monocrotophos Induces the Expression of Xenobiotic Metabolizing Cytochrome P450s (CYP2C8 and CYP3A4) and Neurotoxicity in Human Brain Cells. *Molecular Neurobiology,* 54**,** 3633-3651.

VALE, A. & LOTTI, M. 2015. Chapter 10 - Organophosphorus and carbamate insecticide poisoning. *In:* LOTTI, M. & BLEECKER, M. L. (eds.) *Handbook of Clinical Neurology.* Elsevier.

VAN DER HOEK, W. & KONRADSEN, F. 2005. Risk factors for acute pesticide poisoning in Sri Lanka. *Trop Med Int Health,* 10**,** 589-96.

VANGIPURAM, S. D., GREVER, W. E., PARKER, G. C. & LYMAN, W. D. 2008. Ethanol Increases Fetal Human Neurosphere Size and Alters Adhesion

Molecule Gene Expression. *Alcoholism: Clinical and Experimental Research,* 32**,** 339-347.

VANGIPURAM, S. D. & LYMAN, W. D. 2010. Ethanol Alters Cell Fate of Fetal Human Brain-Derived Stem and Progenitor Cells. *Alcoholism: Clinical and Experimental Research,* 34**,** 1574-1583.

VENDEMIALE, G., GRATTAGLIANO, I. & ALTOMARE, E. 1999. An update on the role of free radicals and antioxidant defense in human disease. *Int J Clin Lab Res,* 29**,** 49-55.

VIDYASAGAR, J., KARUNAKAR, N., REDDY, M., RAJNARAYANA, K., SURENDER, T. & DEVARAKONDA, K. 2004. Oxidative stress and antioxidant status in acute organophosphorus insecticide poisoning. *Indian Journal of Pharmacology (ISSN: 0253-7613) Vol 36 Num 2,* 36.

VIDYASAGAR, J., N, KARUNAKAR, MS, REDDY, K, RAJNARAYANA, T, SURENDER, DEVARAKONDA, KRISHNA, 2004. Oxidative stress and antioxidant status in acute organophosphorus insecticide poisoning. *Indian Journal of Pharmacology (ISSN: 0253-7613) Vol 36 Num 2,* 36.

VILANOVA, E., JOHNSON, M. K. & VICEDO, J. L. 1987. Interaction of some unsubstituted phosphoramidate analogs of methamidophos (O,S-dimethyl phosphorothioamidate) with acetylcholinesterase and neuropathy target esterase of hen brain. *Pesticide Biochemistry and Physiology,* 28**,** 224-238.

VILLA, A., NAVARRO-GALVE, B., BUENO, C., FRANCO, S., BLASCO, M. A. & MARTINEZ-SERRANO, A. 2004. Long-term molecular and cellular stability of human neural stem cell lines. *Exp Cell Res,* 294**,** 559-70.

VON HAEFEN, C., SIFRINGER, M., MENK, M. & SPIES, C. D. 2011. Ethanol enhances susceptibility to apoptotic cell death via down-regulation of autophagy-related proteins. *Alcohol Clin Exp Res,* 35**,** 1381-91.

WALL, S. B., OH, J.-Y., DIERS, A. R. & LANDAR, A. 2012. Oxidative modification of proteins: an emerging mechanism of cell signaling. *Frontiers in physiology,* 3**,** 369-369.

WANG, X., CHU, G., YANG, Z., SUN, Y., ZHOU, H., LI, M., SHI, J., TIAN, B., ZHANG, C. & MENG, X. 2015a. Ethanol directly induced HMGB1 release through NOX2/NLRP1 inflammasome in neuronal cells. *Toxicology,* 334**,** 104-110.

WANG, X., KE, Z., CHEN, G., XU, M., BOWER, K. A., FRANK, J. A., ZHANG, Z., SHI, X. & LUO, J. 2012a. Cdc42-dependent activation of NADPH oxidase is involved in ethanol-induced neuronal oxidative stress. *PloS one,* 7**,** e38075-e38075.

WANG, X., YANG, Z., SUN, Y., ZHOU, H., CHU, G., ZHANG, J. & MENG, X. 2015b. Ethanol Activation of PKA Mediates Single-Minded 2 Expression in Neuronal Cells. *Molecular Neurobiology,* 52**,** 1234-1244.

WANG, Y., YANG, J. & YI, J. 2012b. Redox sensing by proteins: oxidative modifications on cysteines and the consequent events. *Antioxid Redox Signal,* 16**,** 649-57.

WARREN, K. R., HEWITT, B. G. & THOMAS, J. D. 2011. Fetal alcohol spectrum disorders: research challenges and opportunities. *Alcohol research & health : the journal of the National Institute on Alcohol Abuse and Alcoholism,* 34**,** 4-14.

WATAYA, T., NUNOMURA, A., SMITH, M. A., SIEDLAK, S. L., HARRIS, P. L., SHIMOHAMA, S., SZWEDA, L. I., KAMINSKI, M. A., AVILA, J., PRICE, D. L., CLEVELAND, D. W., SAYRE, L. M. & PERRY, G. 2002. High molecular weight neurofilament proteins are physiological substrates of adduction by the lipid peroxidation product hydroxynonenal. *J Biol Chem,* 277**,** 4644-8.

WENK, G. L., MCGANN, K., HAUSS-WEGRZYNIAK, B. & ROSI, S. 2003. The toxicity of tumor necrosis factor-α upon cholinergic neurons within the nucleus basalis and the role of norepinephrine in the regulation of inflammation: implications for alzheimer's disease. *Neuroscience,* 121**,** 719-729.

WEST, J. R., CHEN, W.-J. A. & PANTAZIS, N. J. 1994. Fetal alcohol syndrome: the vulnerability of the developing brain and possible mechanisms of damage. *Metabolic Brain Disease,* 9**,** 291-322.

WEST, J. R., GOODLETT, C. R., BONTHIUS, D. J., HAMRE, K. M. & MARCUSSEN, B. L. 1990. Cell Population Depletion Associated with Fetal Alcohol Brain Damage: Mechanisms of BAC-Dependent Cell Loss. *Alcoholism: Clinical and Experimental Research,* 14**,** 813-818.

WHANG, J. M., SCHOMBURG, C. J., GLOTFELTY, D. E. & TAYLOR, A. W. 1993. Volatilization of Fonofos, Chlorpyrifos, and Atrazine from Conventional and No-Till Surface Soils in the Field. *Journal of Environmental Quality,* 22**,** 173-180.

WHITE, R. E. 1991. The involvement of free radicals in the mechanisms of monooxygenases. *Pharmacology & Therapeutics,* 49**,** 21-42.

WHO 2018. Global status report on alcohol and health 2018. *World Health Organization: Geneva*.

WHO 2019. Alcohol country fact sheets (2019). *World Health Organisation Geneva*.

WILLIAMS, M. 2013. The Merck Index: An Encyclopedia of Chemicals, Drugs, and Biologicals, 15th Edition Edited by M.J. O'Neil , Royal Society of Chemistry, Cambridge, UK ISBN 9781849736701; 2708 pages. April 2013, $150 with 1-year free access to The Merck Index Online. *Drug Development Research,* 74**,** 339-339.

WILSON, M. R. & EASTERBROOK-SMITH, S. B. 2000. Clusterin is a secreted mammalian chaperone. *Trends Biochem Sci,* 25**,** 95-8.

WOREK, F., AURBEK, N., KOLLER, M., BECKER, C., EYER, P. & THIERMANN, H. 2007. Kinetic analysis of reactivation and aging of human acetylcholinesterase inhibited by different phosphoramidates. *Biochemical Pharmacology,* 73**,** 1807-1817.

WU, J. M. & HSIEH, T. C. 2011. Resveratrol: a cardioprotective substance. *Ann N Y Acad Sci,* 1215**,** 16-21.

WU, X., YANG, X., MAJUMDER, A., SWETENBURG, R., GOODFELLOW, F. T., BARTLETT, M. G. & STICE, S. L. 2017. From the Cover: AstrocytesAre Protective Against Chlorpyrifos Developmental Neurotoxicity in Human Pluripotent Stem Cell-Derived Astrocyte-Neuron Cocultures. *Toxicological Sciences,* 157**,** 410-420.

XIA, Y., YANG, X., LU, J., XIE, Q., YE, A. & SUN, W. 2020. The endoplasmic reticulum stress and related signal pathway mediated the glyphosate-induced testosterone synthesis inhibition in TM3 cells. *Environmental Pollution,* 260**,** 113949.

XIANG, Y., KIM, K.-Y., GELERNTER, J., PARK, I.-H. & ZHANG, H. 2015. Ethanol upregulates NMDA receptor subunit gene expression in human embryonic stem cell-derived cortical neurons. *PloS one,* 10**,** e0134907-e0134907.

XIE, H. R., HU, L. S. & LI, G. Y. 2010. SH-SY5Y human neuroblastoma cell line: in vitro cell model of dopaminergic neurons in Parkinson's disease. *Chin Med J (Engl),* 123**,** 1086-92.

XIE, Y., HOU, W., SONG, X., YU, Y., HUANG, J., SUN, X., KANG, R. & TANG, D. 2016. Ferroptosis: process and function. *Cell Death & Differentiation,* 23**,** 369-379.

XU, M.-Y., WANG, P., SUN, Y.-J., YANG, L. & WU, Y.-J. 2017. Joint toxicity of chlorpyrifos and cadmium on the oxidative stress and mitochondrial damage in neuronal cells. *Food and Chemical Toxicology,* 103**,** 246-252.

XU, Y., LIU, P. & LI, Y. 2005. Impaired development of mitochondria plays a role in the central nervous system defects of fetal alcohol syndrome. *Birth Defects Research Part A: Clinical and Molecular Teratology,* 73**,** 83-91.

YAMADA, S., KUBO, Y., YAMAZAKI, D., SEKINO, Y. & KANDA, Y. 2017. Chlorpyrifos inhibits neural induction via Mfn1-mediated mitochondrial dysfunction in human induced pluripotent stem cells. *Scientific Reports,* 7**,** 40925.

YANG, D., HOWARD, A., BRUUN, D., AJUA-ALEMANJ, M., PICKART, C. & LEIN, P. J. 2008. Chlorpyrifos and chlorpyrifos-oxon inhibit axonal growth by interfering with the morphogenic activity of acetylcholinesterase. *Toxicology and applied pharmacology,* 228**,** 32-41.

YANG, D., LAURIDSEN, H., BUELS, K., CHI, L.-H., LA DU, J., BRUUN, D. A., OLSON, J. R., TANGUAY, R. L. & LEIN, P. J. 2011. Chlorpyrifos-Oxon

Disrupts Zebrafish Axonal Growth and Motor Behavior. *Toxicological Sciences,* 121**,** 146-159.

YURUMEZ, Y., CEMEK, M., YAVUZ, Y., BIRDANE, Y. O. & BUYUKOKUROGLU, M. E. 2007. Beneficial Effect of N-Acetylcysteine against Organophosphate Toxicity in Mice. *Biological and Pharmaceutical Bulletin,* 30**,** 490-494.

ZERIN, T., SONG, H., GIL, H. & HONG, S. 2017. Surfactant 4-nonylphenyl-polyethylene glycol stimulates reactive oxygen species generation and apoptosis in human neuroblastoma cells. *Journal of Environmental Sciences,* 53**,** 262-268.

ZHANG, J., GUO, J., WU, C., QI, X., JIANG, S., LU, D., FENG, C., LIANG, W., CHANG, X., ZHANG, Y., CAO, Y., WANG, G. & ZHOU, Z. 2019. Exposure to carbamate and neurodevelopment in children: Evidence from the SMBCS cohort in China. *Environmental Research,* 177**,** 108590.

ZHANG, Q., ZHANG, M., HUANG, X., LIU, X. & LI, W. 2016. Inhibition of cytoskeletal protein carbonylation may protect against oxidative damage in traumatic brain injury. *Experimental and therapeutic medicine,* 12**,** 4107-4112.

ZHANG, X., HASHIMOTO, J. & GUIZZETTI, M. 2018. Developmental Neurotoxicity of Alcohol: Effects and Mechanisms of Ethanol on the Developing Brain.

ZHAO, L., YAN, M., WANG, X., XIONG, G., WU, C., WANG, Z., ZHOU, Z. & CHANG, X. 2018. Modification of Wnt signaling pathway on paraquat-induced inhibition of neural progenitor cell proliferation. *Food and chemical toxicology : an international journal published for the British Industrial Biological Research Association,* 121**,** 311-325.

ZHAO, M.-W., YANG, P. & ZHAO, L.-L. 2019. Chlorpyrifos activates cell pyroptosis and increases susceptibility on oxidative stress-induced toxicity by miR-181/SIRT1/PGC-1α/Nrf2 signaling pathway in human neuroblastoma SH-SY5Y cells. *Environmental Toxicology,* 34**,** 699-707.

ZIMATKIN, S. M., PRONKO, S. P., VASILIOU, V., GONZALEZ, F. J. & DEITRICH, R. A. 2006. Enzymatic Mechanisms of Ethanol Oxidation in the Brain. *Alcoholism: Clinical and Experimental Research,* 30**,** 1500-1505.

ANNEXURE I

CHPATER IV

Effect of NAC on ROS generation of CPO, AZO and Aldicarb treated SH-SY5Y cells.

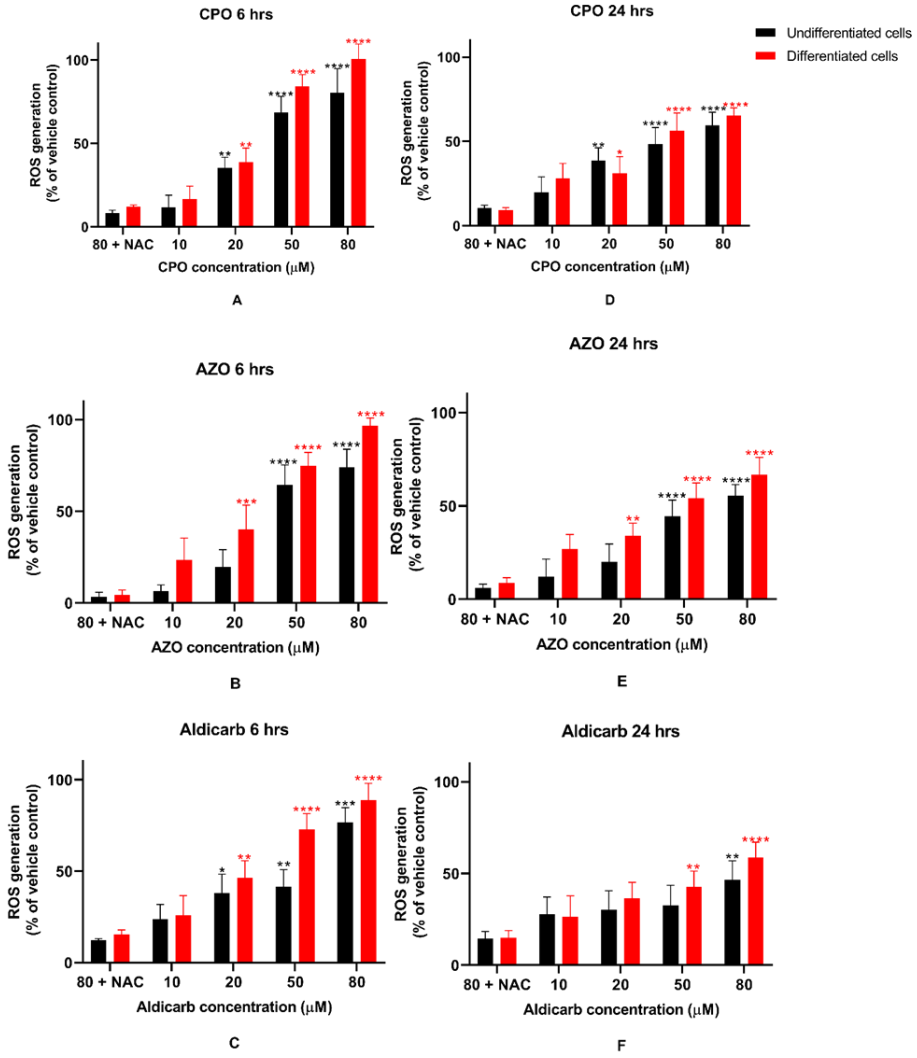


Figure 1: Effect of NAC on ROS generation of CPO, AZO and Aldicarb on undifferentiated and differentiated SH-SY5Y cells for 24 h exposure.
Undifferentiated and differentiated cells were exposed IC_{10}, IC_{20}, IC_{50} and IC_{80} concentrations CPO, AZO, and Aldicarb for 6h (A-C) and 24 h (D-E). 1 mM NAC was added to the cells at the same time cells treated with IC_{80} treatment and incubate for 6 and 24 h. Cellular ROS generation was quantified using DCFDA and readings were normalised to the vehicle control treatments and presented as a percentage of vehicle control. Readings including vehicle control and treatments were obtained from 5 individual experiments (n=5) with triplicates in each treatment. Results were analysed using one-way ANOVA with Tukey's multiple comparison and expressed as the mean ± standard error of the mean (SEM), When SEM bar is not apparent, this means that error is smaller than the symbol size. For significance; *p<0.05, ** p<0.01, **** p<0.0001. * or * indicate the significance difference with IC_{80} + NAC treatment with other treatments.

Quantification of β tubulin II changes in undifferentiated and differentiated SH-SY5Ycells upon exposure of CPO, AZO and Aldicarb for 24 h

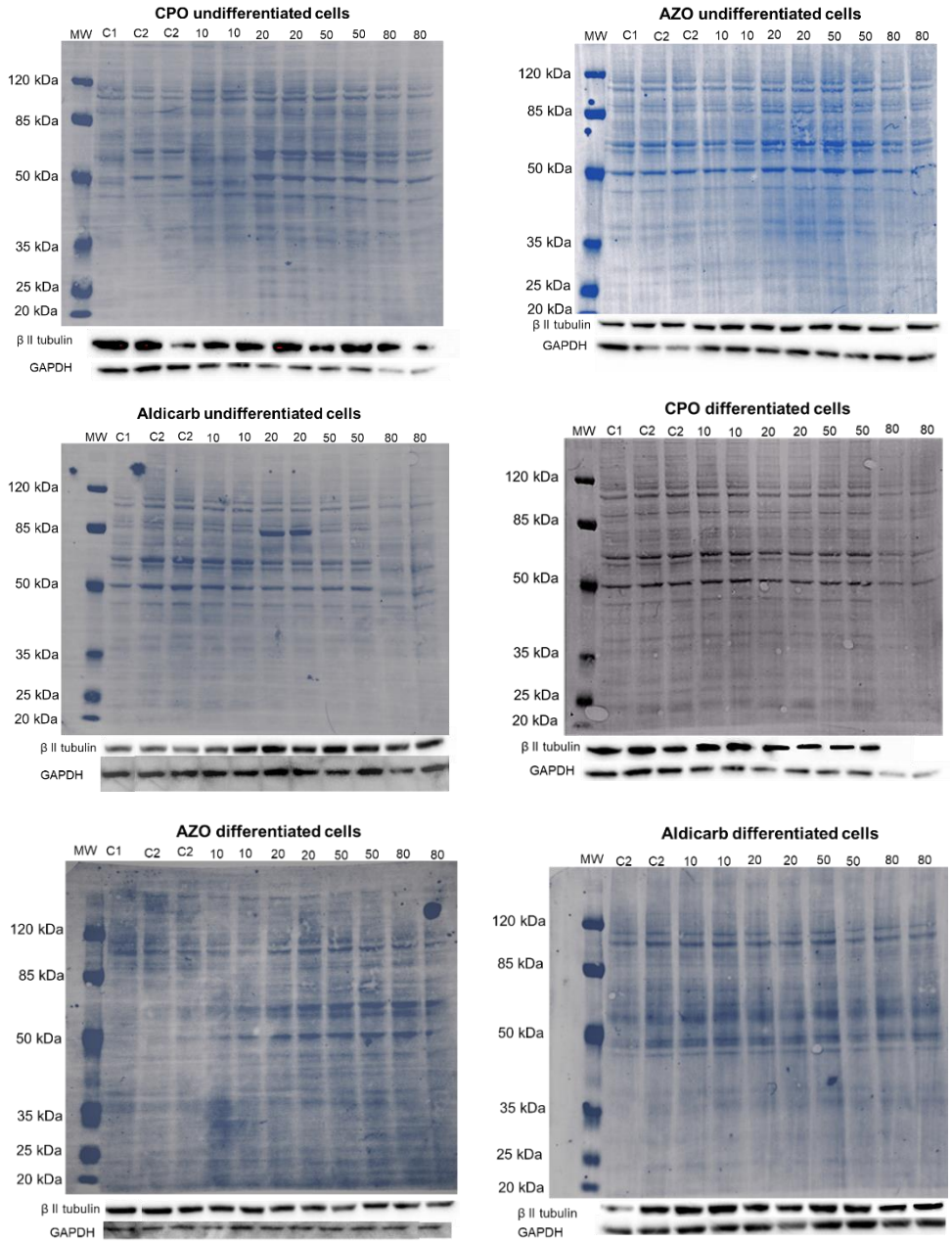


Figure 2: Detection of β II tubulin on western blots of undifferentiated and differentiated neuroblastoma SH-SY5Y cells upon exposure of CPO,AZO and Aldicarb for 24 h.

Expression of βII tubulin expression in undifferentiated and differentiated cells revealed by gel electrophoresis and Western blotting. Equal levels of protein were loaded and the blot reversibly stained (upper panel), with βII and GAPDH detected via immunoblotting. C1 -Control; C2 – vehicle control.

Table 1: Densiometric analysis of western blots probed with β II tubulins in undifferentiated and differentiated cells.

Western blots of cell lysates were probed with β II tubulin, after antibody reactivity was visualized with clarity Western ECL reagents as described in 3.12.4 in methodology. Densiometric peaks were quantified using Imagelab software version 6.0.1 build 64. Band measurements was corrected for background for normalization with total protein and values presented as averages to corresponding controls ± SEM.

Pesticide	Treatment (µM)	Densitometric peak (% control ± SEM)	
		Undifferentiated	Differentiated
CPO	IC_{10}	103 ± 05	110 ± 08
	IC_{20}	104 ± 08	105 ± 05
	IC_{50}	114 ± 10	096 ± 06
	IC_{80}	61 ± 11*	-
AZO	IC_{10}	102 ± 07	102 ± 03
	IC_{20}	103 ± 10	106 ± 06
	IC_{50}	112 ± 08	104 ±12
	IC_{80}	111 ± 06	109 ± 06
Aldicarb	IC_{10}	097 ± 04	100 ± 12
	IC_{20}	101 ± 08	107 ± 10
	IC_{50}	106 ± 06	106 ± 09
	IC_{80}	109 ±11	102 ± 11

CHAPTER V

Effect of NAC on ROS generation of CPO, AZO and Aldicarb treated hNPCs cells.

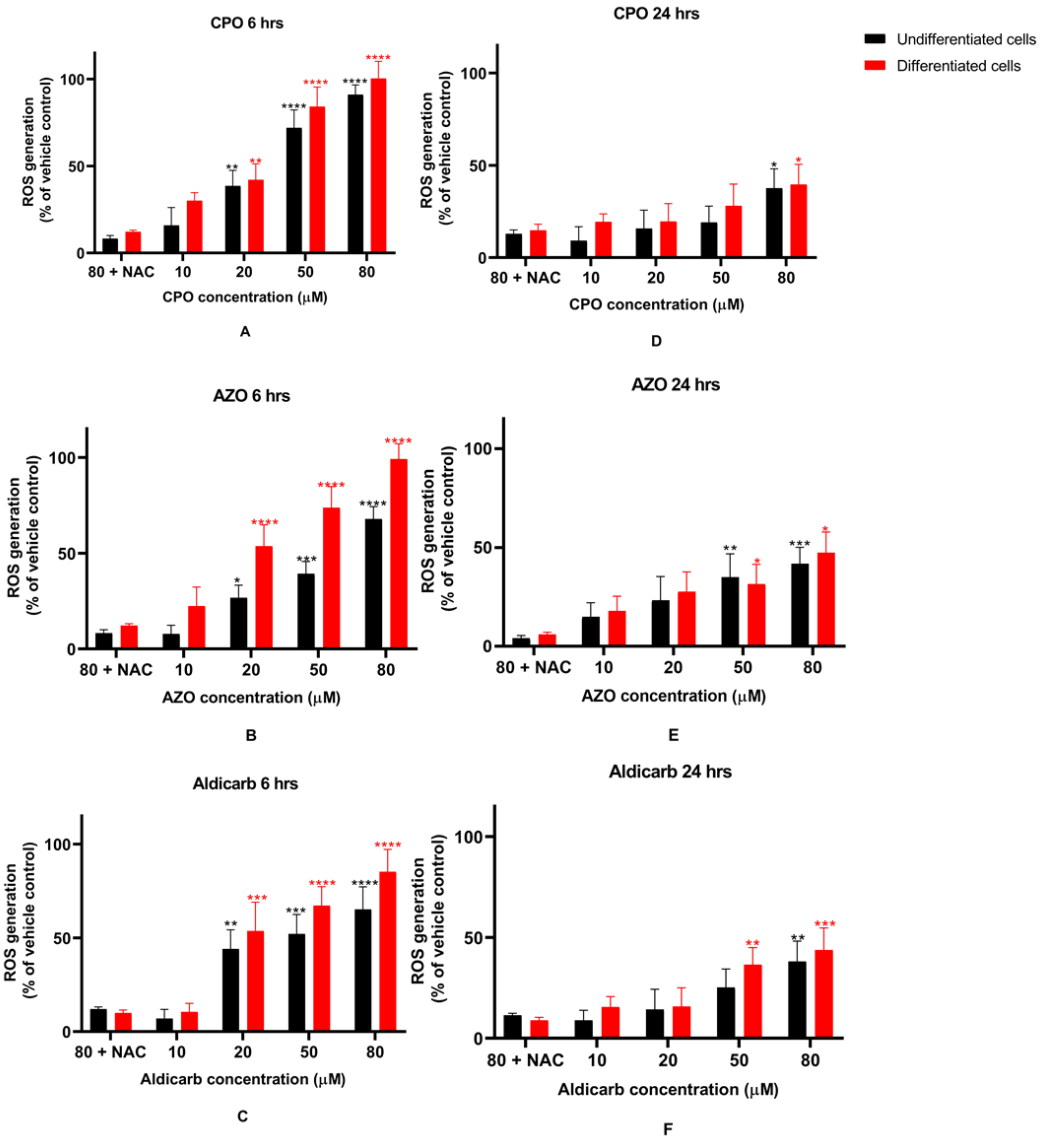


Figure 3: Effect of NAC on ROS generation of CPO, AZO and Aldicarb on undifferentiated and differentiated hNPCs cells for 24 h exposure.
Undifferentiated and differentiated cells were exposed IC_{10}, IC_{20}, IC_{50} and IC_{80} concentrations CPO, AZO, and Aldicarb for 6h (A-C) and 24 h (D-E). 1 mM NAC was added to the cells with the at the same time cells treated with IC_{80} treatment and incubate for 6 and 24 h. Cellular ROS generation was quantified using DCFDA and readings were normalised to the vehicle control treatments and presented as a percentage of vehicle control. Readings including vehicle control and treatments were obtained from 5 individual experiments (n=5) with triplicates in each treatment. Results were analysed using one-way ANOVA with Tukey's multiple comparison and expressed as the mean ± standard error of the mean (SEM), When SEM bar is not apparent, this means that error is smaller than the symbol size. For significance; *p<0.05, ** p<0.01, **** p<0.0001. * or * indicate the comparison with IC_{80} + NAC treatment with other treatments.

Quantification of β tubulin III in differentiated hNPCs cells upon exposure of CPO, AZO and Aldicarb for 24 h.

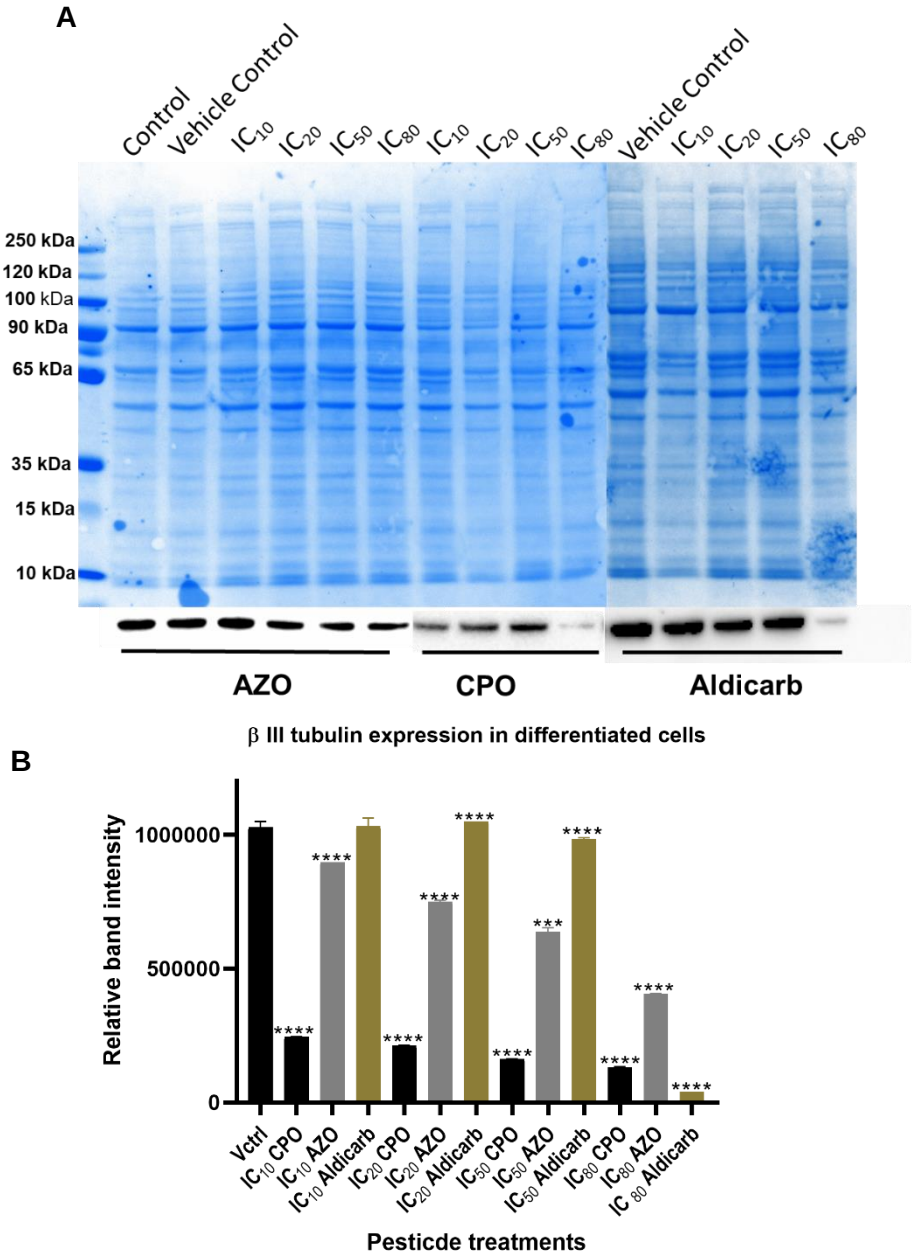


Figure 4: Detection of β III tubulin on western blots of undifferentiated and differentiated hNPCs cells upon exposure of CPO, AZO and Aldicarb for 24 h.

Expression of βIII tubulin expression in differentiated hNPCs cells revealed by gel electrophoresis and Western blotting. Equal levels of protein were loaded and the blot reversibly stained (upper panel), with βII detected via immunoblotting. (A). Western blots of cell lysates were probed with β III tubulin, after antibody reactivity was visualized with clarity Western ECL reagents as described in 3.12.4 in methodology. Densiometric peaks were quantified using Image lab software version 6.0.1 build 64. Band measurements was corrected for background for normalization with total protein. Results were analysed using one-way ANOVA with Tukey's multiple comparison and expressed as the mean ± standard error of the mean (SEM) (B).

CHAPTER VI

Cellular proliferation of SH-SY5Y cells in response to alcohol exposure.

Cell were grown in 96 well plates as described for the MTT assay, and similarly treated with ethanol for 24 hours. Cell proliferation was assessed using a 5-bromo-2'-deoxyuridine (BrdU) cell proliferation assay (QIA58, Millipore, USA) according to the manufacturer's guidelines. After treatment with ethanol, 20 µL of BrdU label was added to the cells at a 1:2000 dilution in growth media and cells returned to the incubator for 24 hours. Cell were fixed and then wells incubated for 1 hour at room temperature with 100 µL of a specific anti-BrdU primary antibody at 1:100 dilution, followed by 100 µL of horse radish peroxidase goat anti-mouse secondary for 30 min at room temperature. After plate washing, 100 µL of substrate solution (3,3',5,5'-tetramethylbenzamine (TMB) Peroxidase) was added to each well and samples incubated in the dark for 15 mins, before 100 µL of stop solution (2.5 N H_2SO_4) was added. The absorbance of each well was measured spectrophotometrically (Multiskan Spectrum, Thermo Electron Corporation, Finland) at dual wavelengths of 450 and 540 nm. The BrdU incorporation was expressed as a percentage of control wells after subtraction of absorbance of blanks. Samples were assayed in triplicate.

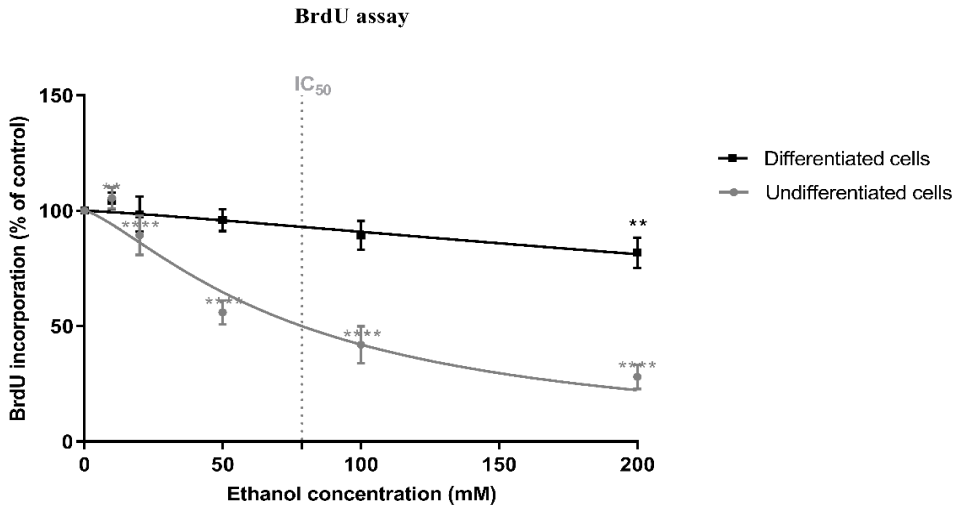


Figure 5: BrdU incorporation of ethanol treated undifferentiated and differentiated SH-SY5Y cells.

Undifferentiated and differentiated cells were exposed 0-200 mM ethanol concentrations for 24 h. BrdU assay readings were normalised to the vehicle control treatments and presented as a percentage of vehicle control. Readings including vehicle control and treatments were obtained from five individual experiments with triplicates in each treatment. Results were analysed using one-way ANOVA with Dunnett's multiple comparison and expressed as the mean ± standard error of the mean (SEM), for significance ** $p< 0.01$; **** $p<0.0001$.

Effect of NAC on ROS generation of SH-SY5Y cells exposed ethanol for 24 h.

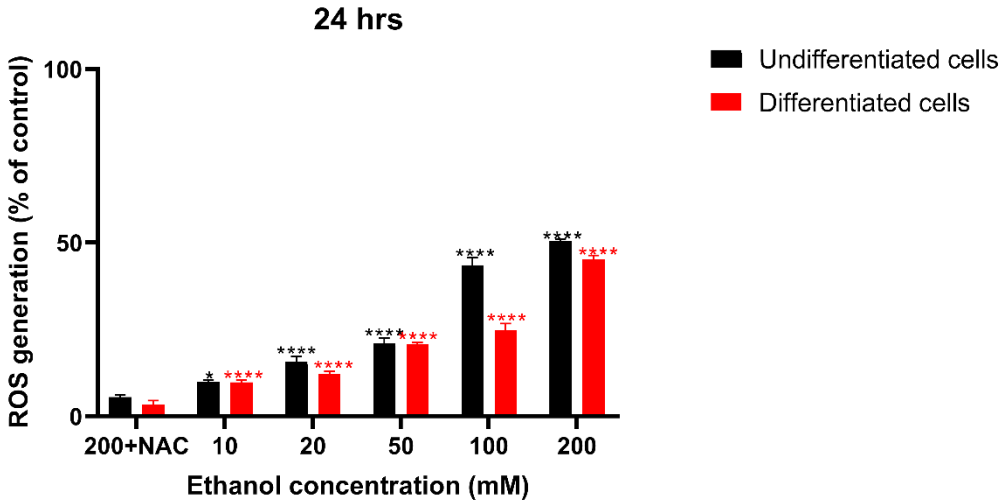


Figure 6: Effect of NAC on ROS generation of ethanol on undifferentiated and differentiated SH-SY5Y cells for 24 h exposure

Undifferentiated and differentiated cells were exposed 0 - 200 mM concentrations ethanol for 24 h.1 mM NAC was added to the cells at the same time cells treated with 200 mM treatment and incubate for 24 h. Cellular ROS generation was quantified using DCFDA and readings were normalised to the vehicle control treatments and presented as a percentage of vehicle control. Readings including vehicle control and treatments were obtained from 5 individual experiments (n=5) with triplicates in each treatment. Results were analysed using one-way ANOVA with Tukey's multiple comparison and expressed as the mean ± standard error of the mean (SEM), When SEM bar is not apparent, this means that error is smaller than the symbol size. For significance; *p<0.05, ** p<0.01, **** p<0.0001. * or * indicate the significance difference with 200 mM + NAC treatment with other treatments.

Table 2: Densitometric analysis of western blots probed with β II tubulins in undifferentiated and differentiated cells.

Western blots of cell lysates were probed with β II tubulin, after antibody reactivity was visualized with clarity Western ECL reagents as described in 3.12.4 in methodology. Densiometric peaks were quantified using Imagelab software version 6.0.1 build 64. Band measurements was corrected for background for normalization with total protein and values presented as averages to corresponding controls ± SEM. * - Significant

Pesticide	Treatment (µM)	Densiometric peak are (% control ± SEM)	
		Undifferentiated	Differentiated
Ethanol	50	105 ± 5	96 ± 7
	100	108 ±8	98 ± 4
	200	115 ± 10*	98 ± 10

Quantification of β tubulin II in SH-SY5Y cells exposed ethanol for 24 h.

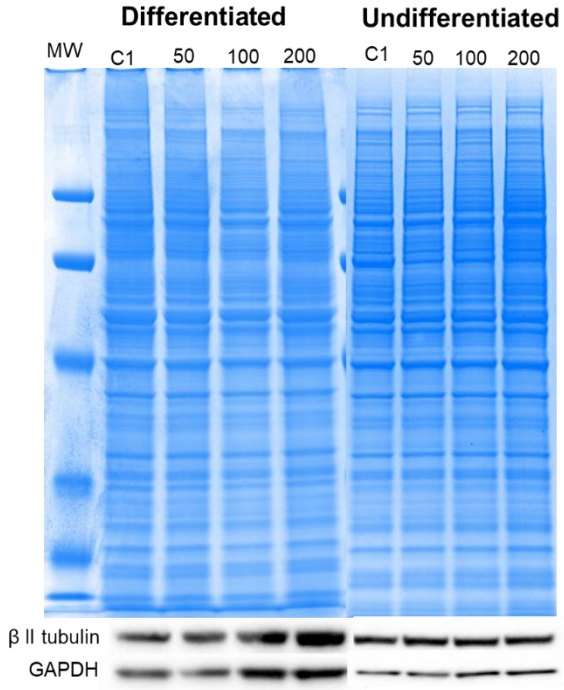


Figure 7: Detection of β II tubulin on western blots of undifferentiated and differentiated neuroblastoma SH-SY5Y cells upon exposure of CPO, AZO and Aldicarb for 24 h.
Expression of βII tubulin expression in undifferentiated and differentiated cells revealed by gel electrophoresis and Western blotting. Equal levels of protein were loaded and the blot reversibly stained (upper panel), with βII and GAPDH detected via immunoblotting. C1 -Control; C2 – vehicle control.

Table 3: Psychiatric diagnosis, age, gender, post-mortem delay (PMD), cause of death, and toxicological characteristics of Control (C), Alcoholic (A) subjects used in this study.

Identifier	Psychiatric diagnosis	Age (years)	Gender (F/M)	PMD (h)	Cause of death	Ethanol in blood (mg/ml)	Other drugs in blood
C1	None	66	M	50	Accident	0	(-)
A1	Alcoholism	71	M	17	Accident	0.35	(-)
C2	Bipolar	50	M	6	Suicide	0	Diazepam
A2	Alcoholism	50	M	3	Suicide	0	(-)
C3	Anxiety	44	M	15	Suicide	0	(-)
A3	Alcoholism	40	M	21	Suicide	0	(-)
C4	Depression	58	F	48	Suicide	Not determined	Not determined
A4	Alcoholism	57	F	24	Suicide	0.23	Methanol
C5	Anxiety	48	F	9	Suicide	0	Ephedrine
A5	Alcoholism	50	F	6	Suicide	0	Hydroclorothiazide
C6	OCD	65	M	19	Suicide	0	Nodiazepam
A6	Alcoholism	71	M	19	Suicide	0.55	(-)
C28	None	64	F	19	Cardiac failure	Not determined	Not determined

CHAPTER VII.

Effect of NAC on ROS generation of hNPCs cells exposed ethanol for 24 h.

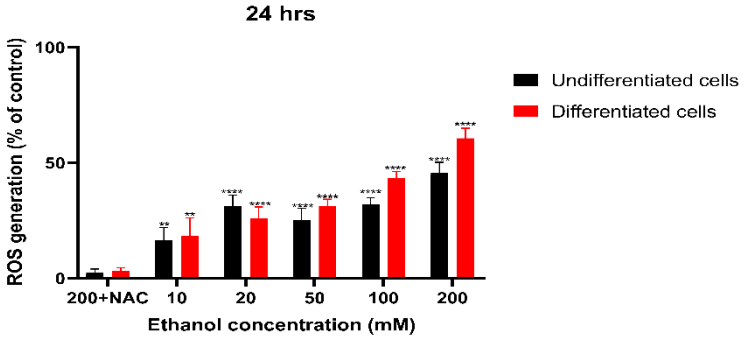


Figure 8: Effect of NAC on ROS generation of ethanol on undifferentiated and differentiated hNPCs cells for 24 h exposure.
Undifferentiated and differentiated cells were exposed 0 - 200 mM concentrations ethanol for 24 h.1 mM NAC was added to the cells at the same time cells treated with 200 mM treatment and incubate for 24 h. Cellular ROS generation was quantified using DCFDA and readings were normalised to the vehicle control treatments and presented as a percentage of vehicle control. Readings including vehicle control and treatments were obtained from 5 individual experiments (n=5) with triplicates in each treatment. Results were analysed using one-way ANOVA with Tukey's multiple comparison and expressed as the mean ± standard error of the mean (SEM), When SEM bar is not apparent, this means that error is smaller than the symbol size. For significance; *p<0.05, ** p<0.01, **** p<0.0001. * or * indicate the significance difference with 200 mM + NAC treatment with other treatments.8

Identification of major cytosolic protein targets of protein carbonylation

2D oxyblots

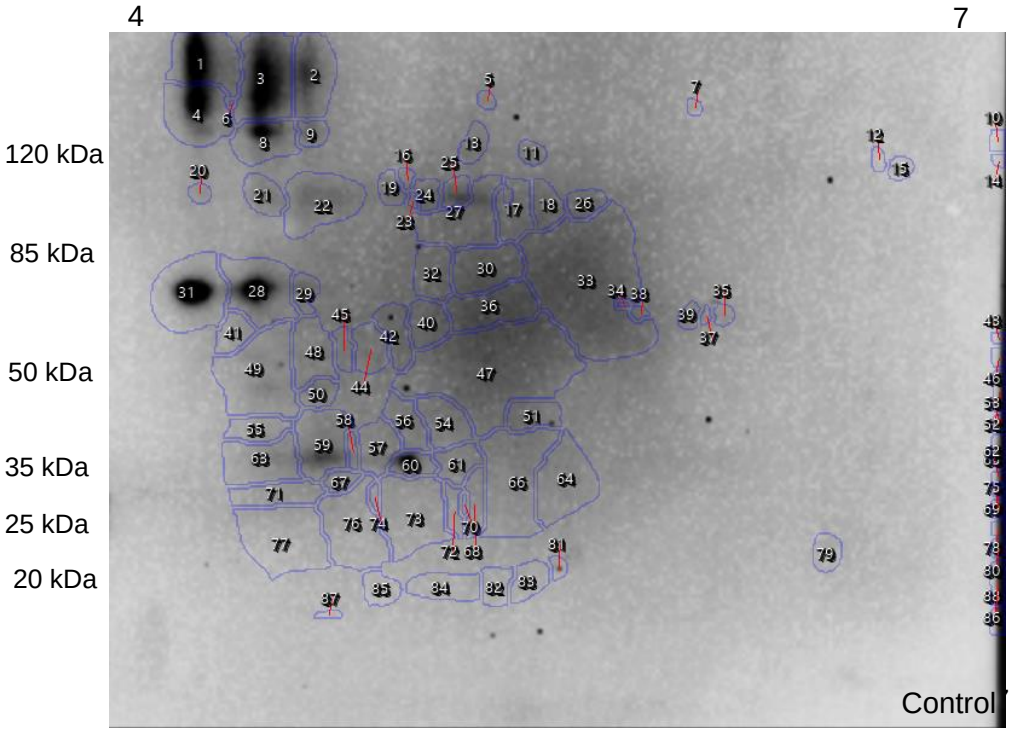
500 µg of SH-SY5Y cells treated with IC_{50} of CPO, AZO, Aldicarb, or 50 mM ethanol or vehicle controls were derivatized with DNPH for 1 h at room temperature by vortex missing at every 15 minutes. Samples were then precipitated by ice cold 20 % TCA on ice for 10 minutes. Then samples were centrifuged at 4 ^{o}C at 500 x g for 5 minutes. Then samples were washed with 20 % TCA and cleaned with 1:1 ethanol: ethyl acetate until the sample was clear to dissolve within a rehydration buffer. Protein in the samples were solubilized

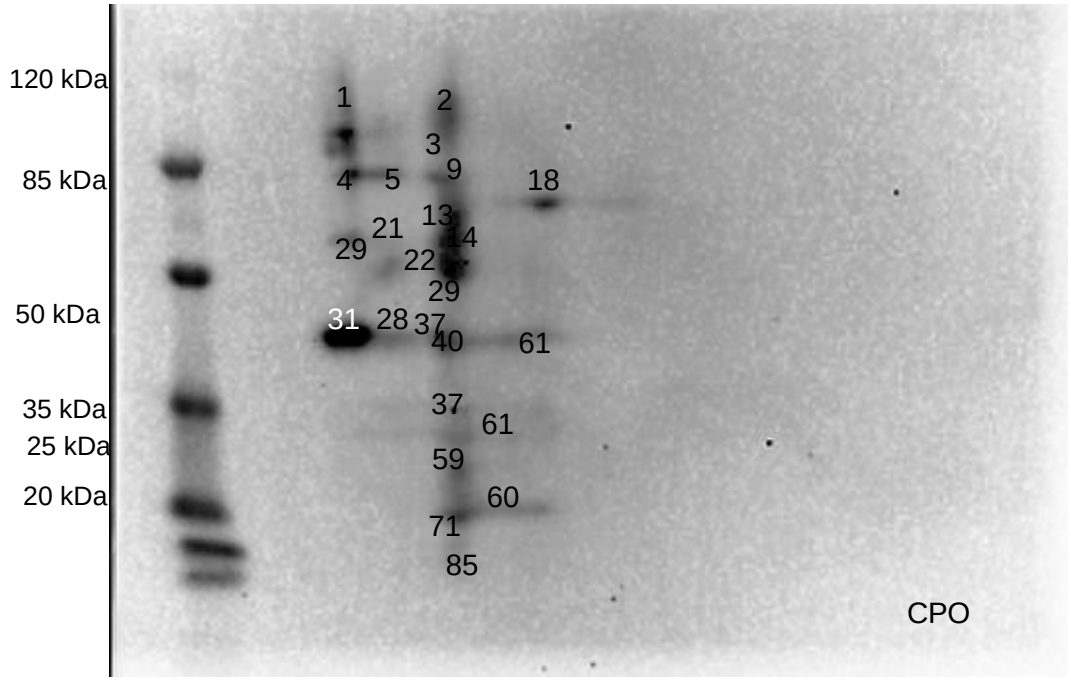
with 8 M urea, 2 M thiourea, 2% CHAPS, 30 mM Tris, 200 mM TBP and 0.8% (V/V) carrier ampholytes and 6 µl of de-streak agent. Samples were vortexed for 30 seconds and then left 1 h at room temperature to dissolve the protein pellets. Then samples were loaded into the rehydration tray with IPG strips (pH 4-7 (non-linear (NL) strips and 1 ml of mineral oil was added to prevent evaporation. Samples allowed to passively rehydrate at room temperature for 1 h and then actively rehydrated using a Protean IEF cell at 50 V for 16 hours. Following active rehydration wetted paper wicks were placed in the focusing tray underneath the gel strips in the place of the cathode and anode wires. Strips were focussed at 20 ^{o}C with a voltage gradient for a total of 25,000 Vh with a limiting current of 50 mA/ strip, rapid ramping and hold settings. Focused time lasted for 16-20 hrs after which strips were run on 2D gels.

Focused strips were run on 2D gels to separate the proteins according to their denatured molecular weight. Strips were first washed in equilibrium buffer containing 2% (w/v) DTT and then 2.5 % (w/v) iodoacetamide for 15 minutes each. Then strips were washed in a running buffer (MOPS) before protein separation using 4-12 % NuPage Bis-Tris protein gels 2D (4-12% gradient) gels. 10 µl of protein standard was pipetted in the first well and IPG strips was overlaid with warm molten 1% agarose to fix in place. Gels were resolved using 125 V for 1 hour and were electro-transferred to PVDF membranes at 80V for 2h for immunoblotting.

PVDF membranes were blocked with 1% BSA in PBST for 1h at room temperature and probed with anti-DNPH antibody at a concentration of 1:150 overnight at 4^{o}C. The following day, blots were probed with 1:300 of horse secondary antibody and images were acquired using Chemi-Doc imaging system (Bio-Rad) using ECL substrates.

Spot analysis was done using same spot 2D gel analysis software to identify the carbonylated proteins compared to vehicle control treatment. IC_{50} concentrations of each pesticides were selected for doing 2D oxyblots since these provided significant levels of protein carbonylation and at the same time maintaining a significant percentage of live cells. In the vehicle control, protein spots corresponding to the carbonylated species covered the acid to neutral pI numbered in CPO, AZO and Aldicarb. Spots showing immunoreactivity and visible in very low levels were not analysed in treatments. However, these experiments were performed only once and need to be repeated several more times to establish the reproducibility of spot identification and to establish fold changes in carbonylation of proteins.


4
7
120 kDa
85 kDa
50 kDa
35 kDa
25 kDa
20 kDa
Control


120 kDa
85 kDa
50 kDa
35 kDa
25 kDa
20 kDa
CPO

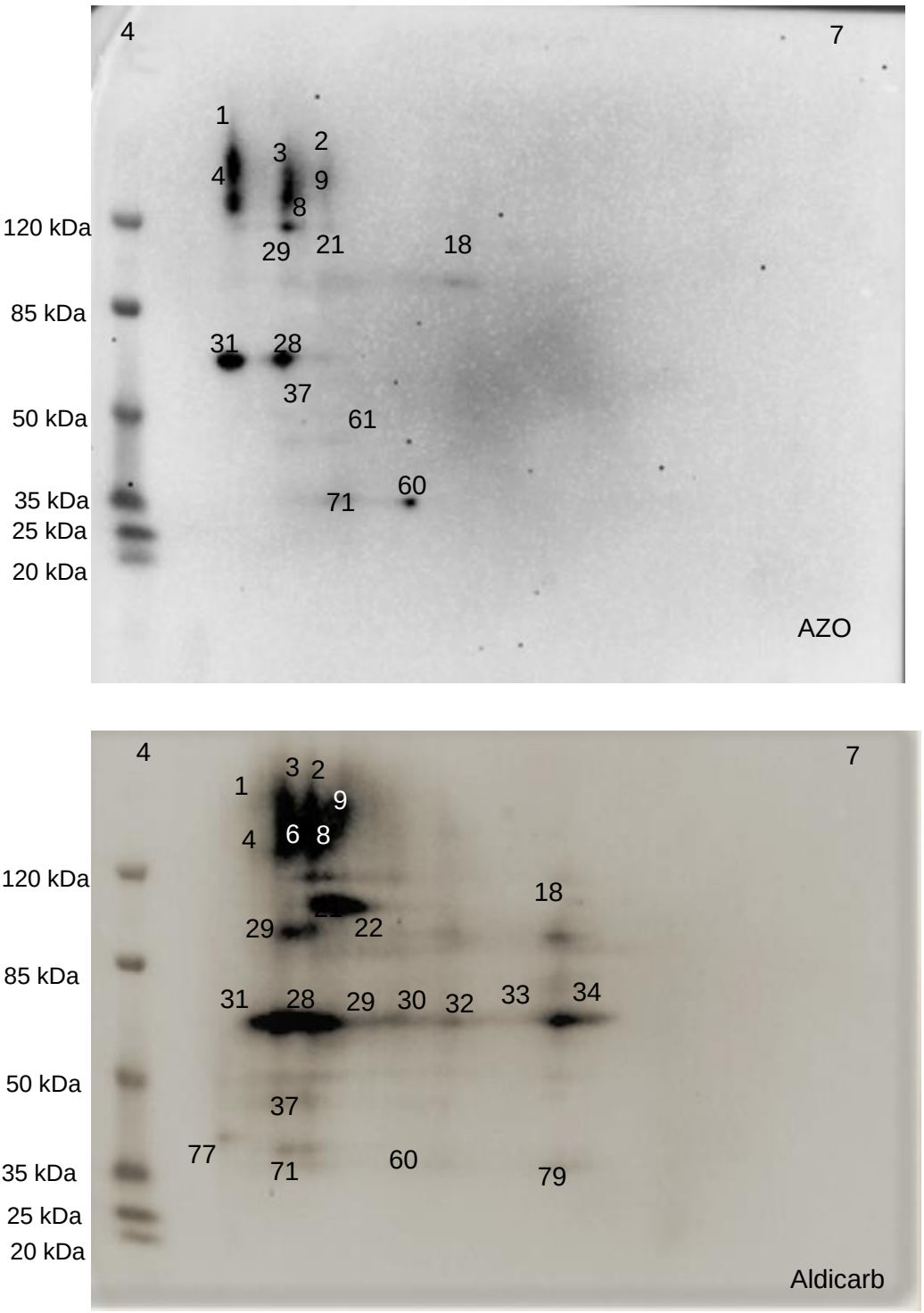


Figure 9: 2D analysis of protein carbonylation in differentiated SH-SY5Y cells exposed to CPO, AZO and Aldicarb. Vehicle control shows total protein staining. CPO, AZO and Aldicarb showed 2D oxyblots.